6.10.93

NASA Contractor Report 191097

Three-Dimensional Water Droplet Trajectory Code Validation Using an ECS Inlet Geometry

Marlin D. Breer and Mark P. Goodman
Boeing Defense and Space Group
Seattle, Washington

May 1993

Prepared for
Lewis Research Center
Under Contract NAS3-25820

NASA
National Aeronautics and
Space Administration

THREE-DIMENSIONAL WATER DROPLET TRAJECTORY CODE VALIDATION USING AN ECS INLET GEOMETRY

Marlin D. Breer
Boeing Commercial Airplane Group
3801 South Oliver M/S K95-05
Wichita, Kansas 67210

Mark P. Goodman
Boeing Defense & Space Group
Military Airplanes Division
P.O. Box 3707 M/S 4C-71
Seattle, WA. 98124-2207

March 31, 1992

Prepared under Contract NAS3-25820 for:

Lewis Research Center
Cleveland, Ohio 44135

ABSTRACT

A task was completed under NASA contract, the purpose of which was to validate a three-dimensional particle trajectory code with existing test data obtained from the Icing Research Tunnel at NASA-Lewis. The geometry analyzed was a flush-mounted ECS inlet. Results of the study indicated good overall agreement between analytical predictions and wind tunnel test results at most flight conditions. Difficulties were encountered when predicting impingement characteristics of the droplets less than or equal to 13.5 microns in diameter. This difficulty was corrected to some degree by modifications to a module of the particle trajectory code; however, additional modifications will be required to accurately predict impingement characteristics of smaller droplets.

TABLE OF CONTENTS

TABLE OF CONTENTS

LIST OF FIGURES

LIST OF FIGURES

LIST OF FIGURES

LIST OF FIGURES

LIST OF FIGURES

LIST OF FIGURES

LIST OF FIGURES

LIST OF FIGURES

LIST OF FIGURES

LIST OF FIGURES

LIST OF FIGURES

LIST OF FIGURES

NOMENCLATURE AND SYMBOLS

AGPS	Aerodynamic Grid and Paneling System
BETA	Postprocessor for 3-D PTA
COMPBETA	Postprocessor for BETA
CONTOUR	Preprocessor for BETA
D1	The smallest diameter droplet in the IRT tunnel cloud distribution--5.6 micron
D2	The second diameter droplet in the IRT tunnel cloud distribution--9.1 micron
D3	The third diameter droplet in the IRT tunnel cloud distribution--13.5 micron
D4	The fourth diameter droplet in the IRT tunnel cloud distribution--20.4 micron
D5	The fifth diameter droplet in the IRT tunnel cloud distribution--32.3 micron
D6	The sixth diameter droplet in the IRT tunnel cloud distribution--46.7 micron
D7	The largest diameter droplet in the IRT tunnel cloud distribution--66.3 micron
FC1	Flight Condition 1 of Table 3.1
FC2	Flight Condition 2 of Table 3.1
FC3	Flight Condition 3 of Table 3.1
FC4	Flight Condition 4 of Table 3.1
IRT	Icing Research Tunnel at NASA-Lewis
LSQGEN	Preprocessor computer program which determines least square velocity coefficients for all flowfield cells which intersect the geometry
MASTER	Modeling of Aerodynamic Surfaces by Three-dimensional Explicit Representation
MVD	Mean Volumetric Diameter
PTA	Particle Trajectory Analysis Computer Code
P582	Transonic Potential Flow Code about Three Dimensional Configurations

NOMENCLATURE AND SYMBOLS

S	Surface distance measured from geometric highlight, in. or cm.
12LY	Refers to ECS inlet lower lip cross section at buttock line Y=12.0 inches
12UY	Refers to ECS inlet upper lip cross section at buttock line Y=12.0 inches
20Y	Refers to ECS wing cross section at buttock line Y=20.0 inches
4Y	Refers to ECS wing cross section at buttock line Y=4.0 inches

1.0 INTRODUCTION

Experimental aerodynamic and local water impingement efficiency data were obtained during ECS inlet testing in the NASA-Lewis Icing Research Tunnel (IRT) in April and May 1989. A task entitled "3-D Trajectory Code Validation" was initiated by NASA-Lewis in May 1990. The overall objective of the task was to compare experimental and analytical aerodynamic and local water impingement efficiency data for the ECS inlet tested in the NASA-Lewis IRT in 1989 and to document the results. An additional objective was to provide the NASA Task Manager the necessary tools to carry out independent trajectory analyses of the ECS inlet. Specific task items identified to meet these objectives are summarized as follows:

a. Obtain an accurate representation of the ECS inlet (including the end cap geometry) to generate patch geometry data needed for flowfield and trajectory calculations.

b. Produce and refine flowfield mesh until no differences exist in trajectory results for successive mesh refinements.

c. Generate suitable flowfields for each of the four conditions tested in the IRT.

d. Produce plots comparing experimental and analytical surface Mach numbers for each of the four conditions tested.

e. Produce individual local collection efficiency curves at each of four geometry locations for each of the four flow conditions tested (maximum number of curves = 7 drop sizes/location x 4 geometry locations/condition x 4 conditions = 112).

f. Combine the individual local collection efficiency curves to produce cumulative local collection efficiency curves at each of the four geometry locations for each of the flow conditions (maximum number of curves = 4 geometry locations/condition x 4 conditions = 16).

g. Produce plots comparing analytical cumulative local collection efficiency to experimental collection data for each of the 16 cases.

h. Prepare informal Task Order Final Report which includes a summary of analysis codes, flowfield comparison plots, local collection efficiency comparison plots and a discussion of overall comparisons.

i. Provide computer data files to NASA Task Manager.

During the course of the project significant difficulties were encountered while obtaining correct water impingement analysis data. The problems were due to water droplets crossing as they got close to the geometry, resulting in irregular and incorrect water impingement patterns on the surface of the geometry. After extensive review and analyses it was determined that the trajectory crossing problem was probably due to inadequate least square fits of the surface cell (i.e., those flowfield mesh cells which are irregular due to intersecting the geometry) velocities. The above described effort was stopped in December 1990 due to budget constraints and technical problems related to the trajectory crossings.

The project was restarted in August 1991 with the same overall objective to compare experimental and analytical aerodynamic and local water impingement efficiency for the ECS inlet and to document the results. Due to the earlier findings, emphasis was placed on correcting the trajectory crossing problem rather than to modifying the flowfield mesh in an attempt to obtain correct analytical water impingement efficiency data. Specific task items identified to correct the trajectory crossing problem and still achieve the overall objective were as follows:

1. Select a previously-run case which exhibited trajectory crossings and analyze it in detail to determine the cause.

2. Determine if the trajectory crossings are affected by the Least Square fit of the surface cell velocities.

3. Correct the Least Square preprocessor if erroneous surface cell velocities are being calculated.

4. Complete the comparison of experimental and analytical aerodynamic and water impingement efficiency data and document results.

1.1 Summary

Analyses of the ECS inlet for the four flight conditions (inlet massflows, W, of 3.0 and 4.3 lbm/sec at 0.0° and 15.0° angle of attack) have been successfully completed. Experimental aerodynamic surface Mach number data were available from NASA-Lewis for the upper and lower geometry surfaces at buttock line Y = 12.0. Surface Mach number experimental data were not available at buttock lines Y= 4.0 and 20. Experimental water impingement data were available for the upper and lower geometry surfaces at buttock line Y = 12.0 as well as buttock lines Y = 4 and Y = 20.0

Comparisons of the analytical surface Mach number data results between an initial mesh (Mesh2) and a refined mesh (Mesh3) showed that the mesh refinement had very little effect on the analytical results. This also provided justification for placing emphasis on improving water impingement efficiency results by investigating and correcting the surface cell least square velocities instead of modifying and refining the flowfield mesh. An added benefit of using a less dense flowfield mesh is a considerable savings in computer time and computer storage requirements. Since only minor differences were found between the surface Mach number results for Mesh2 and Mesh3 for condition 1 (alpha = 0°, W = 3.0 lbm/sec) and condition 3 (alpha = 15.0° and W = 4.3 lbm/sec), Mesh2 was chosen for all comparisons with experimental surface Mach numbers. Comparisons between Mesh2 analytical surface Mach number results and experimental surface Mach numbers show good agreement. The flowfield calculated using Mesh2 was then used as input to the Least Square preprocessor and also as a direct input to the 3-D particle trajectory program.

Particle trajectory runs were made for all flight conditions, geometry locations and droplet sizes. After corrections were made to the least squares generator module of the code, the code was able to predict impingement values for droplet sizes 4 through 7 (20.4 through 66.3 microns). For droplet sizes 1 and 2 (5.6 and 9.1 microns) the code indicated no impingement; this prediction was substantiated by two-dimensional analysis. For droplet size 3 (13.5 microns) several instances of crossing trajectories were still in evidence, indicating the need for further improvements to the module.

Agreement between analytical predictions and test data was good, particularly for flight conditions 2 and 3. At conditions for which impingement distributions did not match as well, overall water collection values were still in good agreement. Thus, although additional code modifications will certainly enhance its capabilities, the code in its present state represents a valuable tool for prediction of three dimensional particle impingement characteristics.

2.0 ECS GEOMETRY

The 3-D geometry of the ECS inlet is shown in Figure 2.1. Figure 2.2 illustrates the inlet imbedded in a constant chord wing. The analytical geometry definition consists of a series of networks, which are divided into sections and members. The complete geometry definition of the ECS inlet imbedded in the wing is made up of sixteen different networks with various numbers of sections and members. Appendix A shows the sixteen networks which define the ECS geometry as well as a summary of the relevant parameters of each of the networks.

The ECS geometry cross sections where detailed aerodynamic analysis data and water impingement data were obtained are at buttock lines Y=4.0, Y=12.0 (upper and lower lip) and Y=20.0. These cross sectional cuts are illustrated in Figures 2.3, 2.4 and 2.5.

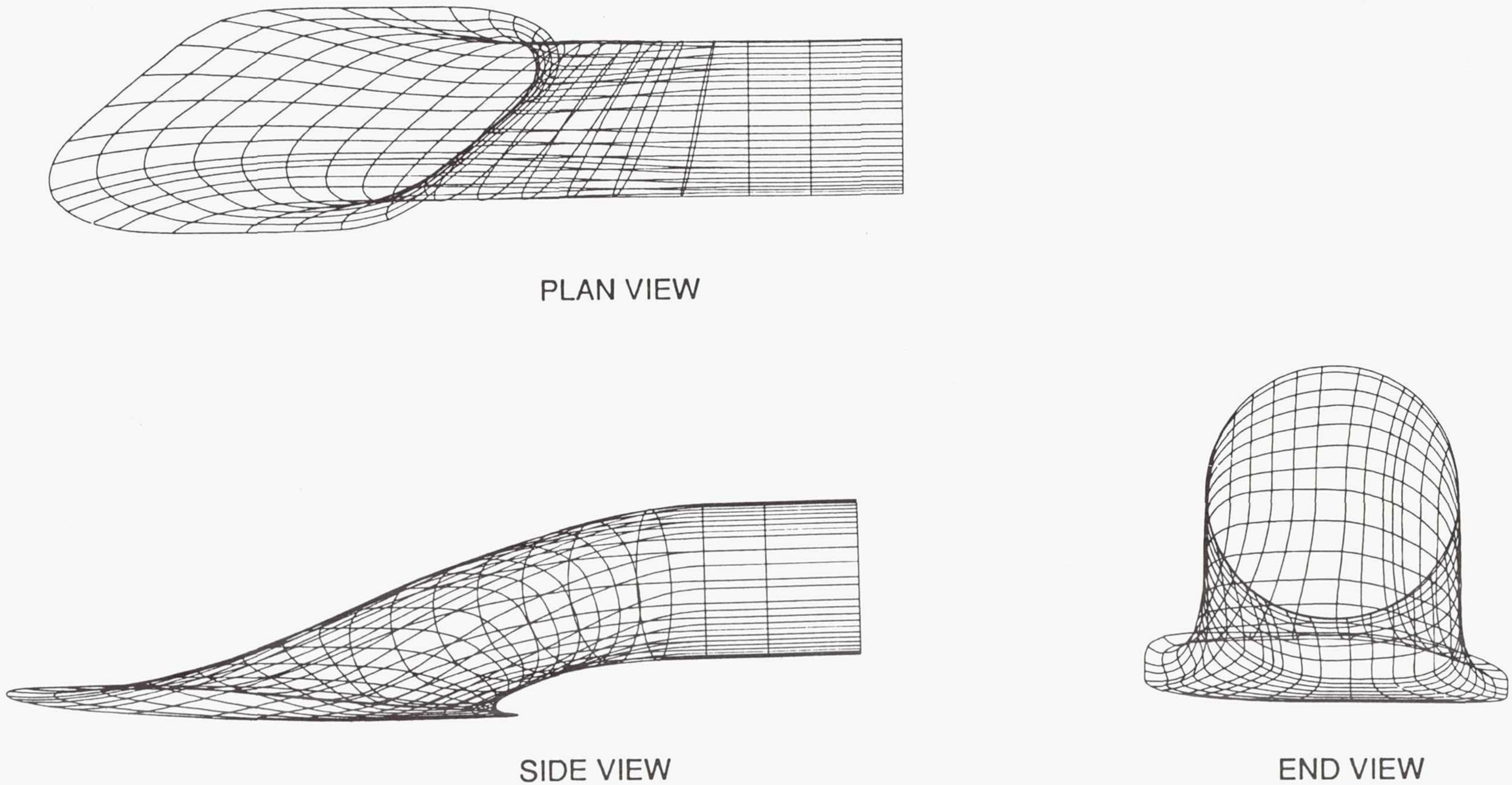

FIGURE 2.1

THREE VIEWS OF ECS INLET

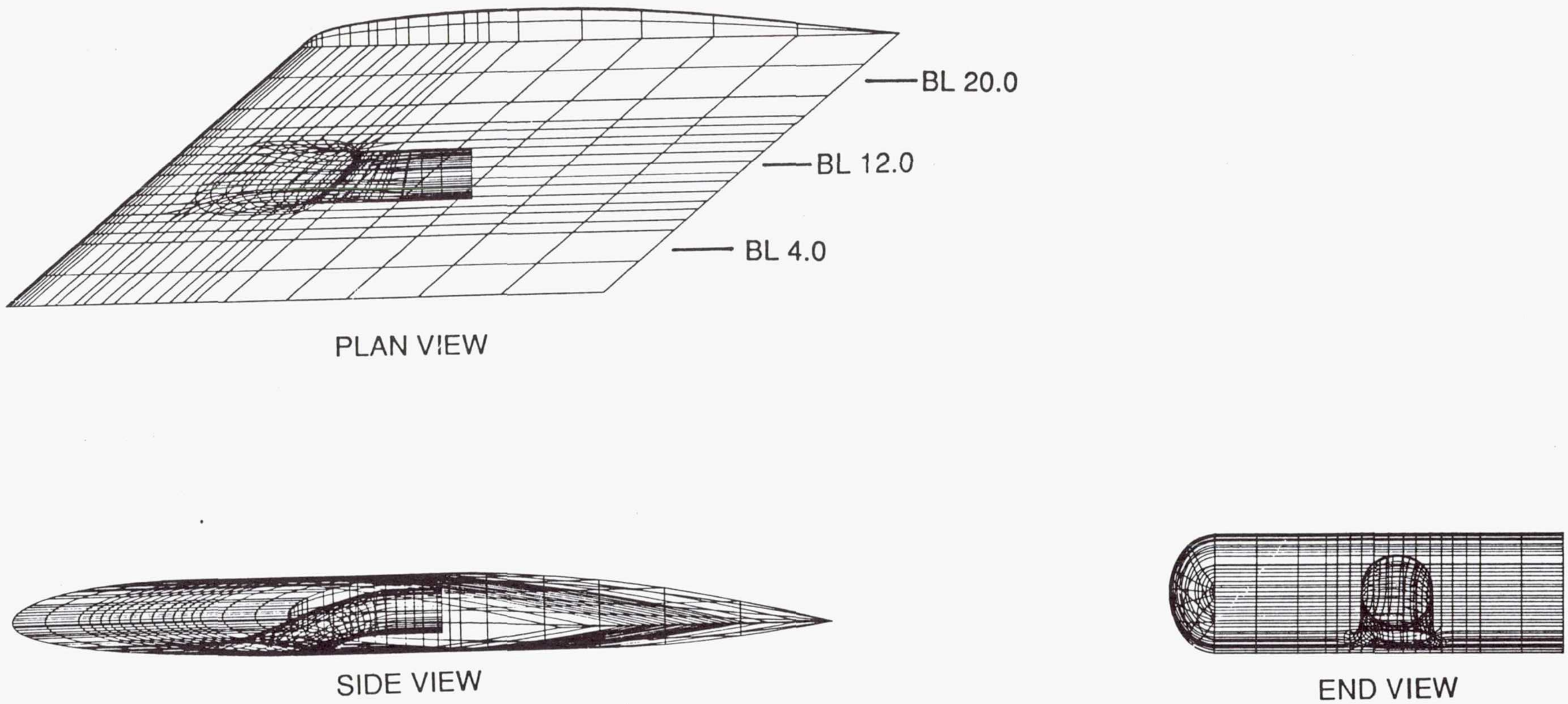

FIGURE 2.2

THREE VIEWS OF ECS INLET IMBEDDED IN A WING

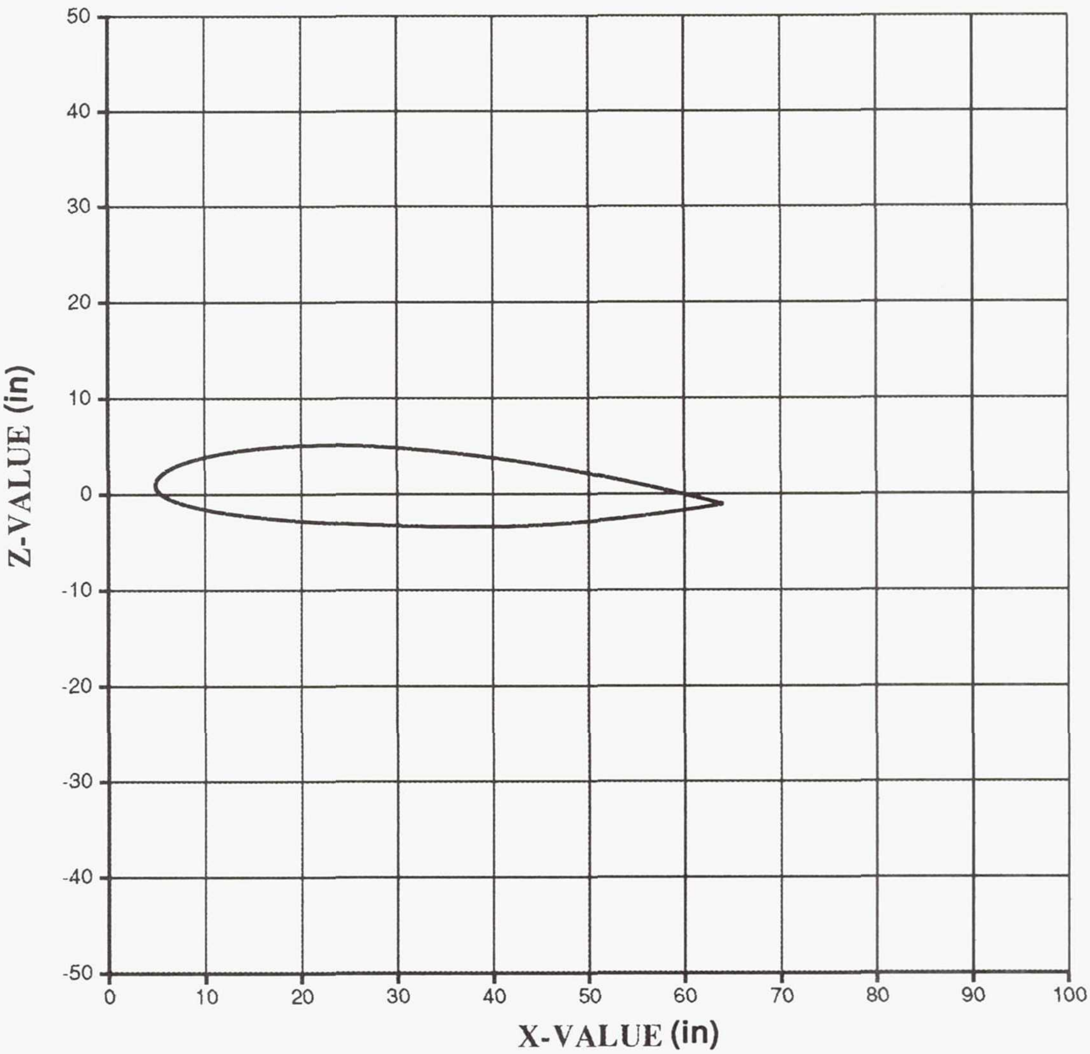

FIGURE 2.3

ECS GEOMETRY CROSS SECTION AT BUTTOCK LINE Y=4.0

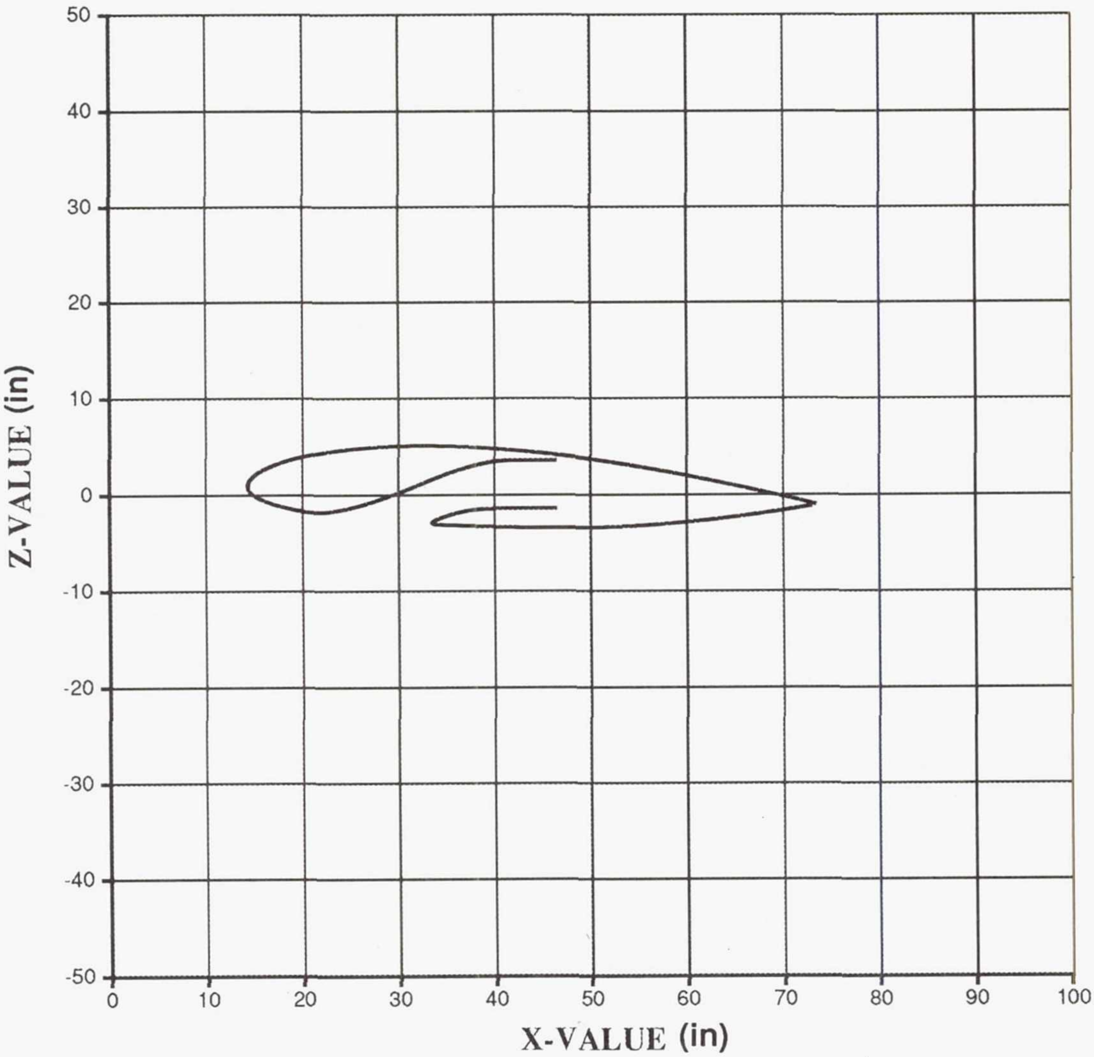

FIGURE 2.4

ECS GEOMETRY CROSS SECTION AT BUTTOCK LINE Y=12.0

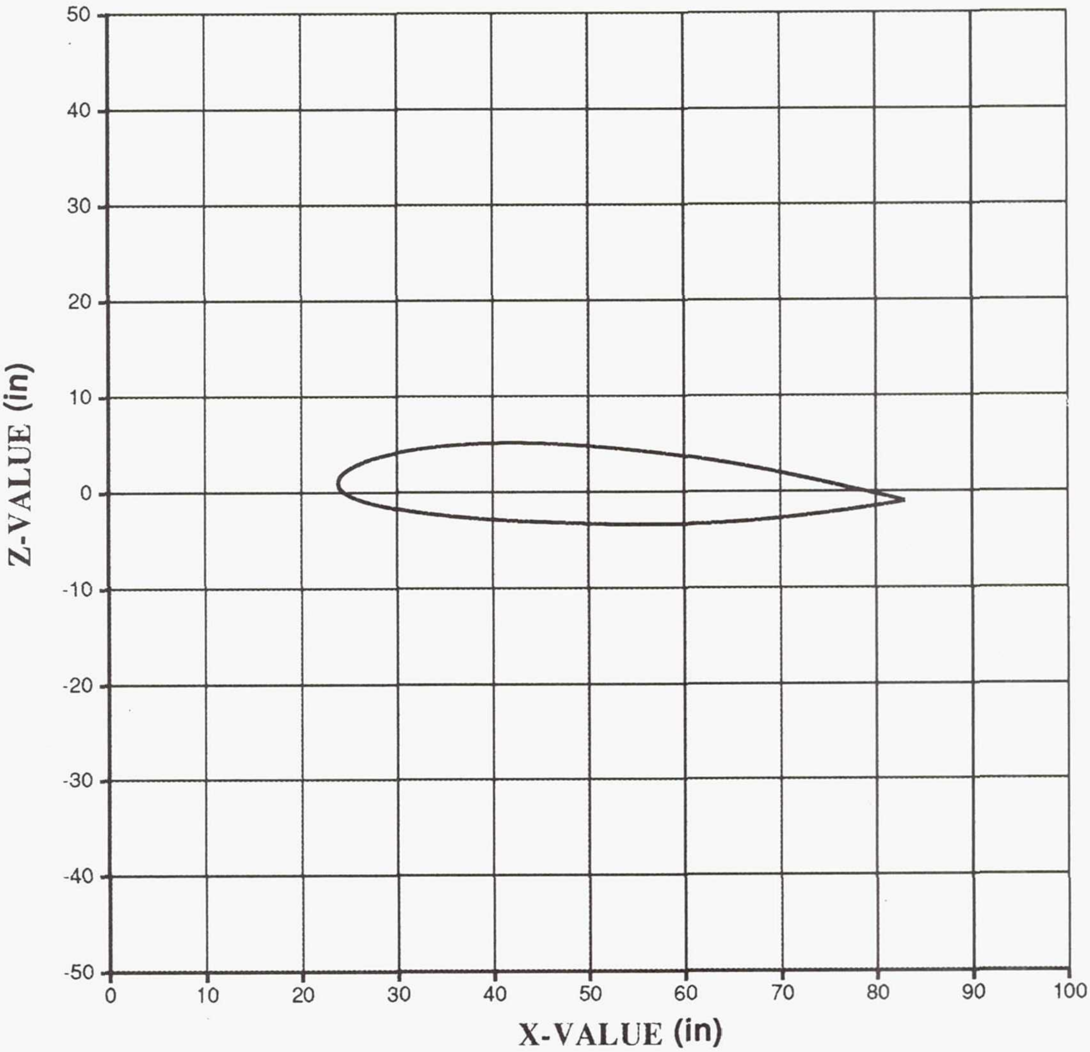

FIGURE 2.5

ECS GEOMETRY CROSS SECTION AT BUTTOCK LINE Y=20.0

3.0 ECS ICING RESEARCH TUNNEL (IRT) TESTING

Aerodynamic and water impingement testing was conducted on the ECS inlet in April and May 1989 in the NASA-Lewis Icing Research Tunnel (IRT). Aerodynamic testing and data reduction were performed by C. Bidwell and R. Woollett of NASA-Lewis. Water impingement testing was conducted by M. Breer and N. Craig of Boeing Military Airplanes and C. Bidwell and R. Woollett of NASA-Lewis.

Water impingement testing was conducted for four "icing type" flight conditions. The testing and data reduction were conducted using the dye-tracer technique discussed in detail in Reference 3.

The four conditions tested were selected in an attempt to obtain variations in water impingement efficiency and impingement limit locations. These types of variations are very beneficial since the results can be utilized to verify computer codes which are used to calculate local water impingement efficiency.

Water impingement efficiency test data is very susceptible to variations in tunnel conditions, including cloud droplet sizes. For this reason, each of the four test conditions were run five times in order to obtain a statistical sample. The nominal parameters for each of the four test conditions are shown in Table 3.1.

TABLE 3.1
NOMINAL WATER IMPINGEMENT TEST CONDITIONS
FOR ECDS INLET

FLIGHT CONDITION	ANGLE OF ATTACK (deg.)	INLET AIRFLOW (lbm/sec)	CLOUD MEAN VOLUMETRIC DROP DIAMETER (micron)
1	0.0	3.0	20.0
2	15.0	3.0	20.0
3	15.0	4.3	20.0
4	0.0	4.3	20.0

Test data logs for the tests conducted are contained in Appendix B. Appendix C contains all data relevant to the Reference collector which is used in the dye-tracer technique (Reference 3) to obtain experimental water impingement efficiency data. The contents of Appendix C are as follows:

a. Photo of Reference Collector

b. A complete list of all Reference Collector masses obtained for the ECS inlet test

c. Figures showing the location of the Reference Collector relative to the four geometry positions where impingement efficiency data were obtained

d. Tabulation of Reference Collector masses used for each of the four geometry positions at both the 0.0° and 15.0° angle of attack

4.0 ECS ANALYSES

One of the tasks of the initial part of this project was to investigate the effect of flowfield mesh density on the aerodynamic and water impingement efficiency analytical results. With the change in emphasis in the 1991 effort to investigate and correct the trajectory crossing problem, the intent of the mesh refinement study became to determine whether Mesh2, the baseline mesh defined in 1990, was adequate.

To determine whether Mesh2 was adequate, Mesh3, a refined mesh, was created and comparisons were made between the aerodynamic results of Mesh2 and Mesh3 as discussed in Section 4.2.3 below. Mesh3 contained increased mesh density in regions where strong flow gradients were expected or where critical flow regions needed to be resolved. Mesh lines were added near the inlet aperture and near the lower lip and wing leading edge. Additionally, care was taken to ensure an adequate mesh around the wing cap in an attempt to avoid trajectory computation problems experienced in the Reference 1 analysis. The resulting refined flowfield mesh, Mesh3, contained approximately twice the number of total grid points as Mesh2. The results of the mesh refinement are discussed in Section 4.2.

To simplify analysis and input geometry preparation, it is practical to rotate the flowfield for angle of attack analyses, rather than rotate the geometry. When this was done during the Reference 1 study, it was found that the water droplets had to be started approximately 300 inches downstream of the upstream boundary of the flowfield, or about 170 inches ahead of the front of the wing for the two angle of attack conditions. Water particles that impinge on the geometry typically follow close to the stagnation streamline. For the angle of attack cases, the stagnation streamline passed through the bottom boundary (located at same distance from geometry as tunnel walls from geometry in NASA IRT) of the flowfield rather than through the left hand boundary. Starting the water particles in the interior of the flowfield can lead to errors, since the velocity of the water particle is only known at the left hand boundary of the flowfield where it is assumed to be equal to the velocity of the air. A brief study, using codes indicated in References 4 and 5, was conducted to determine whether moving the flowfield boundaries might yield the same results as the more complex operation of rotating the geometry within the existing boundaries. The results of this study showed that it was possible to obtain good water impingement results by simply holding the geometry fixed and lowering the bottom flowfield boundary by 200 inches. Mesh4 was then created by simply adding twelve negative z mesh lines to Mesh2 to lower the bottom boundary by 200 inches.

A summary of the parameters for the different flowfield meshes discussed above is shown in Table 4.1.

TABLE 4.1

SUMMARY OF PARAMETERS FOR FOUR FLOWFIELD MESHES

ITEM	MESH1	MESH2	MESH3	MESH4
number of x-mesh lines	141	165	209	165
number of y-mesh lines	49	57	89	57
number of z-mesh lines	57	69	69	81
number of x,y,z mesh intersections	393813	648945	1283469	761805
number of x,y,z mesh/geometry intersections	9243	13919	29735	13919
number of least square cells	9200	13847	-----	13847

NOTES:

1. Mesh1 was the **initial mesh utilized in Reference 1.**
2. Mesh2 is the final mesh used in water impingement analyses for Flight Conditions 1 and 4.
3. Mesh3 is the refined mesh which produced the same aerodynamic results as Mesh2 as discussed in Section 4.2.3.
4. Mesh4 is Mesh2 extended in the negative Z direction and is the final mesh used in water impingement analyses for Flight Conditions 2 and 3.

4.1 ECS Analysis Conditions

The analysis conditions were defined by averaging the relevant tunnel parameters from the repeat conditions of the appropriate test runs shown on the Test Data Log sheets of Appendix B. The averaged tunnel parameters are shown in Figure 4.1 and correspond to the Flight Conditions of Table 3.1 as follows:

FLIGHT CONDITION OF TABLE 3.1	ICING TUNNEL TEST RUN I.D.
1	237,238,239,240,241
2	242,243,244,245,246
3	247,248,252,253
4	254,255,256,257,258

4.2 Aerodynamic Analysis

The following sections describe the analytical aerodynamic analysis conducted with the ECS inlet geometry.

4.2.1 Analytical Approach

The approach for the aerodynamic analysis was the same as that used to obtain the final results in Reference 1. The P582 potential flow solver (Reference 6) was utilized to predict the flowfield around the geometry shown in Figure 4.2. The relationship between the different computer programs and input and output files for the flowfield analysis is illustrated in Figure 4.3. A brief description of the computer programs is given in Section 4.2.2.

4.2.2 P582 Code Description

P582 is a computer program used for the analysis of compressible transonic potential flow about complex geometries. Potential flow is inviscid and isentropic, or irrotational flow. The code uses a cylindrical or cartesian mesh that is not body fitted, thus reducing grid generation requirements. Variable spacing of mesh lines is available and often required to obtain an adequate grid. The program uses the intersections of the mesh lines (field points) and the intersections of the mesh lines with the surfaces (surface points) in the calculation scheme. The code requires as input the mesh values, the coordinates of the surface points, and the unit normal to the surface at each surface point. P582 is capable of solving for the flow field about a geometry defined by up to 57,783 surface/grid intersections and 6 million field grid intersections. The program has been successfully used for analysis of general geometries including flowfield simulation of half a transport aircraft with body, wing, nacelle, and strut.

4.2.2.1 Surface Patch File

The original surface loft of the inlet/wing was lofted on a Boeing geometry package called the Aerodynamics and Grid Paneling System (AGPS). A surface patch file was extracted from the AGPS definition. The patch file, composed of a network of patches, contains the surface points and their first and second derivatives with respect to patch parameters, and represents a very accurate resolution of the original loft.

4.2.2.2 Mesh/Geometry Intersection File

This file contains a list of coordinates and surface normals where the flowfield mesh intersects the model surfaces defined by the patch file. The mesh was created by making various cuts of the geometry and establishing a well defined distribution of mesh lines that intersect the inlet in high curvature regions such as the inlet lip, and the leading and trailing edge of the wing. The mesh is shown in Figures 4.3 through 4.6 with vertical planar cuts through the inlet and wing. The intersection file is created with a utility code called MSHNRM (mesh-norm) which is part of a library of geometry manipulation codes called MASTER. The intersection point normals were checked to ensure that they were pointing in the correct direction.

4.2.2.3 Flowfield File

Intersection point files were prepared for all of the surface networks comprising the geometry. The points were then sorted and duplicate points were eliminated. Preliminary runs were then made with P582 to check the model definition for geometry errors. A complete flow analysis run was then made for each of the flight conditions, saving both the surface flow field file and the field output file, both of which are required for trajectory calculations.

4.2.3 Comparison of MESH 1,2, and 3 Aerodynamic Results

A mesh refinement analysis was undertaken to ensure that the baseline grid (Mesh2) was fine enough in the regions of anticipated high gradients to produce accurate results. Figures 4.4 through 4.9 compare Mesh2 and Mesh3 for the three butt-line cuts used in the analysis. Figures 4.10 through 4.15 compare the results obtained for the two grids for all three locations and for two flight conditions. In order to distinguish between symbols, every fifth data point was plotted for each of the Mach number distributions. It is evident from this figure there was no appreciable difference between the results produced by the two grids thus indicating that Mesh2 was adequate. Mesh2 was used throughout the analysis in place of the refined mesh (Mesh3) since it was much easier to transfer between computers and much faster to run through P582 and the PTA code.

4.2.4 Results of Aerodynamic Analysis

As discussed previously, Mesh2 was used for the analysis. Experimental data, in the form of surface Mach numbers, were available for Y=12.0 upper surface and lower surface for all four flight conditions. Figures 4.17,4.20,4.23,and 4.26 show the comparison between the experimental data and the P582 code at buttock line Y=12. The agreement is excellent for all four flight conditions and for both the upper and lower surfaces. In order to present the data in a consistent format, the Y-axis was limited from M=0.0 to M=0.6 for Figures 4.16 through 4.27. On Figures 4.23 and 4.26 the peak Mach numbers were clipped off by the plot format, however the agreement between the predicted and the experimental data above M=0.6 was the same as below. The data at the other buttock lines, Y=4 and Y=20, also appears to be reasonable although no experimental data was available for verification. The flow at the middle of the highly integrated inlet, Y=12, was far more complex that at either of the other stations which were simple wing sections. In all regions, the calculation predicted Mach numbers were well within the accuracy limits of P582.

4.3 Particle Trajectory Analysis

The particle trajectory analysis, based on the results of the aerodynamic analysis, is discussed in the following sections.

4.3.1 Analytical Approach

The analytical approach is that described in the 3-D Particle Trajectory Analysis (PTA) user manual, Reference 2. This analysis method was also utilized in the Reference 1 report of the ECS inlet, as well as the present report. The relationship between the different computer programs and input and output files for the water drop trajectory analysis is illustrated in Figure 4.28. A discussion of the corrections to one module, LSQGEN, is included below, followed by a brief description of the computer programs.

4.3.1.1 Corrections to LSQGEN Preprocessor

As discussed in Section 1.0, efforts in 1990 on this project were hampered by problems in obtaining correct water impingement analysis data. When the project was restarted in 1991, a very detailed examination of particle trajectories near the body was conducted for a case which had exhibited "apparent crossing trajectories" as shown in Figure 4.29. The four-sided cells of figure 4.29 indicate locations where drops have impinged on the

geometry. Centroids of the cells are indicated by dots. "Folded" cells are an indication of crossed trajectories. The case selected for close examination was as follows:

a. Flight Condition 1 (FC1)

b. Drop size D4 (D=20.4 micron)

c. Buttock line Y=12.0 on the upper lip of the inlet

d. Region of Figure 4.29 roughly defined between S=1.0 to 2.0 inches and Y=11.6 to 12.1 inches

Eight water droplet trajectories which impinged in the above defined region were selected and detailed traces of the trajectories were performed. From inspection of the eight individual traces it was determined that some of the trajectories were crossing. Although the trajectory crossing problem was suspected to be due to bad least square coefficients in certain flowfield cells, other possibilities were checked. Other possibilities for the crossing which were investigated were as follows:

a. Error tolerance of the integrator in the PTA code which solves the particle equation of motion

b. Erroneous surface velocity inputs from the P582 flowfield solution which are used to calculate the least square coefficients of surface cells (i.e., flowfield cells which intersect the geometry)

c. Roughness or discontinuities in the patch data which describe the ECS geometry

After examination of the above, it was determined that the crossings were definitely caused by bad least square coefficients in flowfield cell (X=37,Y=18,Z=50) which was above the wing highlight near Y=12.0 Surface velocities and flowfield velocities for the subject cell were examined. These velocities looked consistent with each other. In contrast to this, velocities computed by the least squares equation at different positions within this cell showed that they did not fall within the maximum and minimum values of the velocities which were initially used to calculate the coefficients for the cell. That is, the least square equation for this cell did not give a good fit because, in some cases, the order of the model was too high.

The LSQGEN program already had the capability to utilize a least square equation of either seven or four coefficients, depending on the number of field points and surface points available within a cell. An additional option is to utilize linear interpolation or extrapolation if the matrix of the least square equation is ill-conditioned, or singular.

With these options available, the fix to LSQGEN was as follows:

a. Evaluate the least squares model at a specified number of points distributed through the cell.

b. Determine if the velocities calculated above lie within a specified tolerance of the input maximum and minimum.

c. Based on the above, the order of the equation is reduced until an acceptable fit is obtained.

After these corrections were made, the trajectory crossings were eliminated for this case, resulting in the impingement field shown on Figure 4.30.

4.3.2 Code Description

The 3-D PTA code is a three dimensional particle trajectory analysis code based on the grid approach. It computes the motion of spherical particles relative to the flowfield of air defined at the computational grid points about a three dimensional body. It solves the non-linear, coupled ordinary differential equations of particle motion to predict particle position and velocity as a function of time. By tracing particle trajectories to target bodies, particle impingement efficiency distributions and particle ingestion rates (in the case of engine inlets with particle separators) can be computed.

4.3.2.1 LSQGEN Code

The preprocessor LSQGEN is used to calculate least square coefficients that are used to calculate the potential flowfield velocity components near the surface. Both input files to LSQGEN (XXX.SFL and XXX.FLW)are generated by the 3-D potential flow code, P582.

4.3.2.2 CONTOUR Code

This CONTOUR code provides a contour definition of a constant cut made on the geometry surface. From the geometry patch file (XXX.PAT), the intersection between any constant cut and patch surface is obtained. From these intersection points, a cubic spline curve fit is made to generate the contour definition to any desired degree of detail. The contour definition is then used in the BETA code to produce plots of water impingement efficiency as a function of surface distance measured from the geometry highlight.

4.3.2.3 BETA Code

The 3-D PTA code generates a set of trajectories starting at the points of an M x N grid in the freestream and impinging on the portion of the geometry surface near a selected cut. Each grid element in the freestream and the corresponding grid element on the body surface represent end surfaces of a droplet flux tube. The impingement efficiency (BETA) is defined as the ratio of the freestream end face area to the impingement surface area for the elemental flux tube. The BETA code computes these ratios and assigns these values at the centroid locations of each grid element on the surface. This (M-1) x (N-1) centroid grid of BETA values defines the beta field. The local impingement efficiency curve at a specified cut is obtained by moving along the contour arc length, s, and evaluating the beta value based on the four corner values of the beta grid element in which the contour point is located. This is accomplished by bi-linear interpolation based on the four corner beta values.

4.3.2.4 COMPBETA Code

The Postprocessor COMPBETA code utilizes the XXX.PLT files generated by the BETA code. After the BETA code is run for all droplet sizes for a given geometry cut, the individual files are combined into one file for further postprocessing by COMPBETA. The COMPBETA code applies the specified weighting value of each droplet to its beta curve and then adds up the individual contributions to obtain a composite beta curve. This composite curve represents the water impingement efficiency due to a cloud having a specified distribution of particles, as opposed to a singular particle size. Commonly, a Langmuir D distribution of cloud particles is assumed in water impingement analyses. For the present study, a slightly different cloud was utilized as determined from data provided by NASA-Lewis and documented in Reference 3.

4.3.3 MESH2 Particle Trajectory Analysis Results

The 3-D PTA code of Reference 2 was utilized to perform water impingement analyses of the ECS geometry of Figure 2.2 to obtain local water impingement efficiency data at the four geometry cross sections shown on Figures 2.3 through 2.5. Input data required by the trajectory code were taken from the averaged IRT values of Figure 4.1, as was done for the flowfield analysis. All analytical 3-D impingement data contained in this report were obtained using Mesh2 for zero alpha cases and extended Mesh2 (i.e., Mesh4) for 15° alpha cases as defined in Table 4.1.

The Mean Volumetric Diameter (MVD) of the cloud droplets in the IRT during water impingement testing was 20.4 microns. The droplet distribution used in the analysis was the seven droplet distribution shown in Table E.5 of Reference 3. Early in the project it was found extremely difficult to obtain water impingement data for the two smallest droplets, 5.6 and 9.1 microns, of the cloud distribution. Some cases were also difficult for the 13.5 micron water droplets. Initially, it was suspected that this was an error in the 3-D PTA computer code, which had not been fully verified.

To investigate the "problems" encountered in obtaining water impingement efficiency data for the smaller droplets, the Reference 4 and 5 2-D/Axi-symmetric computer codes were again utilized (see Section 4.0 for related item). These codes were chosen since they are quite easy to use and are considered by Boeing to be production codes. Also, they have been correlated with previous test data acquired in the NASA-Lewis IRT. Use of the 2-D/Axi-symmetric codes for analysis of the 3-D ECS geometry is an approximation, but will show trends relative to water impingement characteristics of different diameter water droplets for the ECS test conditions.

Flight condition 2 which has an angle of attack of 15 degrees was chosen for use in the 2-D analysis. The geometry chosen was a 2-D cut at buttock line Y=4.0 which, in the 2-D case, would also be applicable for the buttock line Y=20.0 location. The flowfield and water impingement efficiency results for the 2-D analysis are shown on Figures 4.31 and 4.32. Again, only the larger droplets impinged on the geometry. In fact, Figure 4.32 shows that the smallest drop of the seven which will impinge on the airfoil section is the mean drop size. After further consideration, it was decided that the lack of impingement by the small droplets was due to the relatively "fat" airfoil section of the geometry and the relatively slow speed in the IRT. That is, the smaller particles had time to turn and follow the streamlines around the geometry, rather than impinge on the body.

After corrections were made to the LSQGEN preprocessor as discussed in Section 4.3.1.1, water droplet trajectory input data files were prepared for running the 3-D PTA on the NASA-Lewis Cray YMP. A summary of the results of the 74 successful trajectory analysis runs obtained is shown on Figures 4.33 through 4.36. These summary curves show the impingement fields with their corresponding impingement efficiency curves directly below. All plots on these figures were made to fit a given size area and therefore exhibit a large variation in scales. The combined impingement efficiency curves shown at the left side of each of the figures give a relative feel for the contribution of each individual particle to the total water impinging on the ECS geometry. The individual curves were reduced extensively to fit all droplet sizes for a given Y location and Flight condition on

a single figure for easier comparisons between different flight conditions. Full size figures of all the individual summary curves are contained in Appendix D.

Difficulties were also encountered with the droplet size 3 (13.5 microns) trajectory predictions. As the droplet size was reduced from droplet size 7, the amount of time required to isolate the correct droplet release point for a given impingement area increased. For three droplet size 3 runs (FC1, FC2 at buttline 12), impingement was predicted but time constraints did not permit accurate enough refinement of the release point (and therefore impingement location) to permit comparison with test data. Automation of the particle release point calculation would greatly reduce the time required for this operation.

Although the corrections to LSQGEN resulted in an increased range of conditions for which impingement predictions were obtained, several droplet size 3 runs exhibited trajectory crossings or missing intersections. The D3 water droplet was only a 20% contributor to the composite collection efficiency curves of this study, and as shown in Section 4.3.4, did not appear to significantly affect agreement with test data.

Of the droplet size 3 runs, the most severe problem encountered occurred for Flight Condition 3 at buttock line Y=4. The projected impingement field for this case is illustrated in Figure 4.37. This figure suggests that one particle was severely affected by an erroneous least squares calculated flow field velocity, causing trajectories to cross, or that the particle missed its impingement point and that the intersection shown is actually that of the particle emerging from inside the geometry. Similar problems were also encountered with droplet size 3 for FC1 at Y=4, FC2 at Y=12L and FC4 at Y=4, as indicated on Figures 4.33, 4.34 and 4.36 respectively.

As shown in detail in the figures of Appendix D, the small droplets have low local collection efficiencies and cover only a small part of the surface and therefore contribute very little to the composite local impingement efficiency curve and therefore little to the total water collected. The comparison of composite local impingement efficiency curves with test data is discussed in Section 4.3.4.

4.3.4 Comparison of Particle Trajectory Analysis Results and IRT Test Data

Each test condition was run five times in the IRT in order to obtain a statistical sample and then the test data was averaged for comparison with analytical results. Figure 4.38 shows a summary comparison of all the analytical composite impingement efficiency curves (light dash) and averaged test

data (heavy dash). Appendix E contains sixteen full size figures which show the data of Figure 4.38, as well as the individual test data which was averaged. Although there were some large variations in test data for a given geometry location and test condition, these variations were not the sole contributor to the differences shown on Figure 4.38.

At buttock line Y=4, the comparison between the efficiency curves is not very good for FC1 and FC4. However, for both of these conditions the area under the impingement efficiency curves is nearly equal, indicating the same amount of total water catch. For FC2 and FC3, the agreement between analysis and test seems quite good.

At buttock line Y=12 (lower lip) the data indicate high impingement efficiency near the highlight (S=0) for all flight conditions. Test data for all four test conditions also show an extra peak along the lower surface of the geometry at S=-13. This "extra" peak is believed to be caused by the difficulty in getting the blotter strips to conform to the geometry in this region. This region of geometry was slightly rough which usually resulted in a bulge in the blotter paper which apparently caught a large amount of dye water, resulting in the second impingement efficiency peak. The significant characteristic revealed by both the test and analysis data is the relatively high impingement efficiency near the thin highlight of the lower lip. This thin lip is a very good water collector. Utilization of this generic type ECS geometry would require that special consideration be given to ensure that the lower lip of the inlet is provided with adequate anti-ice protection.

The correlation of test and analysis data is generally better at buttock locations Y=12 (upper lip) and Y=20 than at Y=4 and Y=12 (lower lip). As expected, none of the correlations for impingement limit location and maximum beta values are exact. However, the areas under the impingement curves (total water collected) are in fair agreement. This correlation should be sufficient to allow utilization of the 3-D PTA computer code for anti-icing or de-icing system design.

Individual figures of each of the curves shown on Figure 4.38 are shown on Figures 4.39 through 4.54. These figures are presented herein to allow better comparisons between test and analysis to aid in any future correlations between analysis and test data.

P582 INPUT FILE PREPARATION

RUN NUMBER	ANGLE OF ATTACK (deg)	AIR TEMPERATURE (deg F)	TRUE AIR SPEED (V) (mph)	TOTAL PRESSURE (psia)	MASS FLOW-COMPRESSOR (lbm/sec)	SPEED OF SOUND (A) (ft/s)	FREESTREAM MACH NO. (M=V/A)	TOTAL TEMP. Tt = F(T,M) (deg R)	MACH AT COMPRESSOR FACE
237	0	52.0	175	14.261	3.0	1109.2	0.2314	517.5	0.2776
238	0	45.0	175	14.273	3.0	1101.6	0.2330	510.5	0.2753
239	0	47.0	175	14.273	3.0	1103.8	0.2325	512.5	0.2759
240	0	44.0	175	14.273	3.0	1100.5	0.2332	509.5	0.2750
241	0	49.0	175	14.273	3.0	1106.0	0.2321	514.5	0.2765
average values ----------->		47.4	175	14.271	3.0	1104.2	0.2324	512.9	0.2761
242	15	50.0	175	14.224	3.0	1107.1	0.2318	515.5	0.2778
243	15	37.0	175	14.200	3.0	1092.9	0.2349	502.5	0.2744
244	15	40.0	175	14.200	3.0	1096.1	0.2342	505.5	0.2753
245	15	45.0	175	14.200	3.0	1101.6	0.2330	510.5	0.2768
246	15	50.0	175	14.200	3.0	1107.1	0.2318	515.5	0.2783
average values ----------->		44.4	175	14.205	3.0	1100.9	0.2331	509.9	0.2765
247	15	44.0	175	14.200	4.3	1100.5	0.2332	509.5	0.4203
248	15	41.0	175	14.188	4.3	1097.2	0.2339	506.5	0.4192
252	15	54.0	175	14.176	4.3	1111.4	0.2309	519.5	0.4264
253	15	54.0	175	14.176	4.3	1111.4	0.2309	519.5	0.4264
average values ----------->		48.3	175	14.185	4.3	1105.1	0.2323	513.7	0.4231
254	0	54.0	175	14.176	4.3	1111.4	0.2309	519.5	0.4264
255	0	54.0	175	14.163	4.3	1111.4	0.2309	519.5	0.4269
256	0	53.0	175	14.163	4.3	1110.3	0.2312	518.5	0.4264
257	0	53.0	175	14.163	4.3	1110.3	0.2312	518.5	0.4264
258	0	54.0	175	14.163	4.3	1111.4	0.2309	519.5	0.4269
average values ----------->		53.6	175	14.166	4.3	1111.0	0.2310	519.1	0.4266

FIGURE 4.1

AVERAGED TUNNEL TEST PARAMETERS USED FOR FLOWFIELD AND TRAJECTORY ANALYSIS INPUT DATA

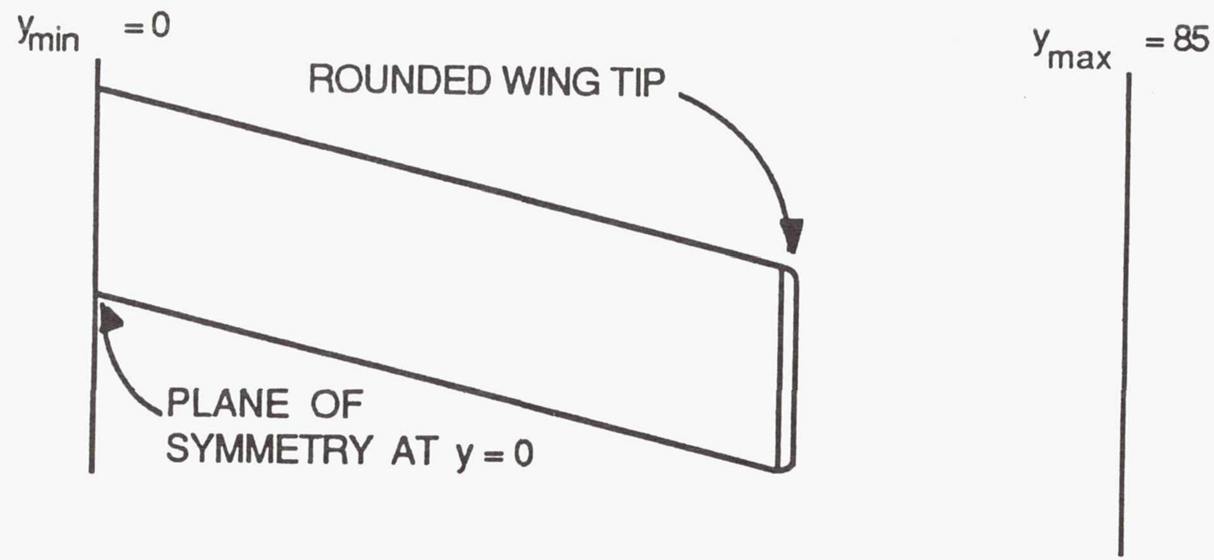

FIGURE 4.2

SCHEMATIC OF ECS GEOMETRY MODELING METHOD

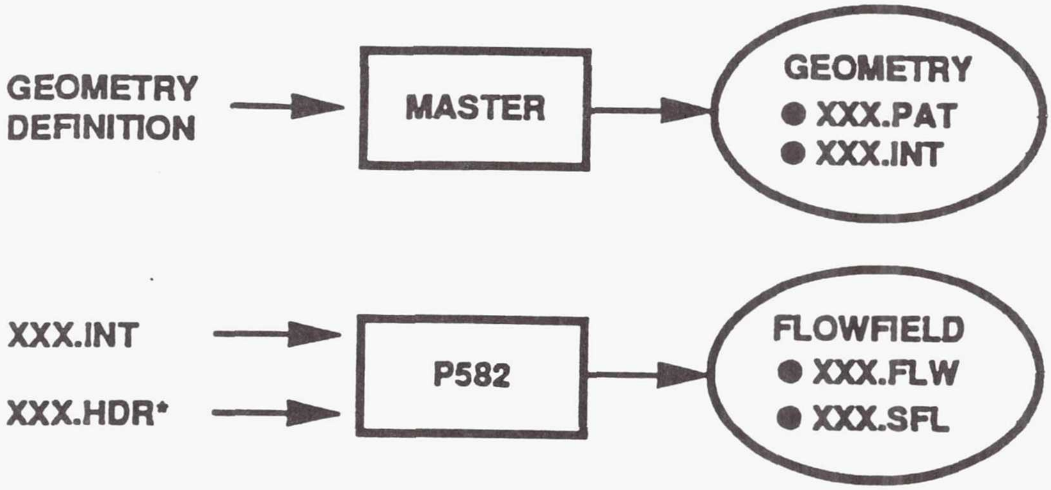

XXX.FLW - Flowfield file; generated by P582.

XXX.PAT - Bicubic patch parameter file; generated by MASTER.

XXX.INT - Contains mesh-surface intersection data; generated by MASTER.

XXX.HDR - Header input file to P582 containing file assignments; user generated.

XXX.SFL - Surface properties file; generated by P582.

FIGURE 4.3

AERODYNAMIC ANALYSIS--FILE/PROGRAM RELATIONSHIPS AND DESCRIPTIONS

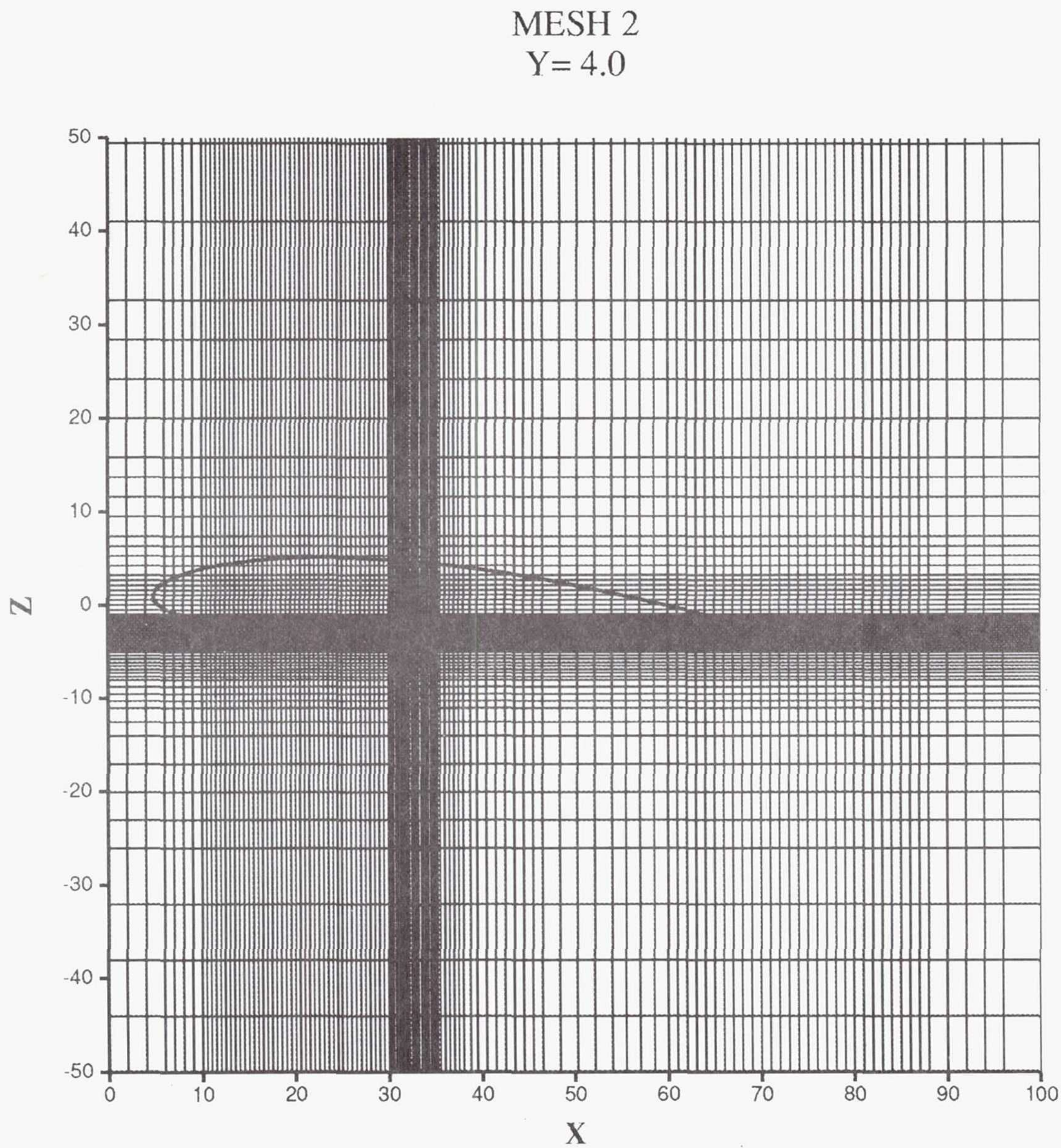

FIGURE 4.4

MESH2 AT Y=4--Z(in) vs X(in)

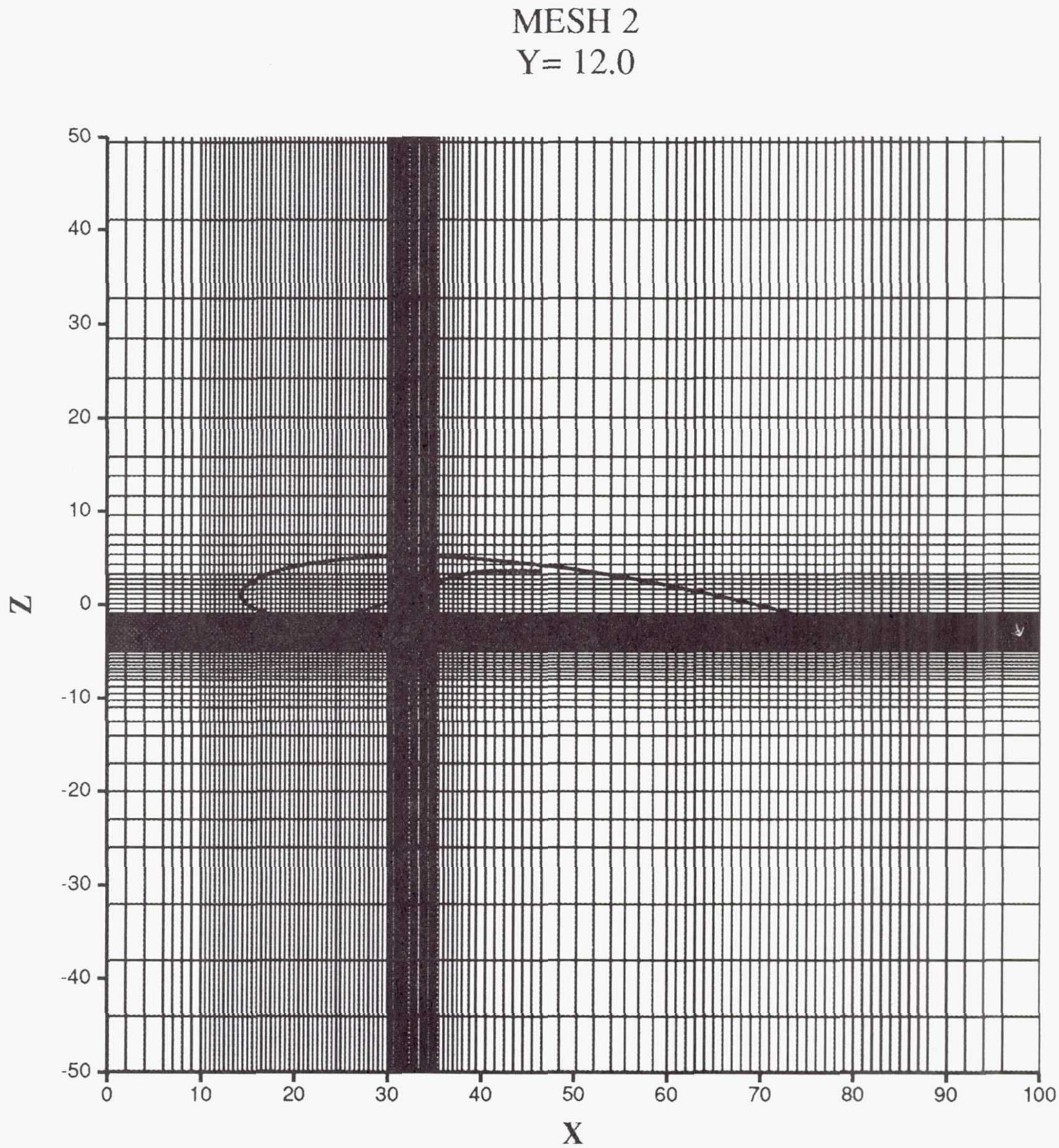

FIGURE 4.5

MESH2 AT Y=12--Z(in) vs X(in)

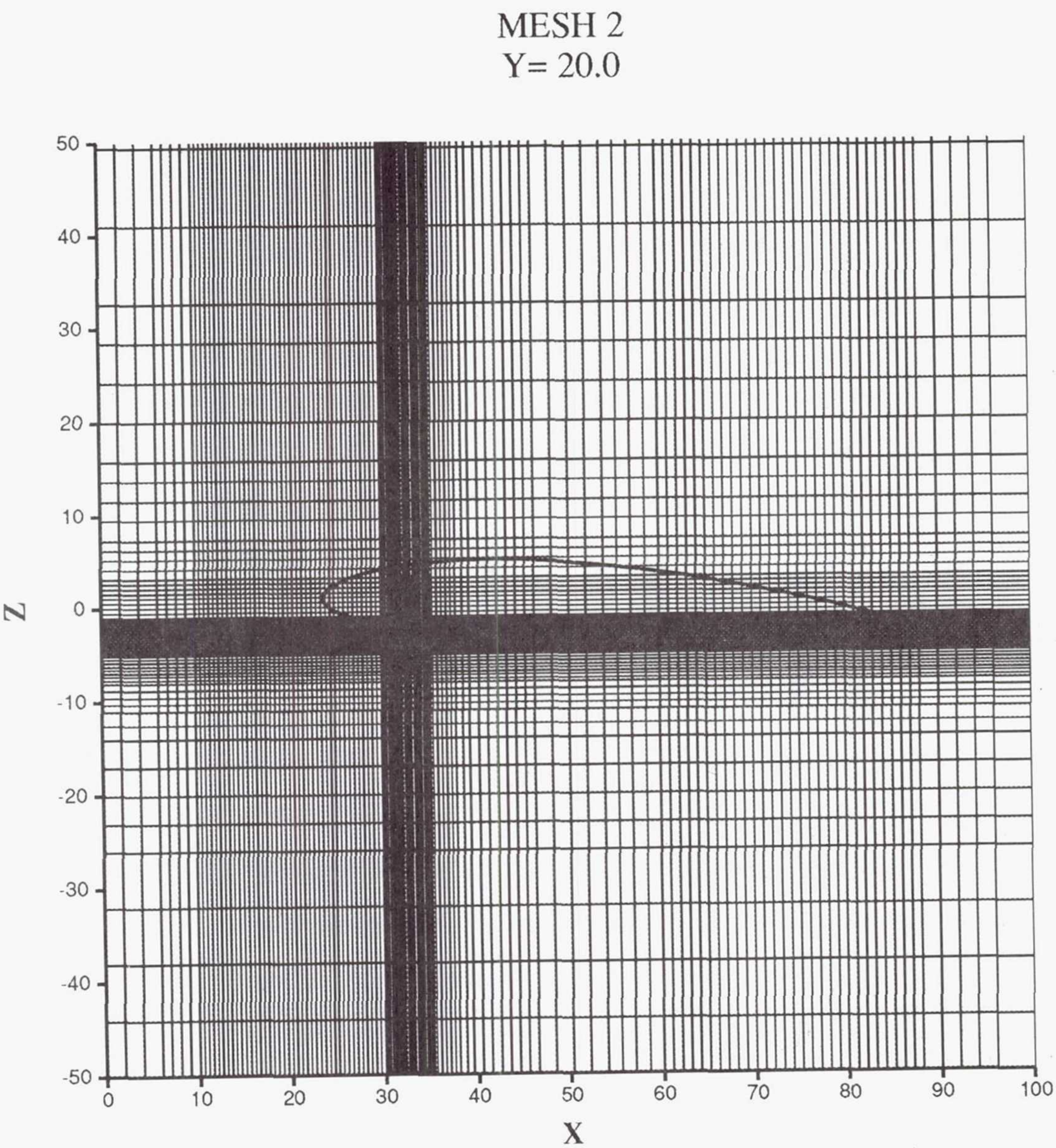

FIGURE 4.6

MESH2 AT Y=20--Z(in) vs X(in)

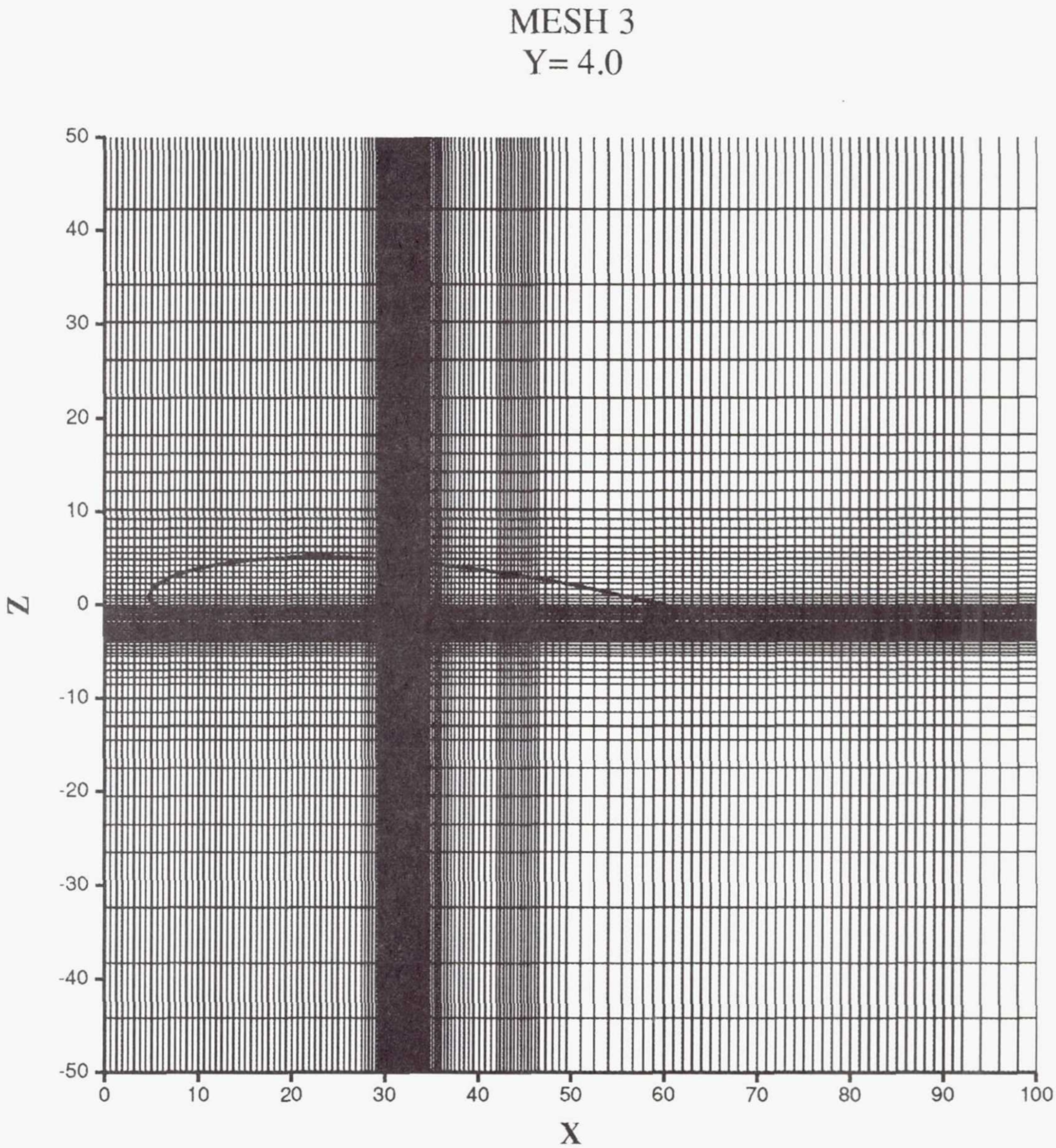

FIGURE 4.7

MESH3 AT Y=4--Z(in) vs X(in)

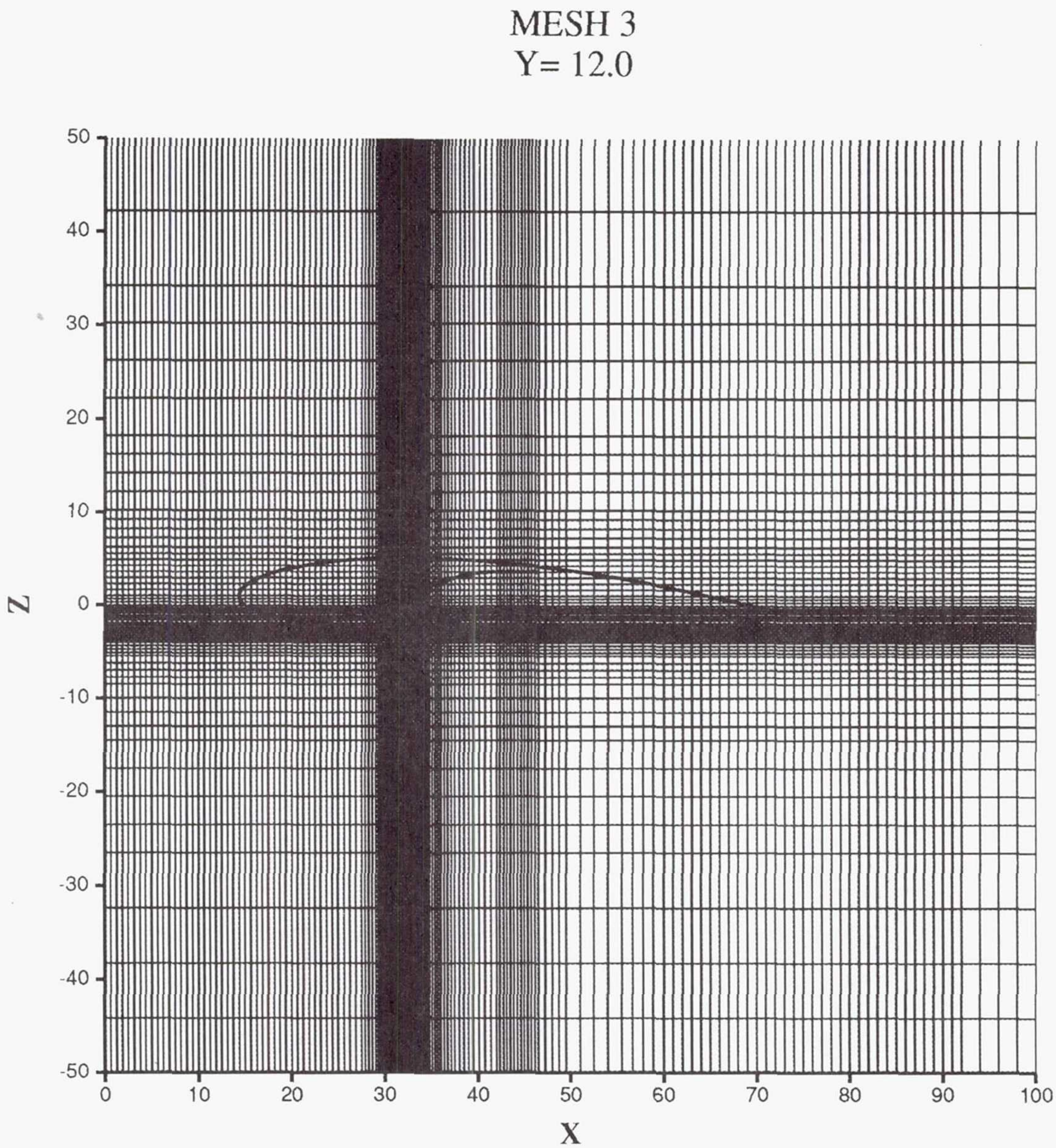

FIGURE 4.8

MESH3 AT Y=12--Z(in) vs X(in)

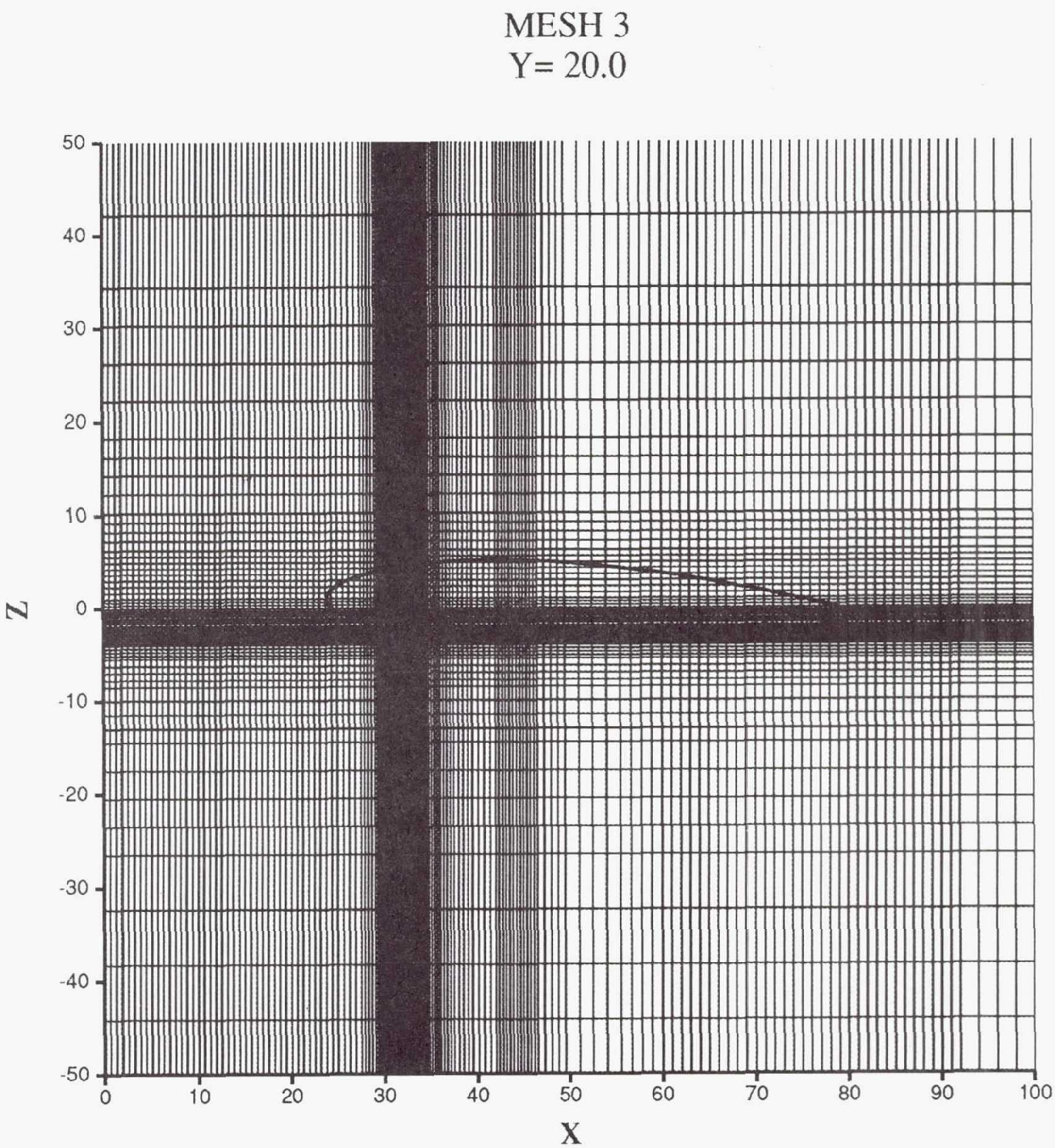

FIGURE 4.9

MESH3 AT Y=20--Z(in) vs X(in)

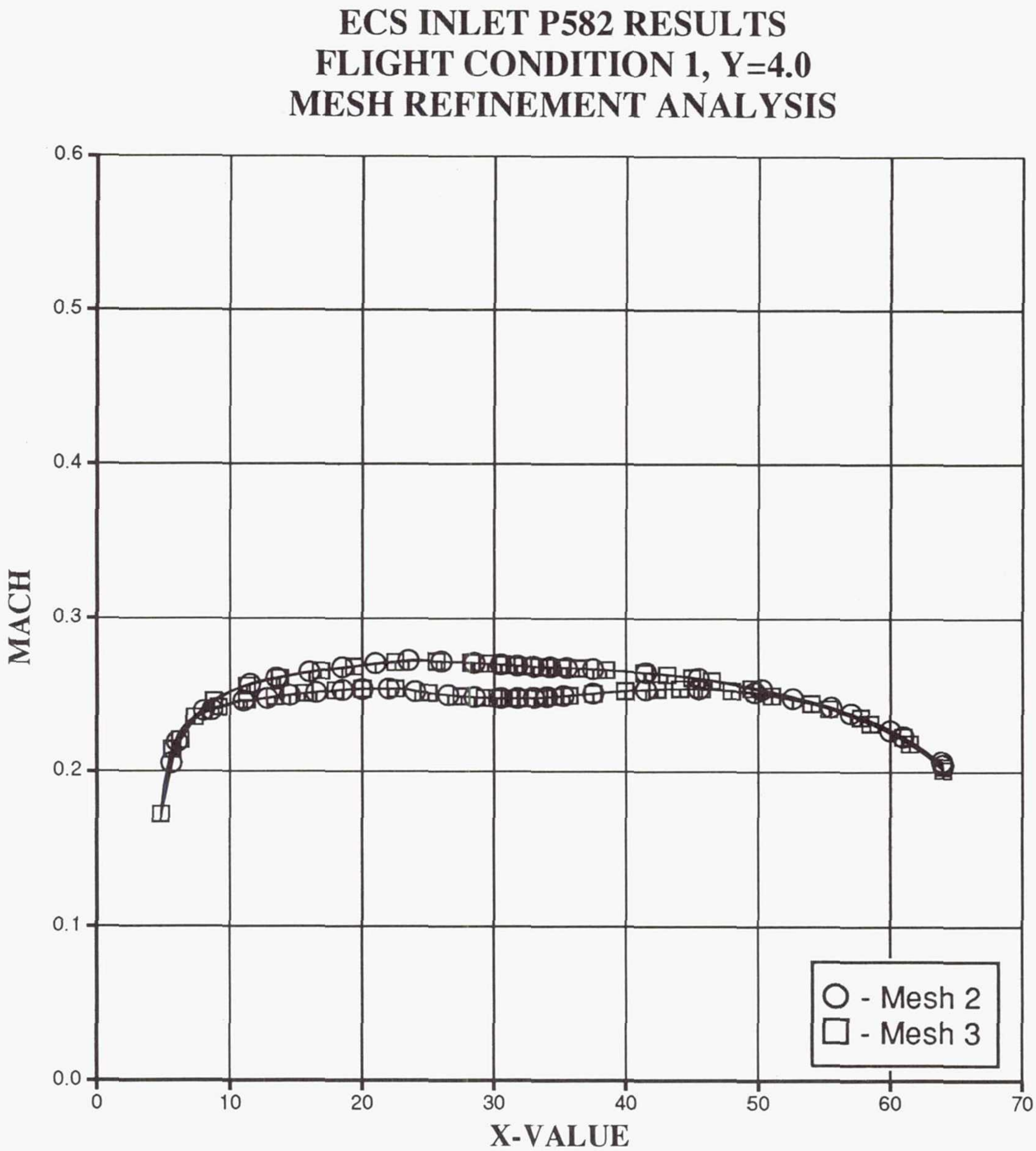

FIGURE 4.10

MESH2 AND MESH3 SURFACE MACH(-) vs X(in)--FC1,Y=4

ECS INLET P582 RESULTS
FLIGHT COND. 1, Y=12.0, UPPER SURFACE
MESH REFINEMENT STUDY

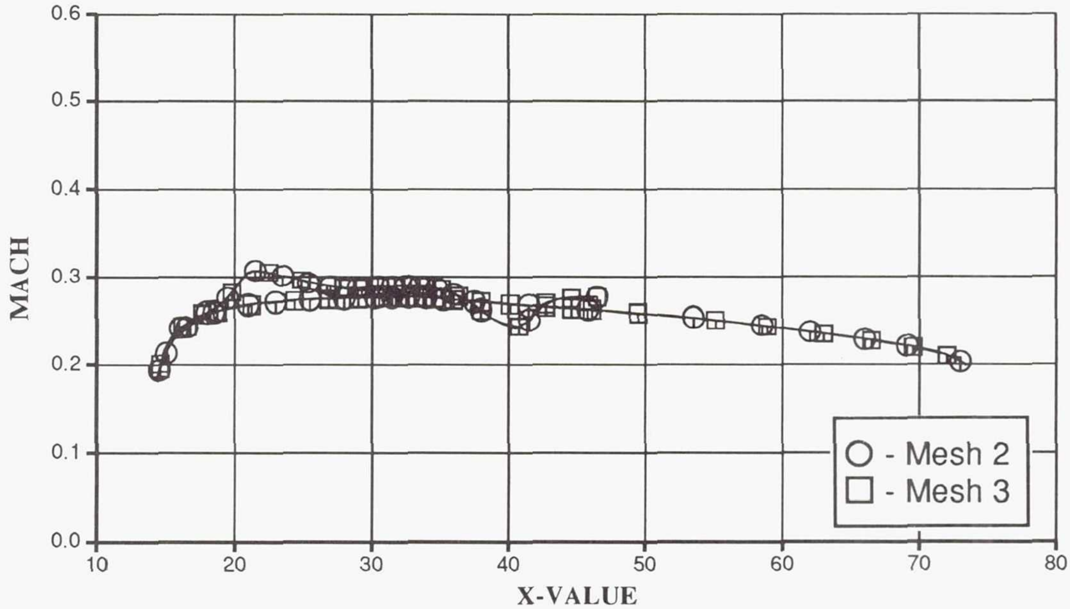

ECS INLET P582 RESULTS
FLIGHT COND. 1, Y=12.0, LOWER SURFACE
MESH REFINEMENT STUDY

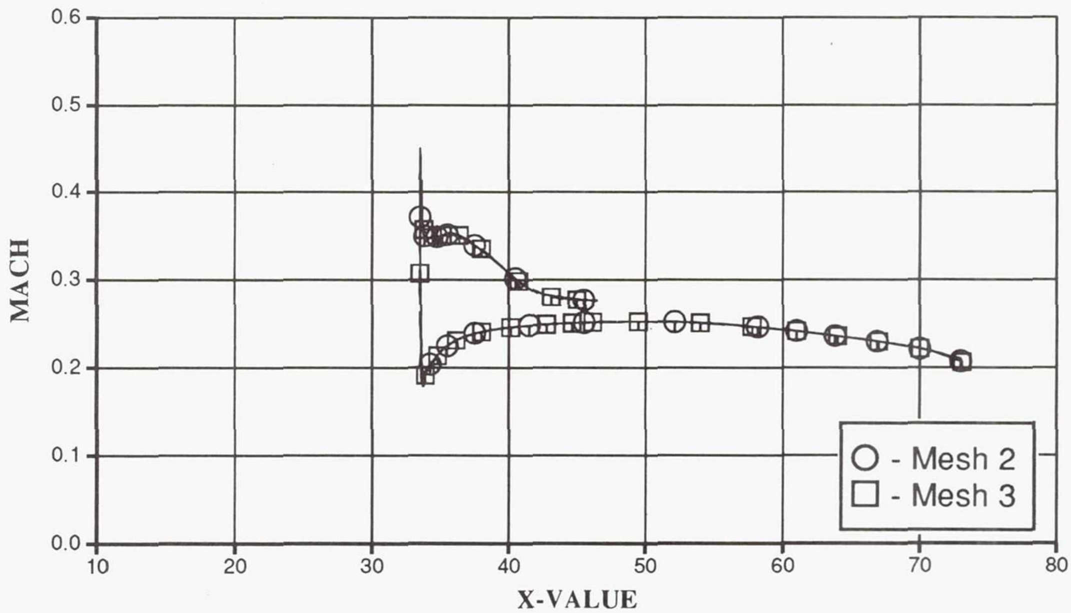

FIGURE 4.11

MESH2 AND MESH3 SURFACE MACH(-) vs X(in)--FC1,Y=12

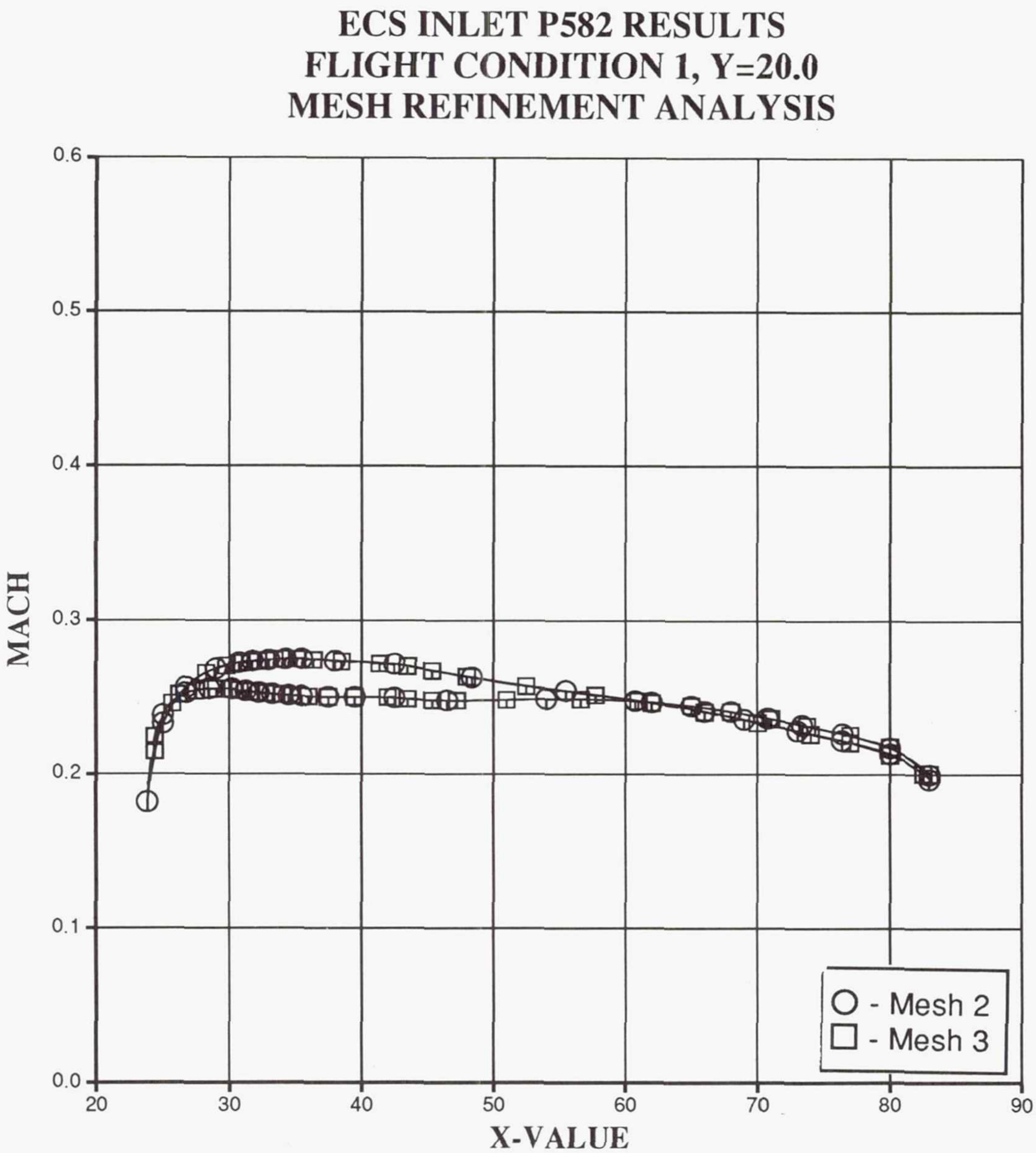

FIGURE 4.12

MESH2 AND MESH3 SURFACE MACH(-) vs X(in)--FC1,Y=20

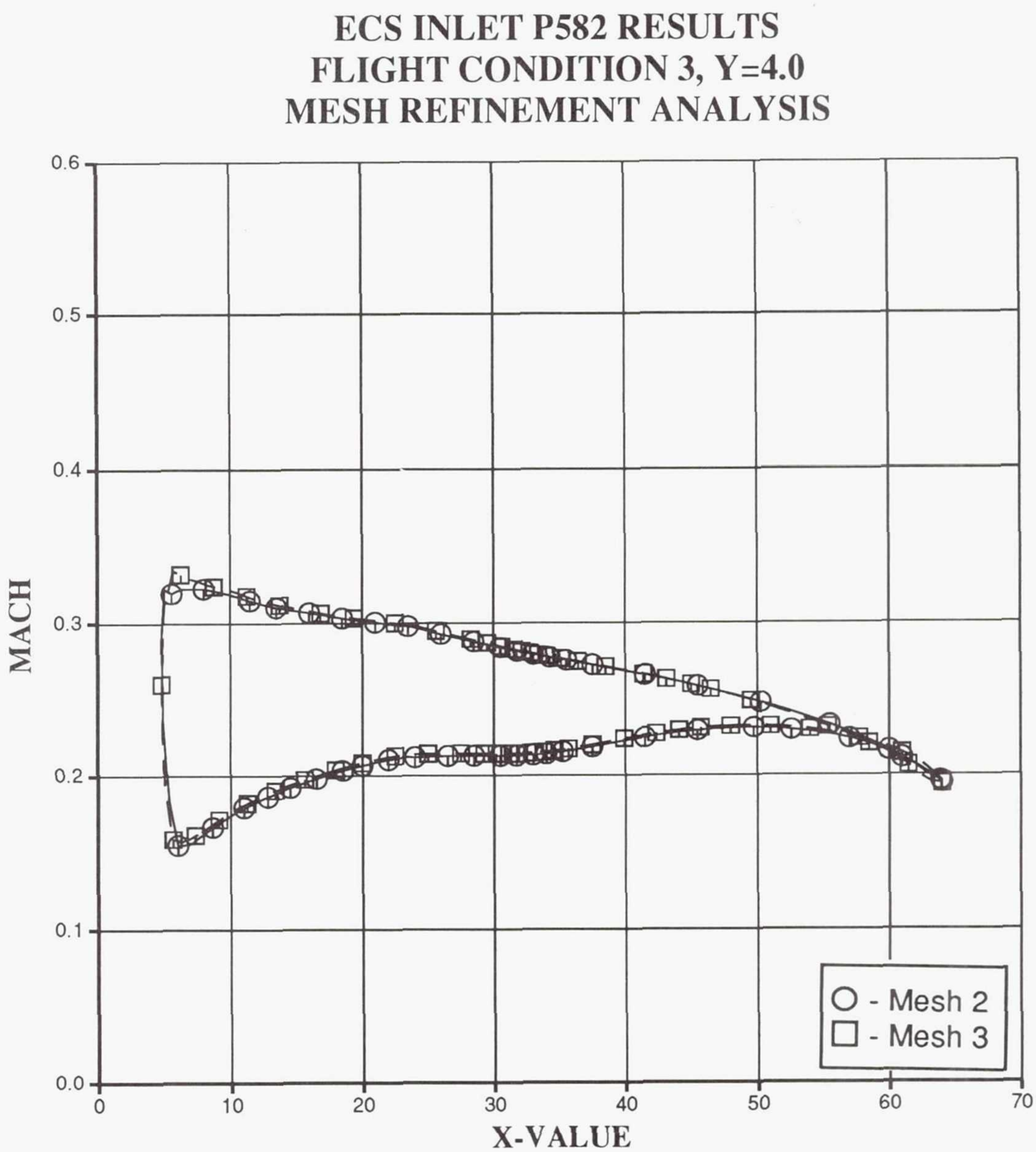

FIGURE 4.13

MESH2 AND MESH3 SURFACE MACH(-) vs X(in)--FC3,Y=4

ECS INLET P582 RESULTS
FLIGHT COND. 3, Y=12.0, UPPER SURFACE
MESH REFINEMENT STUDY

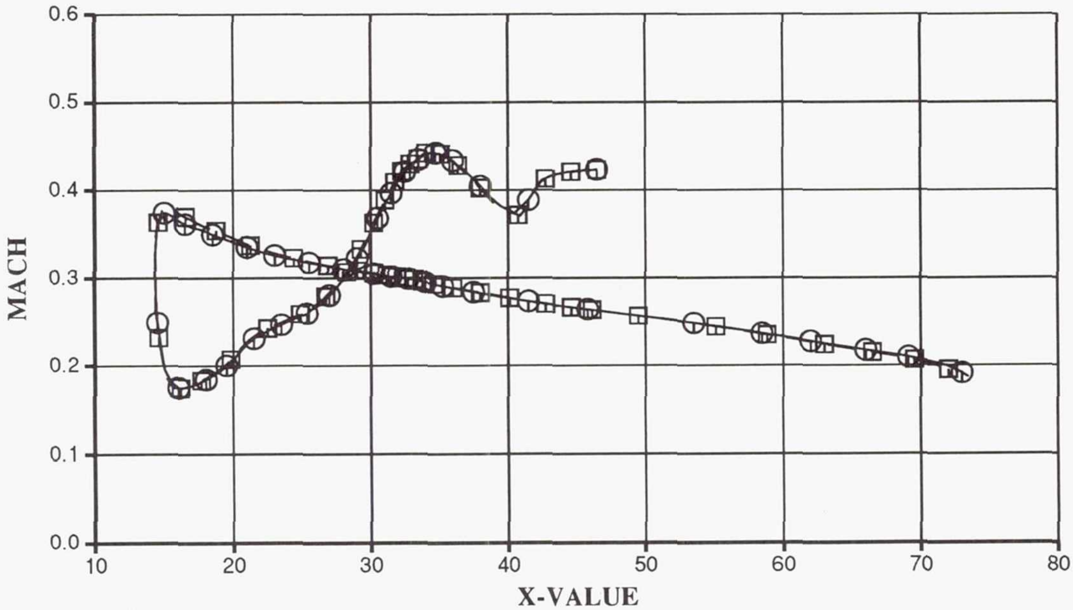

ECS INLET P582 RESULTS
FLIGHT COND. 3, Y=12.0, LOWER SURFACE
MESH REFINEMENT STUDY

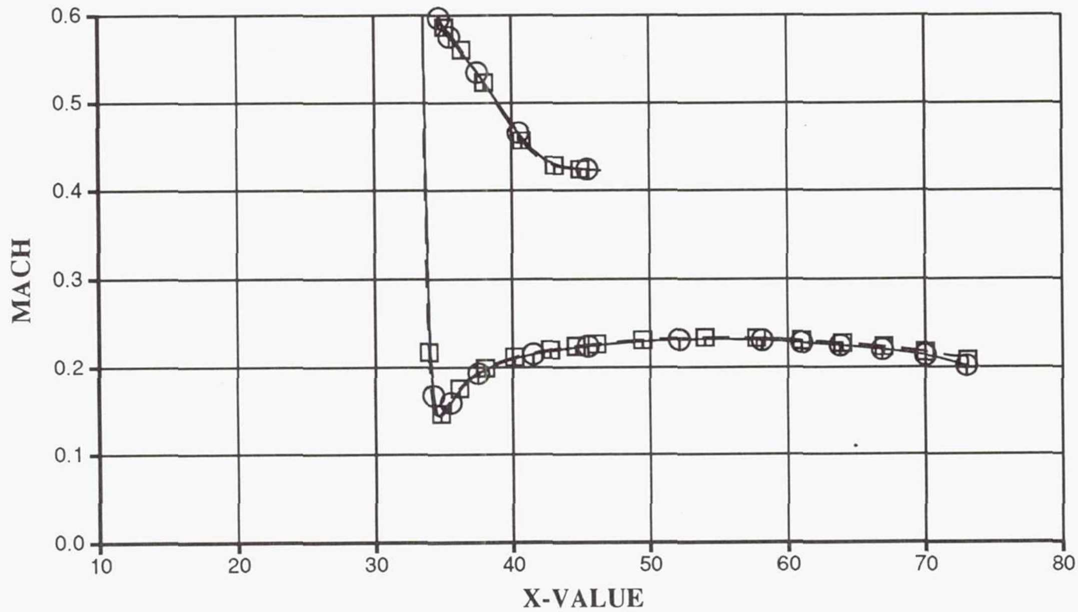

FIGURE 4.14

MESH2 AND MESH3 SURFACE MACH(-) vs X(in)--FC3,Y=12

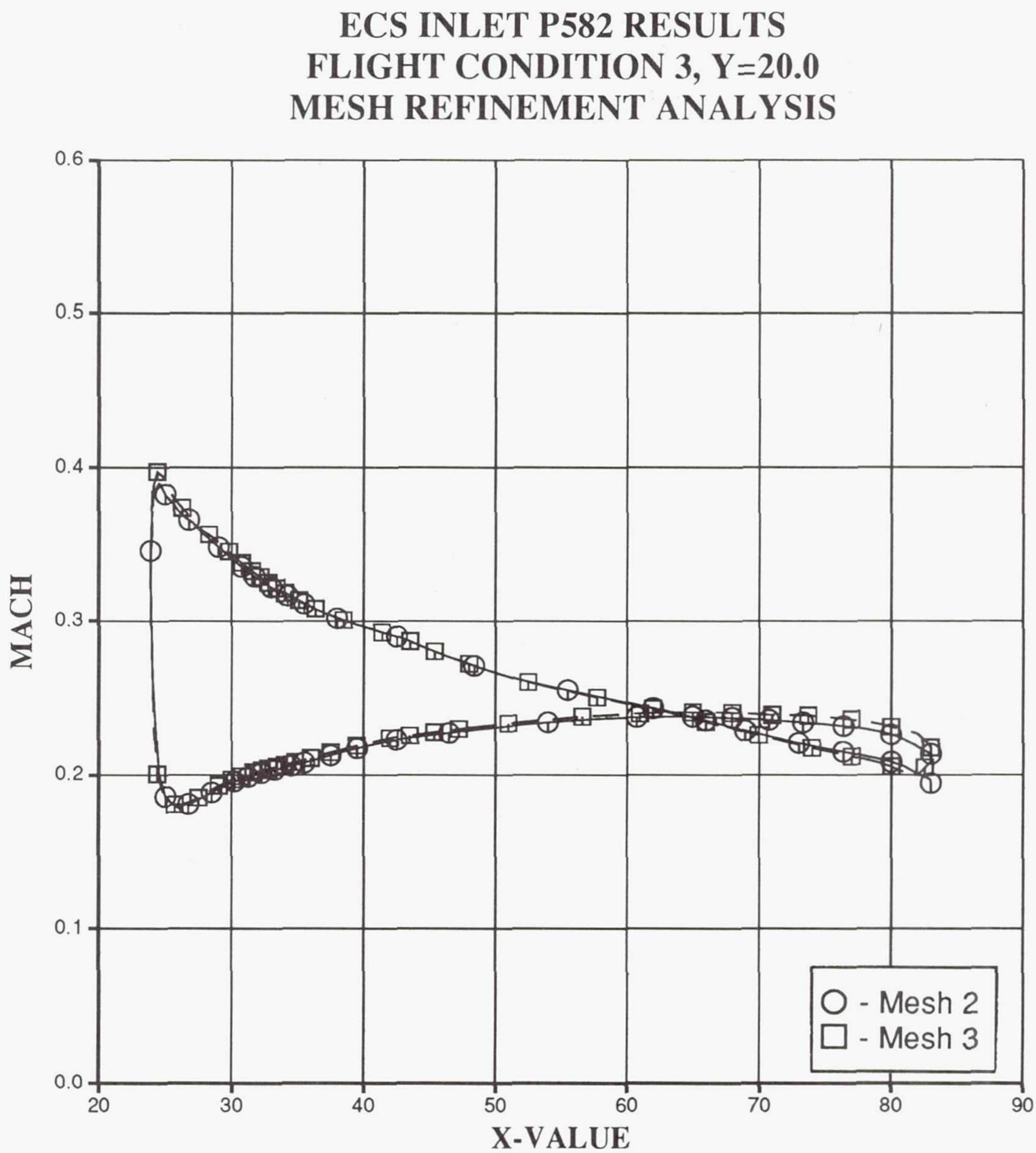

FIGURE 4.15

MESH2 AND MESH3 SURFACE MACH(-) vs X(in)--FC3,Y=20

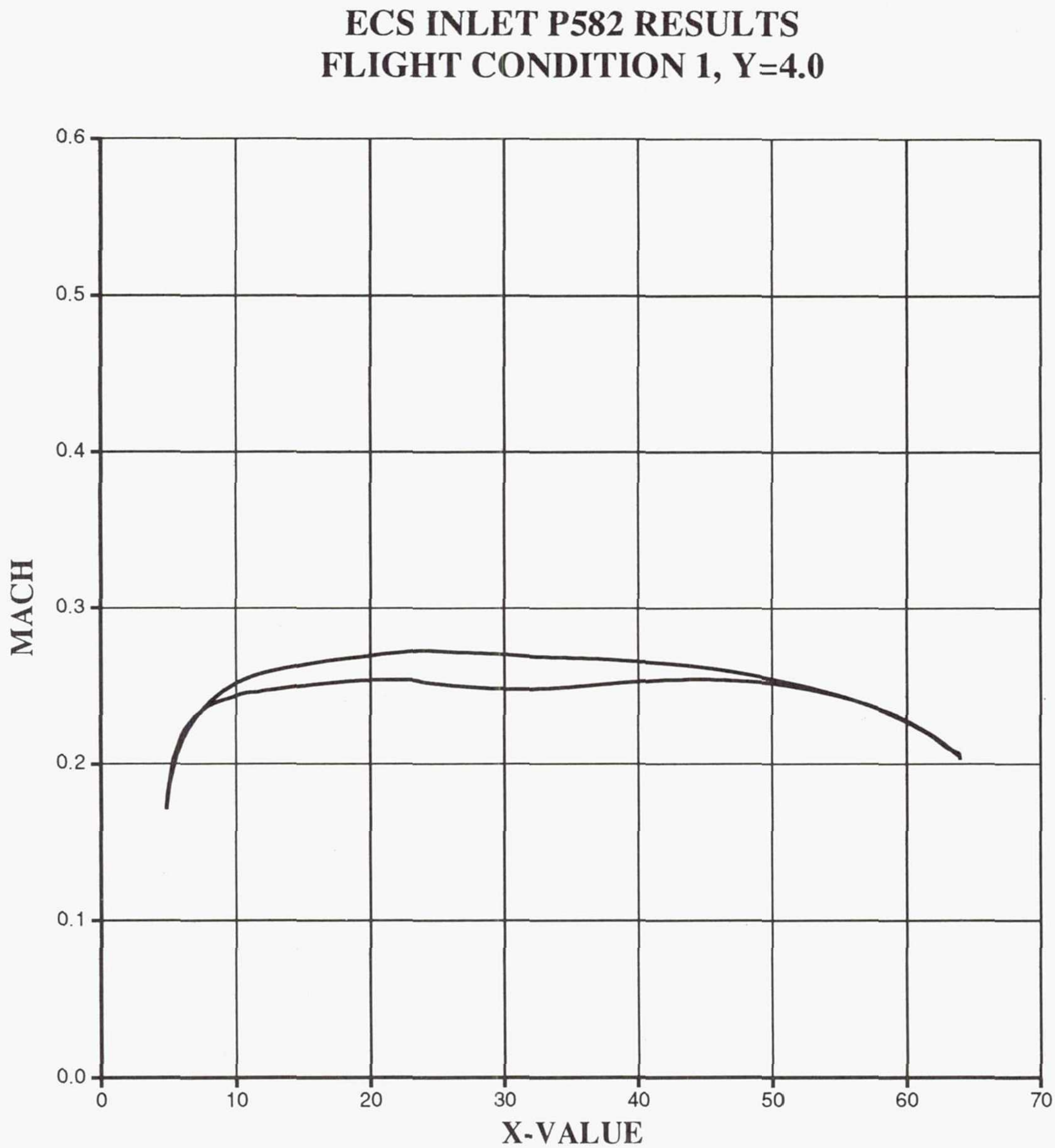

FIGURE 4.16

MESH2 SURFACE MACH(-) vs X(in)--FC1,Y=4

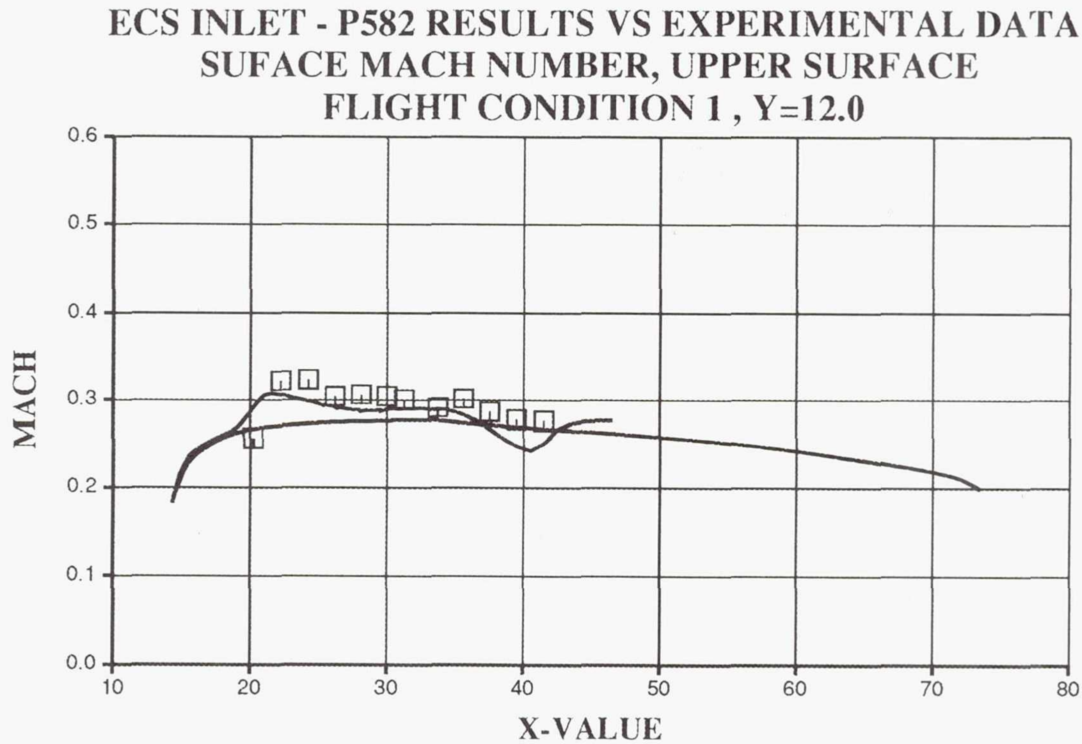

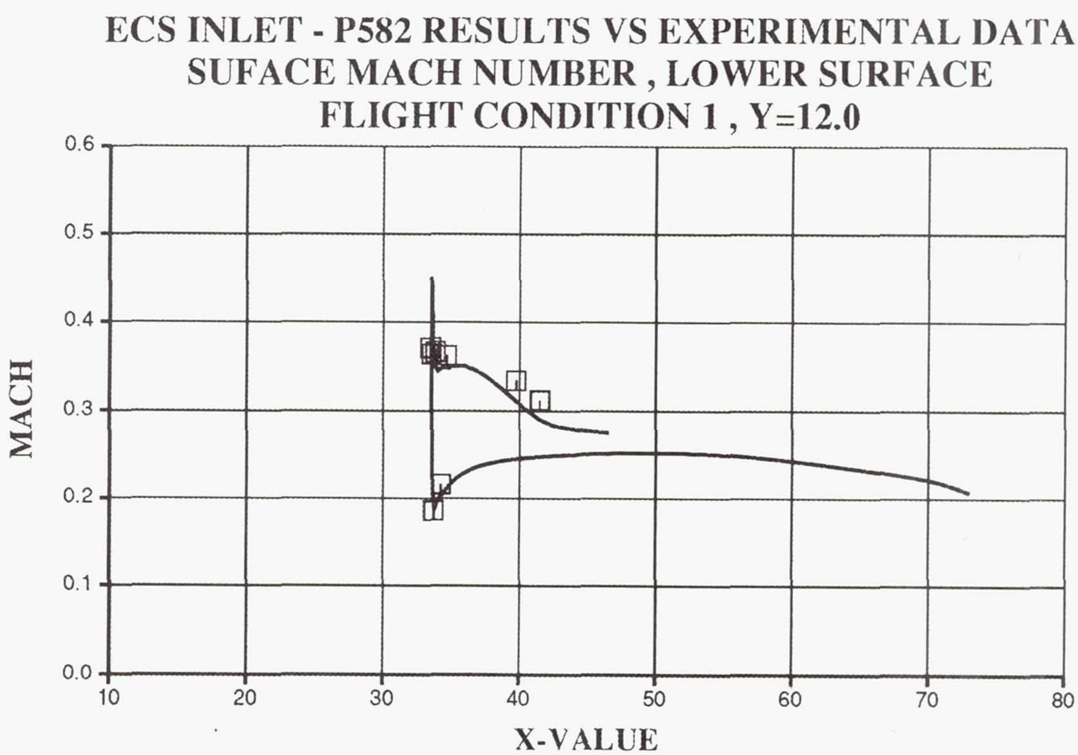

FIGURE 4.17

MESH2 AND TEST DATA SURFACE MACH(-) vs X(in)--FC1,Y=12

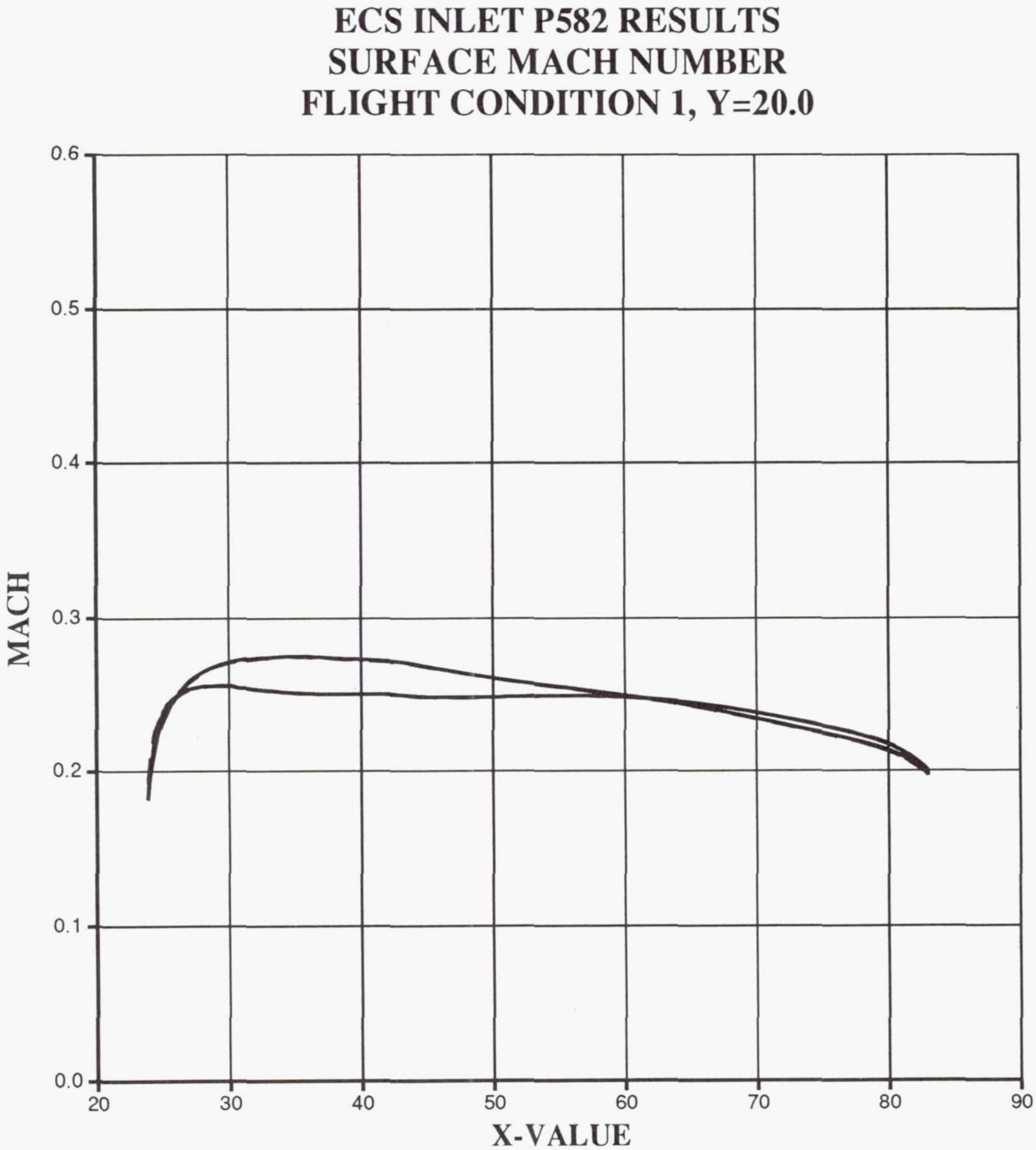

FIGURE 4.18

MESH2 SURFACE MACH(-) vs X(in)--FC1,Y=20

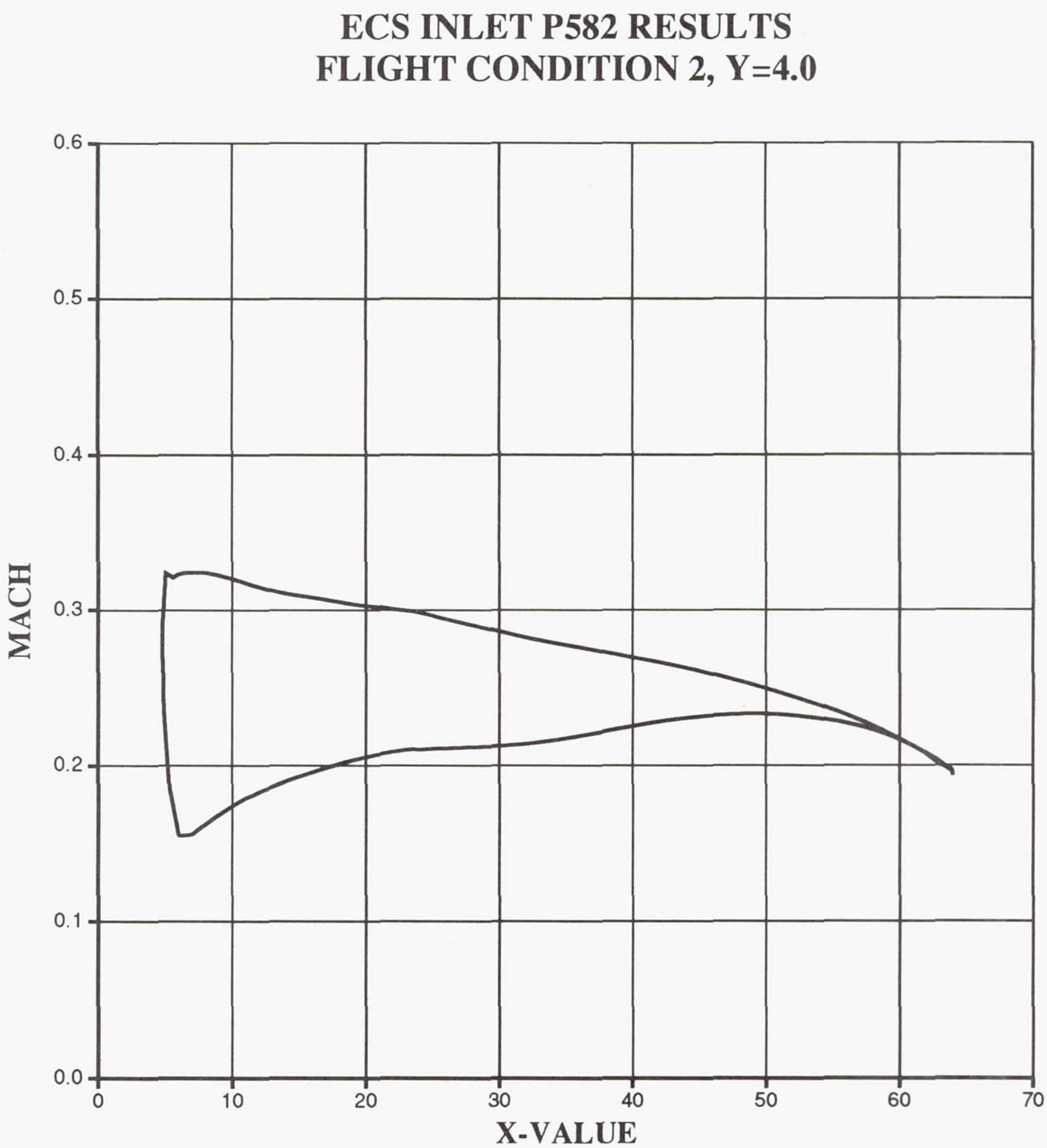

FIGURE 4.19

MESH2 SURFACE MACH(-) vs X(in)--FC2,Y=4

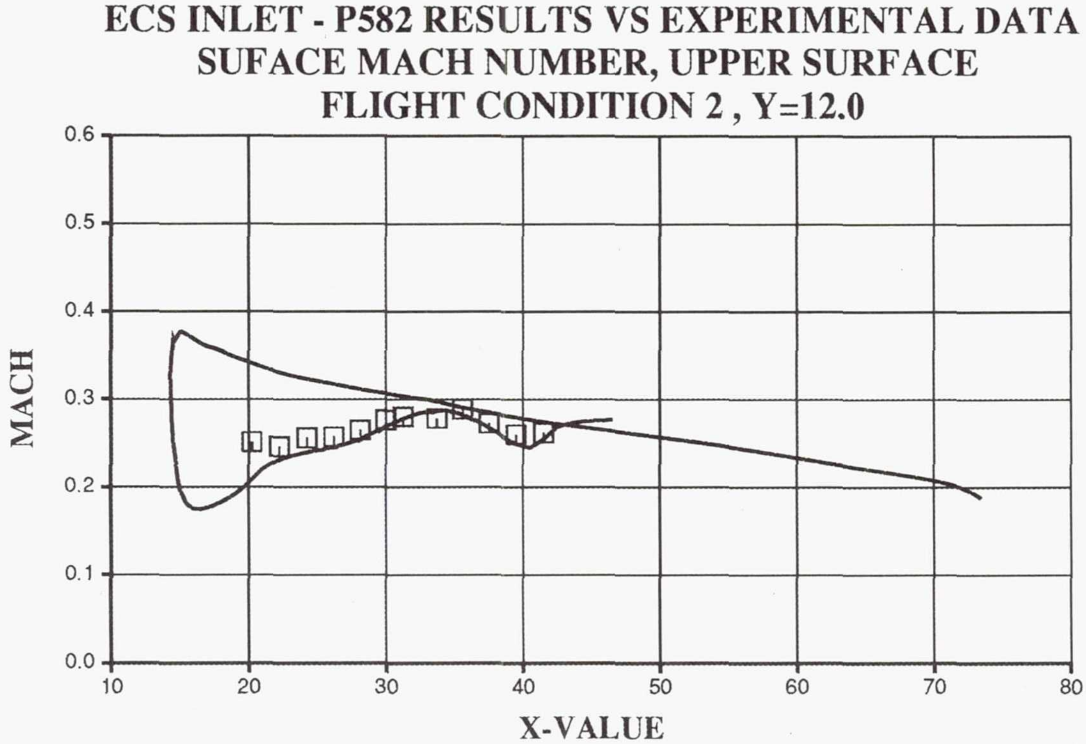

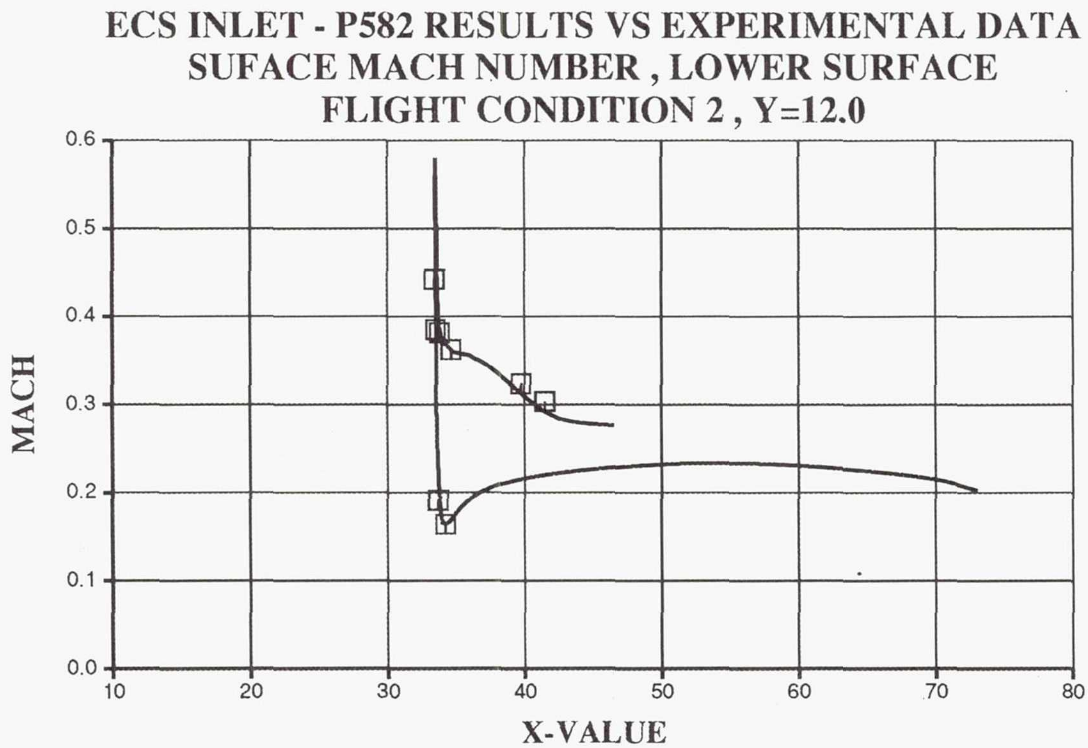

FIGURE 4.20

MESH2 AND TEST DATA SURFACE MACH(-) vs X(in)--FC2,Y=12

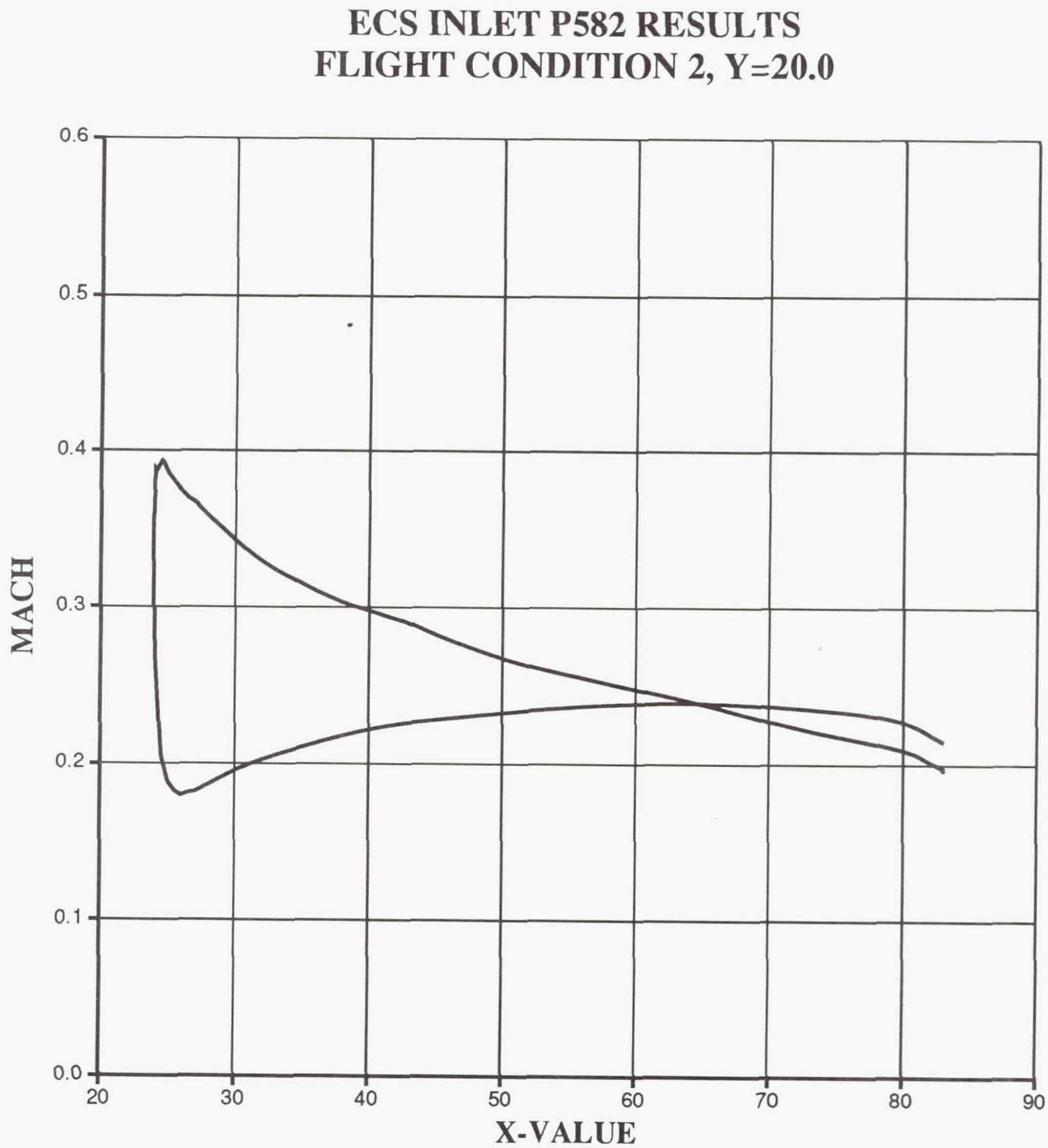

FIGURE 4.21

MESH2 SURFACE MACH(-) vs X(in)—FC2,Y=20

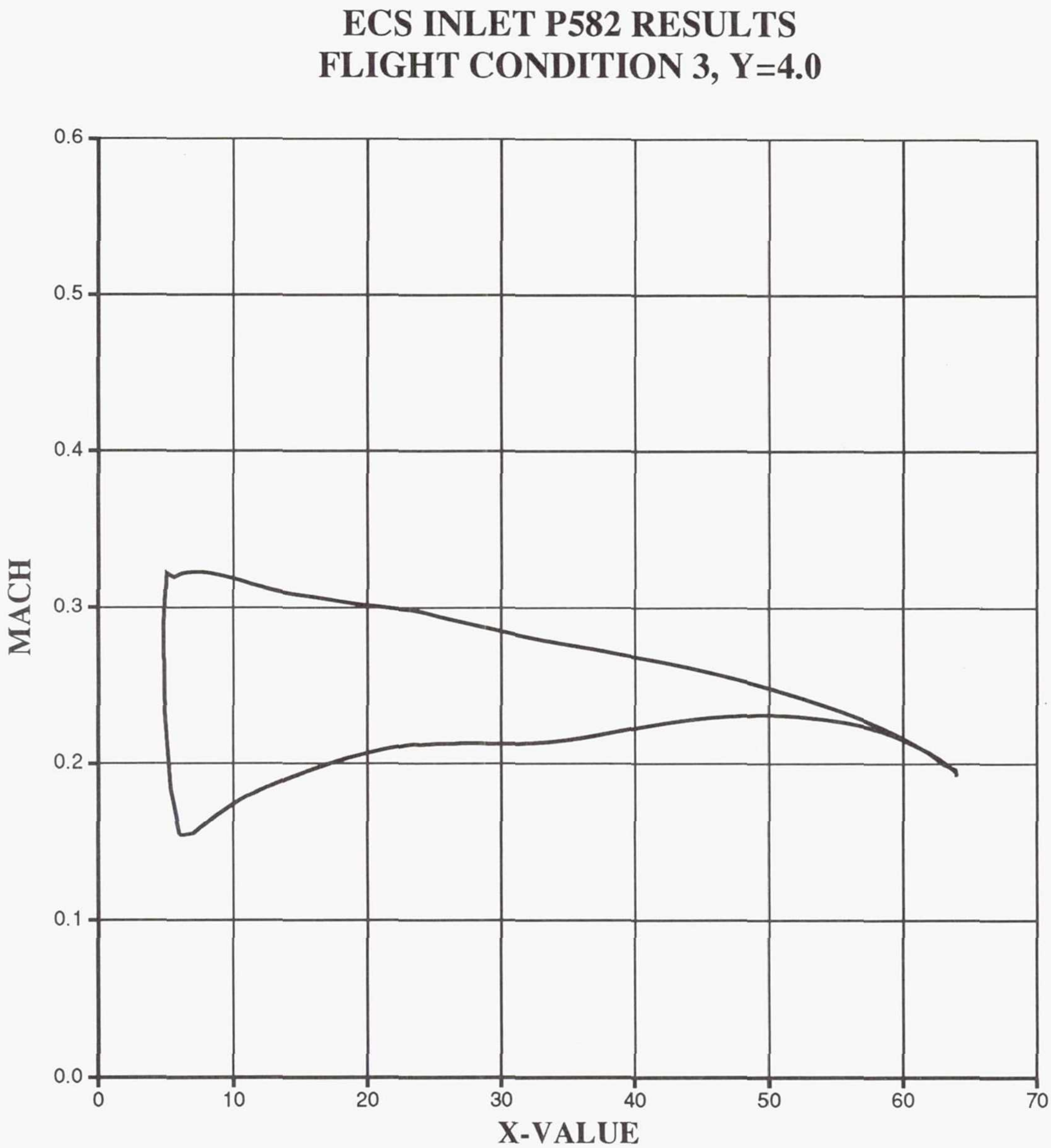

FIGURE 4.22

MESH2 SURFACE MACH(-) vs X(in)—FC3,Y=4

ECS INLET - P582 RESULTS VS EXPERIMENTAL DATA
SUFACE MACH NUMBER, UPPER SURFACE
FLIGHT CONDITION 3, Y=12.0

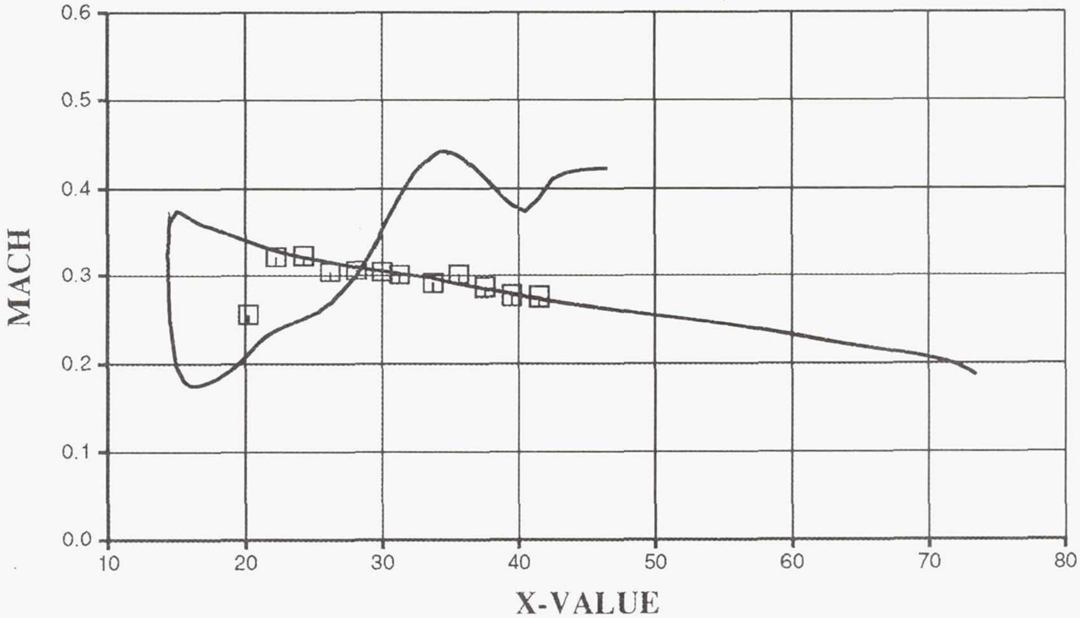

ECS INLET - P582 RESULTS VS EXPERIMENTAL DATA
SUFACE MACH NUMBER , LOWER SURFACE
FLIGHT CONDITION 3 , Y=12.0

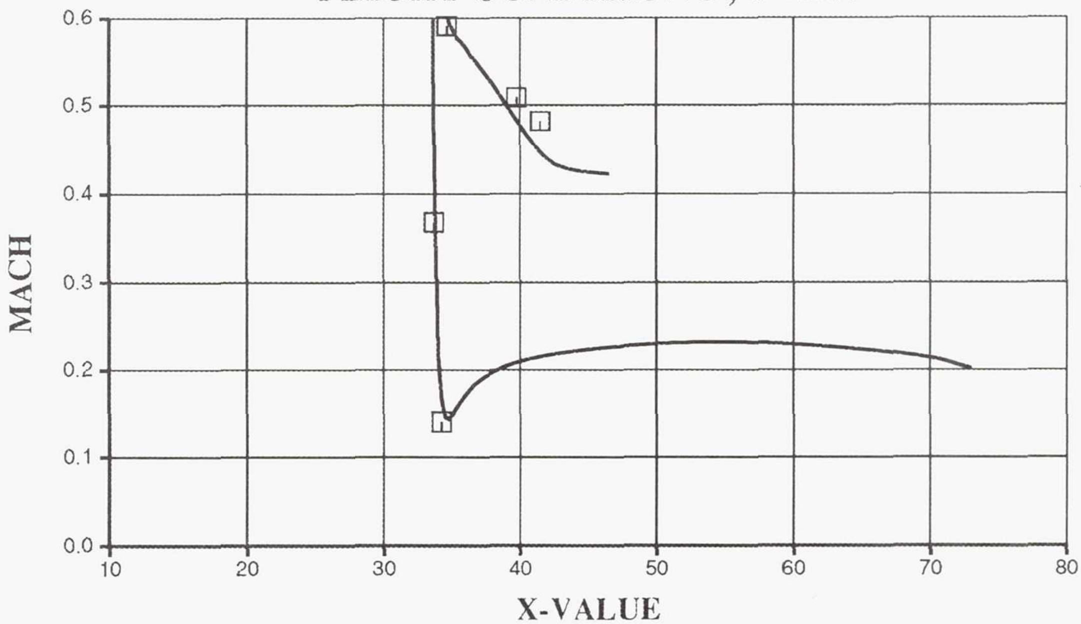

FIGURE 4.23

MESH2 AND TEST DATA SURFACE MACH(-) vs X(in)—FC3,Y=12

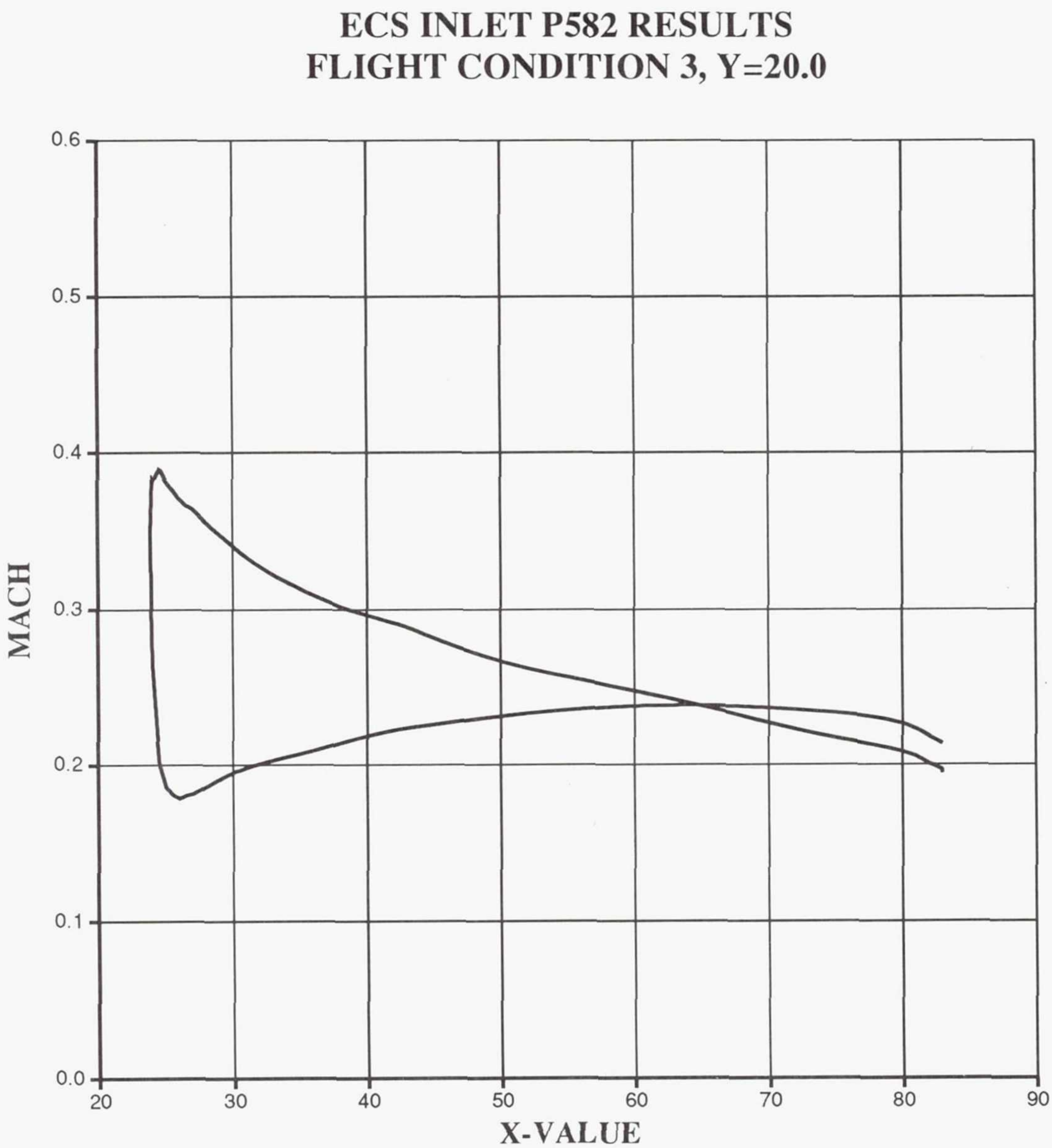

FIGURE 4.24

MESH2 SURFACE MACH(-) vs X(in)—FC3,Y=20

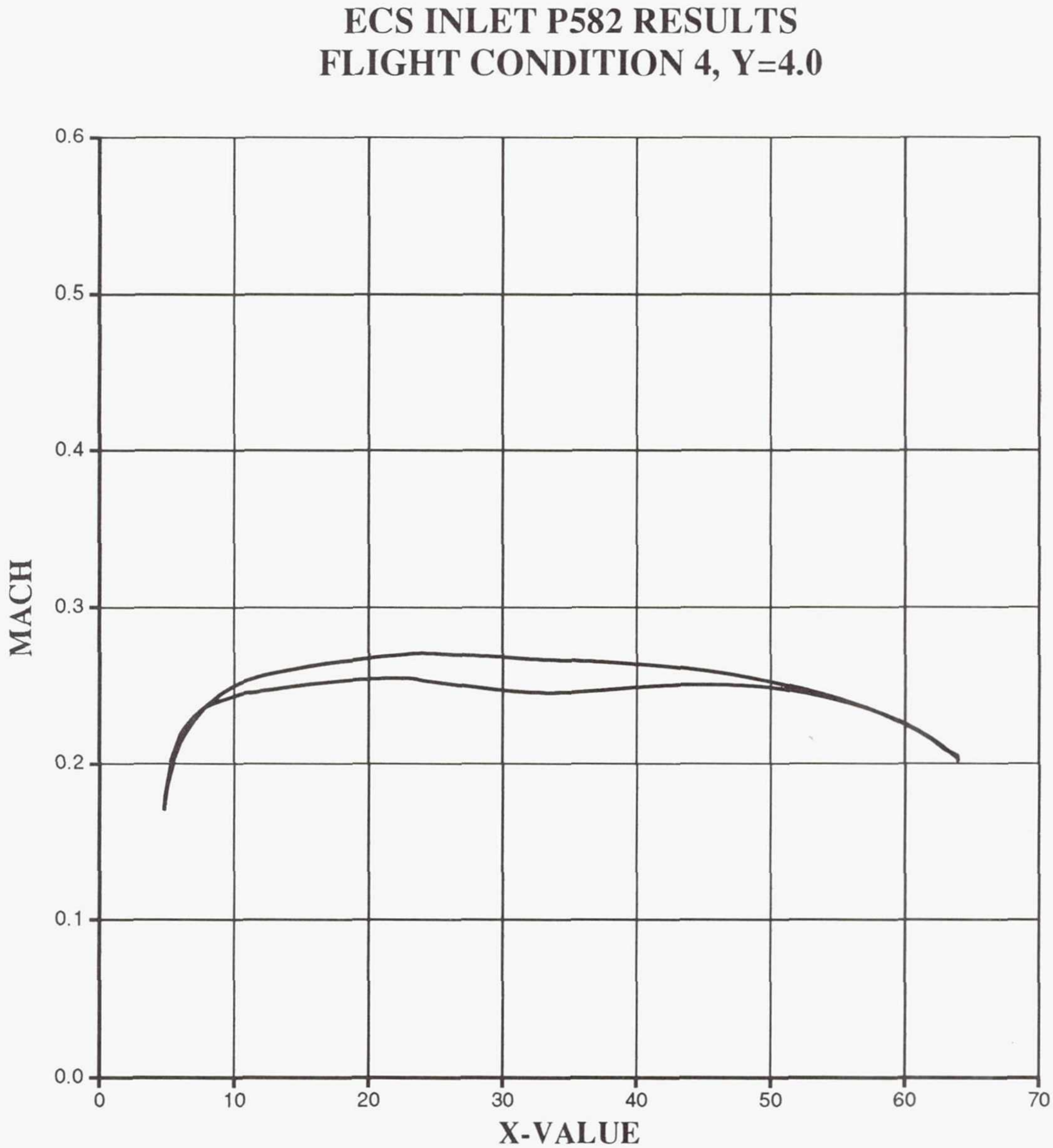

FIGURE 4.25

MESH2 SURFACE MACH(-) vs X(in)--FC4,Y=4

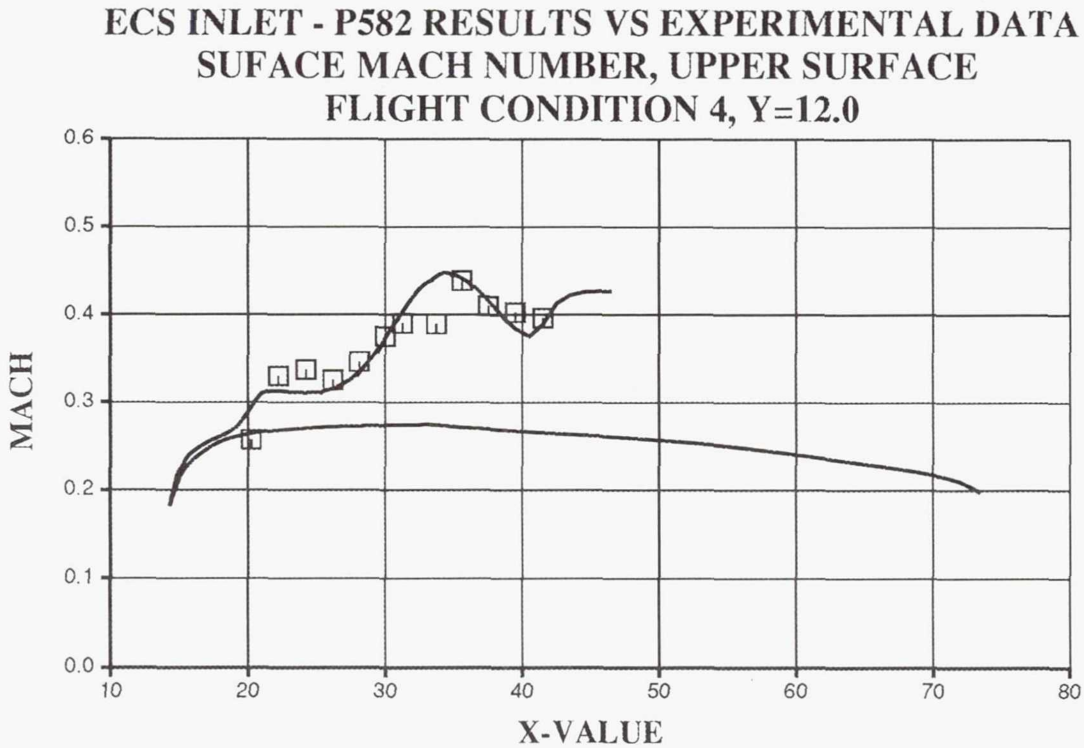

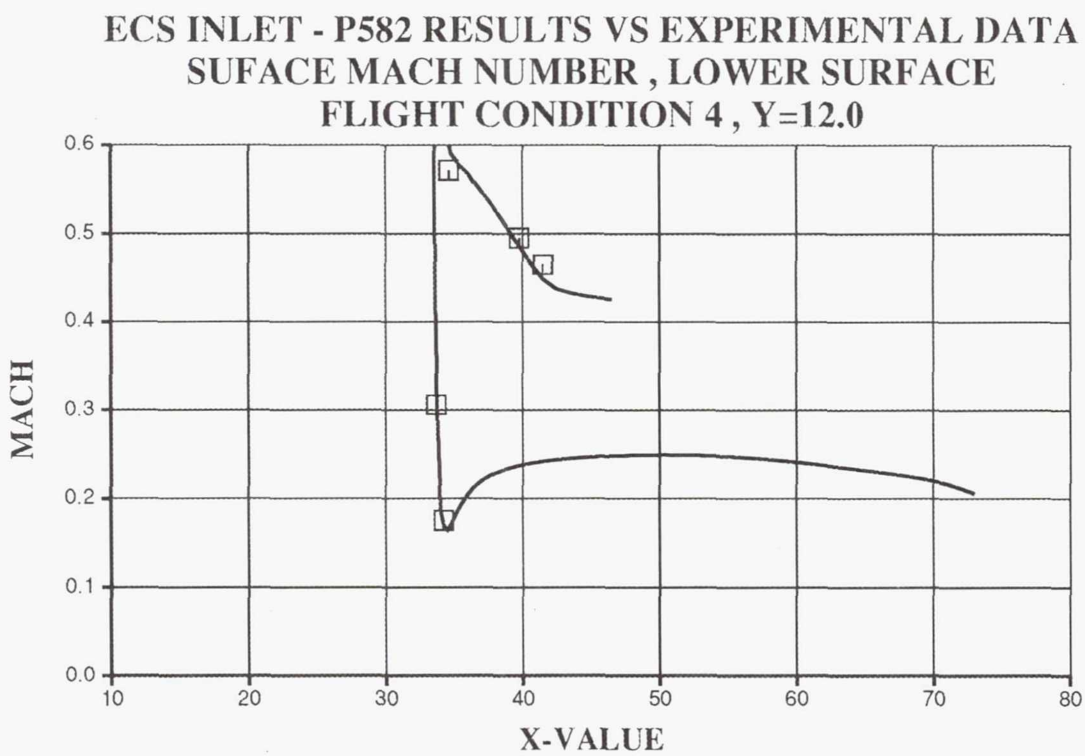

FIGURE 4.26

MESH2 AND TEST DATA SURFACE MACH(-) vs X(in)—FC4,Y=12

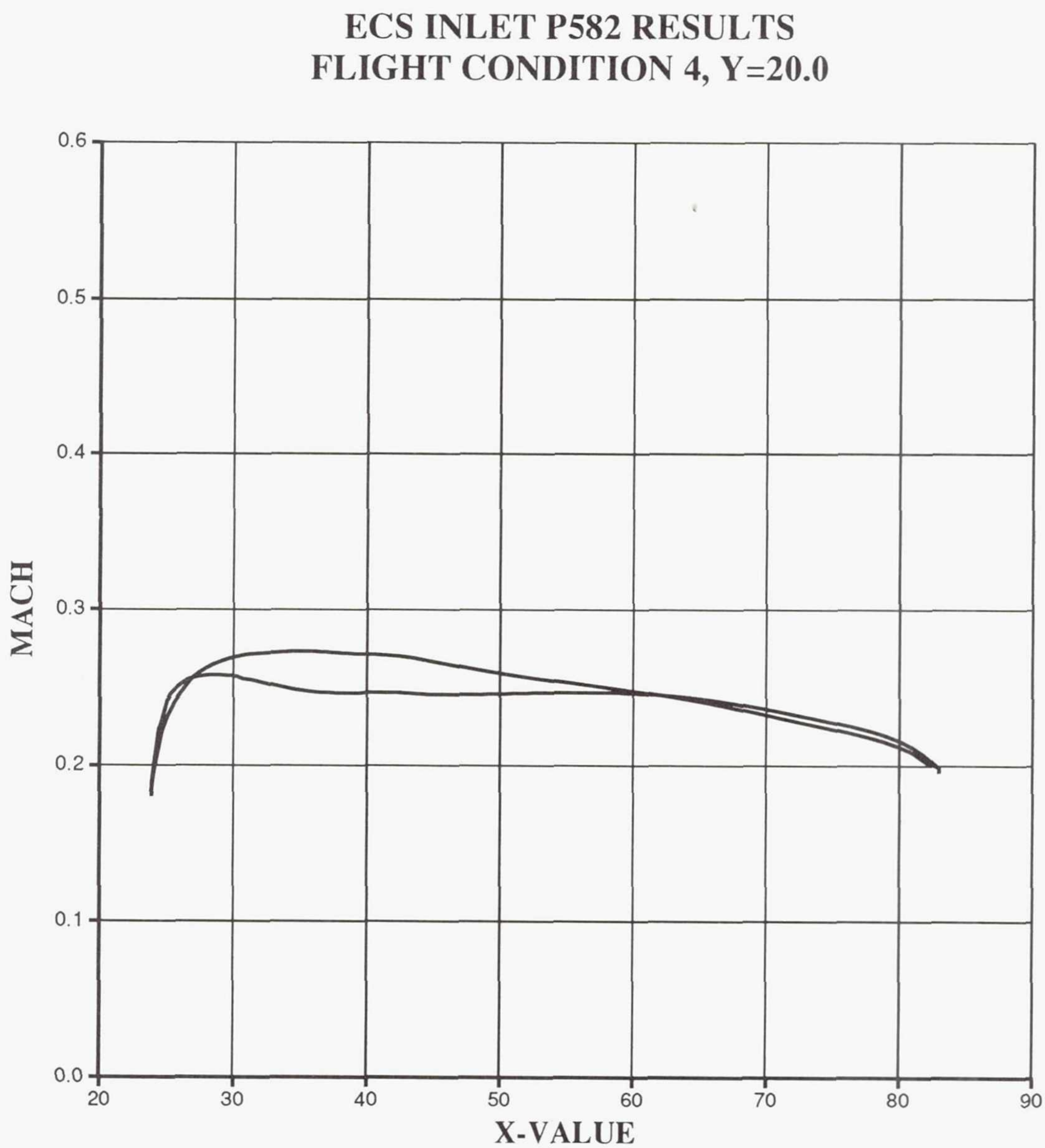

FIGURE 4.27

MESH2 SURFACE MACH(-) vs X(in)—FC4,Y=20

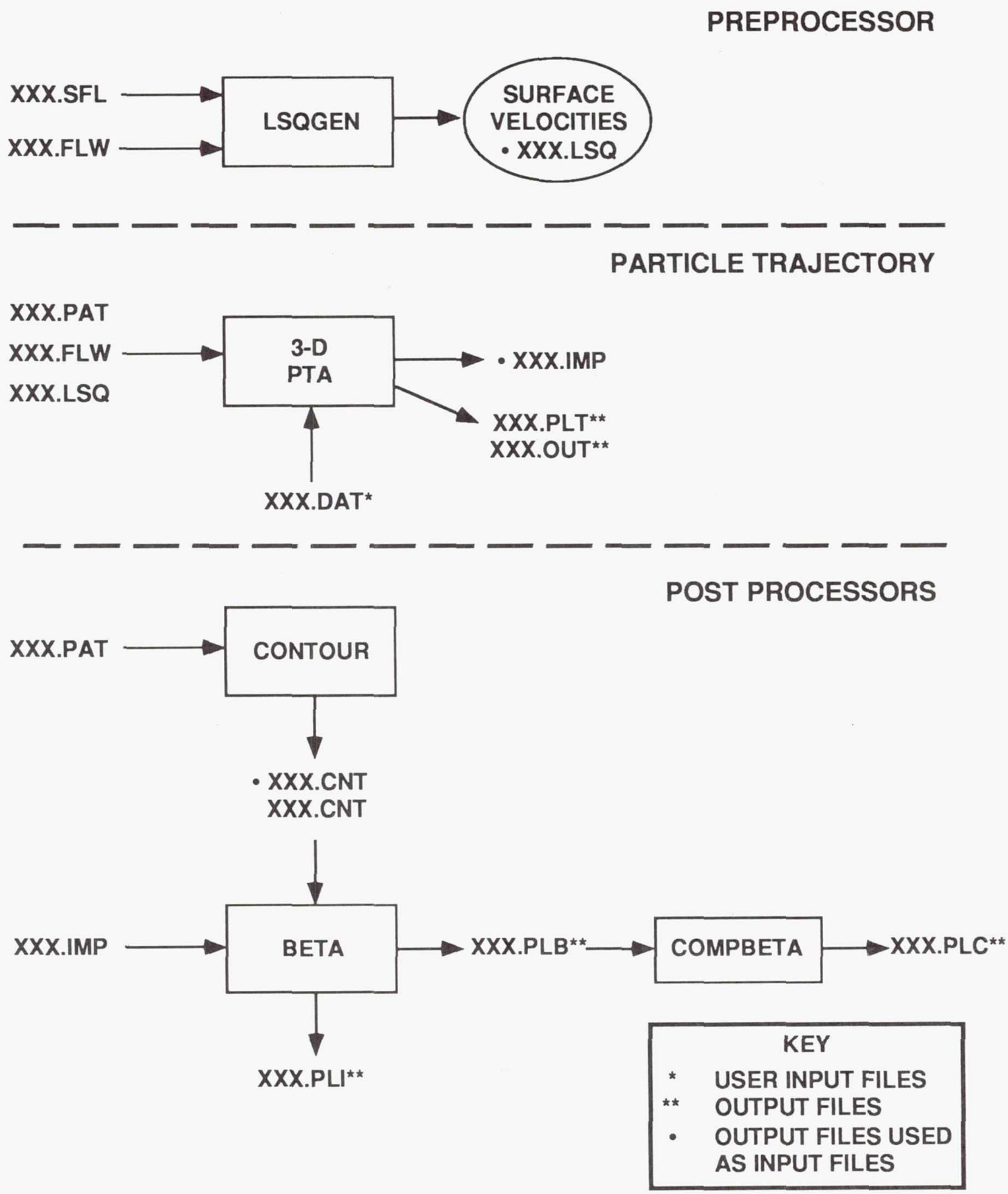

FIGURE 4.28

PARTICLE TRAJECTORY ANALYSIS--FILE/PROGRAM RELATIONSHIPS AND DESCRIPTIONS Page 1 of 2

XXX.PAT - Bicubic patch parameter file; generated by MASTER.

XXX.SFL - Surface properties file; generated by P582.

XXX.FLW - Flowfield file; generated by P582.

XXX.LSQ - Least-square coefficient file; generated by LSQGEN

XXX.DAT - Flow parameter input file to 3-D PTA; user generated.

XXX.OUT - Output file from 3-D PTA; contains diagnostic data for streamline and/or trajectory tracing.

XXX.PLT - Output file from 3-D PTA; contains plot data for streamline and/or trajectory plots.

XXX.IMP - Input file for BETA containing impingement data; generated by 3-D PTA.

XXX.CNT - Input file for BETA containing geometry constant cut data; generated by CONTOUR.

XXX.PLB - Output file from BETA; contains plot data for local impingement efficiency, β.

XXX.PLI - Output file from BETA; contains plot data for projected impingement points along a specified cut.

XXX.PLC — Output File From COMPBETA; contains plot data for local impingement efficiency, β, of all individual drops in cloud distributionas well as the composite drop.

FIGURE 4.28

PARTICLE TRAJECTORY ANALYSIS--FILE/PROGRAM RELATIONSHIPS AND DESCRIPTIONS Page 2 of 2

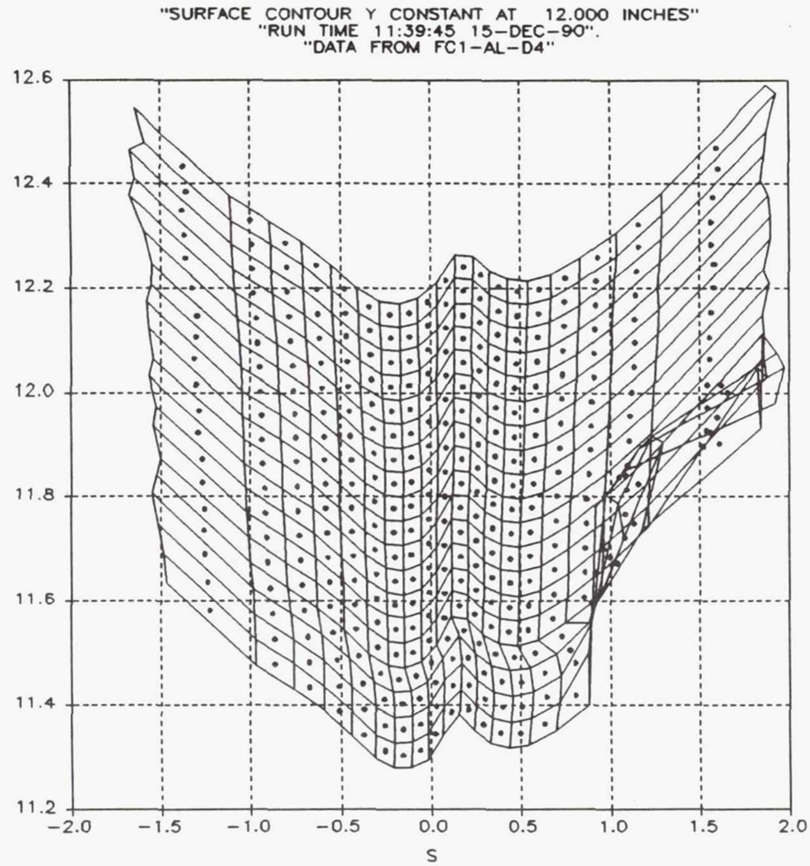

FIGURE 4.29
IMPINGEMENT FIELD Y(in) vs S(in), FC1,Y=12U,D=20.4 micron
--BEFORE LSQGEN CORRECTION

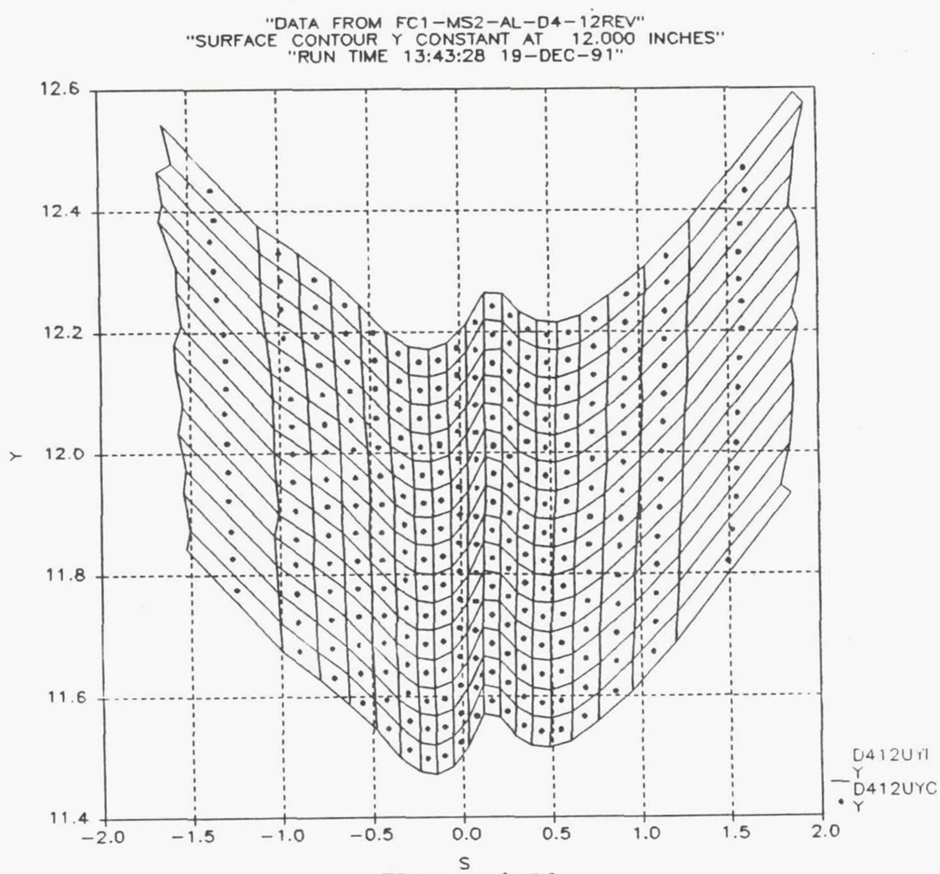

FIGURE 4.30
IMPINGEMENT FIELD Y(in) vs S(in), FC1,Y=12U,D=20.4 micron
--AFTER LSQGEN CORRECTION

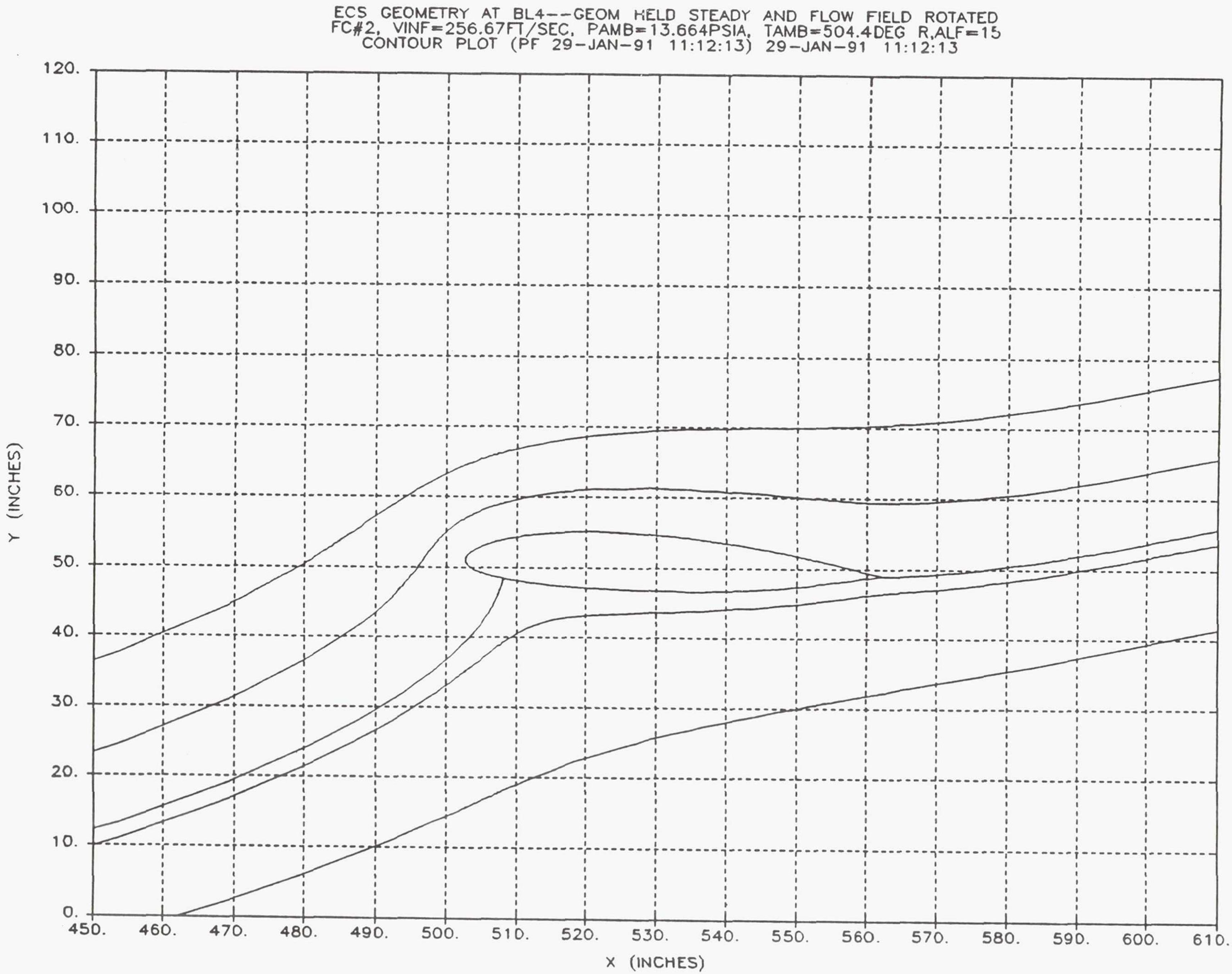

FIGURE 4.31

2-D FLOWFIELD AROUND ECS GEOMETRY, FC2,Y=4

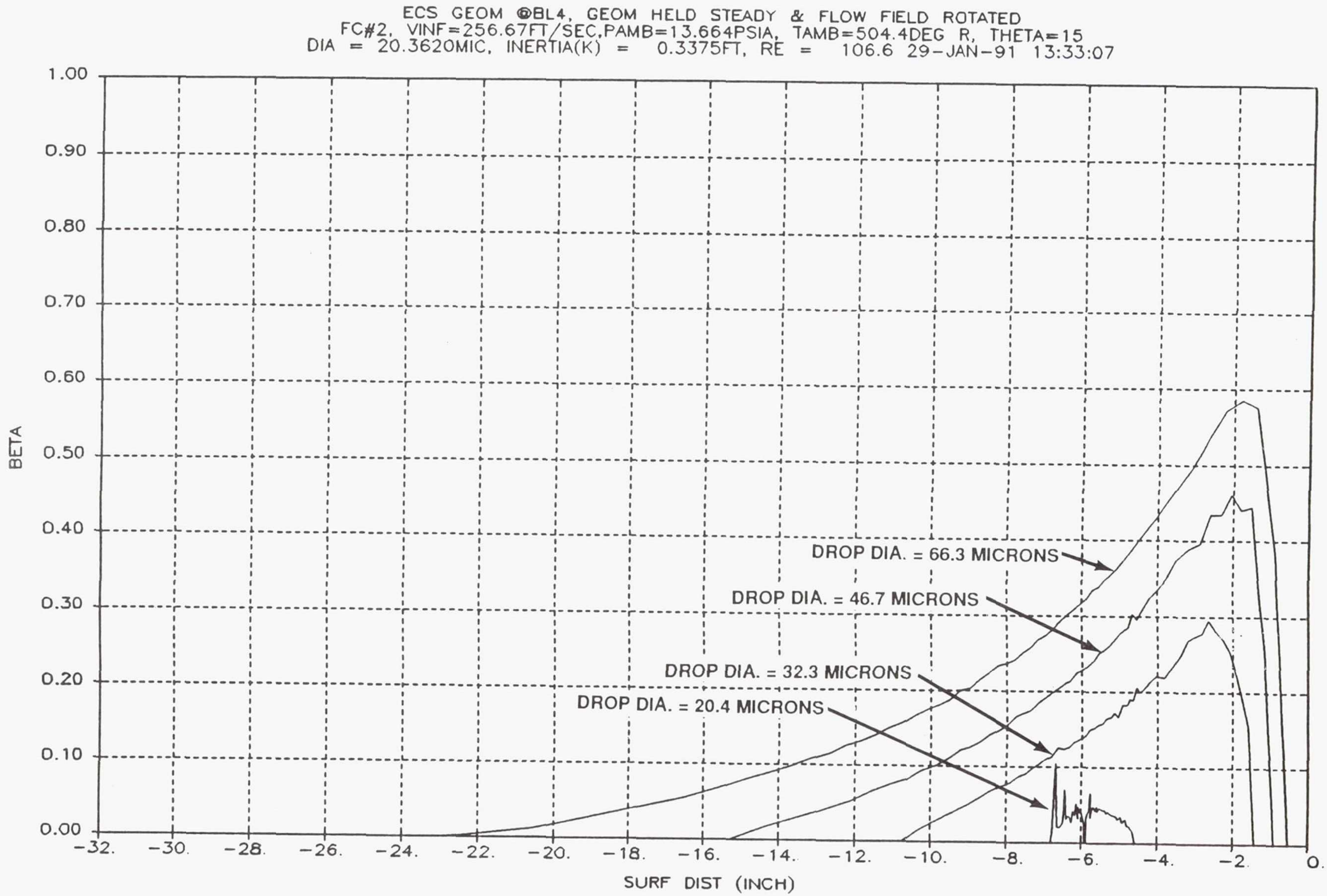

FIGURE 4.32

2-D BETA vs SURF-DIST, FC2,Y=4

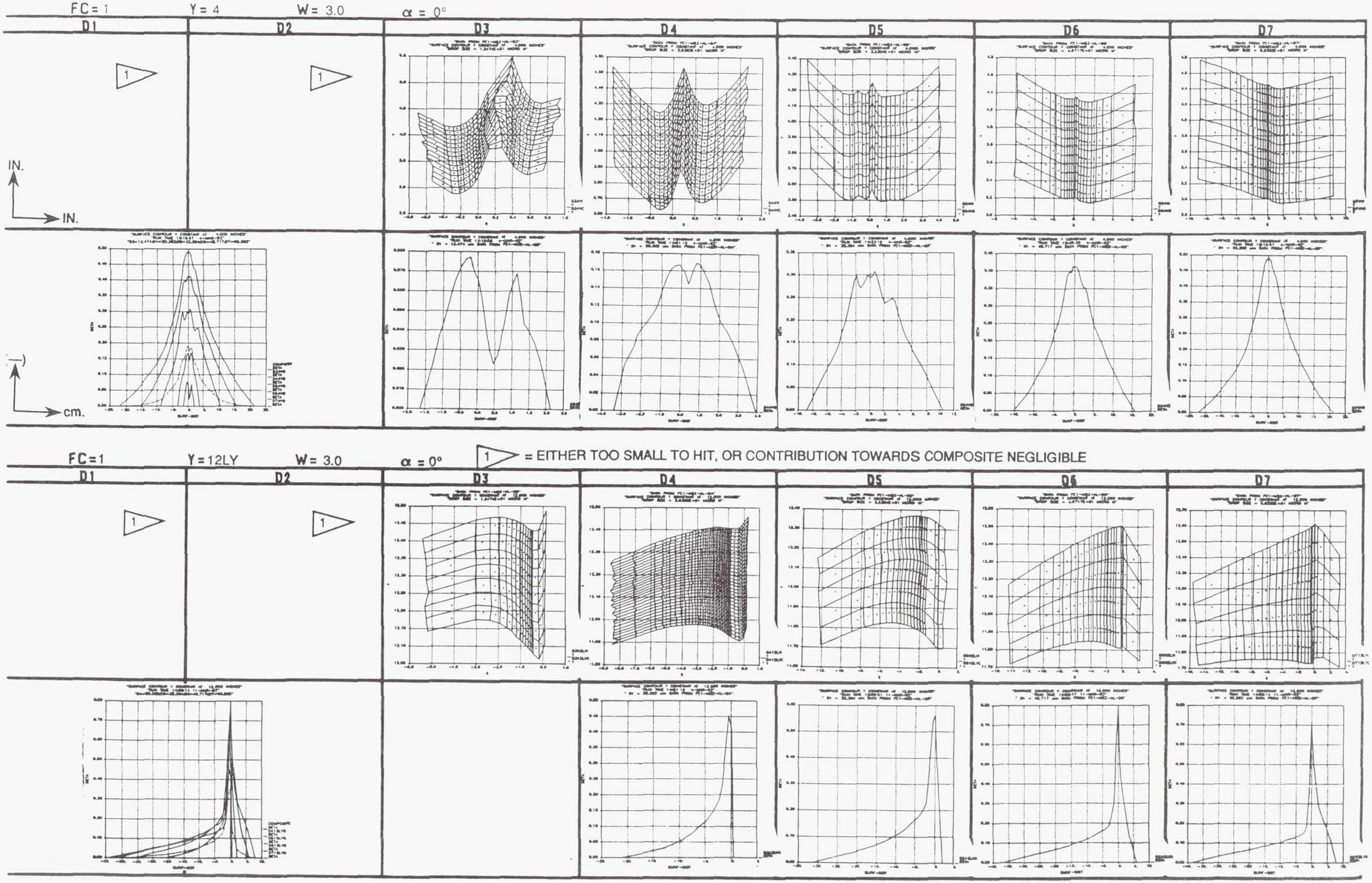

FIGURE 4.33
SUMMARY CURVES FOR IMPINGEMENT ANALYSIS—FC1
Page 1 of 2

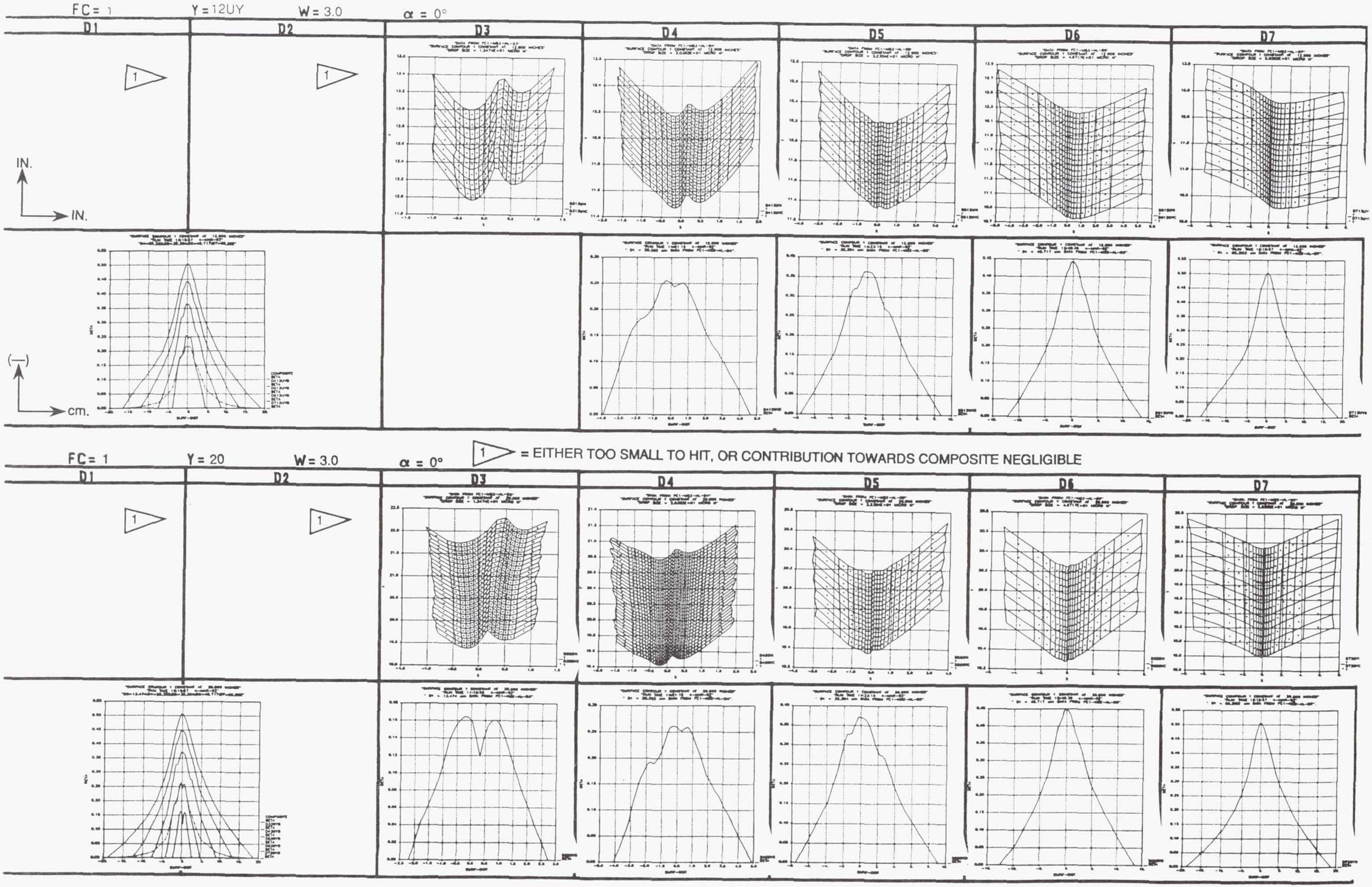

FIGURE 4.33
SUMMARY CURVES FOR IMPINGEMENT ANALYSIS--FC1
Page 2 of 2

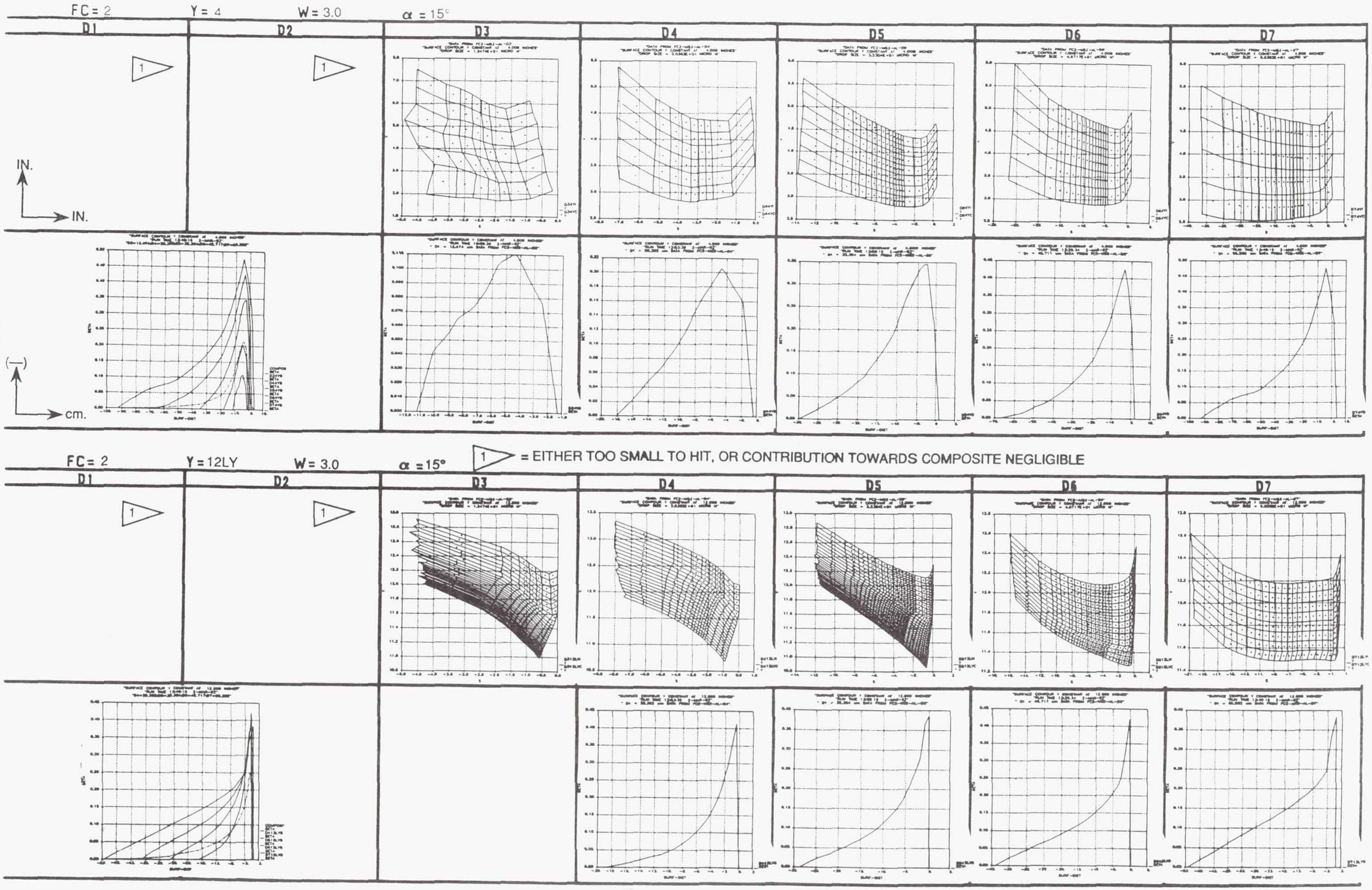

FIGURE 4.34
SUMMARY CURVES FOR IMPINGEMENT ANALYSIS—FC2
Page 1 of 2

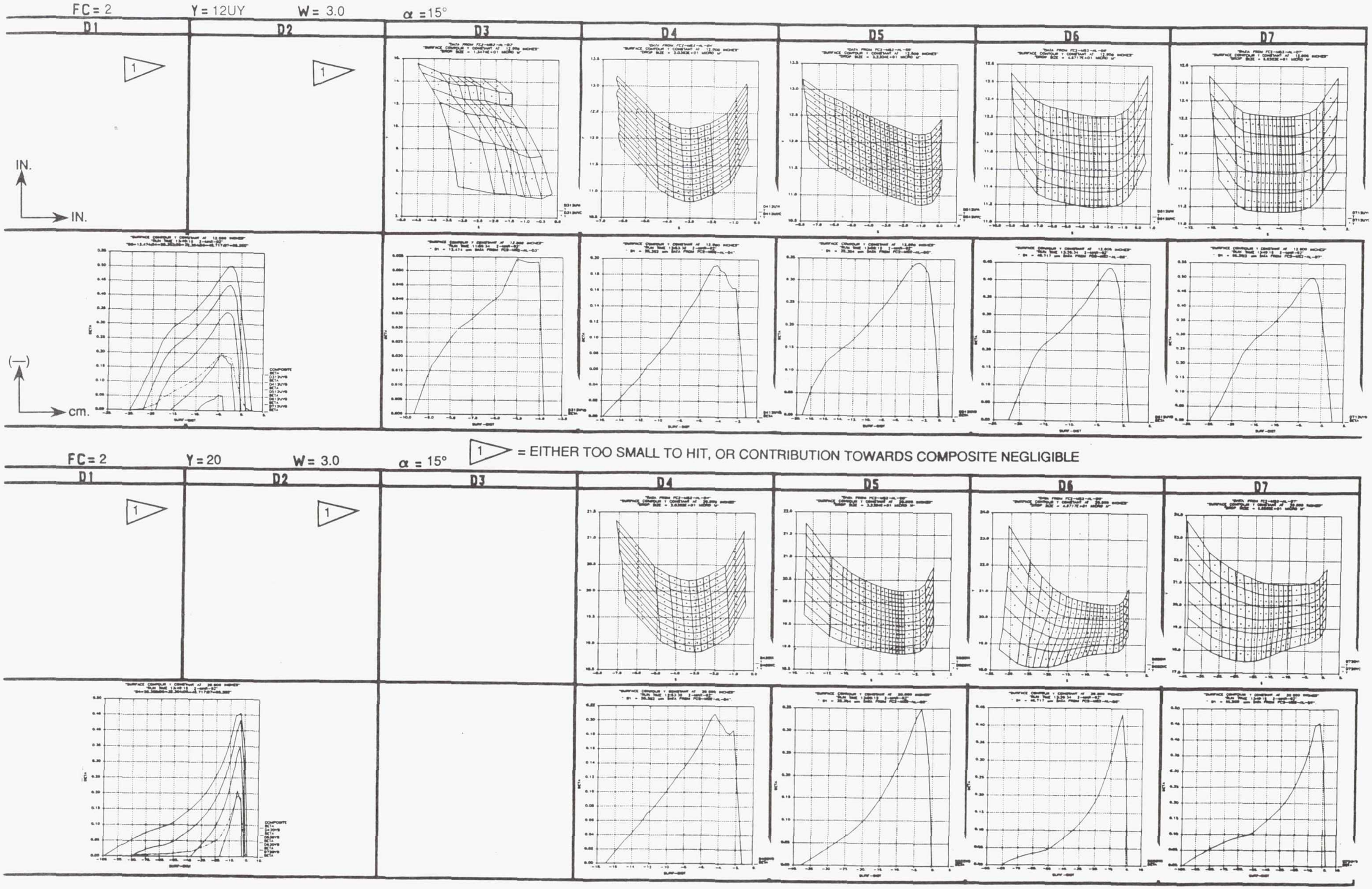

FIGURE 4.34

SUMMARY CURVES FOR IMPINGEMENT ANALYSIS--FC2

Page 2 of 2

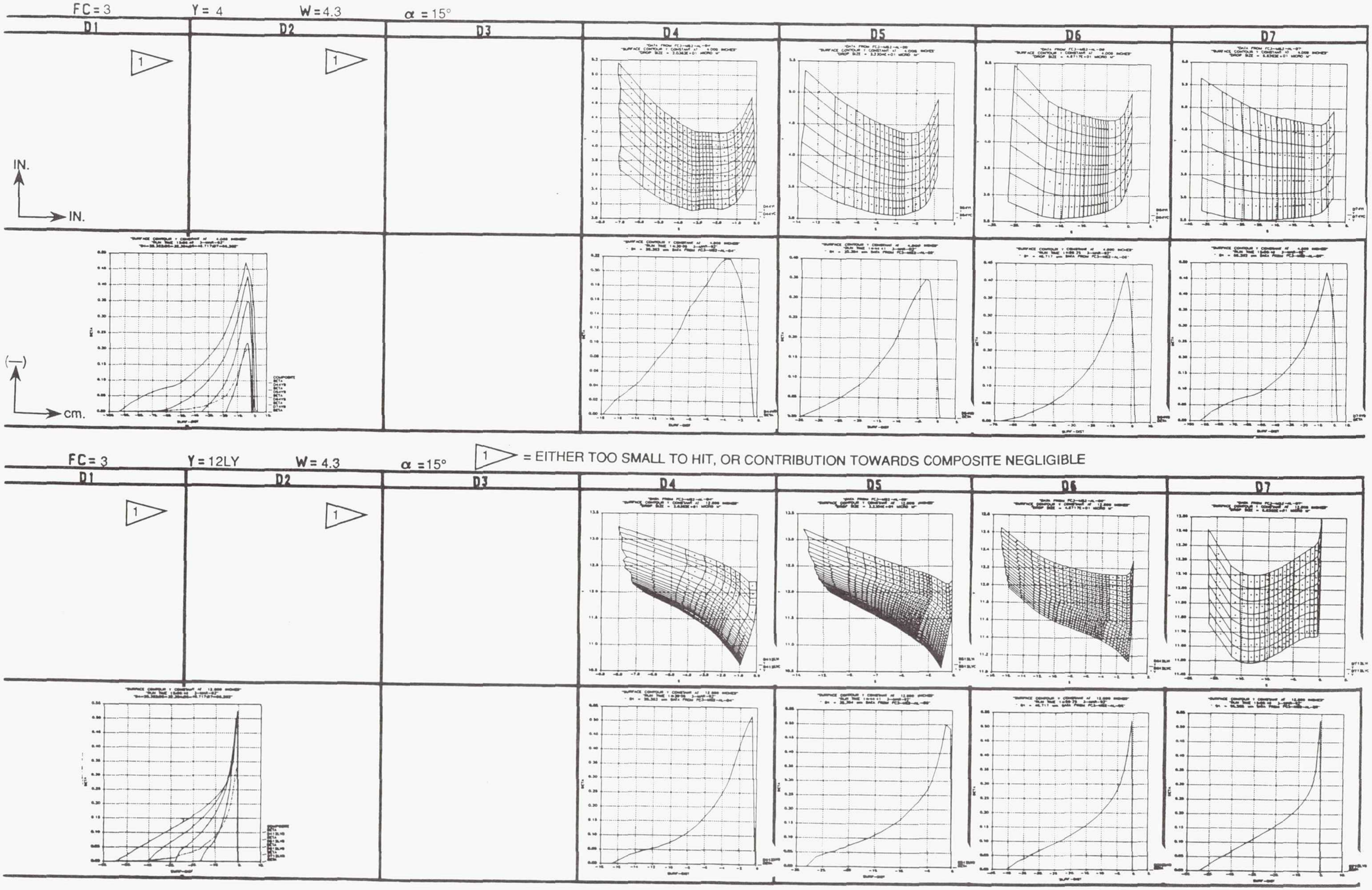

FIGURE 4.35
SUMMARY CURVES FOR IMPINGEMENT ANALYSIS--FC3
Page 1 of 2

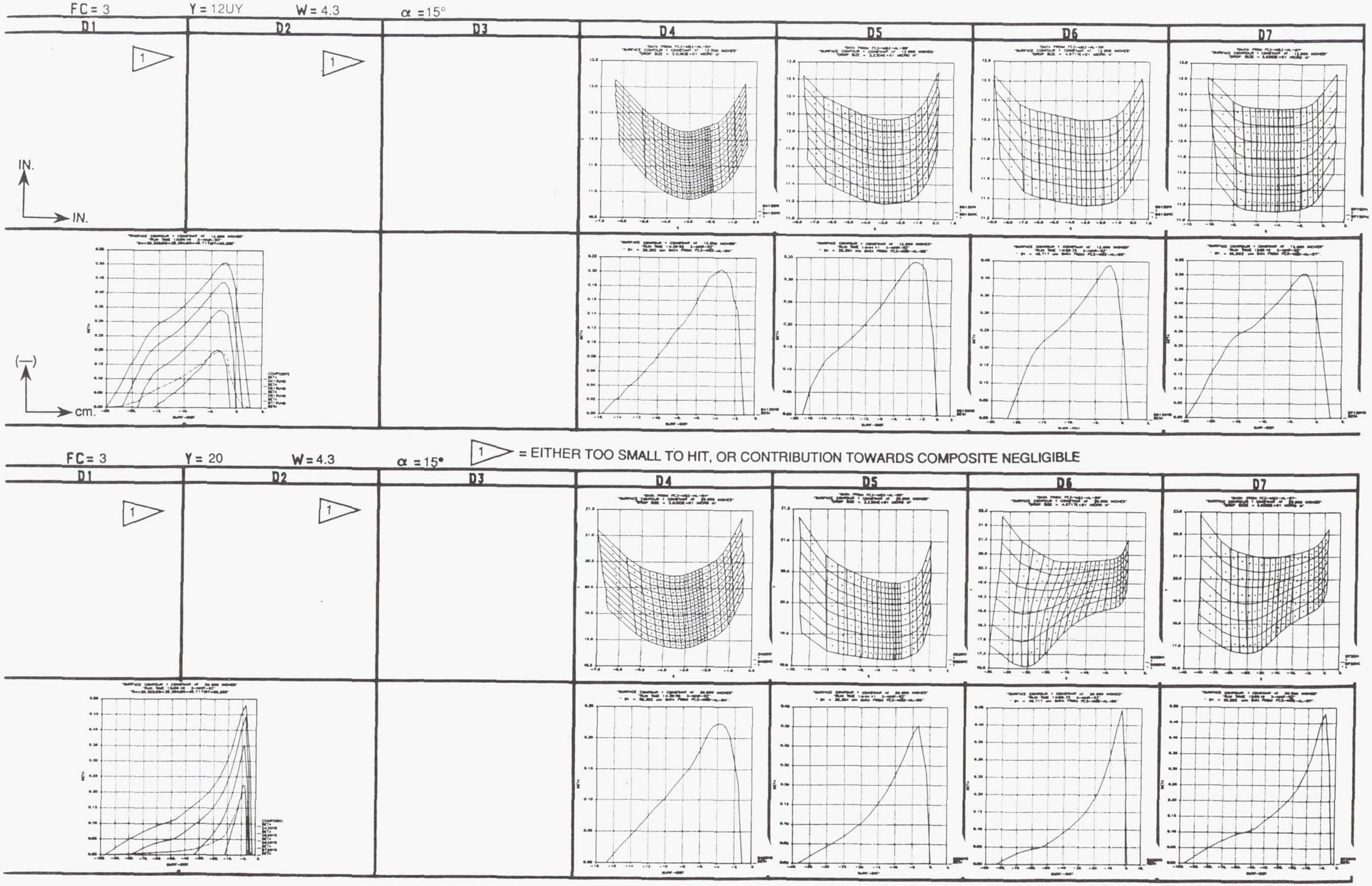

FIGURE 4.35

SUMMARY CURVES FOR IMPINGEMENT ANALYSIS—FC3

Page 2 of 2

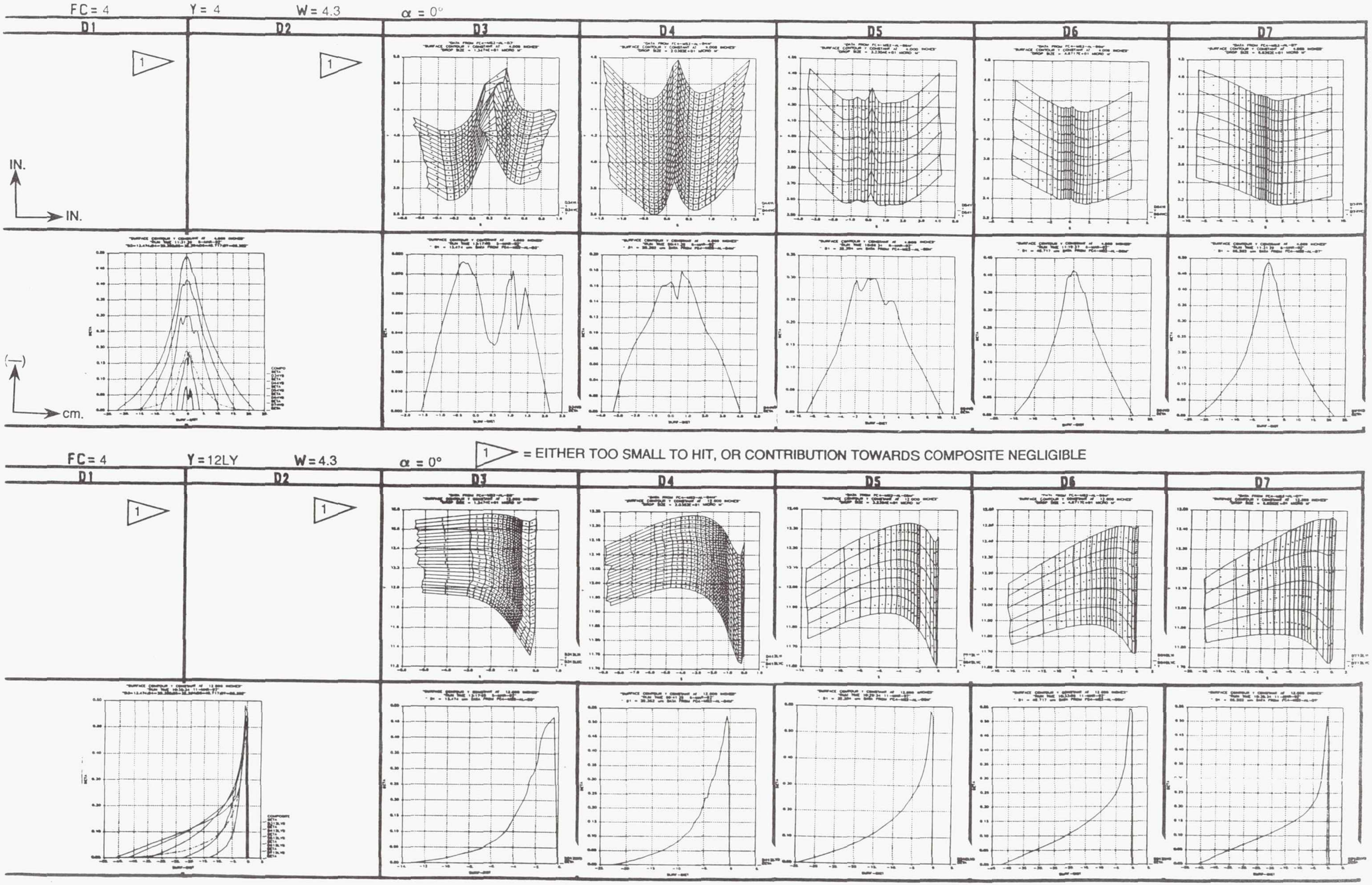

FIGURE 4.36

SUMMARY CURVES FOR IMPINGEMENT ANALYSIS—FC4

Page 1 of 2

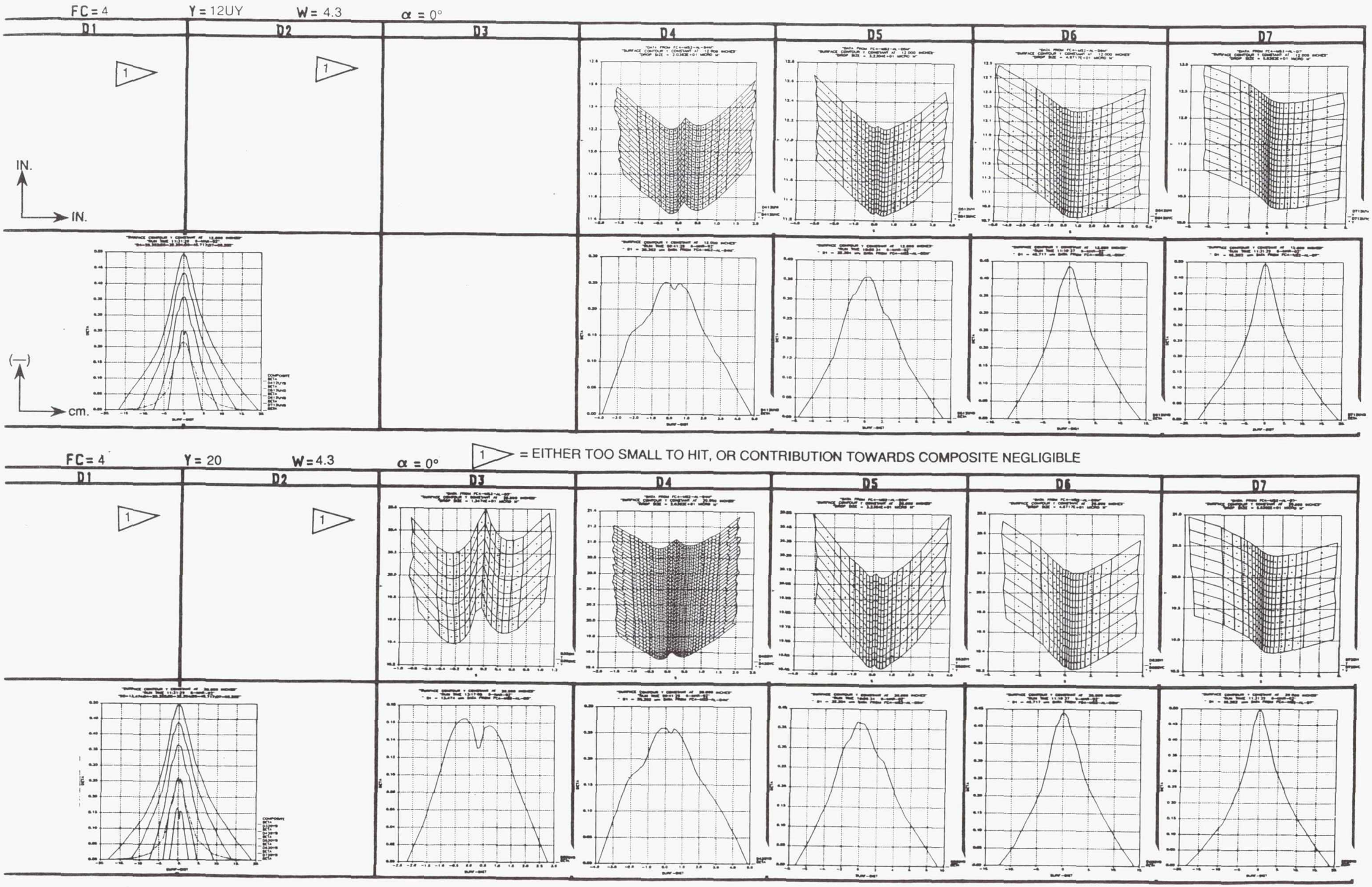

FIGURE 4.36

SUMMARY CURVES FOR IMPINGEMENT ANALYSIS—FC4

Page 2 of 2

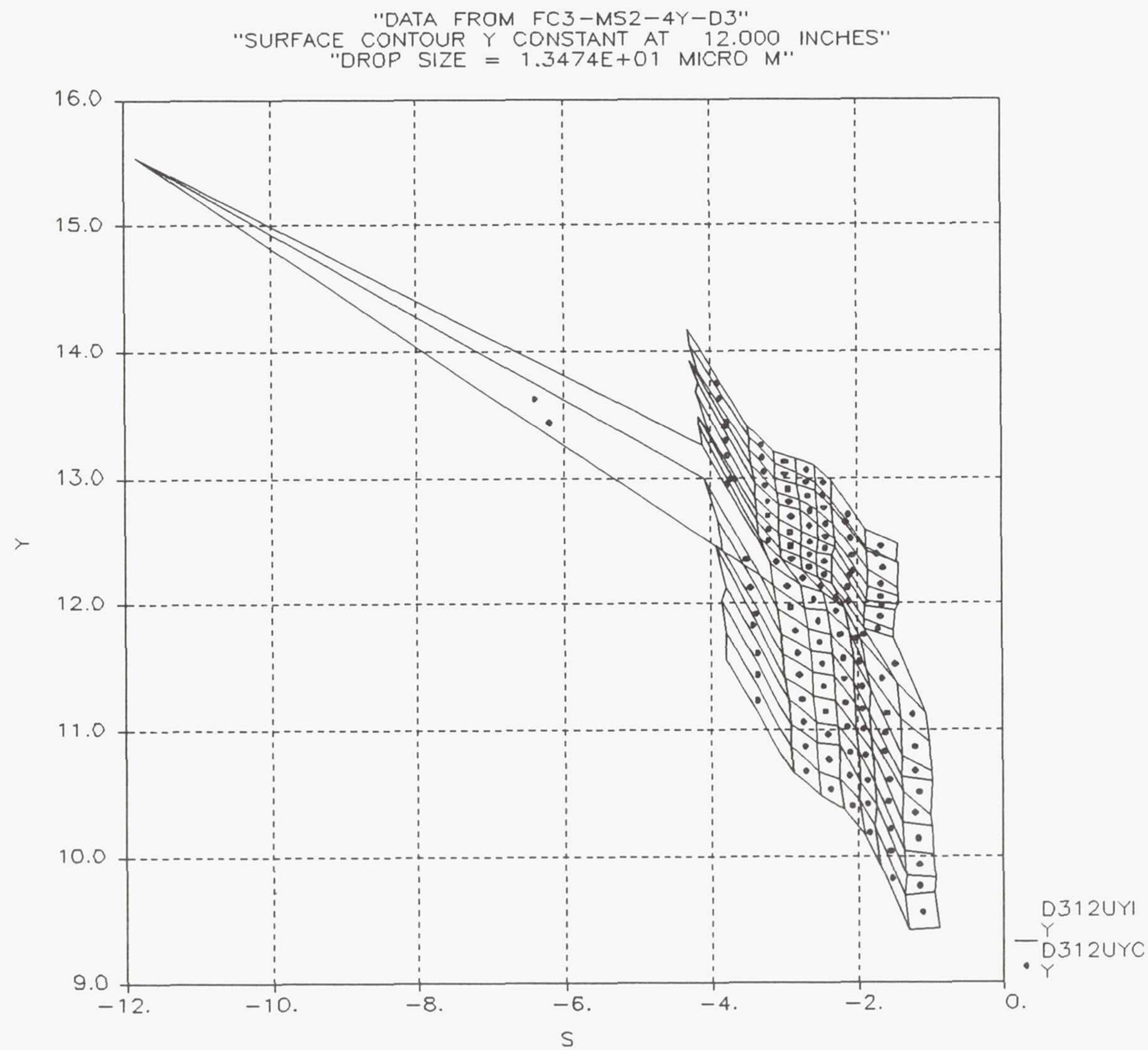

FIGURE 4.37

IMPINGEMENT FIELD Y (in) vs S (in), FC3, Y=12U, D=13.5 MICRON

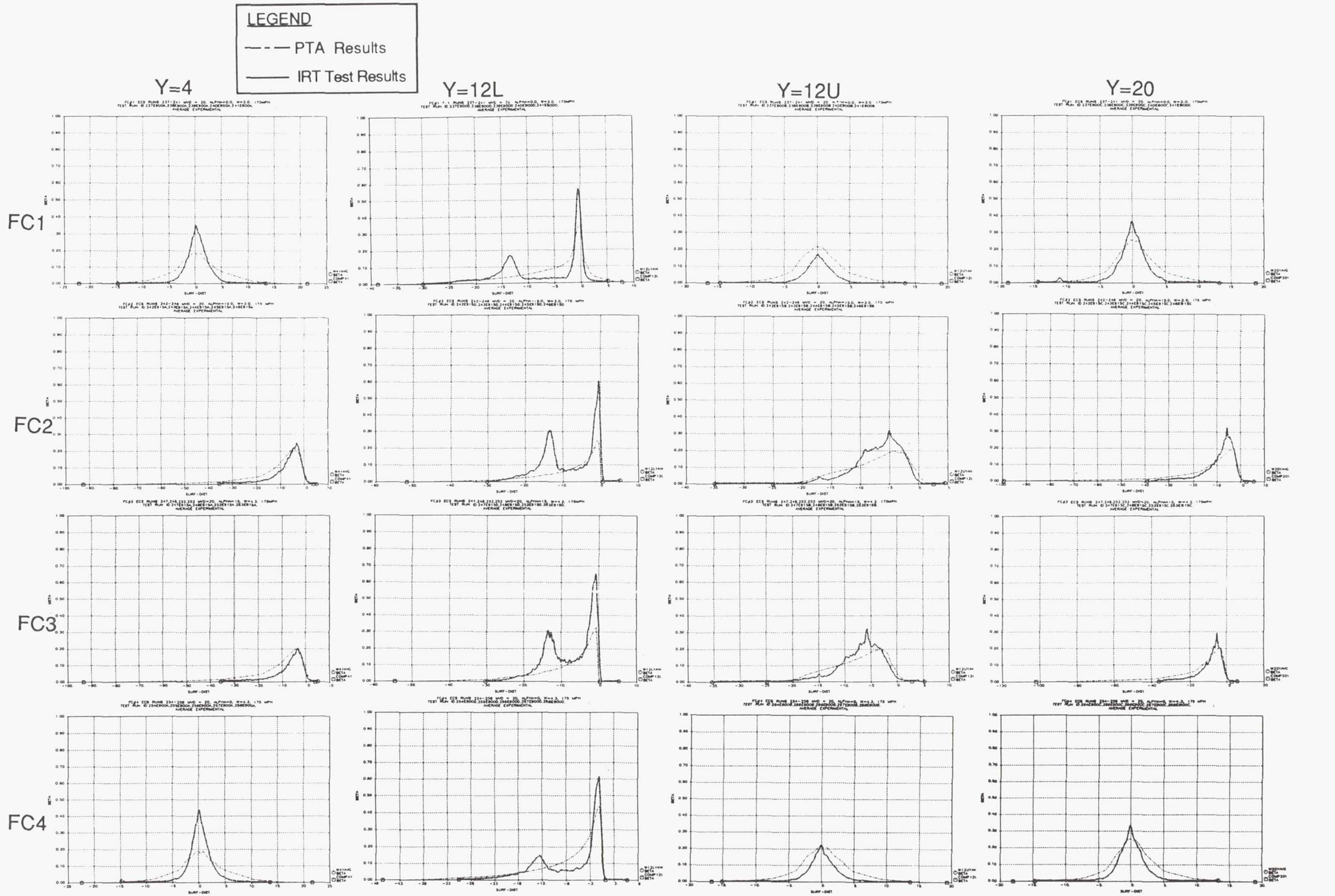

FIGURE 4.38

SUMMARY OF ANALYSIS AND TEST IMPINGEMENT EFFICIENCY DATA--BETA(-) vs SURF-DIST(cm)

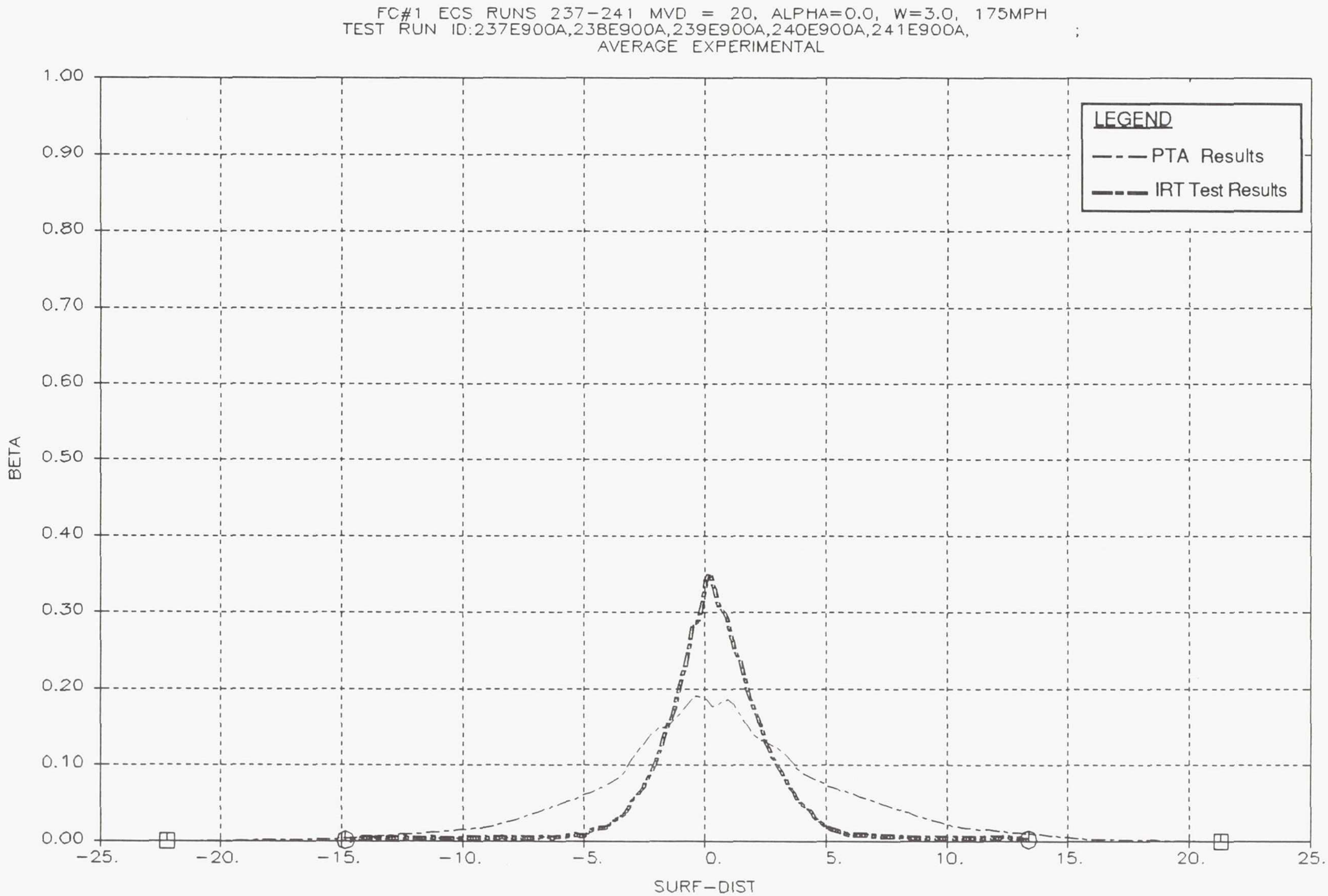

FIGURE 4.39

COMPOSITE ANALYSIS AND AVG TEST BETA RESULTS
—BETA(-) vs SURF-DIST(cm), FC1,Y=4

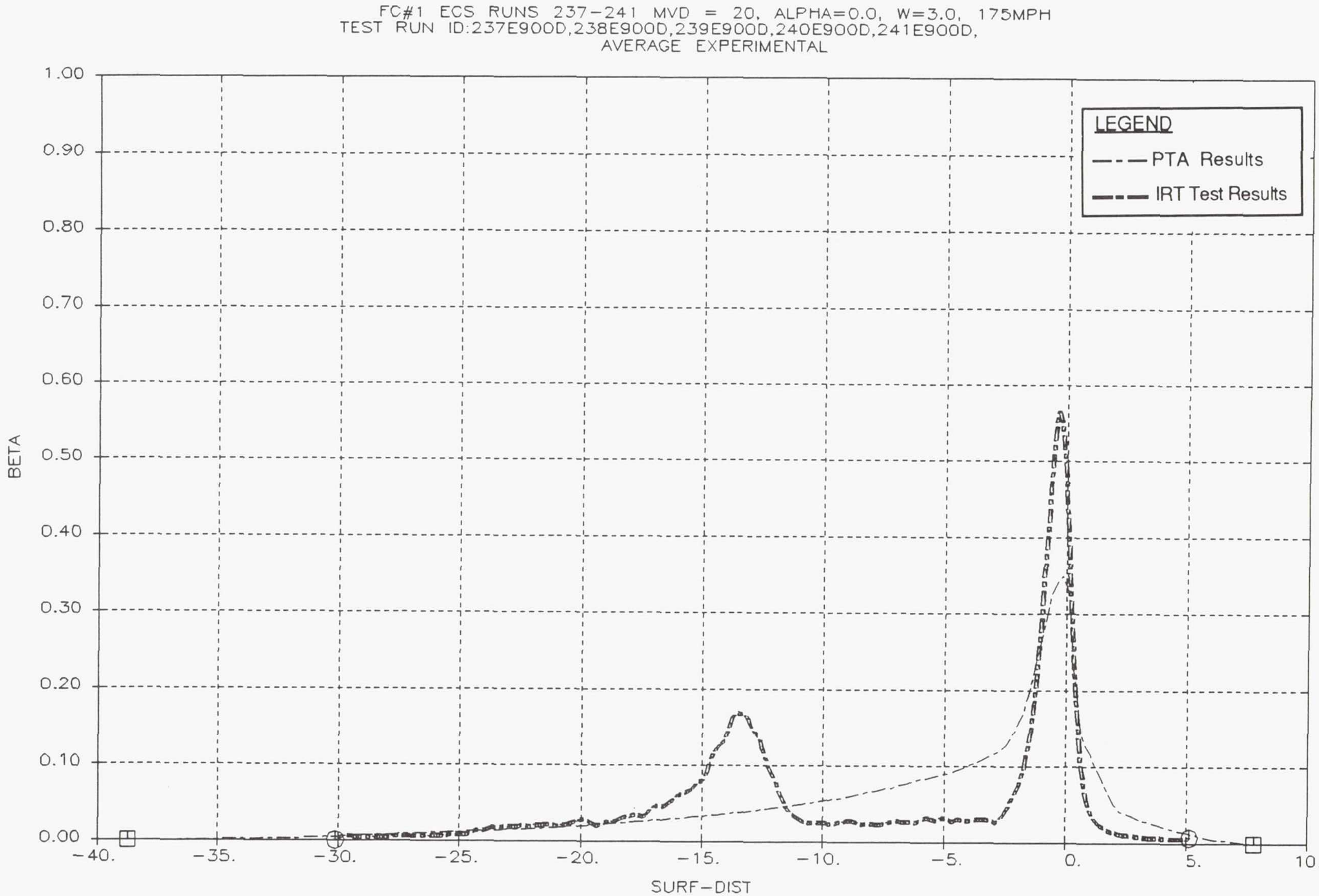

FIGURE 4.40

COMPOSITE ANALYSIS AND AVG TEST BETA RESULTS
- BETA(-) vs SURF-DIST(cm), FC1,Y=12L

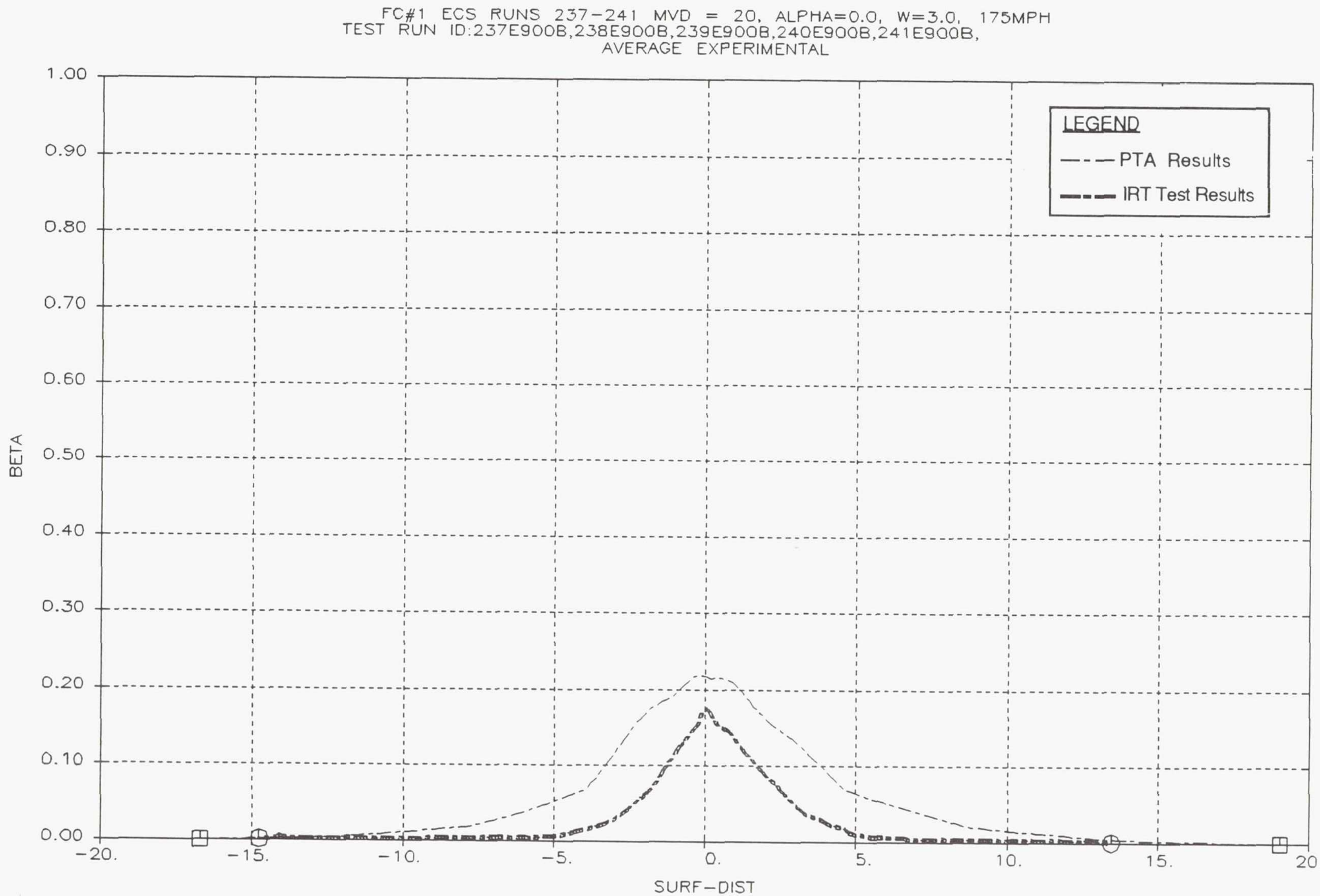

FIGURE 4.41

COMPOSITE ANALYSIS AND AVG TEST BETA RESULTS
---BETA(-) vs SURF-DIST(cm), FC1,Y=12U

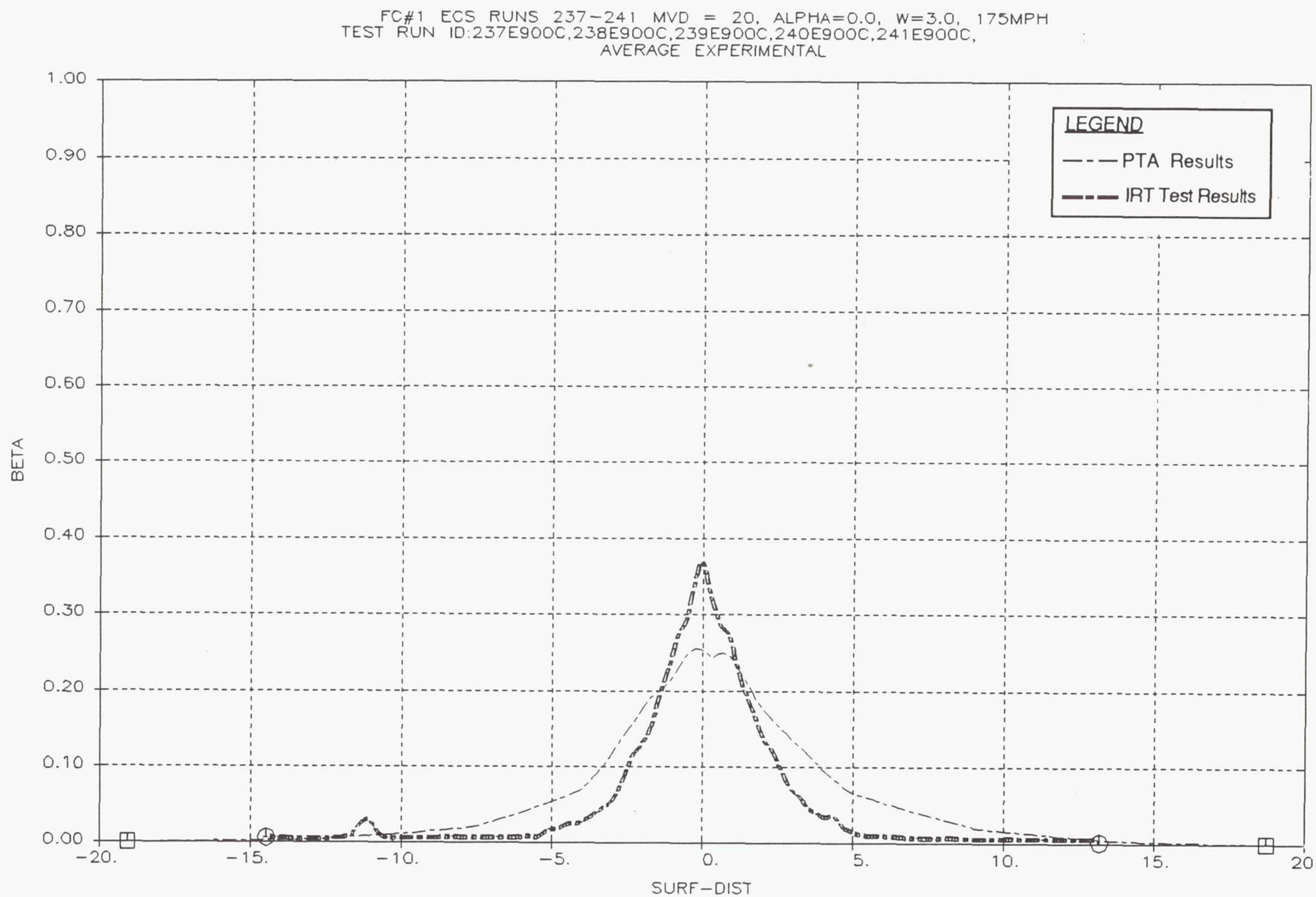

FIGURE 4.42

COMPOSITE ANALYSIS AND AVG TEST BETA RESULTS
--BETA(-) vs SURF-DIST(cm), FC1,Y=20

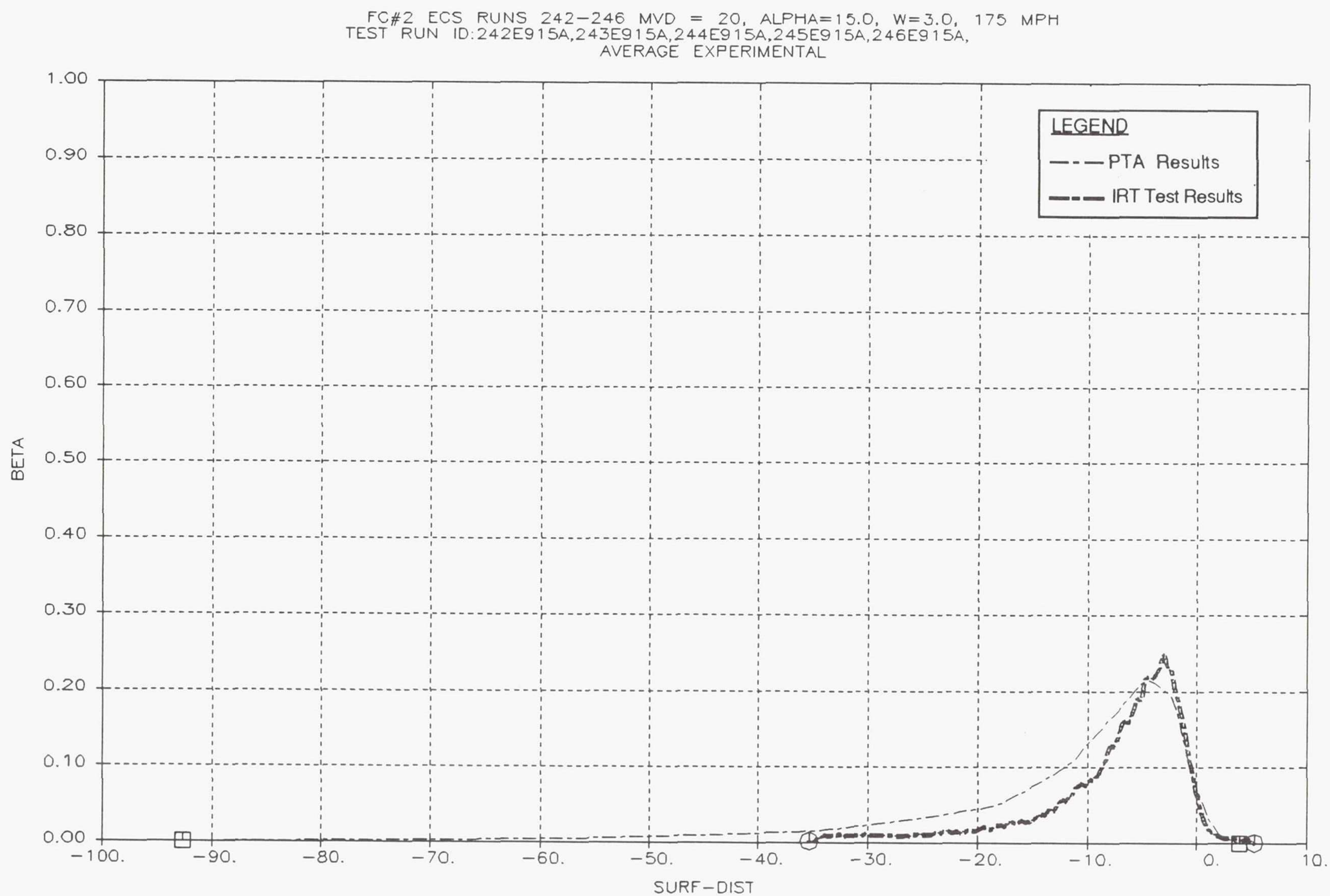

FIGURE 4.43

COMPOSITE ANALYSIS AND AVG TEST BETA RESULTS
—BETA(–) vs SURF-DIST(cm), FC2,Y=4

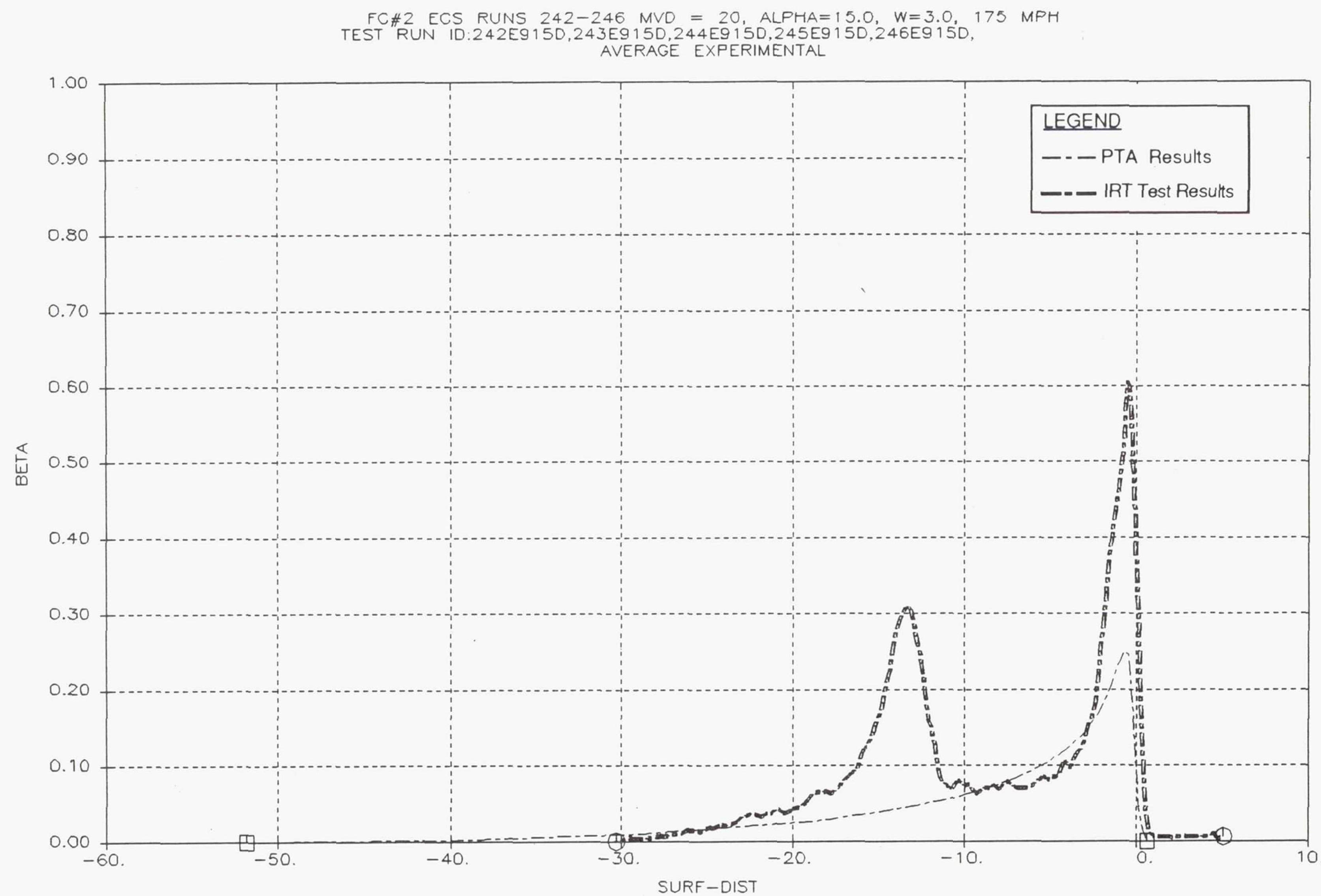

FIGURE 4.44

COMPOSITE ANALYSIS AND AVG TEST BETA RESULTS
--BETA(-) vs SURF-DIST(cm), FC2,Y=12L

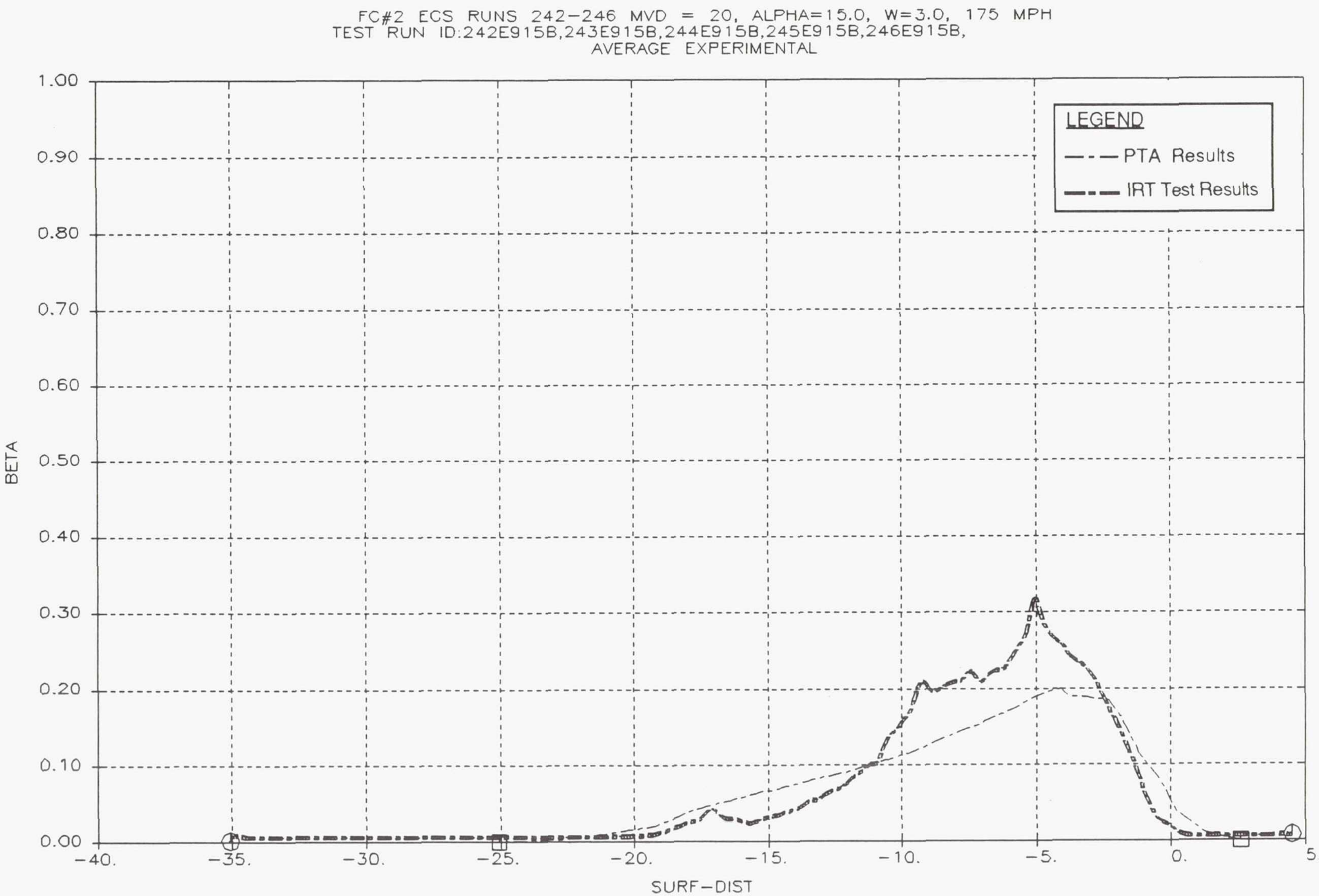

FIGURE 4.45

COMPOSITE ANALYSIS AND AVG TEST BETA RESULTS
--BETA(-) vs SURF-DIST(cm), FC2,Y=12U

FC#2 ECS RUNS 242–246 MVD = 20, ALPHA=15.0, W=3.0, 175 MPH
TEST RUN ID:242E915C,243E915C,244E915C,245E915C,246E915C,
AVERAGE EXPERIMENTAL

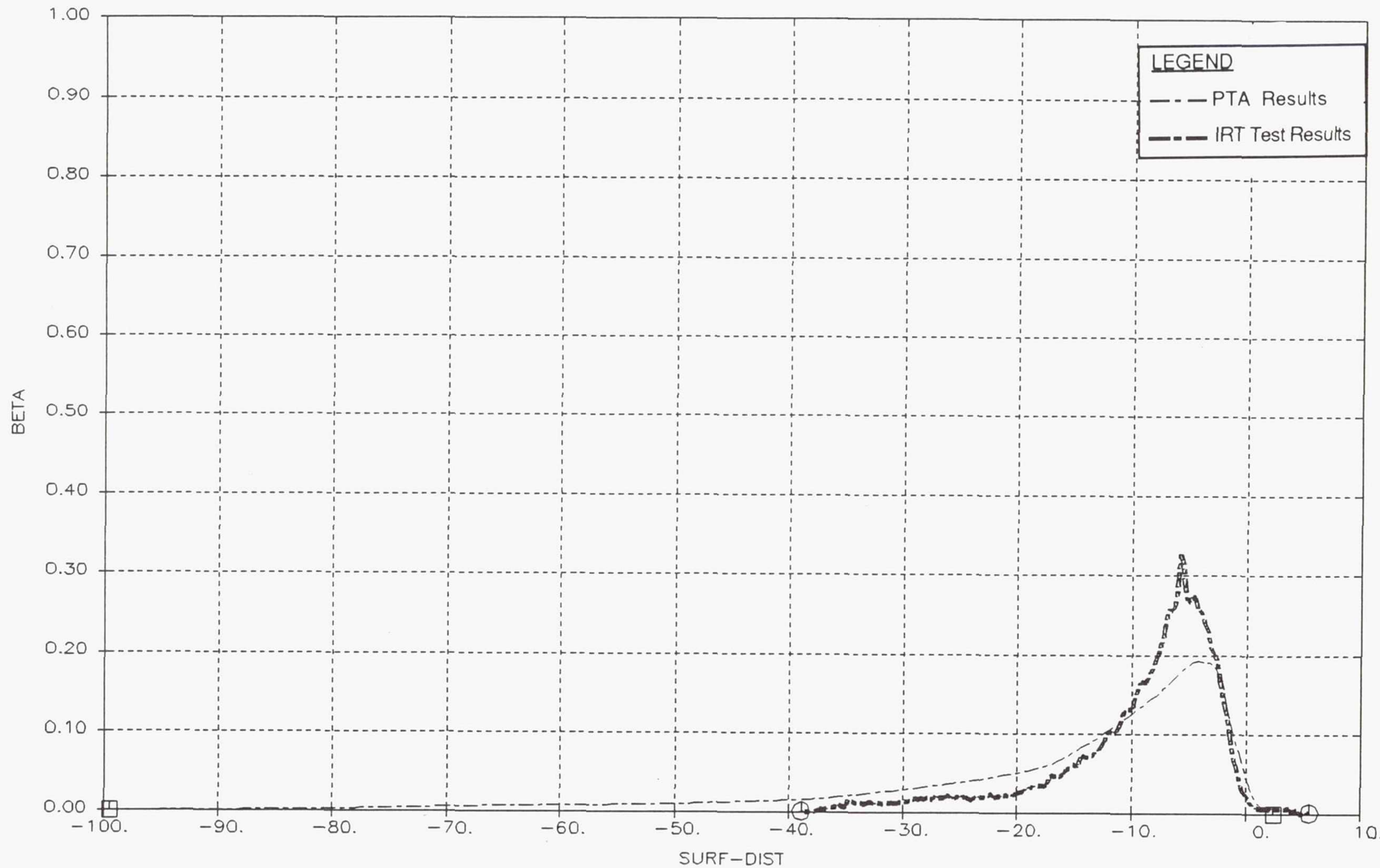

FIGURE 4.46

COMPOSITE ANALYSIS AND AVG TEST BETA RESULTS
--BETA(-) vs SURF-DIST(cm), FC2,Y=20

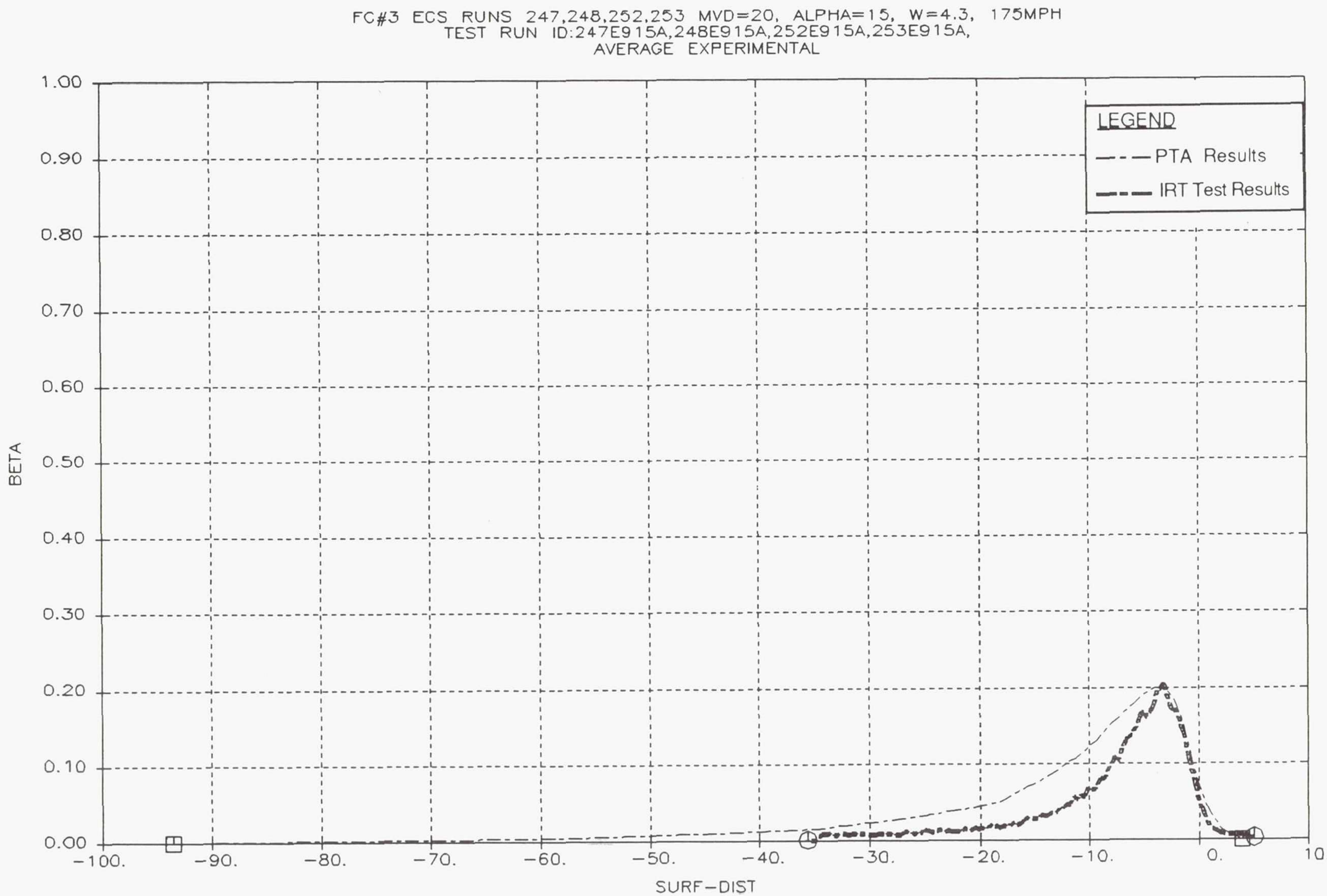

FIGURE 4.47

COMPOSITE ANALYSIS AND AVG TEST BETA RESULTS
—BETA(-) vs SURF-DIST(cm), FC3,Y=4

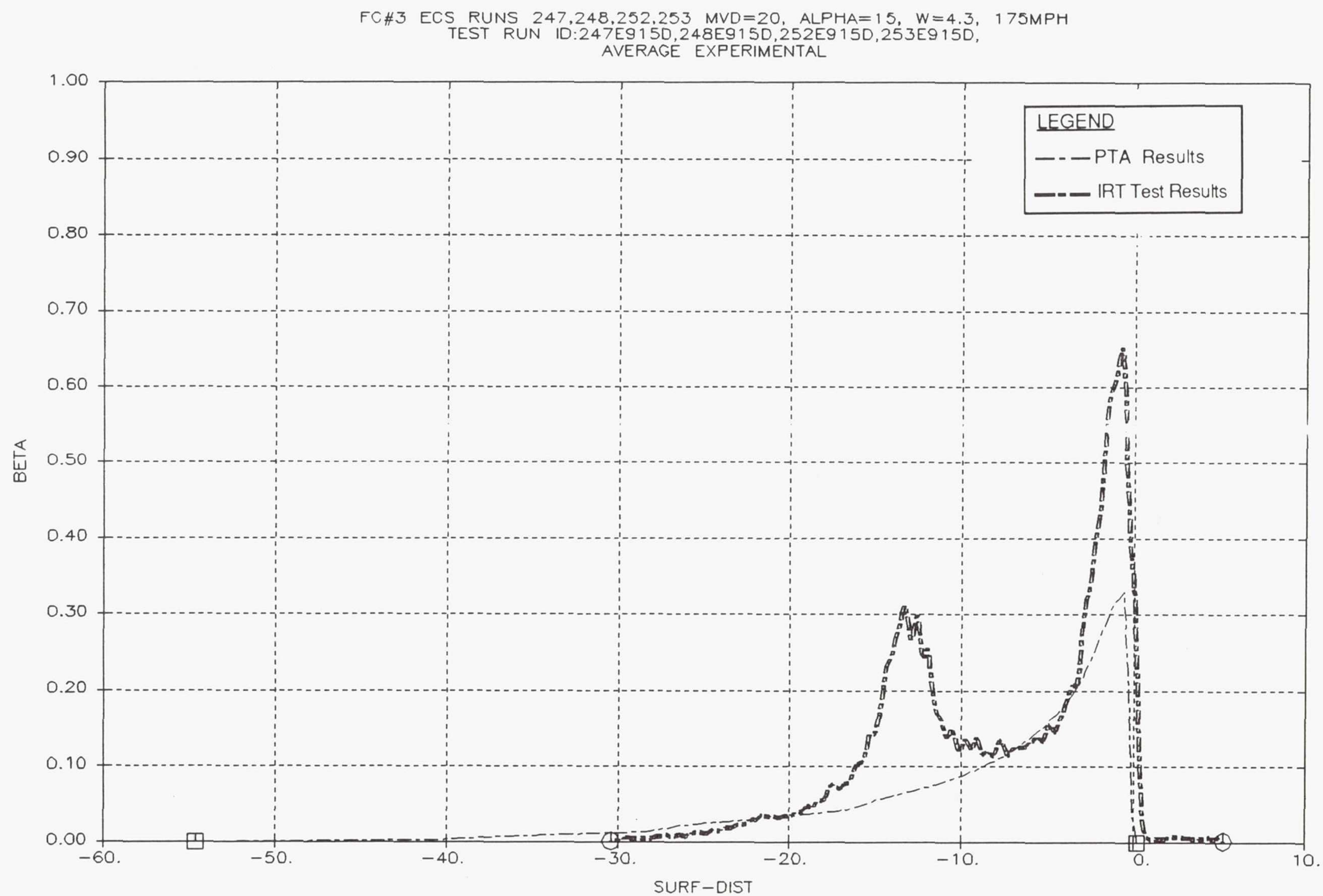

FIGURE 4.48

COMPOSITE ANALYSIS AND AVG TEST BETA RESULTS
—BETA(-) vs SURF-DIST(cm), FC3,Y=12L

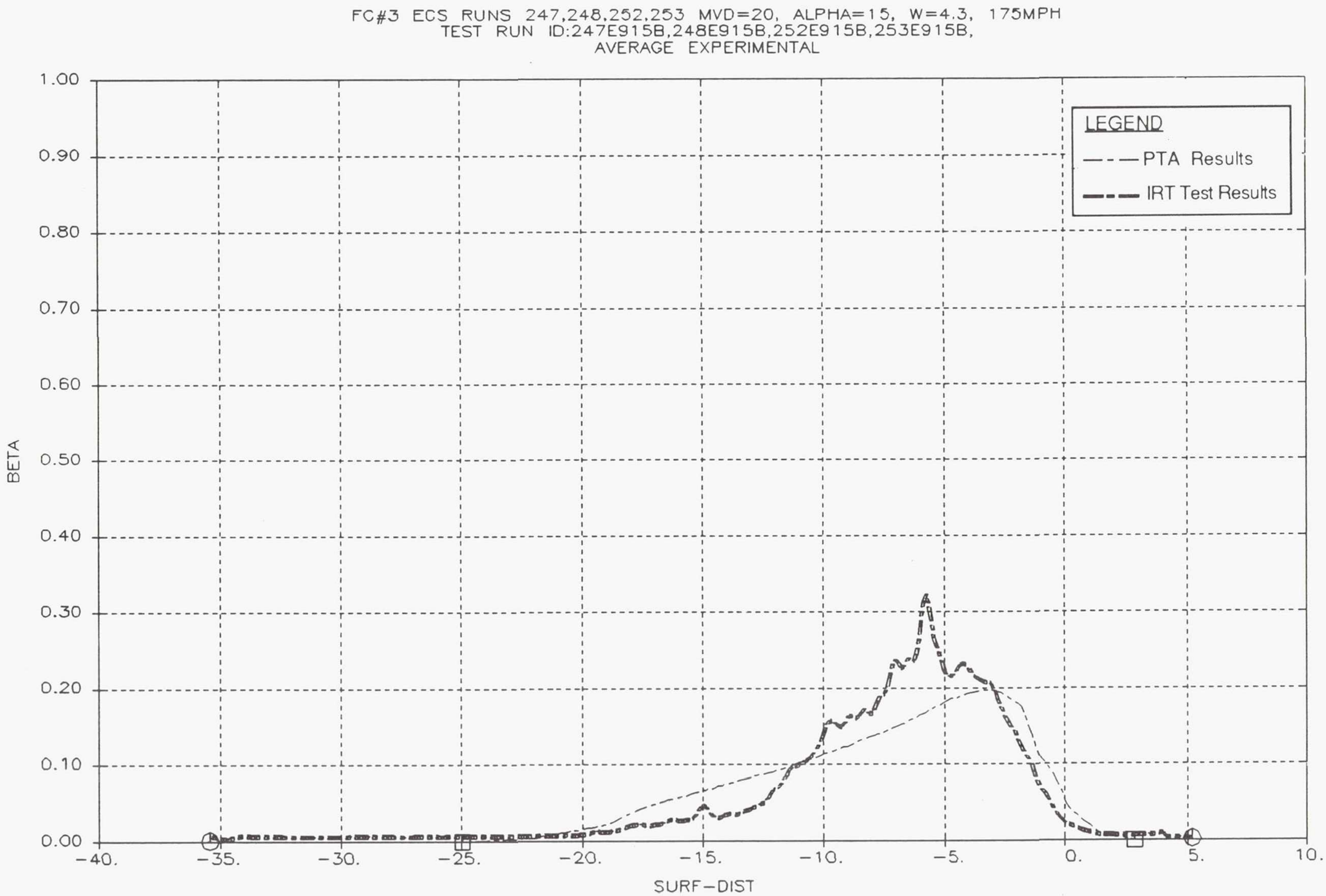

FIGURE 4.49

COMPOSITE ANALYSIS AND AVG TEST BETA RESULTS
--BETA(-) vs SURF-DIST(cm), FC3,Y=12U

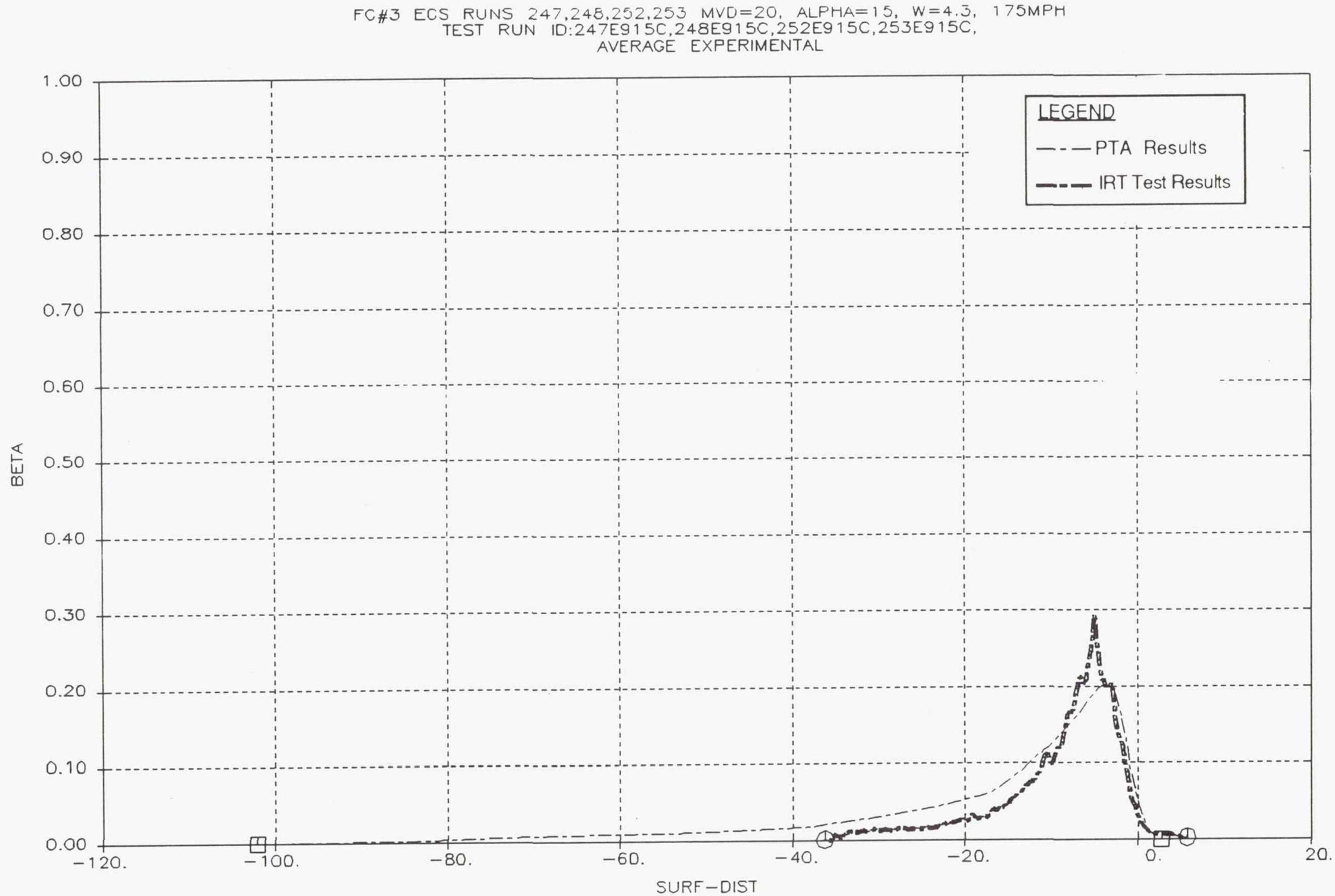

FIGURE 4.50

COMPOSITE ANALYSIS AND AVG TEST BETA RESULTS
--BETA(-) vs SURF-DIST(cm), FC3,Y=20

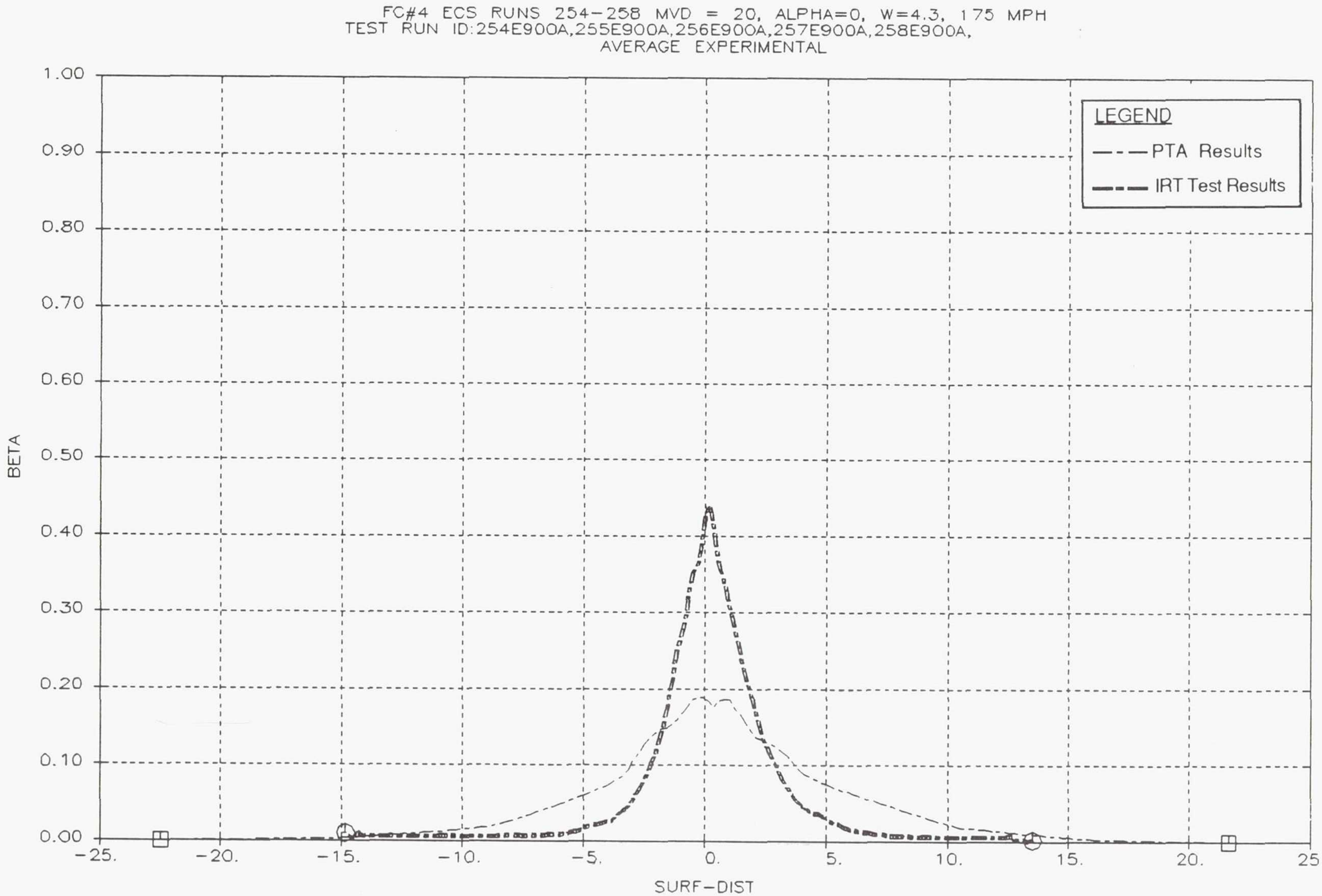

FIGURE 4.51

COMPOSITE ANALYSIS AND AVG TEST BETA RESULTS
—BETA(-) vs SURF-DIST(cm), FC4,Y=4

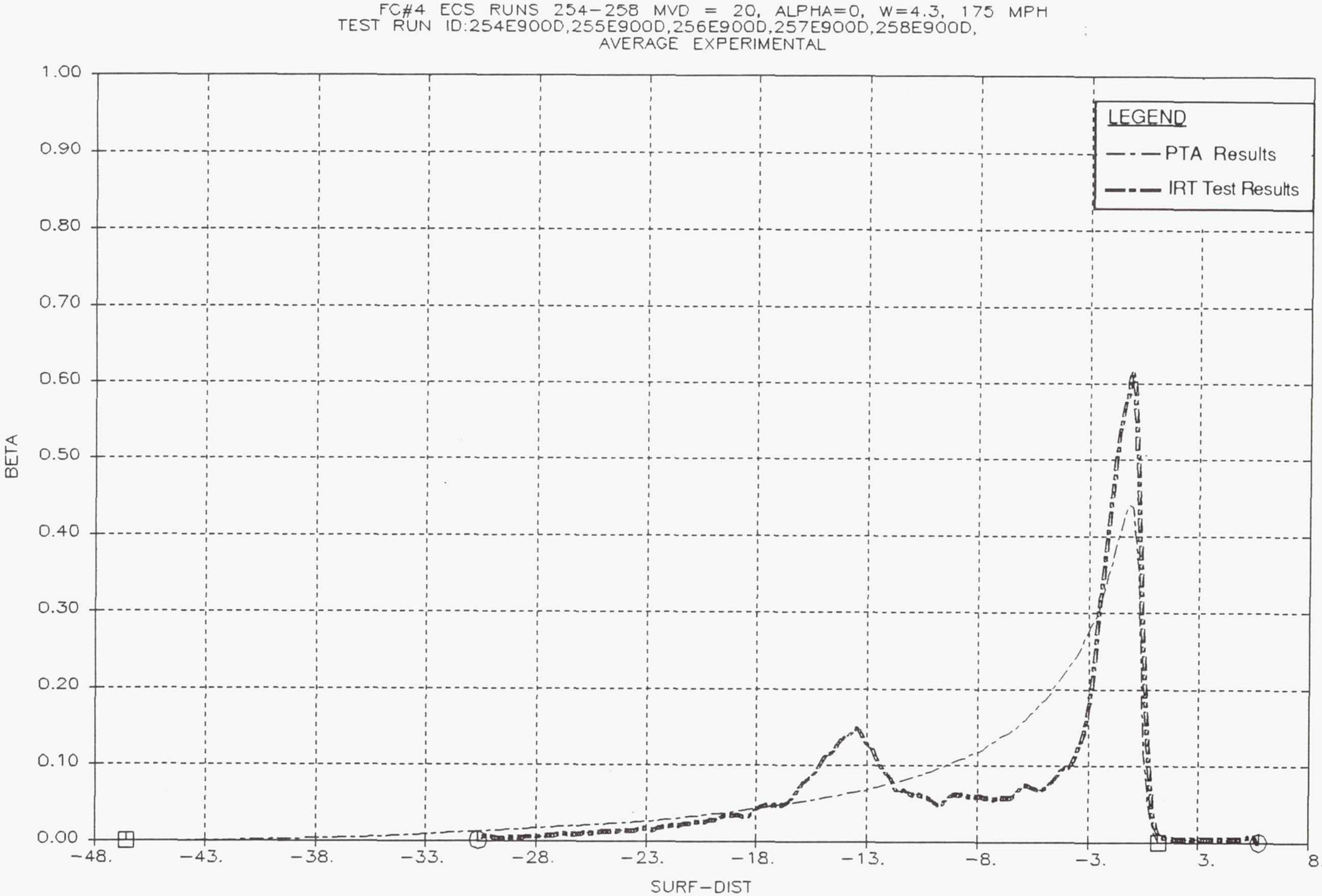

FIGURE 4.52

COMPOSITE ANALYSIS AND AVG TEST BETA RESULTS
—BETA(-) vs SURF-DIST(cm), FC4,Y=12L

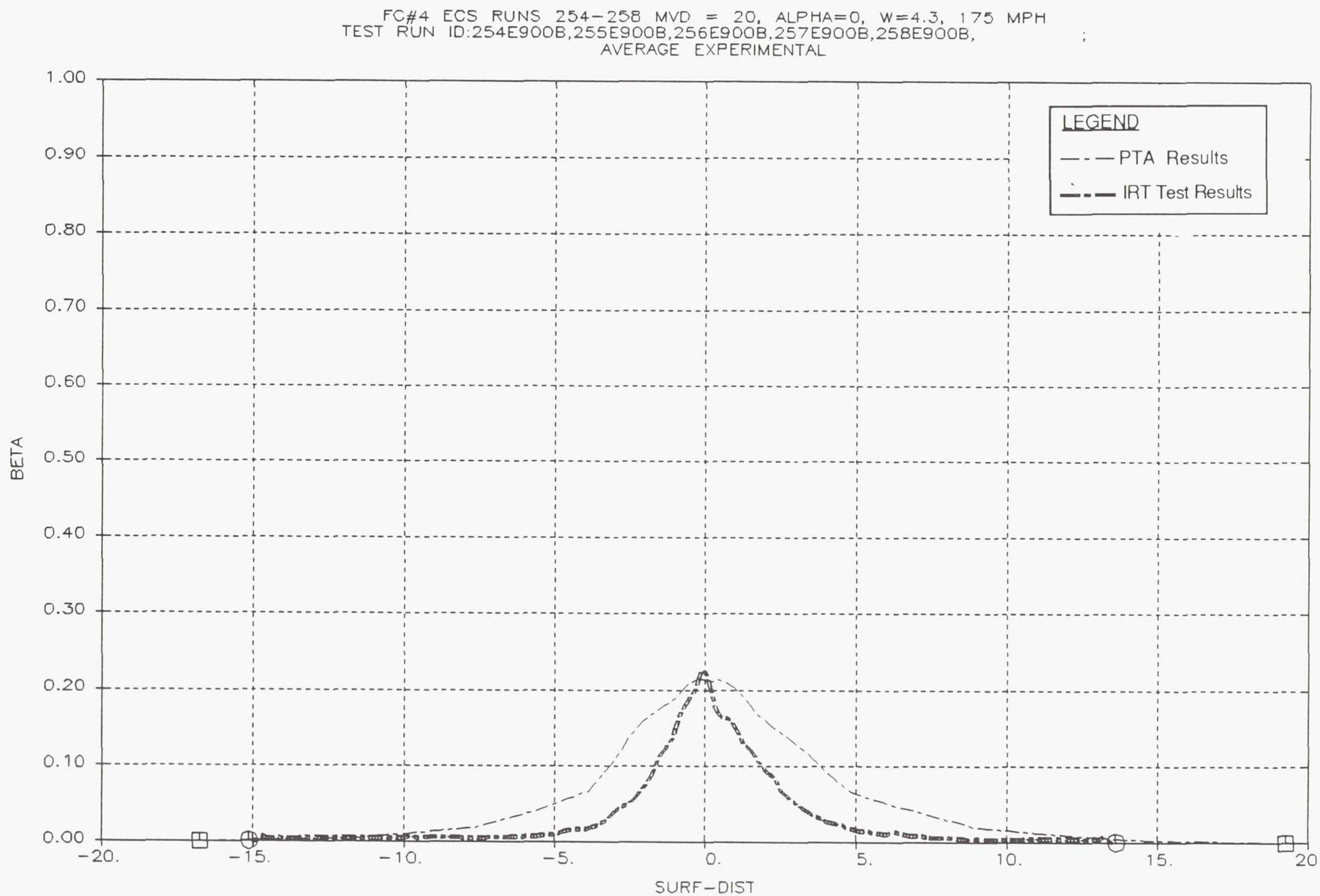

FIGURE 4.53

COMPOSITE ANALYSIS AND AVG TEST BETA RESULTS
—BETA(-) vs SURF-DIST(cm), FC4,Y=12U

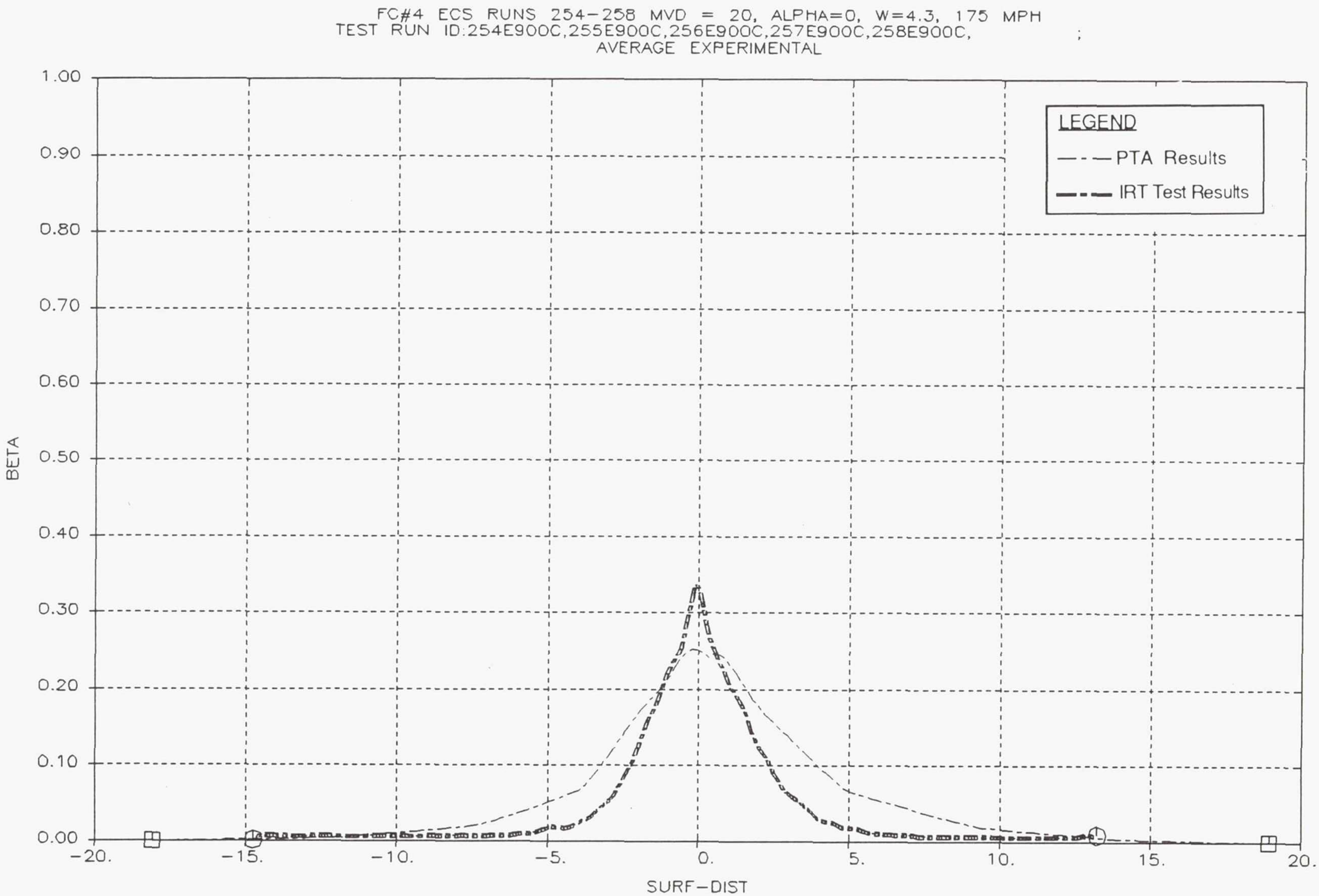

FIGURE 4.54

COMPOSITE ANALYSIS AND AVG TEST BETA RESULTS
--BETA(-) vs SURF-DIST(cm), FC4,Y=20

5.0 CONCLUDING REMARKS

Correlations between test data and the PTA predictions were generally good. However,various problems, as anticipated, were encountered during the course of this project. This is typical for computer codes which are in a development/verification stage rather than a production stage. Fixes and enhancements to the code, beyond the initial fix of the Least Squares correction described in Section 4.3.1.1, were not within the scope or timing of this project. Those items relating to computer code which still need improvements are as follows:

a. **Trajectory Crossings or Missing Intersections**

As discussed in Section 4.3.3, difficulties still exist for prediction of smaller drop sizes, particularly drop size 3. It is possible that the problems exhibited by the 13.5 micron drop size in this study could appear in other analyses with larger drops where the contribution to the composite droplet is larger and, and thus more adversely affects the overall results.

This flowfield velocity problem is, by no means, unique to the cartesian type flowfield of computer code P582 utilized in this study. It is probable that the "near geometry" flowfield velocities obtained from panel method codes are even more susceptible to erroneous results. In any case, it is imperative that accurate and smooth flowfield velocities be available for use in tracing particles as they pass within close proximity of geometry surfaces.

It is recommended that studies be conducted to further investigate and, if necessary, modify the 3-D PTA Least Squares generator and/or particle trajectory intersection routine.

b. **Computer Time Requirements on the NASA-Lewis Cray YMP**

During the present study, computer CPU time varied from a low of 250 seconds to a high of 3600 seconds for a single drop size at a given buttock line cut. The main controlling factors in CPU usage are:

1. Number of particles to be traced between two given tangent (i.e., upper and lower) trajectories

2. Spanwise closeness of projected water impingement field (i.e., Y separation between impinged particles as shown on Figure 4.33 and others).

3. The farfield (X=-498.0 in this study) X, Y, and Z starting coordinates for the particle traces.

In order to expedite the runs in this study, manual plots were constructed to more accurately determine the optimum particle starting coordinates. This manual optimization procedure was successfully used to obtain the 250 CPU second runs mentioned above. This significantly decreased computer turn around time since these runs could be performed during

the day on the NASA-Lewis Cray using the DEBUG Que as opposed to overnight processing.

It is further recommended that the manual methods described above be incorporated into the 3-D PTA computer code. This modification should reduce computer CPU usage by at least fifty percent over that of the present version.

APPENDIX A – ECS GEOMETRY NETWORKS

NNET	NMEM	NSEC	PTR1	PTR2	XMIN	XMAX	YMIN	YMAX	ZMIN	ZMAX	NDIR
1	25	6	1	120	0.00000	69.81300	0.00000	8.80000	-1.04700	5.12300	-1.
2	11	6	121	170	0.00000	19.27100	0.00000	9.52900	-2.03200	0.97300	-1.
3	9	6	171	210	6.69800	29.89600	0.00000	9.52900	-3.04400	-1.84200	-1.
4	7	6	211	240	18.70000	69.81300	0.00000	8.86200	-3.41400	-1.04700	-1.
5	25	8	241	408	10.48700	77.56000	8.80000	15.30000	-1.04700	5.12300	-1.
6	11	8	409	478	10.48700	24.57200	8.80000	15.33800	-2.03200	0.97300	-1.
7	7	8	479	520	29.89600	77.56000	8.80000	15.30000	-3.41400	-1.04700	-1.
8	25	6	521	640	18.23400	89.12000	15.30000	25.00000	-1.04700	5.12300	-1.
9	11	6	641	690	18.23400	36.49200	15.30000	25.00000	-1.84200	0.97300	-1.
10	9	6	691	730	24.57200	48.49300	14.67100	25.00000	-3.01700	-1.76900	-1.
11	7	6	731	760	35.19700	89.12000	14.67100	25.00000	-3.41400	-1.04700	-1.
12	9	18	761	896	24.57200	46.50000	13.16100	15.70000	-2.96300	3.03300	-1.
13	8	18	897	1015	19.06900	46.50000	9.52900	15.33800	-2.06800	3.58800	-1.
14	9	18	1016	1151	19.27100	46.50000	8.50000	10.83900	-3.04400	3.03300	-1.
15	8	18	1152	1270	29.83600	46.50000	8.86200	14.67100	-3.06600	-0.83200	-1.
16	25	7	1271	1414	29.79400	89.12000	25.00000	28.27000	-3.41400	5.12300	-1.

FIGURE A.1

SUMMARY OF RELEVANT PARAMETERS FOR ECS GEOMETRY PATCH DATA WITH TOTAL NUMBER OF NETWORKS IN GEOMETRY = 16

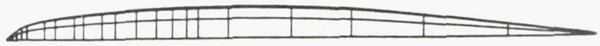

Wing Cap

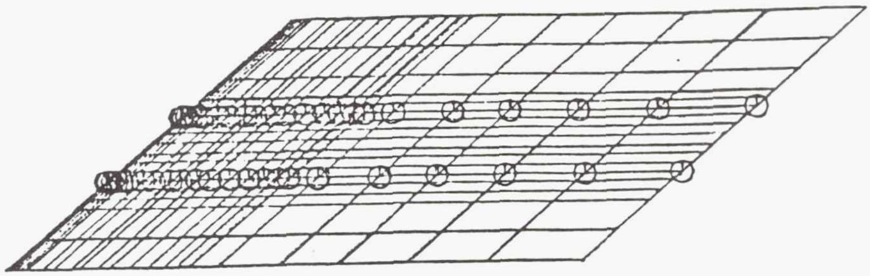

Top Of Wing

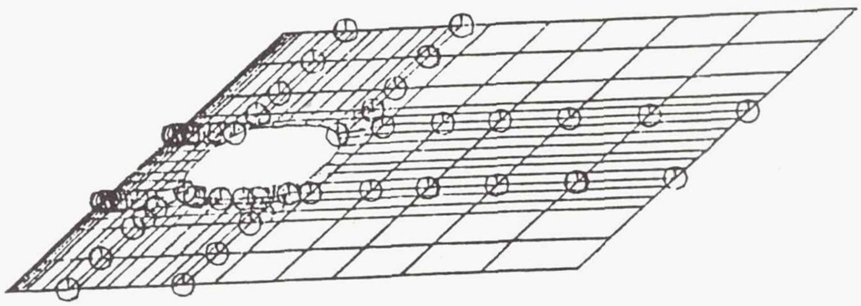

Bottom Of Wing

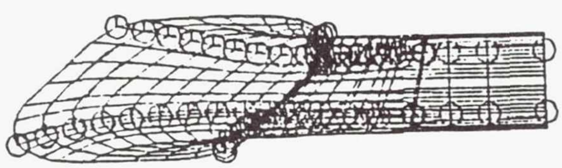

Inlet

FIGURE A.2

FOUR DIVISIONS OF ECS GEOMETRY

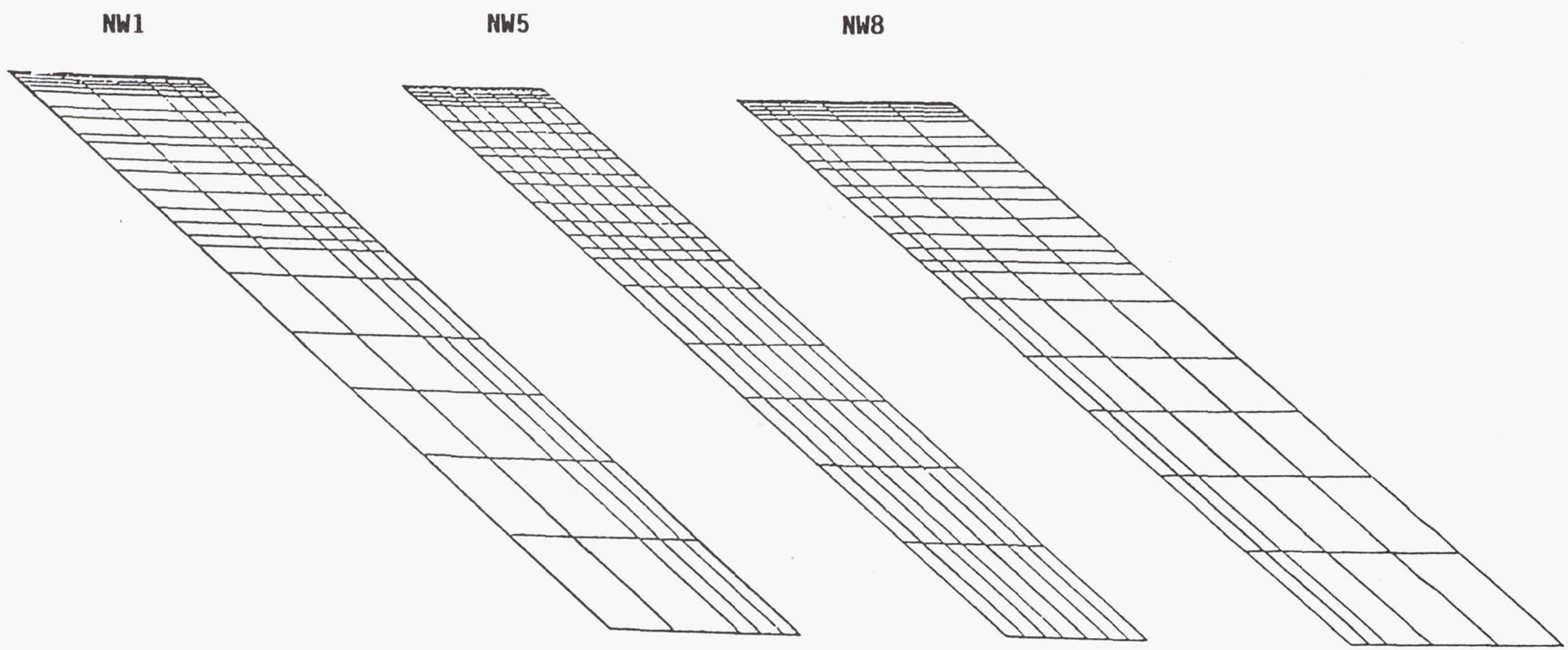

FIGURE A.3
NETWORKS THAT FORM TOP OF WING

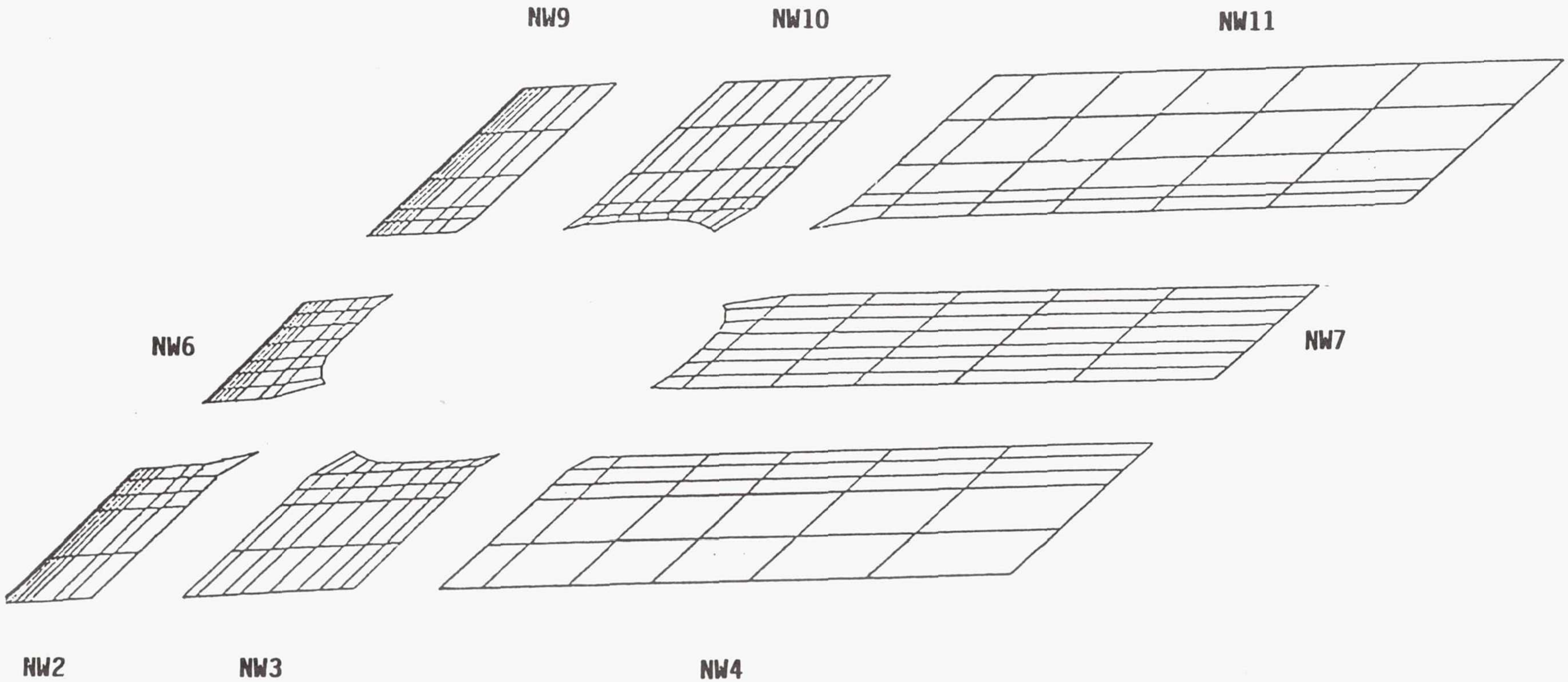

FIGURE A.4

NETWORKS THAT FORM BOTTOM OF WING

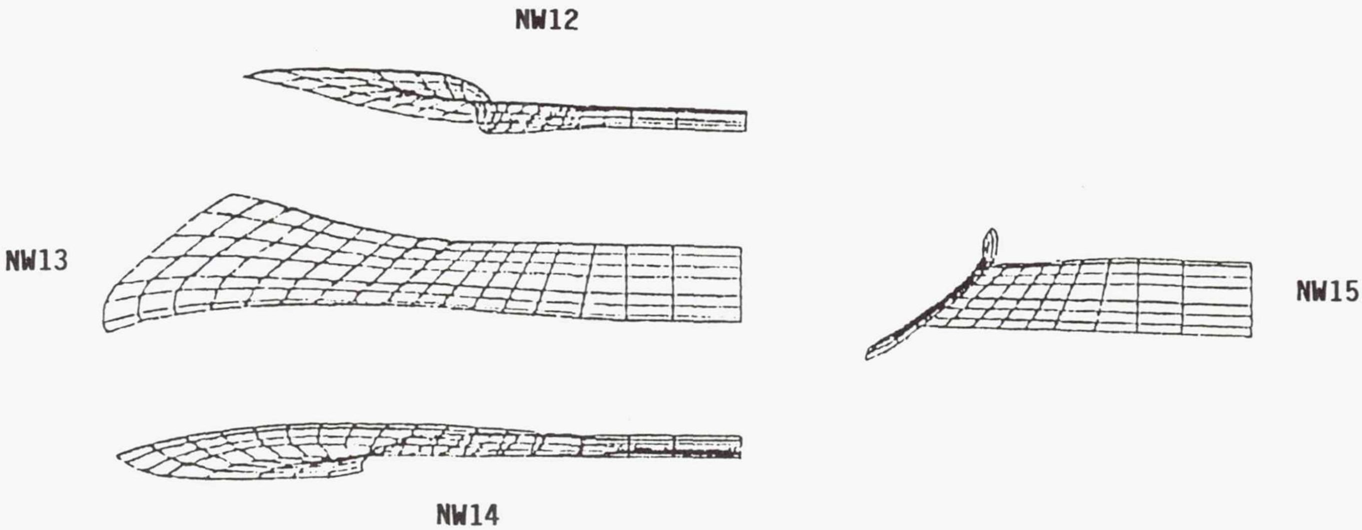

FIGURE A.5

NETWORKS THAT FORM INLET

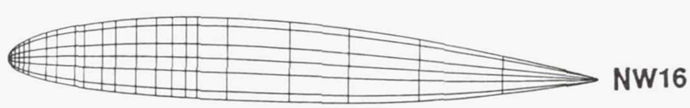

FIGURE A.6

END CAP NETWORK

APPENDIX B – TEST DATA LOG FROM ECS ICING RESEARCH TUNNEL TESTING

#22

☐ SPRAY UNIFORMITY TEST
■ REFERENCE COLLECTOR TEST

DATE: APRIL 21, 1989 (FRIDAY)

P_{BAR} = 14.375 PSIA

DYE CONCENTRATION = 0.0002 GRM/CC

PSYCHROMETER READINGS = ________ °F DB

= ________ °F WB

RELATIVE HUMIDITY = ________ PERCENT

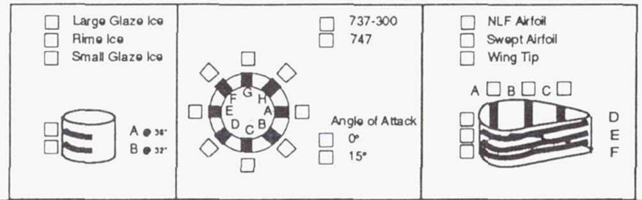

RUN NO.	RUN ID.	TUNNEL CONDITIONS: AIR TEMP (°F)	TAS (MPH)	P_∞ (PSIA)	PRESS TOTAL (PSIA)	DEW POINT (°F)	SPRAY CONDITIONS / MASS FLOW — SUPPLY PRESSURE: P_{AIR}/P_{H_2O}	P_{AIR} (PSIG)	P_{H_2O} (PSIG)	* PLENUM PRESSURE: P_{AIR} (PSIG)	P_{H_2O} (PSIG)	TRANSDUCER READINGS: TANK PRES-SURE	NOZZLE #1	NOZZLE #3	NOZZLE #4	NOZZLE #6	NOZZLE #7	NOZZLE #11	MASS FLOW: (VOLTS)	(LBS/SEC)	TIME (SEC): SPRAY (SEC.)	SPRAY TIME	REMARKS
191	CALIBRATION	–	165	13.882	–	20.0	0.65	65	100	65	106	106	114	103	104	103	101	60			3.52	8:26P	
192	CALIBRATION	47	165	13.885	–	22.0	0.65	65	100	65	106	106	117	103	104	103	101	60			4.00	8:33P	
193	ECS α=15 COL	49	175	13.847	14.334	14.5	0.65	65	100	65	106	106	106	104	103	103	101	60			2.65	9:25P	
194	ECS α=15 COL	51	175	13.853	14.334	24.0	0.65	65	100	65	106	106	105	103	104	102	101	60			2.65	9:37P	
195	ECS α=15 COL	51	175	13.858	14.334	33.4	0.65	65	100	65	106	106	107	103	104	102	101	60			2.66	9:47P	
196	ECS α=15 COL	52	175	13.860	14.334	37.3	0.65	65	100	65	106	106	110	103	104	102	101	60			2.66	9:55P	
197	ECS α=15 COL	53	175	13.862	14.346	37.3	0.65	65	100	65	106	105	115	103	104	102	101	60			2.65	10:05P	
198	ECS α=0 COL	53	175	13.861	14.334	35.3	0.65	65	100	65	106	106	116	103	104	102	101	60			2.64	10:17P	
199	ECS α=0 COL	54	175	13.866	14.334	35.2	0.65	65	100	65	106	106	115	103	104	102	101	60			2.65	10:26P	
200	ECS α=0 COL	54	175	13.865	14.334	33.9	0.65	65	100	65	106	106	115	103	104	102	101	60			2.66	10:34P	

COL = COLLECTOR

* PRESSURE GAUGES ON WATER TANK AND NOZZLE AIR REGULATOR

#23

DATE: APRIL 21, 1989 (FRIDAY)

P_{BAR} = ______ PSIA

DYE CONCENTRATION = 0.0002 GRM/CC

PSYCHROMETER READINGS = ______ °F DB

= ______ °F WB

RELATIVE HUMIDITY = ______ PERCENT

☐ SPRAY UNIFORMITY TEST
■ REFERENCE COLLECTOR TEST

☐ Large Glaze Ice
☐ Rime Ice
☐ Small Glaze Ice

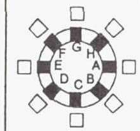

☐ 737-300
☐ 747

Angle of Attack
☐ 0°
☐ 15°

☐ NLF Airfoil
☐ Swept Airfoil
☐ Wing Tip

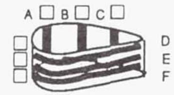

RUN NO.	RUN ID.	TUNNEL CONDITIONS: AIR TEMP (°F)	TAS (MPH)	P_∞ (PSIA)	PRESS TOTAL (PSIA)	DEW POINT (°F)	SPRAY CONDITIONS / MASS FLOW — SUPPLY PRESSURE: $\frac{P_{AIR}}{P_{H_2O}}$	P_{AIR} (PSIG)	P_{H_2O} (PSIG)	* PLENUM PRESSURE: P_{AIR} (PSIG)	P_{H_2O} (PSIG)	TRANSDUCER READINGS: TANK PRES-SURE	NOZZLE #1	NOZZLE #3	NOZZLE #4	NOZZLE #6	NOZZLE #7	NOZZLE #11	MASS FLOW: (VOLTS)	$\left(\frac{LBS}{SEC}\right)$	TIME (SEC): SPRAY (SEC.)	SPRAY TIME	REMARKS
201	ECS α=0 COL	54	175	13.870	14.334	33.2	0.65	65	100	65	106	106	115	103	104	102	101	60			2.66	10:42P	
202	ECS α=0 COL	54	175	13.873	14.334	32.0	0.65	65	100	65	106	106	114	103	104	102	101	60			2.65	10:50P	
203	ECS α=0 COL	55	210	13.630	14.346	32.0	0.65	65	100	65	106	106	114	103	104	103	101	60			2.65	10:59P	
204	ECS α=0 COL	56	210	13.634	14.234	31.5	0.65	65	100	65	106	106	115	103	104	102	101	60			2.65	11:08P	LAST RUN: BIG COLLECTOR BLADE CAME LOOSE

COL = COLLECTOR

* PRESSURE GAUGES ON WATER TANK AND NOZZLE AIR REGULATOR

#24

☐ SPRAY UNIFORMITY TEST
■ REFERENCE COLLECTOR TEST

DATE: APRIL 24, 1989 (MONDAY)

P_{BAR} = 14.341 PSIA

DYE CONCENTRATION = 0.0002 GRM/CC

PSYCHROMETER READINGS = ______ °F DB

= ______ °F WB

RELATIVE HUMIDITY = ______ PERCENT

☐ Large Glaze Ice
☐ Rime Ice
☐ Small Glaze Ice

☐ 737-300
☐ 747

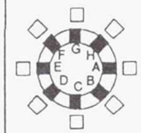

Angle of Attack
☐ 0°
☐ 15°

☐ NLF Airfoil
☐ Swept Airfoil
☐ Wing Tip

A ☐ B ☐ C ☐

		TUNNEL CONDITIONS					SPRAY CONDITIONS / MASS FLOW																REMARKS
							SUPPLY PRESSURE			* PLENUM PRESSURE		TRANSDUCER READINGS							MASS FLOW		TIME (SEC)		
RUN NO.	RUN ID.	AIR TEMP (°F)	TAS (MPH)	P_∞ (PSIA)	PRESS TOTAL (PSIA)	DEW POINT (°F)	$\frac{P_{AIR}}{P_{H_2O}}$	P_{AIR} (PSIG)	P_{H_2O} (PSIG)	P_{AIR} (PSIG)	P_{H_2O} (PSIG)	TANK PRES-SURE	NOZZLE #1	NOZZLE #3	NOZZLE #4	NOZZLE #6	NOZZLE #7	NOZZLE #11	(VOLTS)	$\left(\frac{LBS}{SEC}\right)$	SPRAY (SEC.)	SPRAY TIME	
205	ECS α=0 COL	46	215	13.537	14.285	21.4	0.65	65	100	65	106	106	124	103	105	103	102	60			2.65	5:36P	
206	ECS α=0 COL	42	215	13.543	14.285	12.0	0.65	65	100	65	106	106	117	103	104	103	101	59			2.66	6:13P	BLADE BROKE BETWEEN RUN 205 AND RUN 206
207	ECS α=0 COL	45	215	14.536	14.273	9.9	0.65	65	100	65	106	105	112	102	103	102	100	58			2.65	6:25P	
208	ECS α=0 COL	45	215	13.545	14.285	15.6	0.65	65	100	65	106	105	109	102	103	102	100	59			2.64	6:37P	
209	ECS α=0 COL	44	215	13.540	14.285	13.8	0.65	65	100	65	106	105	107	102	104	102	100	58			2.64	647P	
210	ECS α=0 COL	45	227	13.444	14.285	13.8	0.65	65	100	65	106	105	106	102	103	102	100	58			2.65	6:58P	
211	ECS α=0 COL	45	227	13.450	14.273	14.2	0.65	65	100	65	106	105	108	102	103	102	100	58			2.66	7:09P	
212	ECS α=0 COL	45	227	13.454	14.285	13.5	0.65	65	100	65	106	105	109	102	103	102	100	58			2.65	7:19P	
213	ECS α=0 COL	44	227	13.449	14.273	12.9	0.65	65	100	65	106	105	113	102	103	102	100	58			2.66	7:29P	
214	ECS α=0 COL	44	227	13.452	14.285	13.3	0.65	65	100	65	106	105	117	102	103	102	100	–			2.66	7:39P	

COL = COLLECTOR

* PRESSURE GAUGES ON WATER TANK AND NOZZLE AIR REGULATOR

#25

DATE: APRIL 25, 1989 (TUESDAY)

P_{BAR} = 14.265 PSIA

DYE CONCENTRATION = 0.0002 GRM/CC

PSYCHROMETER READINGS = ______ °F DB

= ______ °F WB

RELATIVE HUMIDITY = ______ PERCENT

☐ SPRAY UNIFORMITY TEST
☐ REFERENCE COLLECTOR TEST

☐ Large Glaze Ice
☐ Rime Ice
☐ Small Glaze Ice

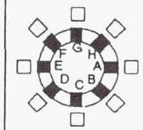

☐ 737-300
☐ 747

Angle of Attack
☐ 0°
☐ 15°

■ NLF Airfoil
☐ Swept Airfoil
☐ Wing Tip

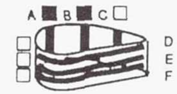

		TUNNEL CONDITIONS					SPRAY CONDITIONS / MASS FLOW																REMARKS
							SUPPLY PRESSURE			* PLENUM PRESSURE		TRANSDUCER READINGS							MASS FLOW		TIME (SEC)		
RUN NO.	RUN ID.	AIR TEMP (°F)	TAS (MPH)	P_∞ (PSIA)	PRESS TOTAL (PSIA)	DEW POINT (°F)	$\frac{P_{AIR}}{P_{H_2O}}$	P_{AIR} (PSIG)	P_{H_2O} (PSIG)	P_{AIR} (PSIG)	P_{H_2O} (PSIG)	TANK PRES-SURE	NOZZLE #1	NOZZLE #3	NOZZLE #4	NOZZLE #6	NOZZLE #7	NOZZLE #11	(VOLTS)	$\left(\frac{LBS}{SEC}\right)$	SPRAY (SEC.)	SPRAY TIME	
215	NLF α=8	49	165	13.801	14.188	34.3	0.65	65	100	65	106	106	120	104	105	104	102	60			2.67	4:52P	
216	NLF α=8	45	165	13.797	14.188	32.8	0.65	65	100	65	106	106	122	104	105	104	102	60			2.67	502P	
217	NLF α=8	37	80	13.797	14.188	21.5	0.65	65	100	65	106	106	121	103	104	103	101	58			2.66	5:21P	
218	NLF α=8	40	165	13.797	14.188	17.5	0.65	65	100	65	106	106	117	103	104	103	101	58			2.67	5:29P	
219	NLF α=8	43	165	13.800	14.188	19.5	0.65	65	100	65	106	106	112	103	104	103	101	58			2.67	5:39P	
220	NLF α=0	39	165	13.780	14.188	19.1	0.65	65	100	65	106	105	104	102	103	102	100	58			2.67	5:51P	
221	NLF α=0	40	165	13.786	14.188	17.4	0.65	65	100	65	106	105	95	102	103	102	100	58			2.67	5:59P	
222	NLF α=0	34	165	13.782	14.188	17.3	0.65	65	100	65	106	105	86	101	103	102	100	60			2.66	6:15P	STRIP LOOKS DIFFERENT THAN 220 AND 221
223	NLF α=0	39	165	13.784	14.188	15.9	0.65	65	100	65	106	105	85	102	103	102	100	59			2.66	6:23P	
224	NLF α=0	43	165	13.787	14.200	16.8	0.65	65	100	65	106	104	86	101	103	101	100	59			2.66	6:32P	

* PRESSURE GAUGES ON WATER TANK AND NOZZLE AIR REGULATOR

#26

DATE: APRIL 25, 1989 (TUESDAY)

P_{BAR} = 14.265 PSIA

DYE CONCENTRATION = 0.0002 GRM/CC

PSYCHROMETER READINGS = ________ °F DB

= ________ °F WB

RELATIVE HUMIDITY = ________ PERCENT

☐ SPRAY UNIFORMITY TEST
☐ REFERENCE COLLECTOR TEST

☐ Large Glaze Ice
☐ Rime Ice
☐ Small Glaze Ice

☐ A ● 38"
☐ B ● 32"

☐ 737-300
☐ 747

Angle of Attack
☐ 0°
☐ 15°

■ NLF Airfoil
☐ Swept Airfoil
☐ Wing Tip

A ■ B ■ C ☐

☐ D
☐ E
☐ F

		TUNNEL CONDITIONS					SPRAY CONDITIONS / MASS FLOW: SUPPLY PRESSURE			* PLENUM PRESSURE		TRANSDUCER READINGS							MASS FLOW		TIME (SEC)		REMARKS
RUN NO.	RUN ID.	AIR TEMP (°F)	TAS (MPH)	P_∞ (PSIA)	PRESS TOTAL (PSIA)	DEW POINT (°F)	$\frac{P_{AIR}}{P_{H_2O}}$	P_{AIR} (PSIG)	P_{H_2O} (PSIG)	P_{AIR} (PSIG)	P_{H_2O} (PSIG)	TANK PRES-SURE	NOZZLE #1	NOZZLE #3	NOZZLE #4	NOZZLE #6	NOZZLE #7	NOZZLE #11	(VOLTS)	$\left(\frac{LBS}{SEC}\right)$	SPRAY (SEC.)	SPRAY TIME	
225	NLF α=0	47	165	13.790	14.188	20.6	0.65	65	100	65	106	105	90	103	104	102	100	59			2.67	6:42P	
226	NLF α=0	49	165	13.797	14.200	24.1	0.80	80	100	80	106	105	95	103	104	102	101	73			4.53	6:52P	
227	NLF α=0	51	165	13.798	14.200	28.1	0.80	80	100	80	106	106	98	104	105	103	101	73			4.53	6:59P	
228	NLF α=0	52	165	13.801	14.200	30.9	0.80	80	100	80	106	106	99	104	105	103	101	73			4.54	7:05P	
229	NLF α=0	53	165	13.801	14.200	33.7	0.80	80	100	80	106	106	103	104	105	103	101	73			4.53	7:11P	
230	NLF α=0	54	165	13.800	14.200	36.1	0.80	80	100	80	106	106	109	104	105	103	101	74			4.53	7:18P	
231	NLF α=8	54	165	13.803	14.188	40.2	0.80	80	100	80	106	105	117	104	105	103	101	73			4.53	7:33P	STRIP B BROKE / AIR 73 → 75 (WHILE SPRAYING)
232	NLF α=8	55	165	13.809	14.200	41.9	0.80	80	100	80	106	105	115	104	105	103	101	73			4.54	7:40P	AIR 73 → 75 (WHILE SPRAYING)
233	NLF α=8	56	165	13.808	14.188	43.3	0.80	80	100	80	106	105	116	104	105	103	101	73			4.53	7:48P	
234	NLF α=8	57	165	13.809	14.188	44.6	0.80	80	100	80	106	105	116	104	105	103	101	73			4.53	7:55P	

* PRESSURE GAUGES ON WATER TANK AND NOZZLE AIR REGULATOR

#27

DATE: APRIL 25, 1989 (TUESDAY)

P_{BAR} = 14.265 PSIA

DYE CONCENTRATION = 0.0002 GRM/CC

PSYCHROMETER READINGS = ________ °F DB

= ________ °F WB

RELATIVE HUMIDITY = ________ PERCENT

☐ SPRAY UNIFORMITY TEST
☐ REFERENCE COLLECTOR TEST

☐ Large Glaze Ice
☐ Rime Ice
☐ Small Glaze Ice

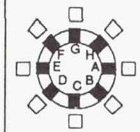

☐ 737-300
☐ 747

Angle of Attack
☐ 0°
☐ 15°

■ NLF Airfoil
☐ Swept Airfoil
☐ Wing Tip

A ■ B ■ C ☐

		TUNNEL CONDITIONS					SPRAY CONDITIONS / MASS FLOW: SUPPLY PRESSURE			* PLENUM PRESSURE		TRANSDUCER READINGS							MASS FLOW		TIME (SEC)		REMARKS
RUN NO.	RUN ID.	AIR TEMP (°F)	TAS (MPH)	P_∞ (PSIA)	PRESS TOTAL (PSIA)	DEW POINT (°F)	P_{AIR}/P_{H_2O}	P_{AIR} (PSIG)	P_{H_2O} (PSIG)	P_{AIR} (PSIG)	P_{H_2O} (PSIG)	TANK PRES-SURE	NOZZLE #1	NOZZLE #3	NOZZLE #4	NOZZLE #6	NOZZLE #7	NOZZLE #11	(VOLTS)	(LBS/SEC)	SPRAY (SEC.)	SPRAY TIME	
235	NLF α=8	57	165	13.813	14.188	45.8	0.80	80	100	80	106	106	114	104	105	103	102	71			4.53	8:03P	AIR 71 → 74 (WHILE SPRAYING)
236	NLF α=8	58	165	13.809	14.188	46.8	0.80	80	100	80	106	106	114	104	105	103	102	73			4.53	8:09P	AIR 73 → 76 (WHILE SPRAYING)

* PRESSURE GAUGES ON WATER TANK AND NOZZLE AIR REGULATOR

#28

☐ SPRAY UNIFORMITY TEST
☐ REFERENCE COLLECTOR TEST

DATE: MAY 3, 1989 (WEDNESDAY)

P_{BAR} = 14.368 PSIA

DYE CONCENTRATION = 0.0002 GRM/CC

PSYCHROMETER READINGS = ______ °F DB

= ______ °F WB

RELATIVE HUMIDITY = ______ PERCENT

☐ Large Glaze Ice
☐ Rime Ice
☐ Small Glaze Ice

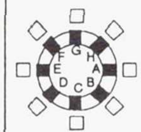

☐ 737-300
■ 747

Angle of Attack
■ 0°
☐ 15°

☐ NLF Airfoil
☐ Swept Airfoil
☐ Wing Tip

A ☐ B ☐ C ☐

		TUNNEL CONDITIONS					SPRAY CONDITIONS / MASS FLOW: SUPPLY PRESSURE			* PLENUM PRESSURE		TRANSDUCER READINGS							MASS FLOW		TIME (SEC)		REMARKS
RUN NO.	RUN ID.	AIR TEMP (°F)	TAS (MPH)	P_∞ (PSIA)	PRESS TOTAL (PSIA)	DEW POINT (°F)	$\frac{P_{AIR}}{P_{H_2O}}$	P_{AIR} (PSIG)	P_{H_2O} (PSIG)	P_{AIR} (PSIG)	P_{H_2O} (PSIG)	TANK PRES-SURE	NOZZLE #1	NOZZLE #3	NOZZLE #4	NOZZLE #6	NOZZLE #7	NOZZLE #11	(VOLTS)	$\left(\frac{LBS}{SEC}\right)$	SPRAY (SEC.)	SPRAY TIME	
237	ECS α=0	52	175	13.752	14.261	29.7	0.65	65	100	65	106	106	103	103	104	102	99	60	0.41	3.0	2.66	9:19P	
238	ECS α=0	45	175	13.752	14.273	27.5	0.65	65	100	65	106	106	103	103	104	102	101	59	0.42	3.0	2.67	9:44P	
239	ECS α=0	47	175	13.756	14.273	22.9	0.65	65	100	65	106	105	102	102	103	101	100	58	0.41	3.0	2.66	10:05P	PHOTOS BY COLIN B.
240	ECS α=0	44	175	13.756	14.273	18.1	0.65	65	100	65	106	105	102	102	103	102	100	58	0.42	3.0	2.66	10:42P	
241	ECS α=0	49	175	13.763	14.273	15.5	0.65	65	100	65	106	105	102	102	103	101	99	58	-	3.0	2.66	11:00P	

* PRESSURE GAUGES ON WATER TANK AND NOZZLE AIR REGULATOR

#29

☐ SPRAY UNIFORMITY TEST
☐ REFERENCE COLLECTOR TEST

DATE: MAY 4, 1989 (THURSDAY)

P_{BAR} = ______ PSIA

DYE CONCENTRATION = 0.0002 GRM/CC

PSYCHROMETER READINGS = ______ °F DB

= ______ °F WB

RELATIVE HUMIDITY = ______ PERCENT

☐ Large Glaze Ice
☐ Rime Ice
☐ Small Glaze Ice

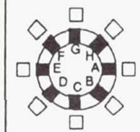

☐ 737-300
■ 747

Angle of Attack
■ 0°
☐ 15°

☐ NLF Airfoil
☐ Swept Airfoil
☐ Wing Tip

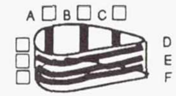

		TUNNEL CONDITIONS					SPRAY CONDITIONS / MASS FLOW: SUPPLY PRESSURE			* PLENUM PRESSURE		TRANSDUCER READINGS							MASS FLOW		TIME (SEC)		REMARKS
RUN NO.	RUN ID.	AIR TEMP (°F)	TAS (MPH)	P_∞ (PSIA)	PRESS TOTAL (PSIA)	DEW POINT (°F)	$\frac{P_{AIR}}{P_{H_2O}}$	P_{AIR} (PSIG)	P_{H_2O} (PSIG)	P_{AIR} (PSIG)	P_{H_2O} (PSIG)	TANK PRES-SURE	NOZZLE #1	NOZZLE #3	NOZZLE #4	NOZZLE #6	NOZZLE #7	NOZZLE #11	(VOLTS)	$\left(\frac{LBS}{SEC}\right)$	SPRAY (SEC.)	SPRAY TIME	
242	ECS α=15	50	175	13.683	14.224	42.2	0.65	65	100	65	106	106	104	104	105	103	102	60	0.42	3.0	2.65	4:17P	
243	ECS α=15	37	175	13.659	14.200	35.4	0.65	65	100	65	106	106	103	102	104	102	101	59	0.44	3.0	2.66	4:36P	
244	ECS α=15	40	175	13.659	14.200	31.1	0.65	65	100	65	106	104	102	101	103	101	99	59	0.42	3.0	2.64	4:54P	
245	ECS α=15	45	175	13.660	14.200	28.6	0.65	65	100	65	106	104	102	102	103	101	100	58	0.42	3.0	2.65	5:10P	
246	ECS α=15	50	175	13.659	14.200	28.4	0.65	65	100	65	106	105	102	102	104	102	99	58	0.42	3.0	2.66	5:24P	
247	ECS α=15	44	175	13.648	14.200	27.4	0.65	65	100	65	106	105	102	102	104	102	99	58	0.56	4.3	2.65	5:40P	BCAD – PHOTOS
248	ECS α=15	41	175	13.643	14.188	25.3	0.65	65	100	65	106	105	102	102	103	102	100	57	0.56	4.3	2.65	5:56P	
249	ECS α=15	41	175	13.640	14.188	24.4	0.65	65	100	65	106	105	103	102	104	102	99	58	0.56	4.3	2.65	6:20P	NO GOOD → TOO LIGHT: PROBABLY FREEZE OUT
250	ECS α=15	43	175	13.640	14.188	23.5	0.65	65	100	65	106	105	102	102	104	102	99	58	0.56	4.3	2.64	6:33P	NO GOOD → TOO LIGHT: PROBABLY FREEZE OUT
251	ECS α=15	40	175	13.633	14.176	22.9	0.65	65	100	65	106	105	102	102	122	121	117	58	0.55	4.2	2.65	6:50P	NO GOOD →TOO LIGHT: LINES FROZE: NOT ALL NOZZLES WORKED

* PRESSURE GAUGES ON WATER TANK AND NOZZLE AIR REGULATOR

#30

☐ SPRAY UNIFORMITY TEST
☐ REFERENCE COLLECTOR TEST

DATE: MAY 4, 1989 (THURSDAY)

P_{BAR} = ____________ PSIA

DYE CONCENTRATION = 0.0002 GRM/CC

PSYCHROMETER READINGS = ____________ °F DB

= ________ °F WB

RELATIVE HUMIDITY = ________ PERCENT

☐ Large Glaze Ice
☐ Rime Ice
☐ Small Glaze Ice

☐ 737-300
■ 747

Angle of Attack
■ 0°
■ 15°

☐ NLF Airfoil
☐ Swept Airfoil
☐ Wing Tip

A ☐ B ☐ C ☐

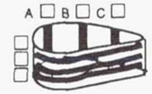

		TUNNEL CONDITIONS					SPRAY CONDITIONS / MASS FLOW: SUPPLY PRESSURE			* PLENUM PRESSURE		TRANSDUCER READINGS							MASS FLOW		TIME (SEC)		REMARKS
RUN NO.	RUN ID.	AIR TEMP (°F)	TAS (MPH)	P_∞ (PSIA)	PRESS TOTAL (PSIA)	DEW POINT (°F)	P_{AIR}/P_{H_2O}	P_{AIR} (PSIG)	P_{H_2O} (PSIG)	P_{AIR} (PSIG)	P_{H_2O} (PSIG)	TANK PRES-SURE	NOZZLE #1	NOZZLE #3	NOZZLE #4	NOZZLE #6	NOZZLE #7	NOZZLE #11	(VOLTS)	$\left(\frac{LBS}{SEC}\right)$	SPRAY (SEC.)	SPRAY TIME	
252	ECS α=15	54	175	13.654	14.176	41.2	0.65	65	100	65	106	106	103	104	105	103	101	60	.58	4.3	2.66	9:41P	
253	ECS α=15	54	175	13.653	14.176	37.5	0.65	65	100	65	106	105	102	103	104	102	101	59	.57	4.3	2.66	9:55P	
254	ECS α=0	54	175	13.664	14.176	31.6	0.65	65	100	65	106	105	103	103	104	102	101	59	.58	4.3	2.66	10:24P	
255	ECS α=0	54	175	13.663	14.163	28.4	0.65	65	100	65	106	106	103	103	104	102	101	59	.57	4.3	2.66	10:37P	
256	ECS α=0	53	175	13.660	14.163	28.7	0.65	65	100	65	106	106	103	103	105	103	101	59	.58	4.3	2.66	10:48P	
257	ECS α=0	53	175	13.662	14.163	28.8	0.65	65	100	65	106	105	103	103	104	102	101	59	.58	4.3	2.65	10:58P	
258	ECS α=0	54	175	13.660	14.163	27.5	0.65	65	100	65	106	105	103	103	104	102	101	59	.58	4.3	2.65	11:09P	
259	ECS α=0	60	227	13.242	14.127	27.0	0.65	65	100	65	106	106	103	103	105	103	101	59	.51	3.7	2.65	11:22P	
260	ECS α=0	51	227	13.237	14.127	28.4	0.65	65	100	65	106	106	103	103	104	102	101	59	.51	3.7	2.65	11:34P	
261	ECS α=0	54	227	13.239	14.127	29.0	0.65	65	00	65	106	106	103	103	105	103	101	59	.50	3.7	2.65	11:46P	

* PRESSURE GAUGES ON WATER TANK AND NOZZLE AIR REGULATOR

#31

☐ SPRAY UNIFORMITY TEST
☐ REFERENCE COLLECTOR TEST

DATE: MAY 4, 1989 (THURSDAY)

P_{BAR} = ________ PSIA

DYE CONCENTRATION = 0.0002 GRM/CC

PSYCHROMETER READINGS = ________ °F DB

= ________ °F WB

RELATIVE HUMIDITY = ________ PERCENT

☐ Large Glaze Ice
☐ Rime Ice
☐ Small Glaze Ice

☐ A ● 3"
☐ B ● 1"

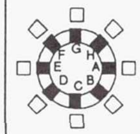

☐ 737-300
■ 747

Angle of Attack
■ 0°
☐ 15°

☐ NLF Airfoil
☐ Swept Airfoil
☐ Wing Tip

A ☐ B ☐ C ☐

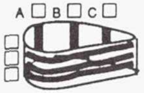

☐ D
☐ E
☐ F

		TUNNEL CONDITIONS					SPRAY CONDITIONS / MASS FLOW: SUPPLY PRESSURE			* PLENUM PRESSURE		TRANSDUCER READINGS							MASS FLOW		TIME (SEC)		REMARKS
RUN NO.	RUN ID.	AIR TEMP (°F)	TAS (MPH)	P_∞ (PSIA)	PRESS TOTAL (PSIA)	DEW POINT (°F)	P_{AIR}/P_{H_2O}	P_{AIR} (PSIG)	P_{H_2O} (PSIG)	P_{AIR} (PSIG)	P_{H_2O} (PSIG)	TANK PRES-SURE	NOZZLE #1	NOZZLE #3	NOZZLE #4	NOZZLE #6	NOZZLE #7	NOZZLE #11	(VOLTS)	$\left(\frac{LBS}{SEC}\right)$	SPRAY (SEC.)	SPRAY TIME	
262	ECS α=0	57	227	13.240	14.139	29.2	0.65	65	100	65	106	106	103	103	105	102	101	59	.50	3.7	2.65	11:58P	
263	ECS α=0	56	227	13.236	14.127	29.9	0.65	65	100	65	106	106	103	103	105	102	101	59	.50	3.7	2.65	12:11A	

* PRESSURE GAUGES ON WATER TANK AND NOZZLE AIR REGULATOR

APPENDIX C – REFERENCE COLLECTOR LOCATIONS AND REFERENCE COLLECTOR VALUES FROM ECS ICING RESEARCH TUNNEL TESTING

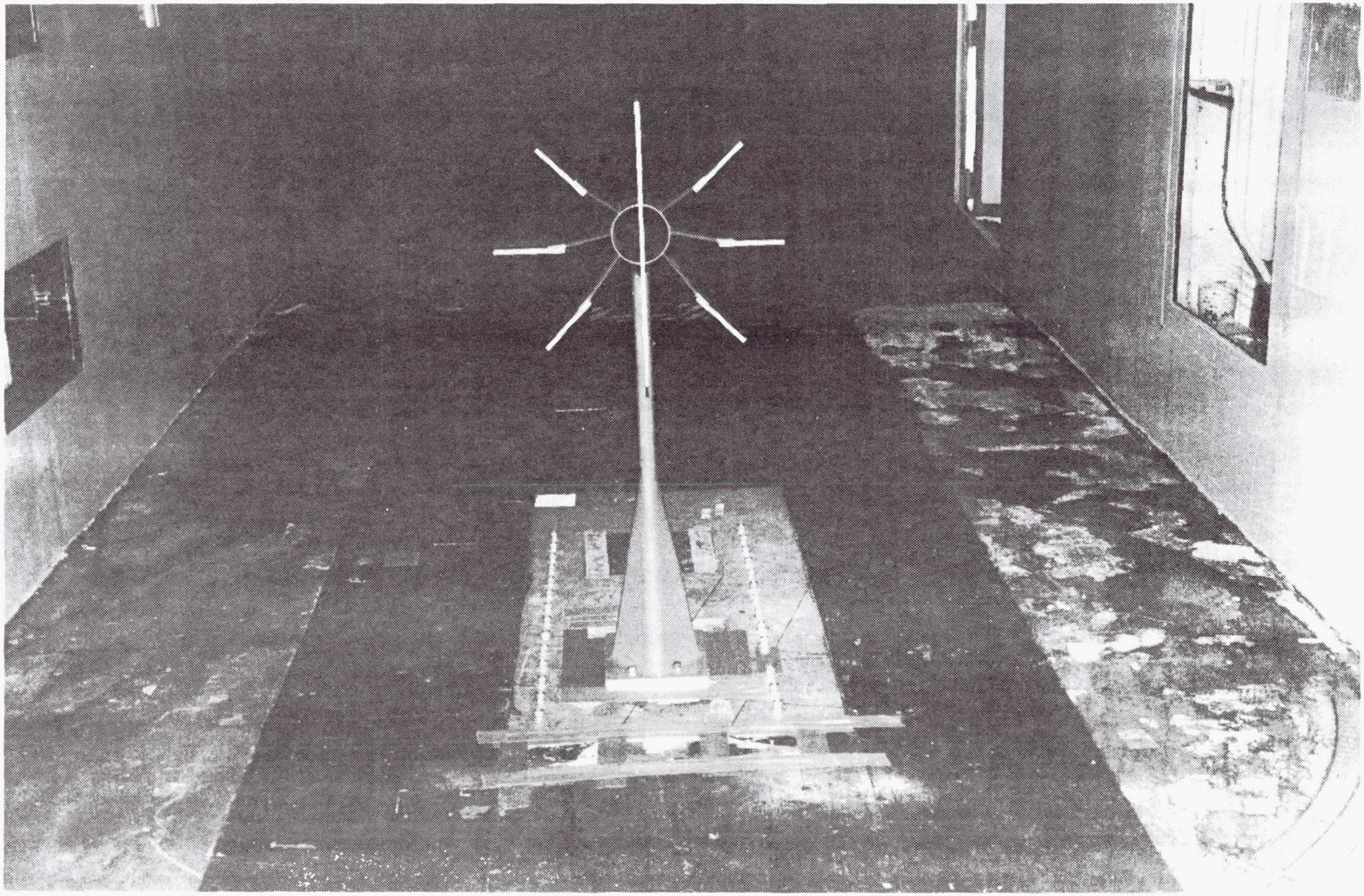

NOTE: CENTER BLADE WAS TURNED HORIZONTAL
FOR ECS INLET TESTING

FIGURE C.1

REFERENCE COLLECTOR MECHANISM USED IN ALL 1989 TESTS

FILE: ECS COLECTOR A1 10/01/91 11:19 WSU -- UCATC

AVERAGE	193	194	195	196	197		
46572	.46081	.47010	.46889	.46316	.46562	A	
.47512	.47167	.47067	.46841	.46371	.50116	B	
.48156	.48845	.49676	.49291	.47032	.45936	C	
.47565	.50411	.47423	.46683	.46758	.46549	D	alpha = 15
.48871	.48851	.47065	.51294	.49912	.47235	E	mvd = 20
.48963	.47930	.50643	.50115	.47921	.48206	F	175 mph
$\boxed{.47290}$	.46724	.47310	.46689	.46352	.49373	G	
.48100	.46561	.50619	.49085	.47294	.46939	H	
.41907	.41325	.41439	.43552	.42813	.40405	CENTER	

AVERAGE	198	199	200	201	202		
.47126	.46882	.4877[illegible]	.45852	.46130	.47991	A	
.48690	.50182	.498[illegible]	.46305	.48550	.48564	B	
$\boxed{.48766}$	.49203	.48970	.51383	.46245	.48029	C	
$\boxed{.47363}$	.48172	.45127	.46553	.48243	.48721	D	alpha = 0
$\boxed{.48196}$	.49484	.47243	.46679	.48794	.48780	E	mvd = 20
.47018	.47106	.50050	.45692	.46096	.46146	F	175 mph
$\boxed{.47321}$	.49658	.46494	.46531	.45561	.48360	G	
.49904	.48436	.51099	.48866	.50066	.51054	H	
$\boxed{.40845}$	.40659	.42624	.42198	.39213	.39529	CENTER	

AVERAGE	203	204		
.45422	.46844	.440	A	
.45876	.45688	.46065	B	
.47078	.45976	.48181	C	
.44396	.44284	.44507	D	alpha = 0
.46042	.47792	.44292	E	mvd = 20
.47499	.48317	.46681	F	210 mph
.47618	.48482	.46753	G	
.49437	.49455	.49420	H	
.40472	.39644	.413	CENTER	

AVERAGE	205	206	207	208	209		
.45146	.44046	.44626	.44182	.44986	.47888	A	
.46670	.45455	.45020	.48319	.48471	.46086	B	
.47193	.48626	.46262	.48677	.45781	.46620	C	
.46490	.47636	.44852	.45583	.45590	.48791	D	alpha = 0
.45724	.44221	.48610	.45723	.44981	.45087	E	mvd = 20
.46577	.45911	.47485	.46765	.45055	.47670	F	215 mph
.46378	.47169	.45447	.48299	.46306	.44668	G	
.47274	.45612	.47555	.48299	.46256	.48649	H	
.40574	.41311	.41939	.39723	.39735	.40160	CENTER	

AVERAGE	210	211	212	213	214		
.45952	.44695	.45096	.48017	.47226	.44726	A	
.46601	.46386	.45136	.47419	.46096	.47968	B	
.46472	.46825	.47857	.46459	.46133	.45085	C	
.46497	.45032	.48239	.45808	.47996	.45410	D	alpha = 0
.46877	.47647	.47822	.47057	.46156	.45702	E	mvd = 20
.45373	.44154	.47602	.45323	.44416	.45370	F	227 mph
.44923	.44695	.44502	.45107	.45031	.45279	G	
.47847	.48400	.46421	.48280	.47002	.49131	H	
.41336	.42138	.39494	.41744	.42973	.40332	CENTER	

NOTE: $\boxed{}$ Denotes Selected Values Shown On Figure C.5

NOTE: ECS-204A AND 204-CENT STRIPS MISSING. 9/19/91.

FIGURE C.2

REFERENCE COLLECTOR DYE MASS ($\mu g/cm^2$) AS FUNCTION OF RUN NUMBER AND REFERENCE COLLECTOR POSITION

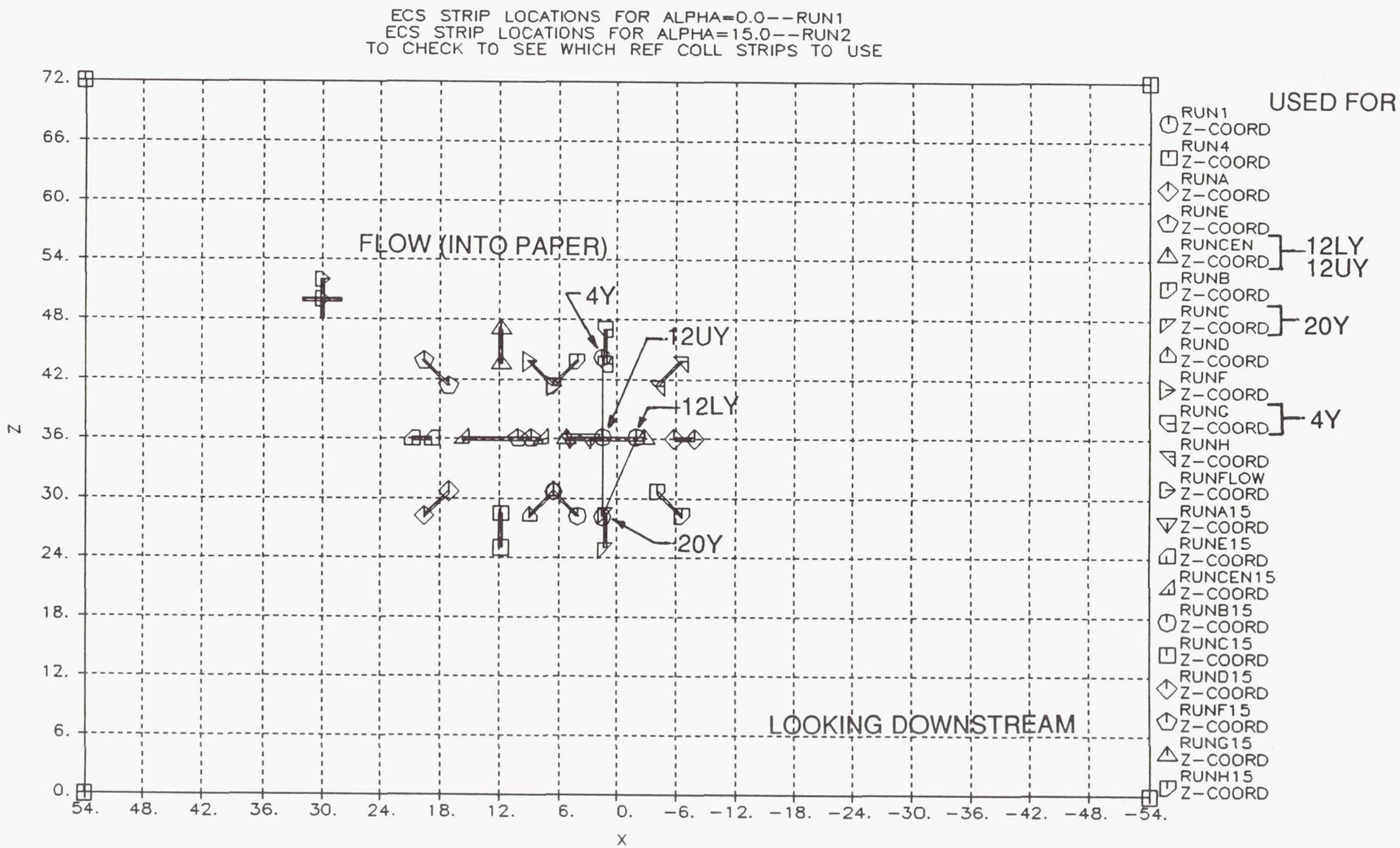

FIGURE C.3 (Page 1 of 3)

REFERENCE COLLECTION ALPHA=0 AND ALPHA=15 POSITION IN TUNNEL
RELATIVE TO ECS GEOMETRY ALPHA=0

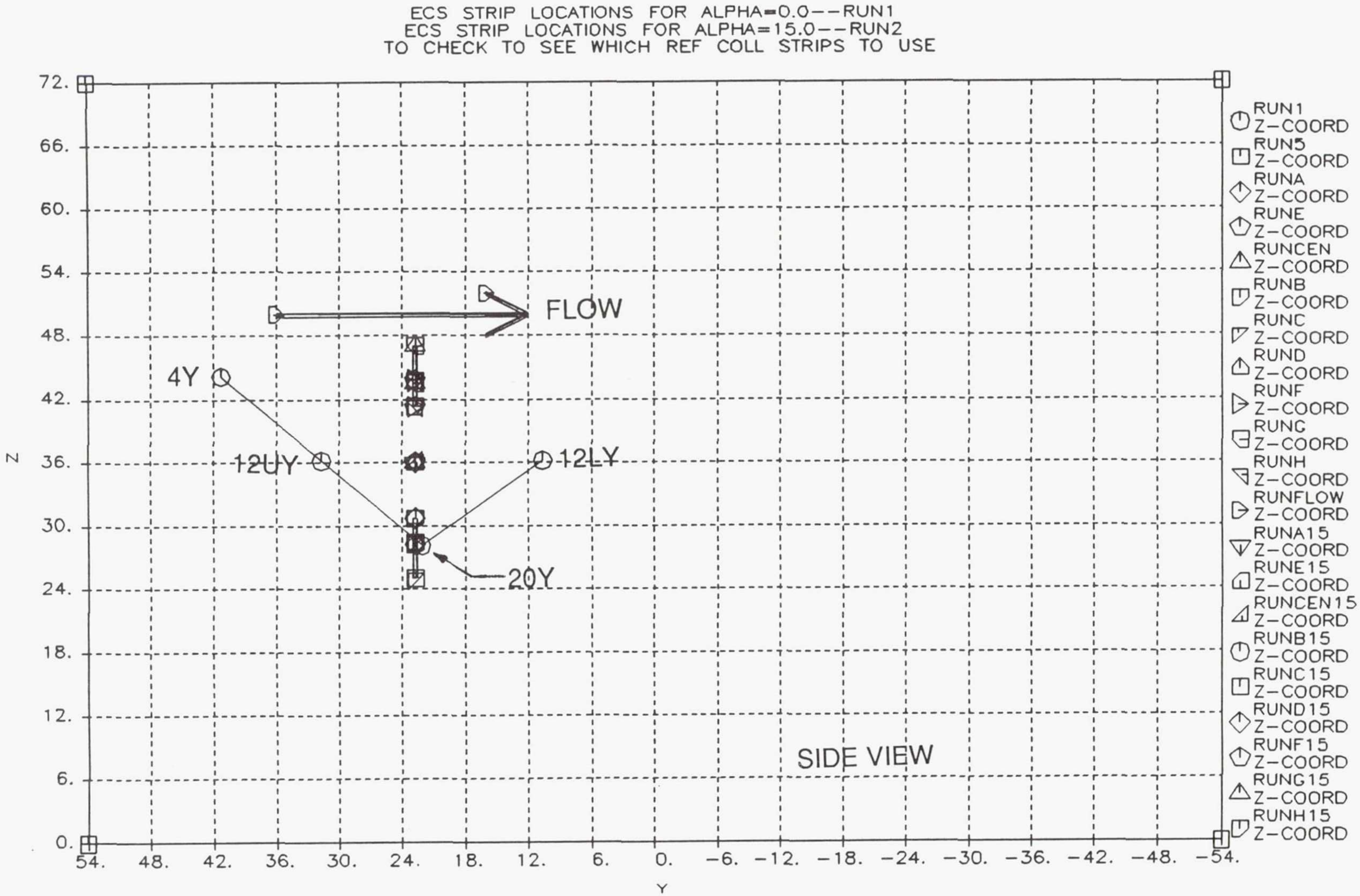

FIGURE C.3 (Page 2 of 3)

REFERENCE COLLECTION ALPHA=0 AND ALPHA=15 POSITION IN TUNNEL RELATIVE TO ECS GEOMETRY ALPHA=0

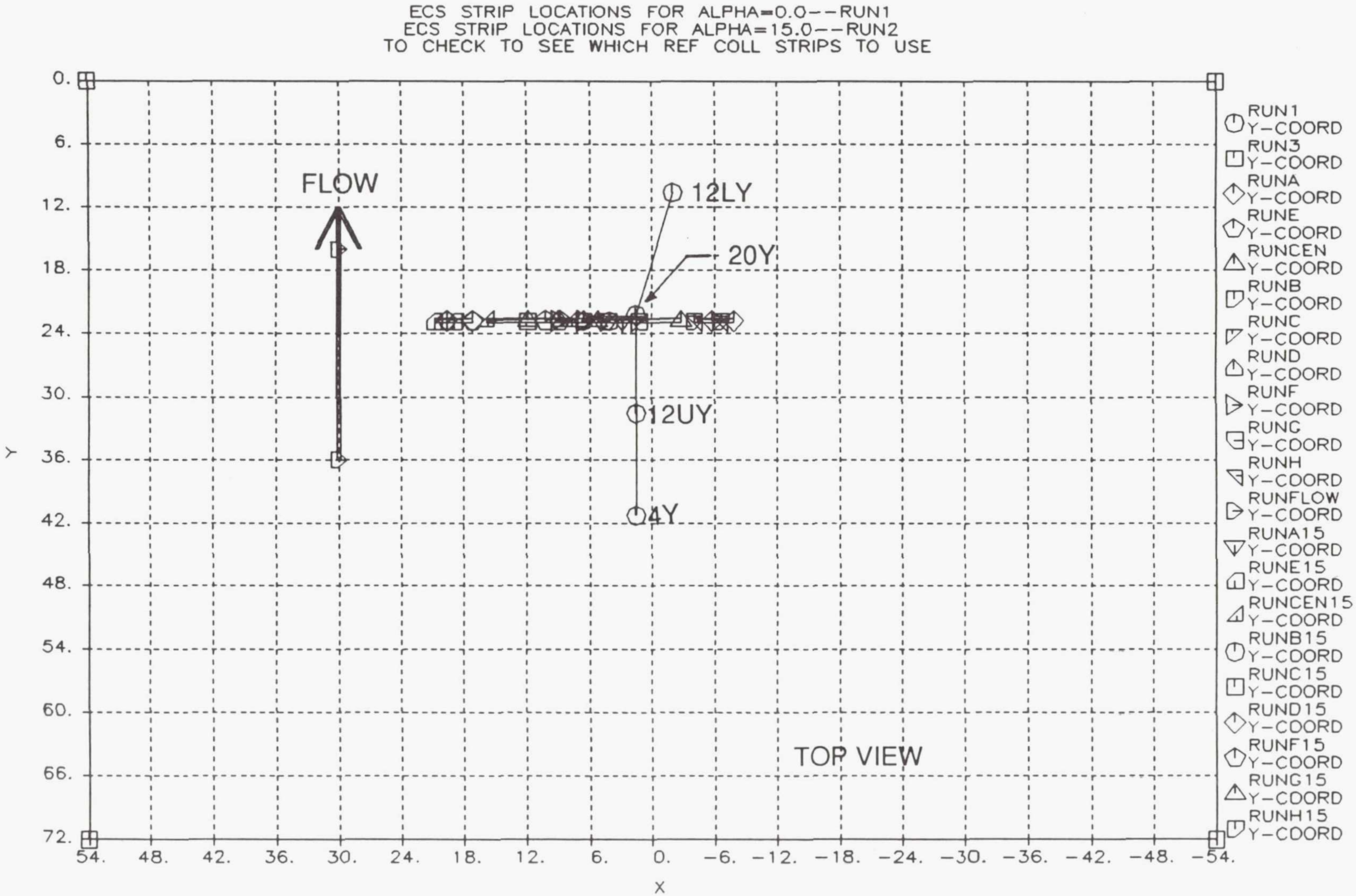

FIGURE C.3 (Page 3 of 3)

REFERENCE COLLECTION ALPHA=0 AND ALPHA=15 POSITION IN TUNNEL
RELATIVE TO ECS GEOMETRY ALPHA=0

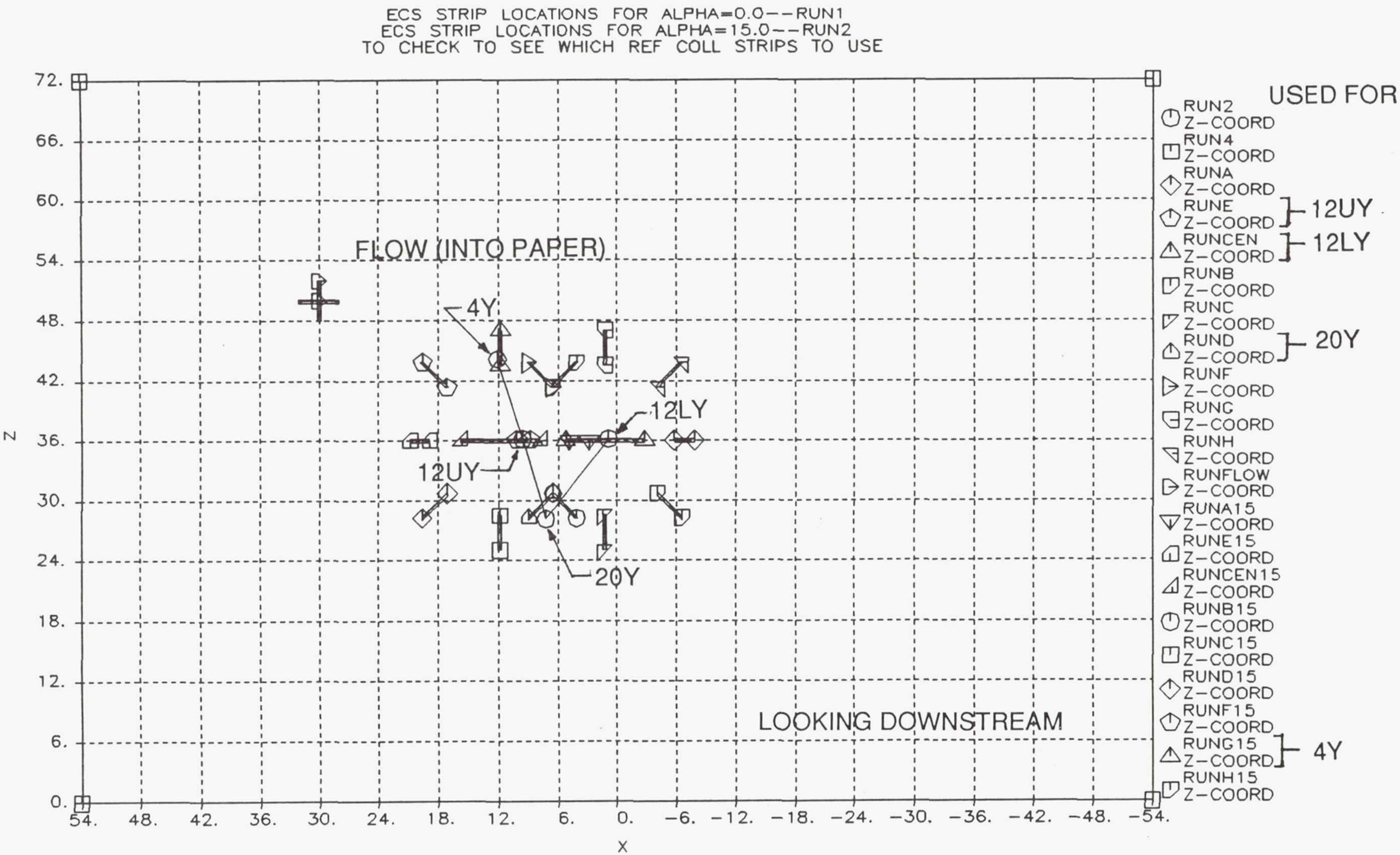

FIGURE C.4 (Page 1 of 3)

REFERENCE COLLECTION ALPHA=0 AND ALPHA=15 POSITION IN TUNNEL
RELATIVE TO ECS GEOMETRY ALPHA=15

ECS STRIP LOCATIONS FOR ALPHA=0.0--RUN1
ECS STRIP LOCATIONS FOR ALPHA=15.0--RUN2
TO CHECK TO SEE WHICH REF COLL STRIPS TO USE

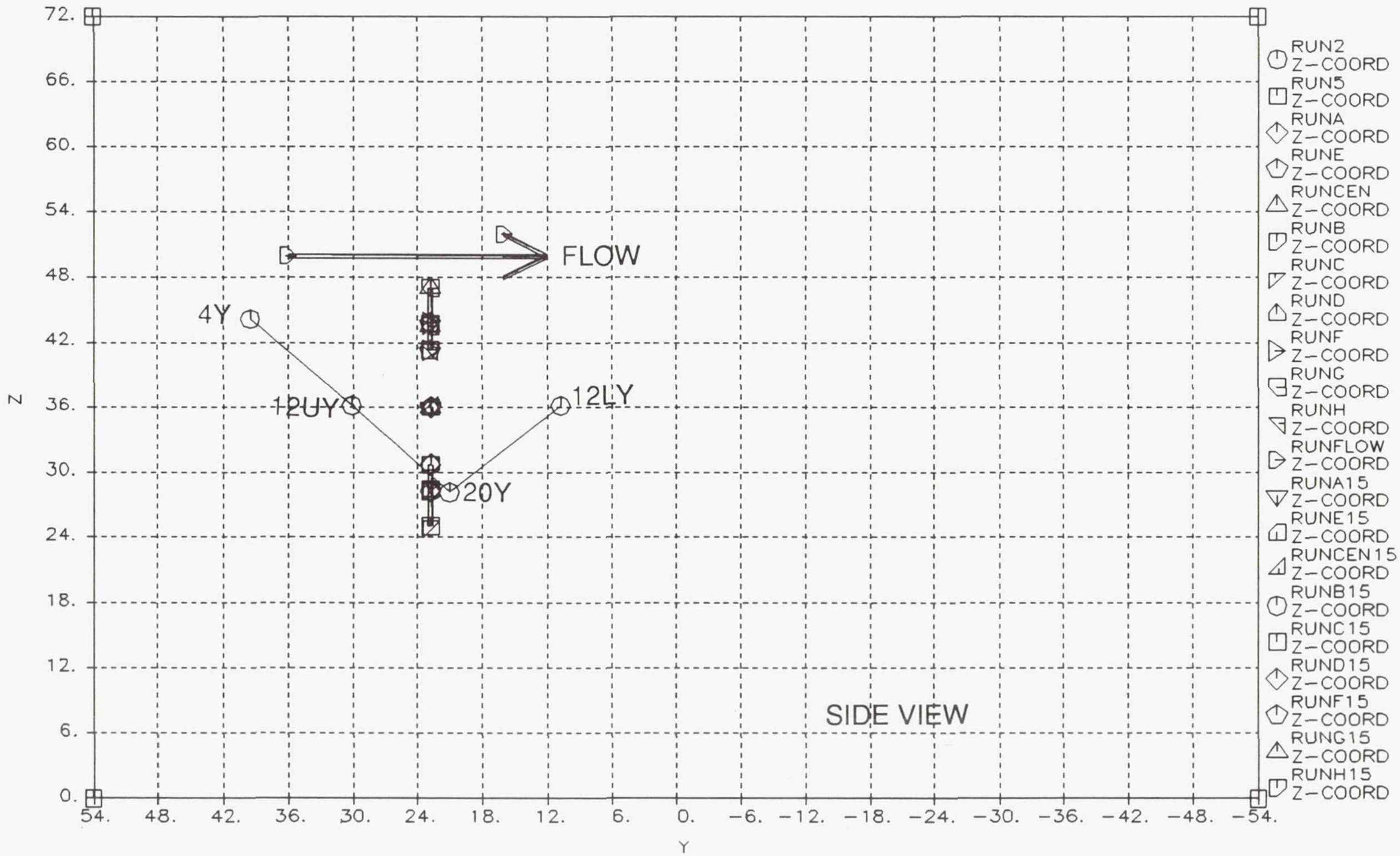

FIGURE C.4 (Page 2 of 3)

REFERENCE COLLECTION ALPHA=0 AND ALPHA=15 POSITION IN TUNNEL
RELATIVE TO ECS GEOMETRY ALPHA=15

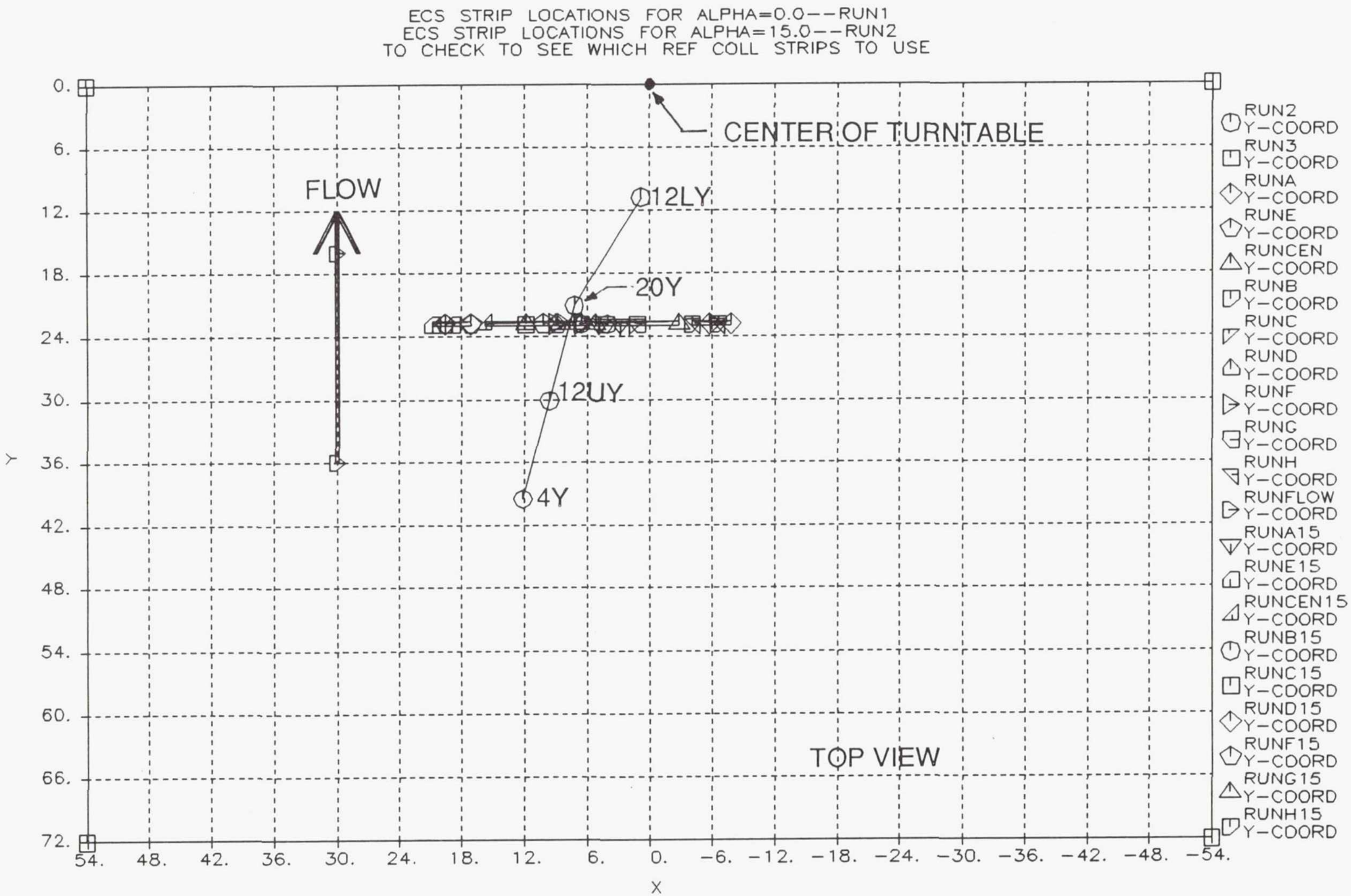

FIGURE C.4 (Page 3 of 3)

REFERENCE COLLECTION ALPHA=0 AND ALPHA=15 POSITION IN TUNNEL
RELATIVE TO ECS GEOMETRY ALPHA=15

ECS INLET ALPHA (deg.)	ECS STRIP (letter)	REFERENCE COLLECTOR MASS (micro gram) (per cm**2)	GEOMETRY LOCATION (buttock) (position)	REFERENCE COLLECTOR POSITION/ALPHA (letter/alpha)
0.0	A	0.473	4Y	G/0.0
0.0	B	0.408	12UY	CENT/0.0
0.0	C	0.488	20Y	C/0.0
0.0	D	0.408	12LY	CENT/0.0
15.0	A	0.473	4Y	G/15.0
15.0	B	0.482	12UY	E/0.0
15.0	C	0.474	20Y	D/0.0
15.0	D	0.408	12LY	CENT/0.0

FIGURE C.5

REFERENCE COLLECTOR MASSES USED IN FINAL DATA REDUCTION

APPENDIX D – INDIVIDUAL IMPINGEMENT EFFICIENCY PLOTS AND IMPINGEMENT FIELD PLOTS FOR MESH 2 ANALYSES

The contents of Appendix D include each individual local water impingement efficiency curve and corresponding impingement field curve for all analysis runs conducted using the Mesh 2 flowfield. These data are shown here to provide detail which may be lost in the summary curves presented in Section 4.3.4. The contents of the Appendix are arranged per flight condition (i.e., tunnel test condition) as follows:

- Flight Condition 1
  - Location–4Y (buttock line Y=4)
  - Location–12LY (lower lip at buttock line Y=12)
  - Location–12UY (upper lip at buttock line Y=12)
  - Location–20Y (buttock line Y=20)
- Flight Condition 2
  - Location–4Y
  - Location–12LY
  - Location–12UY
  - Location–20Y
- Flight Condition 3
  - Location–4Y
  - Location–12LY
  - Location–12UY
  - Location–20Y
- Flight Condition 4
  - Location–4Y
  - Location–12LY
  - Location–12UY
  - Location–20Y

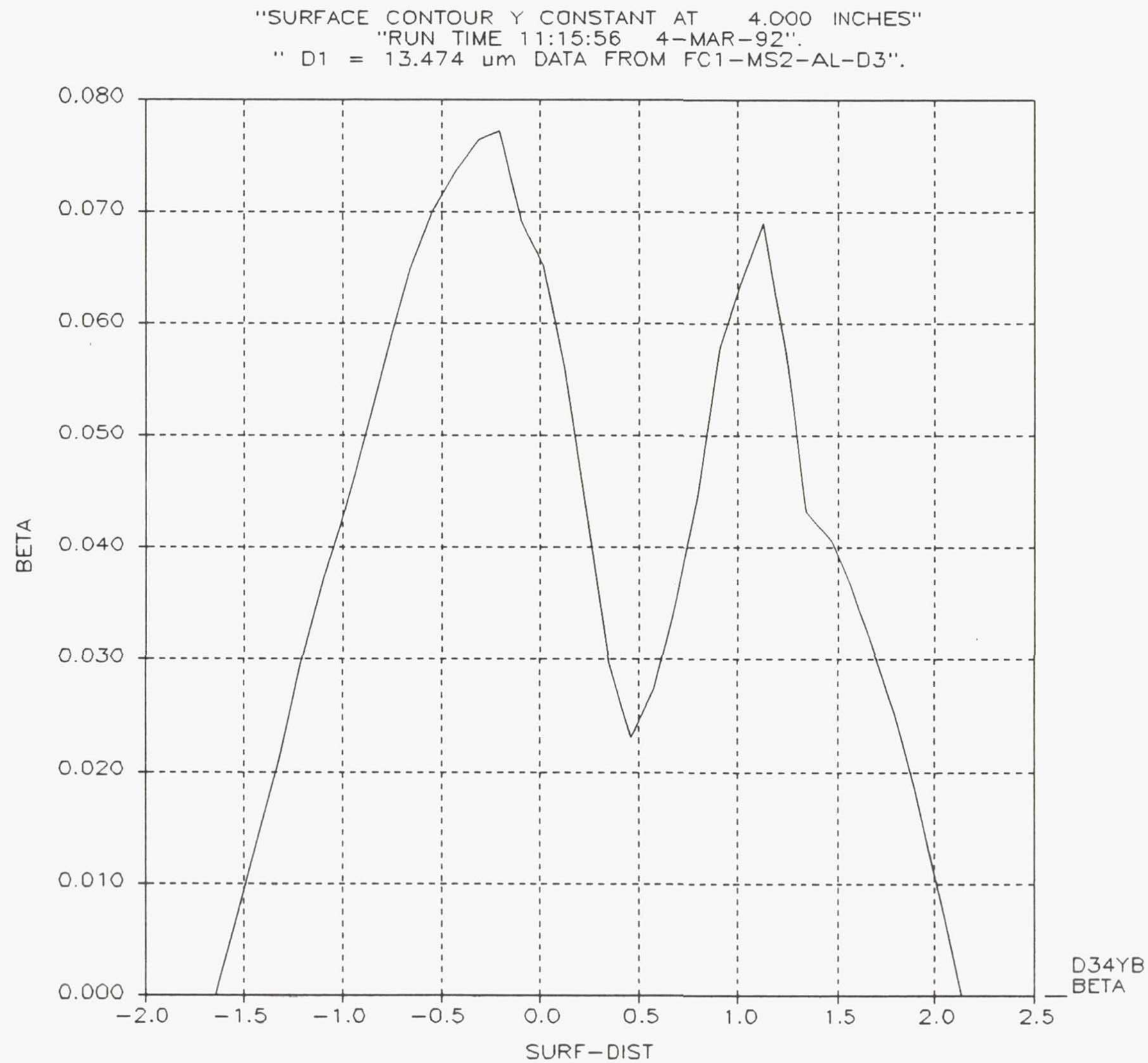

FIGURE D.1

BETA vs SURF-DIST(cm), FC1,Y=4,D=13.5 micron

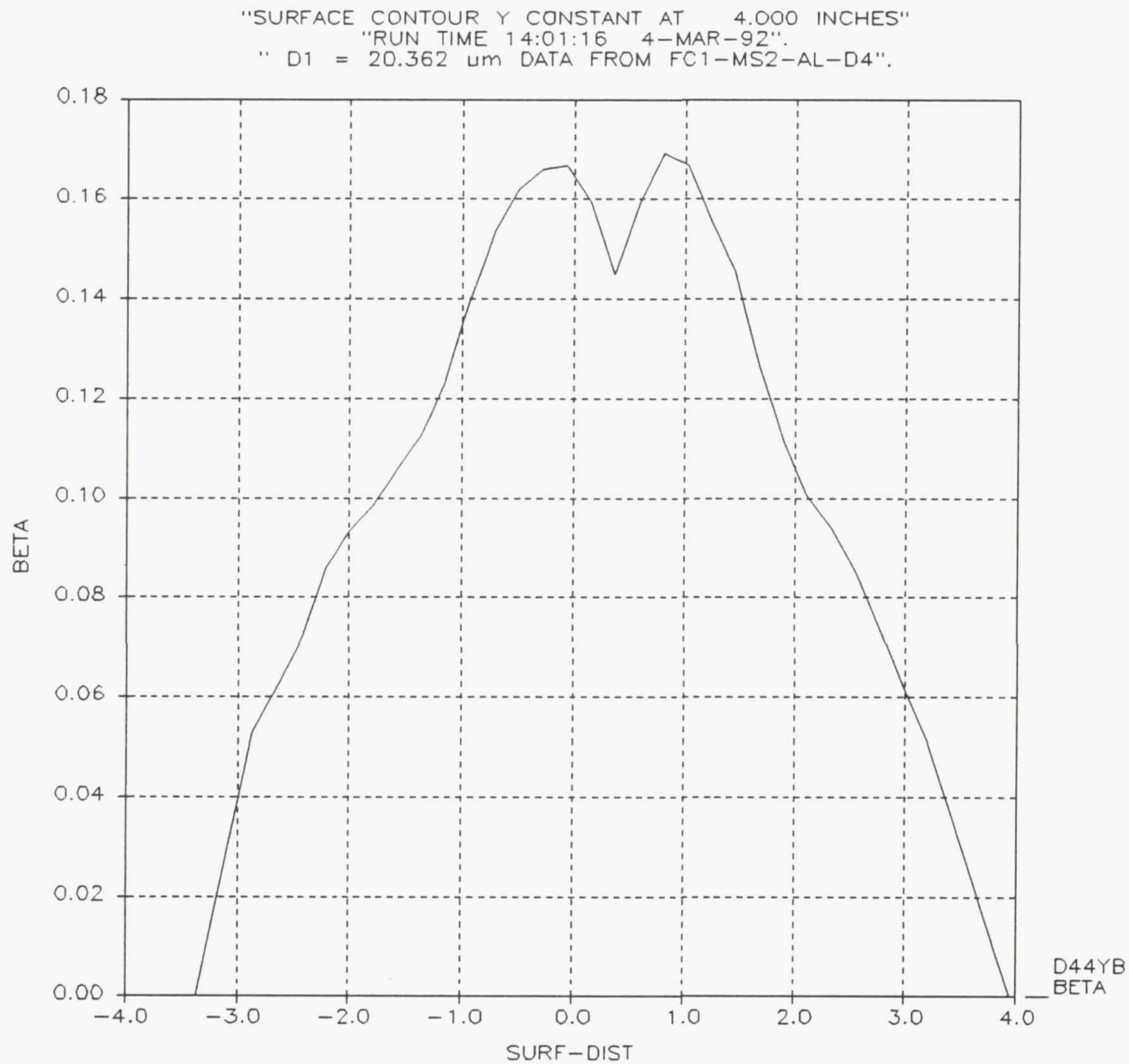

FIGURE D.2

BETA vs SURF-DIST(cm), FC1,Y=4,D=20.4 micron

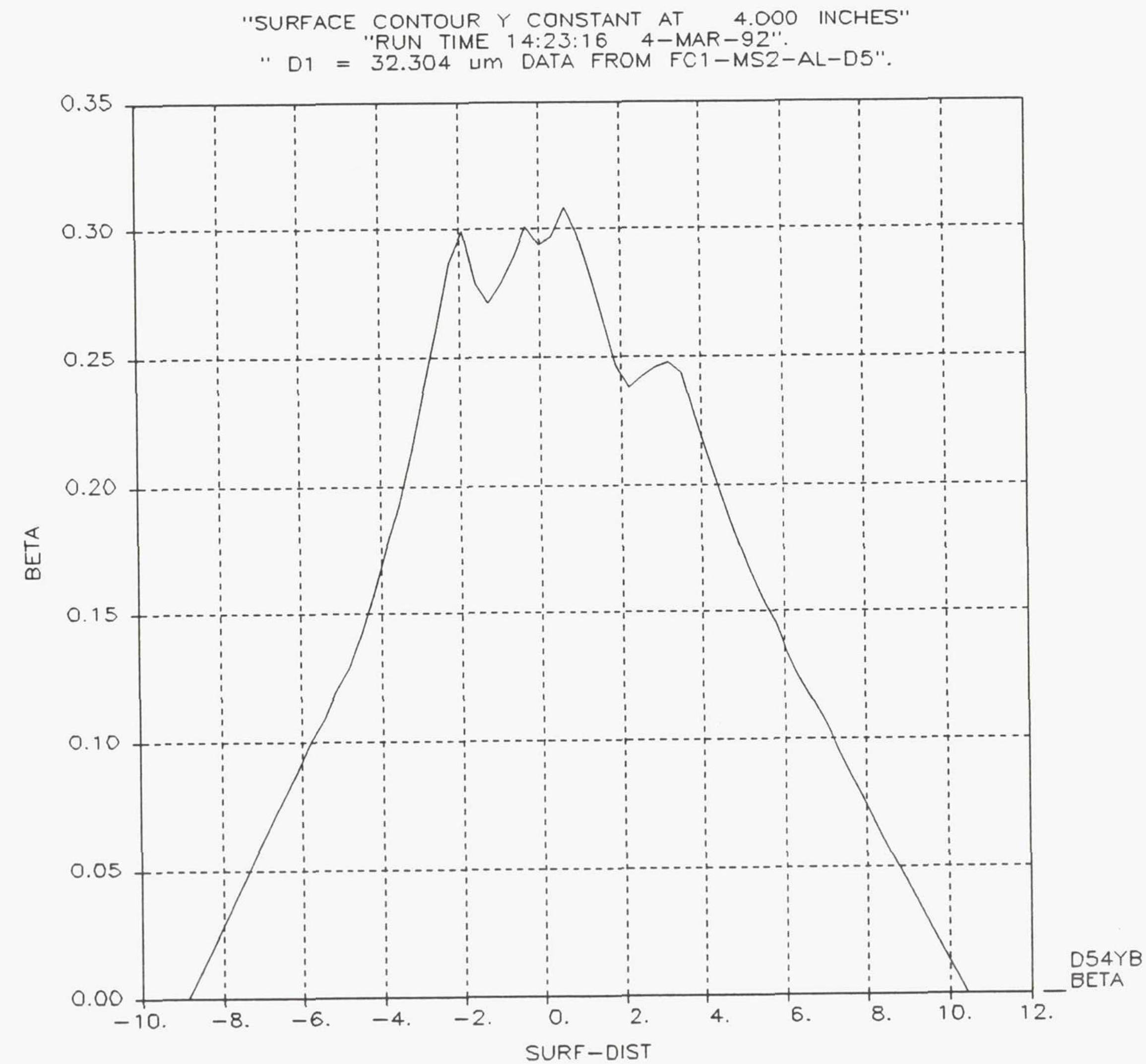

FIGURE D.3

BETA vs SURF-DIST(cm), FC1,Y=4,D=32.3 micron

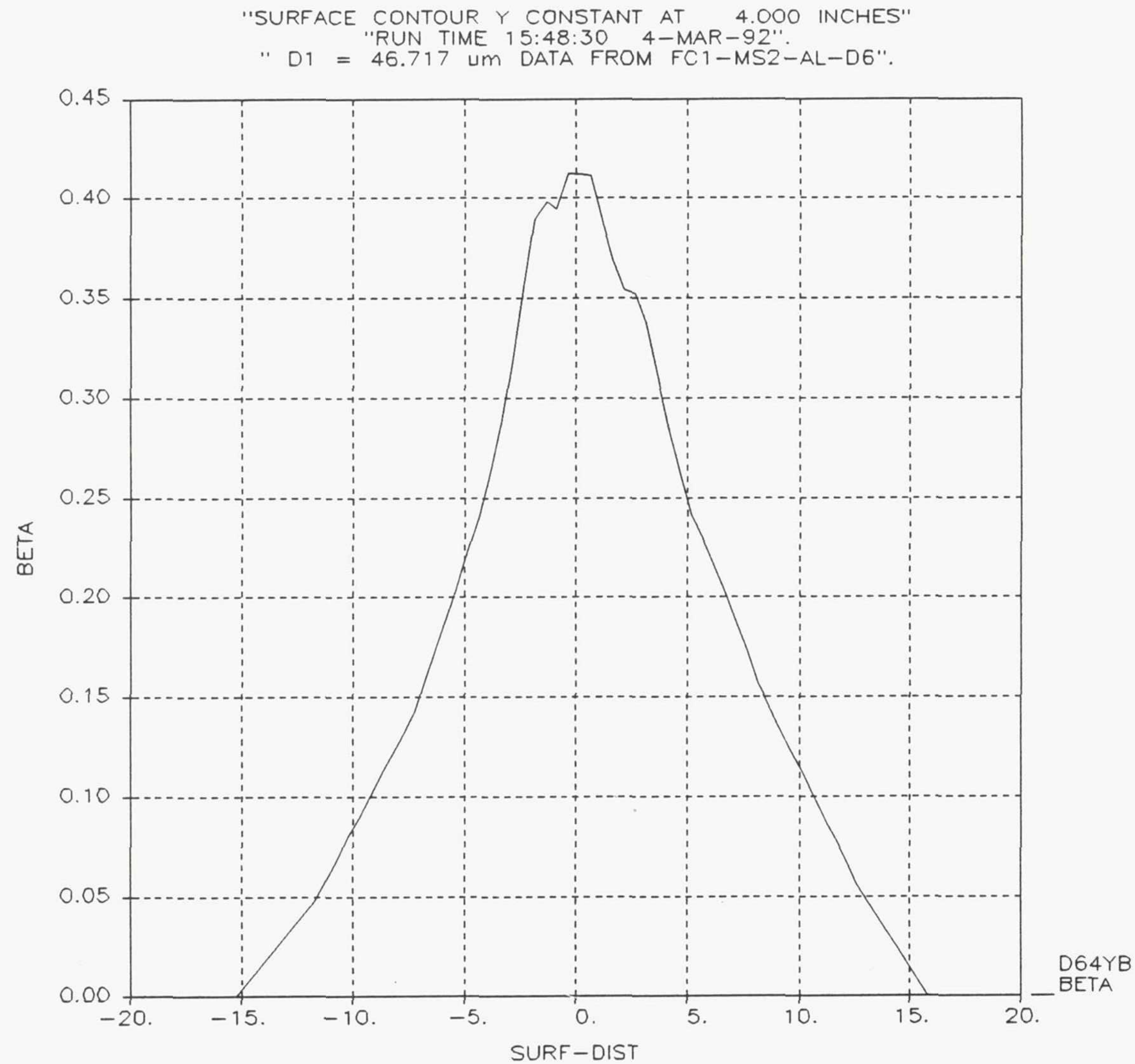

FIGURE D.4

BETA vs SURF-DIST(cm), FC1,Y=4,D=46.7 micron

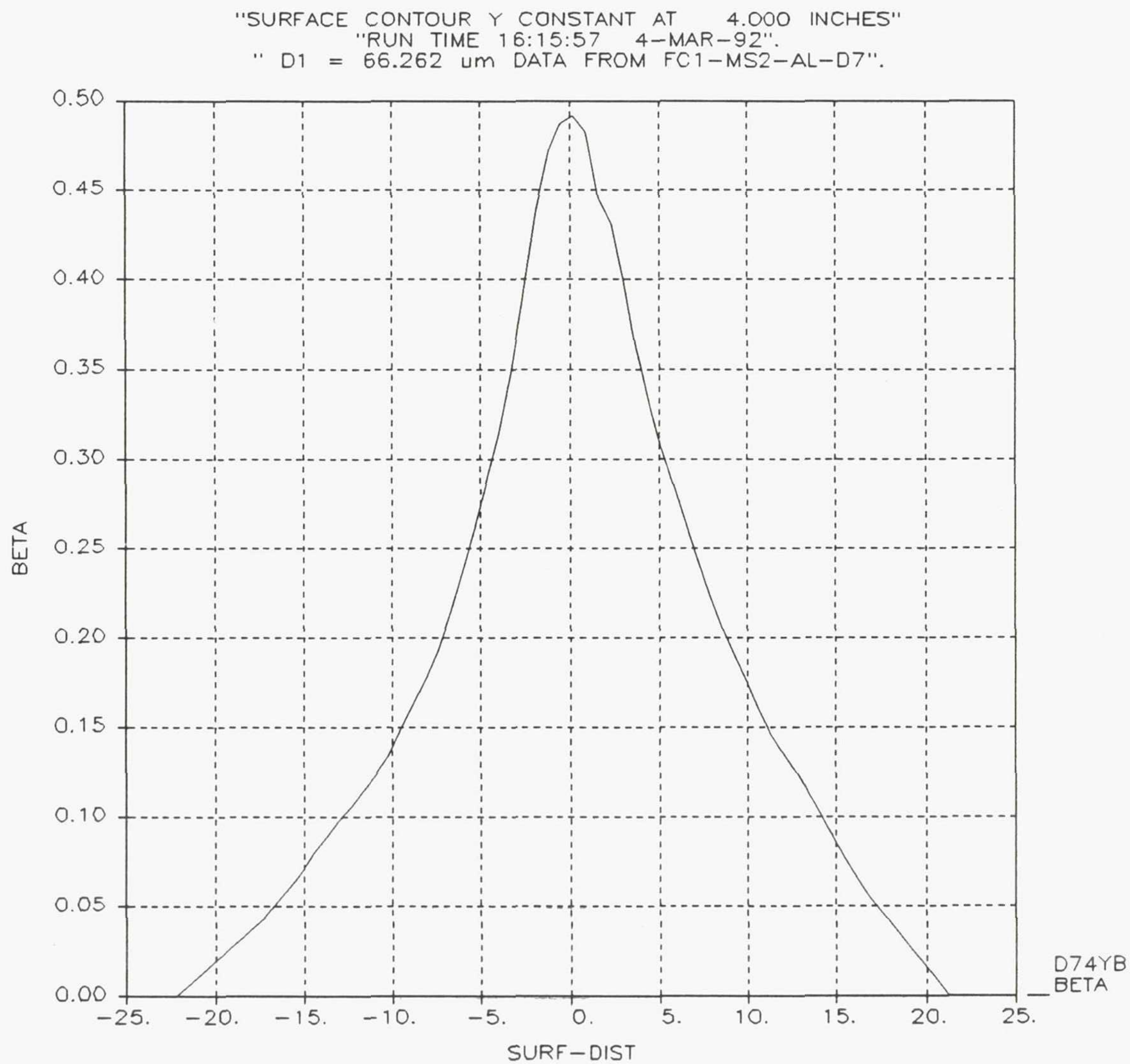

FIGURE D.5

BETA vs SURF-DIST(cm), FC1,Y=4,D=66.3 micron

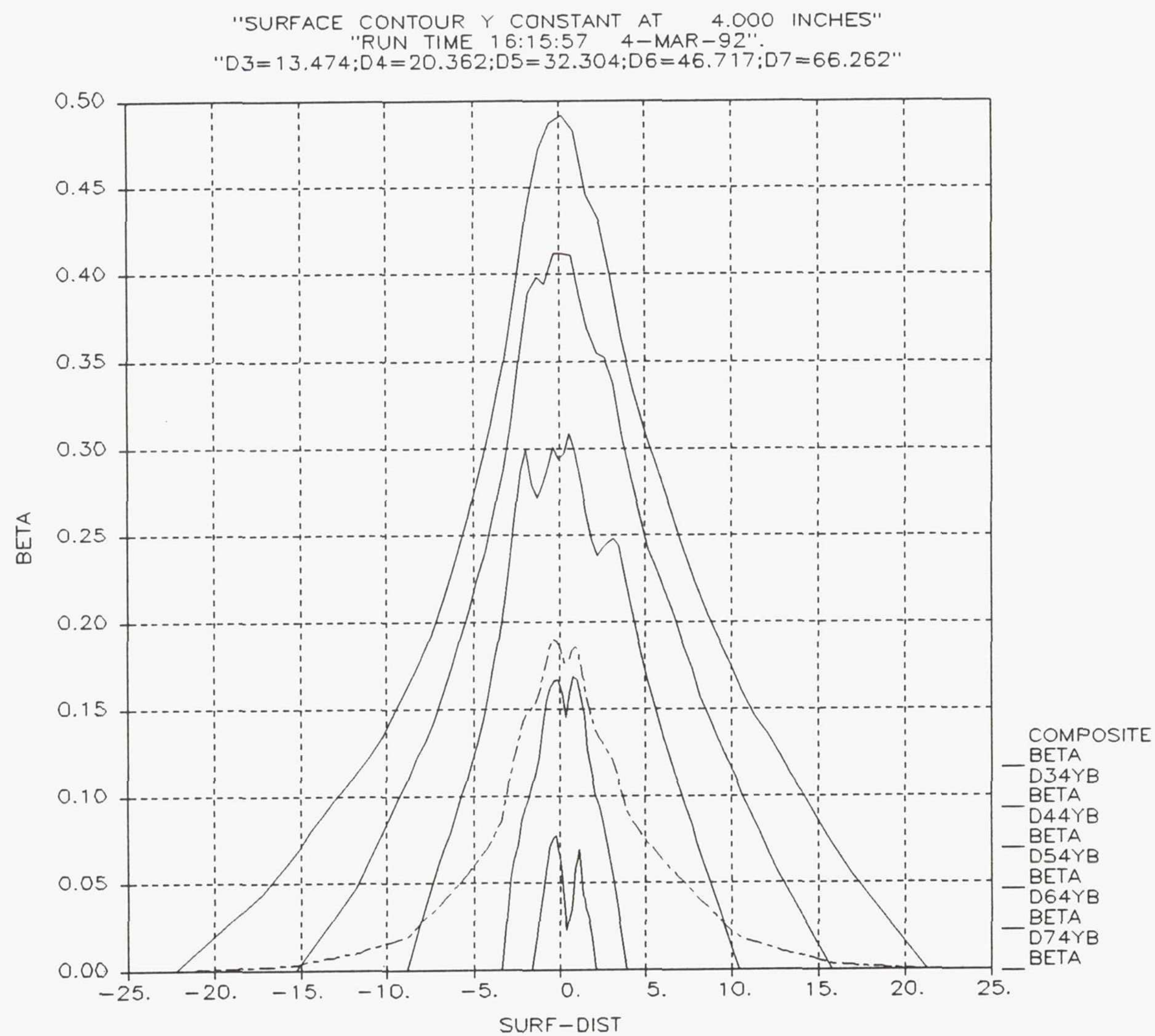

FIGURE D.6

BETA vs SURF-DIST(cm), FC1,Y=4,COMPOSITE AND INDIVIDUAL DROPS

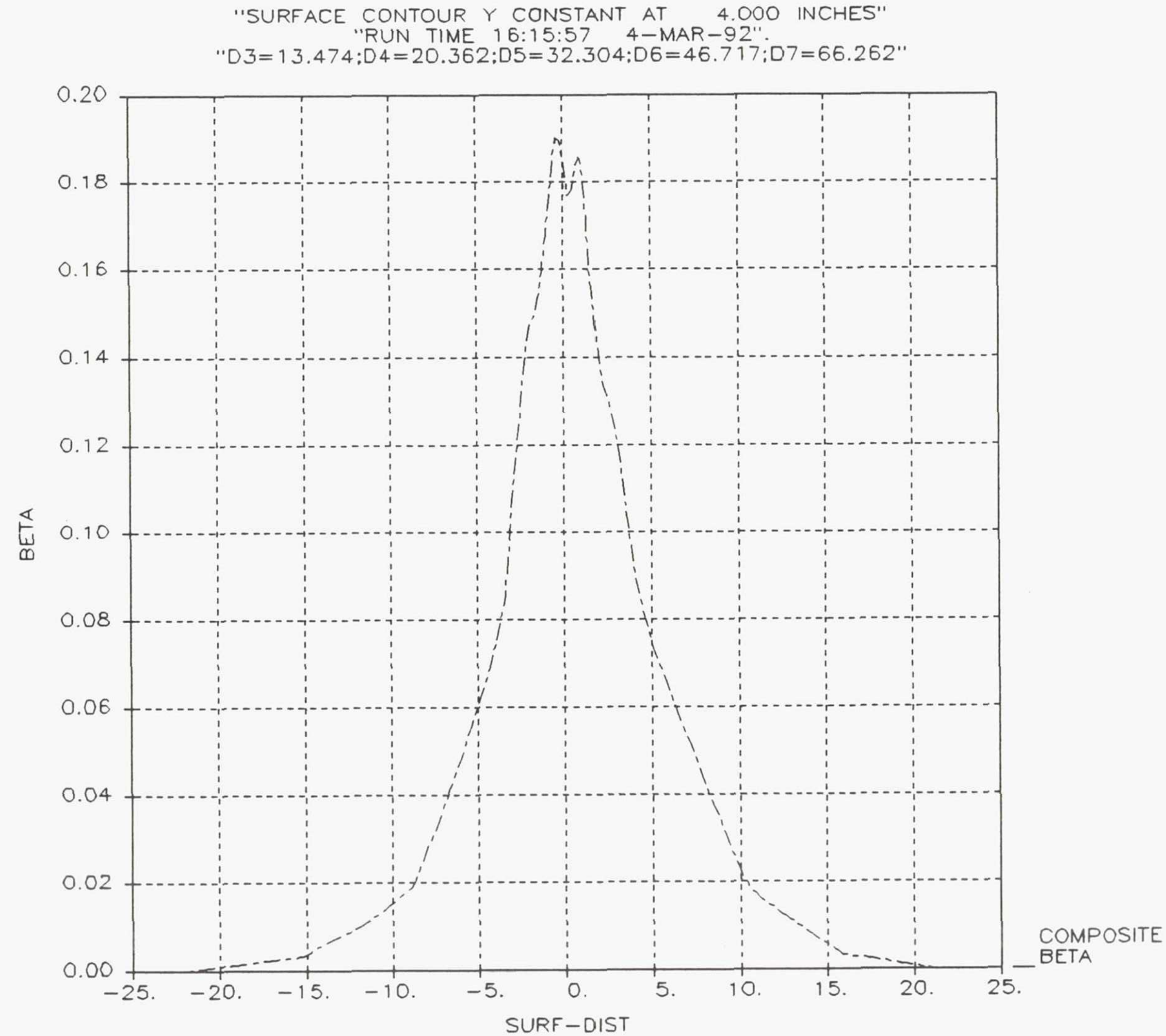

FIGURE D.7

BETA vs SURF-DIST(cm), FC1,Y=4,D=20.4 micron
COMPOSITE DROP

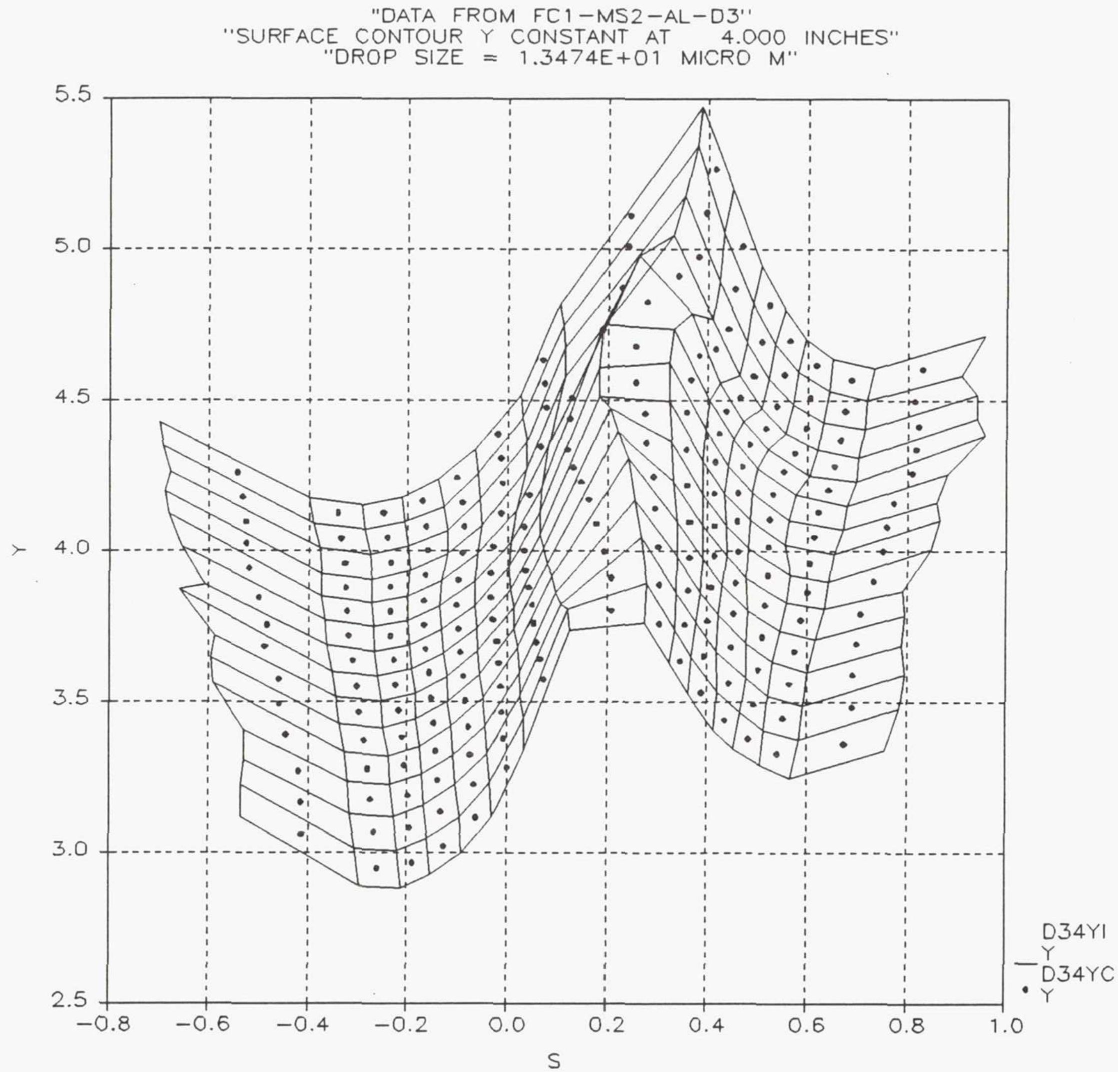

FIGURE D.8

IMPINGEMENT FIELD Y(in) vs S(in), FC1,Y=4,D=13.5 micron

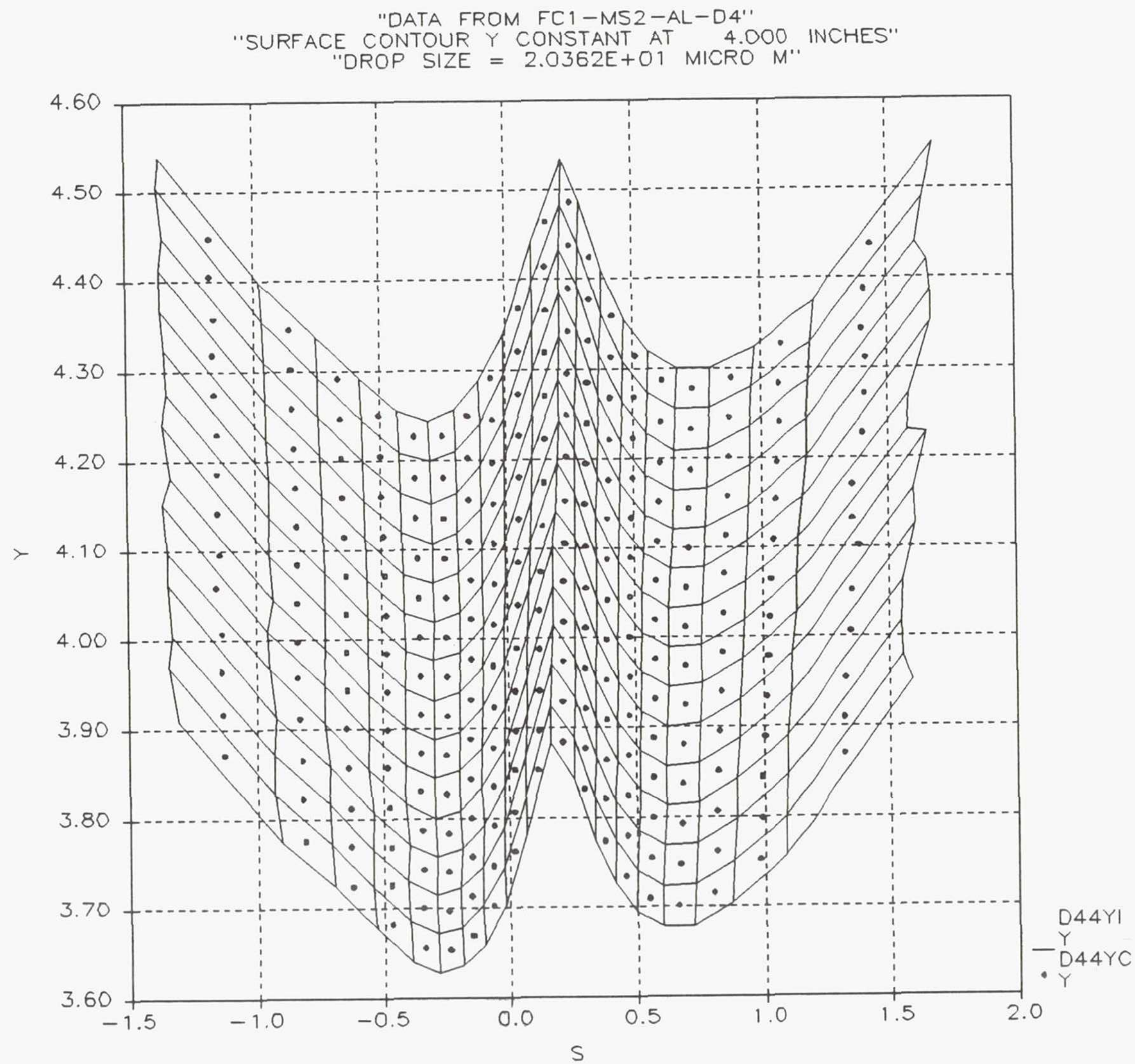

FIGURE D.9

IMPINGEMENT FIELD Y(in) vs S(in), FC1,Y=4,D=20.4 micron

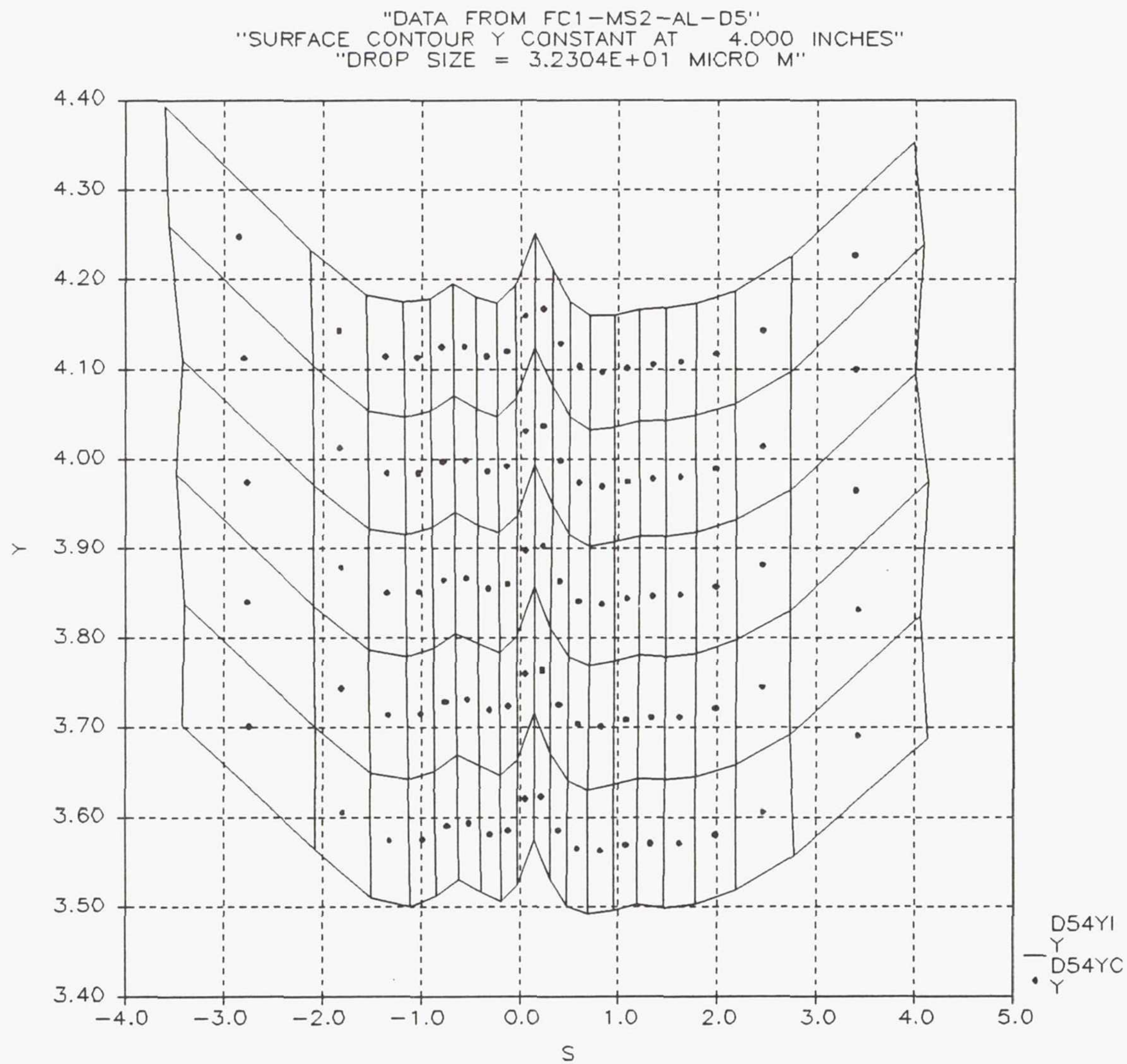

FIGURE D.10

IMPINGEMENT FIELD Y(in) vs S(in), FC1,Y=4,D=32.3 micron

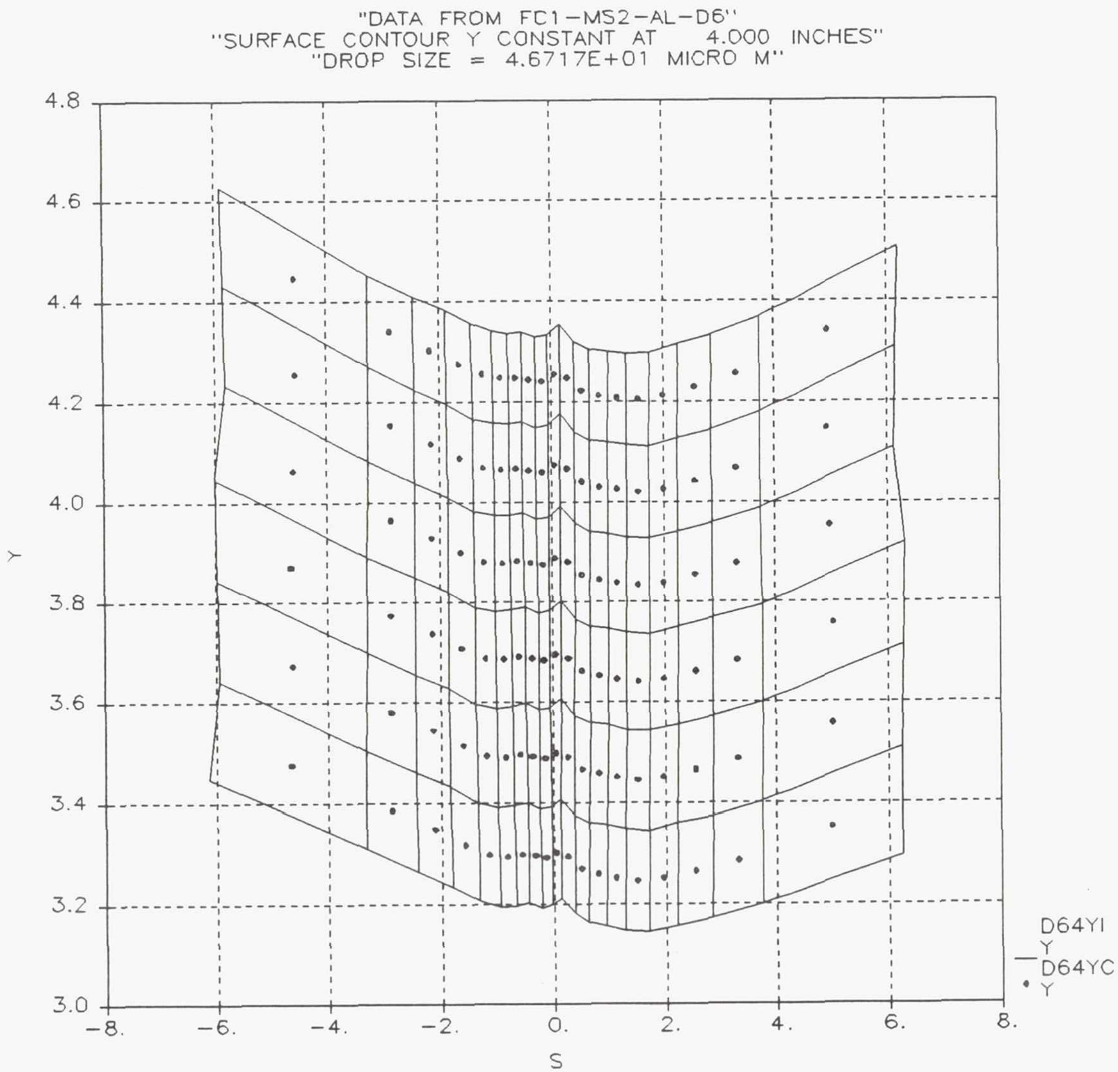

FIGURE D.11

IMPINGEMENT FIELD Y(in) vs S(in), FC1,Y=4,D=46.7 micron

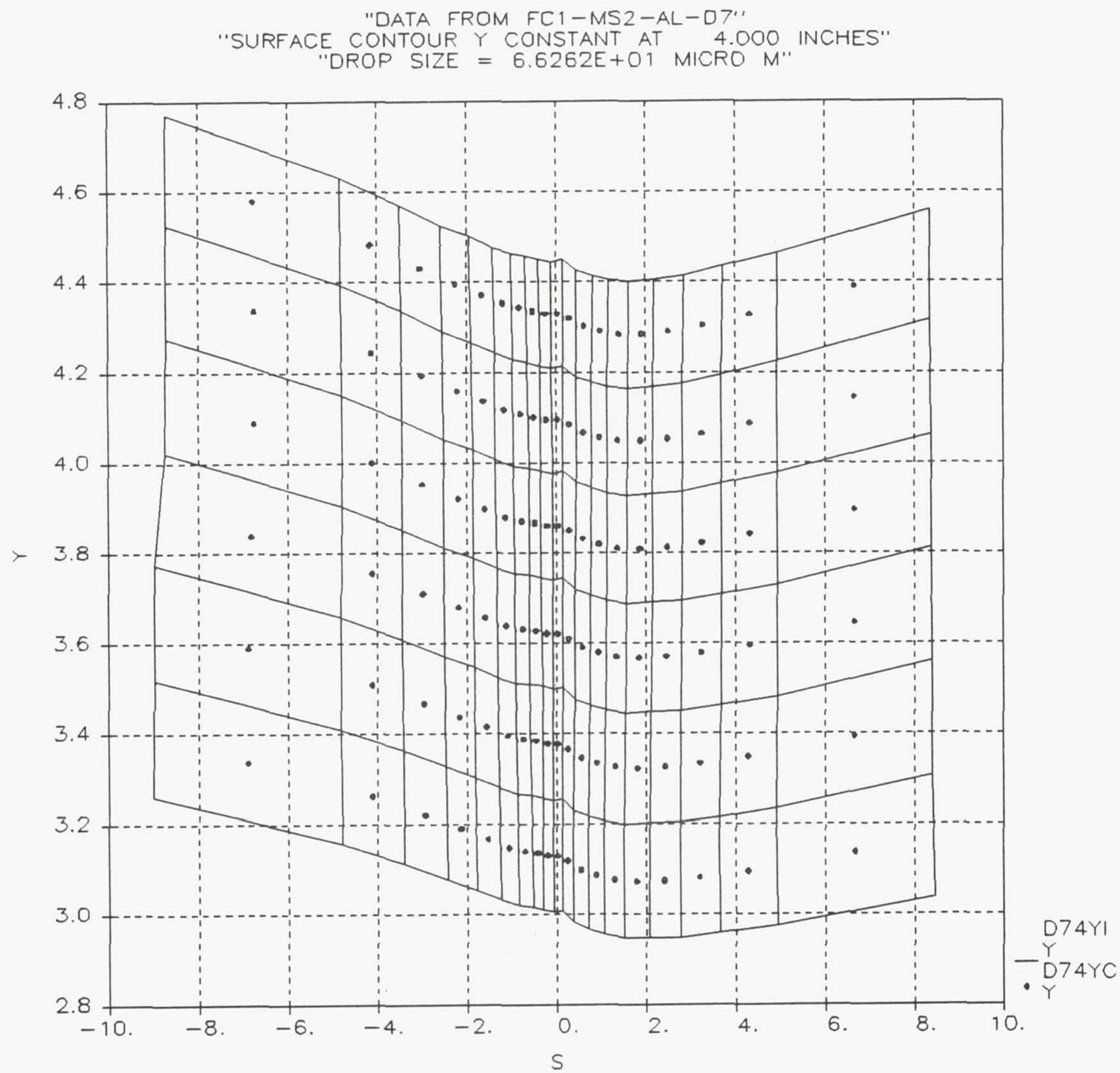

FIGURE D.12

IMPINGEMENT FIELD Y(in) vs S(in), FC1,Y=4,D=66.3 micron

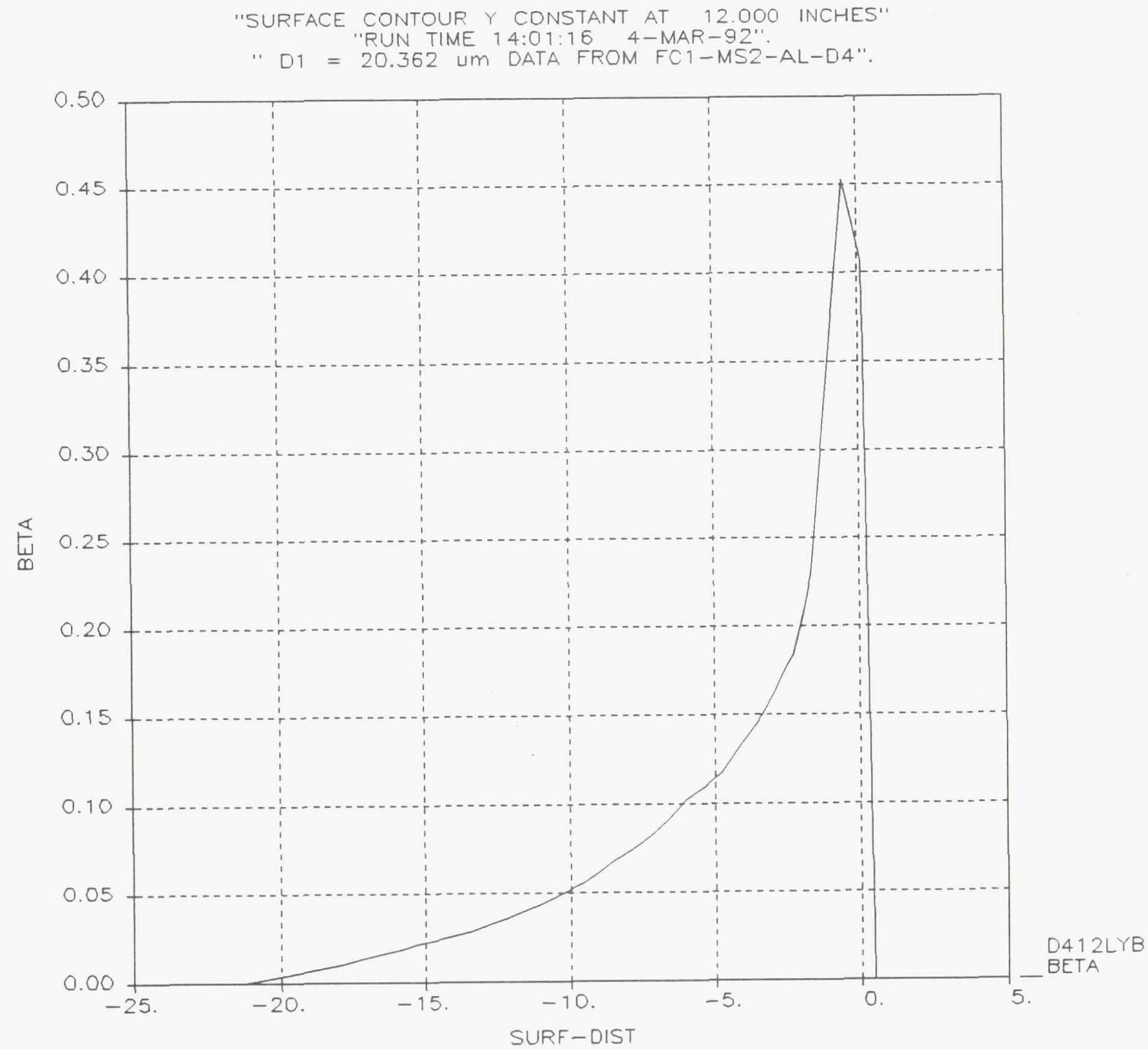

FIGURE D.13

BETA vs SURF-DIST(cm), FC1,Y=12L,D=20.4 micron

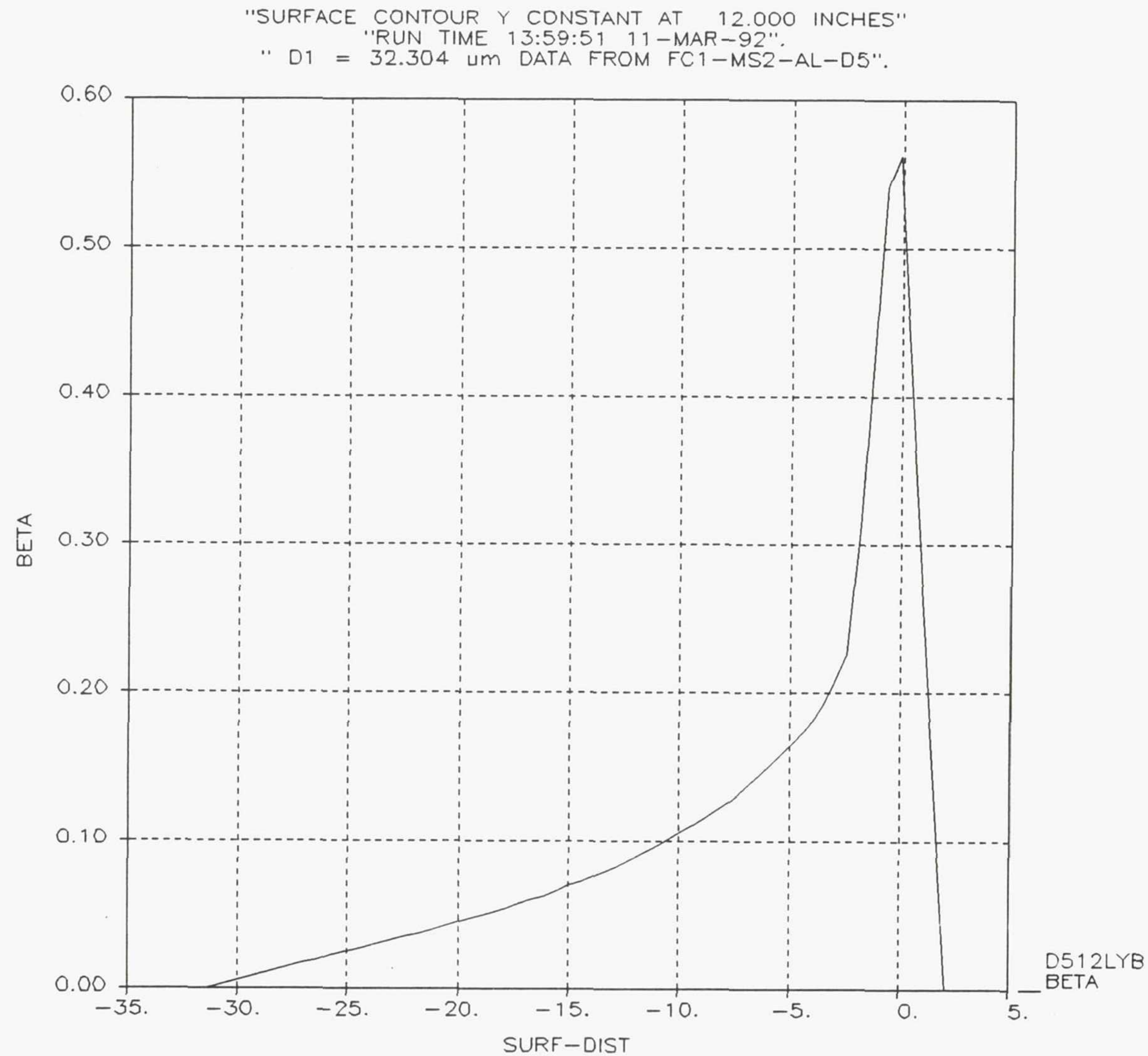

FIGURE D.14

BETA vs SURF-DIST(cm), FC1,Y=12L,D=32.3 micron

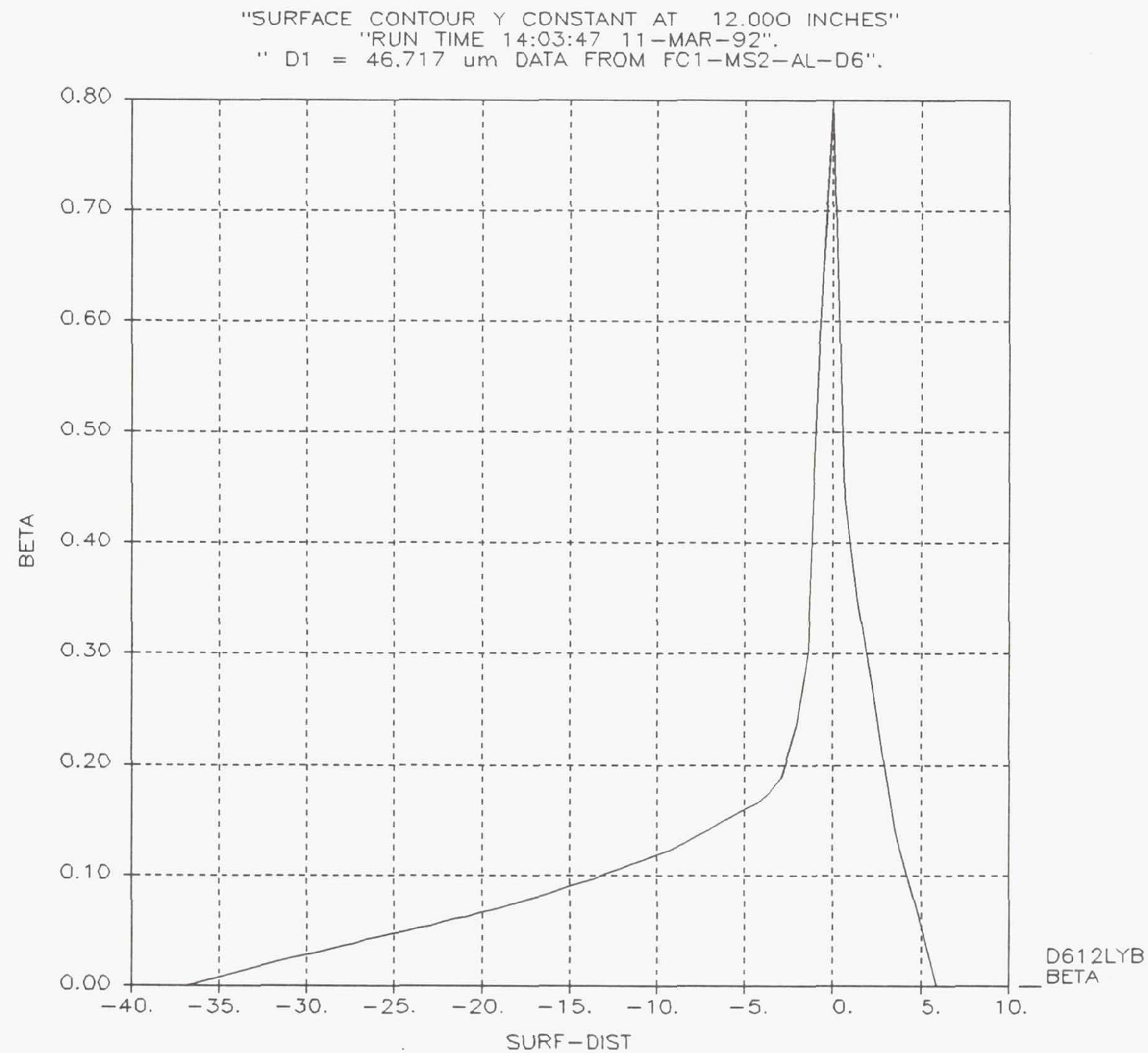

FIGURE D.15

BETA vs SURF-DIST(cm), FC1,Y=12L,D=46.7 micron

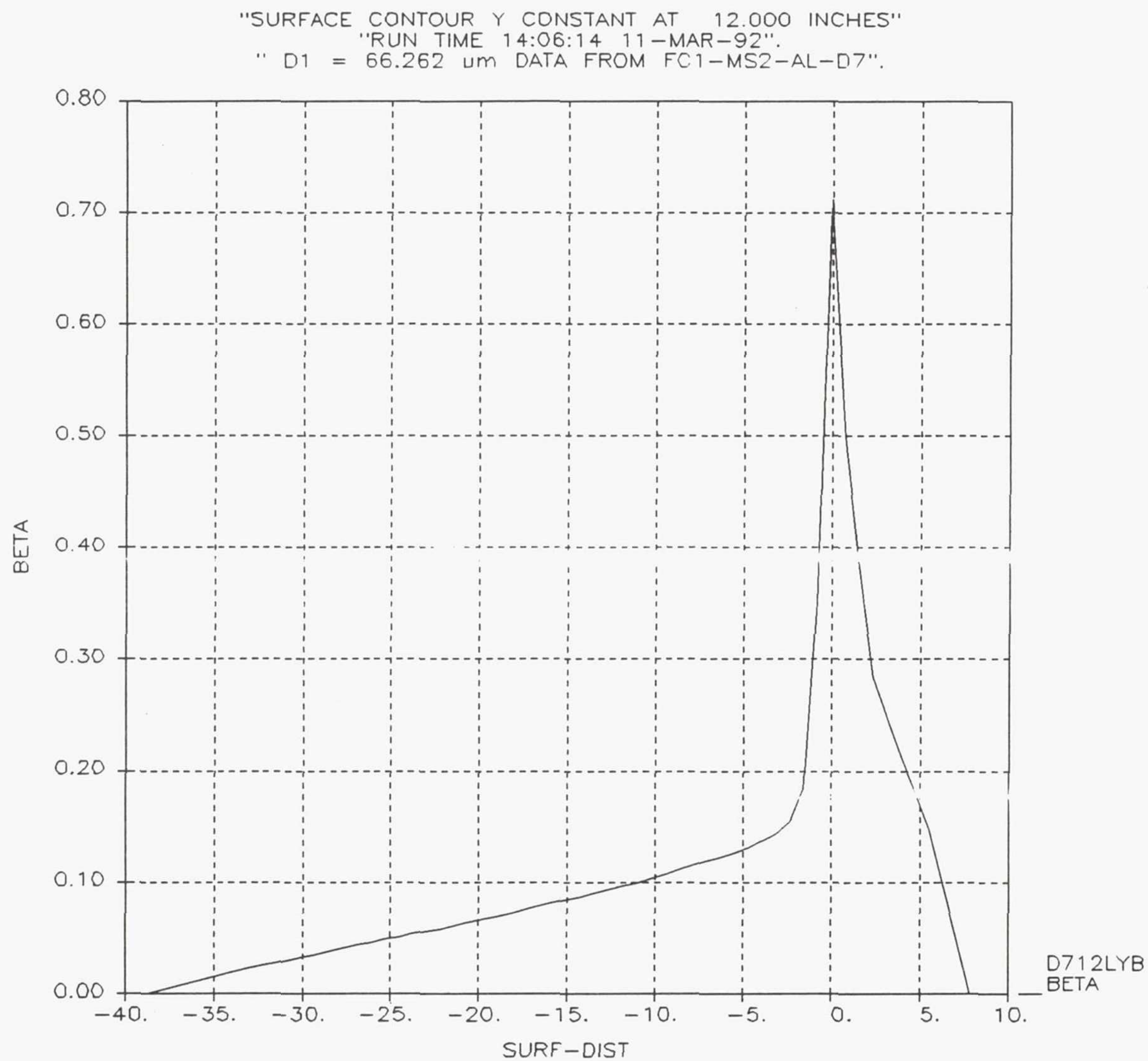

FIGURE D.16

BETA vs SURF-DIST(c 1), FC1,Y=12L,D=66.3 micron

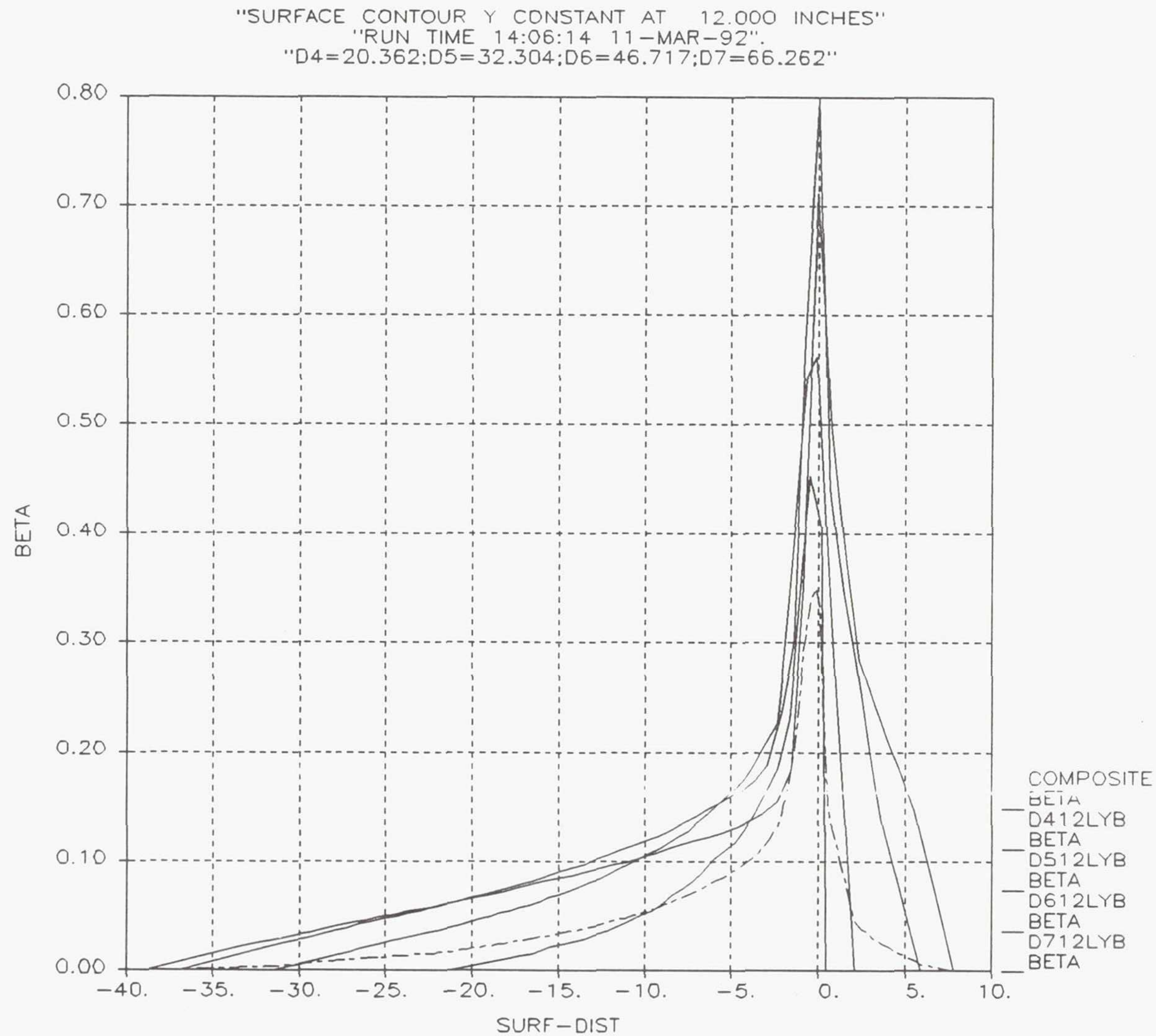

FIGURE D.17

BETA vs SURF-DIST(cm), FC1,Y=12L,COMPOSITE AND INDIVIDUAL DROPS

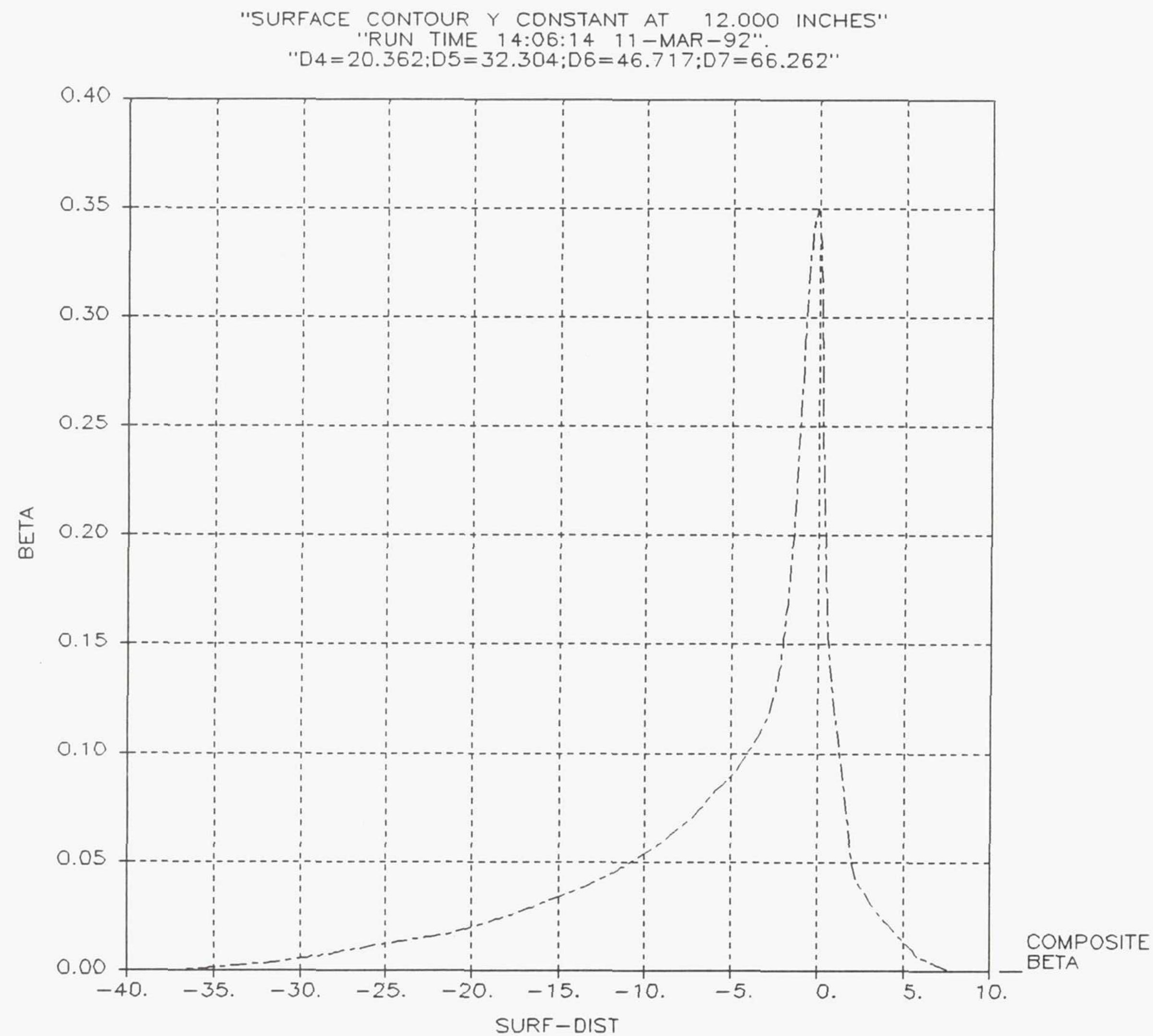

FIGURE D.18

BETA vs SURF-DIST(cm), FC1,Y=12L,D=20.4 micron
COMPOSITE DROP

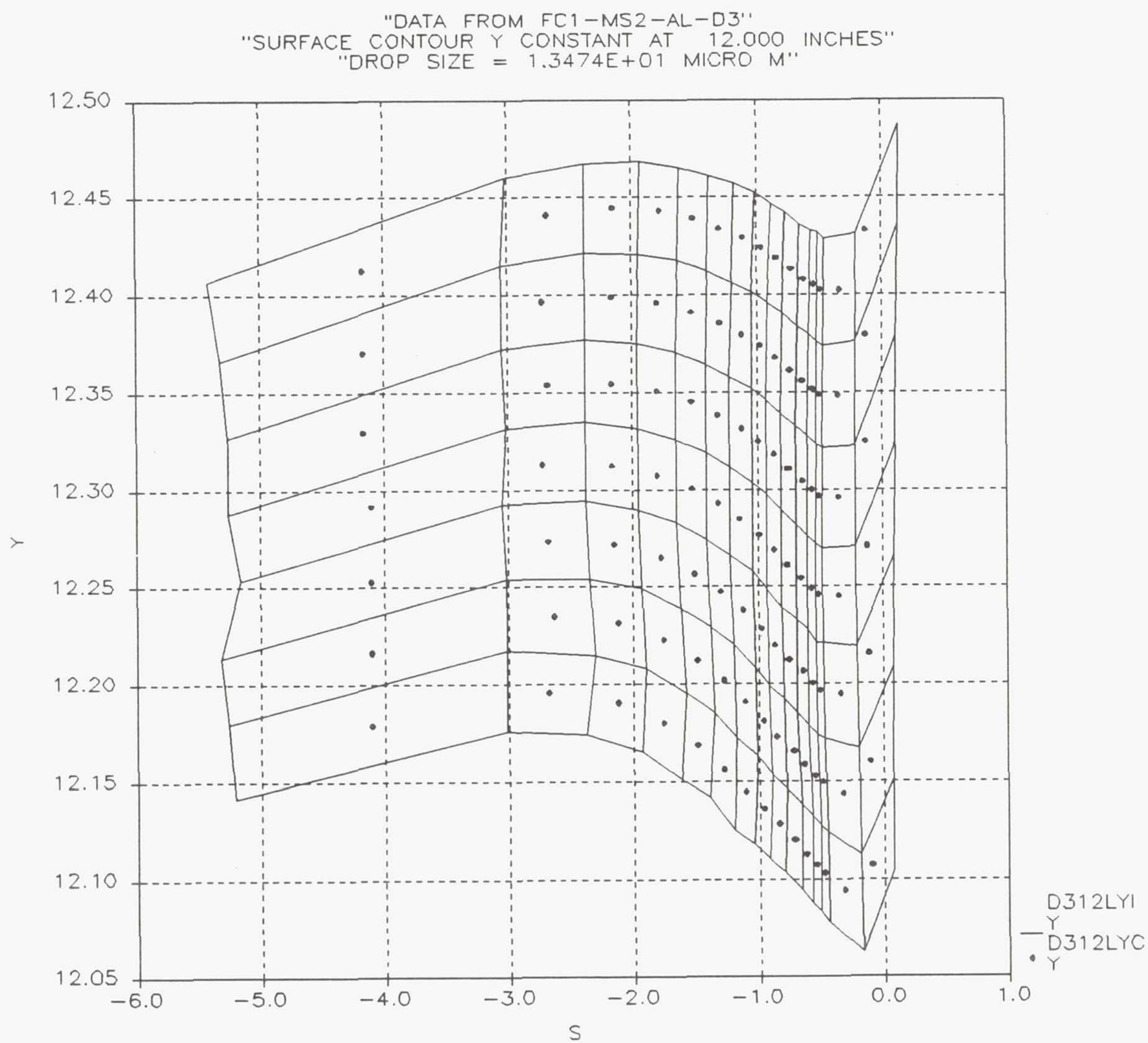

FIGURE D.19

IMPINGEMENT FIELD Y(in) vs S(in), FC1,Y=12L,D=13.5 micron

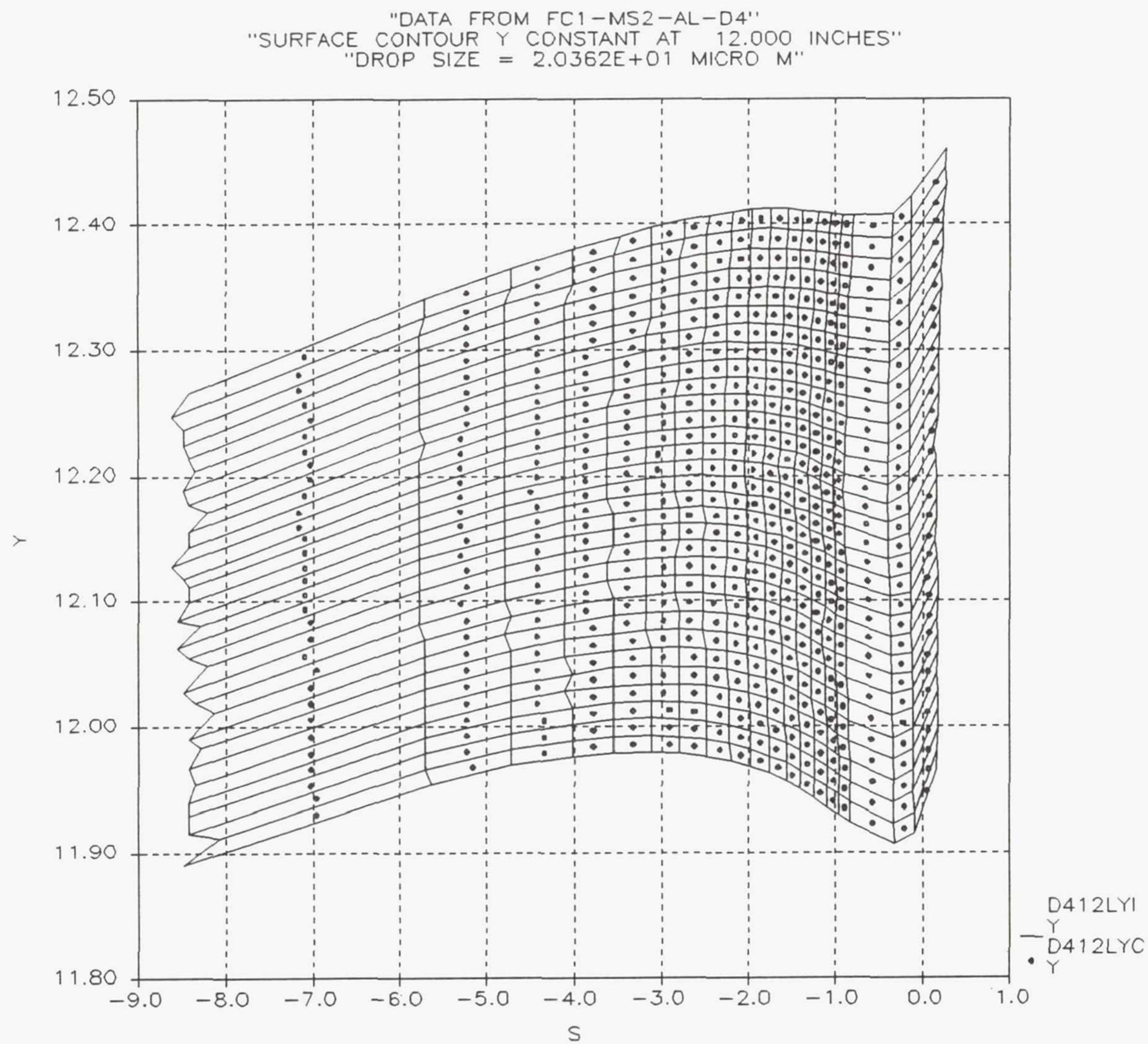

FIGURE D.20

IMPINGEMENT FIELD Y(in) vs S(in), FC1,Y=12L,D=20.4 micron

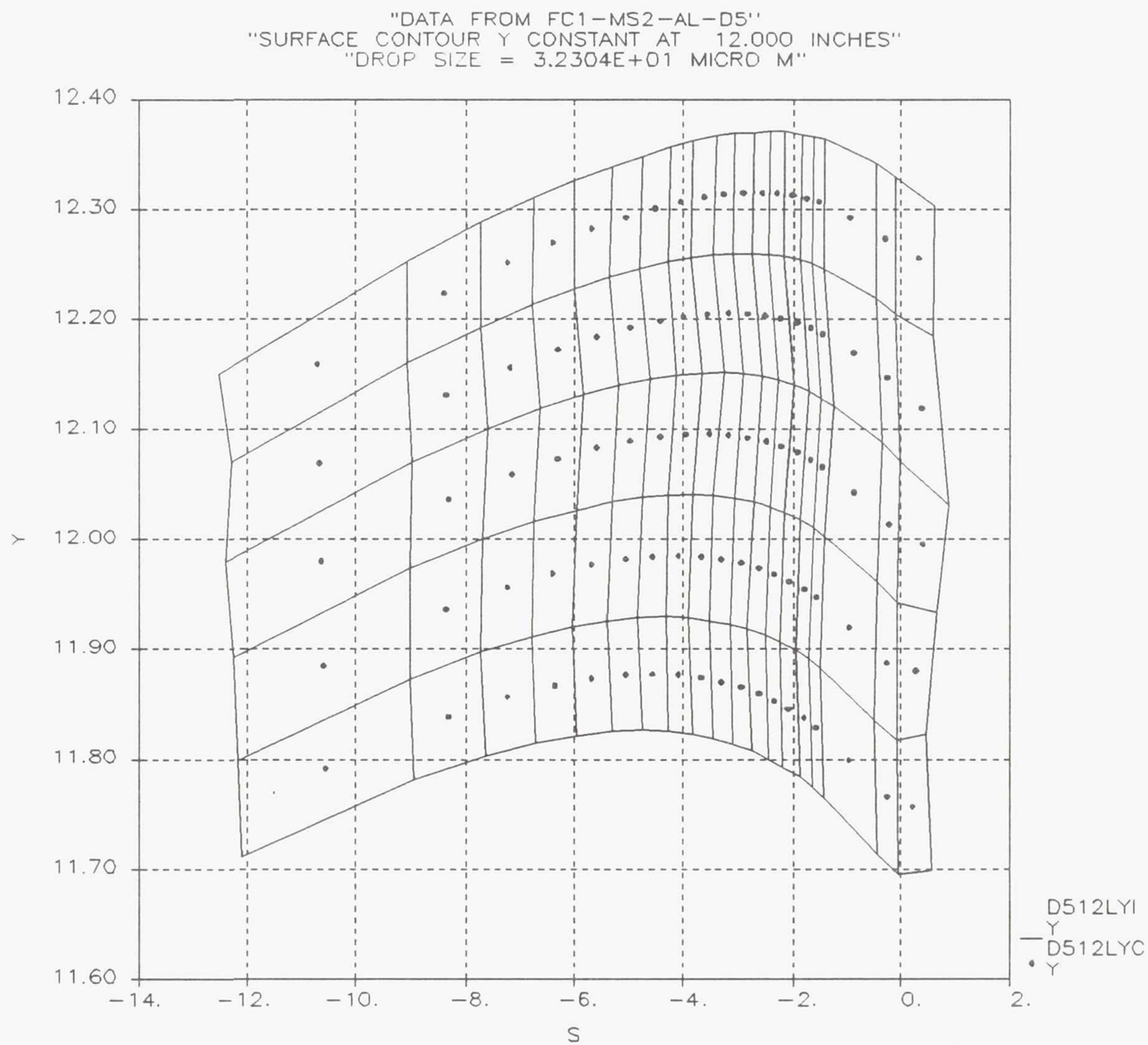

FIGURE D.21

IMPINGEMENT FIELD Y(in) vs S(in), FC1,Y=12L,D=32.3 micron

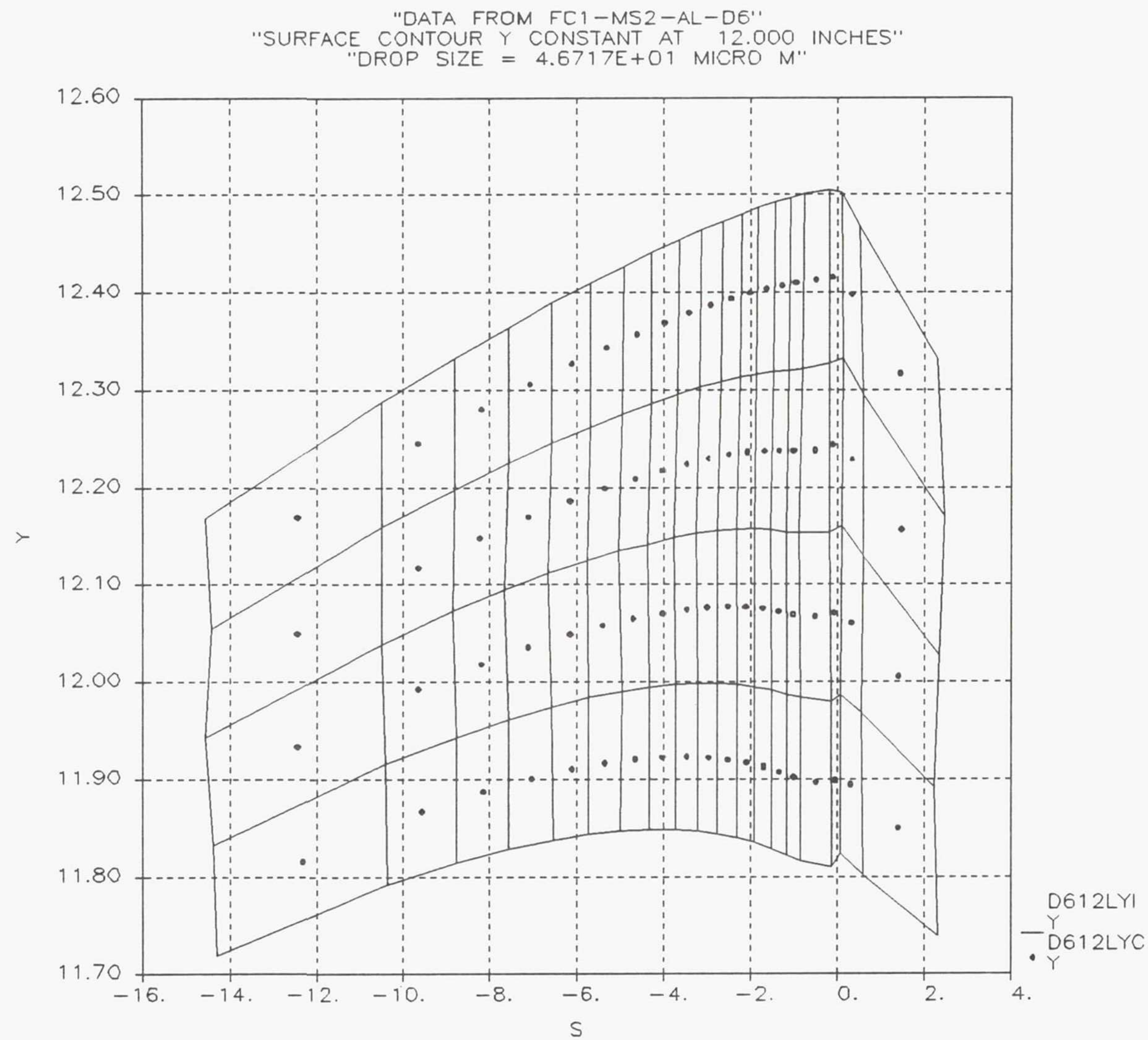

FIGURE D.22

IMPINGEMENT FIELD Y(in) vs S(in), FC1,Y=12L,D=46.7 micron

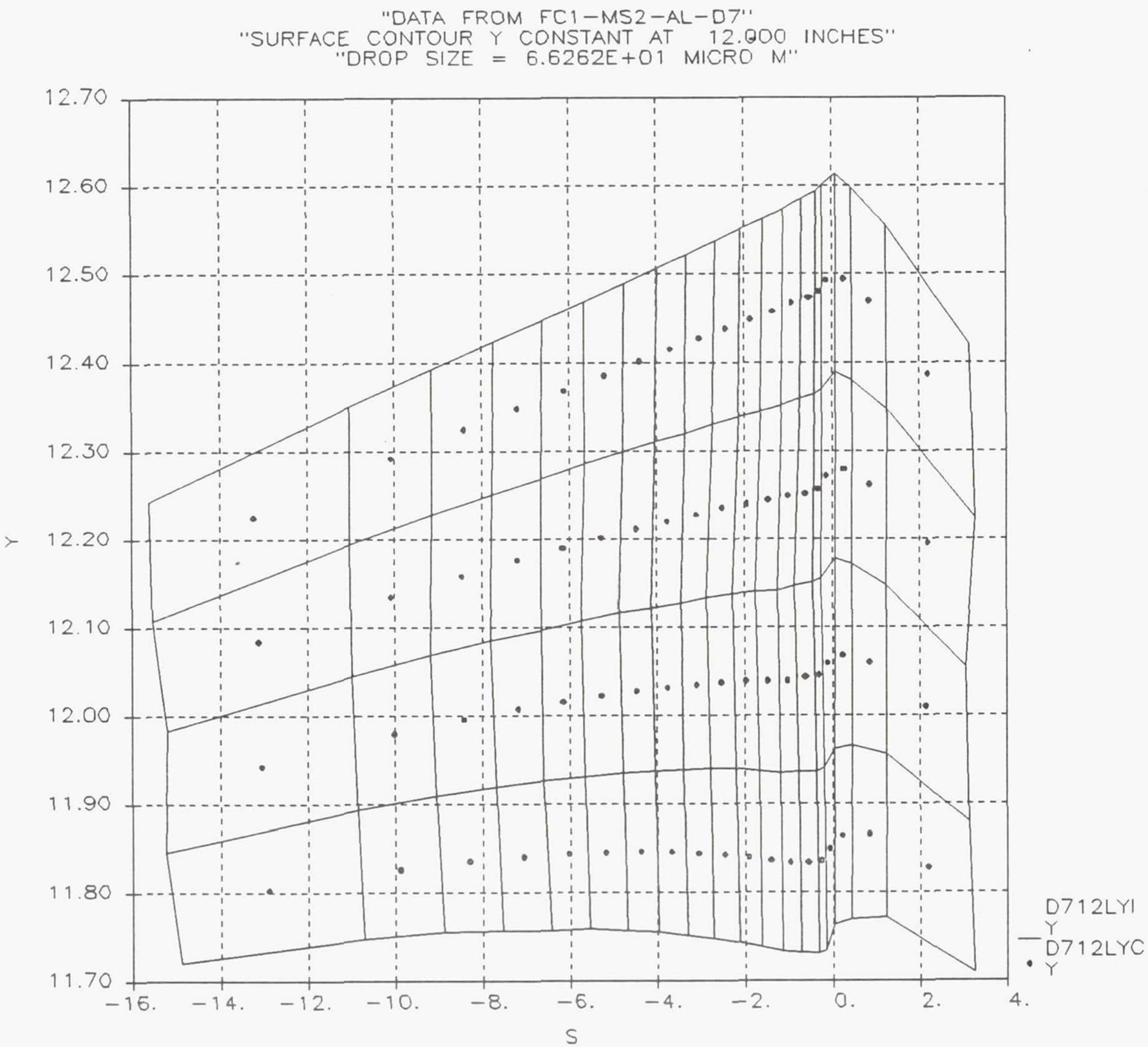

FIGURE D.23

IMPINGEMENT FIELD Y(in) vs S(in), FC1,Y=12L,D=66.3 micron

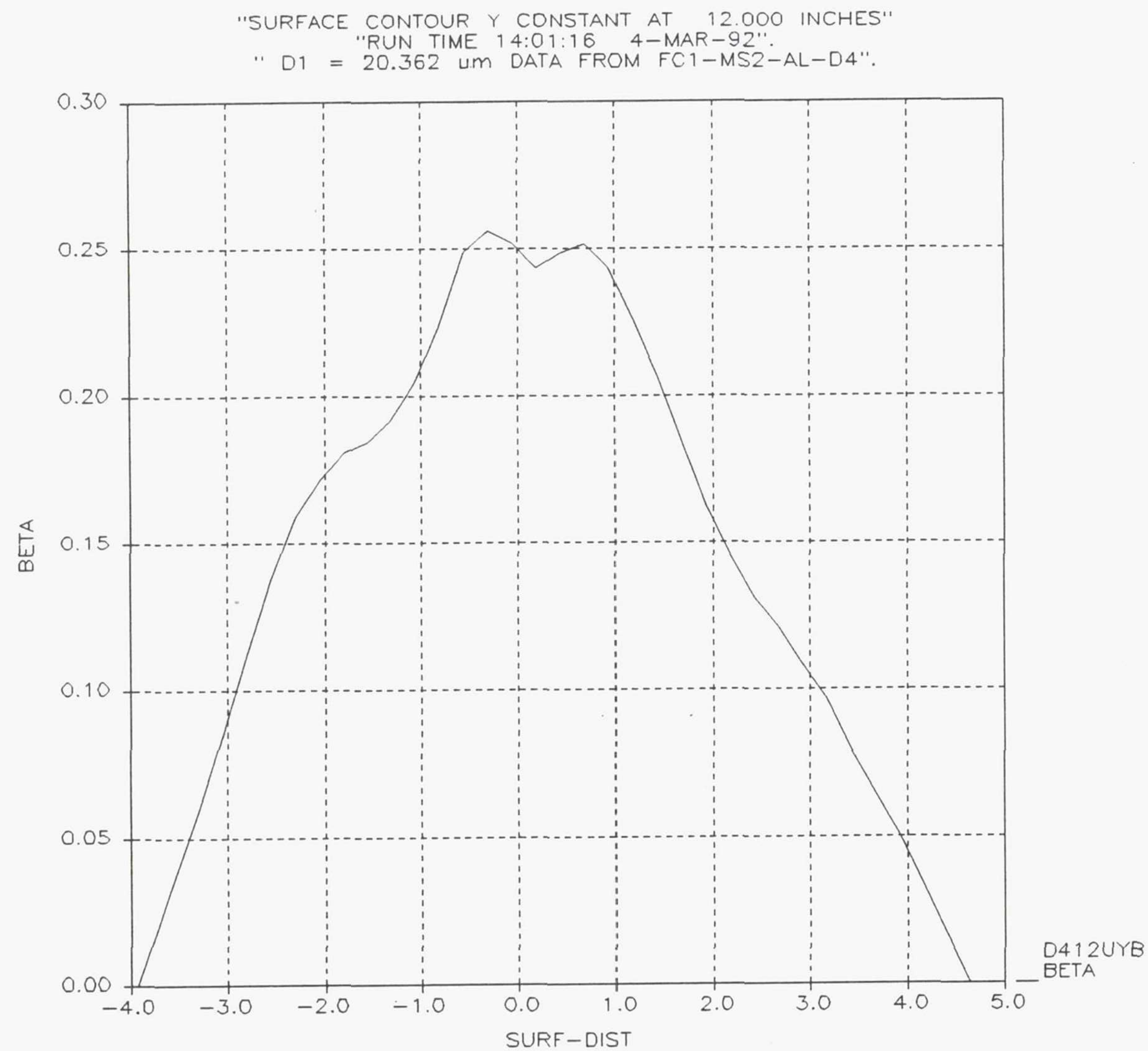

FIGURE D.24

BETA vs SURF-DIST(cm), FC1,Y=12U,D=20.4 micron

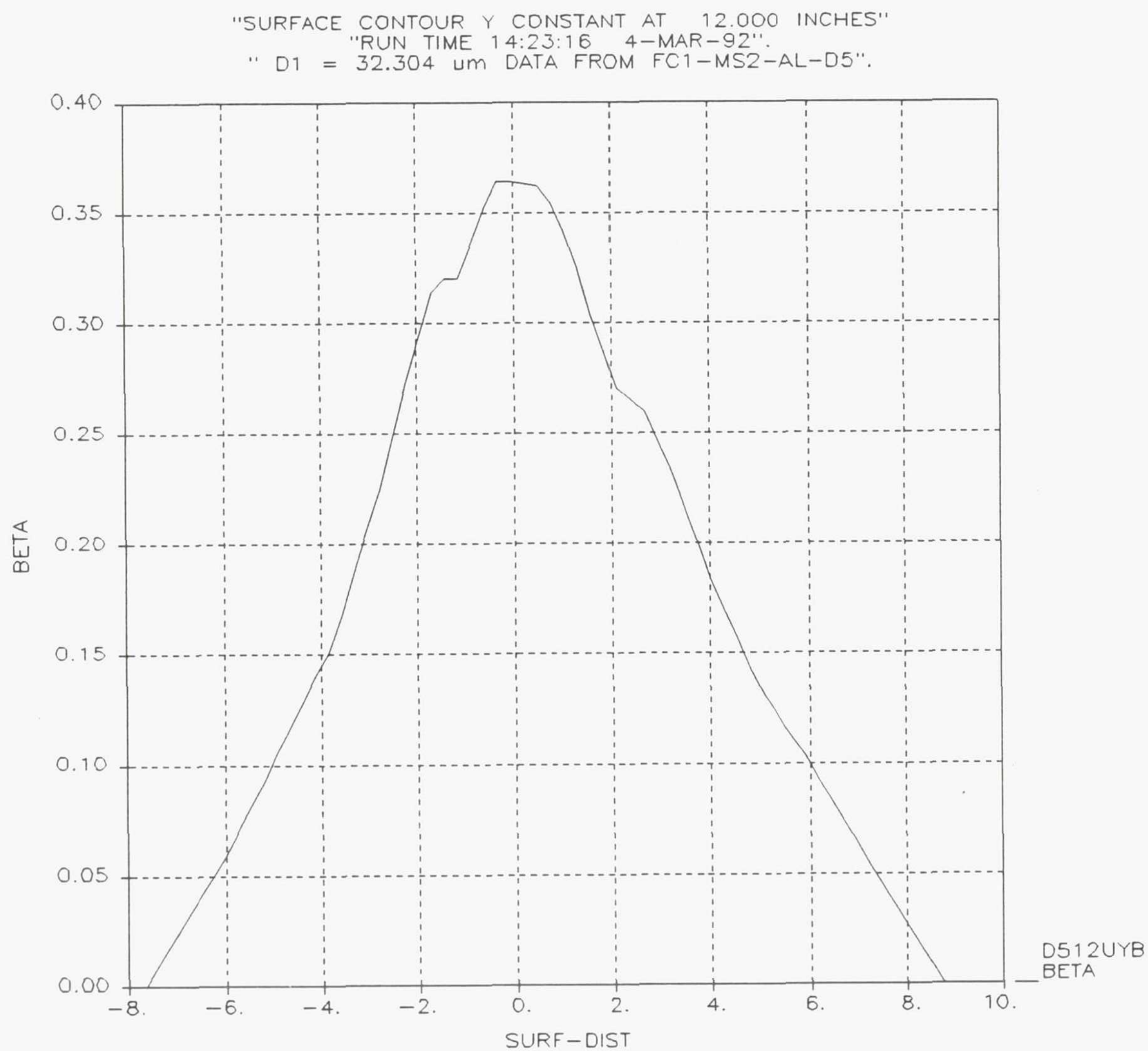

FIGURE D.25

BETA vs SURF-DIST(cm), FC1,Y=12U,D=32.3 micron

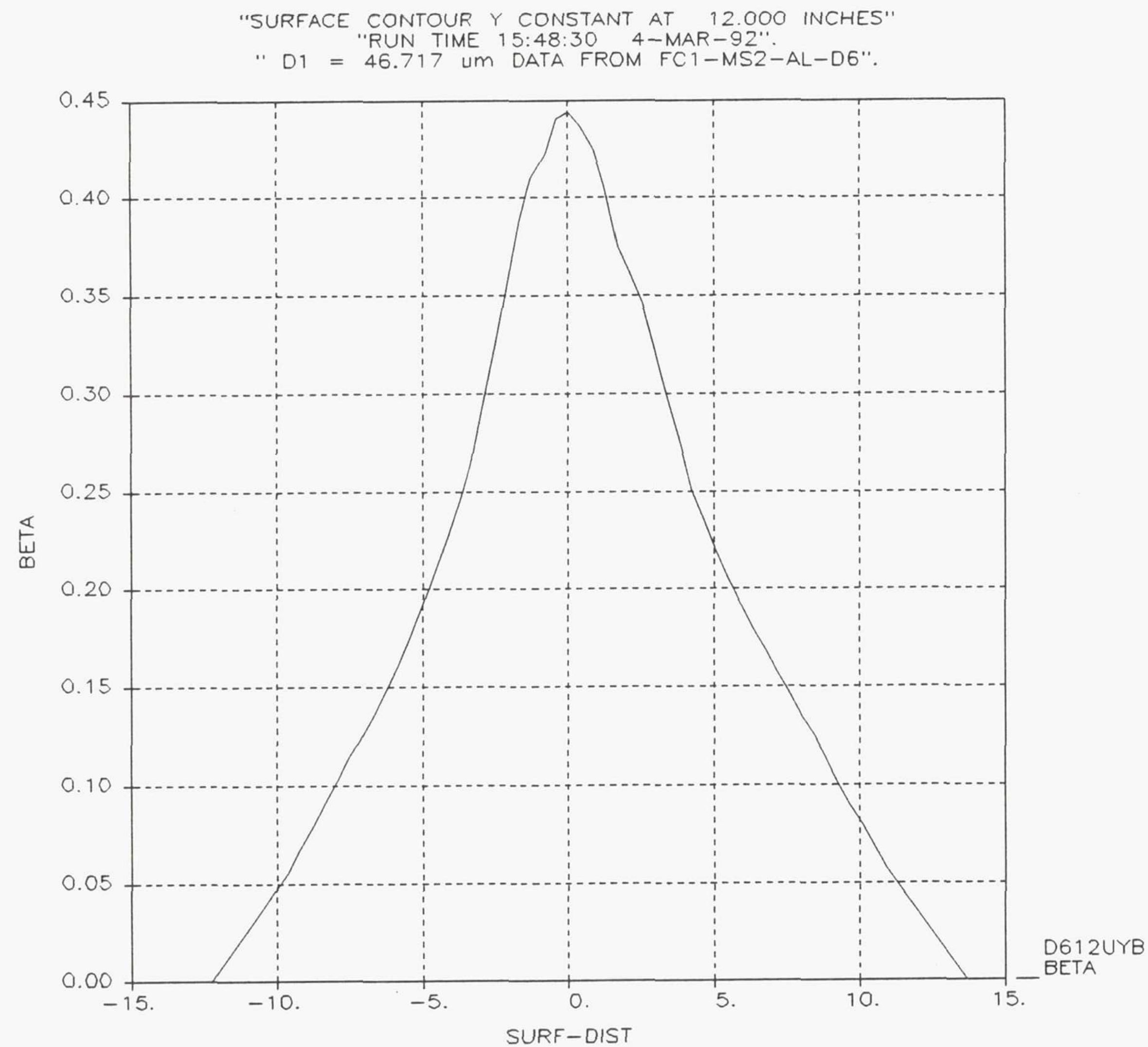

FIGURE D.26

BETA vs SURF-DIST(cm), FC1,Y=12U,D=46.7 micron

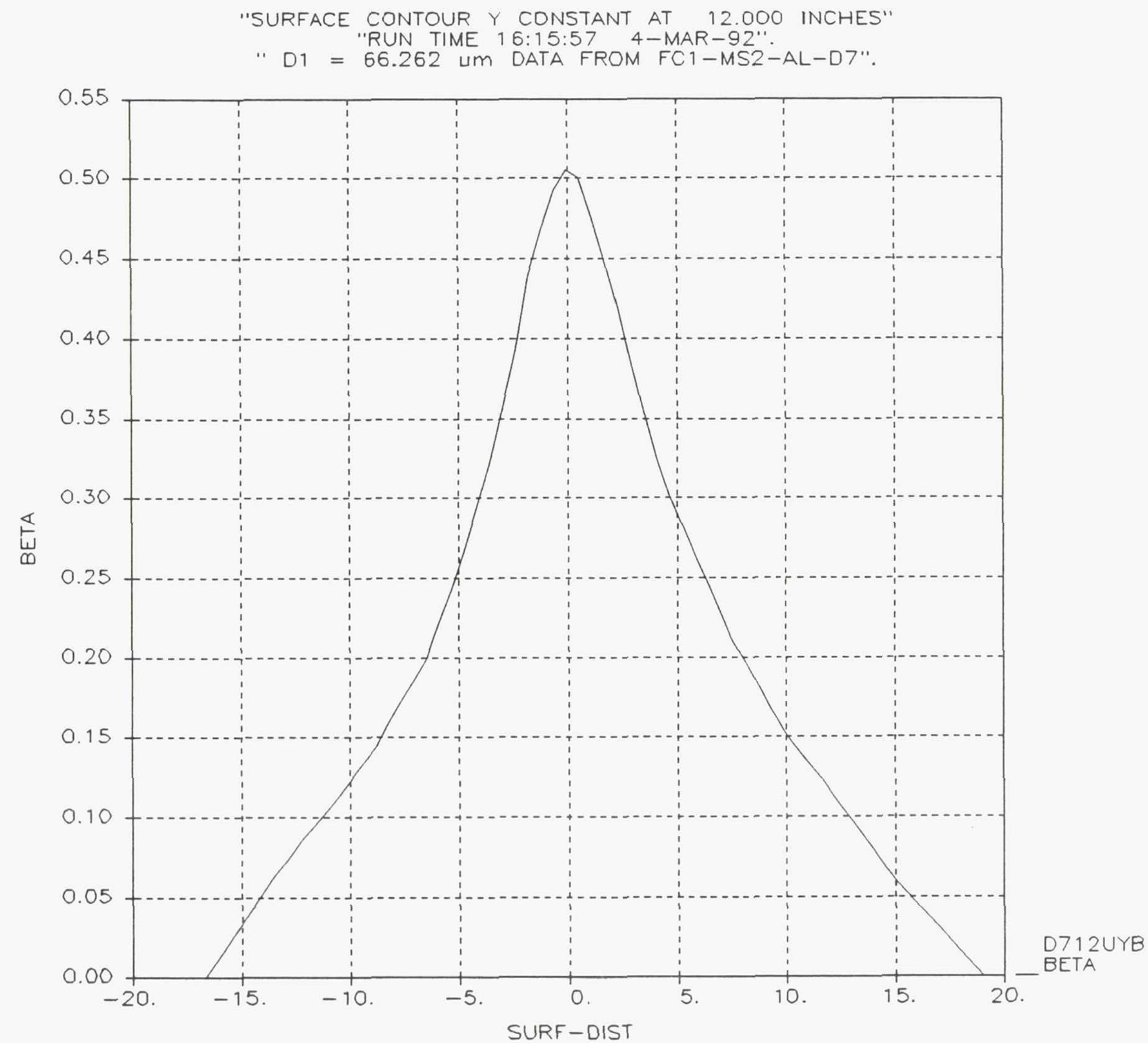

FIGURE D.27

BETA vs SURF-DIST(cm), FC1,Y=12U,D=66.3 micron

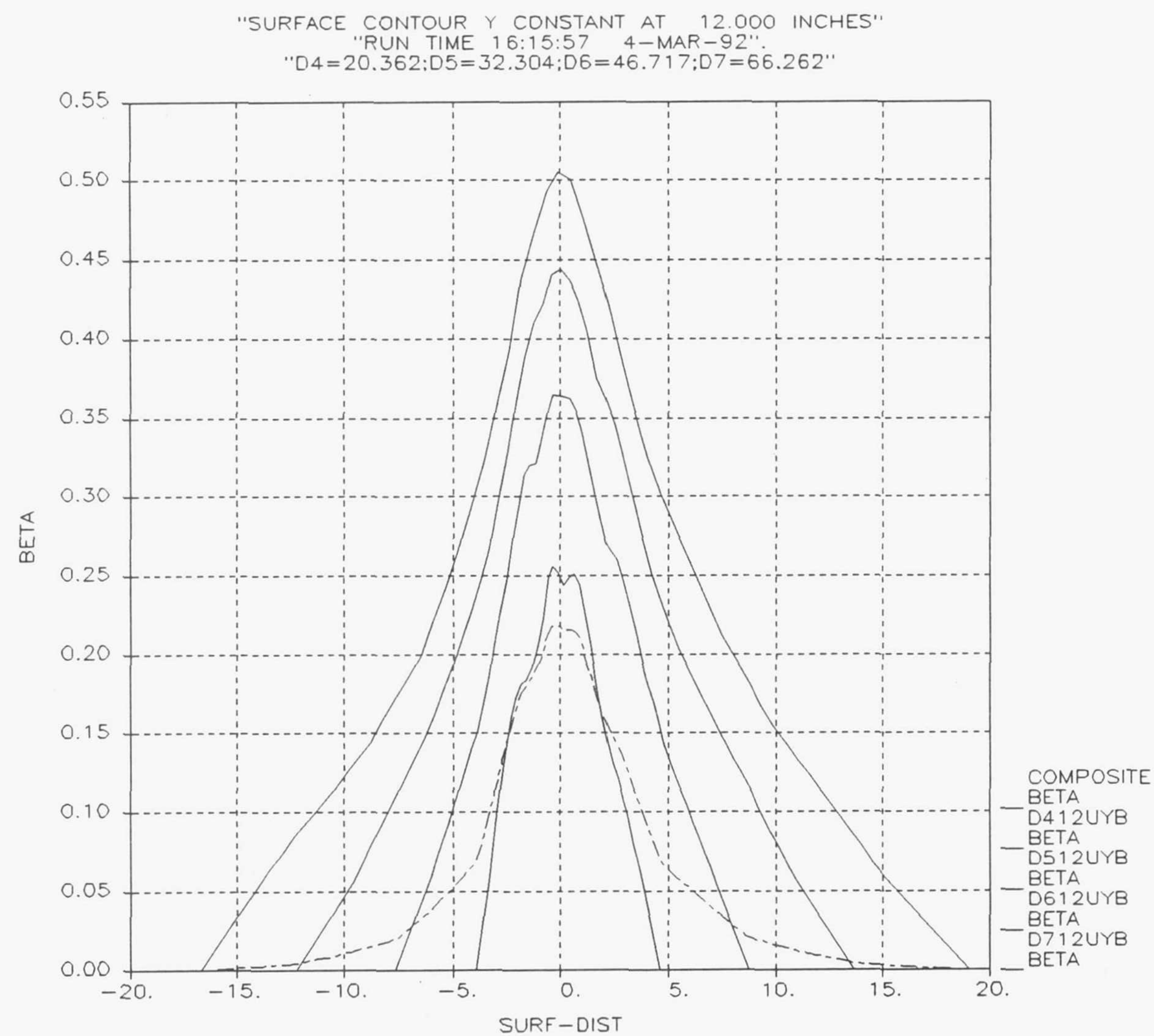

FIGURE D.28

BETA vs SURF-DIST(cm), FC1,Y=12U,COMPOSITE AND INDIVIDUAL DROPS

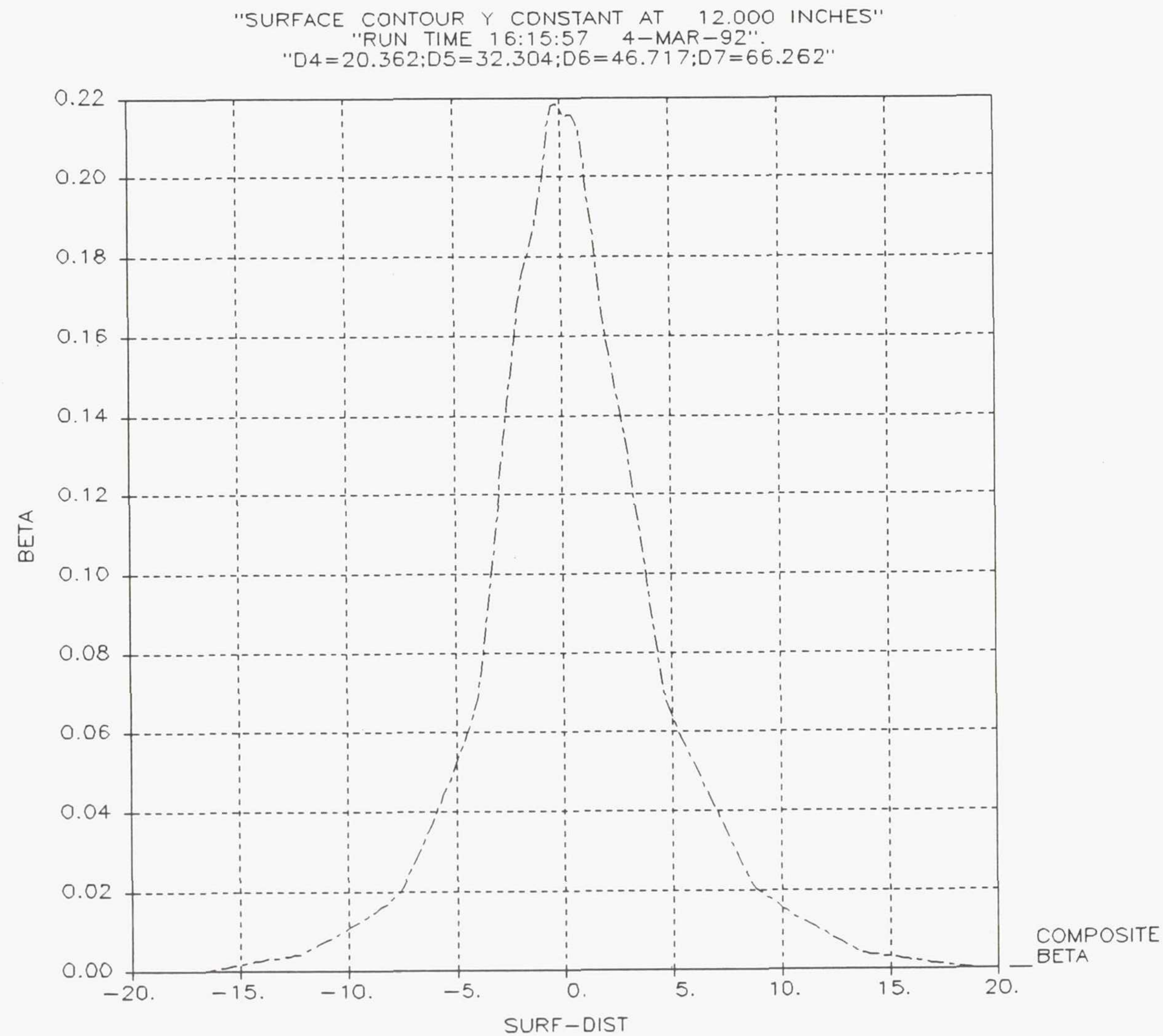

FIGURE D.29

BETA vs SURF-DIST(cm), FC1,Y=12U,D=20.4 micron
COMPOSITE DROP

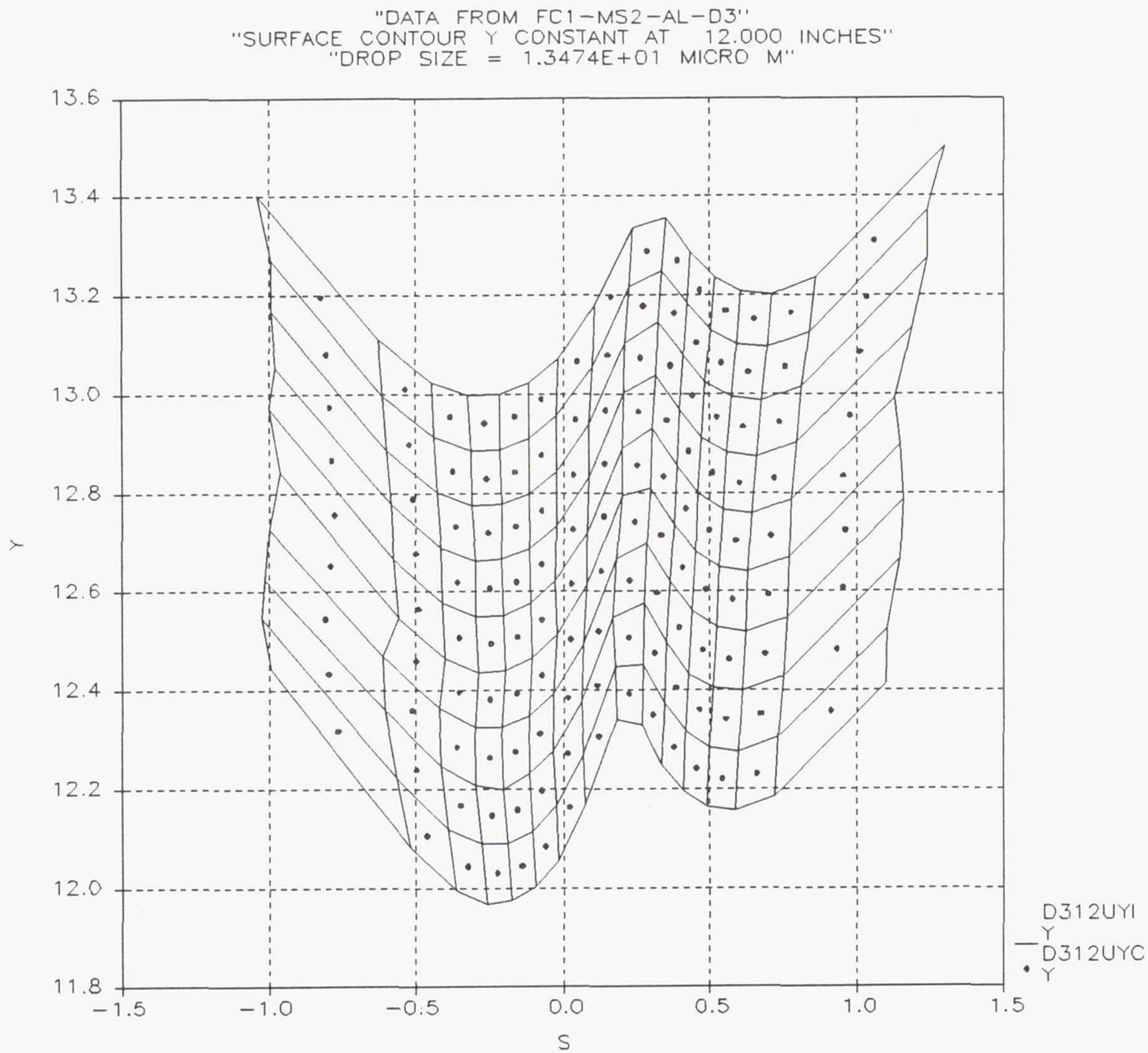

FIGURE D.30

IMPINGEMENT FIELD Y(in) vs S(in), FC1,Y=12U,D=13.5 micron

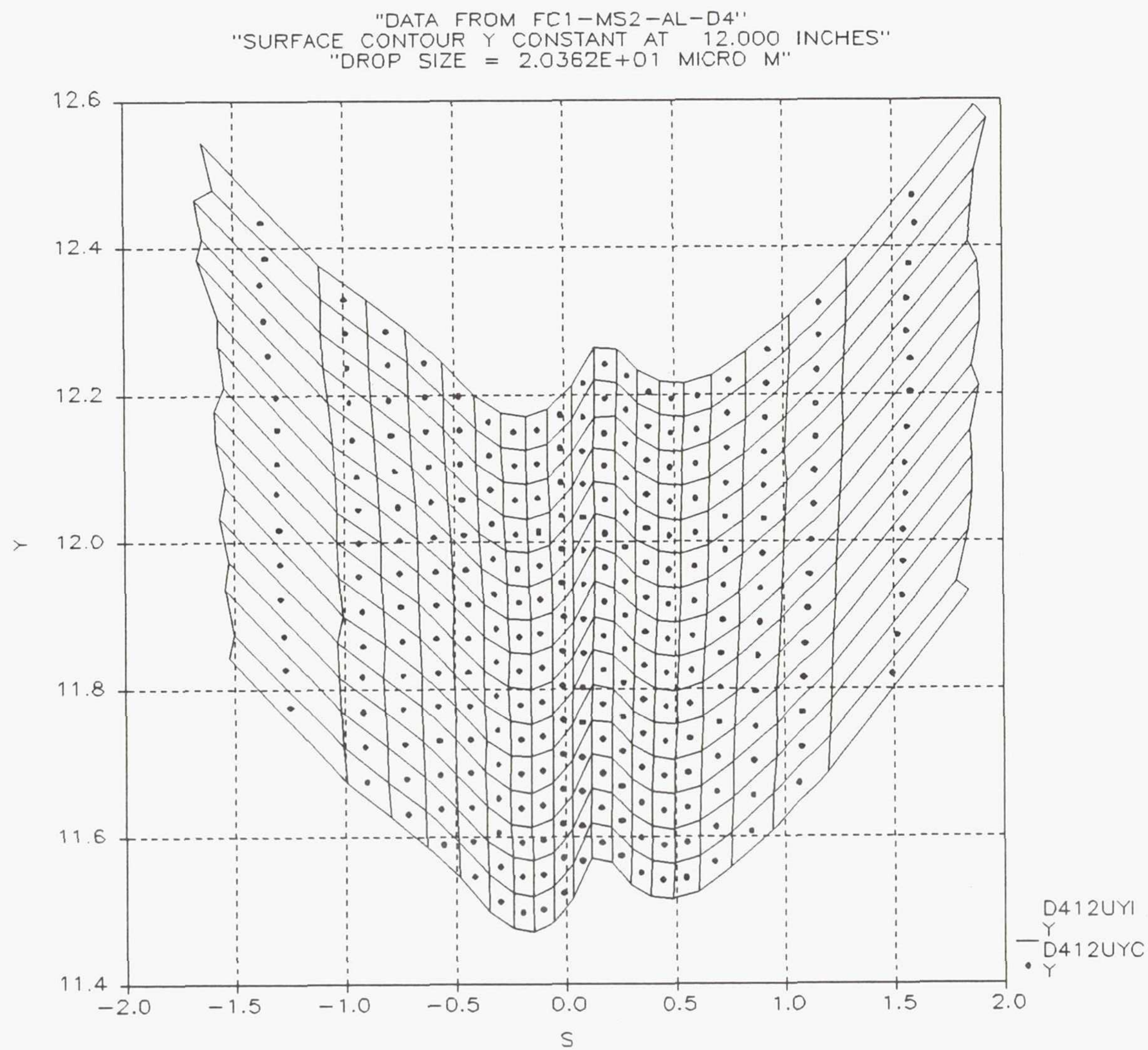

FIGURE D.31

IMPINGEMENT FIELD Y(in) vs S(in), FC1,Y=12U,D=20.4 micron

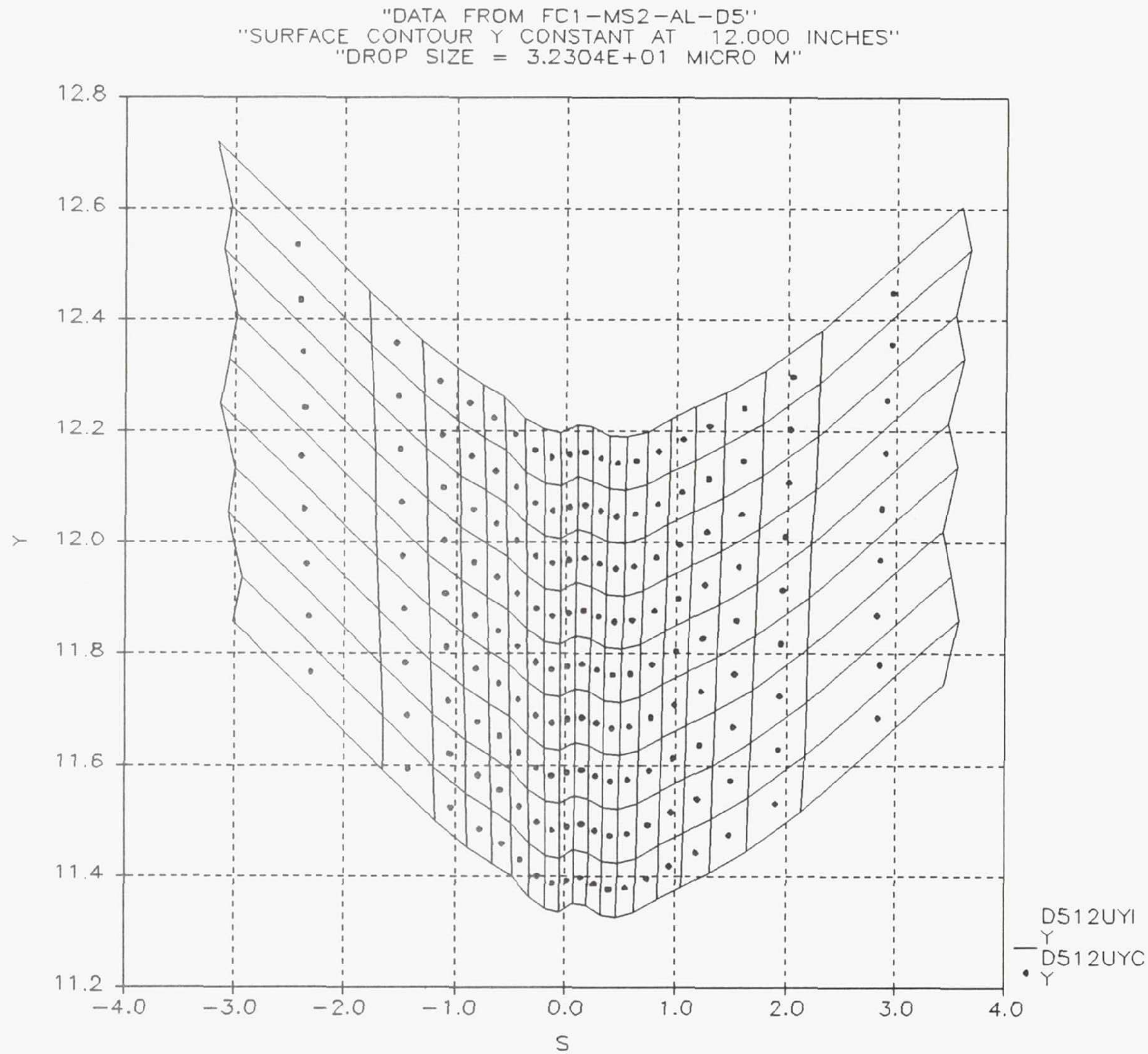

FIGURE D.32

IMPINGEMENT FIELD Y(in) vs S(in), FC1,Y=12U,D=32.3 micron

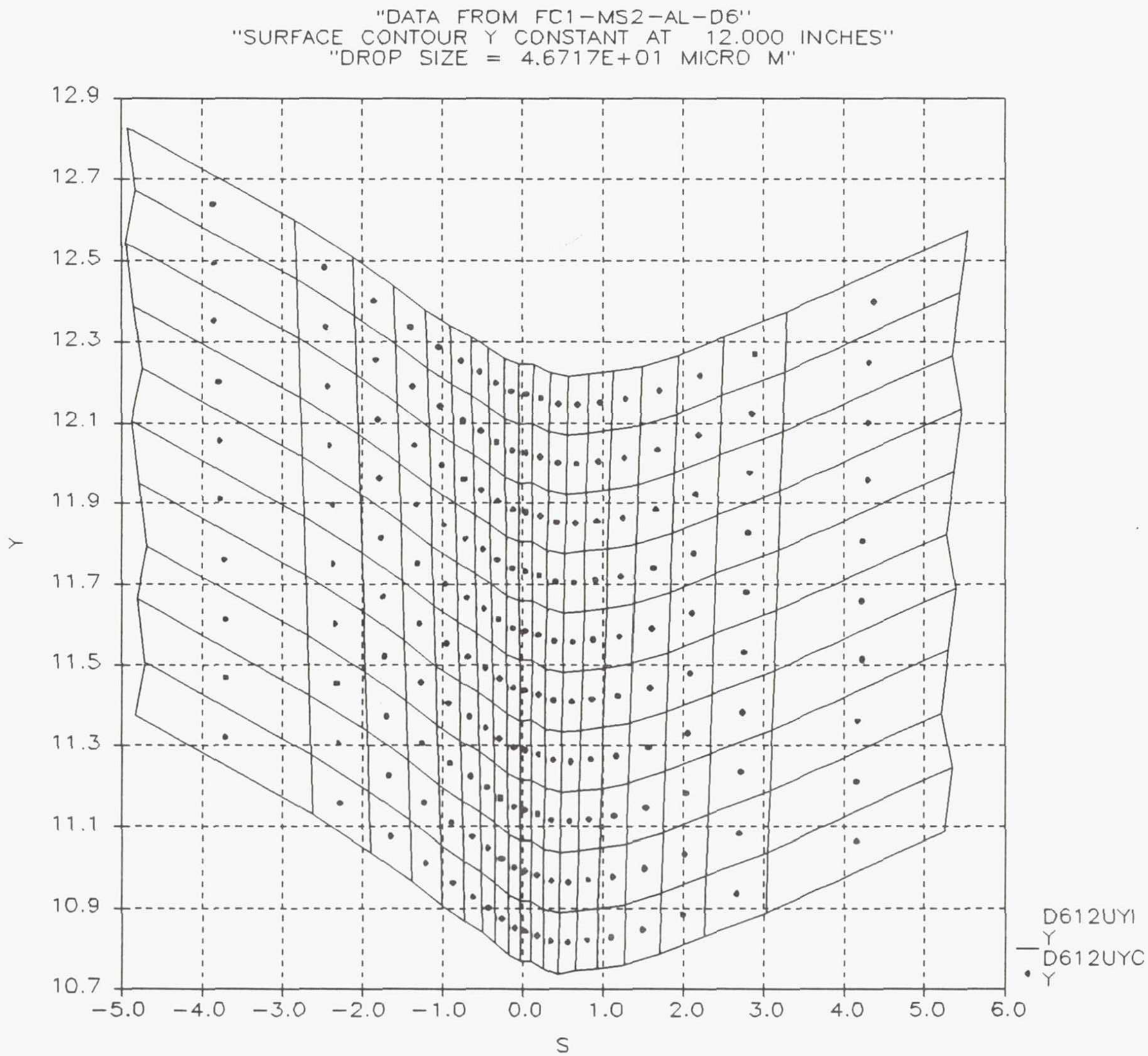

FIGURE D.33

IMPINGEMENT FIELD Y(in) vs S(in), FC1,Y=12U,D=46.7 micron

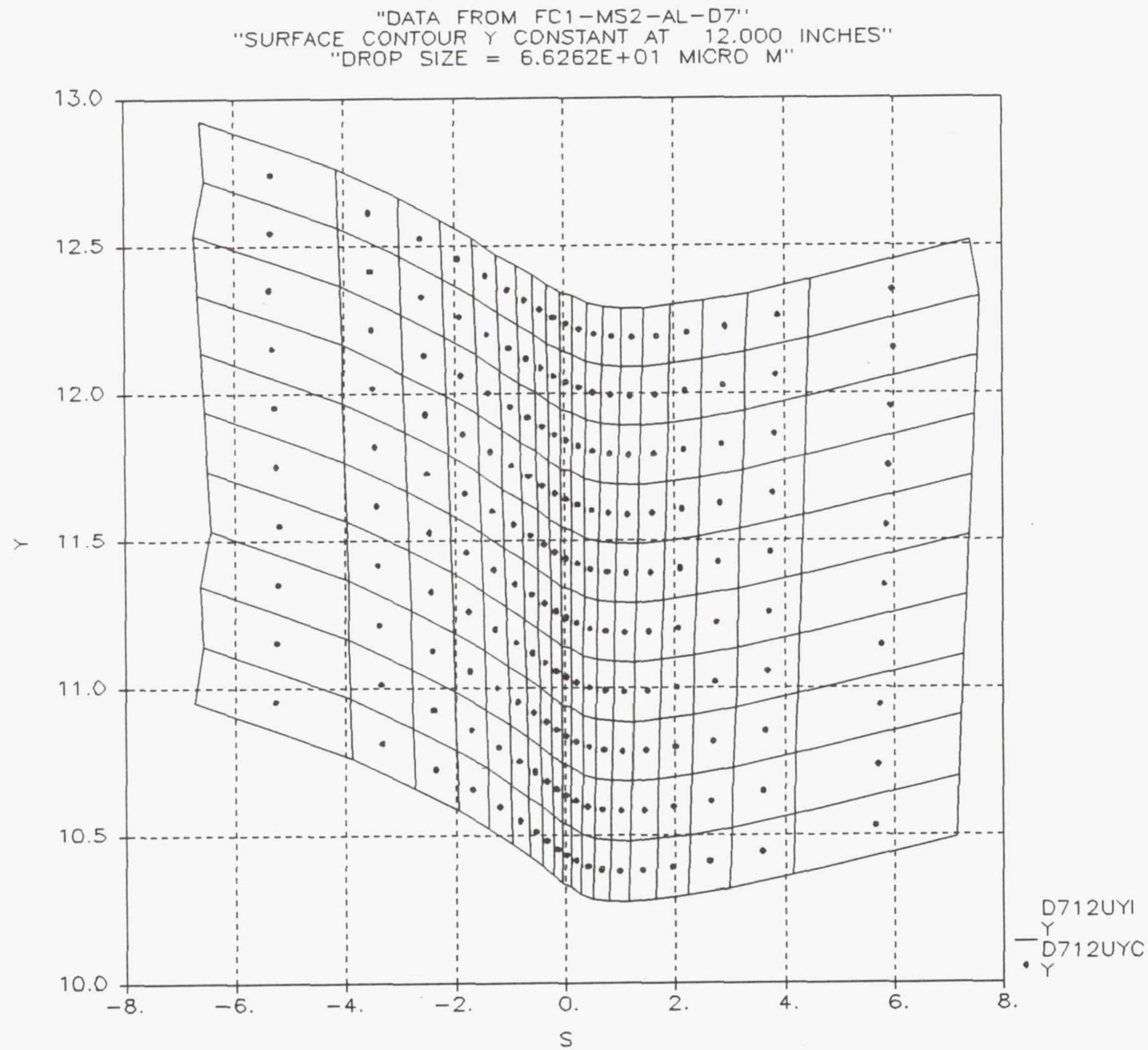

FIGURE D.34

IMPINGEMENT FIELD Y(in) vs S(in), FC1,Y=12U,D=66.3 micron

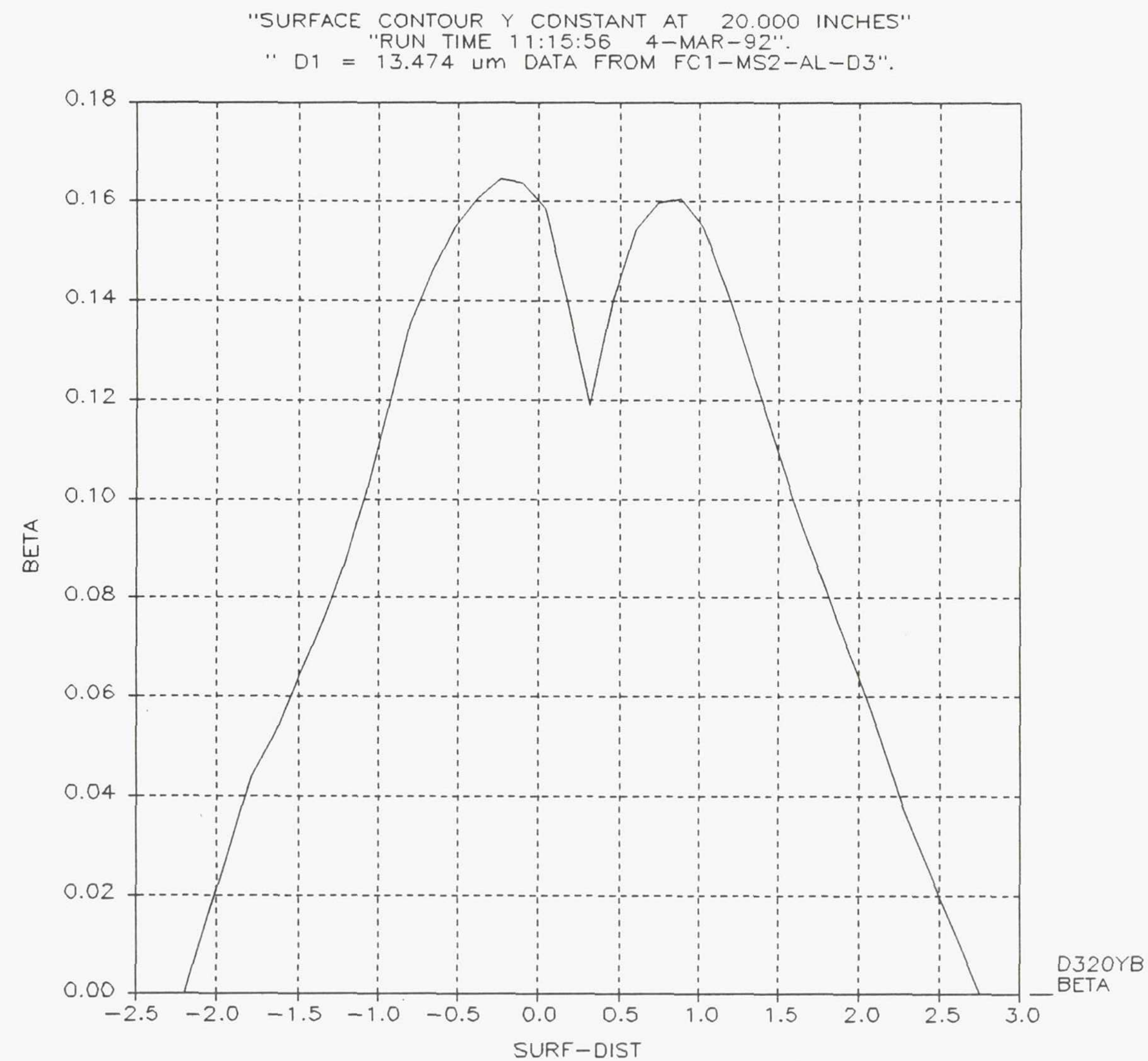

FIGURE D.35

BETA vs SURF-DIST(cm), FC1,Y=20,D=13.5 micron

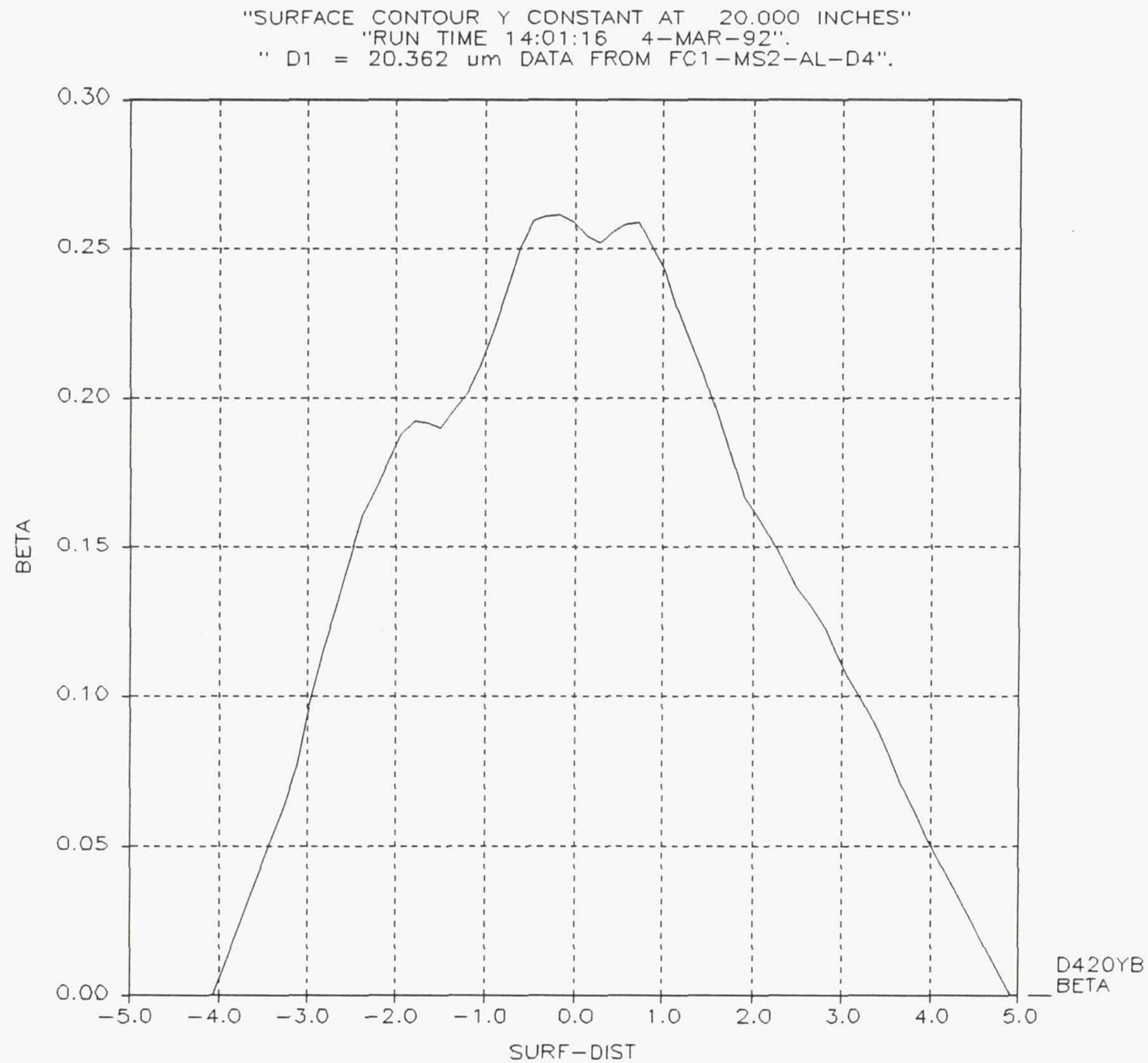

FIGURE D.36

BETA vs SURF-DIST(cm), FC1,Y=20,D=20.4 micron

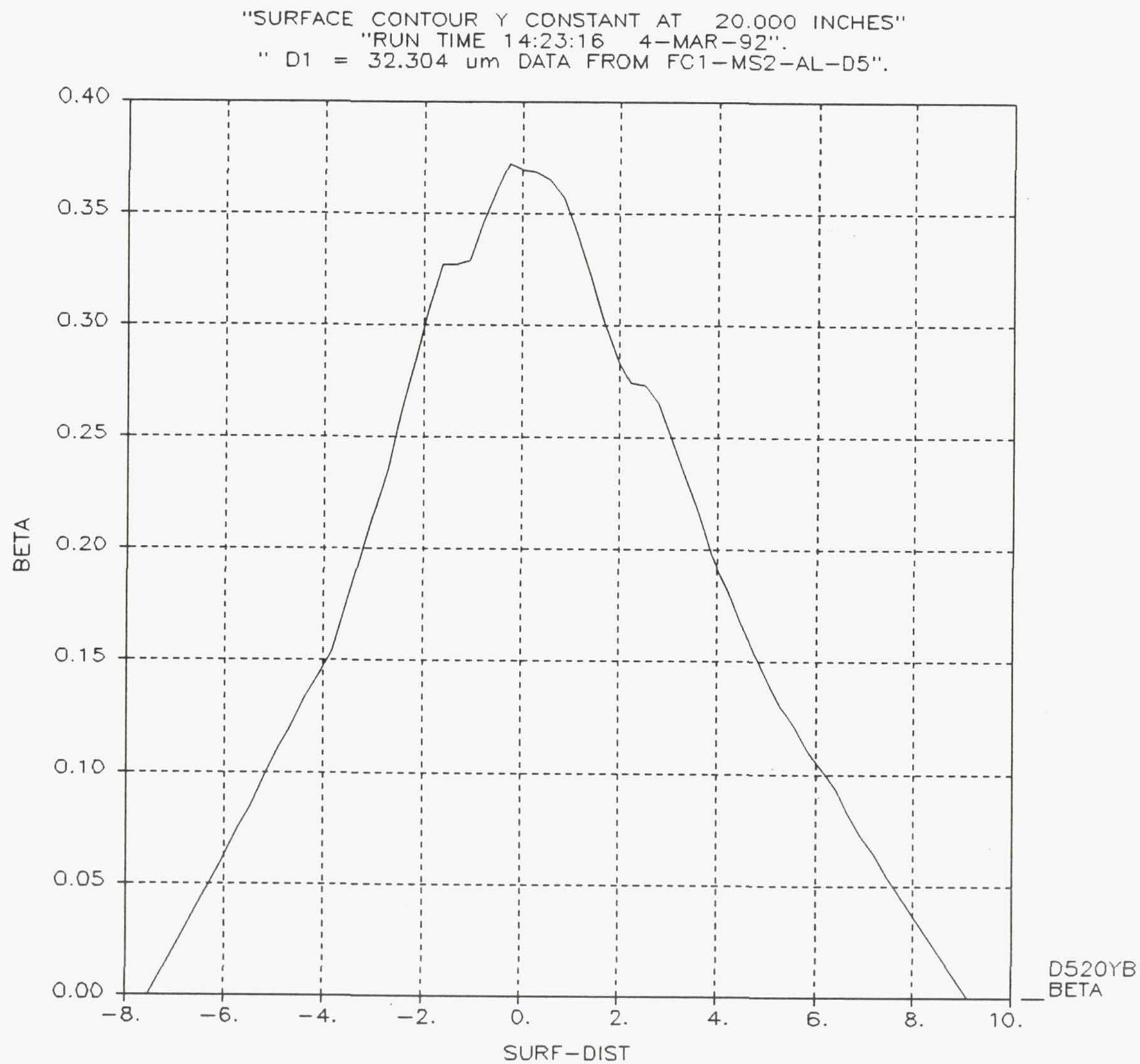

FIGURE D.37

BETA vs SURF-DIST(cm), FC1,Y=20,D=32.3 micron

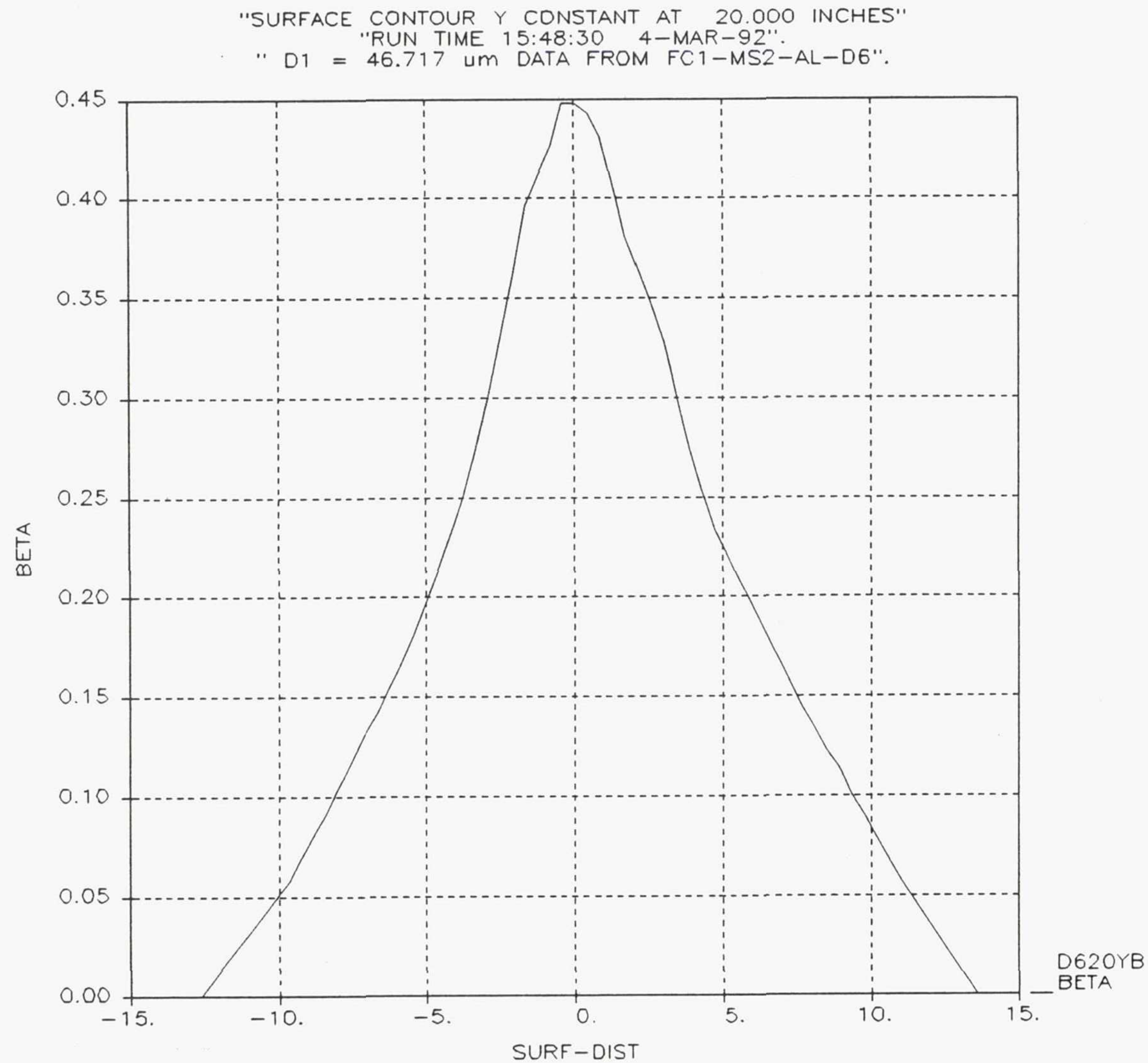

FIGURE D.38

BETA vs SURF-DIST(cm), FC1,Y=20,D=46.7 micron

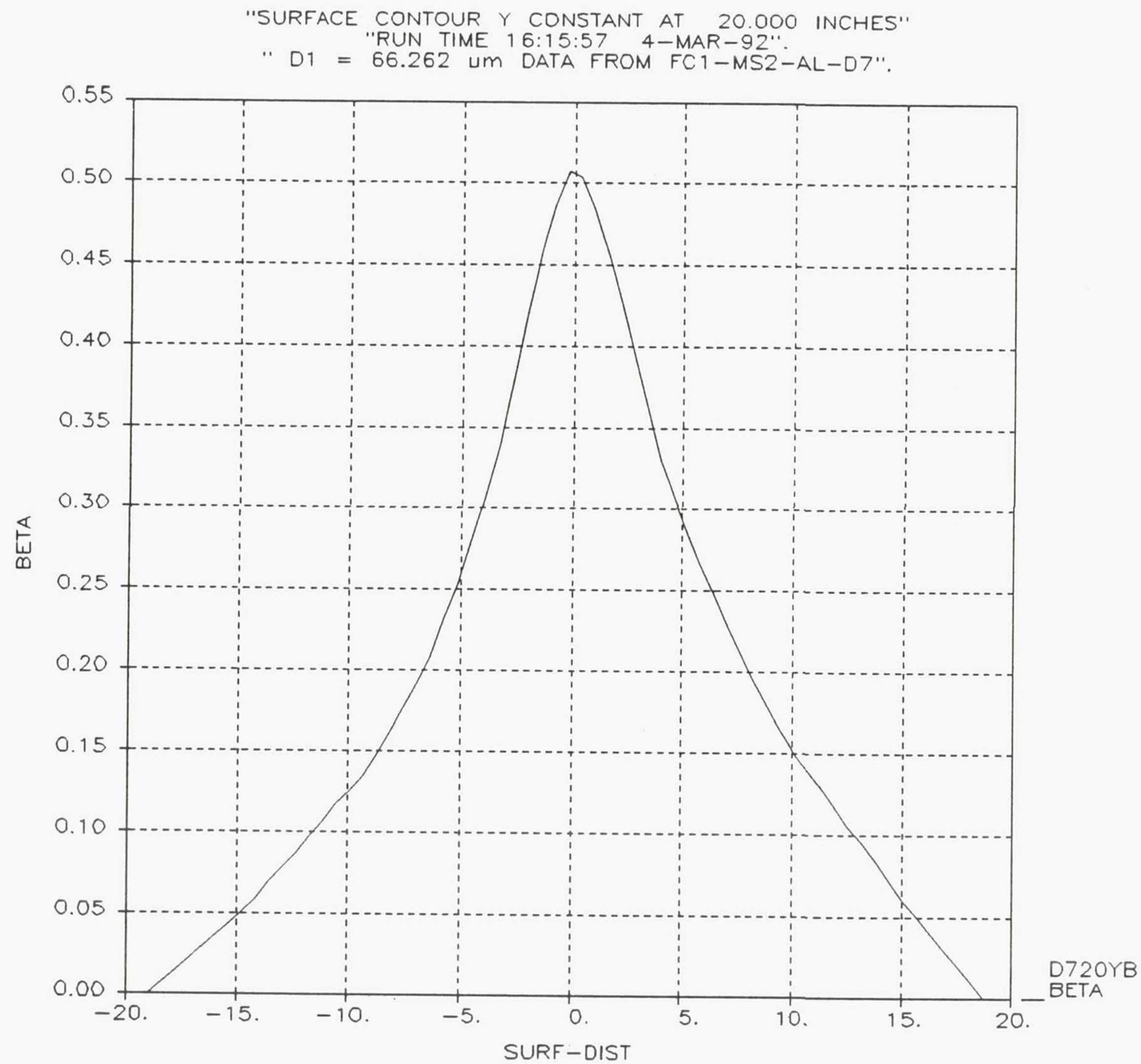

FIGURE D.39

BETA vs SURF-DIST(cm), FC1,Y=20,D=66.3 micron

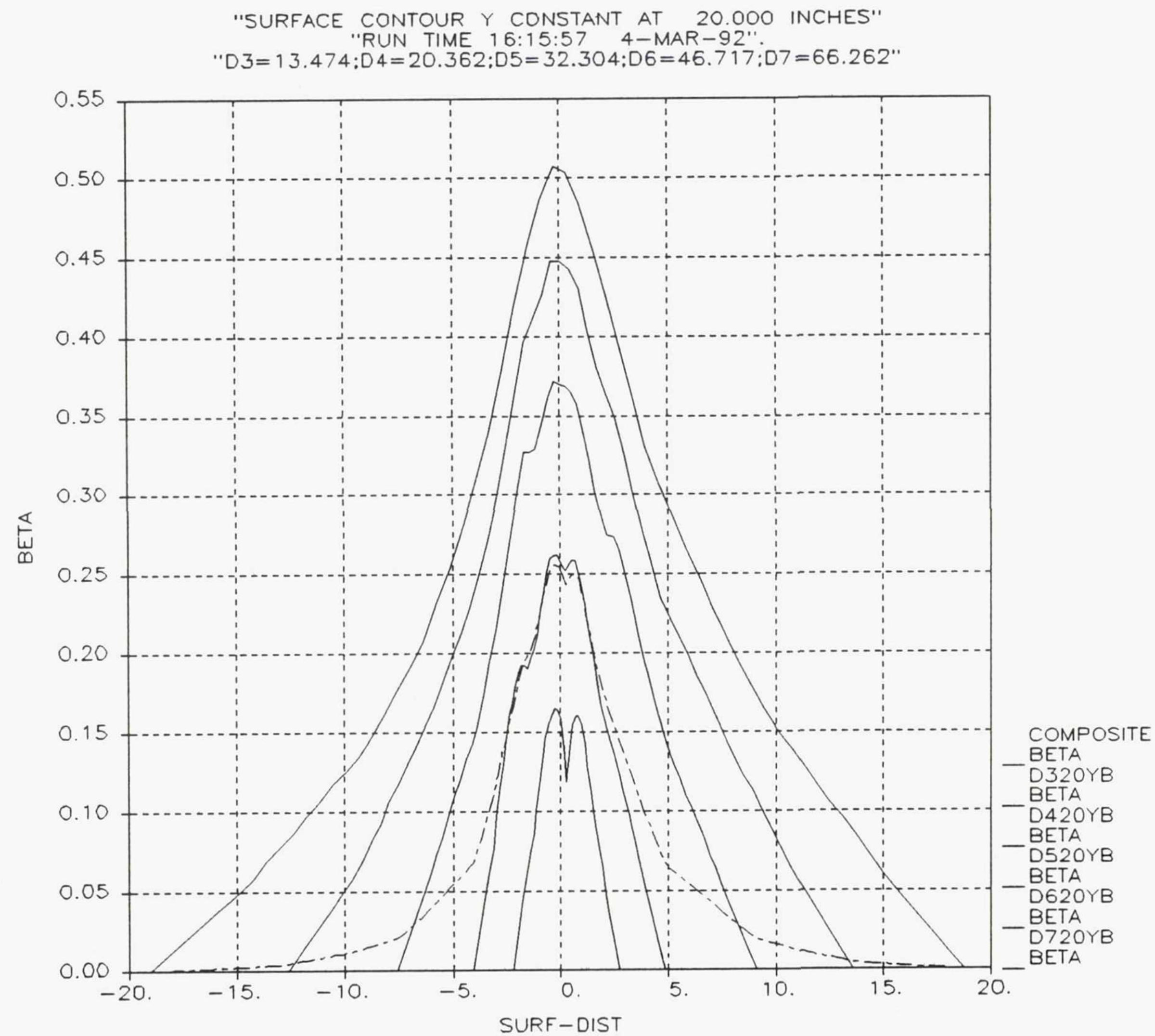

FIGURE D.40

BETA vs SURF-DIST(cm), FC1,Y=20,COMPOSITE AND INDIVIDUAL DROPS

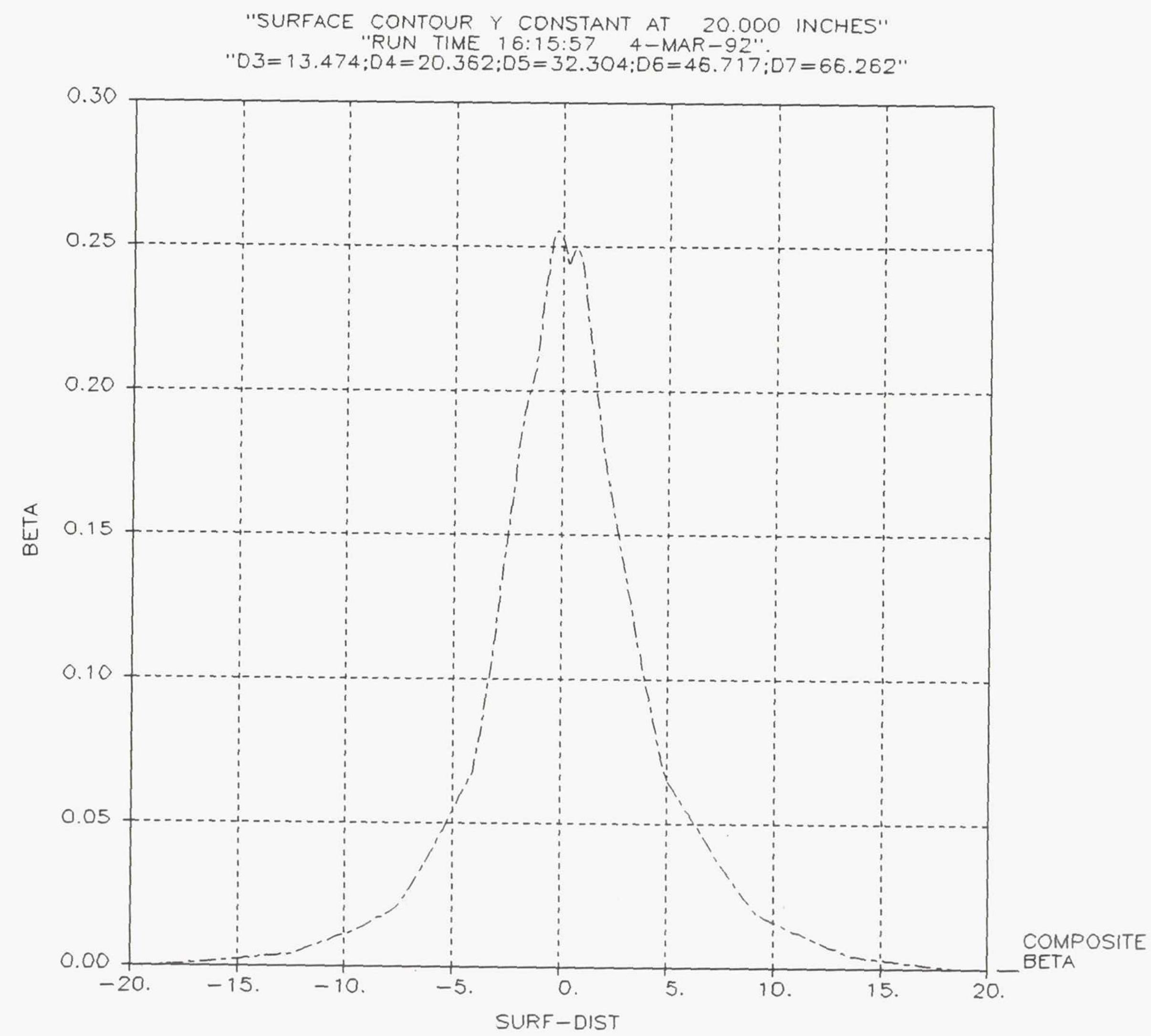

FIGURE D.41

BETA vs SURF-DIST(cm), FC1,Y=20,D=20.4 micron
COMPOSITE DROP

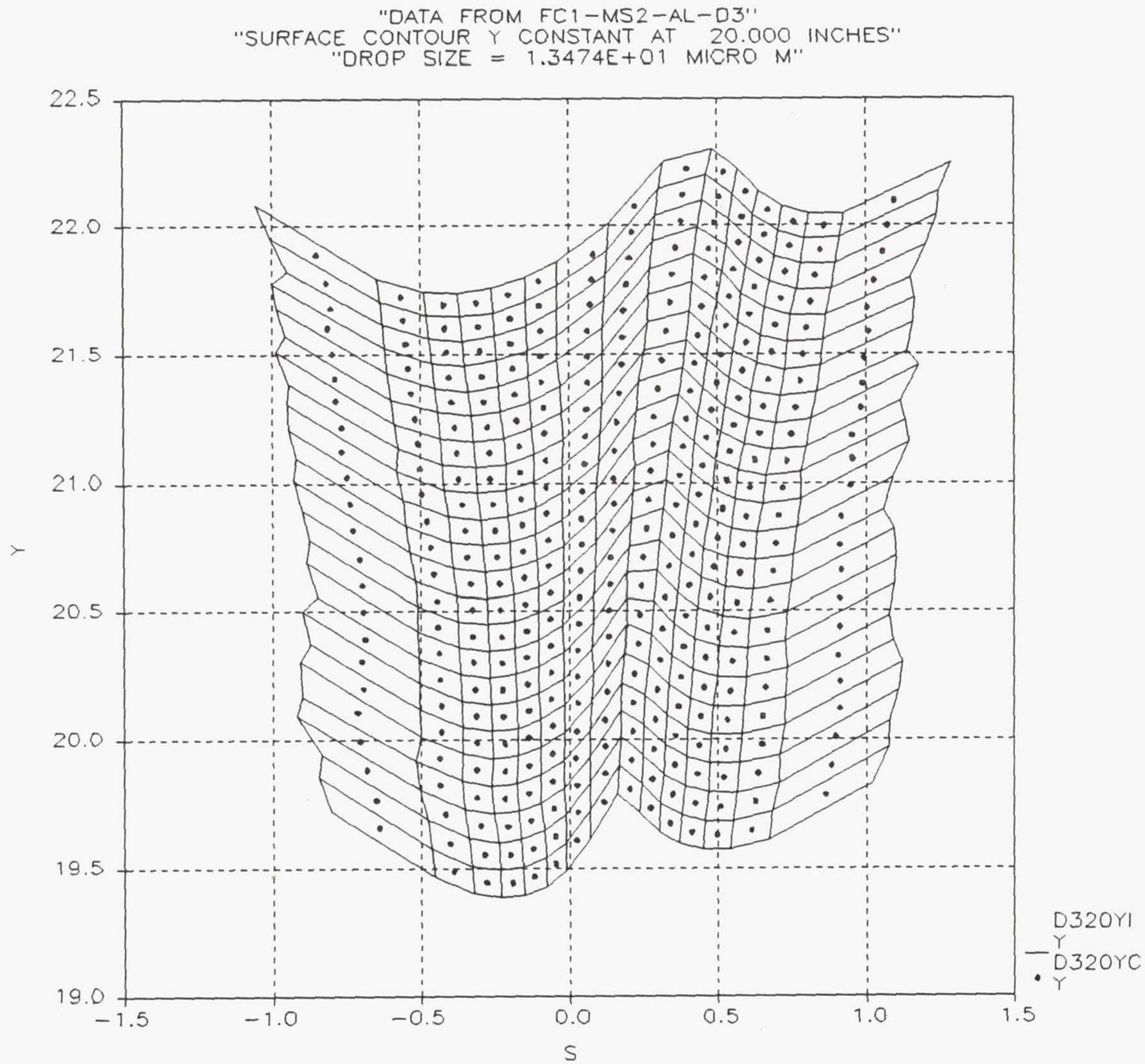

FIGURE D.42

IMPINGEMENT FIELD Y(in) vs S(in), FC1,Y=20,D=13.5 micron

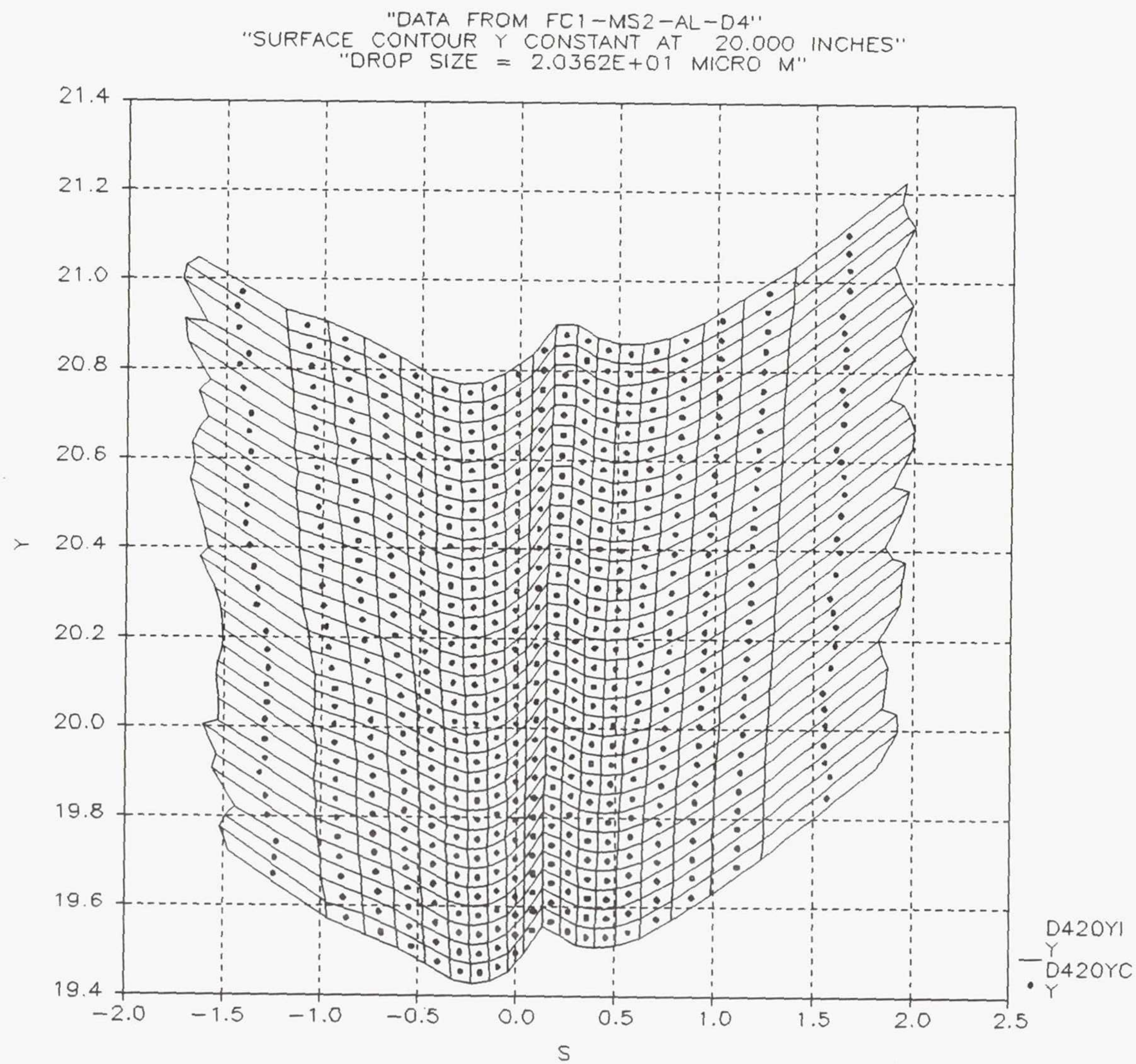

FIGURE D.43

IMPINGEMENT FIELD Y(in) vs S(in), FC1,Y=20,D=20.4 micron

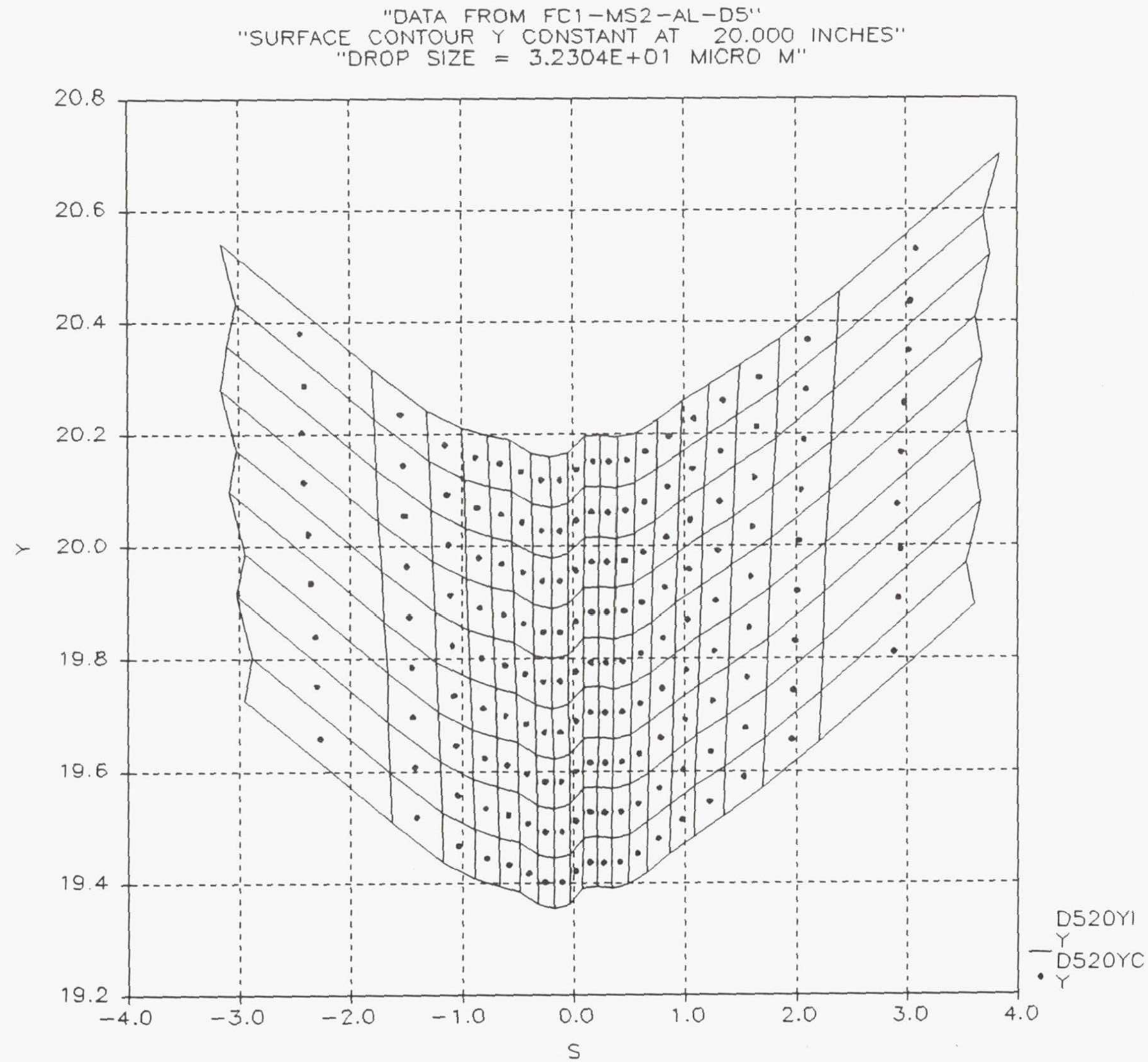

FIGURE D.44

IMPINGEMENT FIELD Y(in) vs S(in), FC1,Y=20,D=32.3 micron

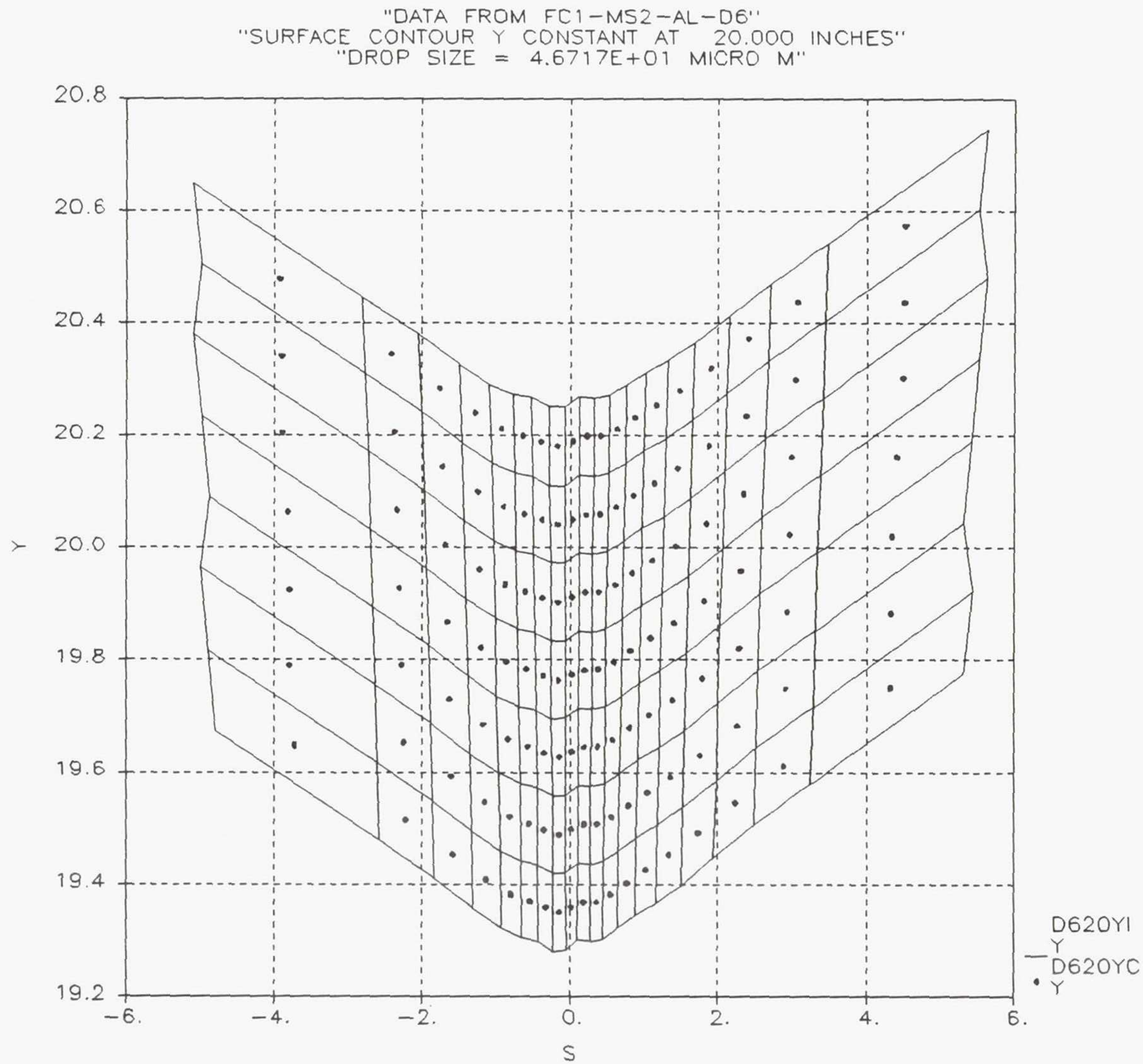

FIGURE D.45

IMPINGEMENT FIELD Y(in) vs S(in), FC1,Y=20,D=46.7 micron

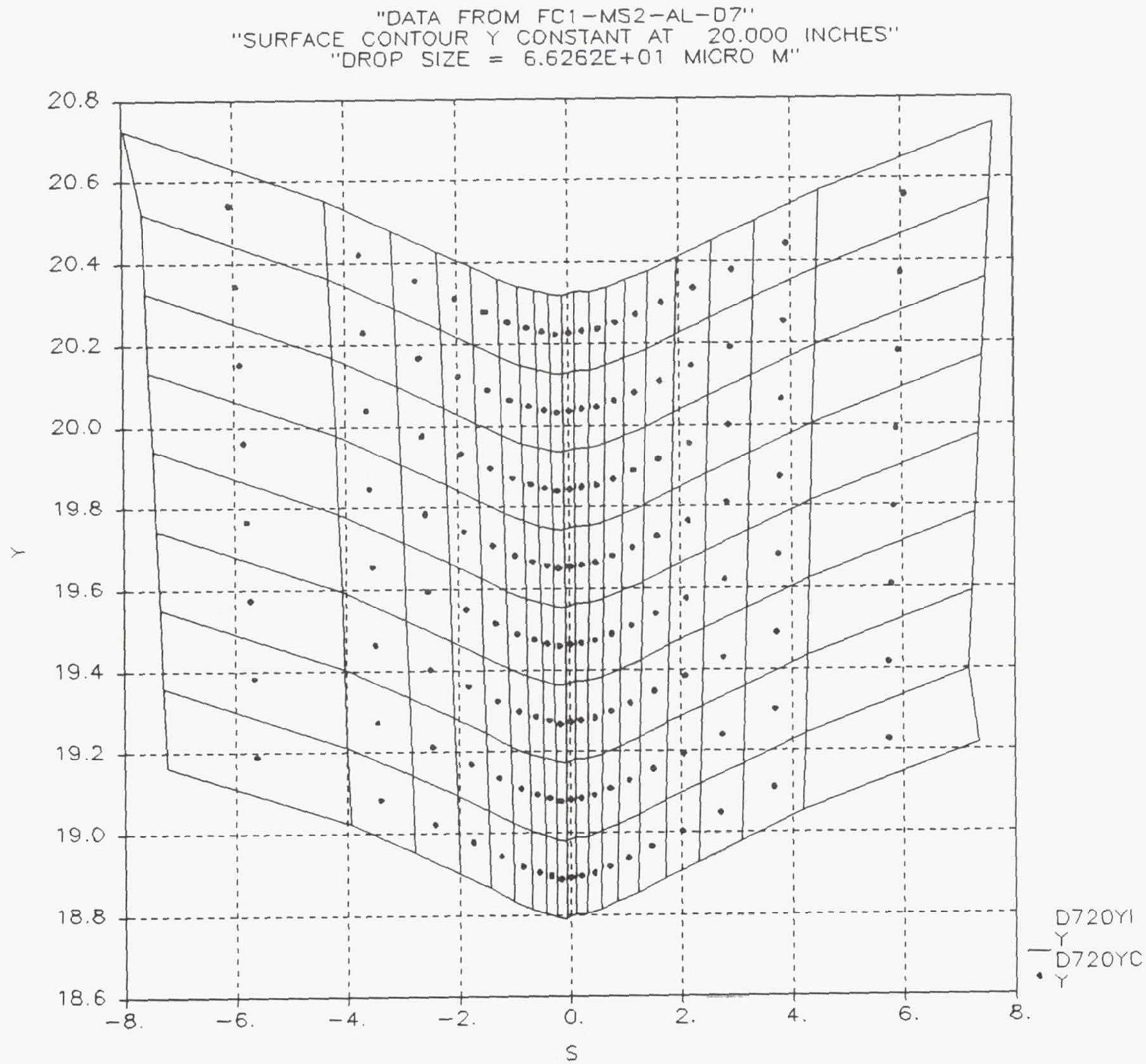

FIGURE D.46

IMPINGEMENT FIELD Y(in) vs S(in), FC1,Y=20,D=66.3 micron

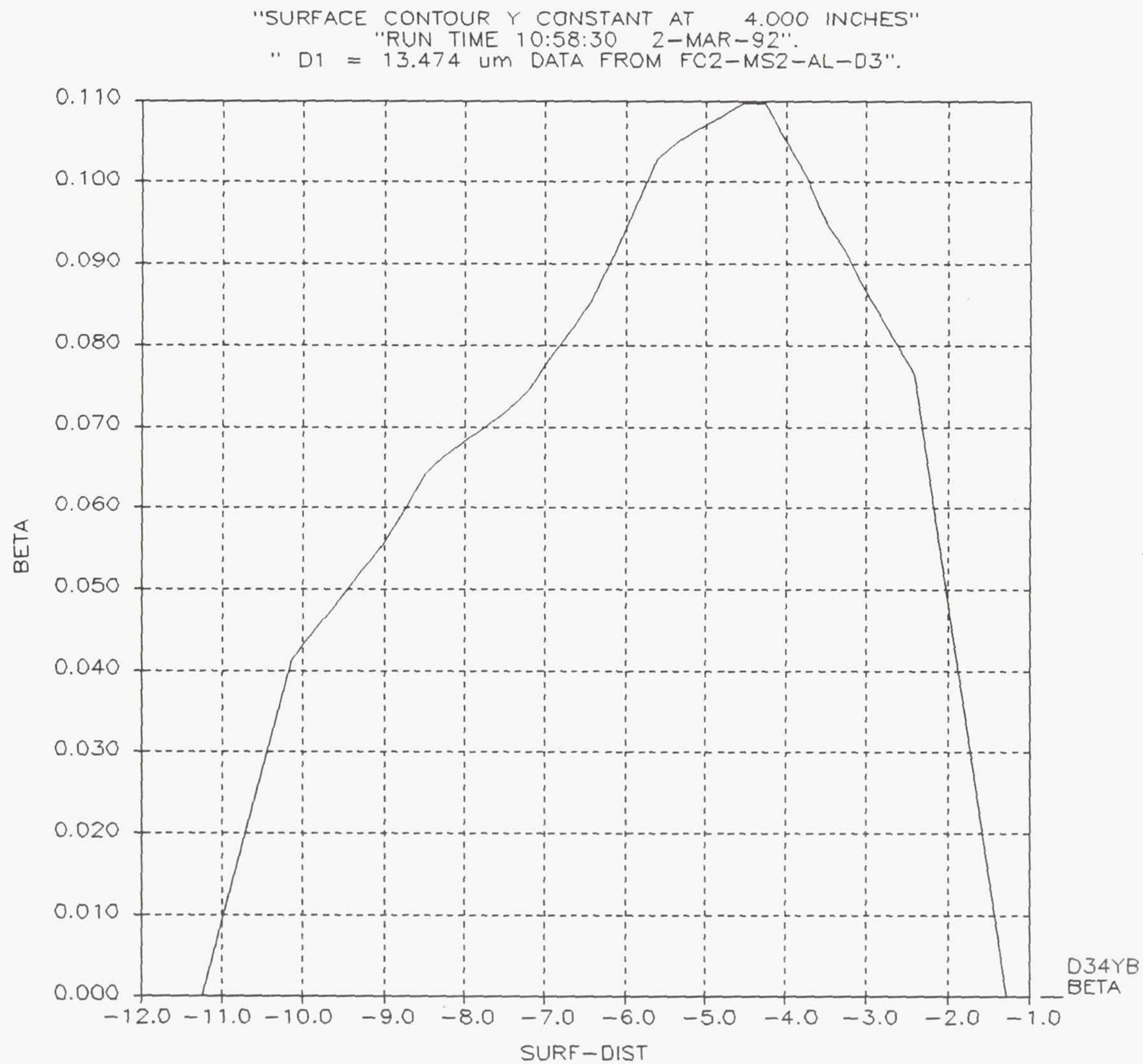

FIGURE D.47

BETA vs SURF-DIST(cm), FC2,Y=4,D=13.5 micron

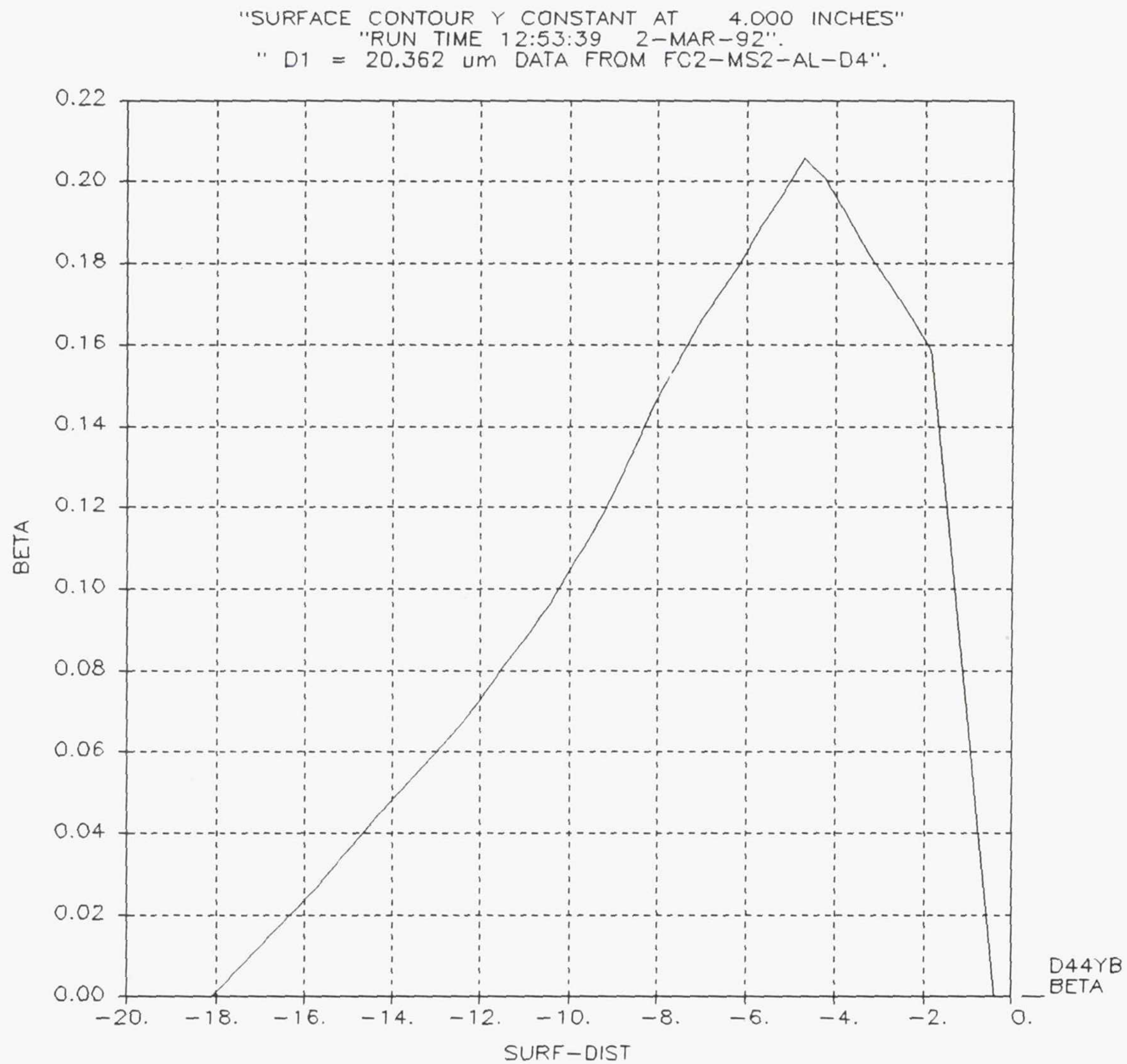

FIGURE D.48

BETA vs SURF-DIST(cm), FC2,Y=4,D=20.4 micron

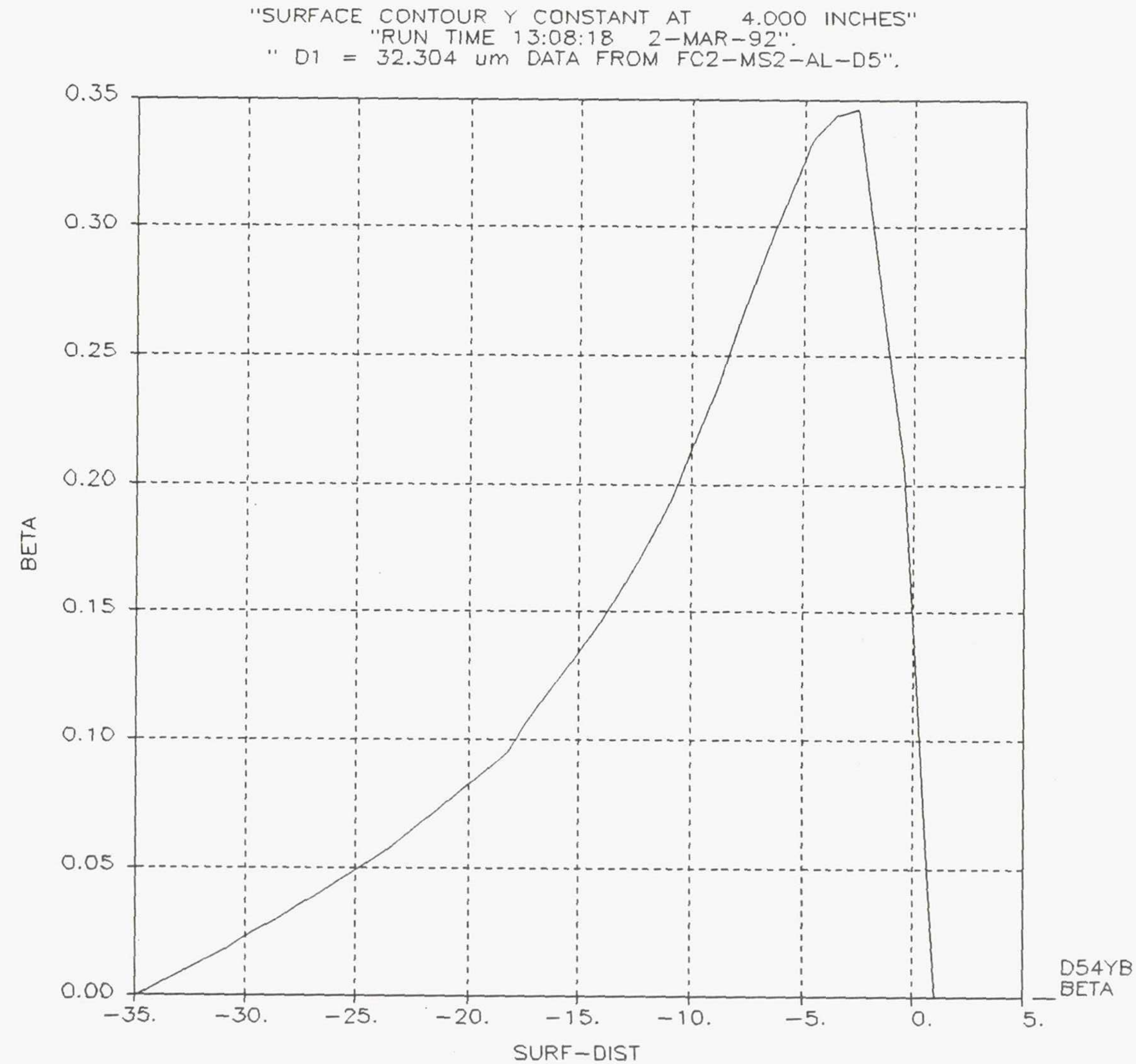

FIGURE D.49

BETA vs SURF-DIST(cm), FC2,Y=4,D=32.3 micron

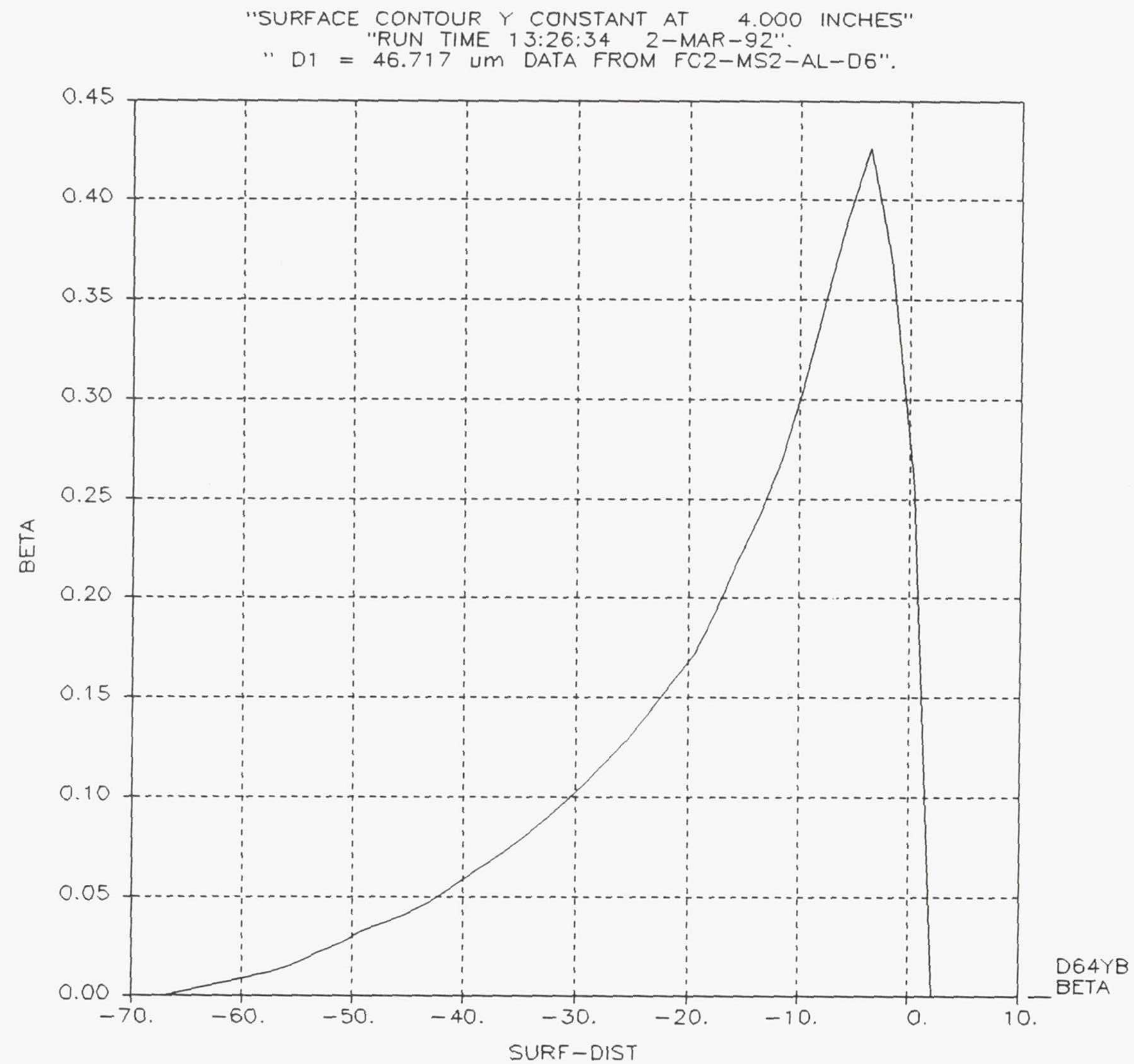

FIGURE D.50

BETA vs SURF-DIST(cm), FC2,Y=4,D=46.7 micron

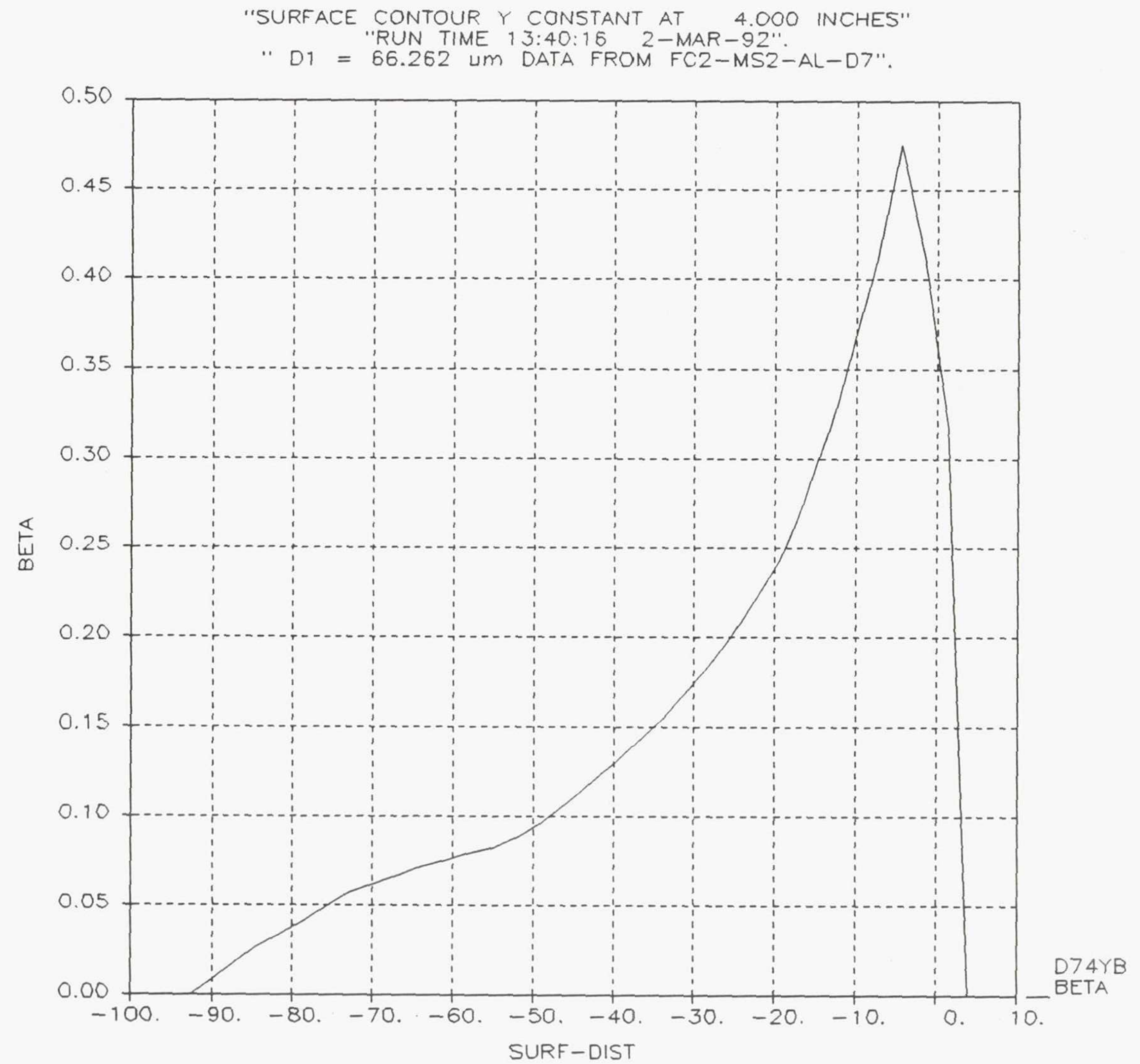

FIGURE D.51

BETA vs SURF-DIST(cm), FC2,Y=4,D=66.3 micron

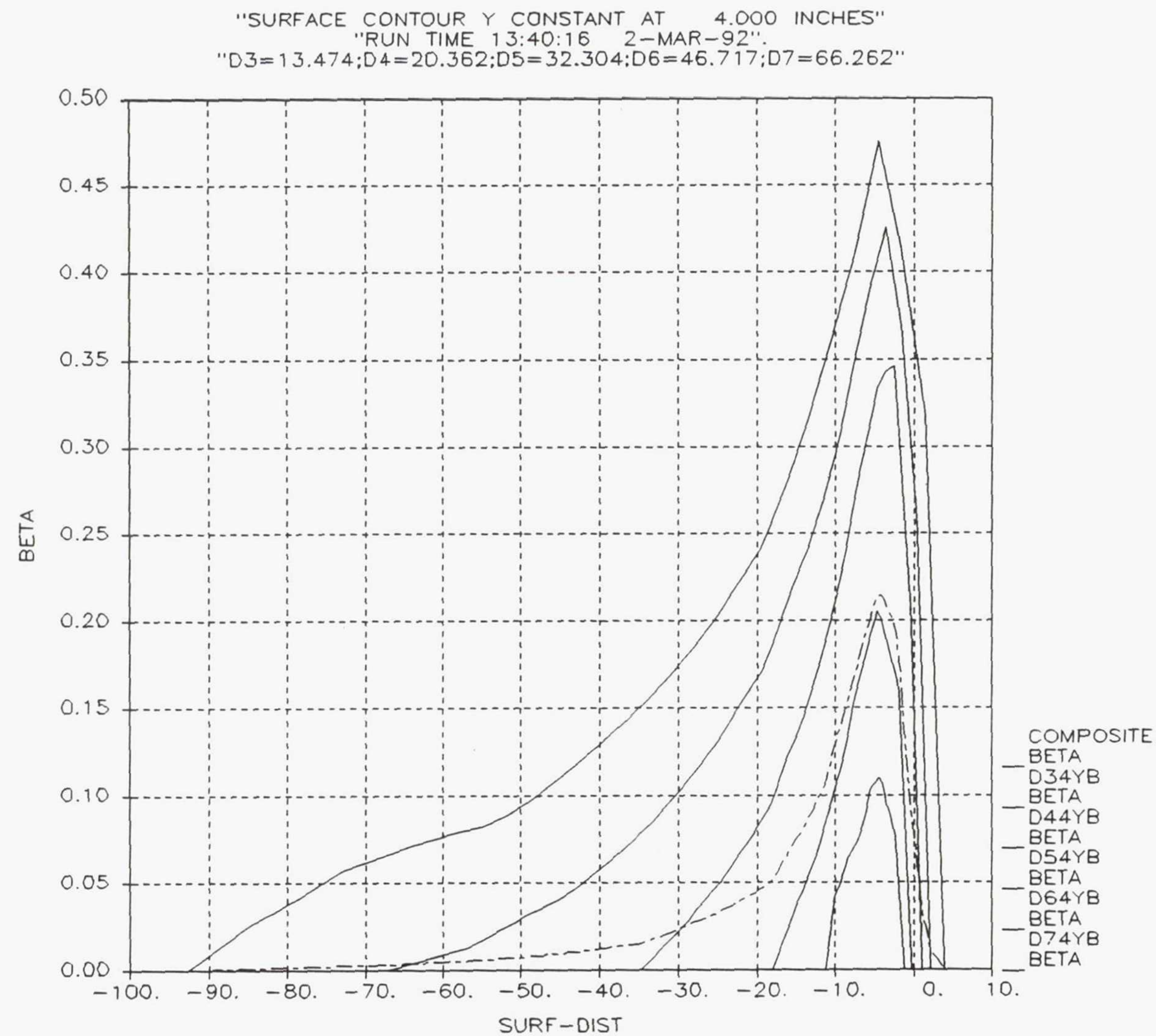

FIGURE D.52

BETA vs SURF-DIST(cm), FC2,Y=4,COMPOSITE AND INDIVIDUAL DROPS

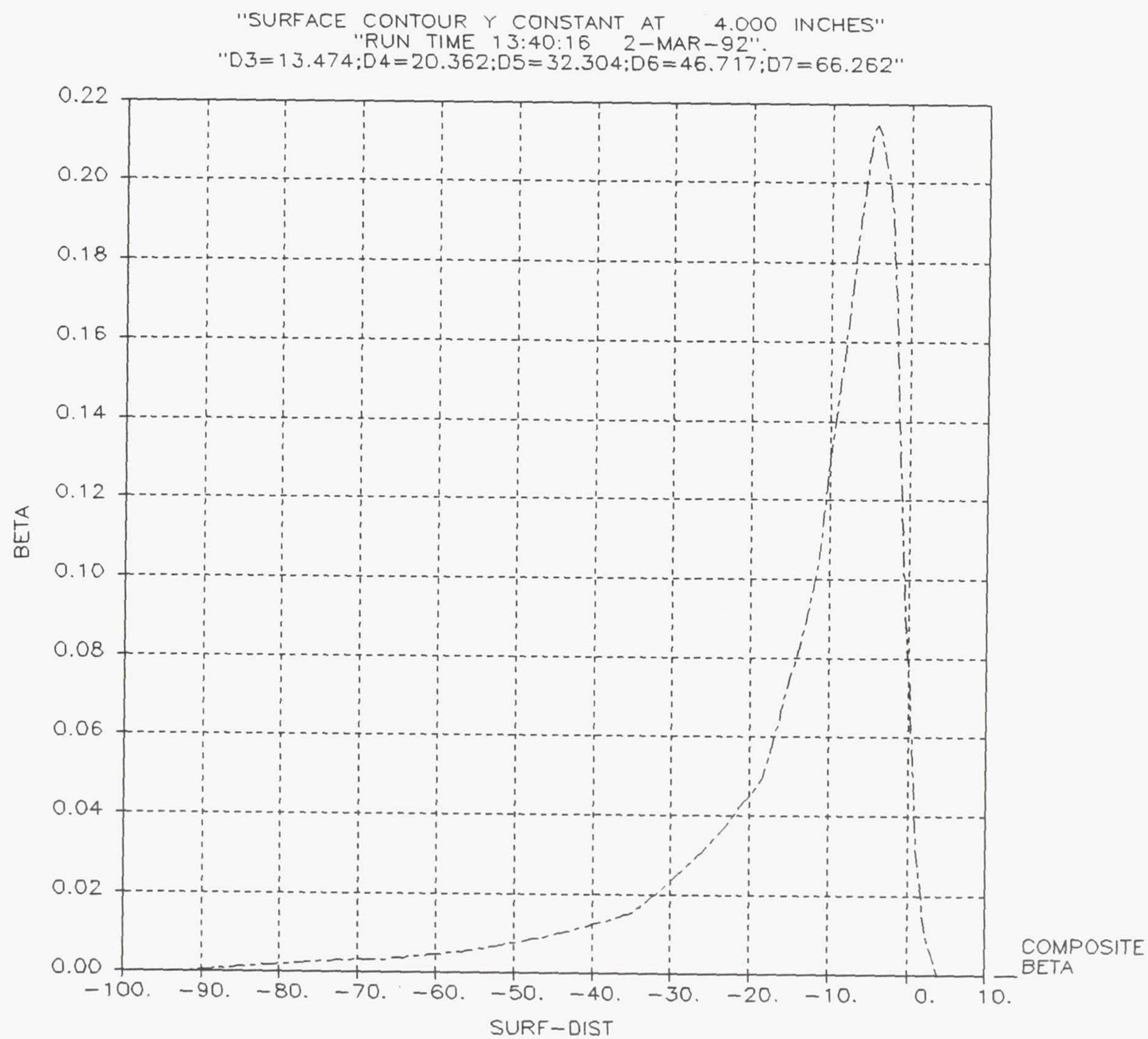

FIGURE D.53

BETA vs SURF-DIST(cm), FC2,Y=4,D=20.4 micron
COMPOSITE DROP

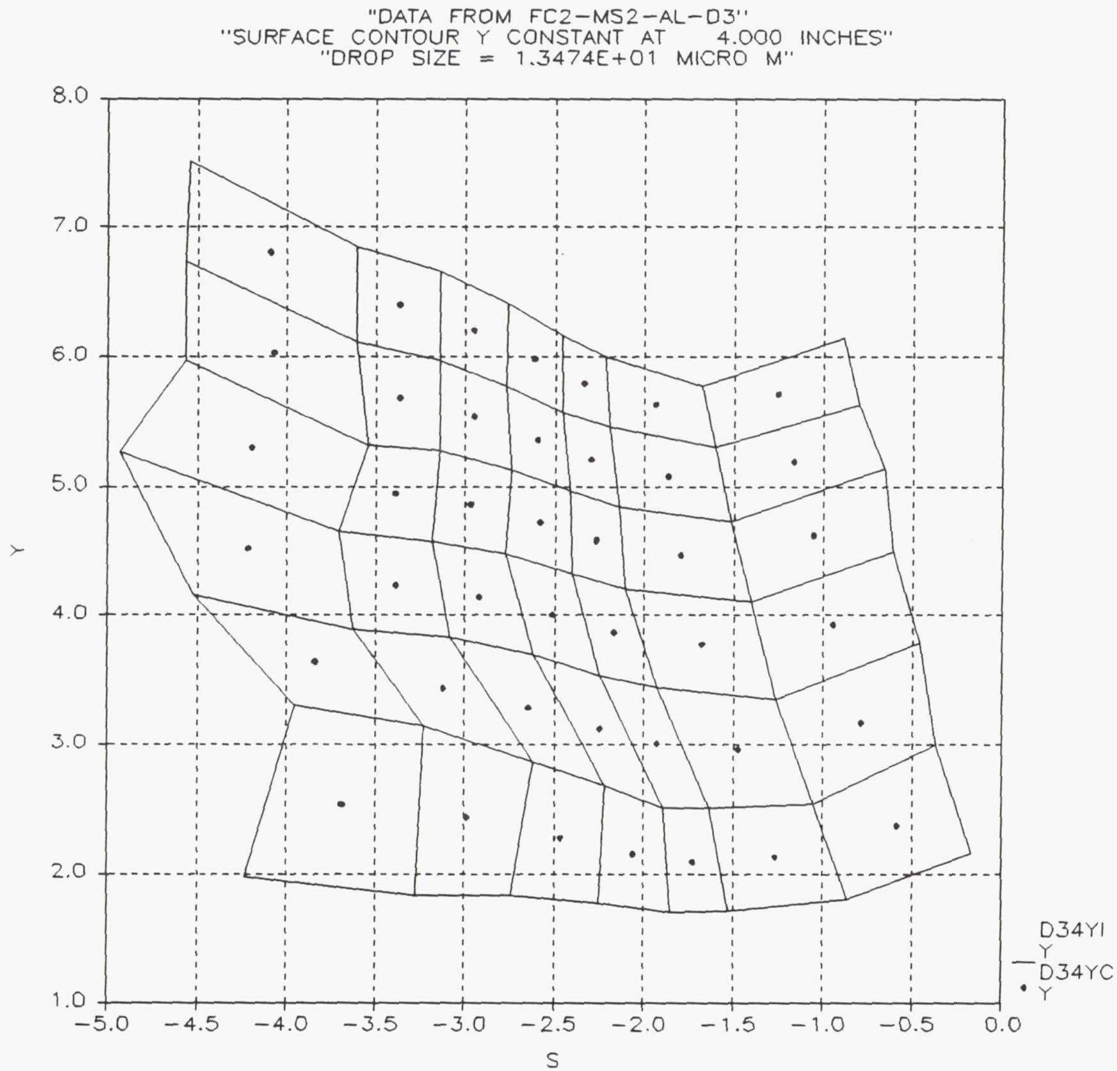

FIGURE D.54

IMPINGEMENT FIELD Y(in) vs S(in), FC2,Y=4,D=13.5 micron

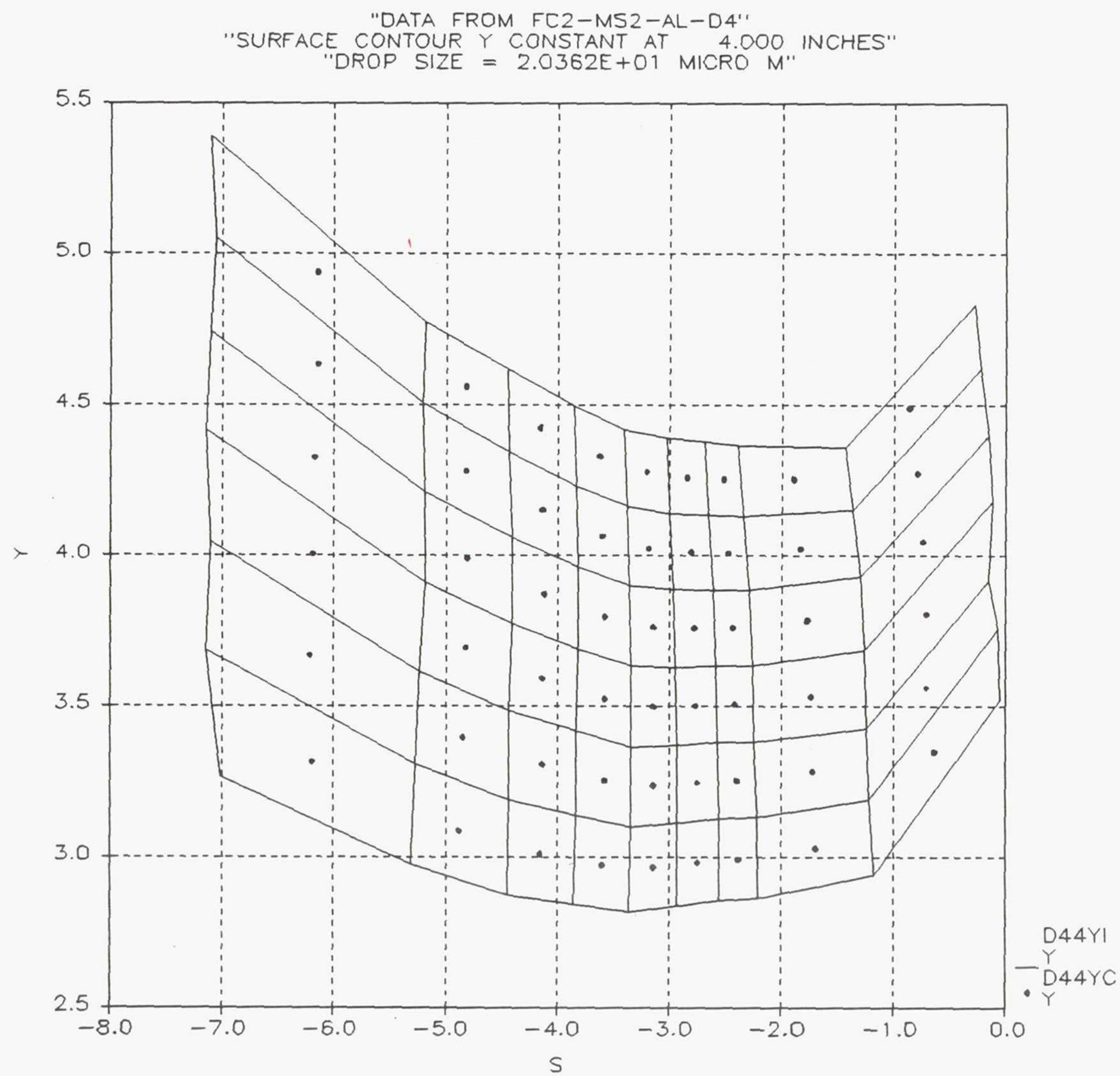

FIGURE D.55

IMPINGEMENT FIELD Y(in) vs S(in), FC2,Y=4,D=20.4 micron

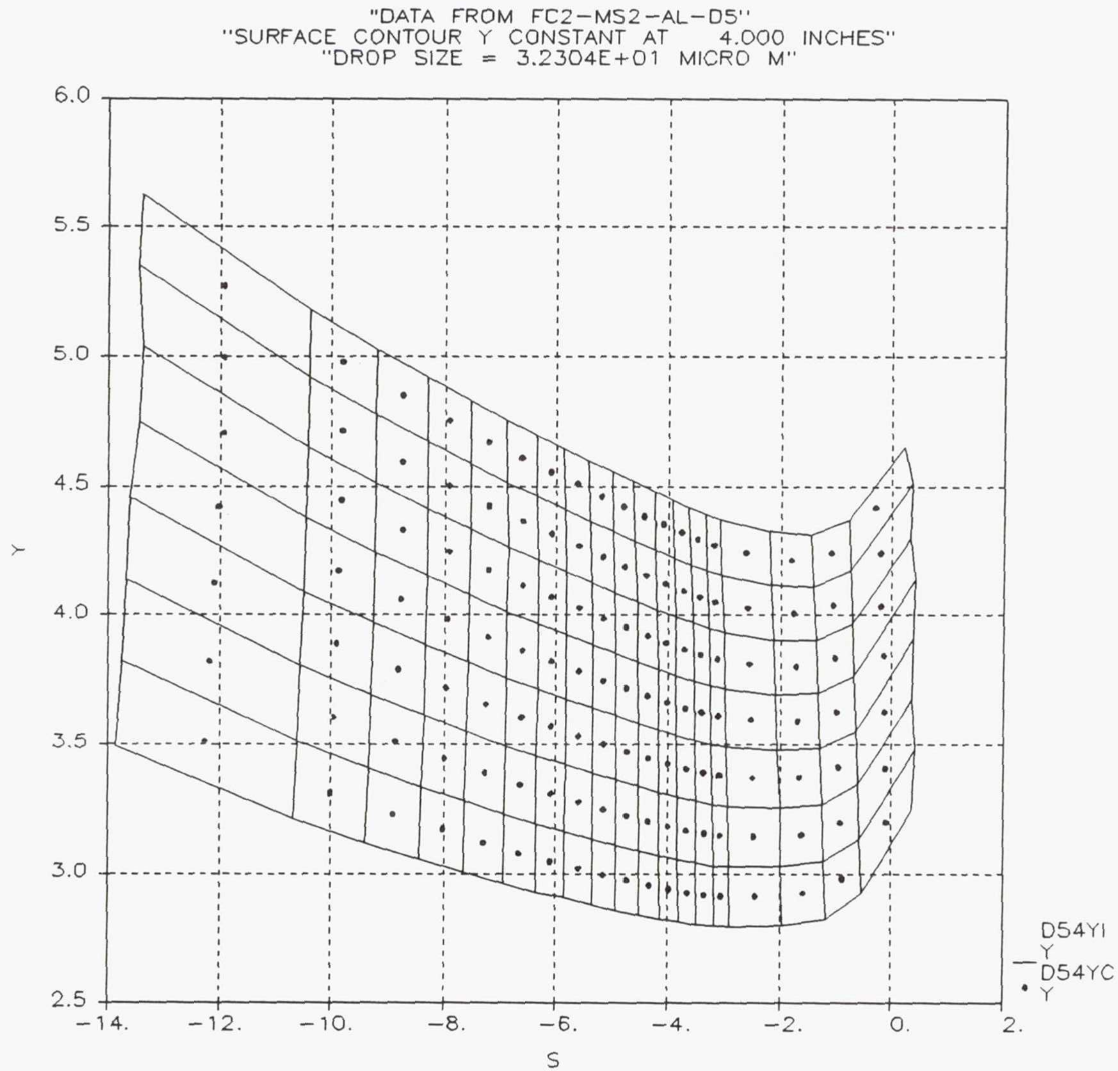

FIGURE D.56

IMPINGEMENT FIELD Y(in) vs S(in), FC2,Y=4,D=32.3 micron

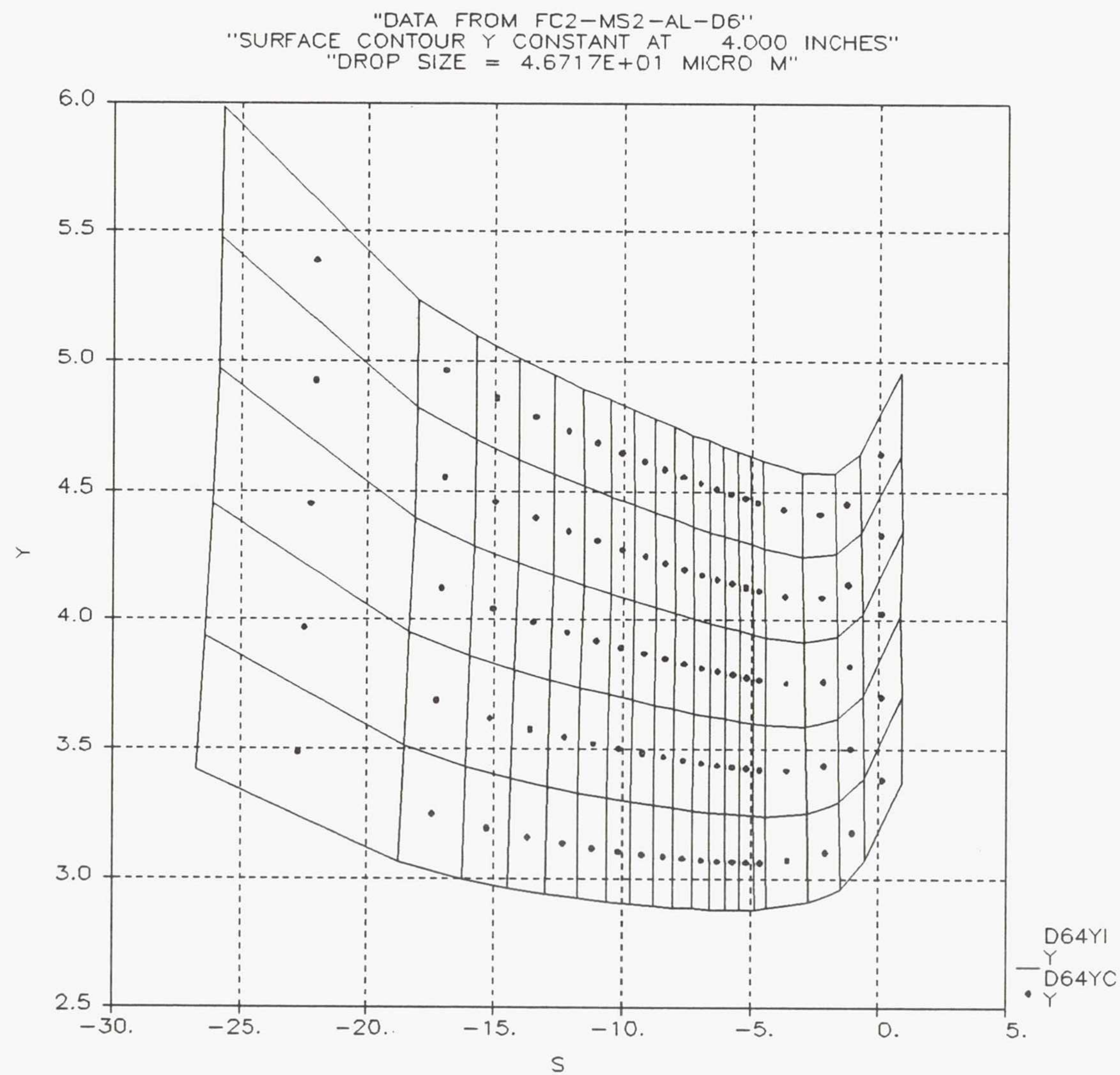

FIGURE D.57

IMPINGEMENT FIELD Y(in) vs S(in), FC2,Y=4,D=46.7 micron

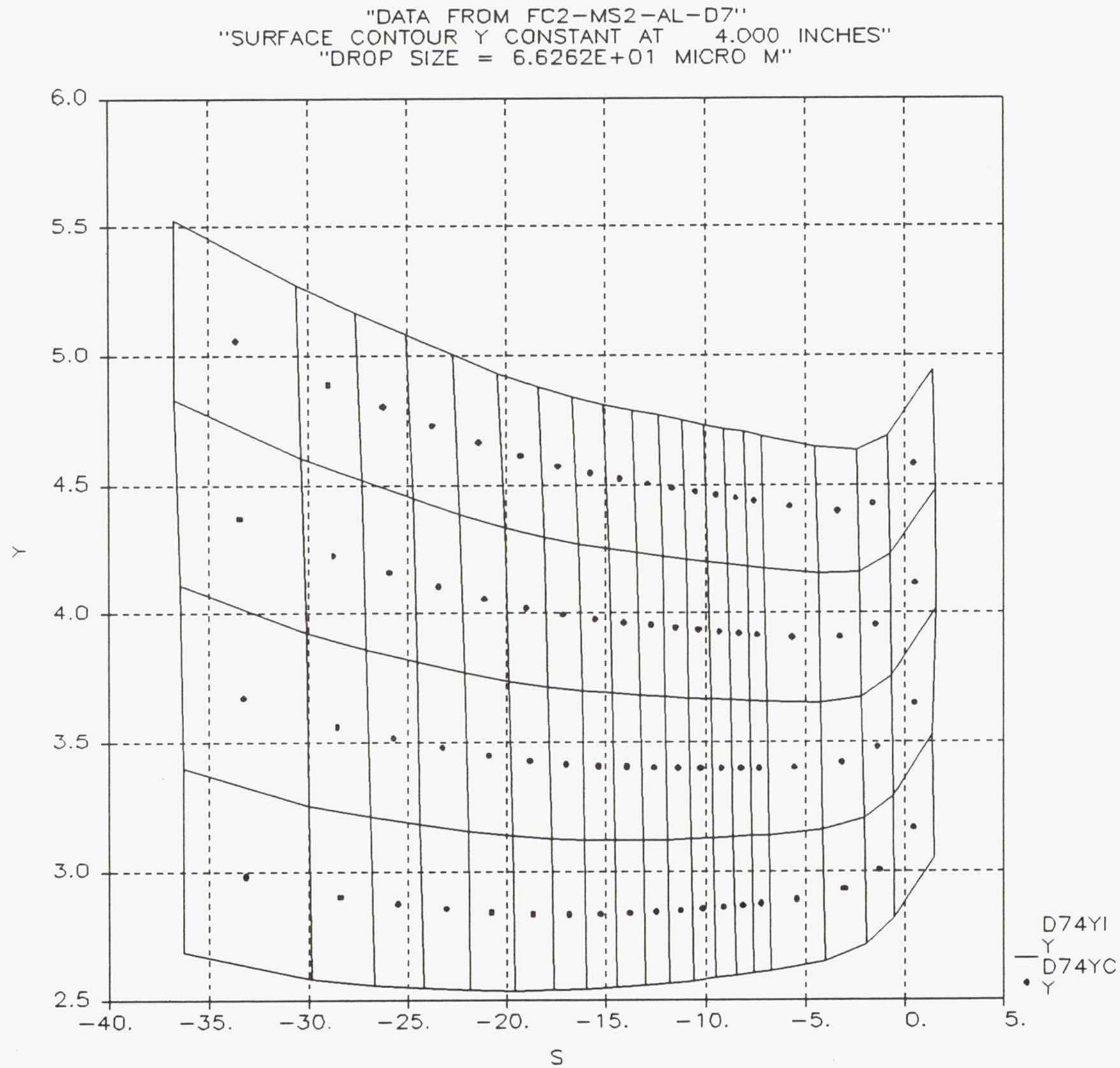

FIGURE D.58

IMPINGEMENT FIELD Y(in) vs S(in), FC2,Y=4,D=66.3 micron

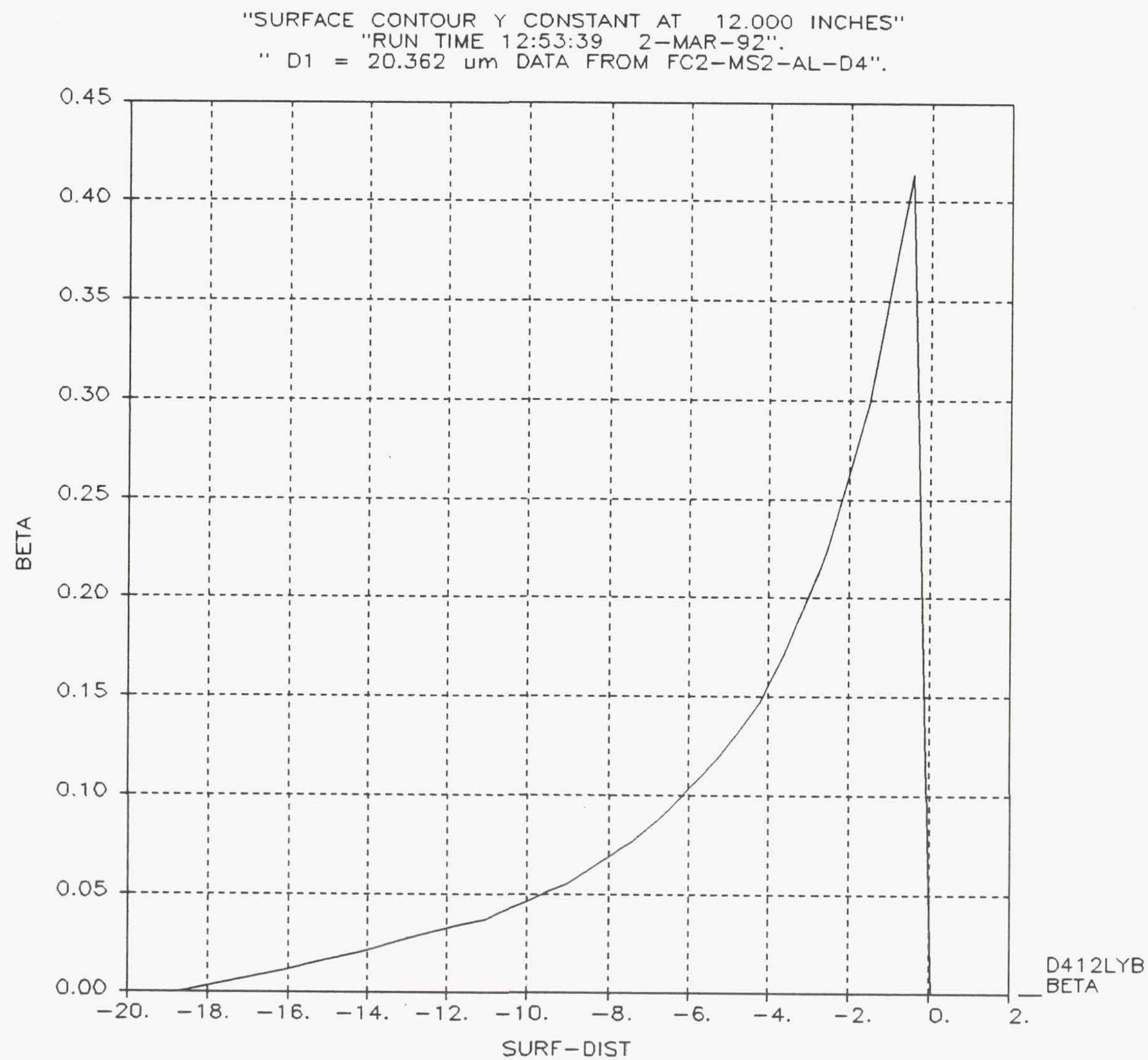

FIGURE D.59

BETA vs SURF-DIST(cm), FC2,Y=12L,D=20.4 micron

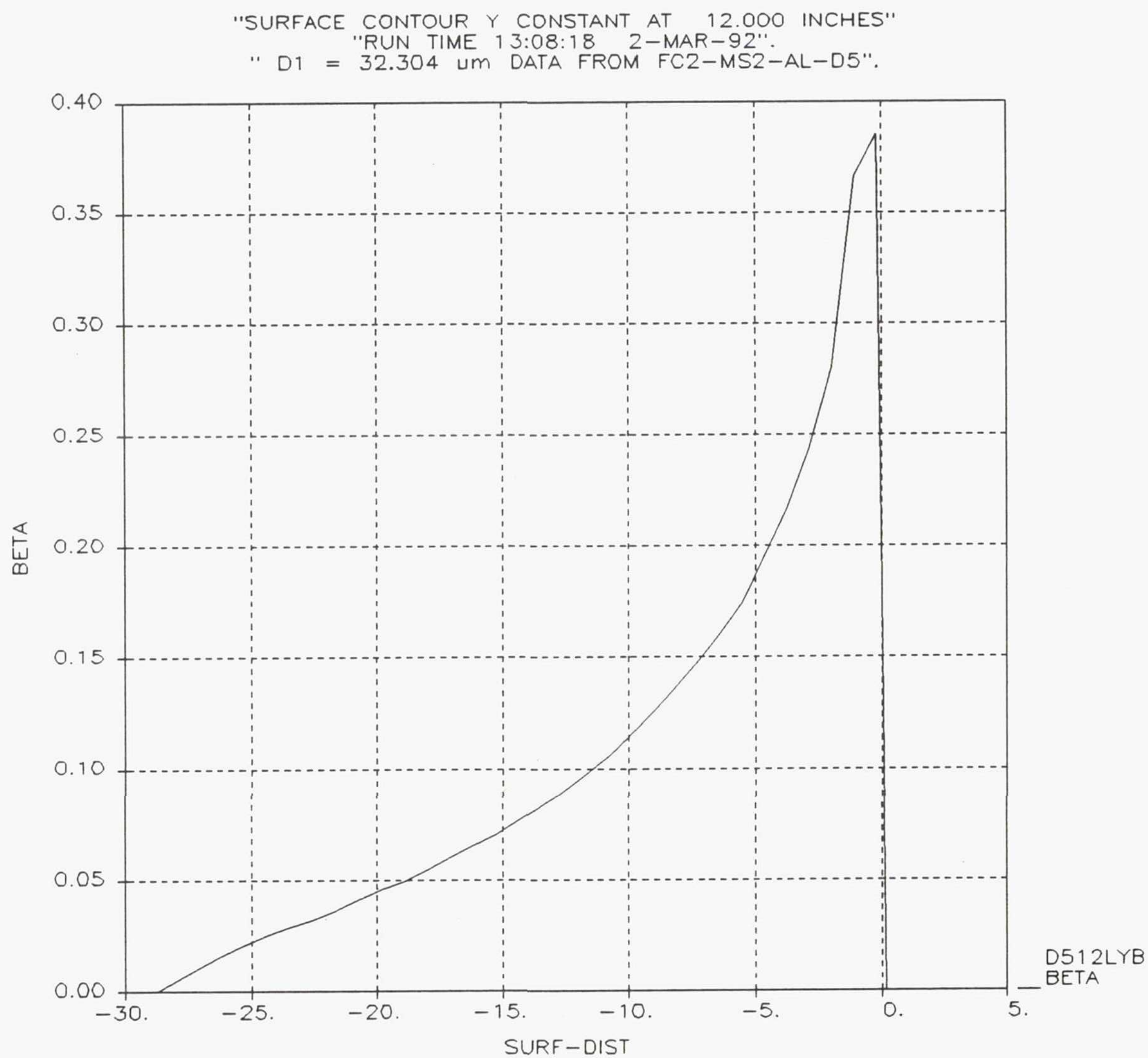

FIGURE D.60

BETA vs SURF-DIST(cm), FC2,Y=12L,D=32.3 micron

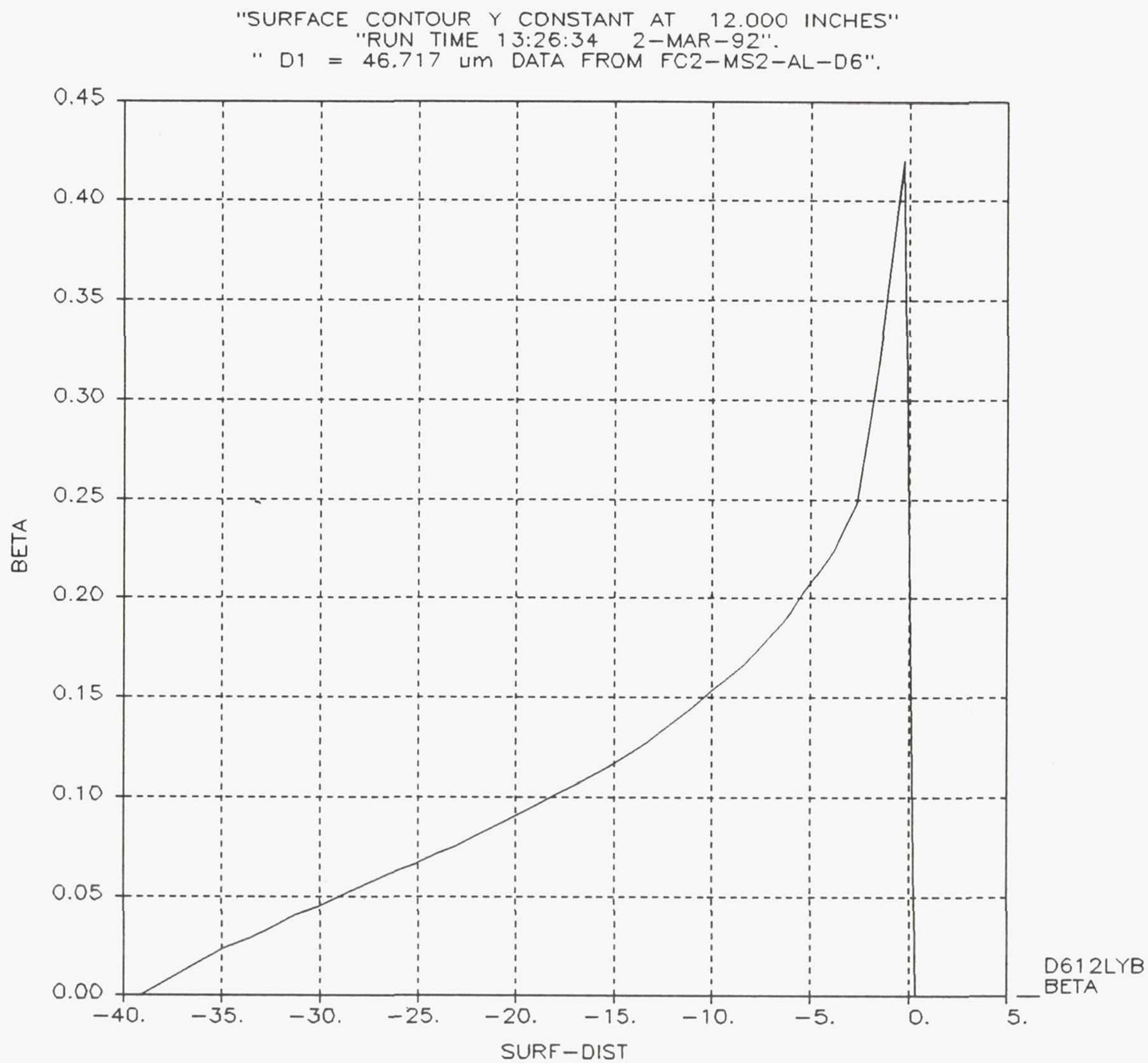

FIGURE D.61

BETA vs SURF-DIST(cm), FC2,Y=12L,D=46.7 micron

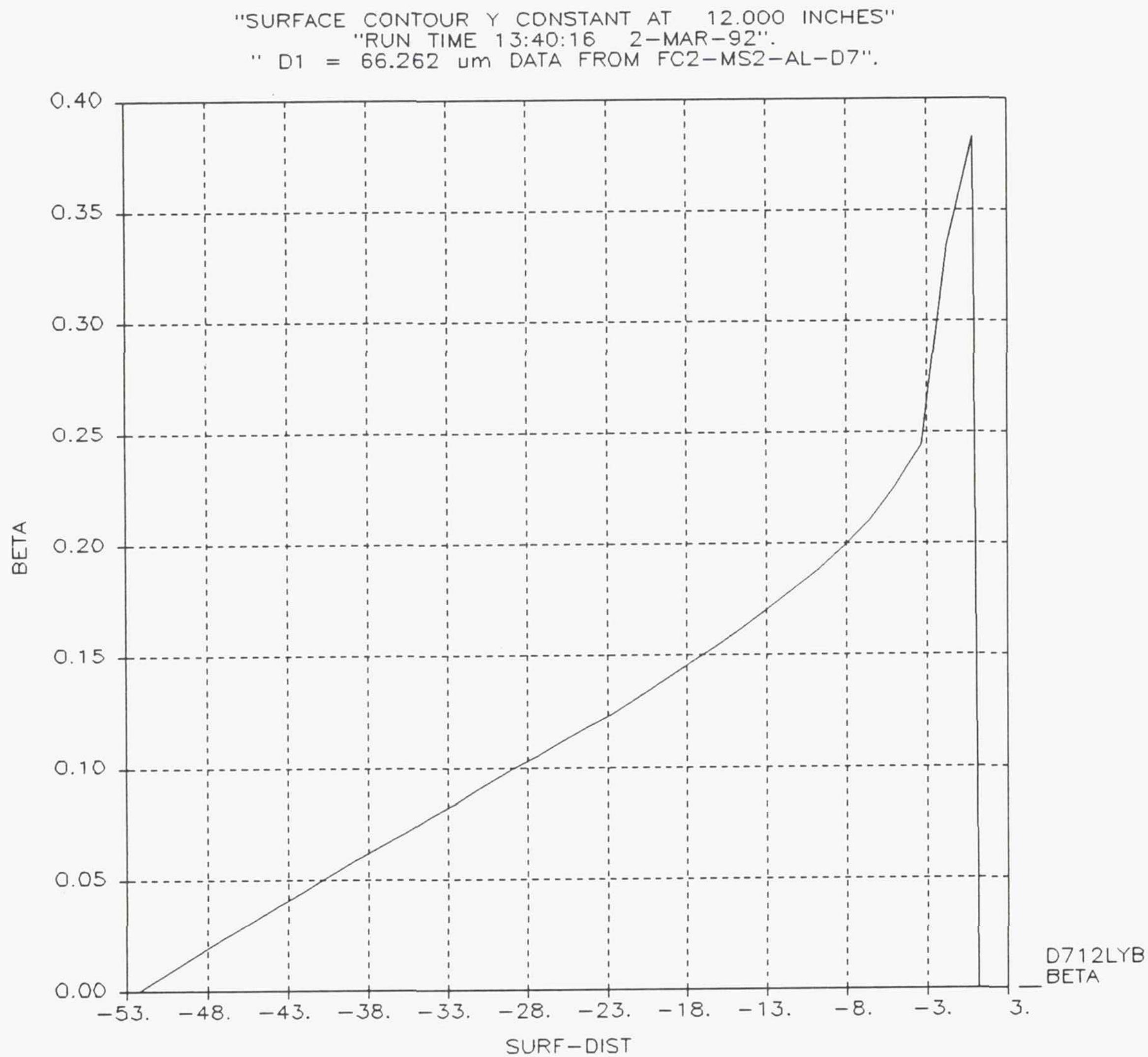

FIGURE D.62

BETA vs SURF-DIST(cm), FC2,Y=12L,D=66.3 micron

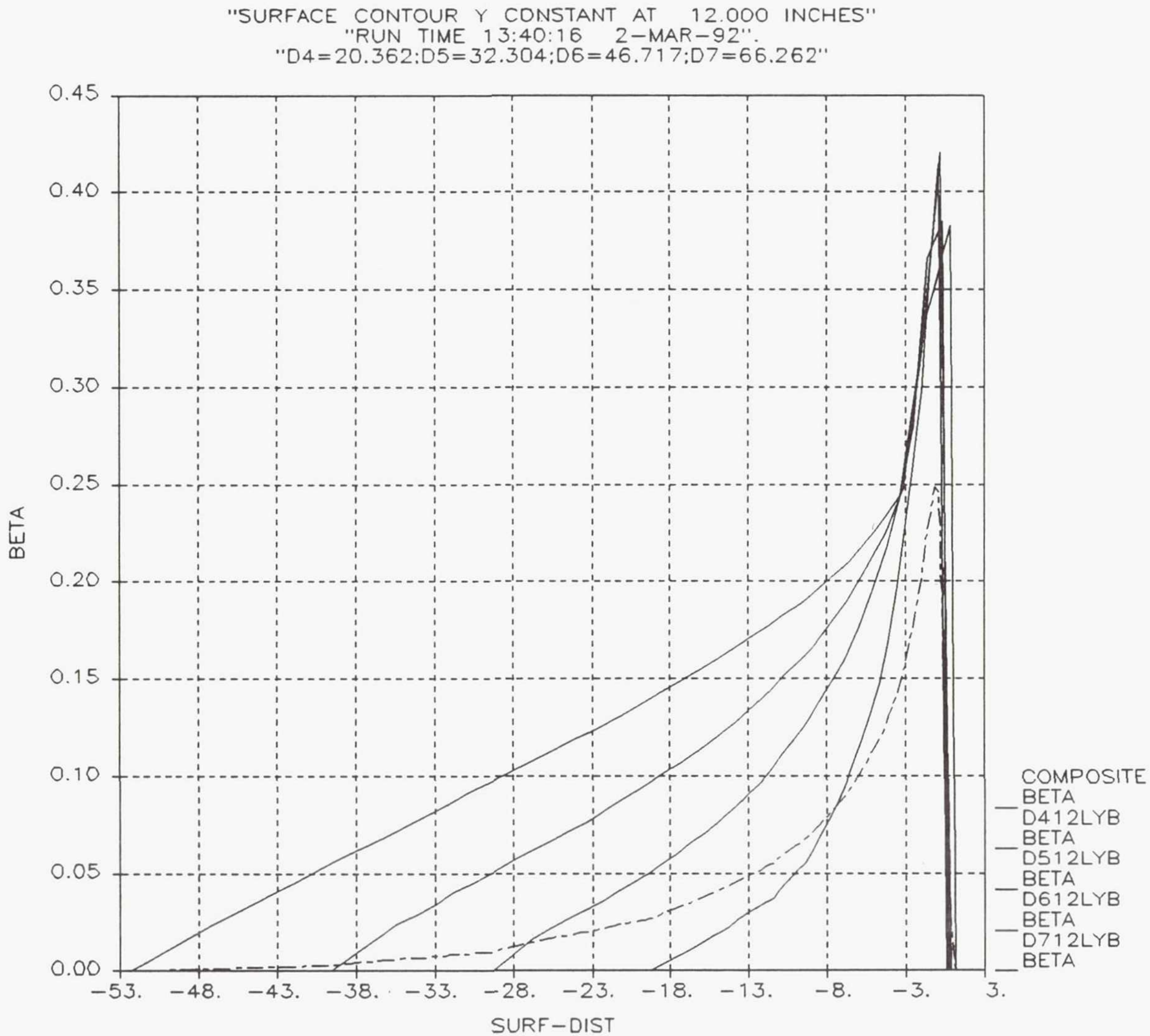

FIGURE D.63

BETA vs SURF-DIST(cm), FC2,Y=12L,COMPOSITE AND INDIVIDUAL DROPS

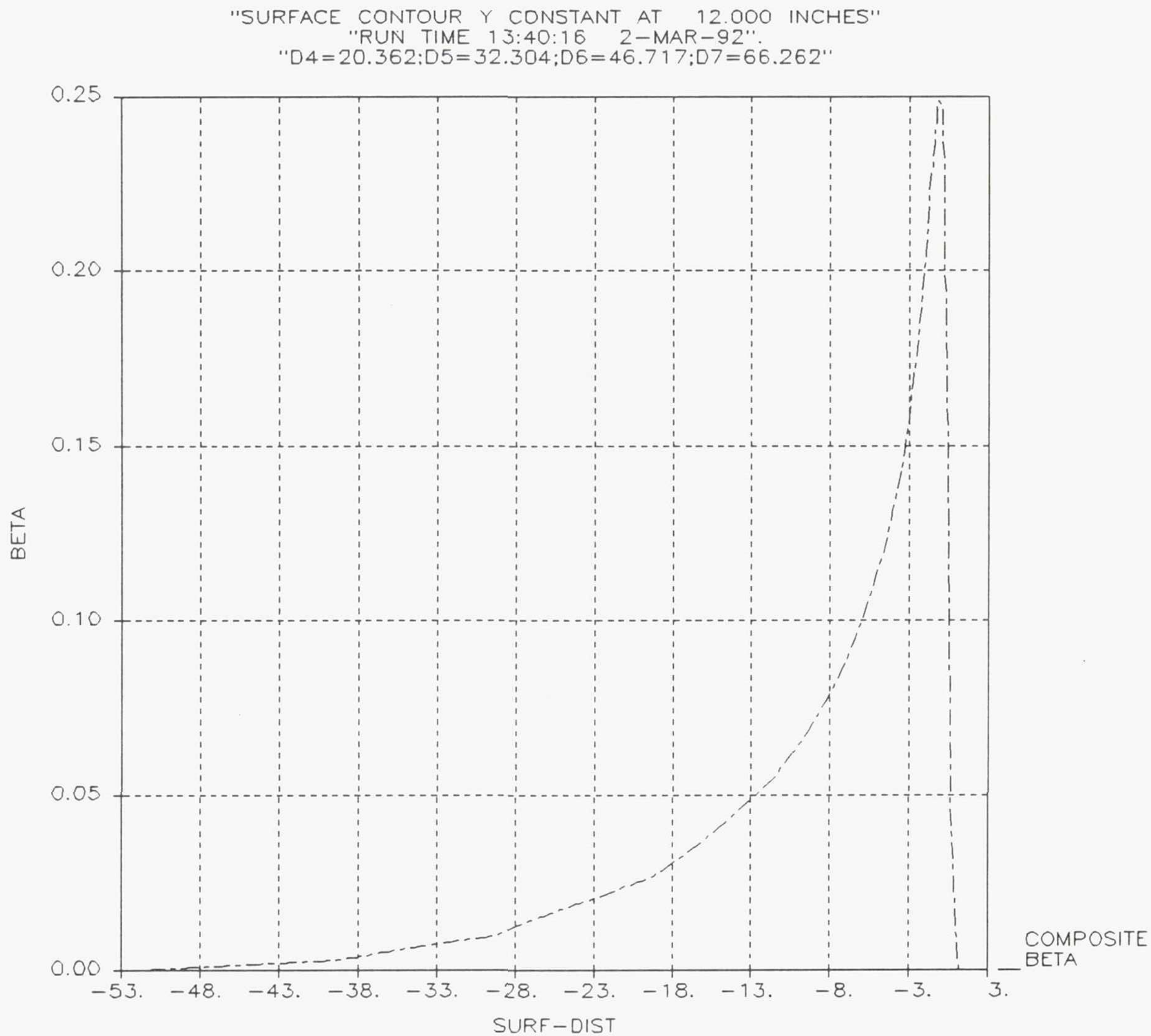

FIGURE D.64

BETA vs SURF-DIST(cm), FC2,Y=12L,D=20.4 micron
COMPOSITE DROP

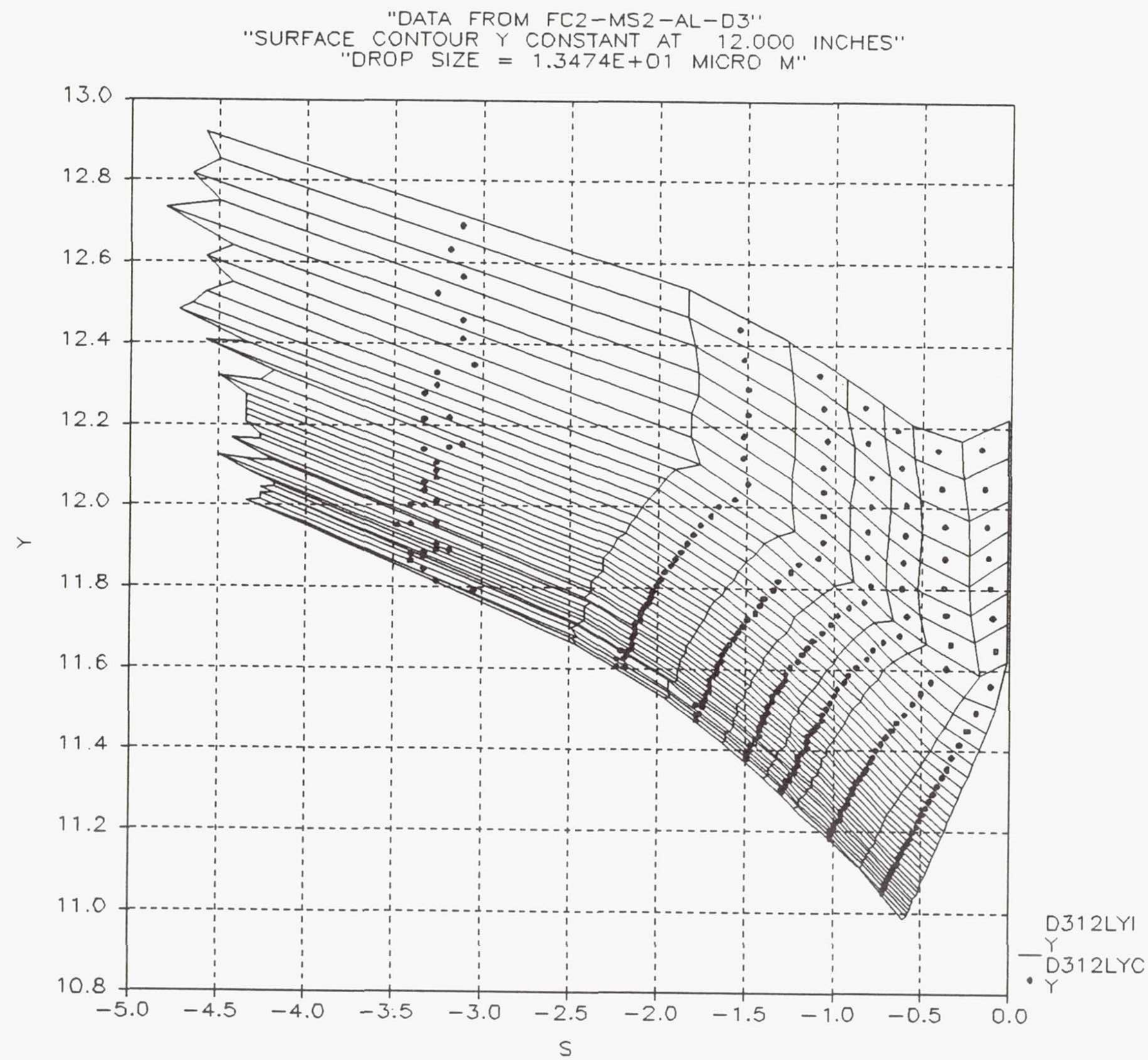

FIGURE D.65

IMPINGEMENT FIELD Y(in) vs S(in), FC2,Y=12L,D=13.5 micron

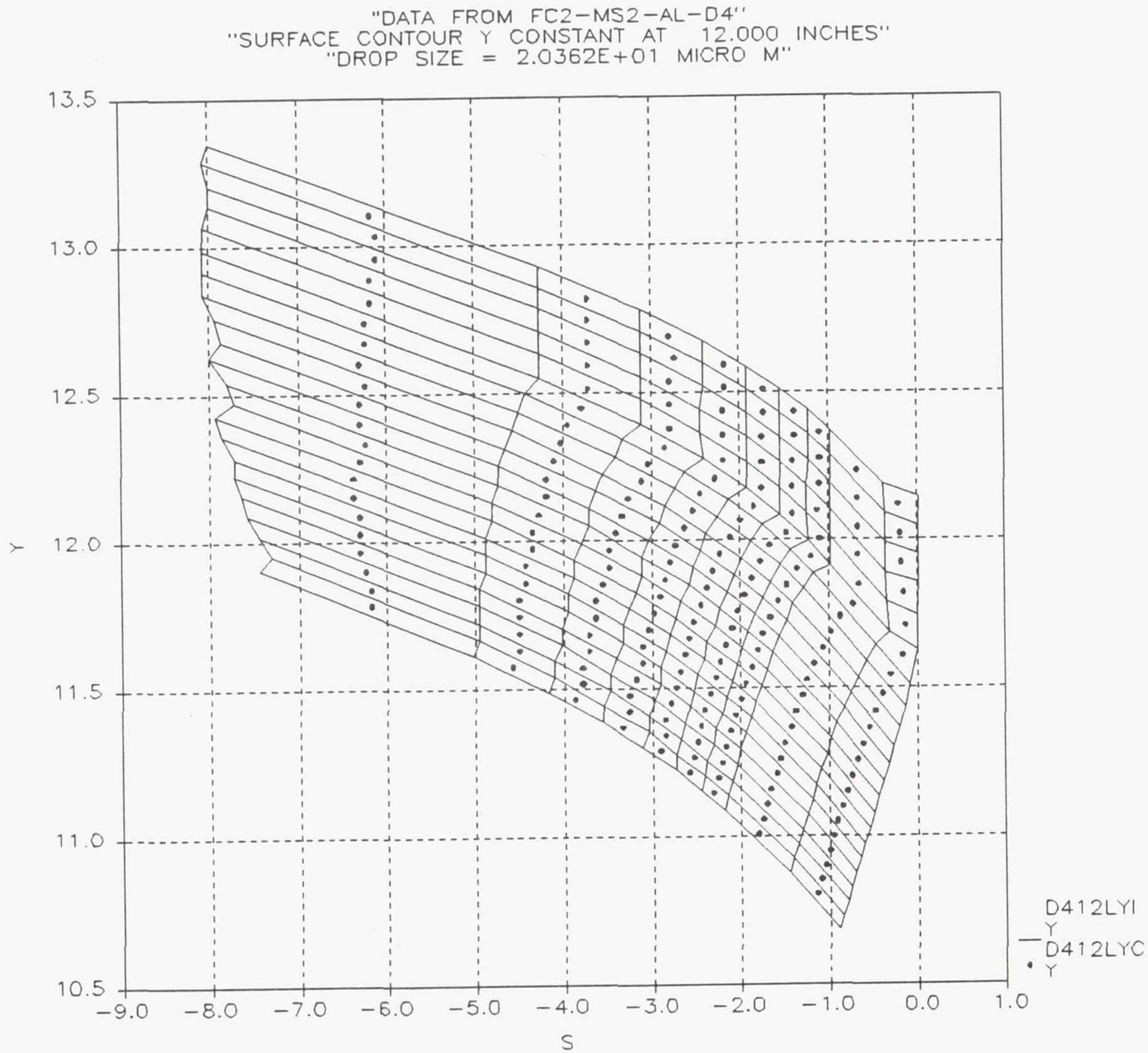

FIGURE D.66

IMPINGEMENT FIELD Y(in) vs S(in), FC2,Y=12L,D=20.4 micron

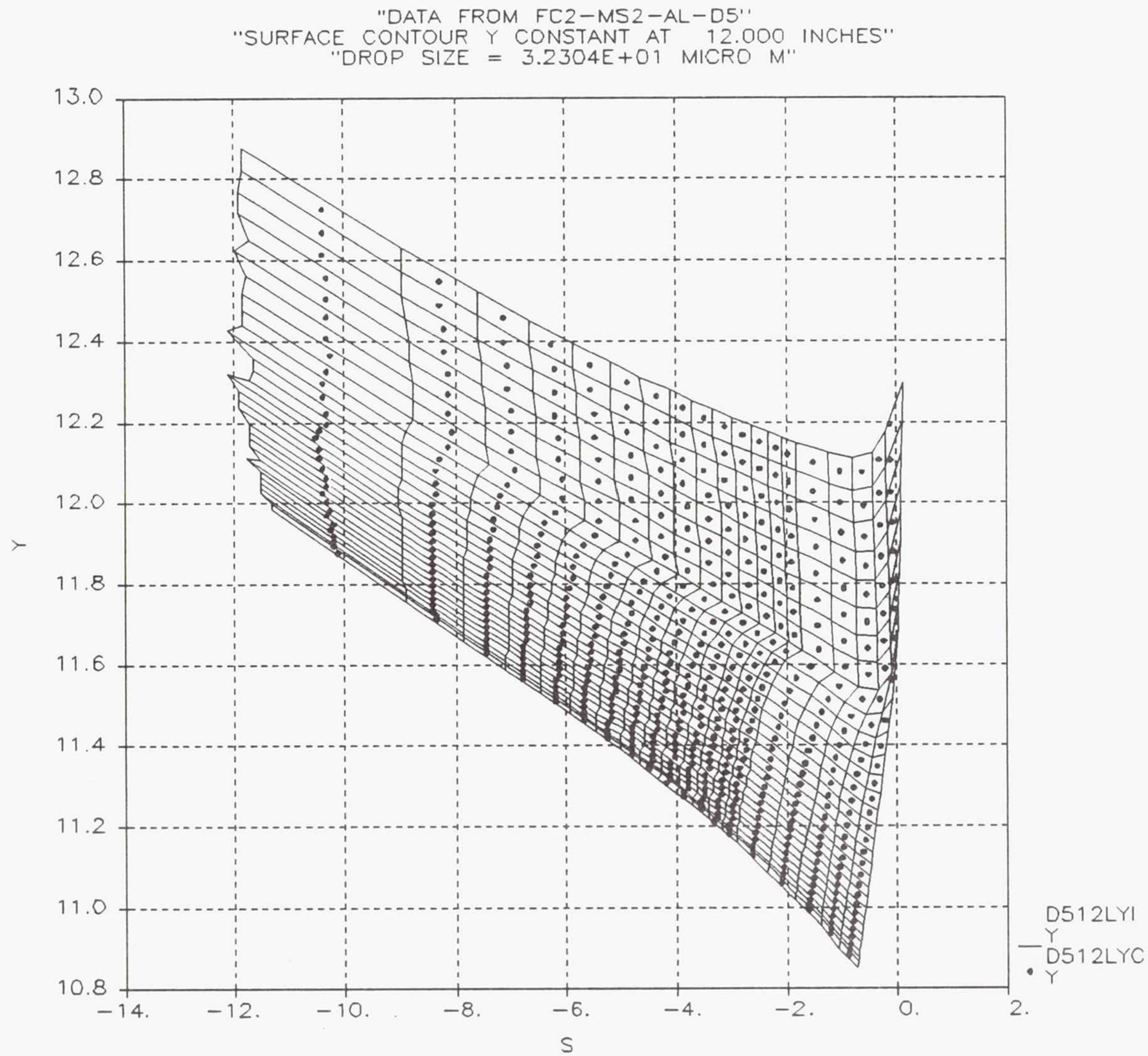

FIGURE D.67

IMPINGEMENT FIELD Y(in) vs S(in), FC2,Y=12L,D=32.3 micron

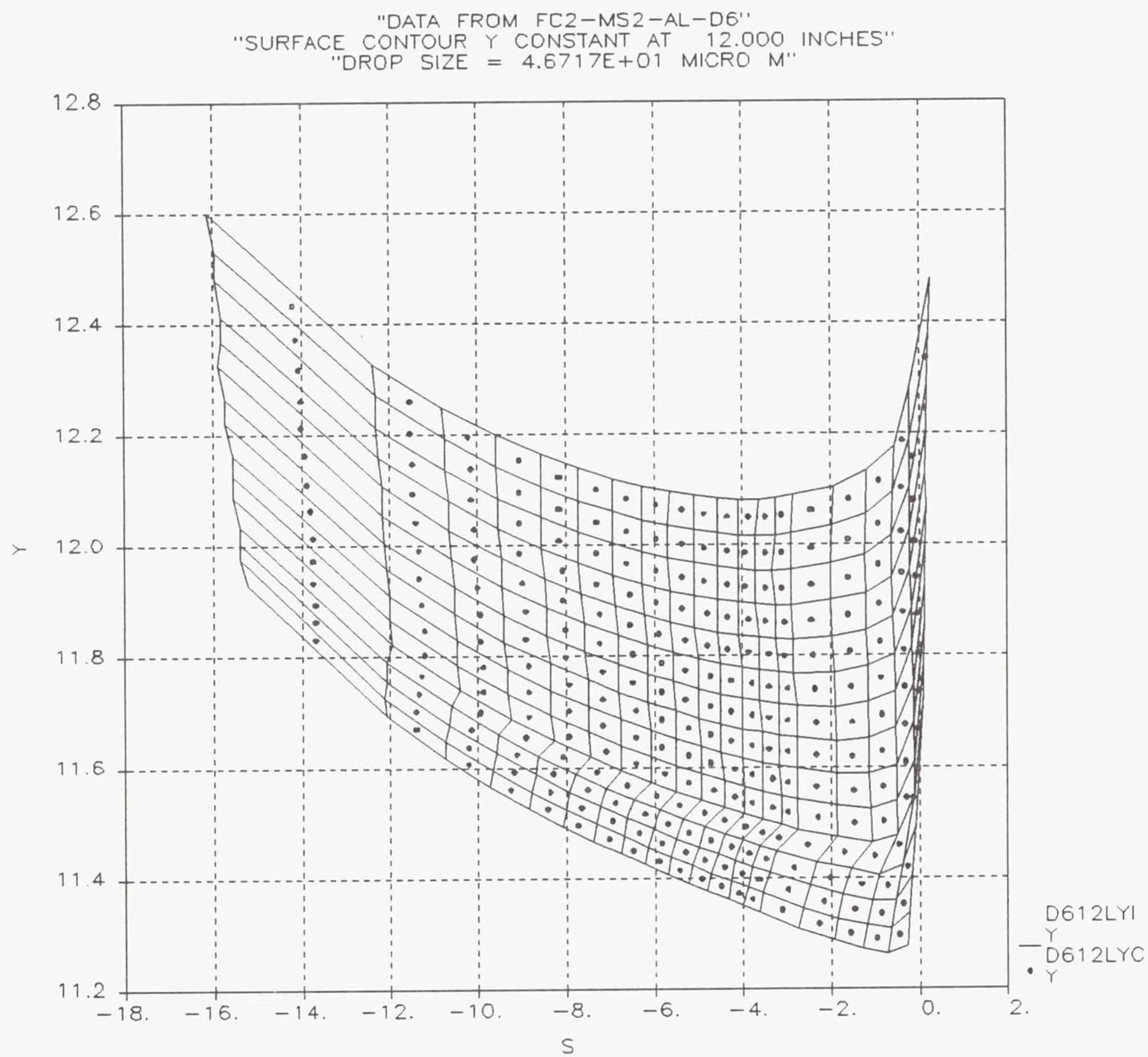

FIGURE D.68

IMPINGEMENT FIELD Y(in) vs S(in), FC2,Y=12L,D=46.7 micron

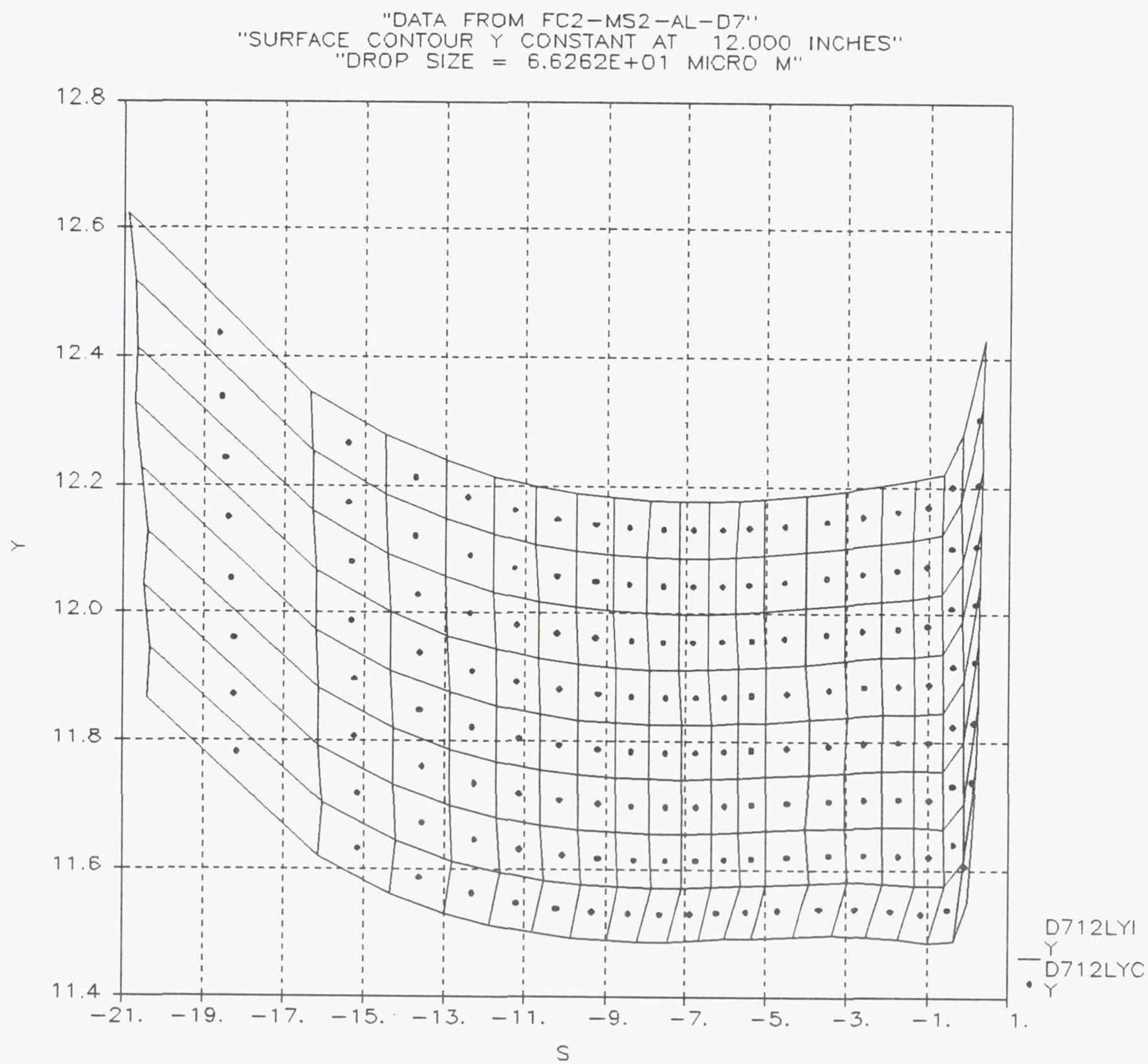

FIGURE D.69

IMPINGEMENT FIELD Y(in) vs S(in), FC2,Y=12L,D=66.3 micron

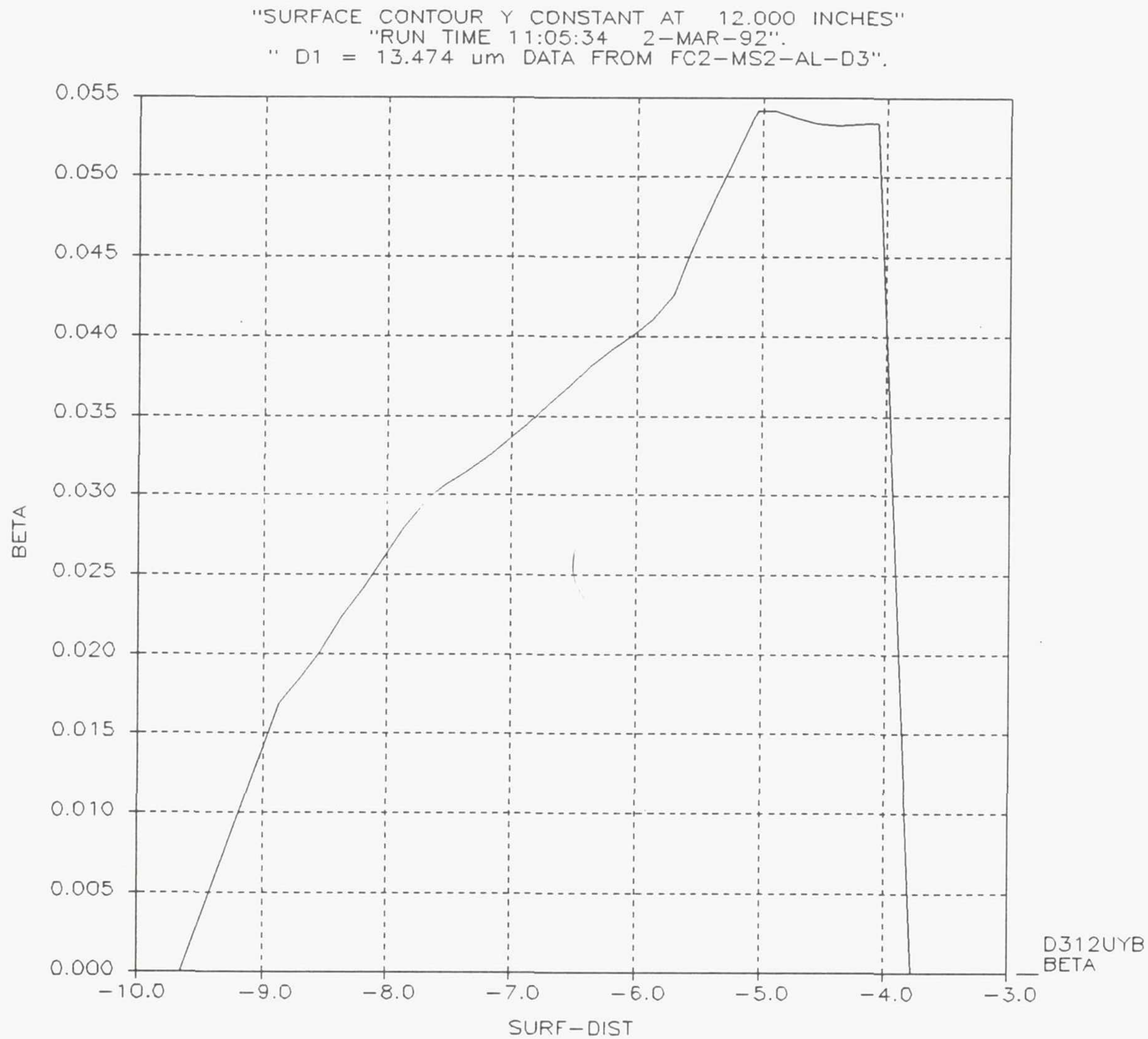

FIGURE D.70

BETA vs SURF-DIST(cm), FC2,Y=12U,D=13.5 micron

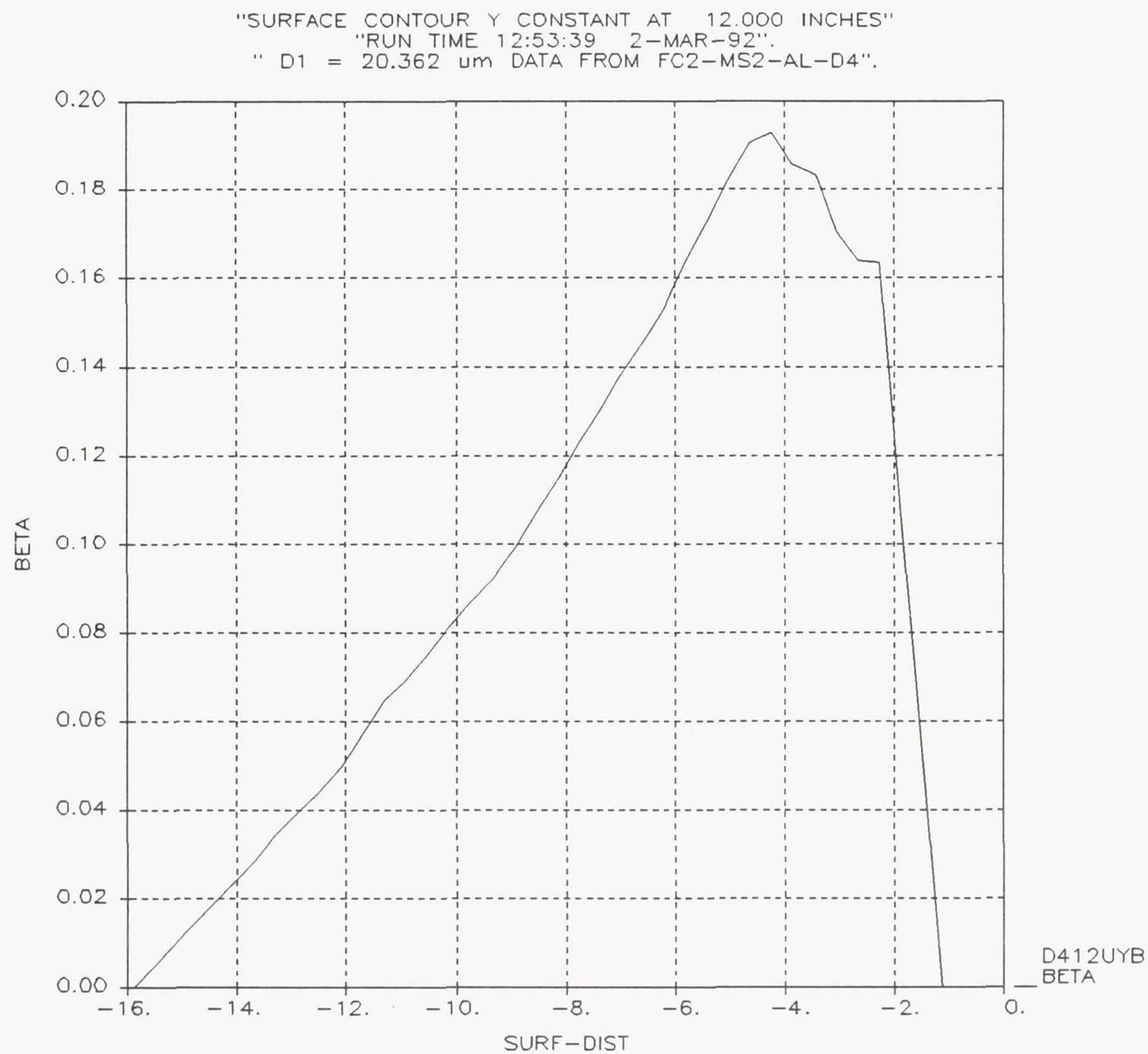

FIGURE D.71

BETA vs SURF-DIST(cm), FC2,Y=12U,D=20.4 micron

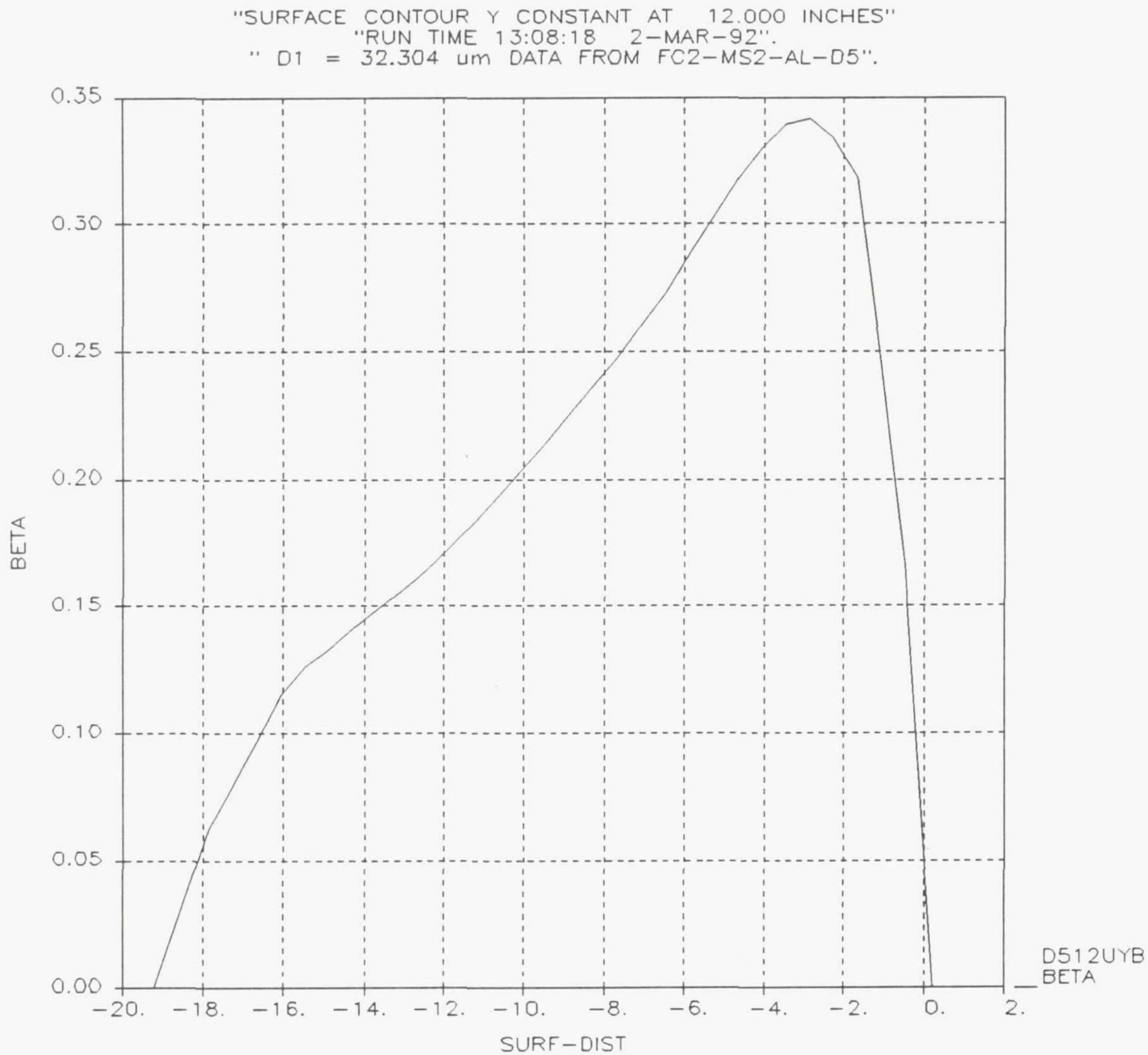

FIGURE D.72

BETA vs SURF-DIST(cm), FC2,Y=12U,D=32.3 micron

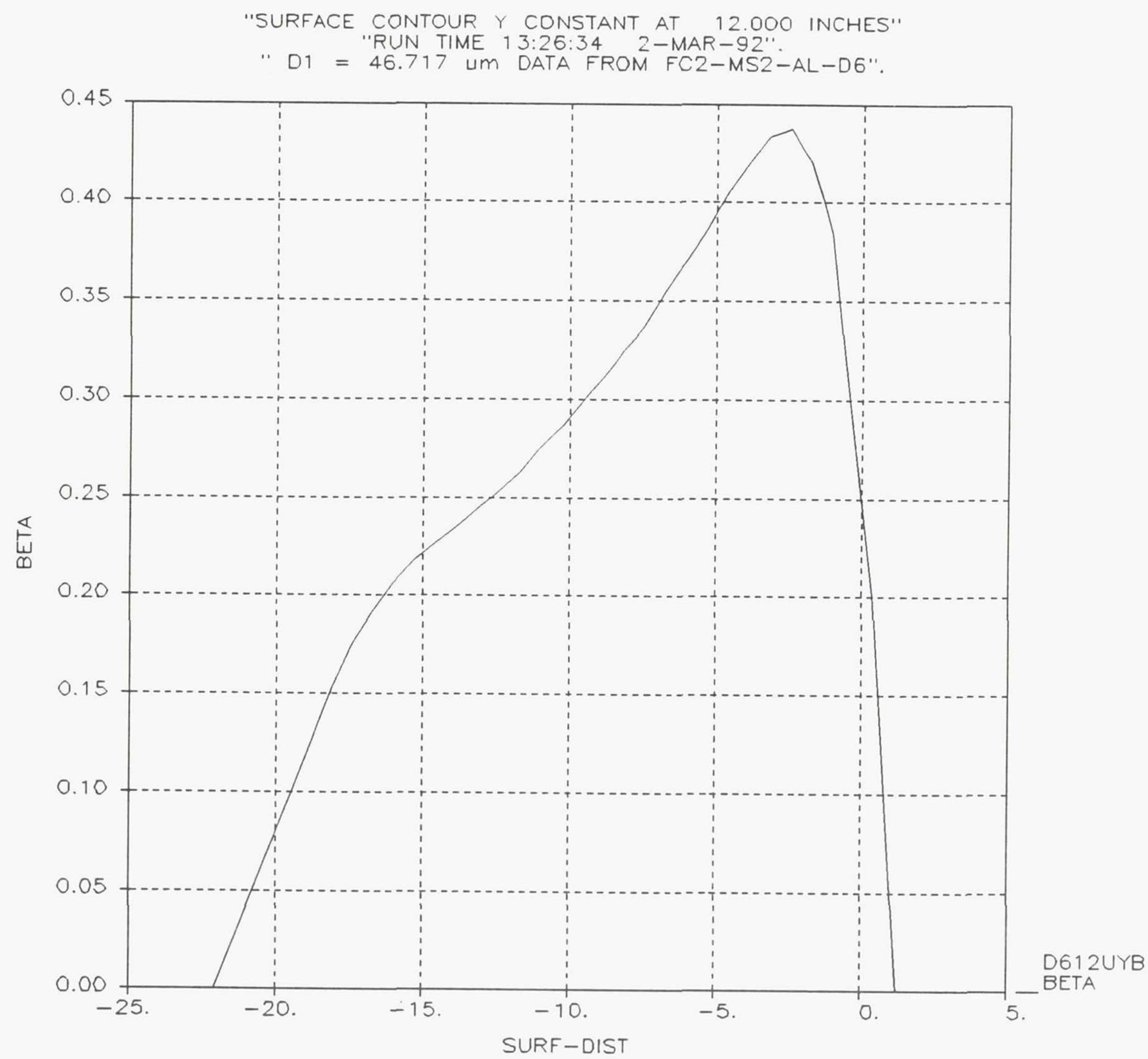

FIGURE D.73

BETA vs SURF-DIST(cm), FC2,Y=12U,D=46.7 micron

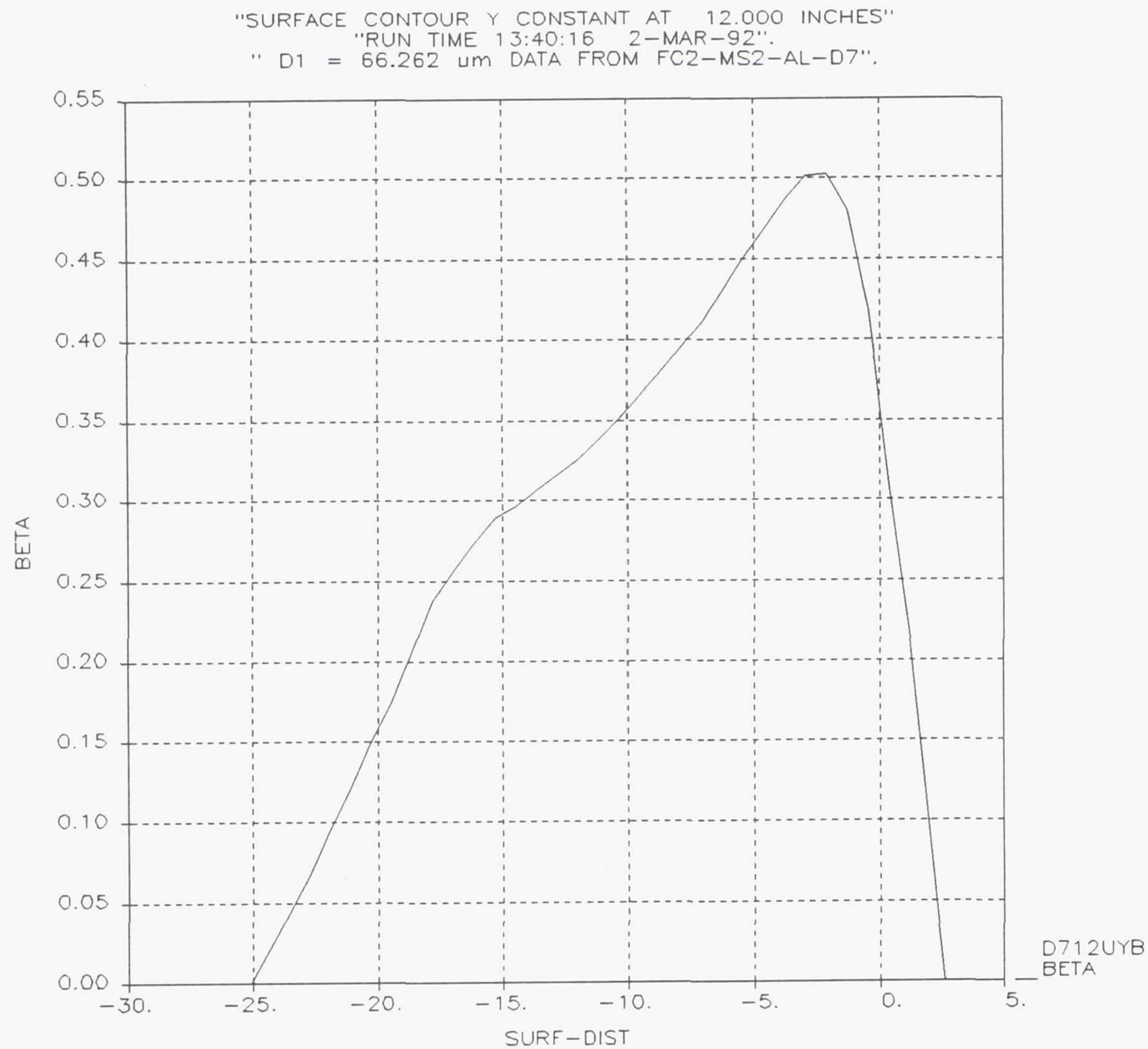

FIGURE D.74

BETA vs SURF-DIST(cm), FC2,Y=12U,D=66.3 micron

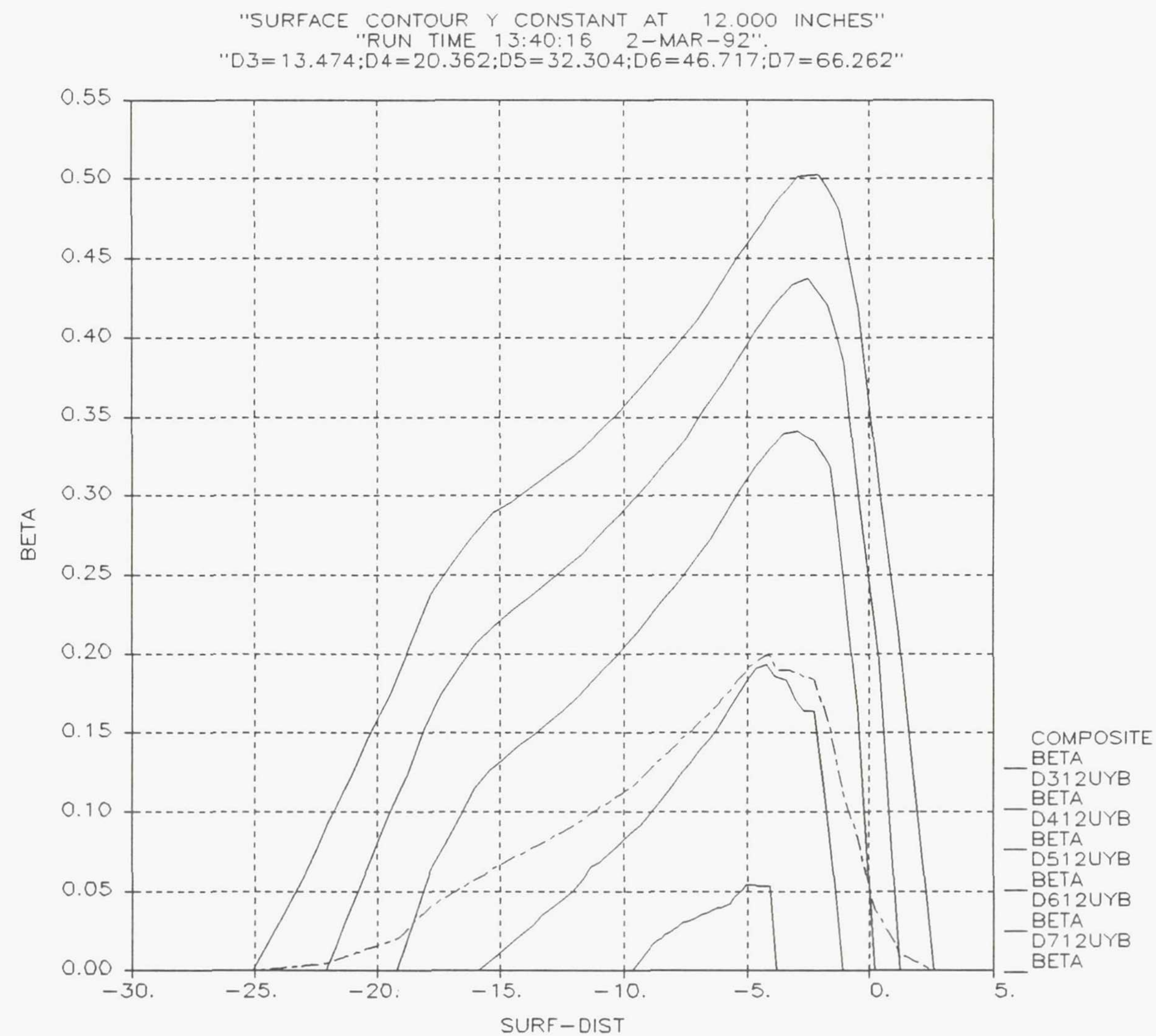

FIGURE D.75

BETA vs SURF-DIST(cm), FC2,Y=12U,COMPOSITE AND INDIVIDUAL DROPS

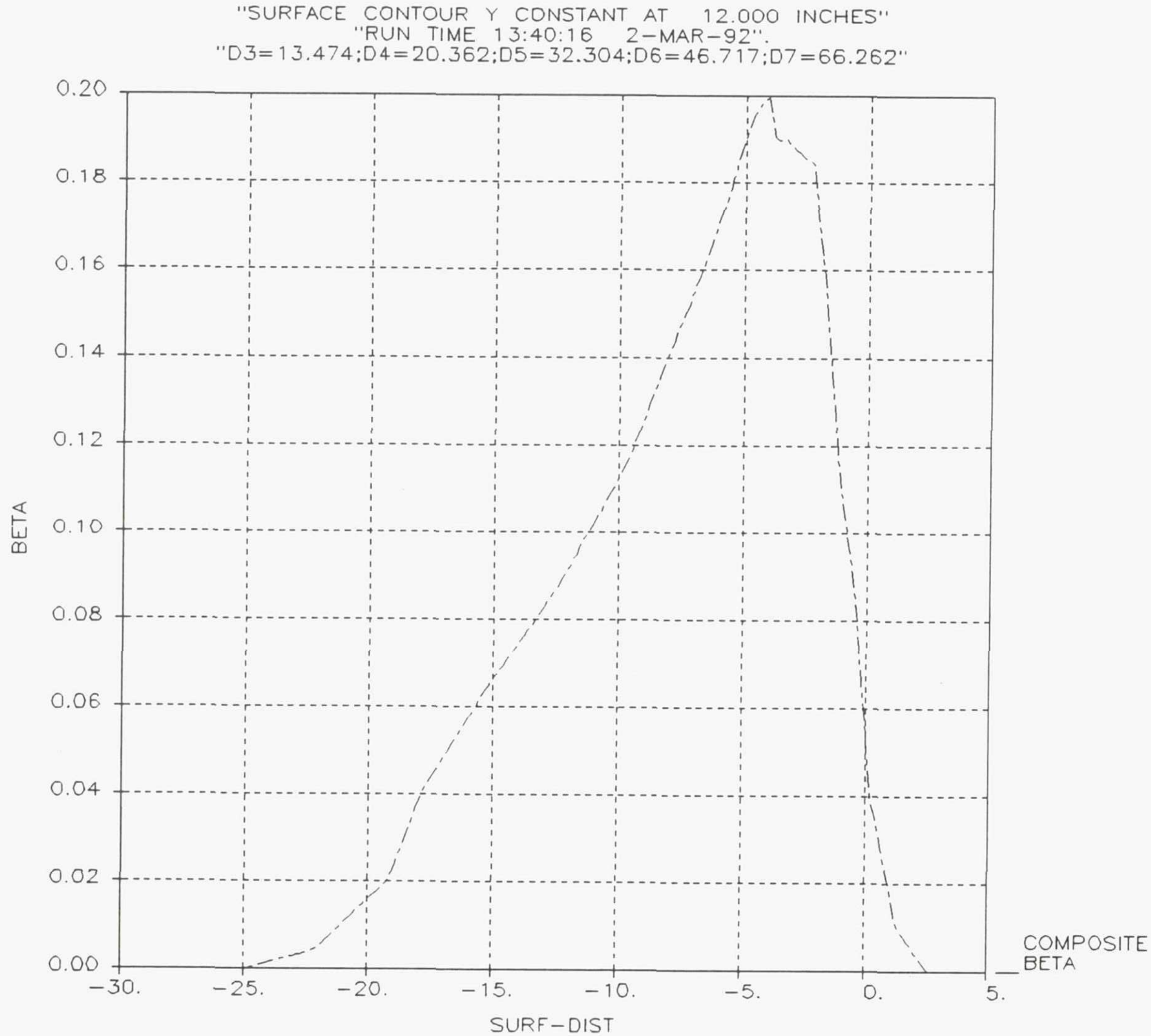

FIGURE D.76

BETA vs SURF-DIST(cm), FC2,Y=12U,D=20.4 micron
COMPOSITE DROP

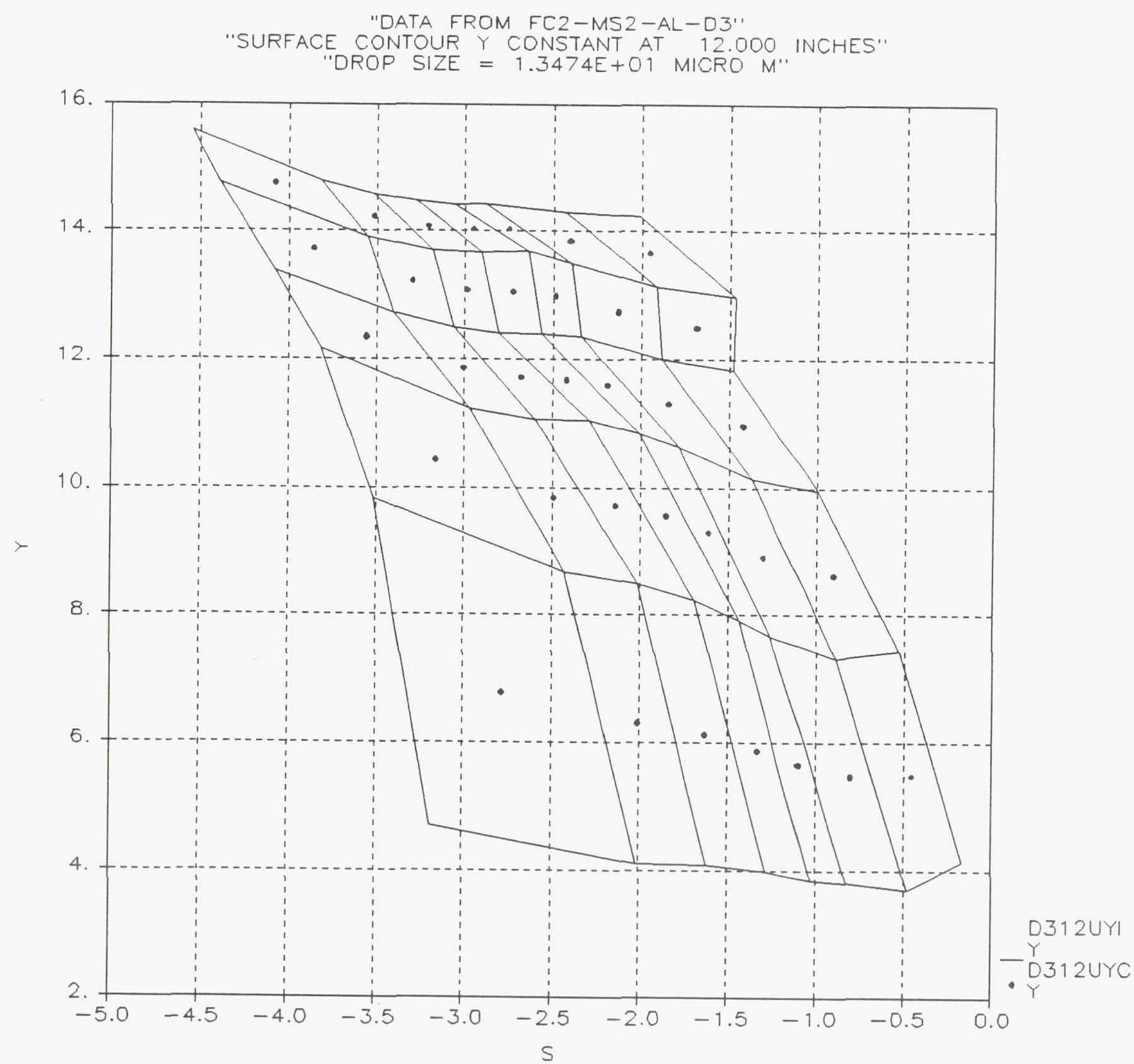

FIGURE D.77

IMPINGEMENT FIELD Y(in) vs S(in), FC2,Y=12U,D=13.5 micron

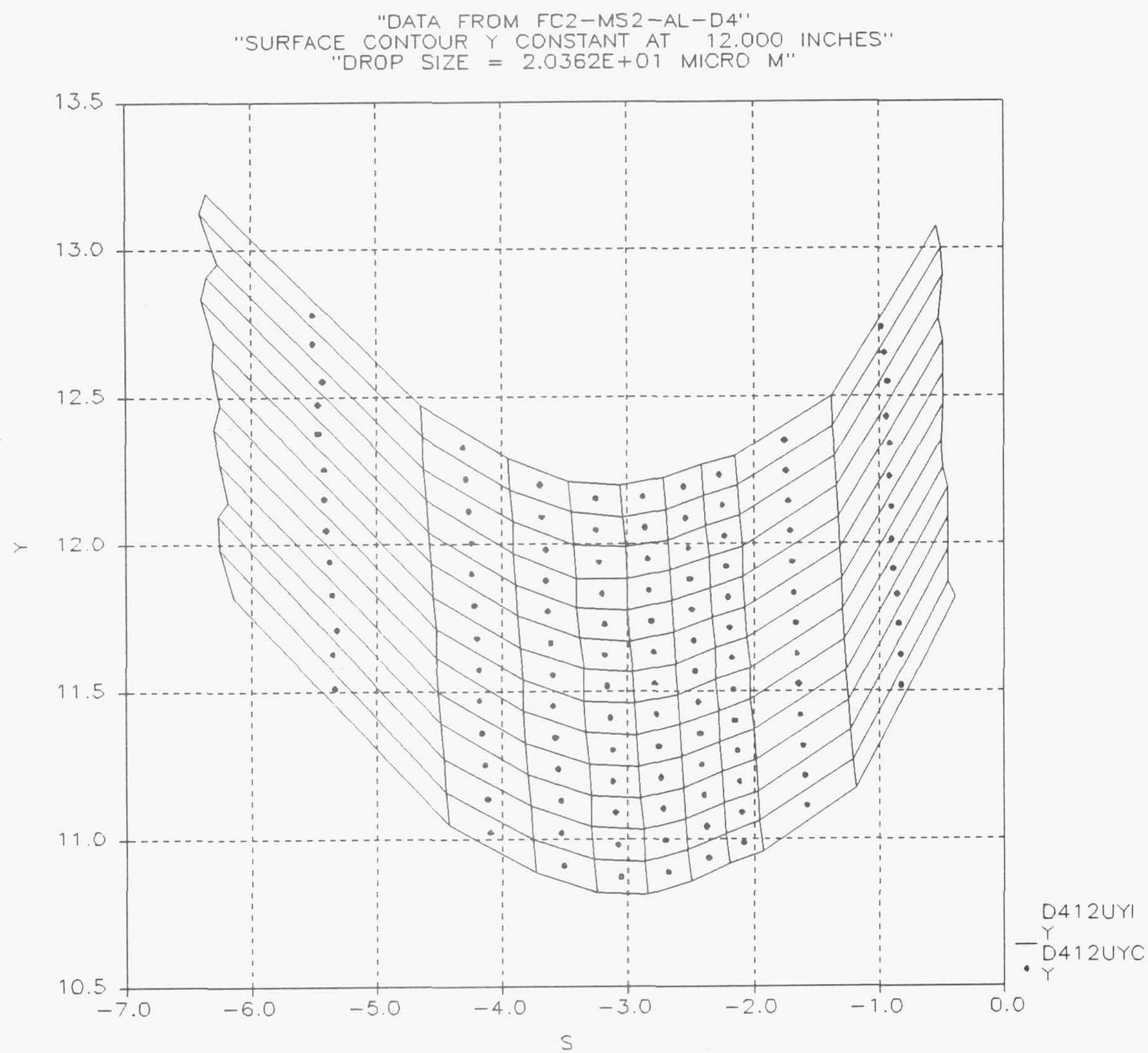

FIGURE D.78

IMPINGEMENT FIELD Y(in) vs S(in), FC2,Y=12U,D=20.4 micron

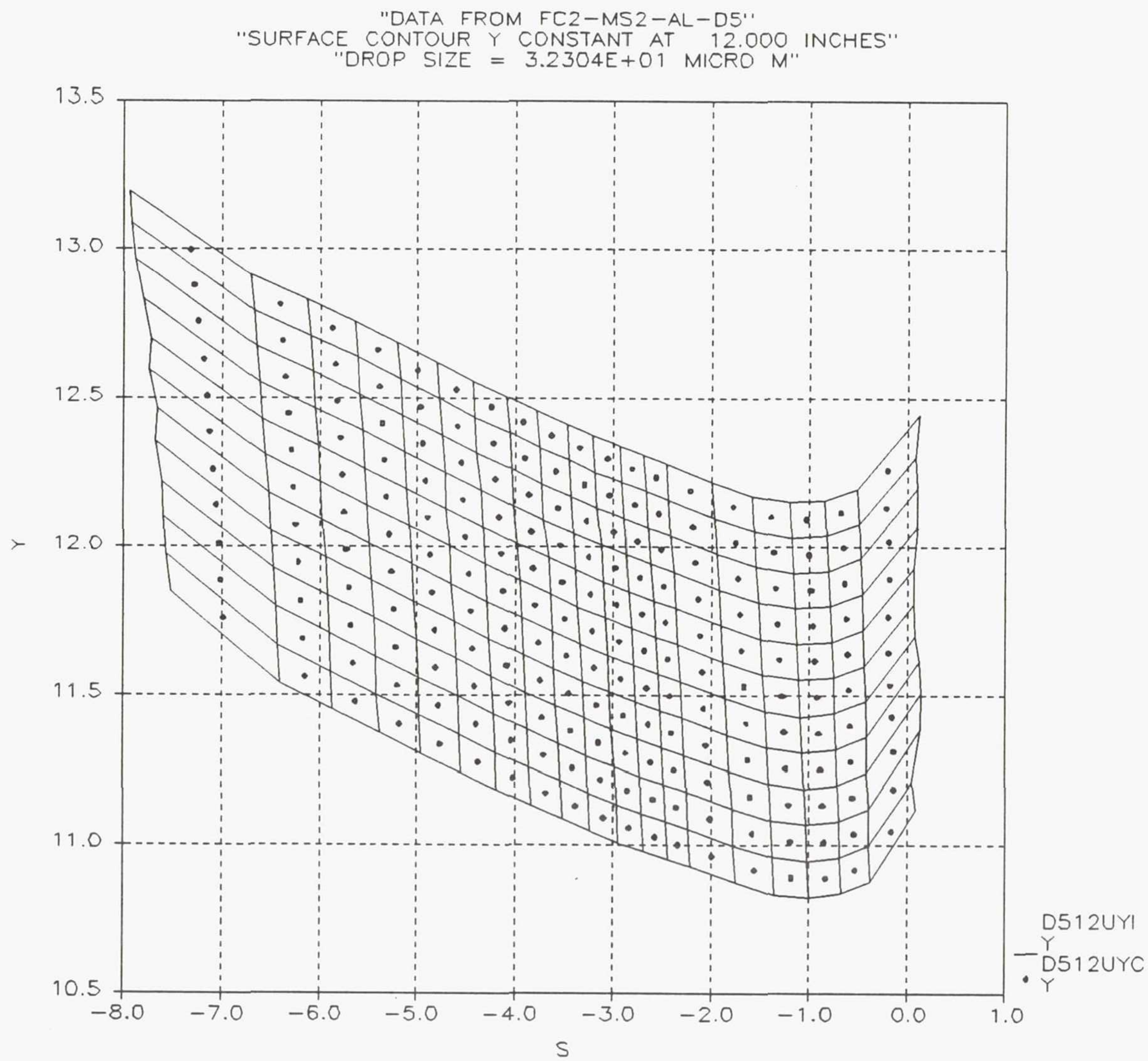

FIGURE D.79

IMPINGEMENT FIELD Y(in) vs S(in), FC2,Y=12U,D=32.3 micron

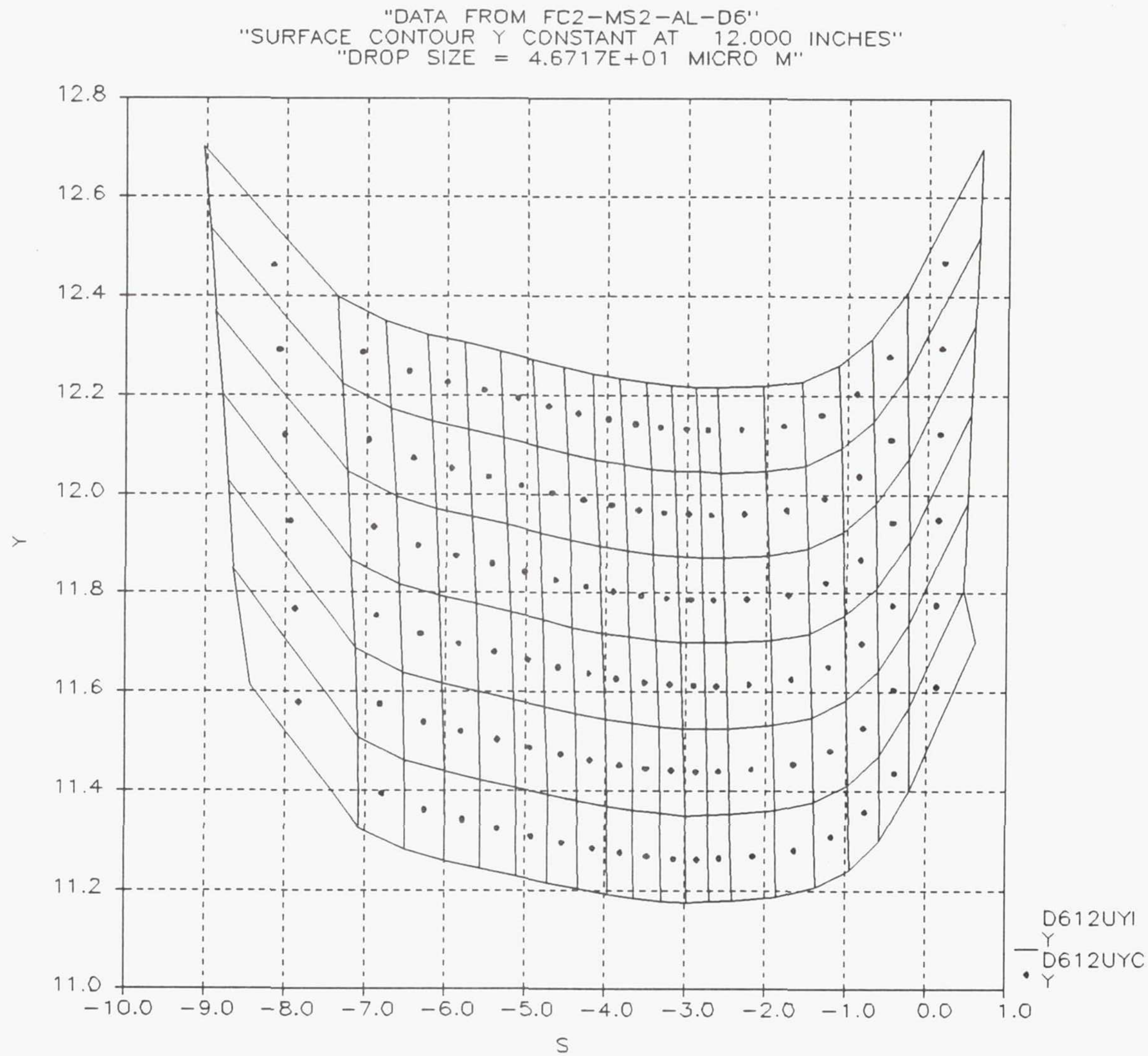

FIGURE D.80

IMPINGEMENT FIELD Y(in) vs S(in), FC2,Y=12U,D=46.7 micron

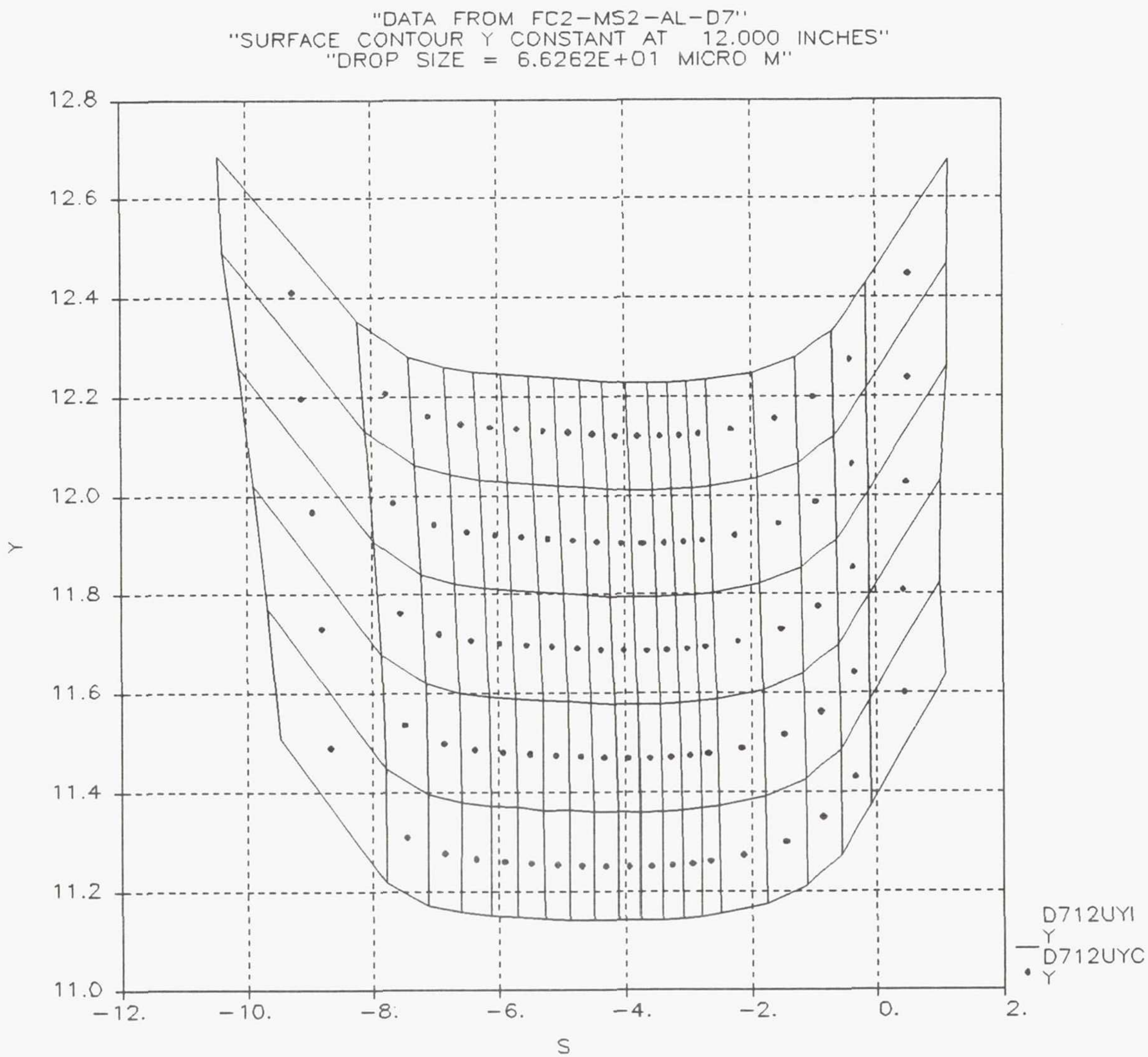

FIGURE D.81

IMPINGEMENT FIELD Y(in) vs S(in), FC2,Y=12U,D=66.3 micron

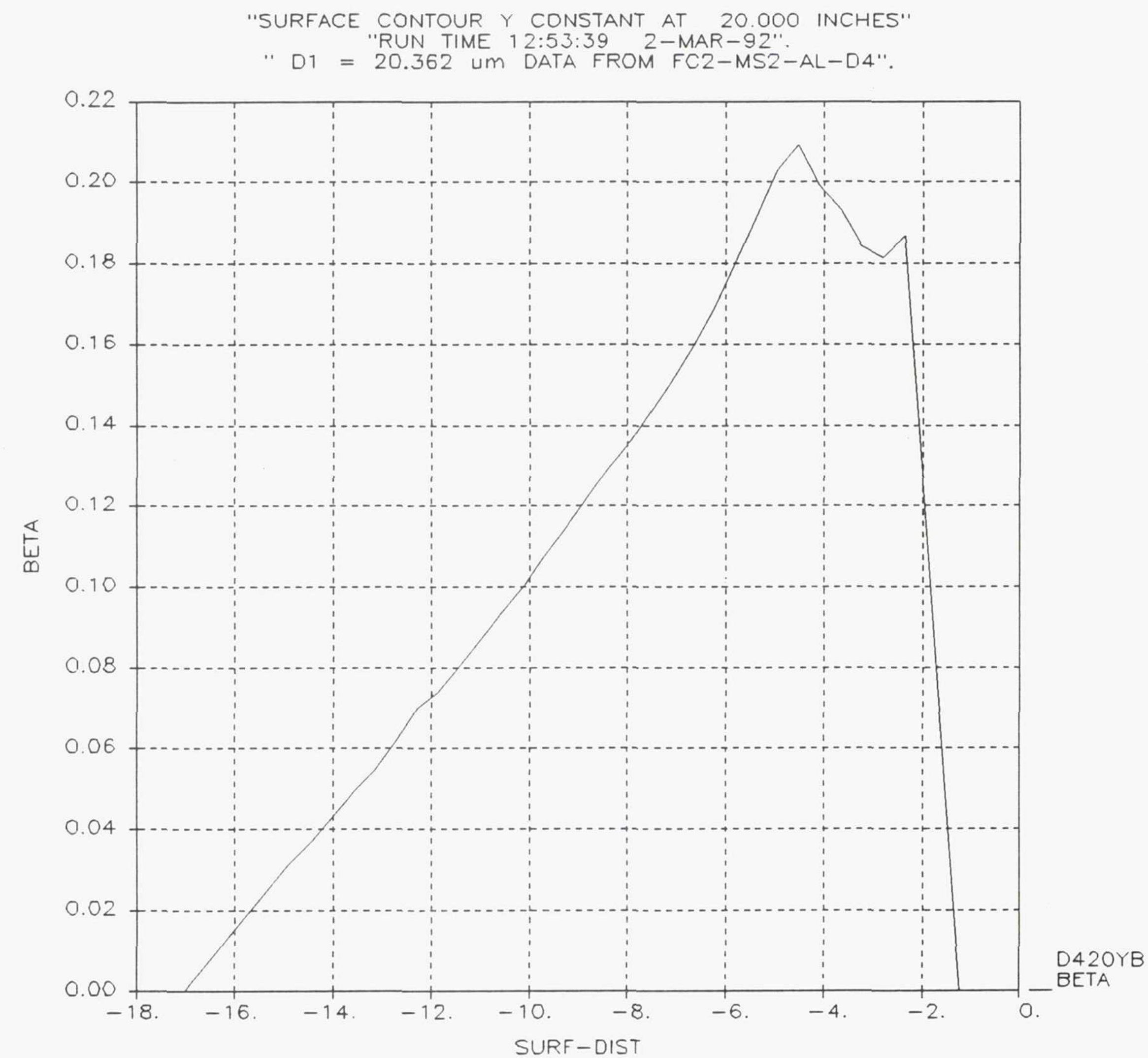

FIGURE D.82

BETA vs SURF-DIST(cm), FC2,Y=20,D=20.4 micron

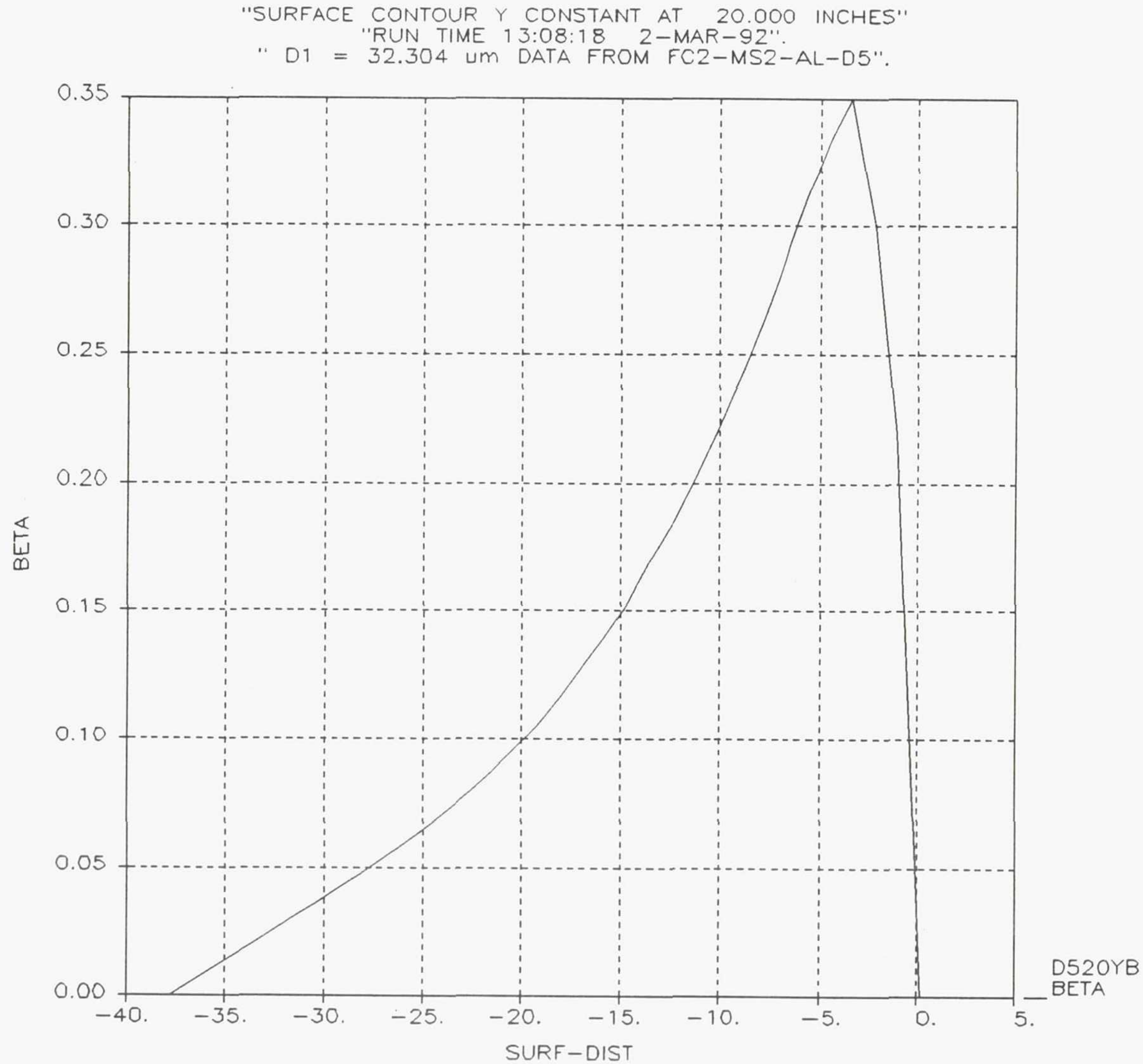

FIGURE D.83

BETA vs SURF-DIST(cm), FC2,Y=20,D=32.3 micron

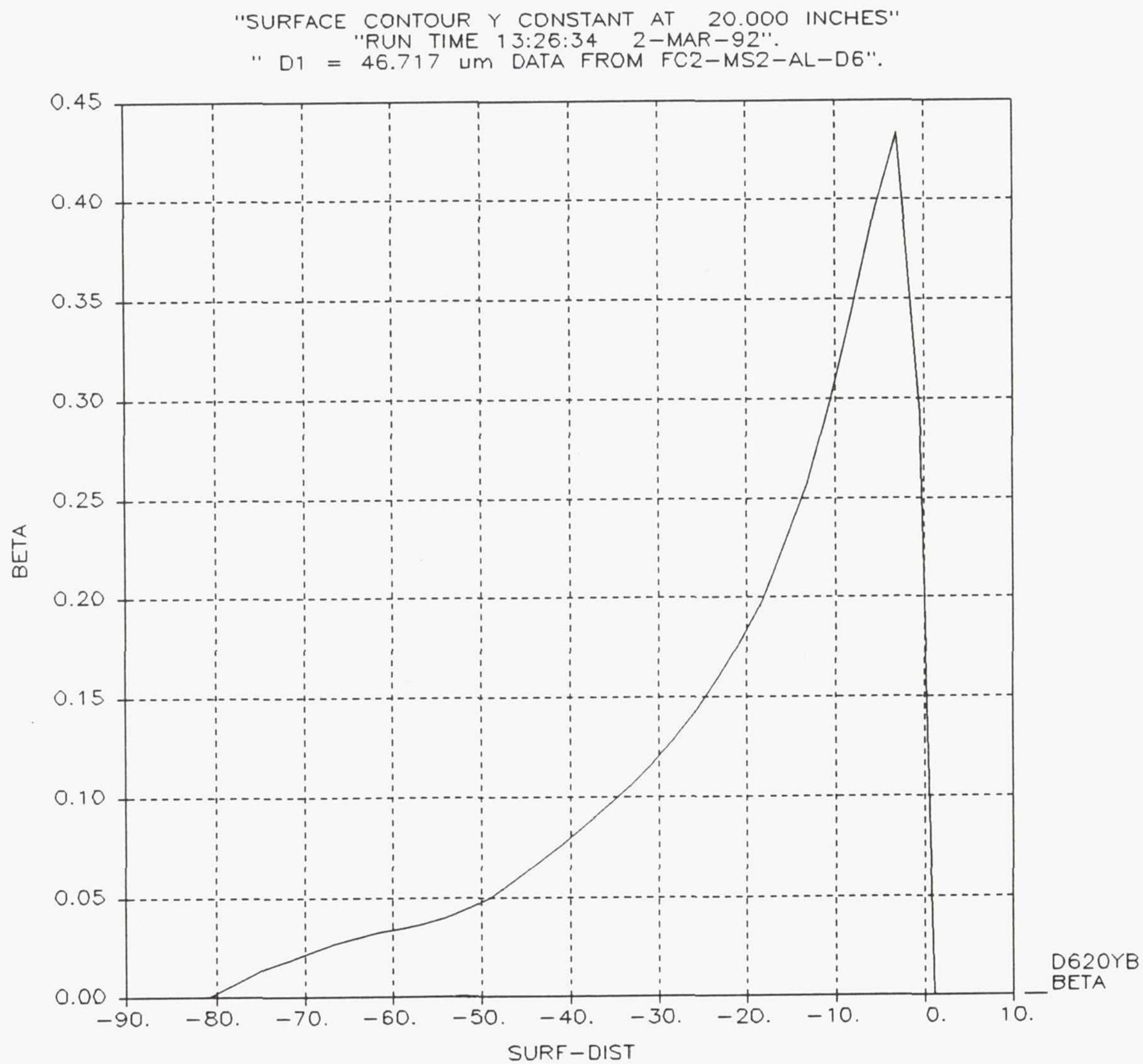

FIGURE D.84

BETA vs SURF-DIST(cm), FC2,Y=20,D=46.7 micron

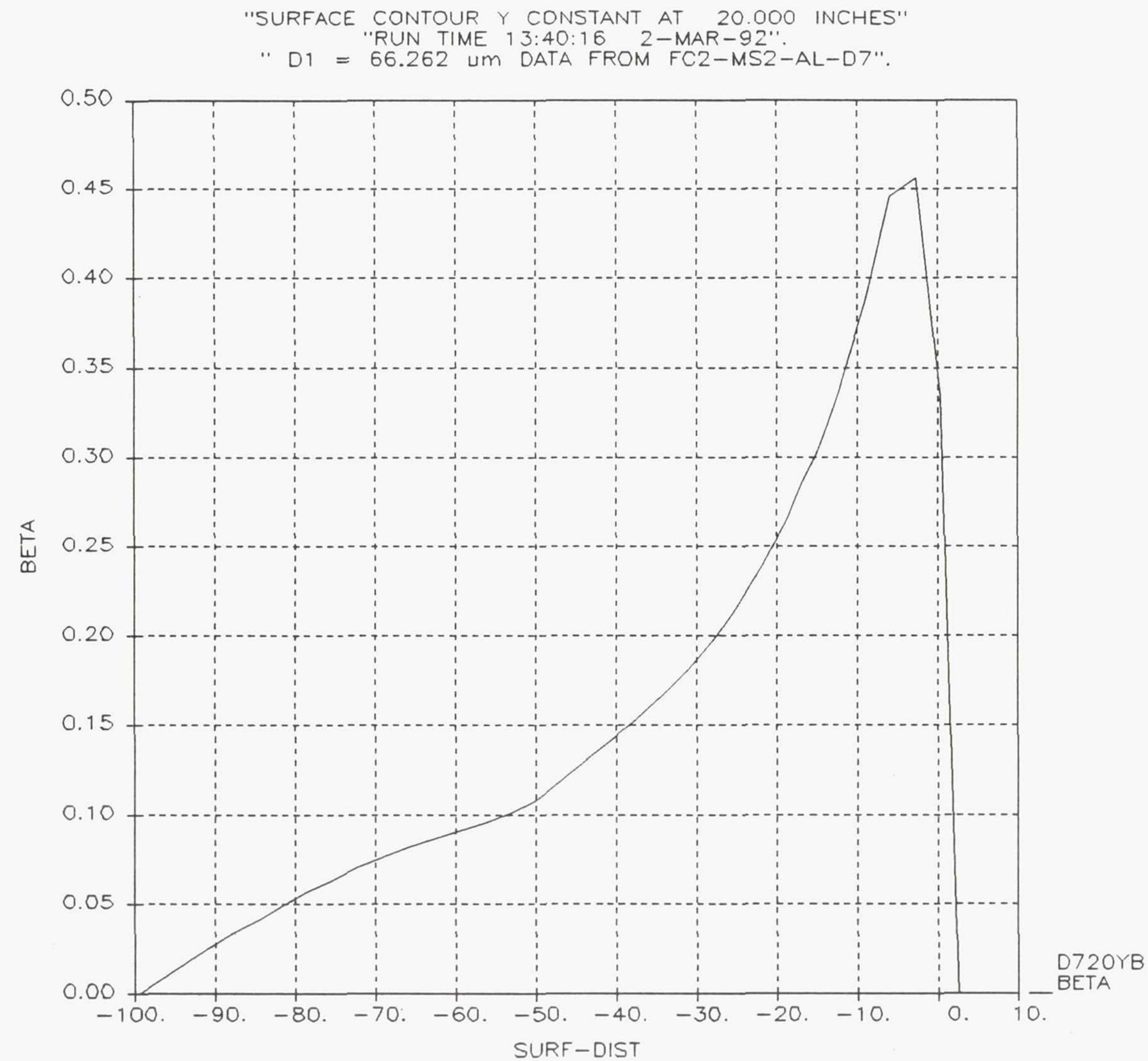

FIGURE D.85

BETA vs SURF-DIST(cm), FC2,Y=20,D=66.3 micron

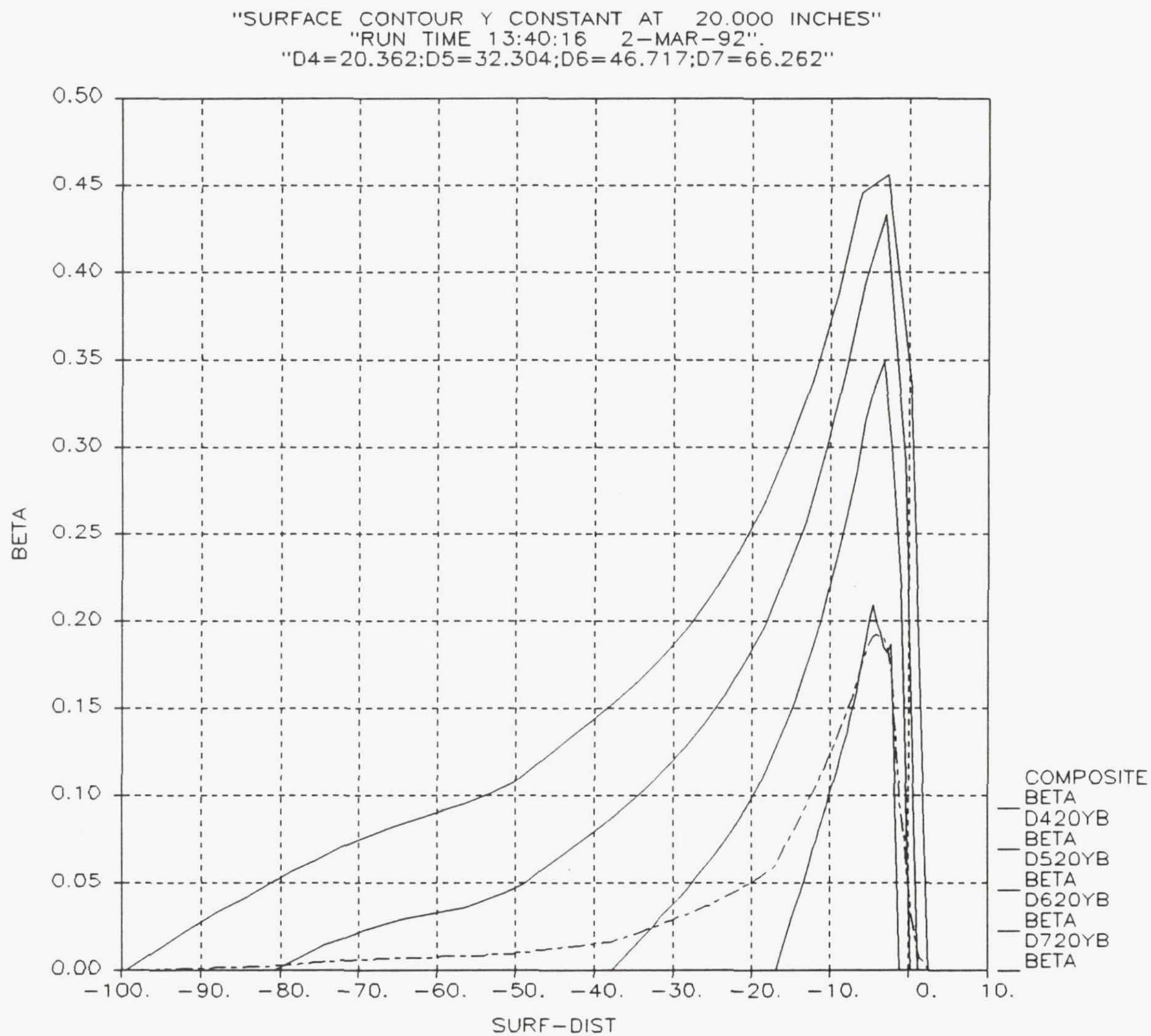

FIGURE D.86

BETA vs SURF-DIST(cm), FC2, Y=20, COMPOSITE AND INDIVIDUAL DROPS

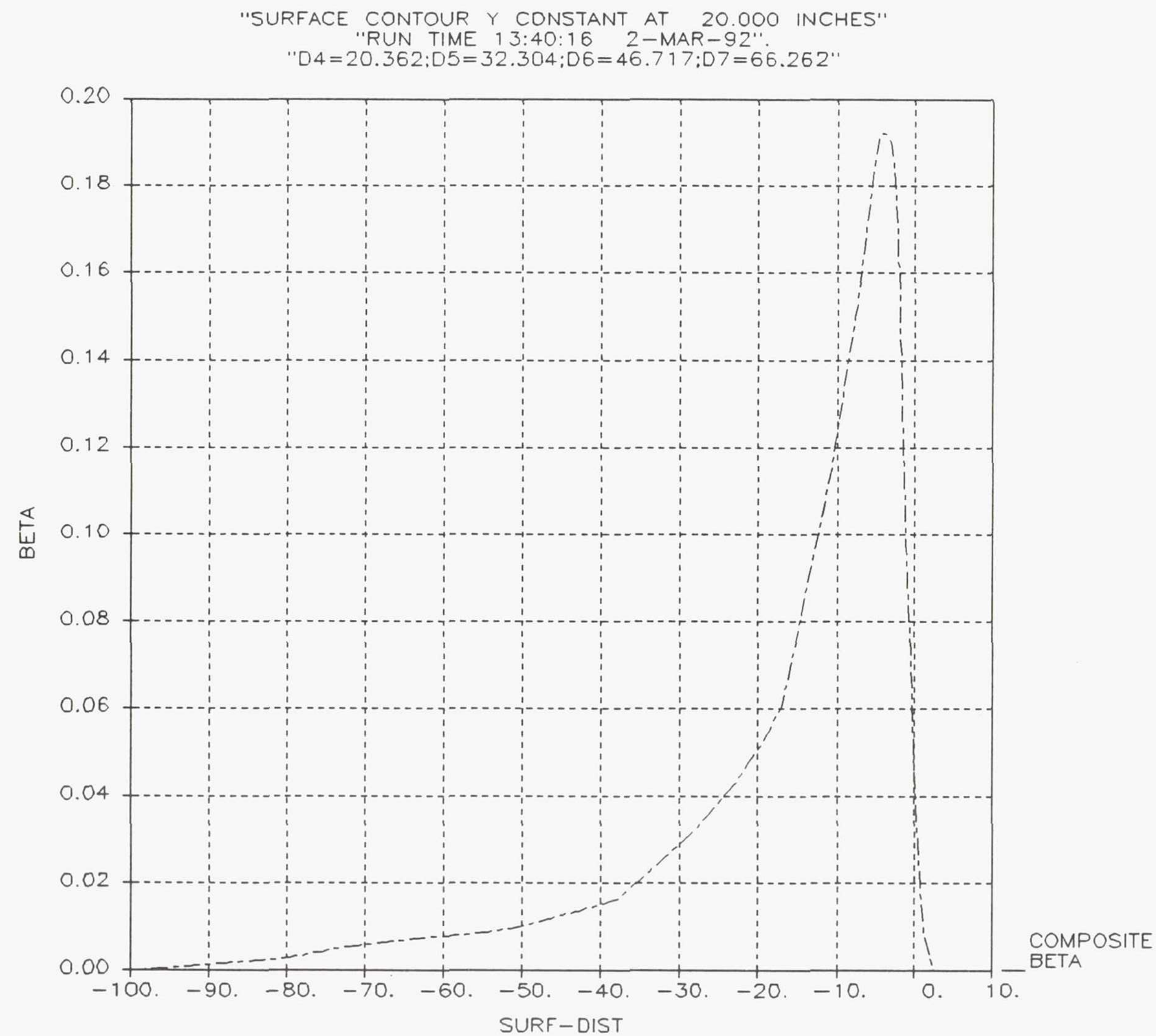

FIGURE D.87

BETA vs SURF-DIST(cm), FC2,Y=20,D=20.4 micron
COMPOSITE DROP

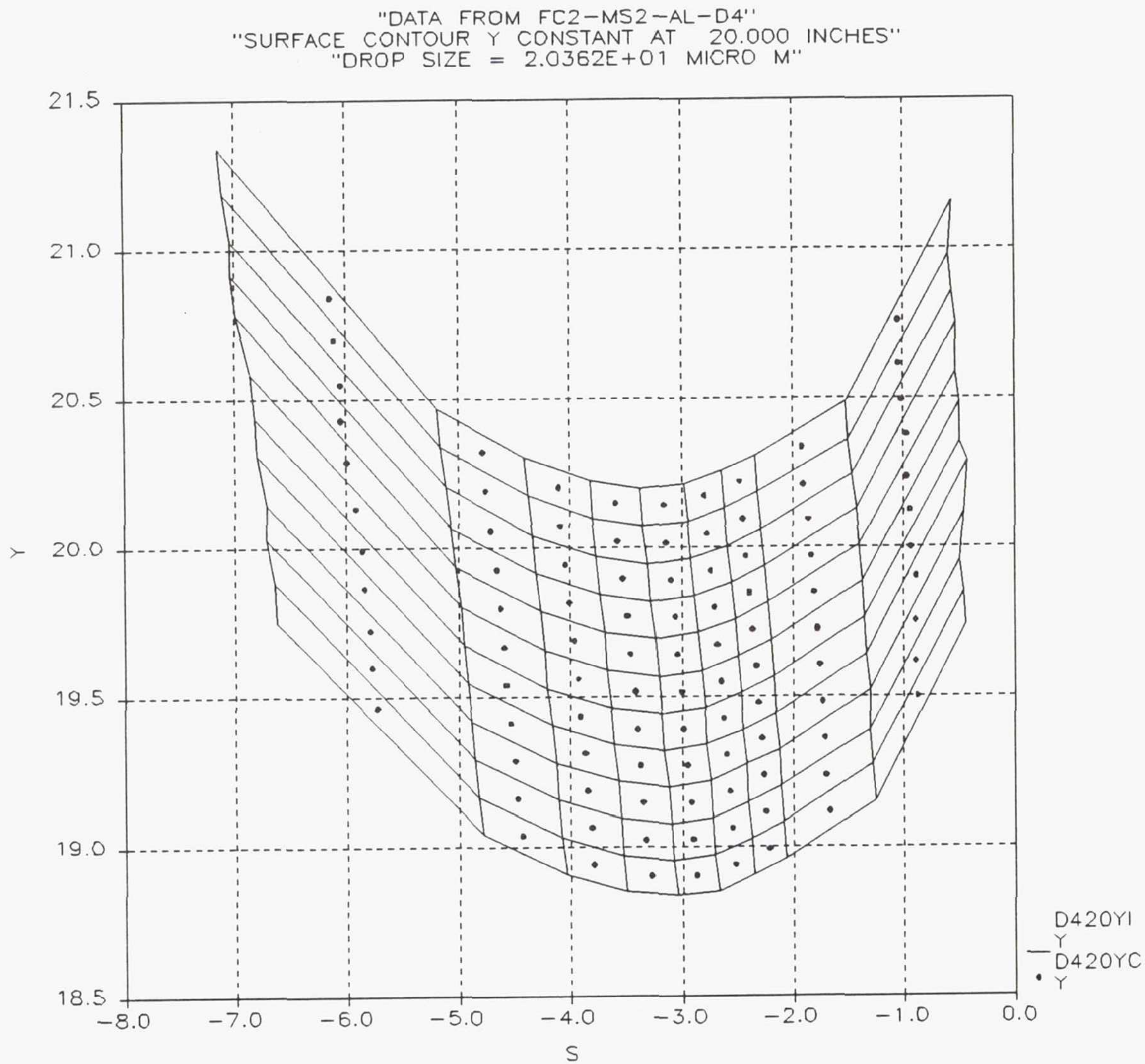

FIGURE D.88

IMPINGEMENT FIELD Y(in) vs S(in), FC2,Y=20,D=20.4 micron

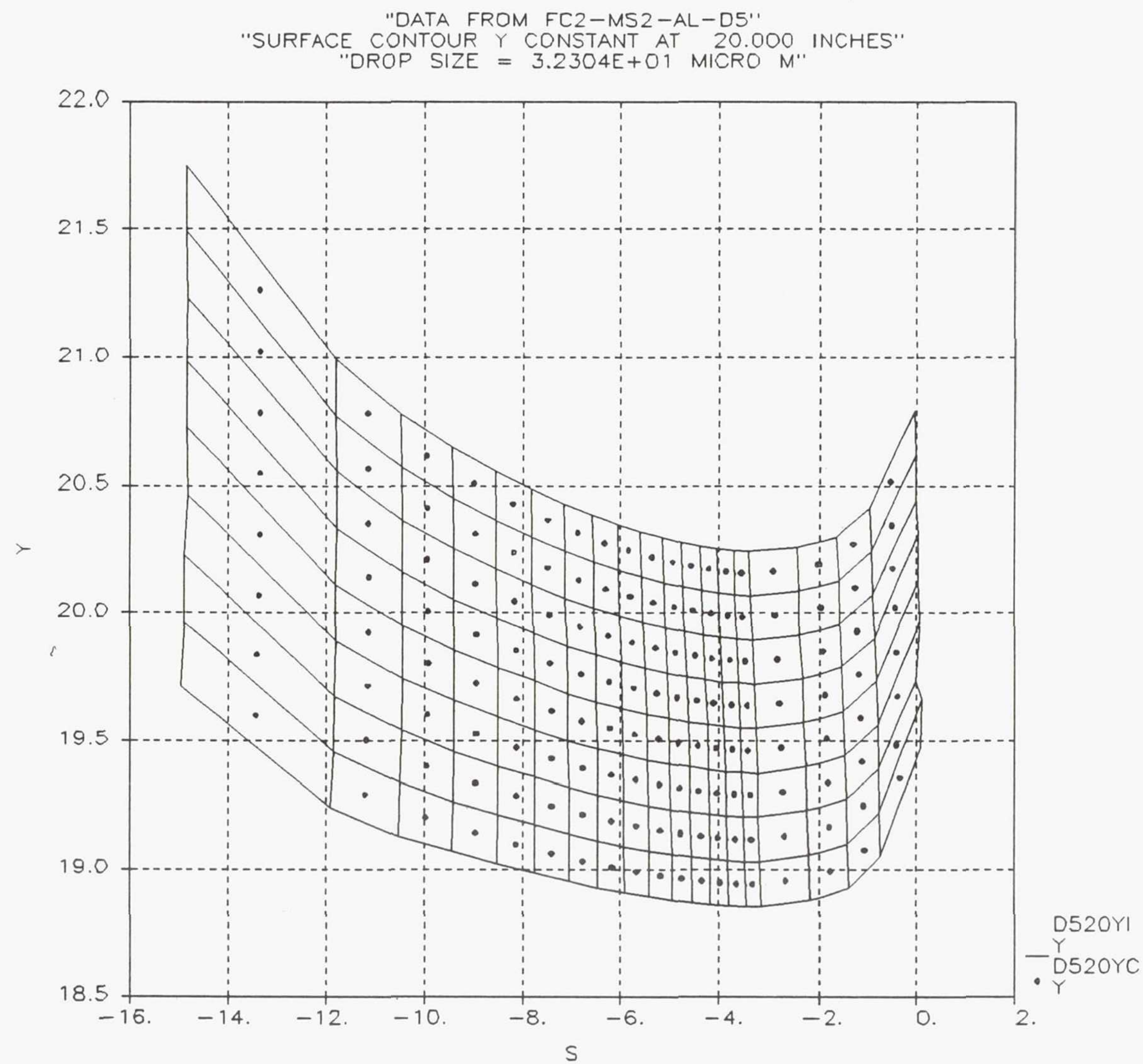

FIGURE D.89

IMPINGEMENT FIELD Y(in) vs S(in), FC2,Y=20,D=32.3 micron

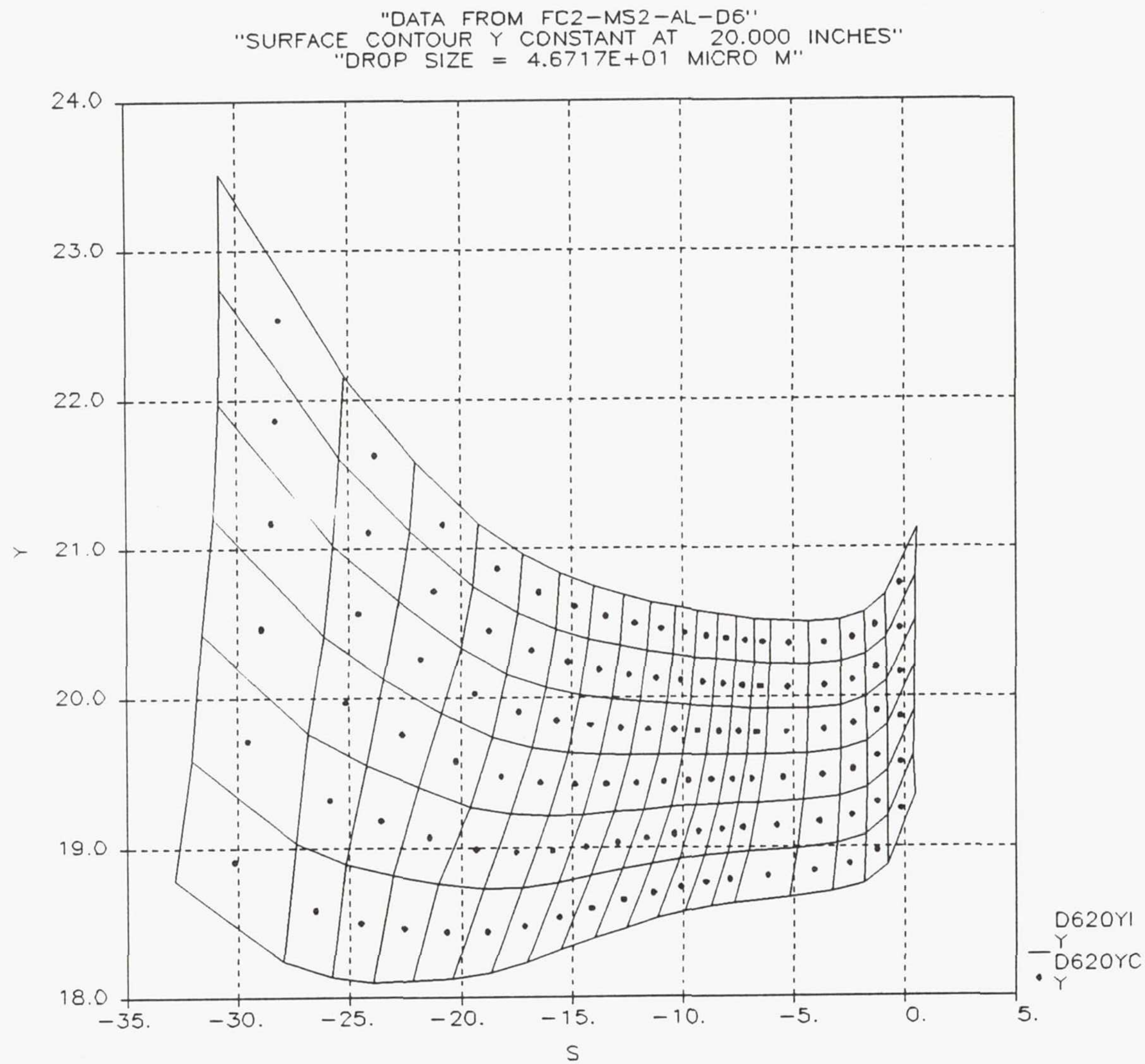

FIGURE D.90

IMPINGEMENT FIELD Y(in) vs S(in), FC2,Y=20,D=46.7 micron

FIGURE D.91

IMPINGEMENT FIELD Y(in) vs S(in), FC2,Y=20,D=66.3 micron

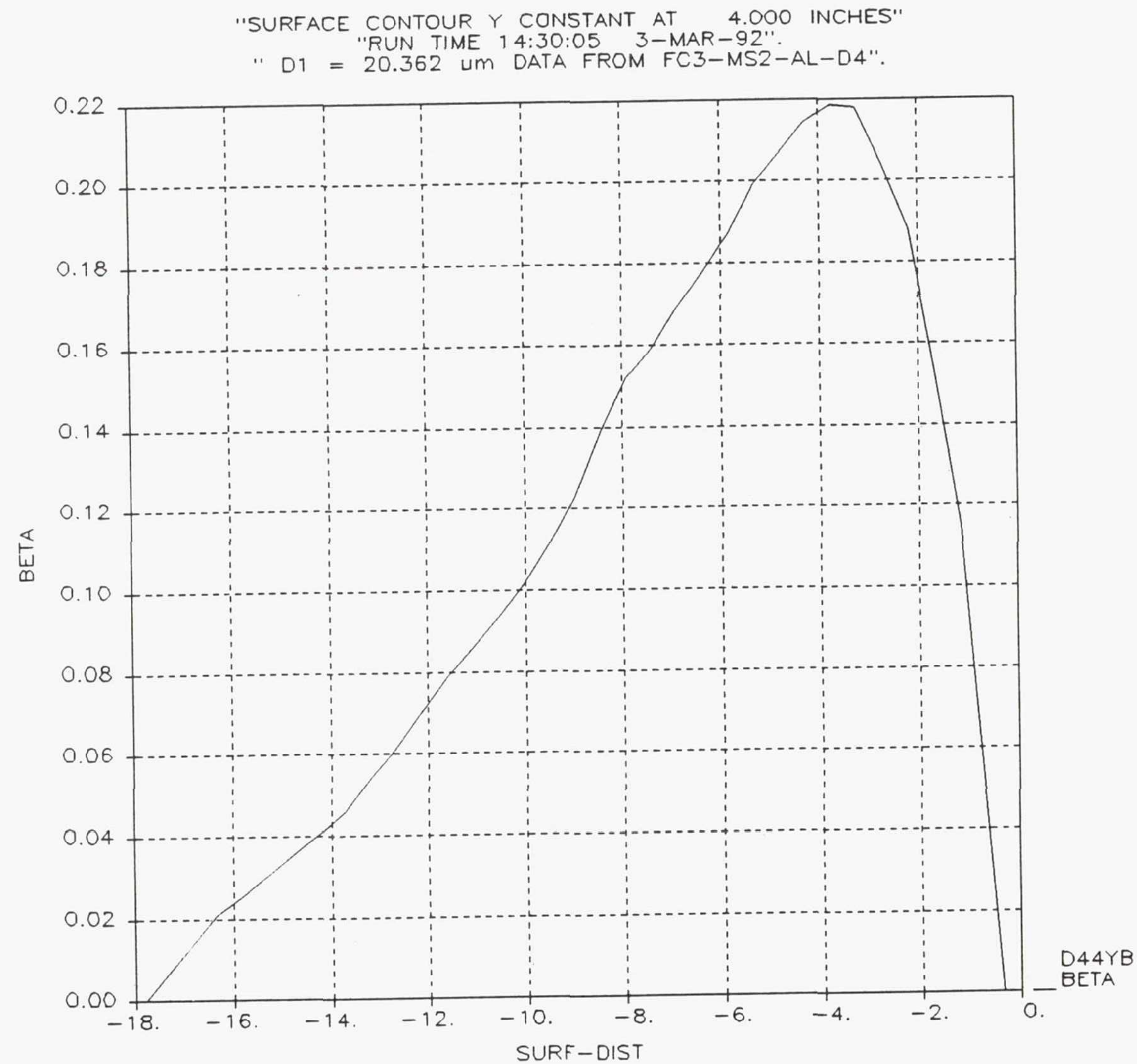

FIGURE D.92

BETA vs SURF-DIST(cm), FC3,Y=4,D=20.4 micron

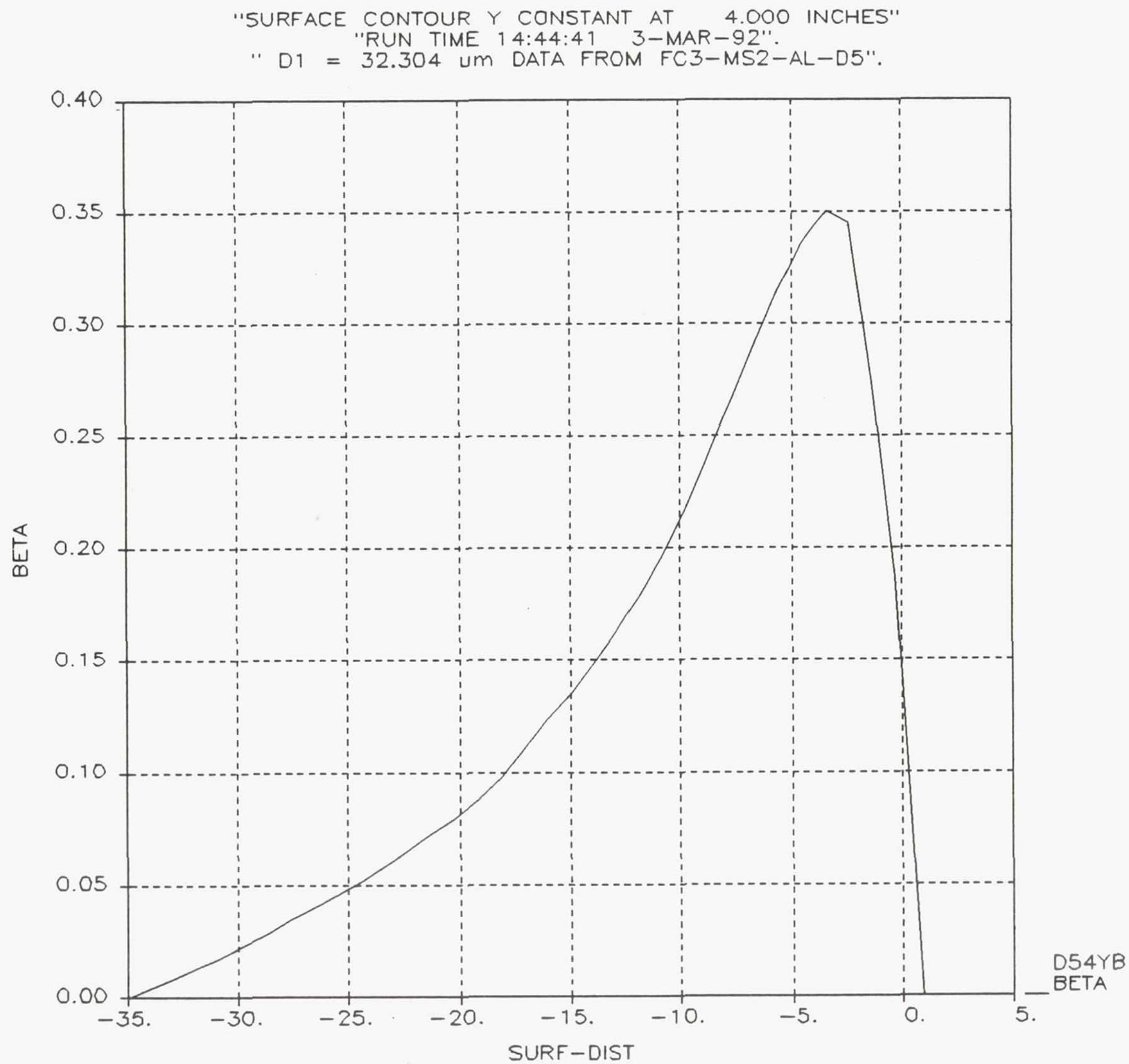

FIGURE D.93

BETA vs SURF-DIST(cm), FC3,Y=4,D=32.3 micron

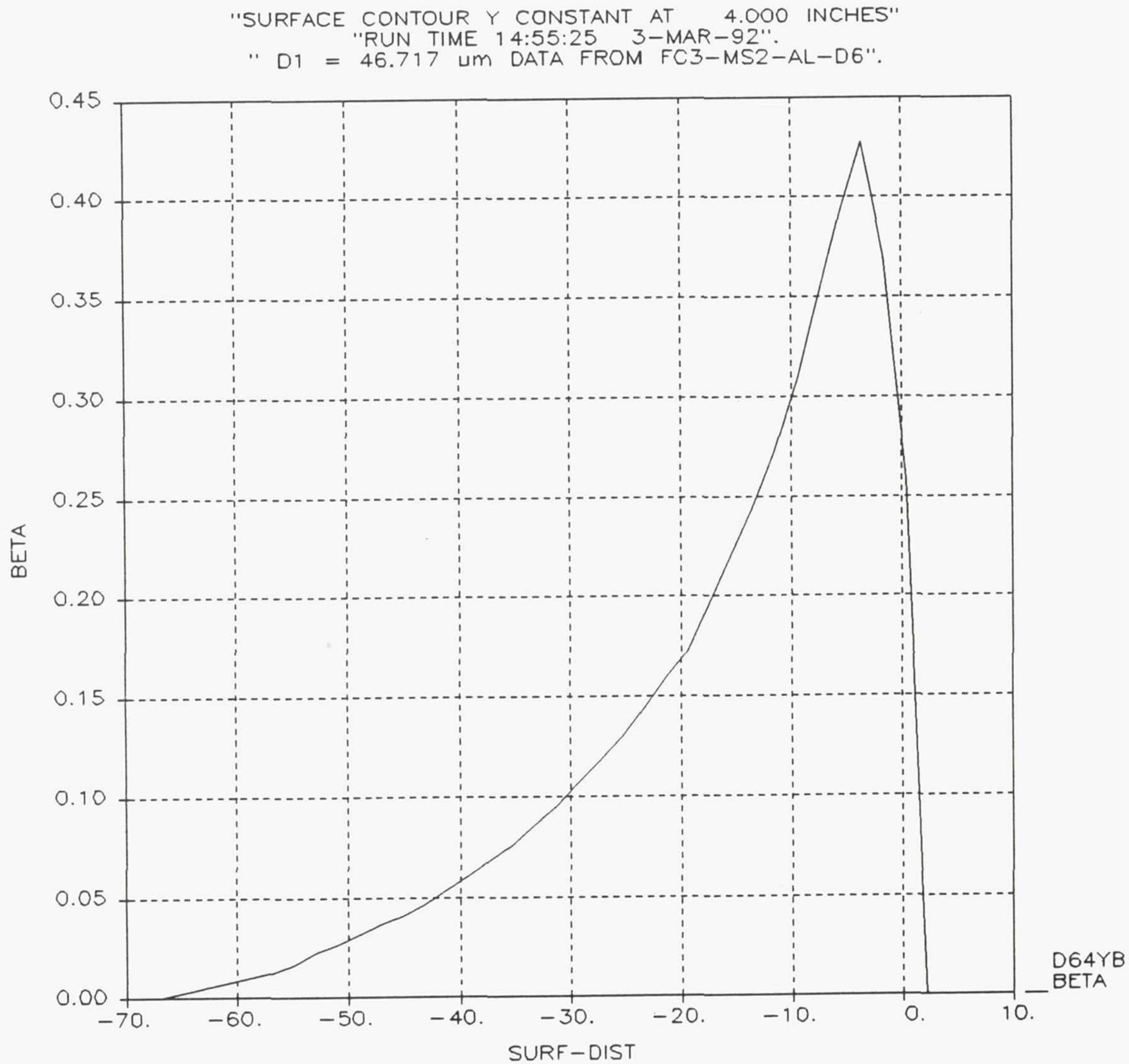

FIGURE D.94

BETA vs SURF-DIST(cm), FC3,Y=4,D=46.7 micron

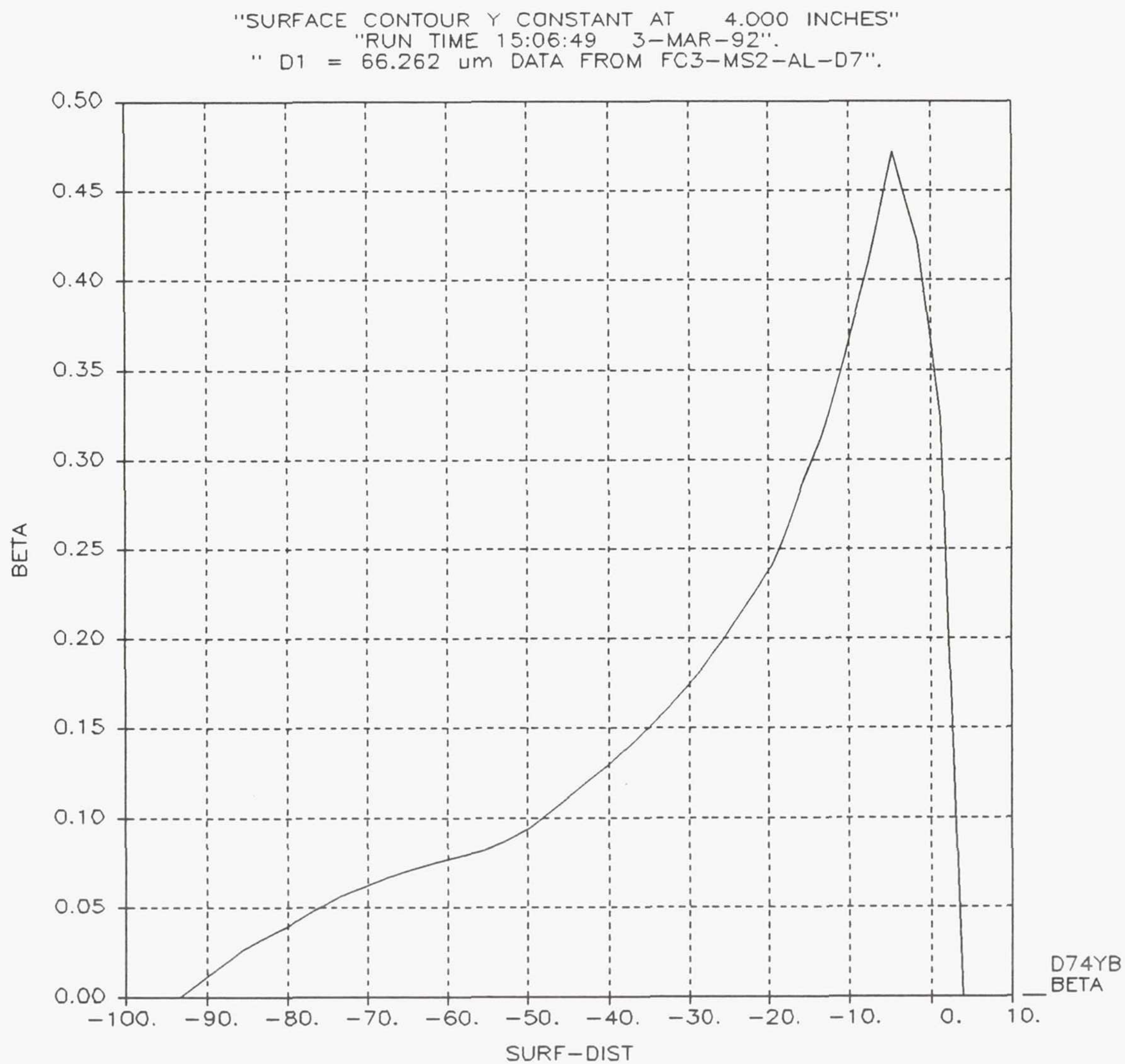

FIGURE D.95

BETA vs SURF-DIST(cm), FC3,Y=4,D=66.3 micron

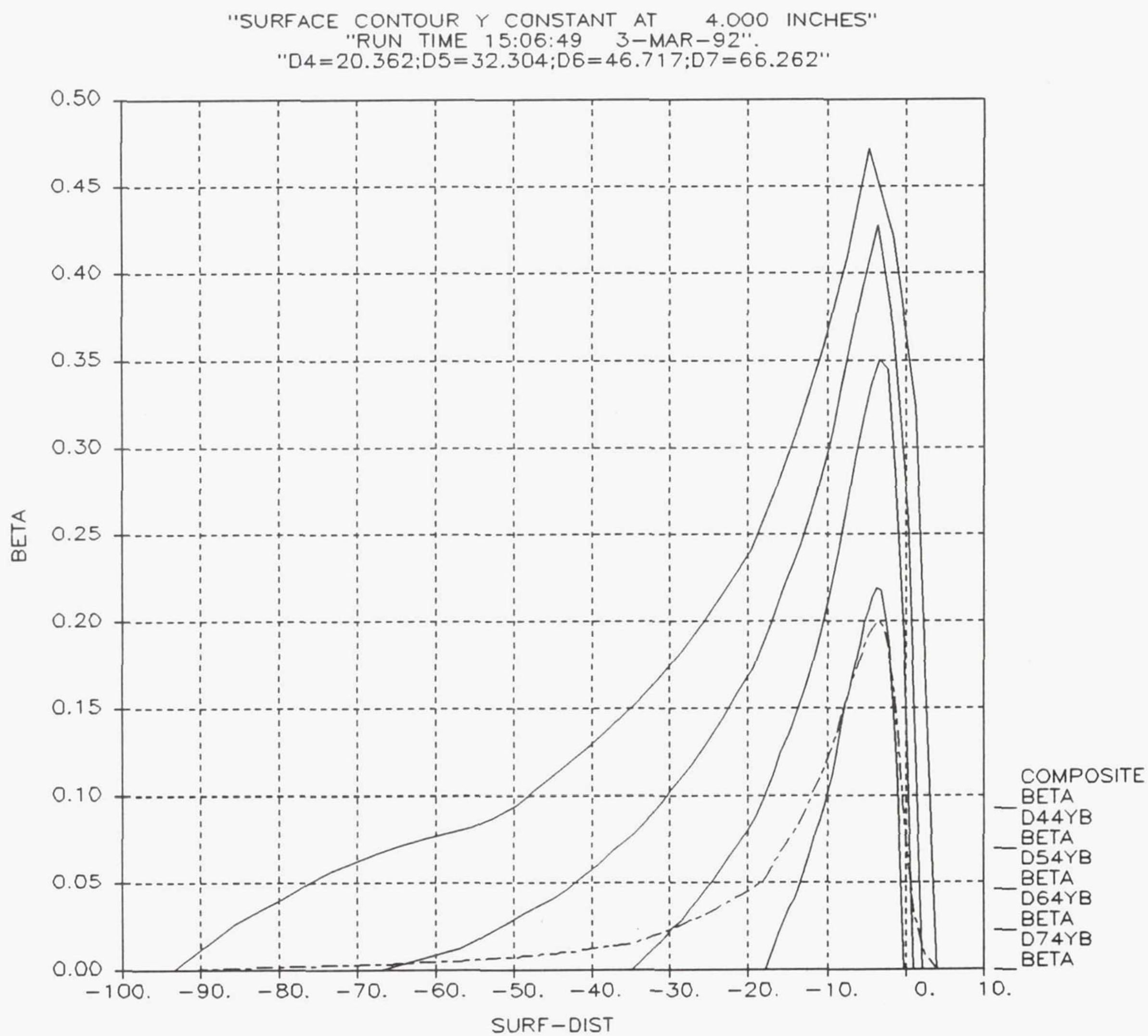

FIGURE D.96

BETA vs SURF-DIST(cm), FC3,Y=4,COMPOSITE AND INDIVIDUAL DROPS

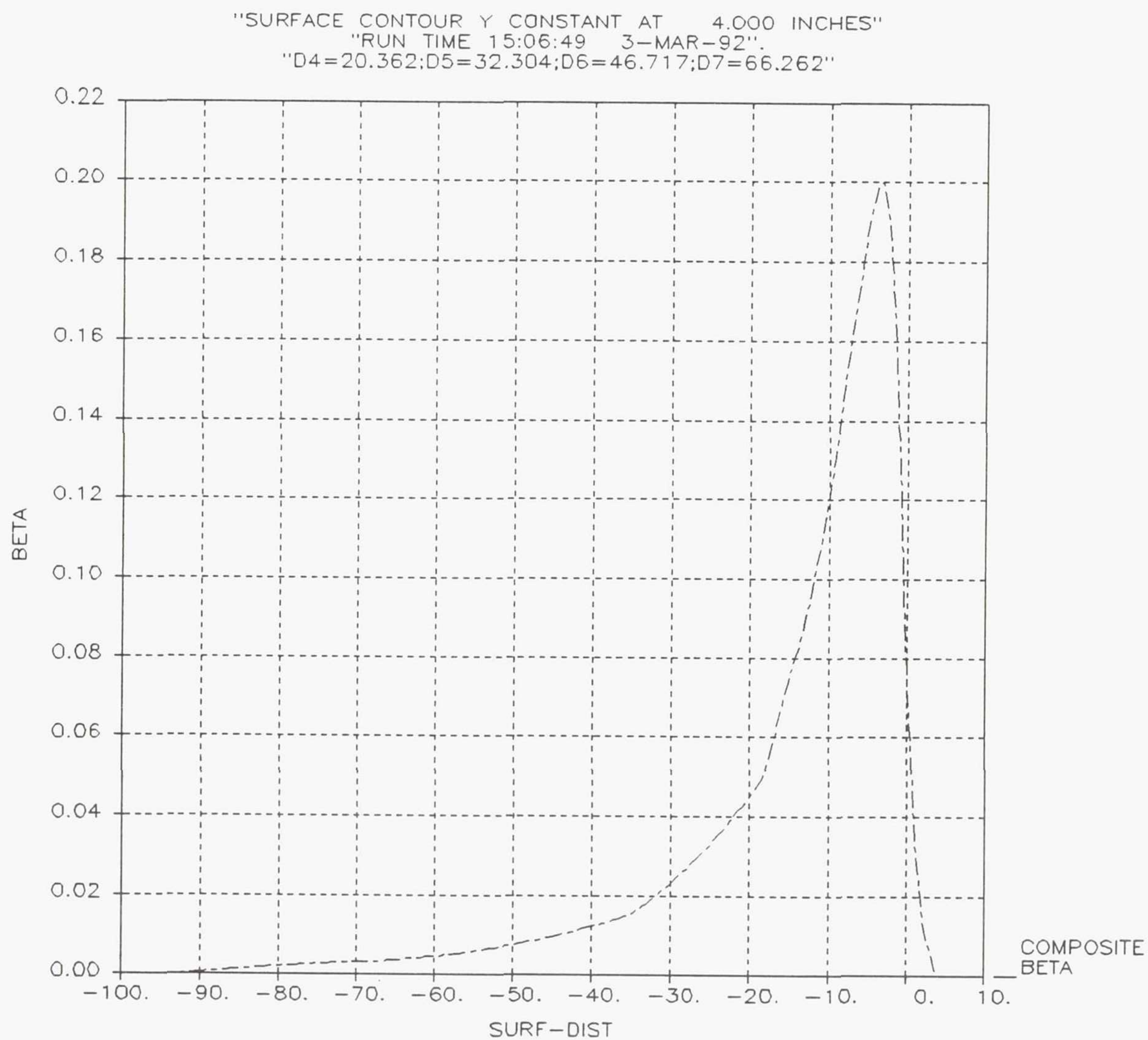

FIGURE D.97

BETA vs SURF-DIST(cm), FC3,Y=4,D=20.4 micron
COMPOSITE DROP

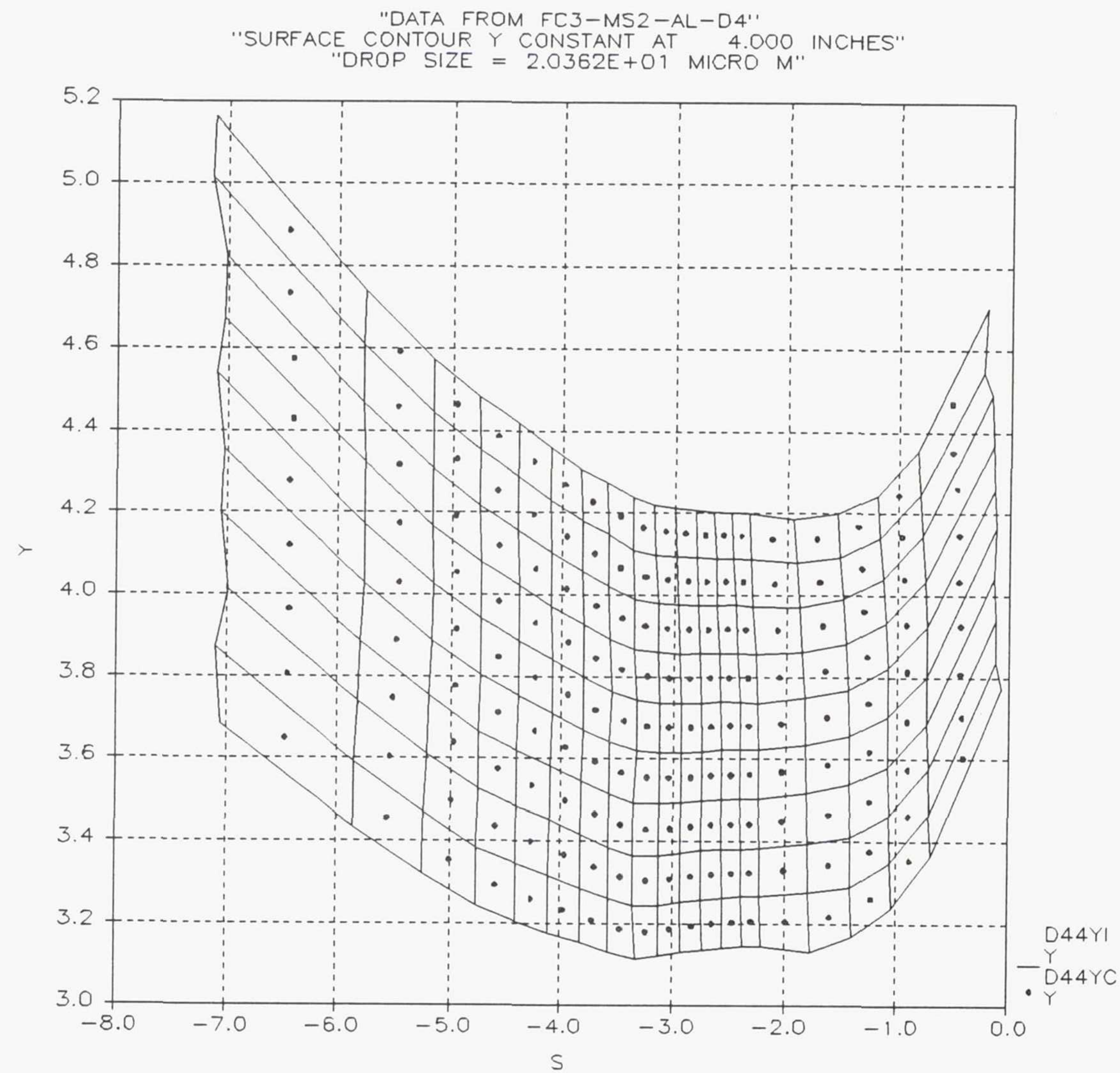

FIGURE D.98

IMPINGEMENT FIELD Y(in) vs S(in), FC3,Y=4,D=20.4 micron

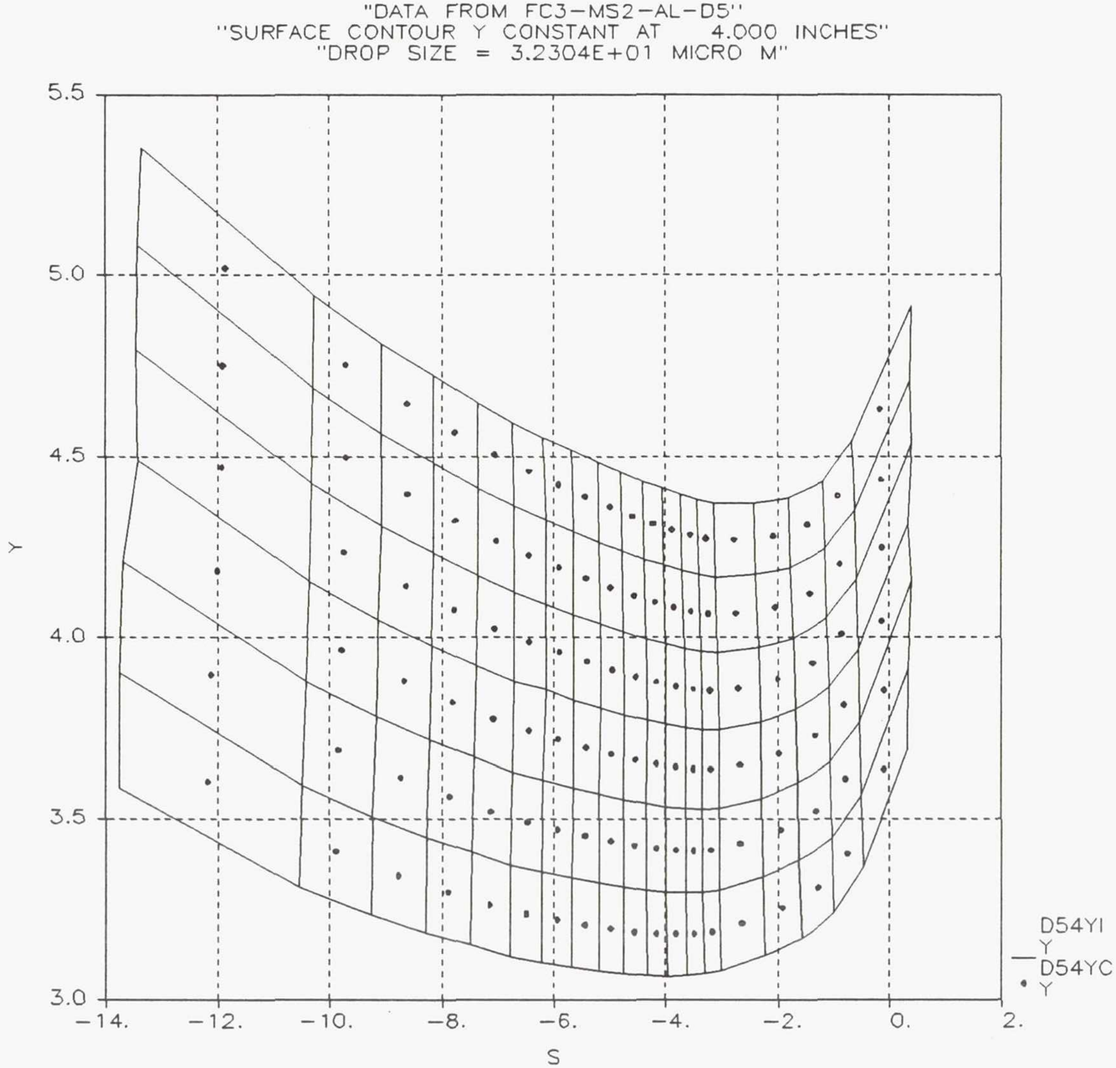

FIGURE D.99

IMPINGEMENT FIELD Y(in) vs S(in), FC3,Y=4,D=32.3 micron

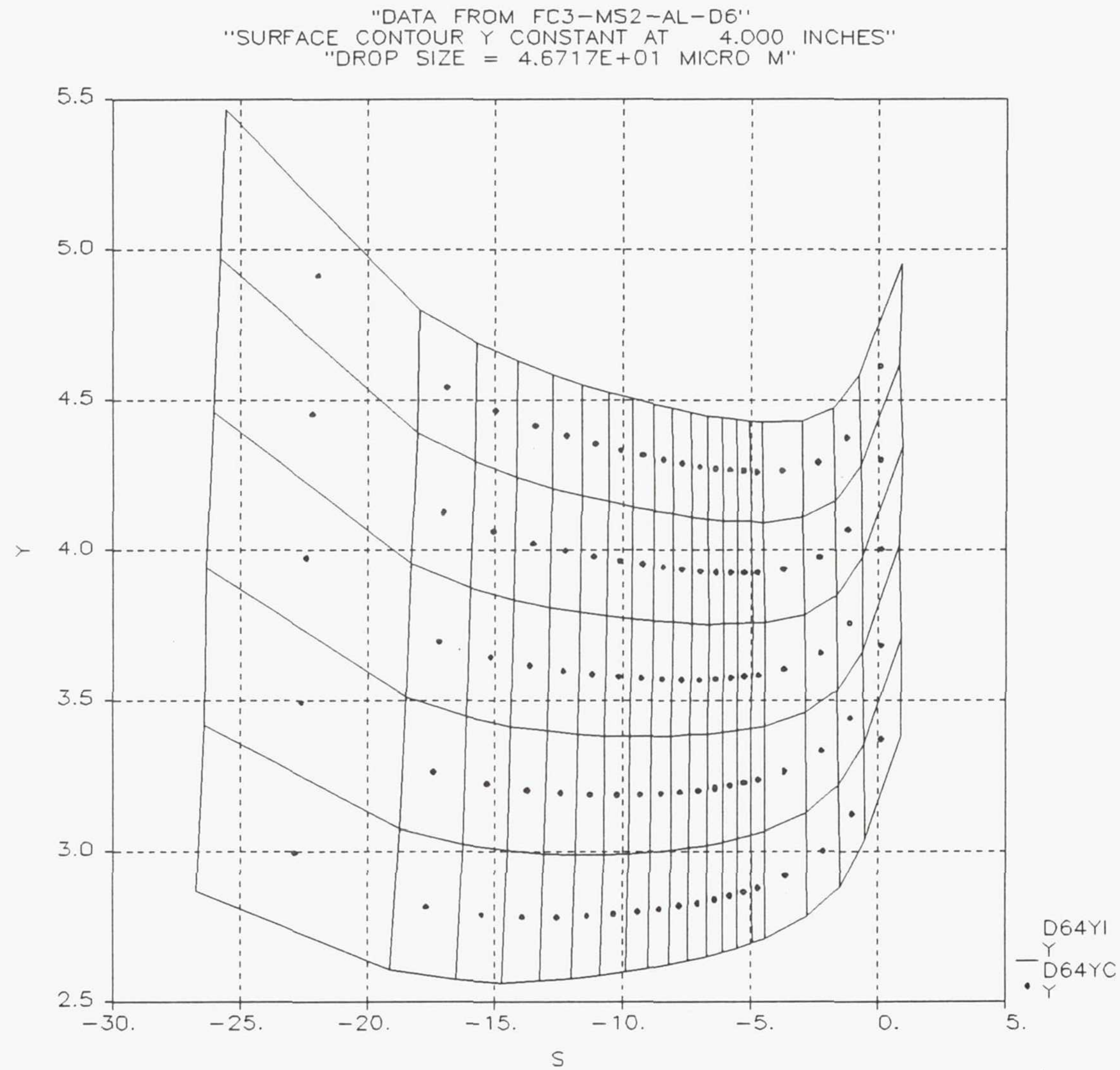

FIGURE D.100

IMPINGEMENT FIELD Y(in) vs S(in), FC3,Y=4,D=46.7 micron

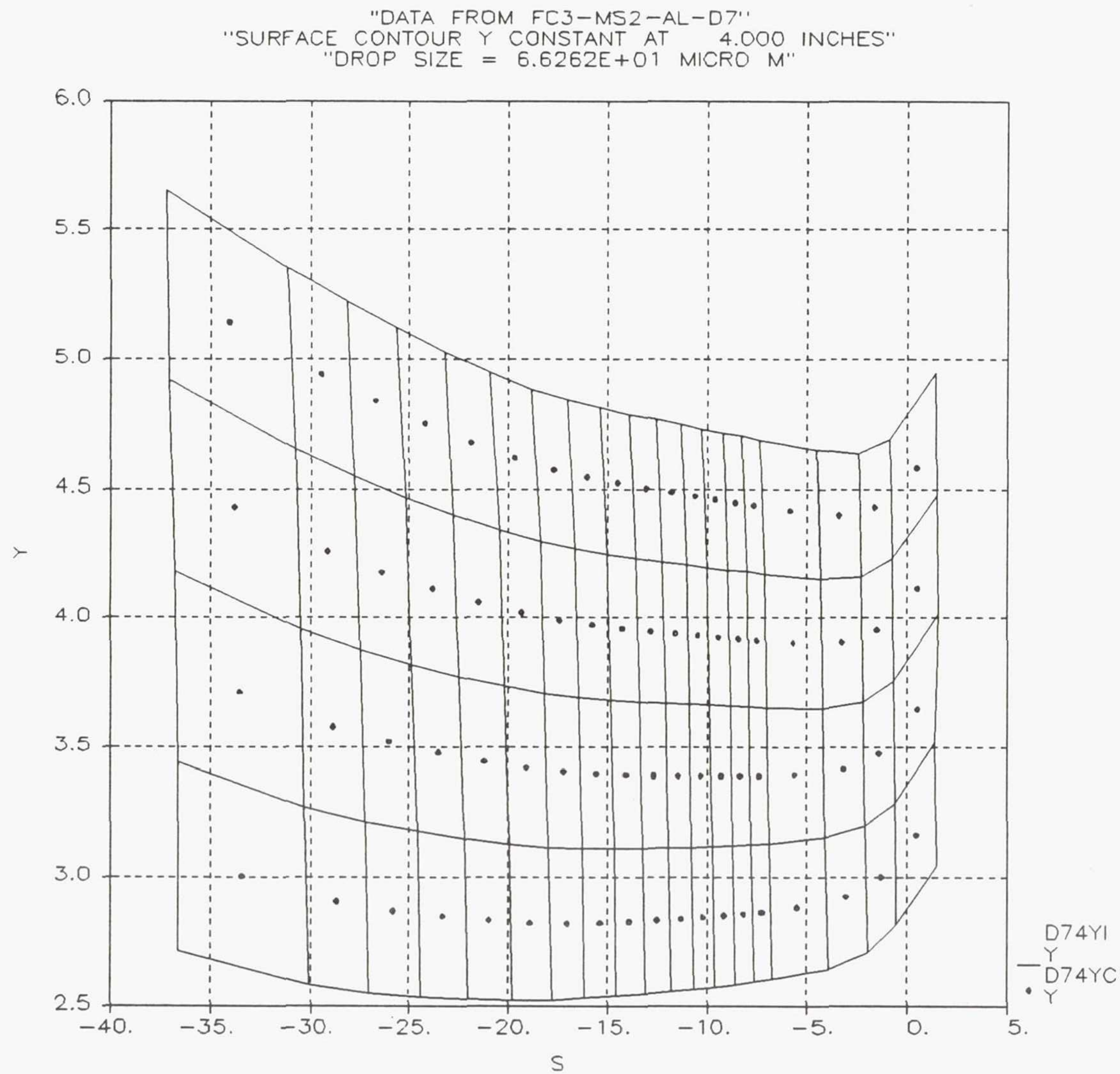

FIGURE D.101

IMPINGEMENT FIELD Y(in) vs S(in), FC3,Y=4,D=66.3 micron

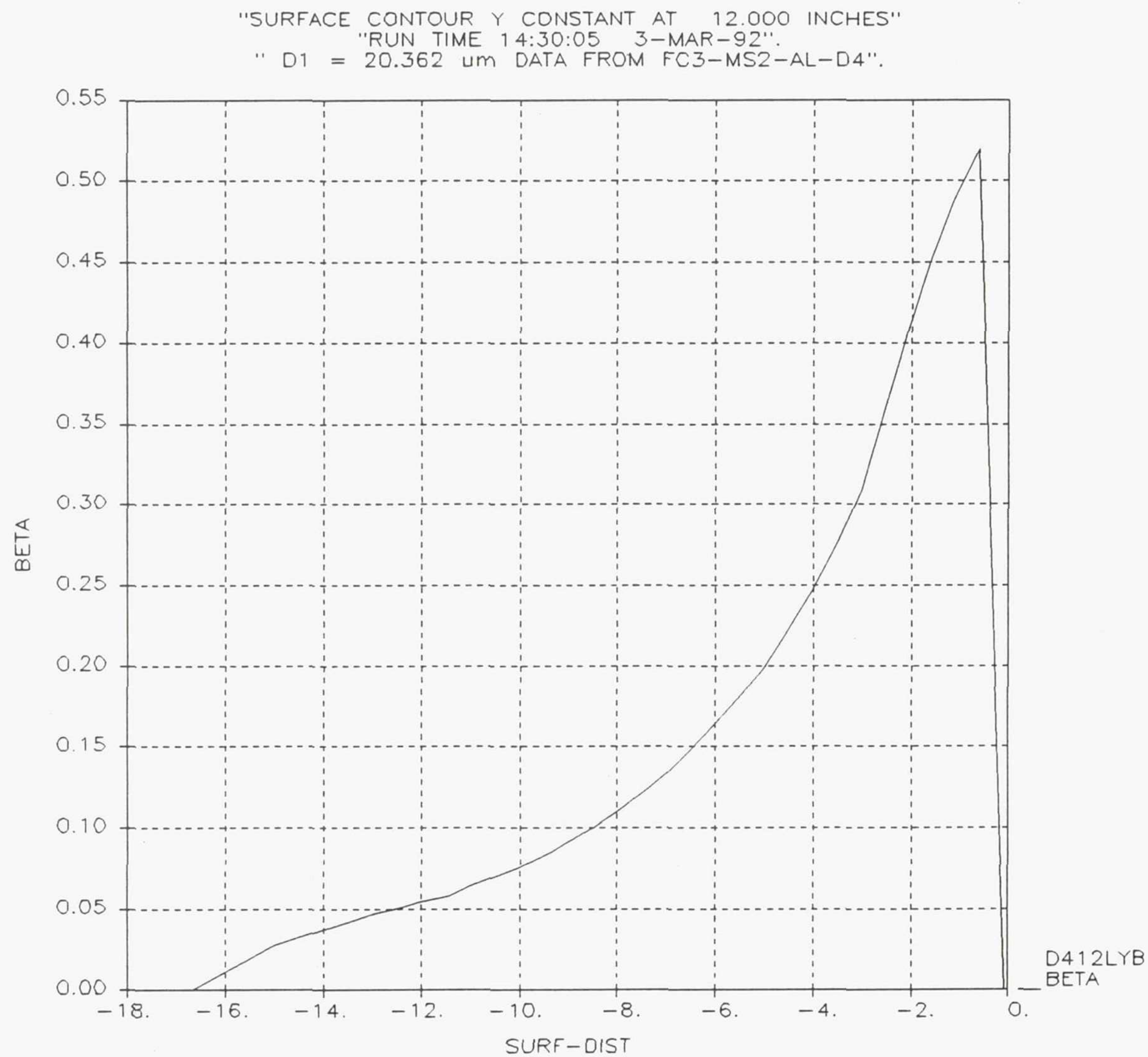

FIGURE D.102

BETA vs SURF-DIST(cm), FC3,Y=12L,D=20.4 micron

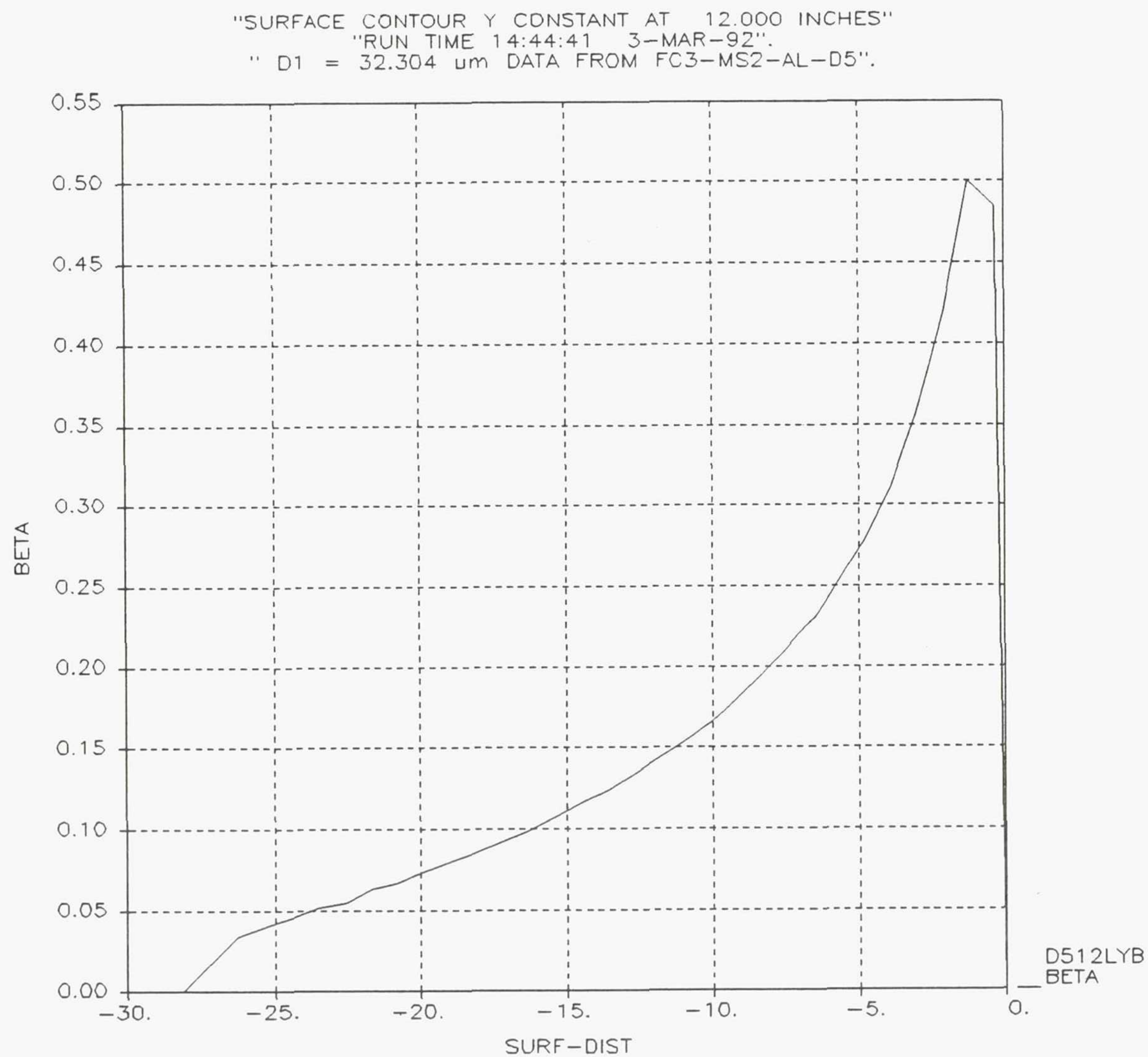

FIGURE D.103

BETA vs SURF-DIST(cm), FC3,Y=12L,D=32.3 micron

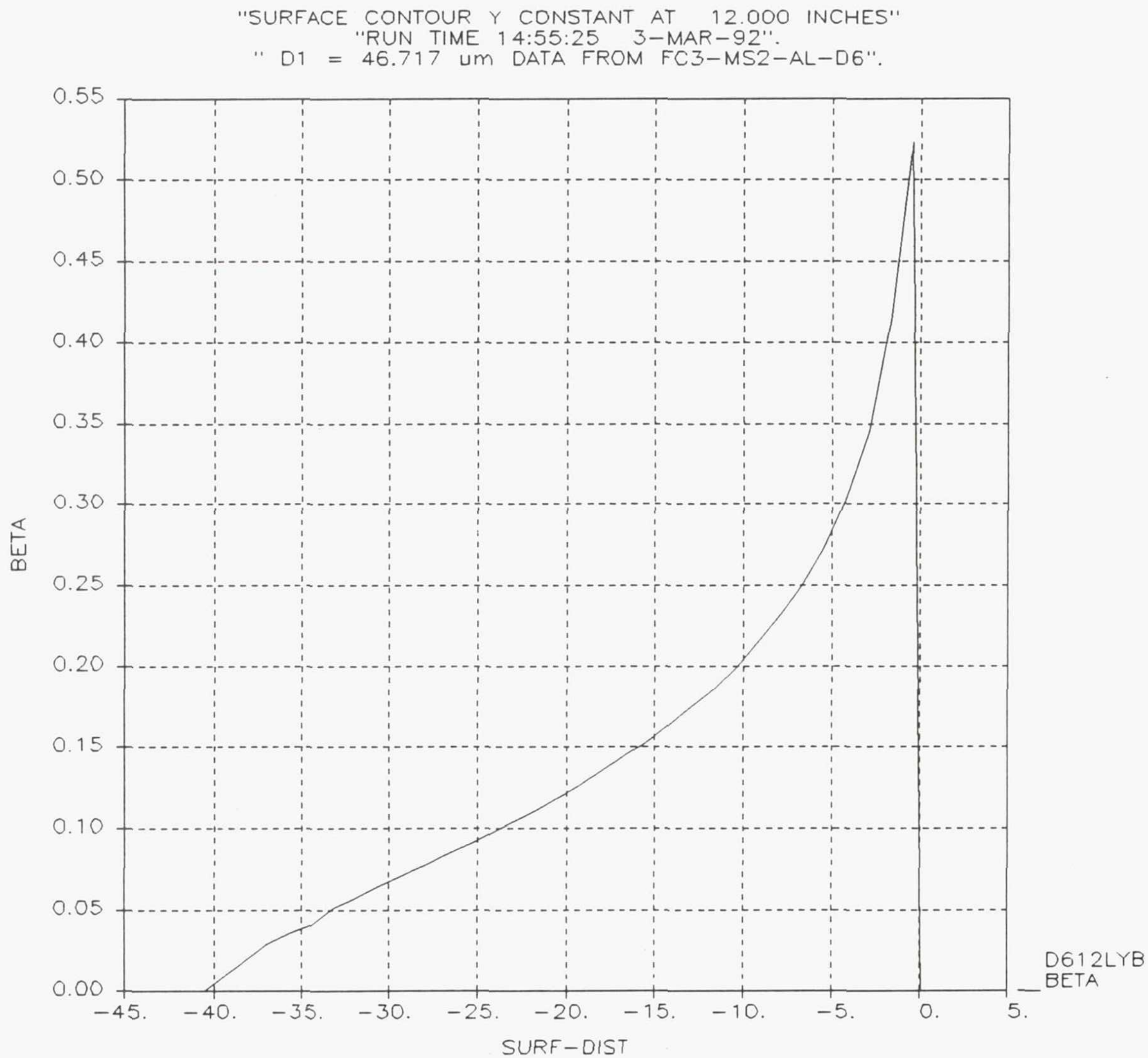

FIGURE D.104

BETA vs SURF-DIST(cm), FC3,Y=12L,D=46.7 micron

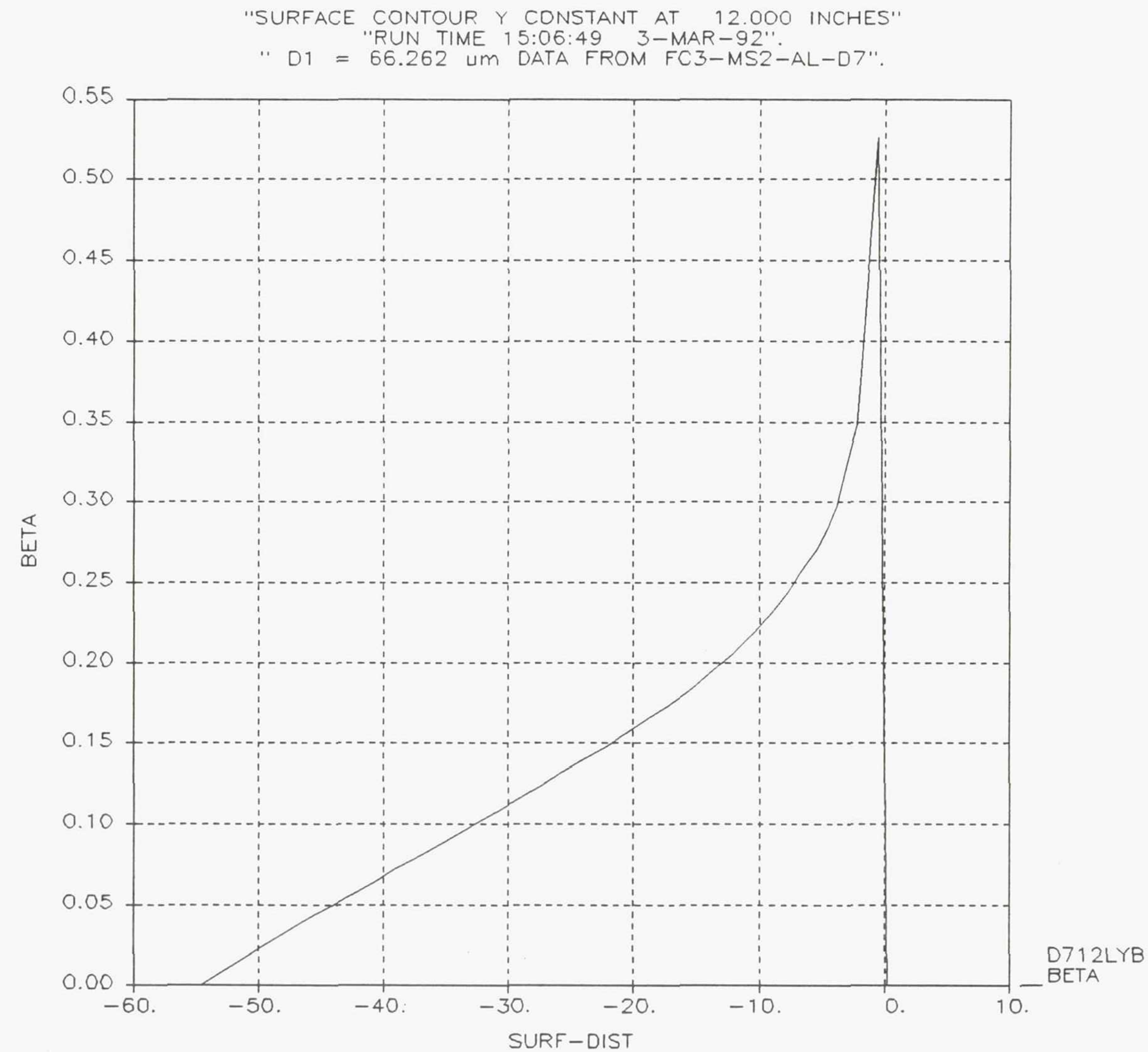

FIGURE D.105

BETA vs SURF-DIST(cm), FC3,Y=12L,D=66.3 micron

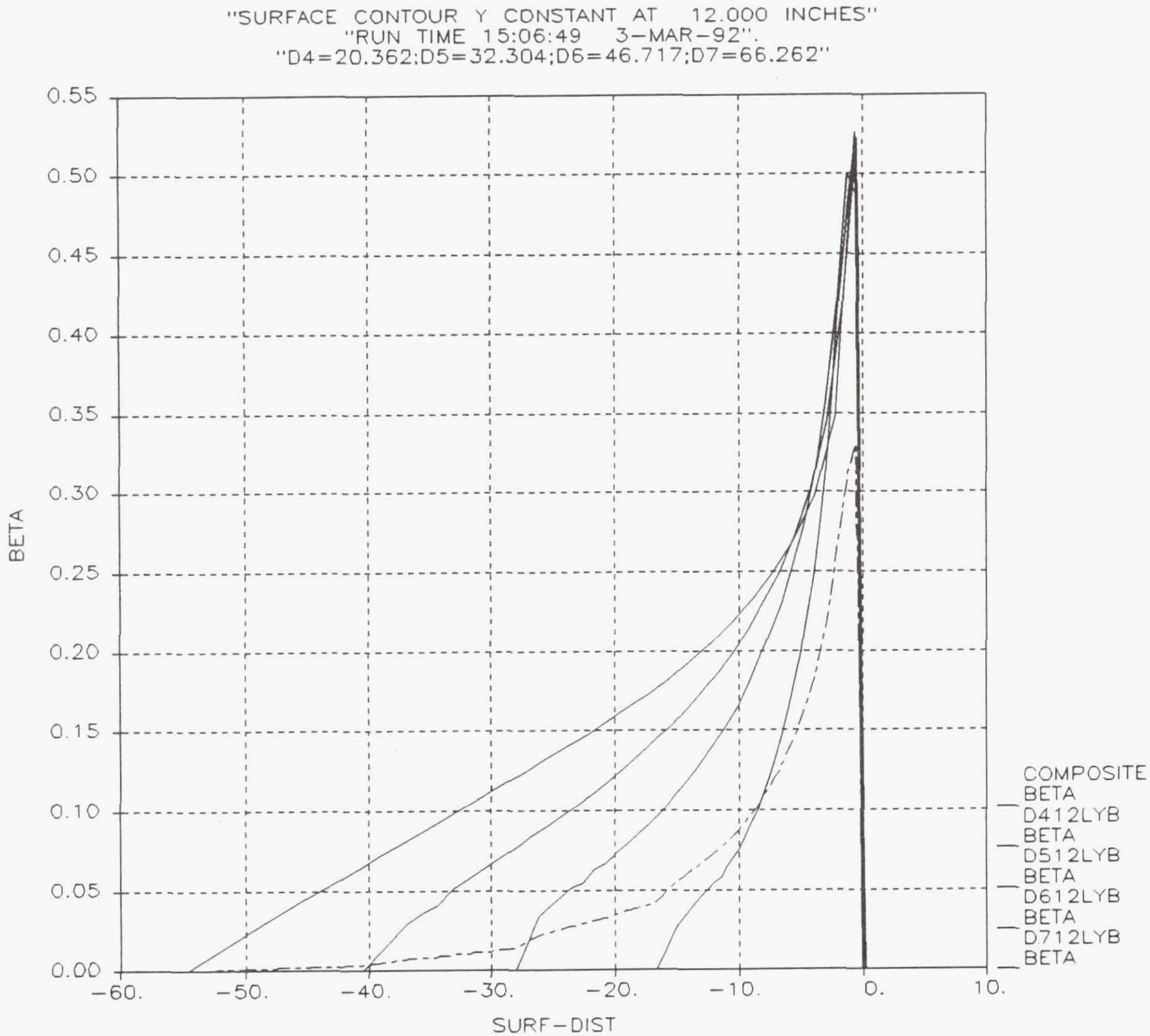

FIGURE D.106

BETA vs SURF-DIST(cm), FC3,Y=12L,COMPOSITE AND INDIVIDUAL DROPS

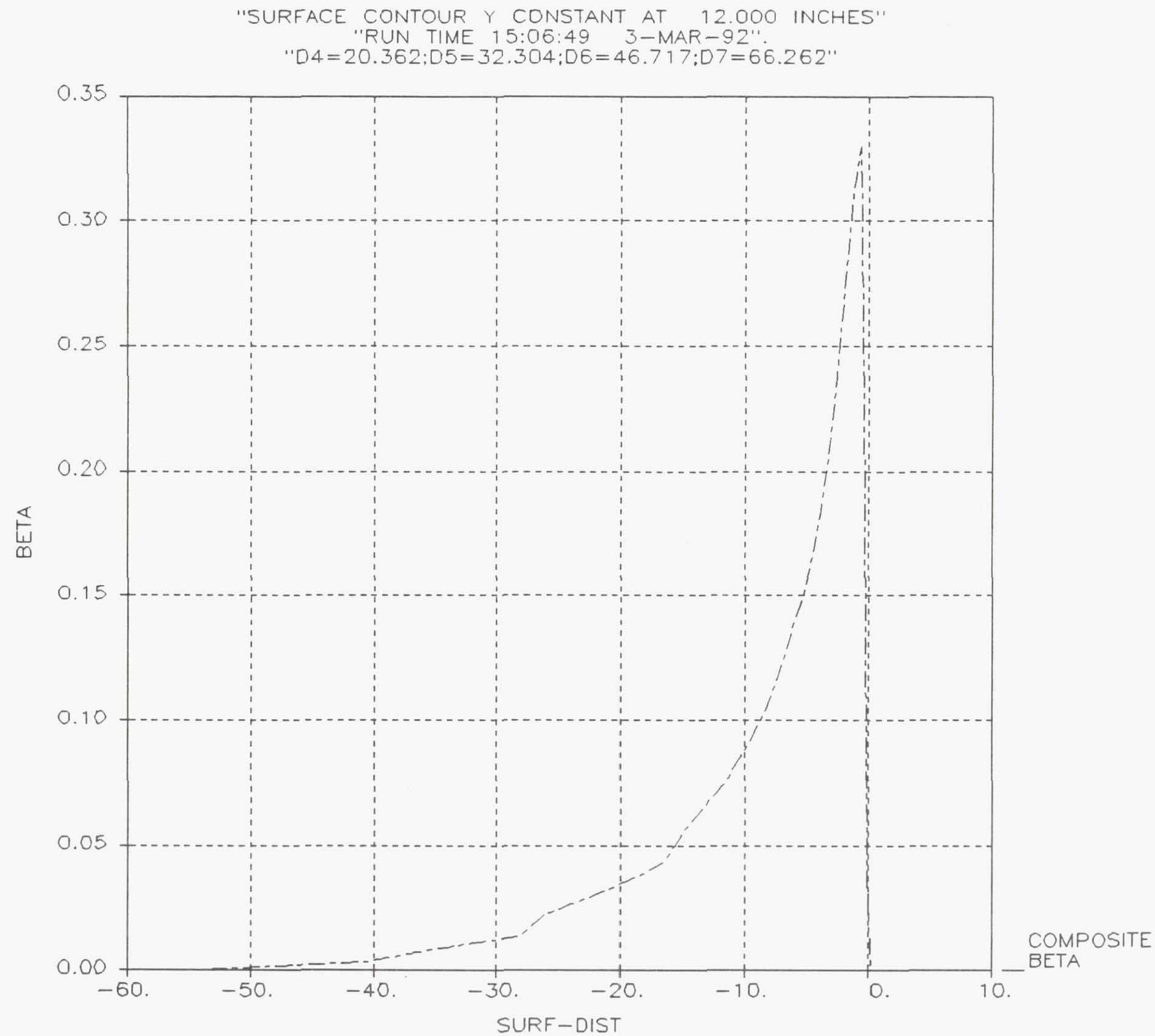

FIGURE D.107

BETA vs SURF-DIST(cm), FC3,Y=12L,D=20.4 micron
COMPOSITE DROP

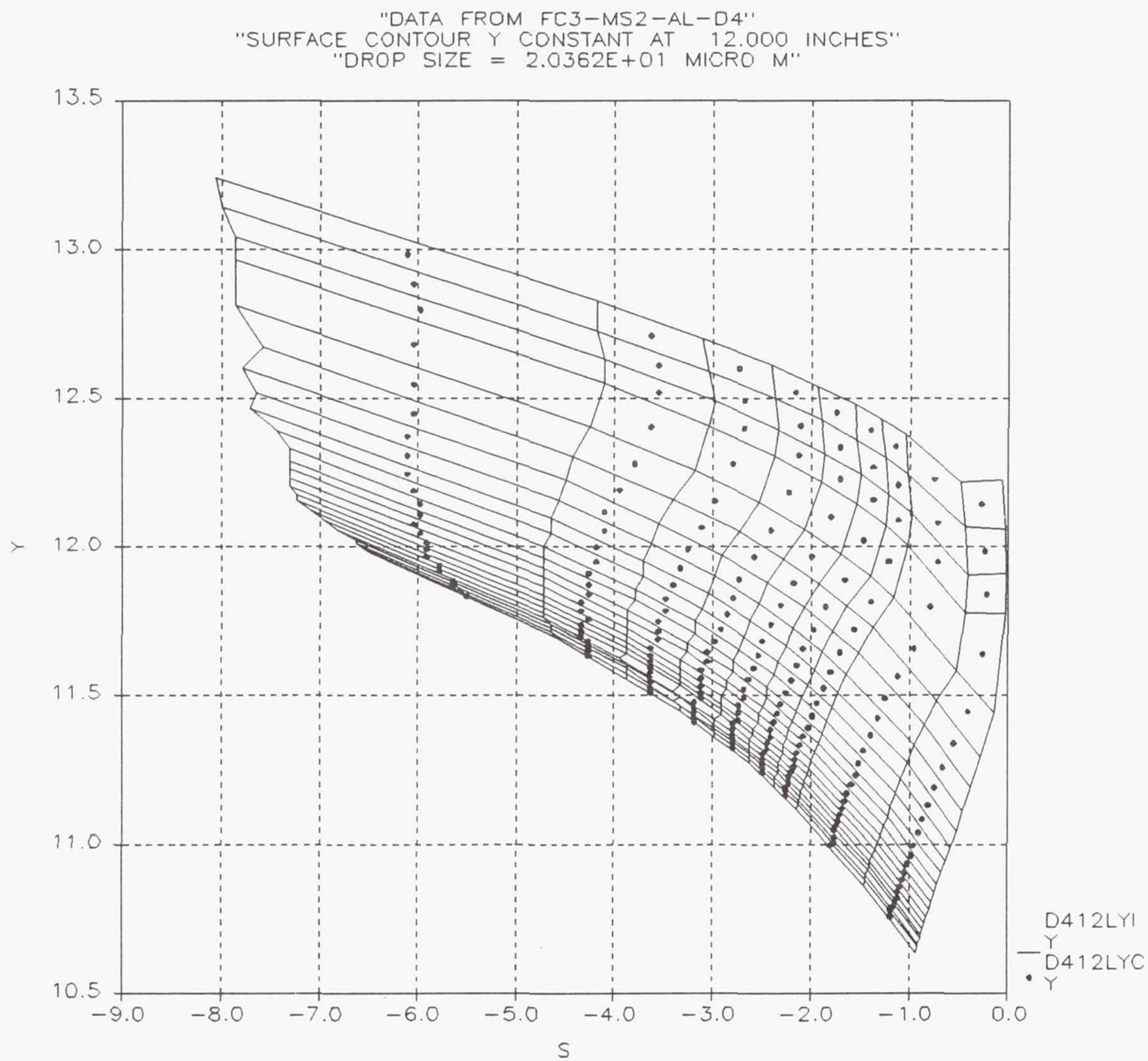

FIGURE D.108

IMPINGEMENT FIELD Y(in) vs S(in), FC3,Y=12L,D=20.4 micron

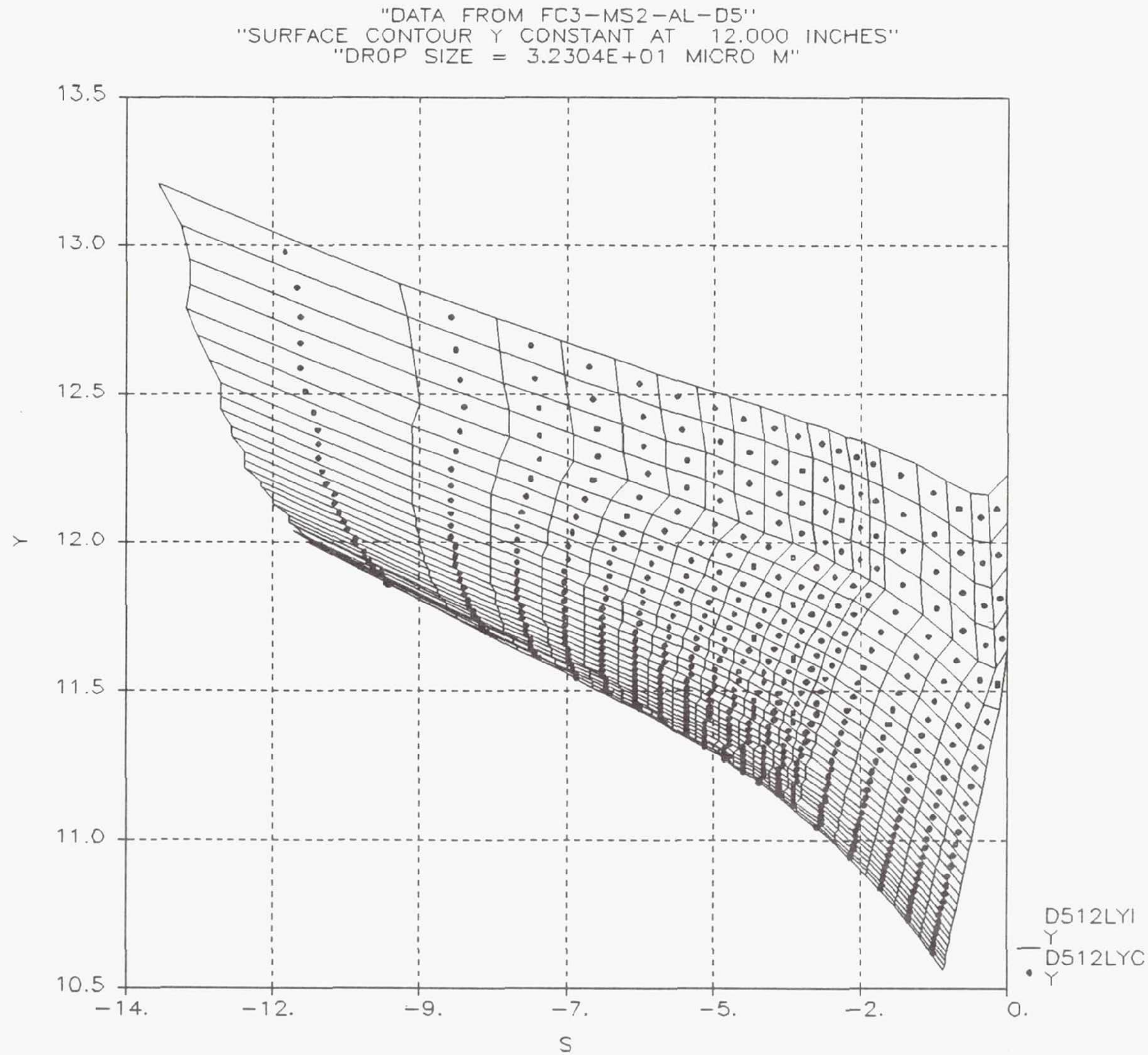

FIGURE D.109

IMPINGEMENT FIELD Y(in) vs S(in), FC3,Y=12L,D=32.3 micron

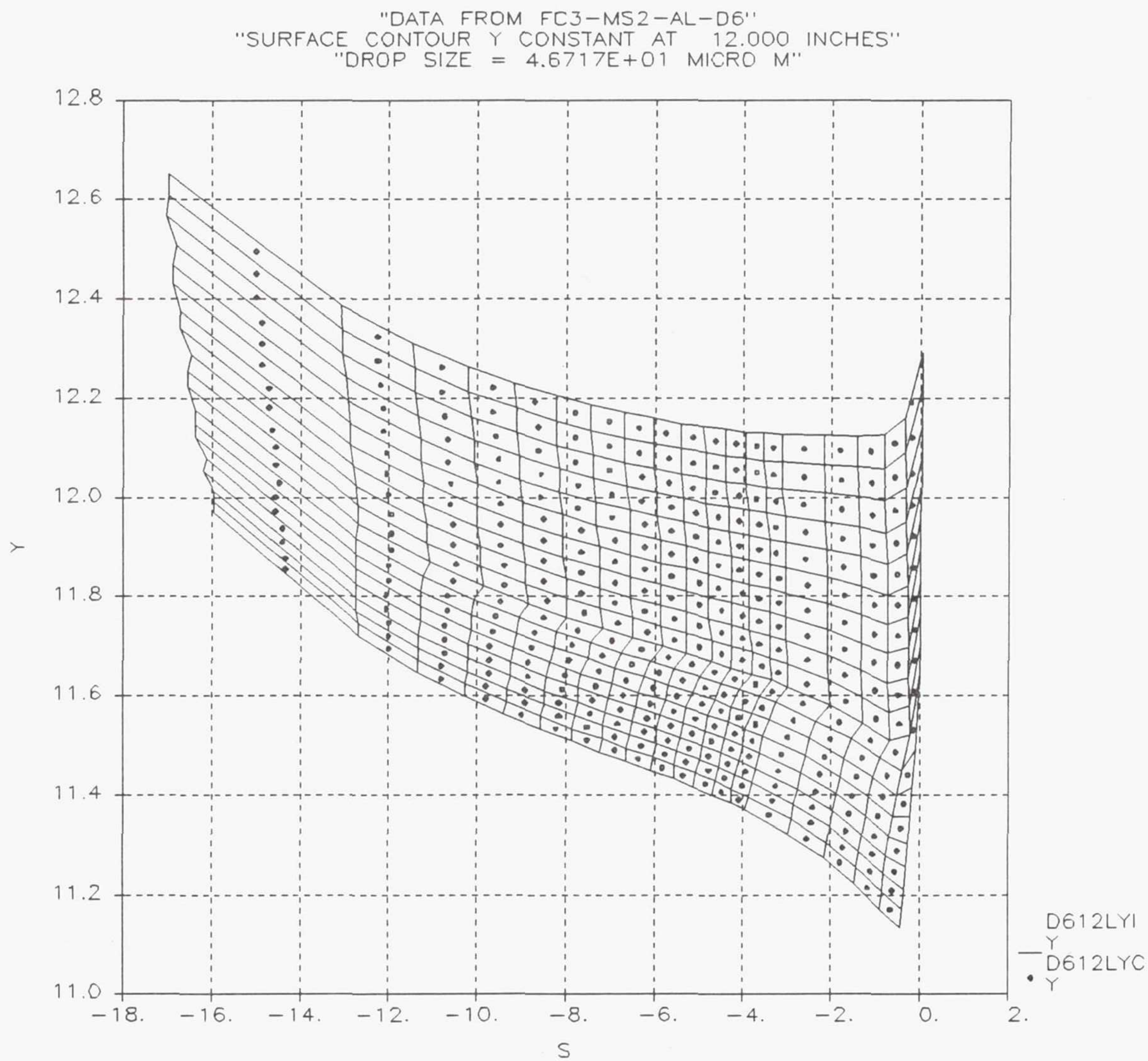

FIGURE D.110

IMPINGEMENT FIELD Y(in) vs S(in), FC3,Y=12L,D=46.7 micron

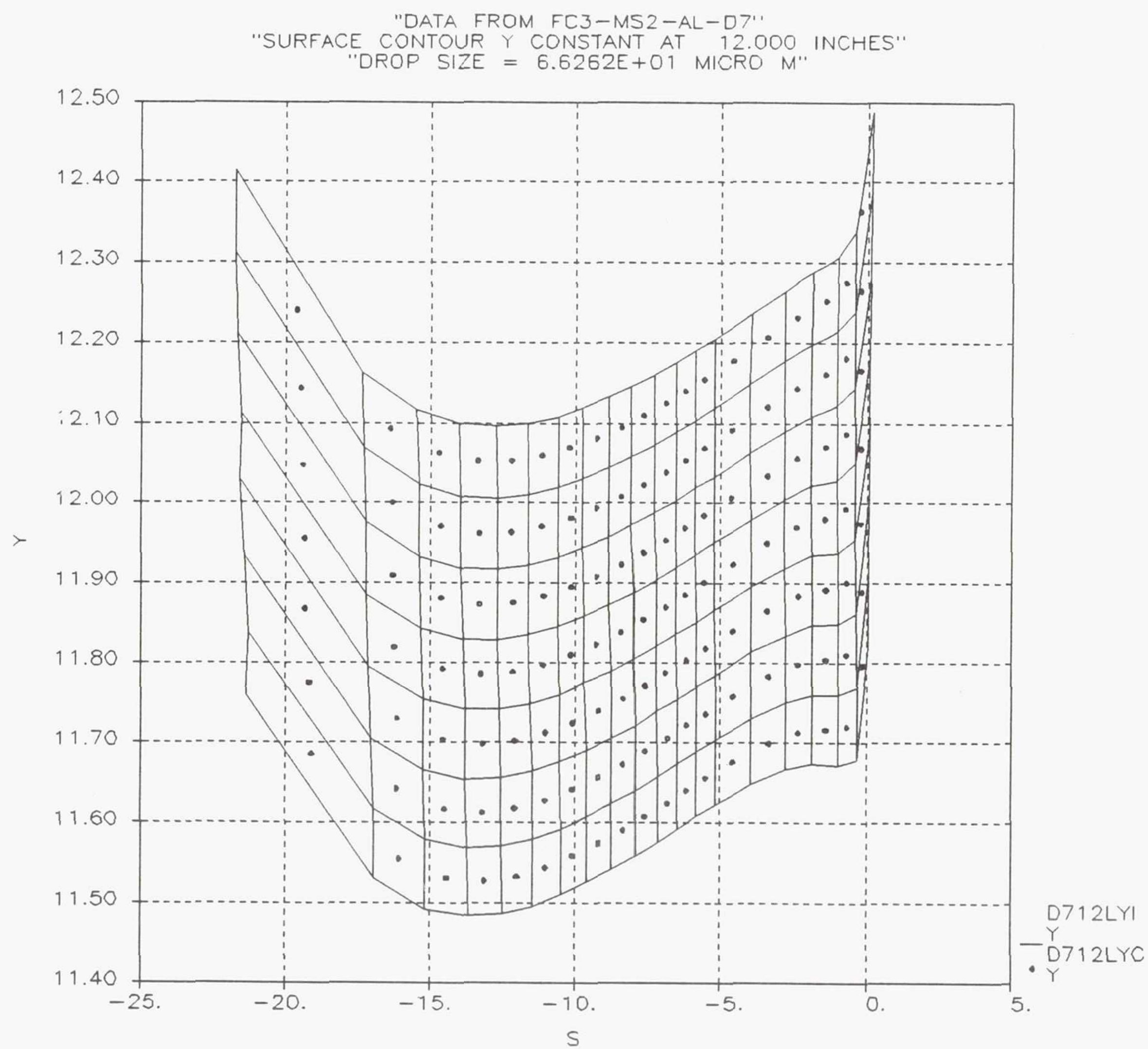

FIGURE D.111

IMPINGEMENT FIELD Y(in) vs S(in), FC3,Y=12L,D=66.3 micron

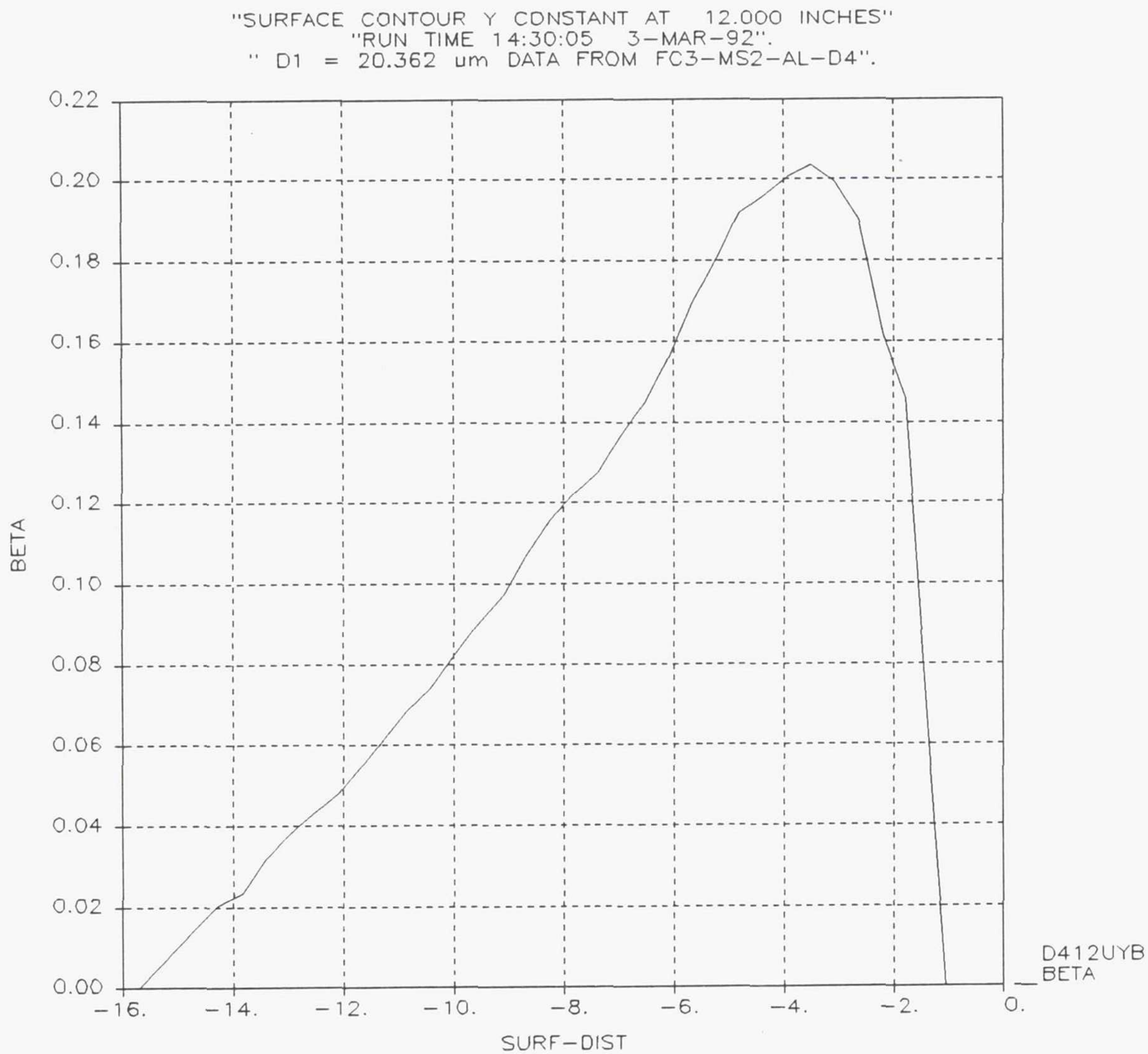

FIGURE D.112

BETA vs SURF-DIST(cm), FC3,Y=12U,D=20.4 micron

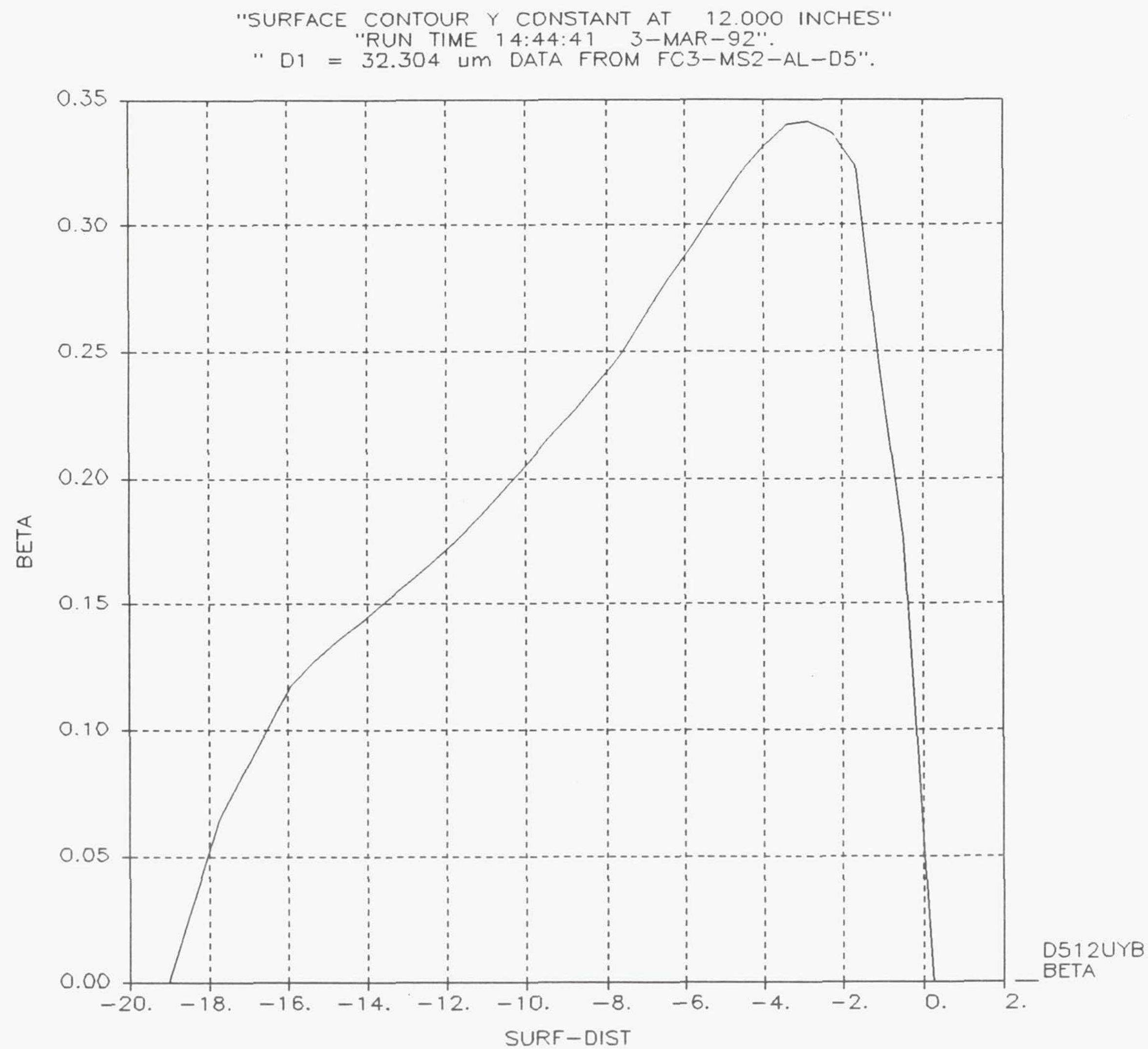

FIGURE D.113

BETA vs SURF-DIST(cm), FC3,Y=12U,D=32.3 micron

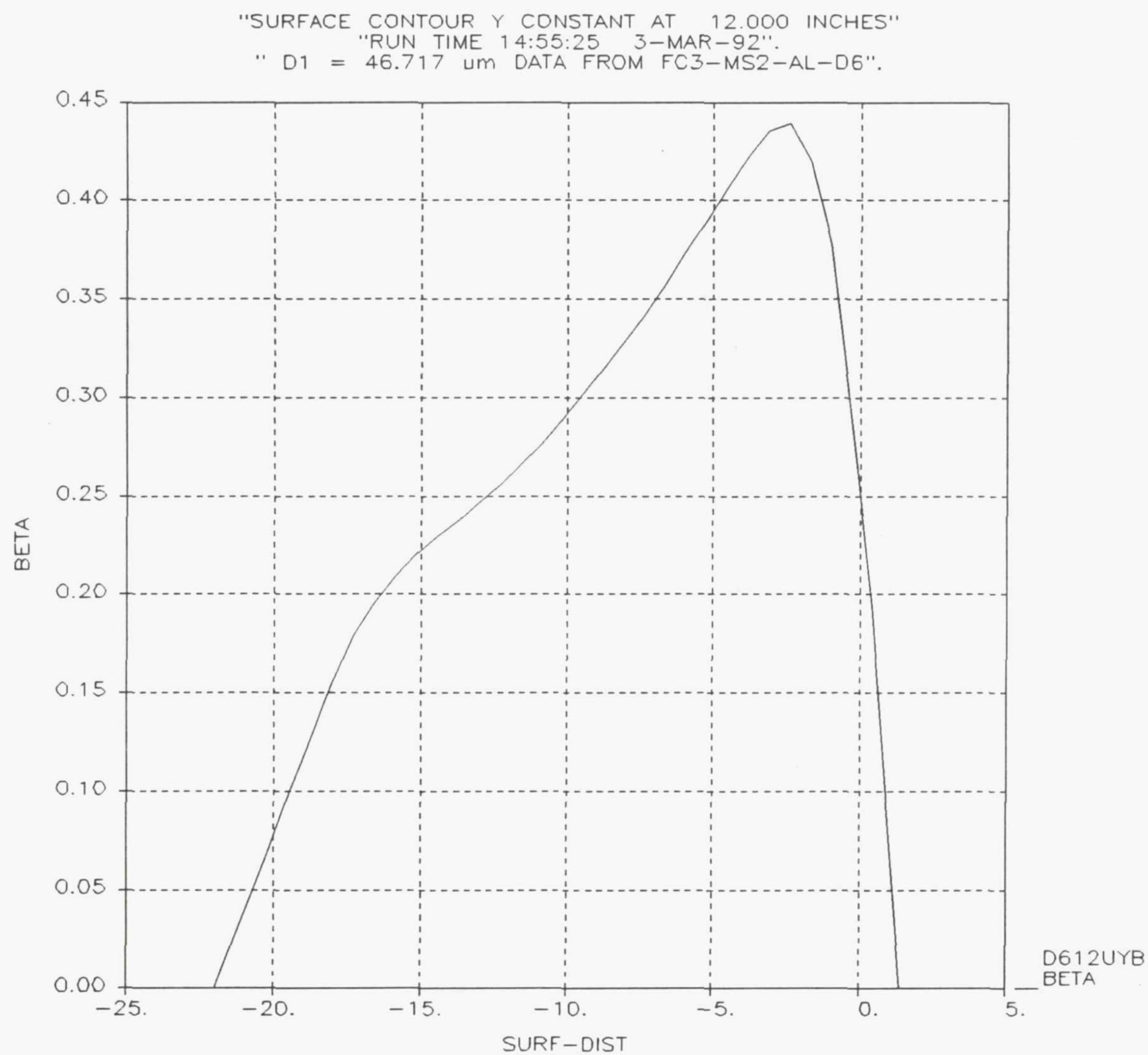

FIGURE D.114

BETA vs SURF-DIST(cm), FC3,Y=12U,D=46.7 micron

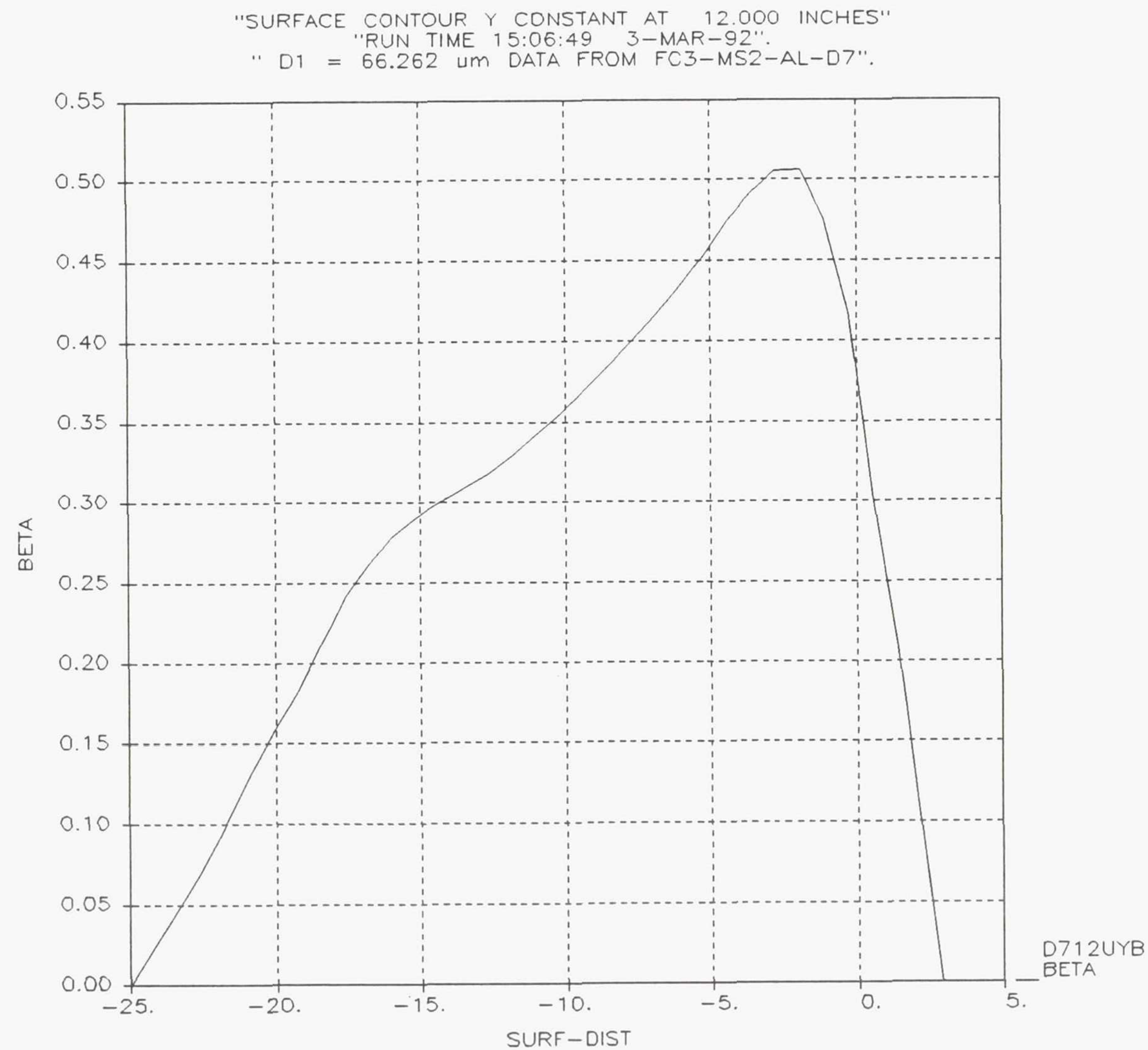

FIGURE D.115

BETA vs SURF-DIST(cm), FC3,Y=12U,D=66.3 micron

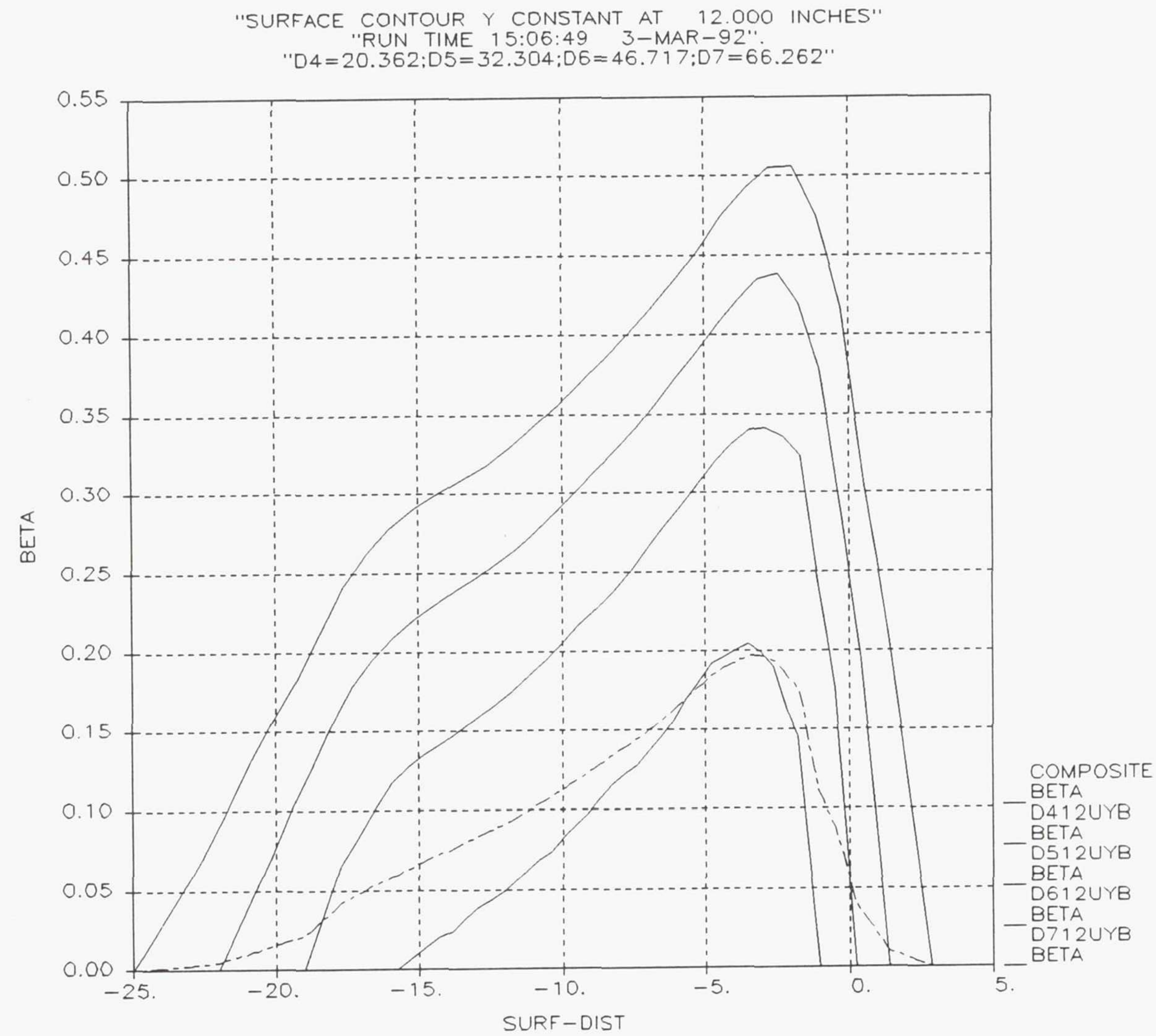

FIGURE D.116

BETA vs SURF-DIST(cm), FC3,Y=12U,COMPOSITE AND INDIVIDUAL DROPS

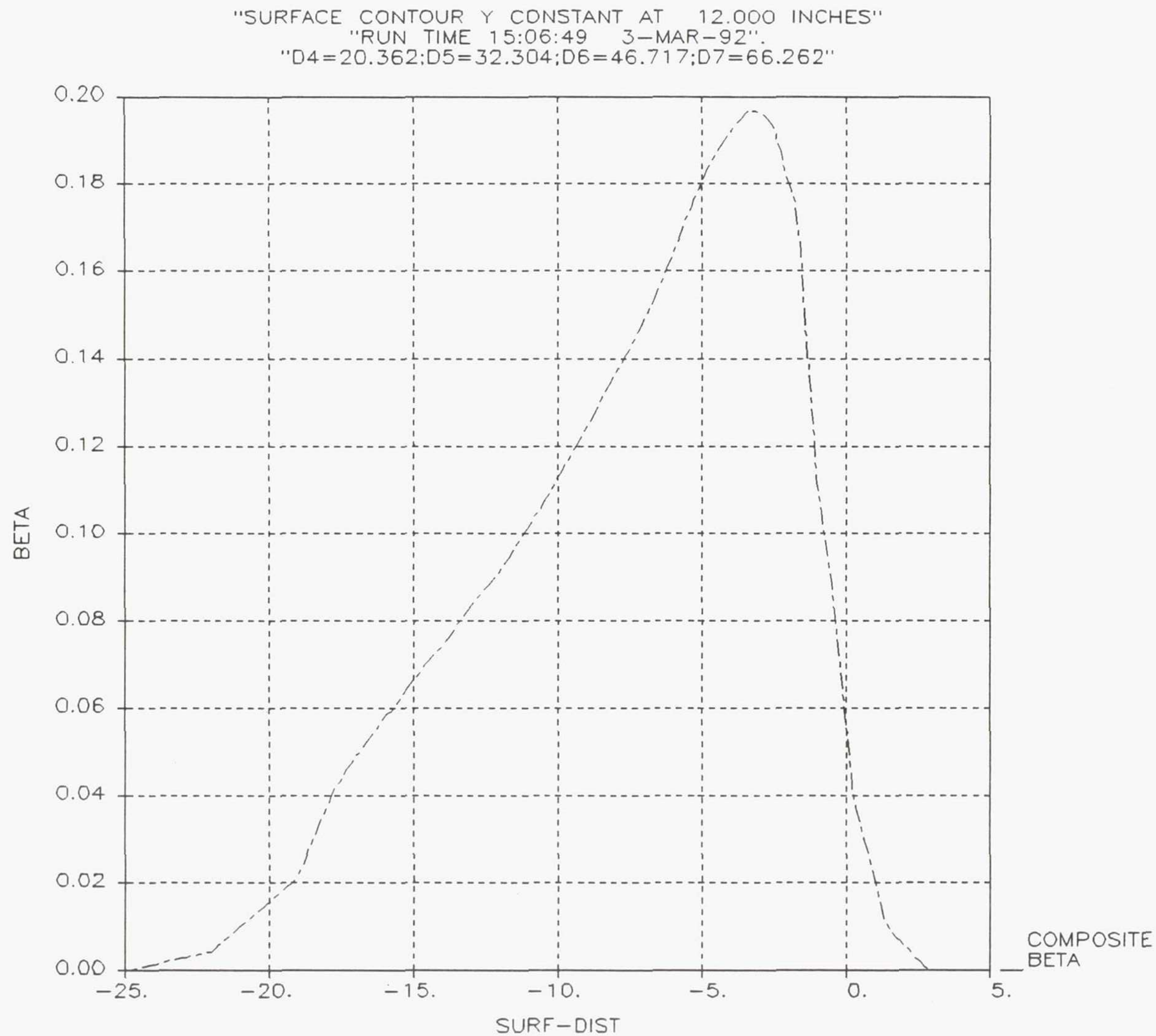

FIGURE D.117

BETA vs SURF-DIST(cm), FC3,Y=12U,D=20.4 micron
COMPOSITE DROP

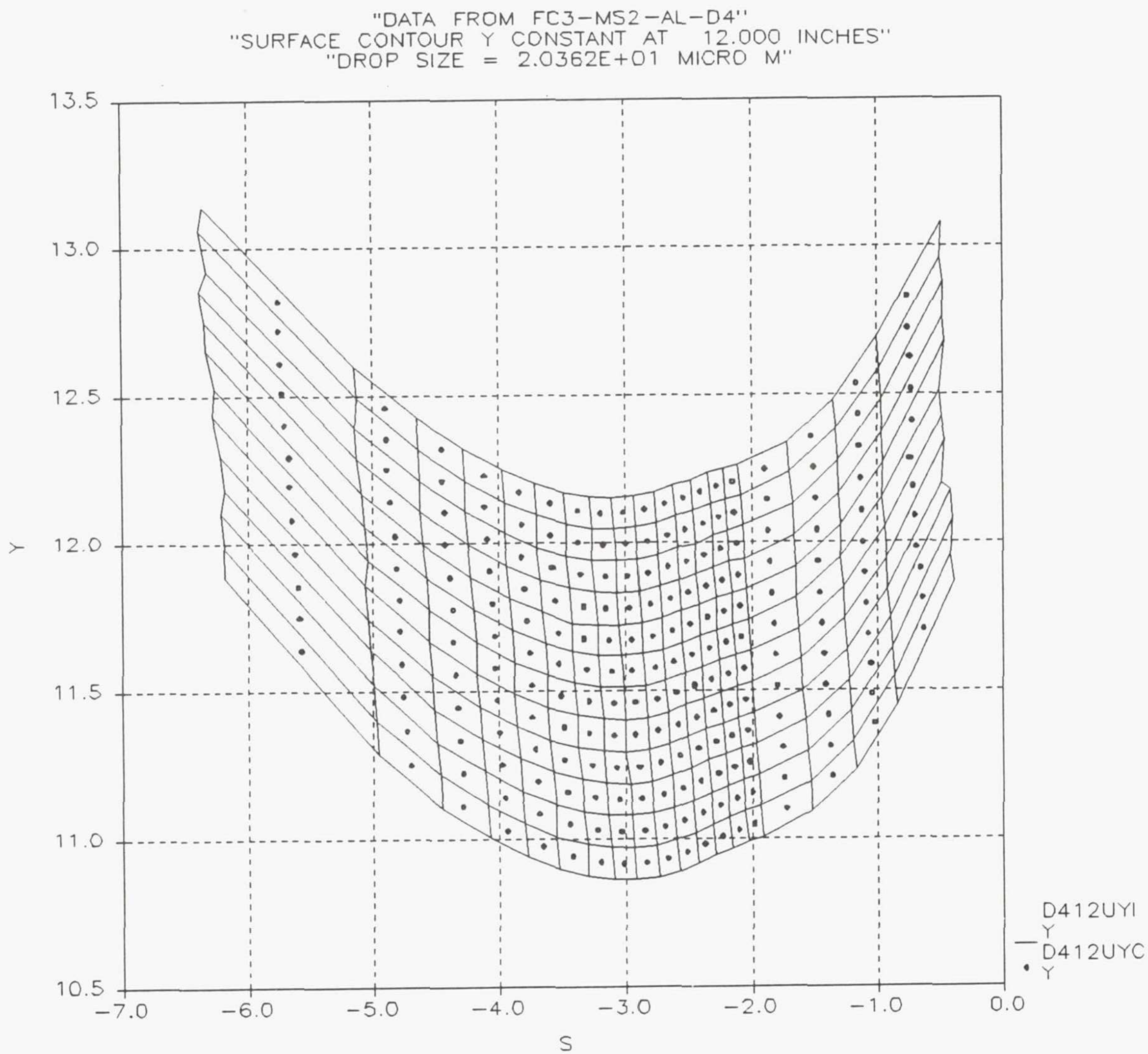

FIGURE D.118

IMPINGEMENT FIELD Y(in) vs S(in), FC3,Y=12U,D=20.4 micron

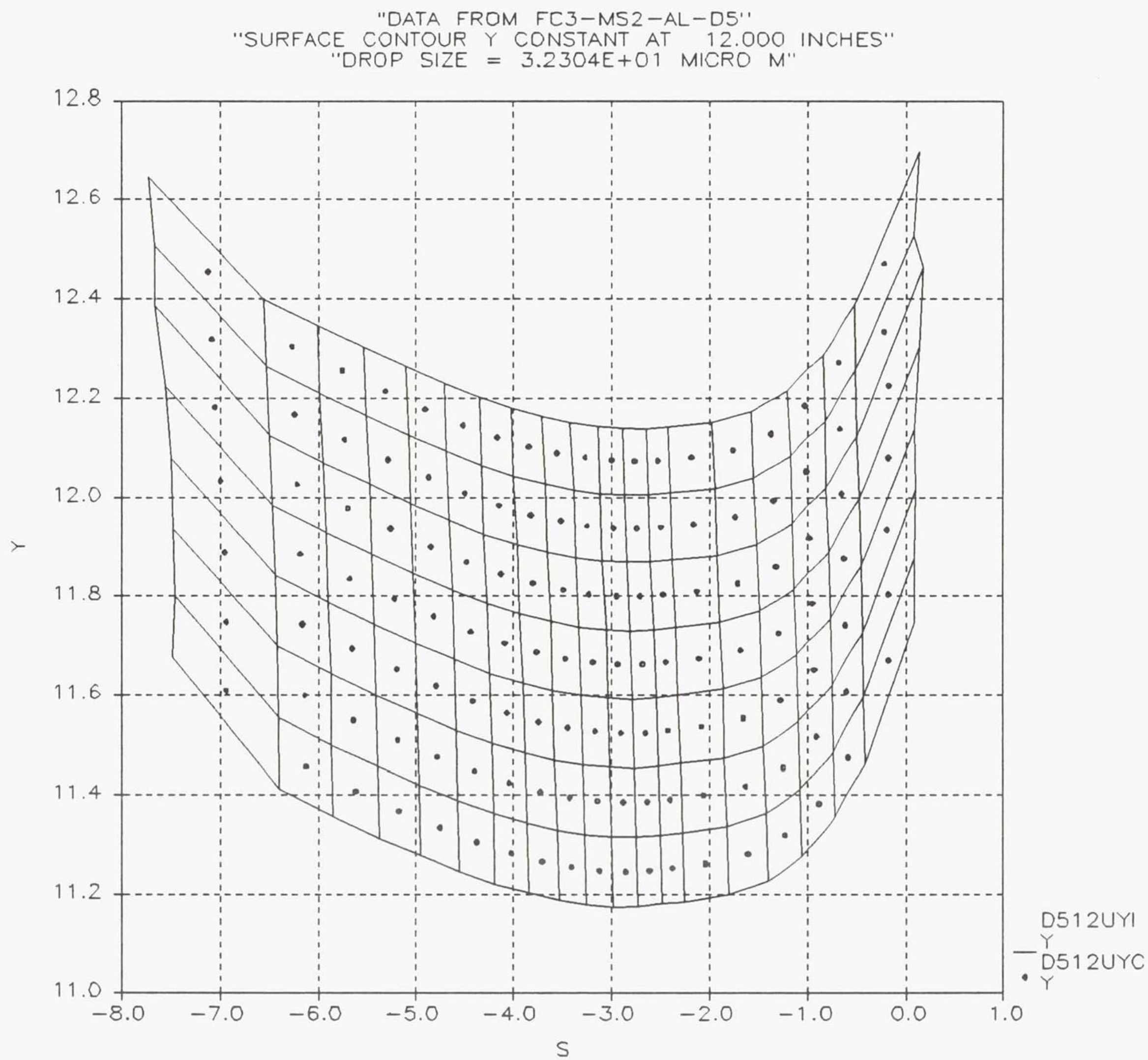

FIGURE D.119

IMPINGEMENT FIELD Y(in) vs S(in), FC3,Y=12U,D=32.3 micron

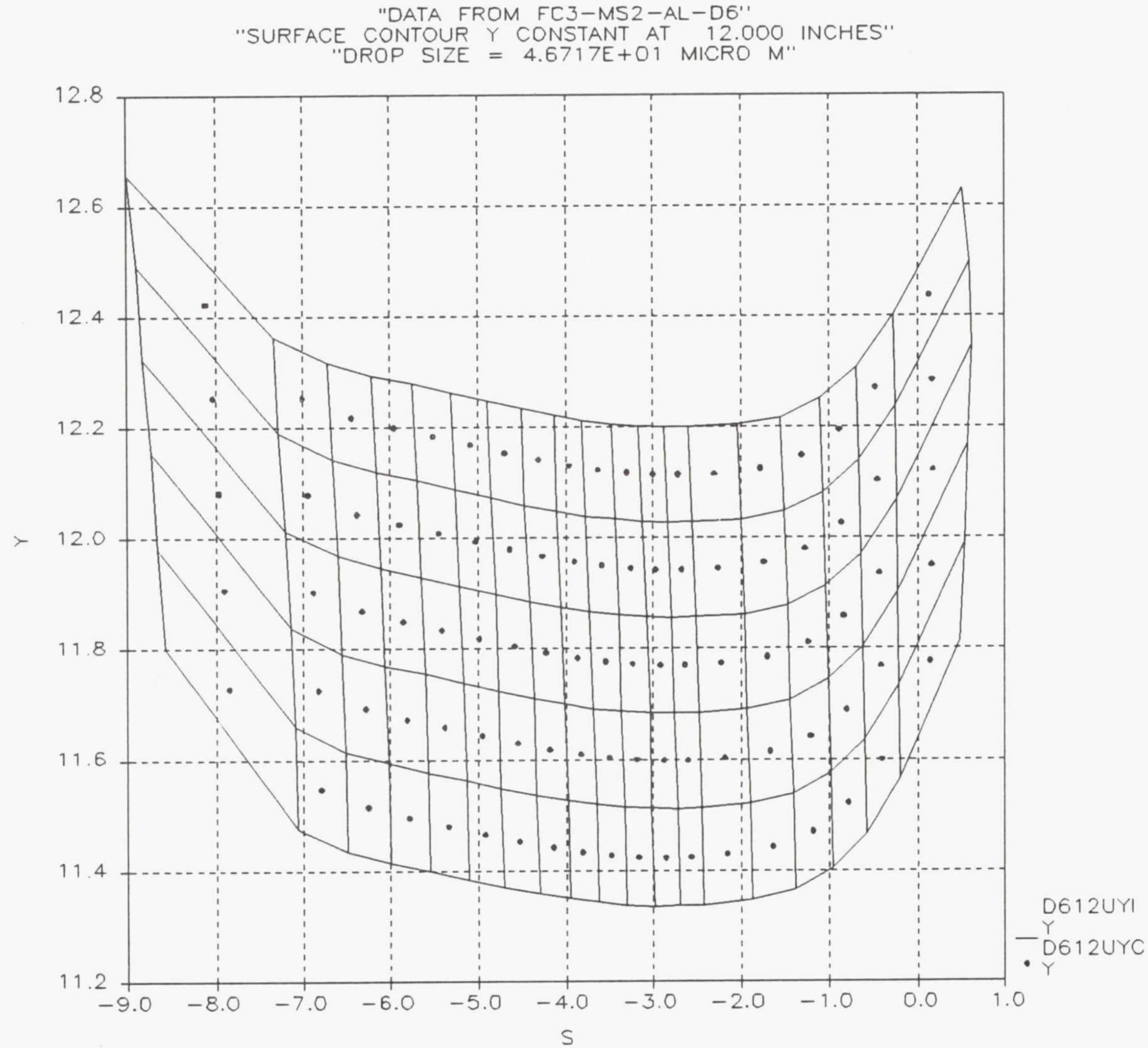

FIGURE D.120

IMPINGEMENT FIELD Y(in) vs S(in), FC3,Y=12U,D=46.7 micron

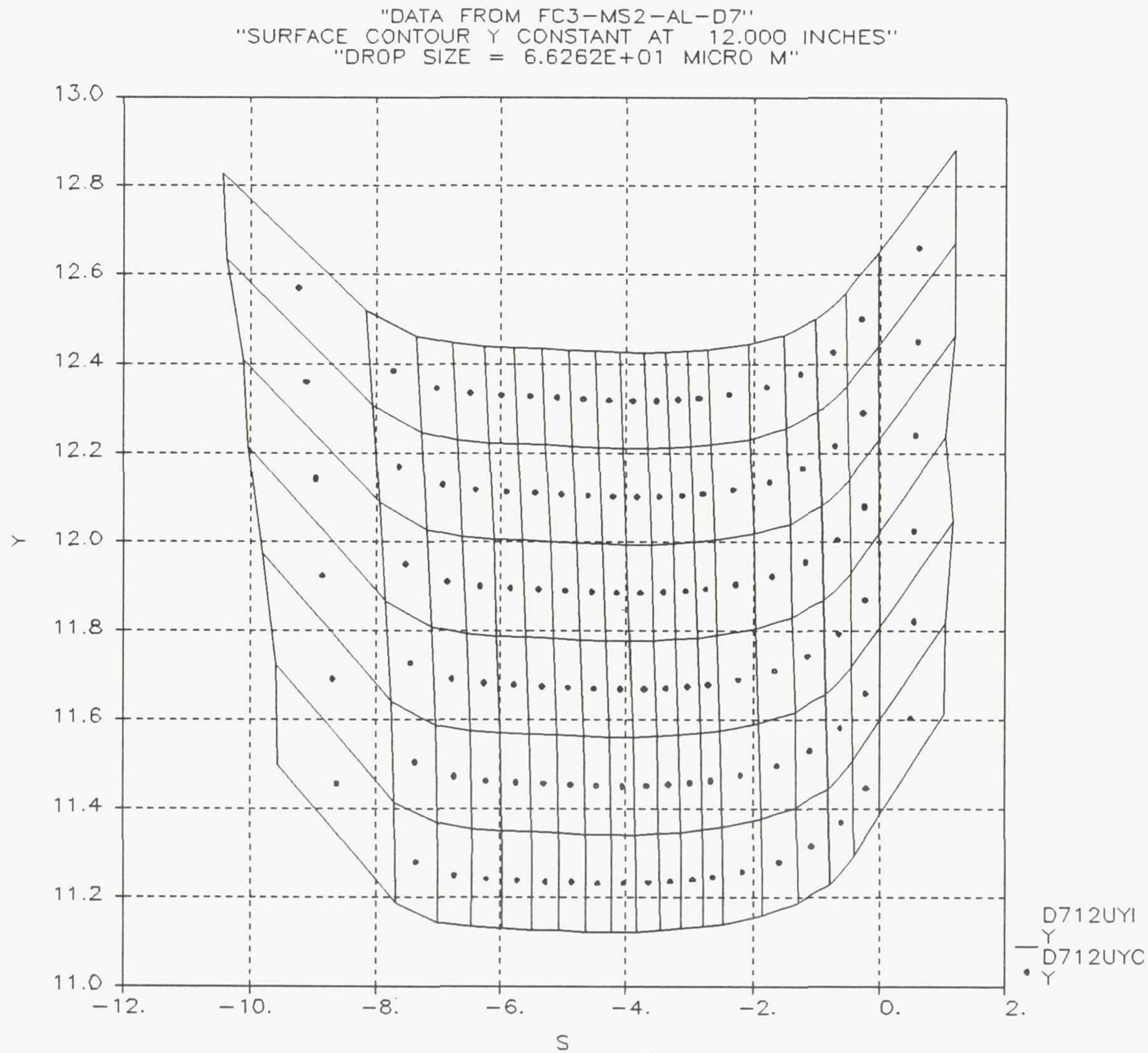

FIGURE D.121

IMPINGEMENT FIELD Y(in) vs S(in), FC3,Y=12U,D=66.3 micron

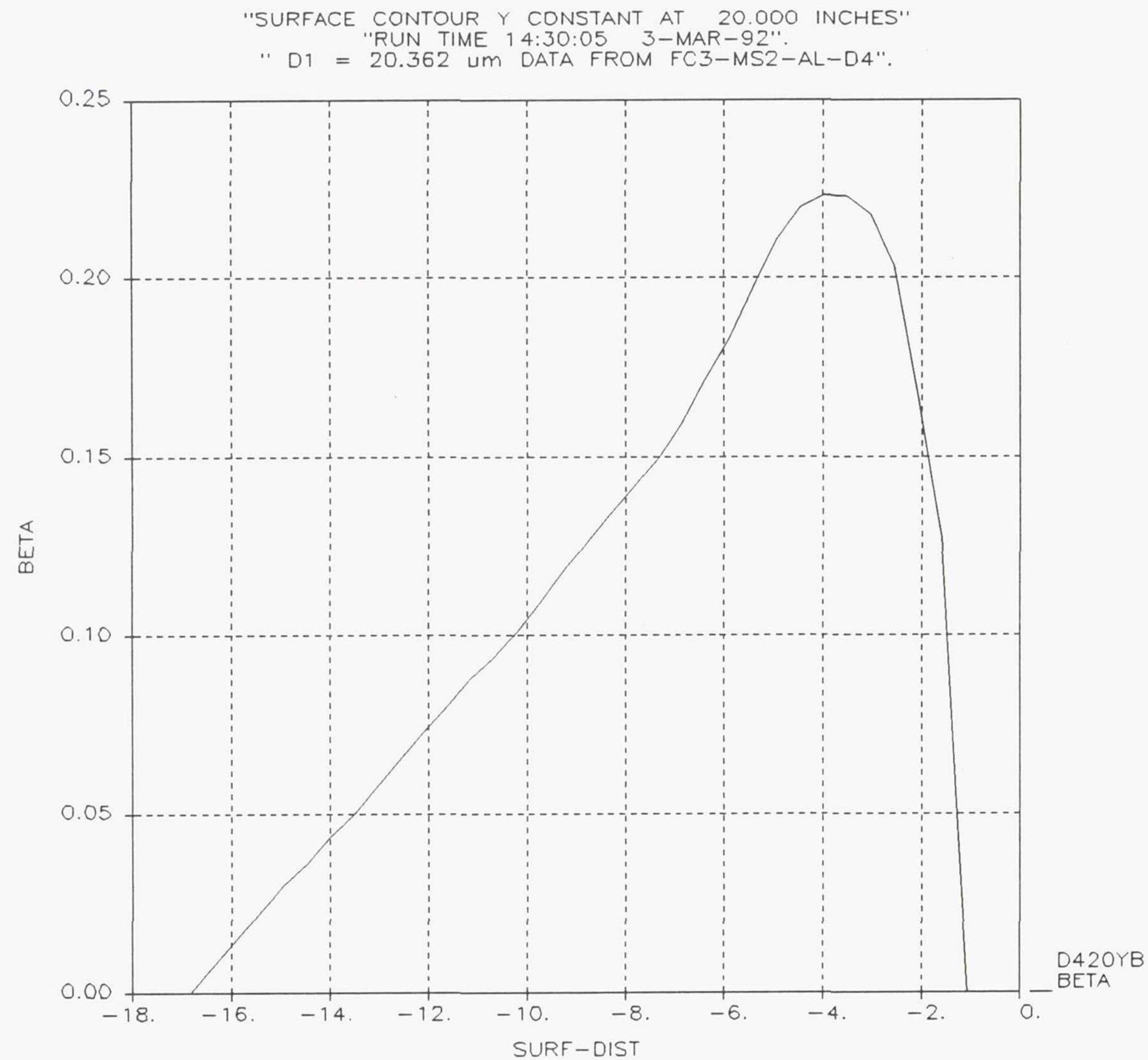

FIGURE D.122

BETA vs SURF-DIST(cm), FC3,Y=20,D=20.4 micron

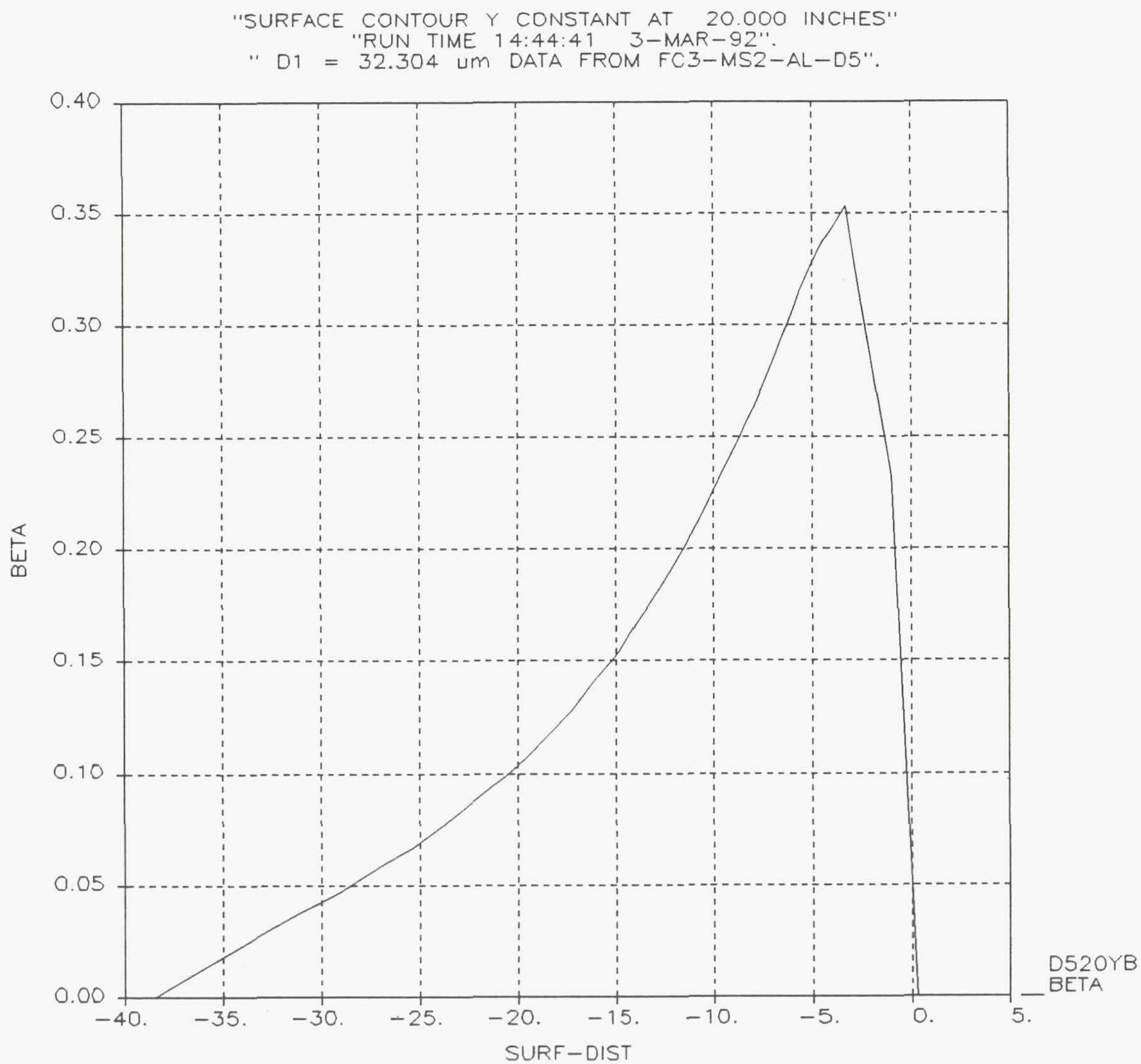

FIGURE D.123

BETA vs SURF-DIST(cm), FC3,Y=20,D=32.3 micron

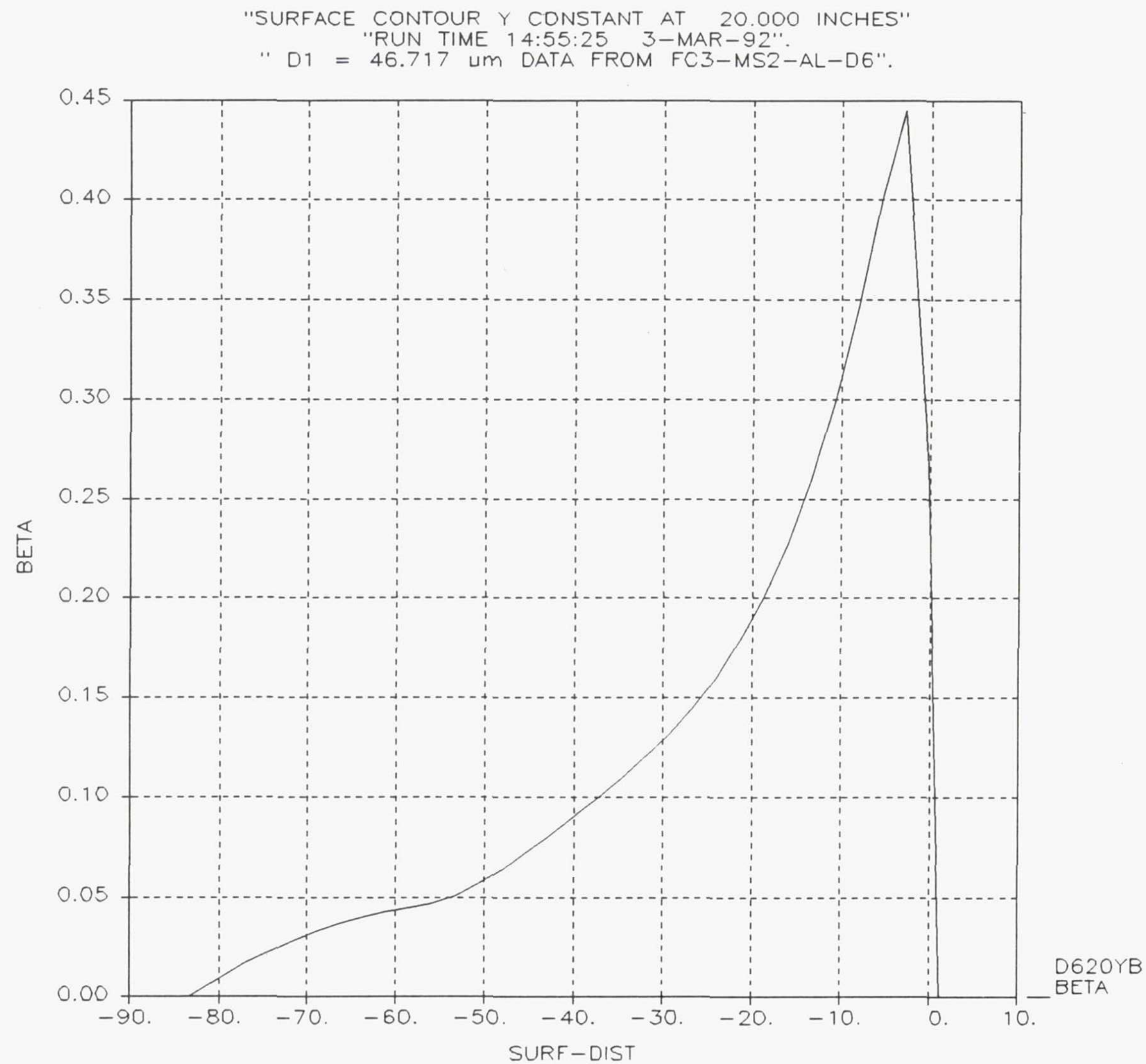

FIGURE D.124

BETA vs SURF-DIST(cm), FC3,Y=20,D=46.7 micron

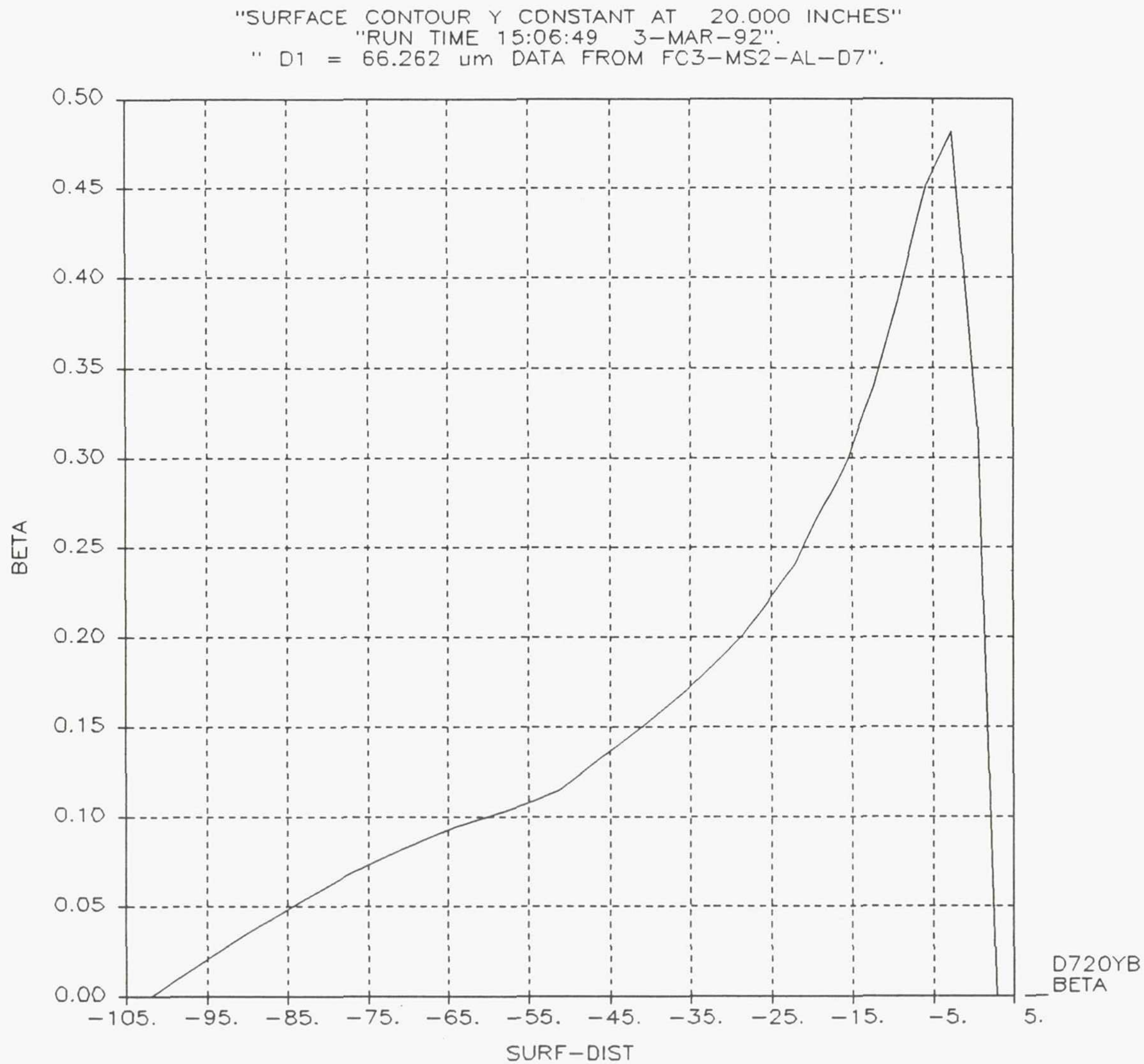

FIGURE D.125

BETA vs SURF-DIST(cm), FC3,Y=20,D=66.3 micron

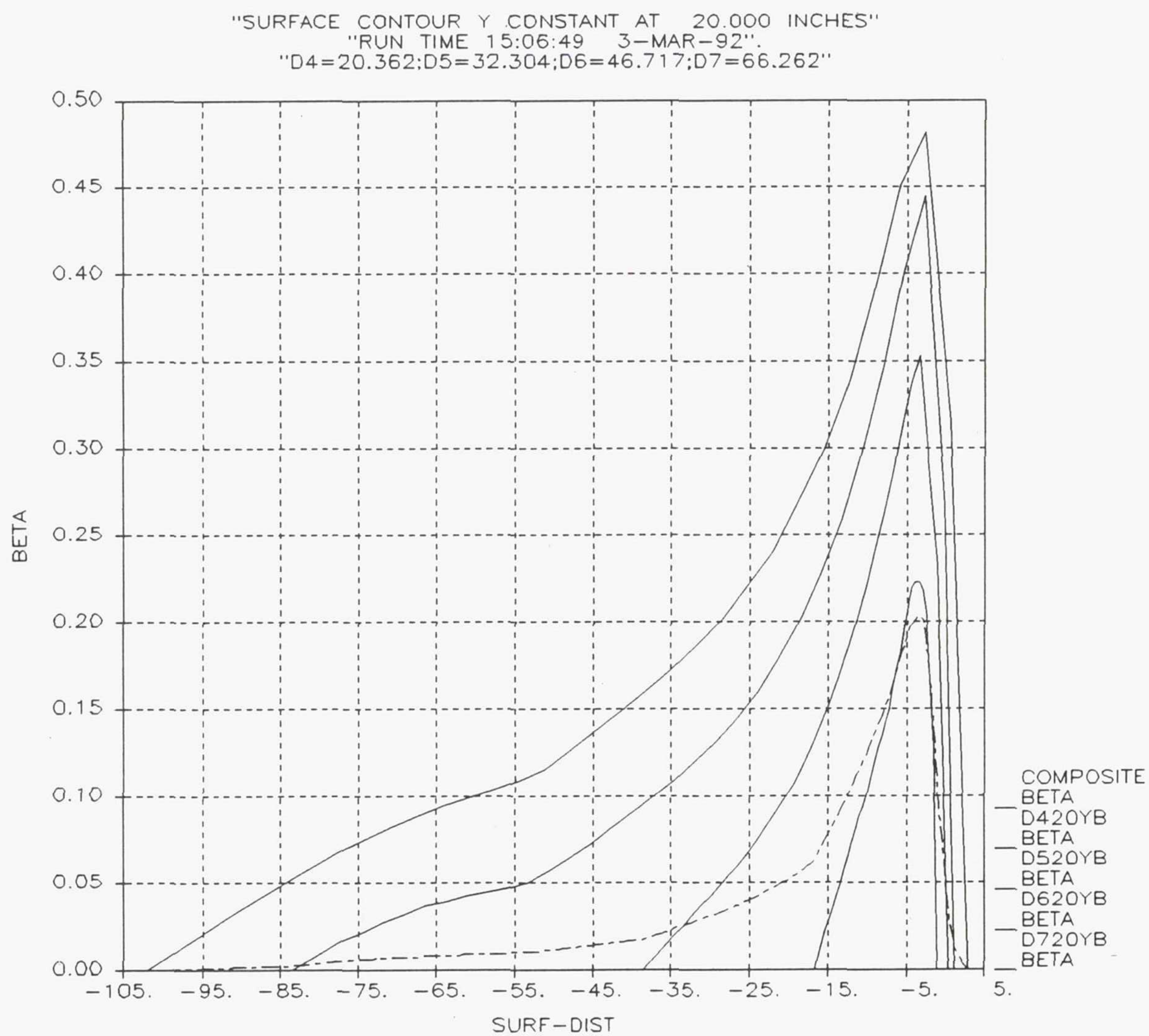

FIGURE D.126

BETA vs SURF-DIST(cm), FC3,Y=20,COMPOSITE AND INDIVIDUAL DROPS

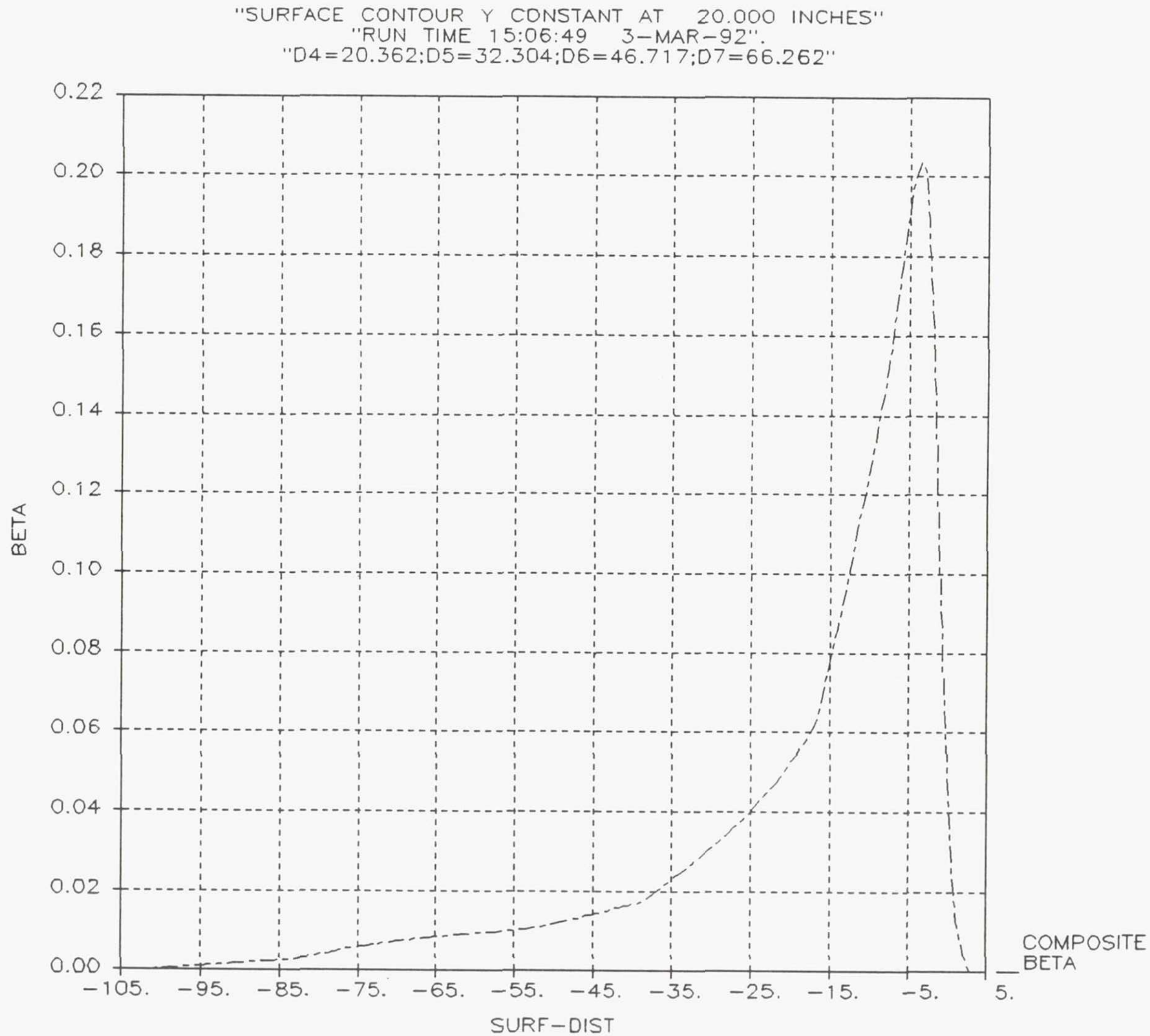

FIGURE D.127

BETA vs SURF-DIST(cm), FC3,Y=20,D=20.4 micron
COMPOSITE DROP

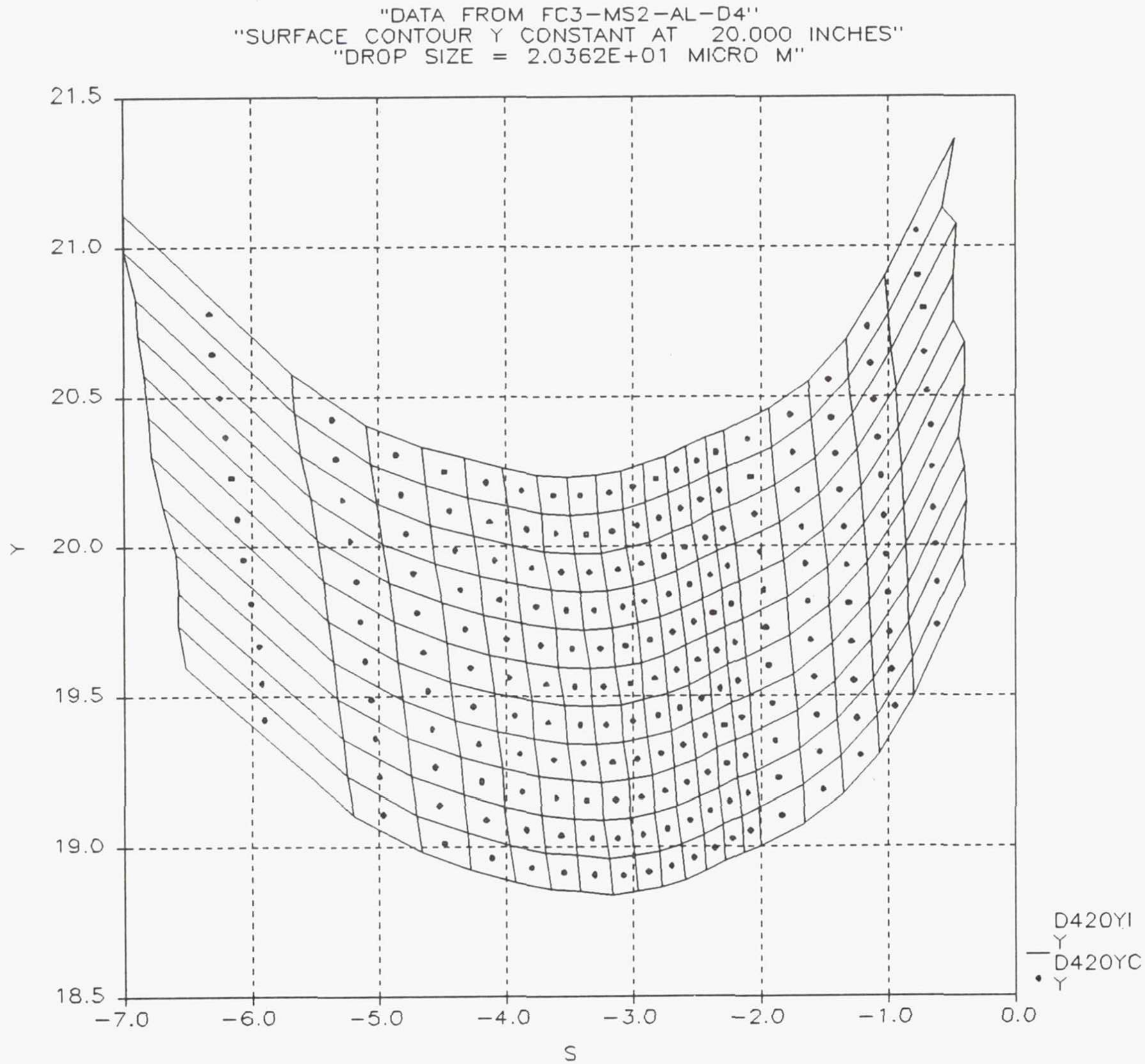

FIGURE D.128

IMPINGEMENT FIELD Y(in) vs S(in), FC3,Y=20,D=20.4 micron

FIGURE D.129

IMPINGEMENT FIELD Y(in) vs S(in), FC3,Y=20,D=32.3 micron

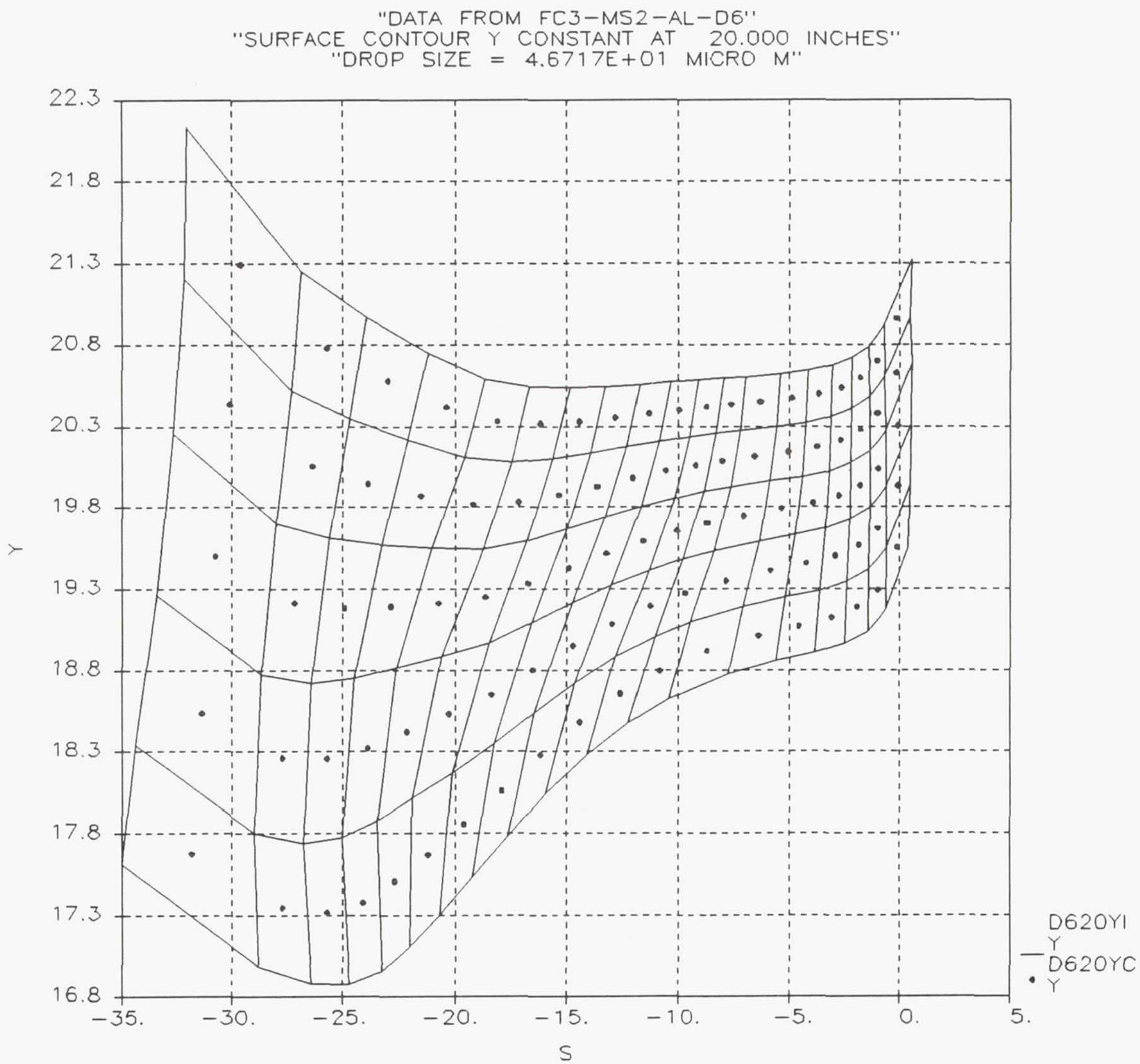

FIGURE D.130

IMPINGEMENT FIELD Y(in) vs S(in), FC3,Y=20,D=46.7 micron

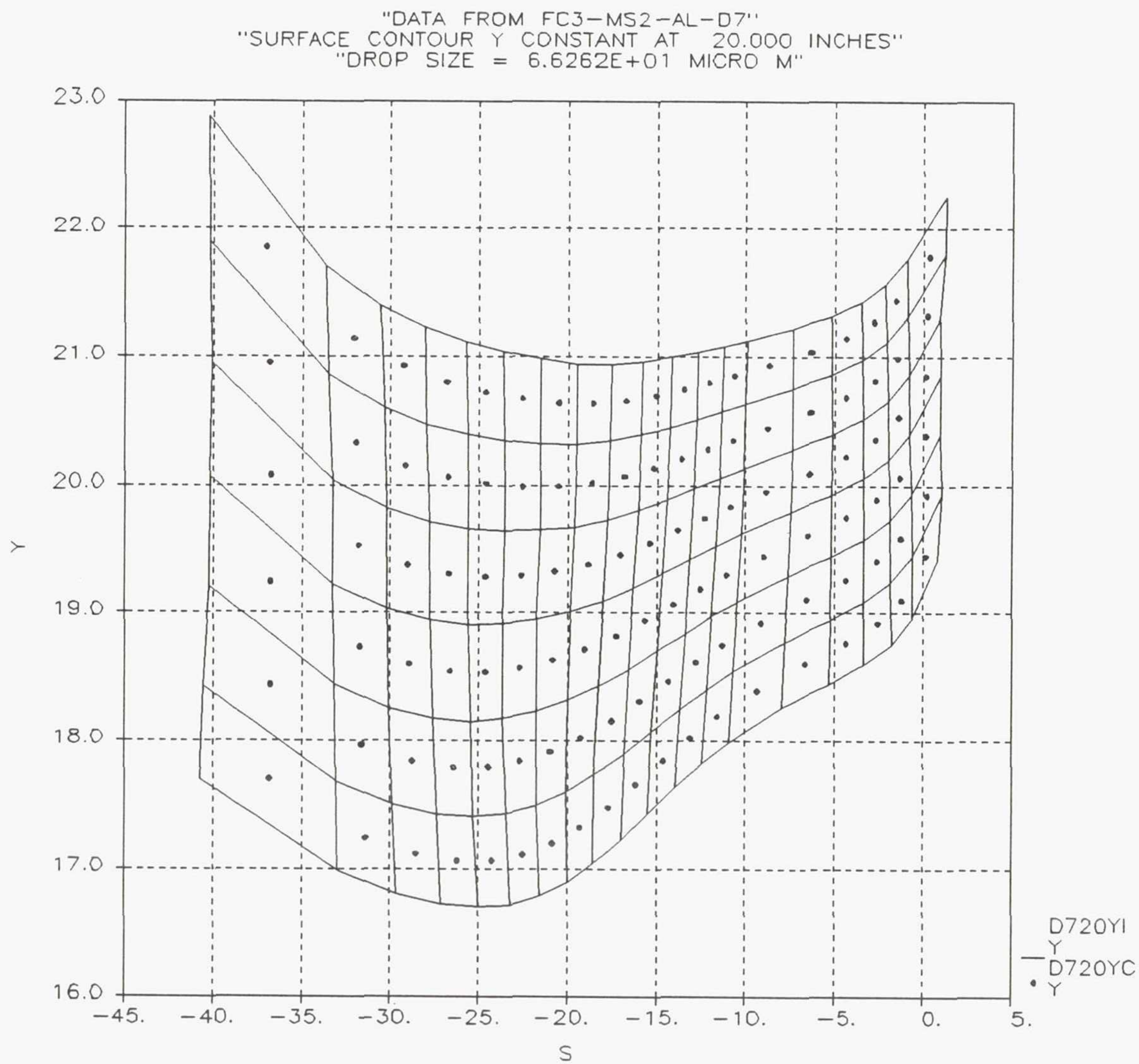

FIGURE D.131

IMPINGEMENT FIELD Y(in) vs S(in), FC3,Y=20,D=66.3 micron

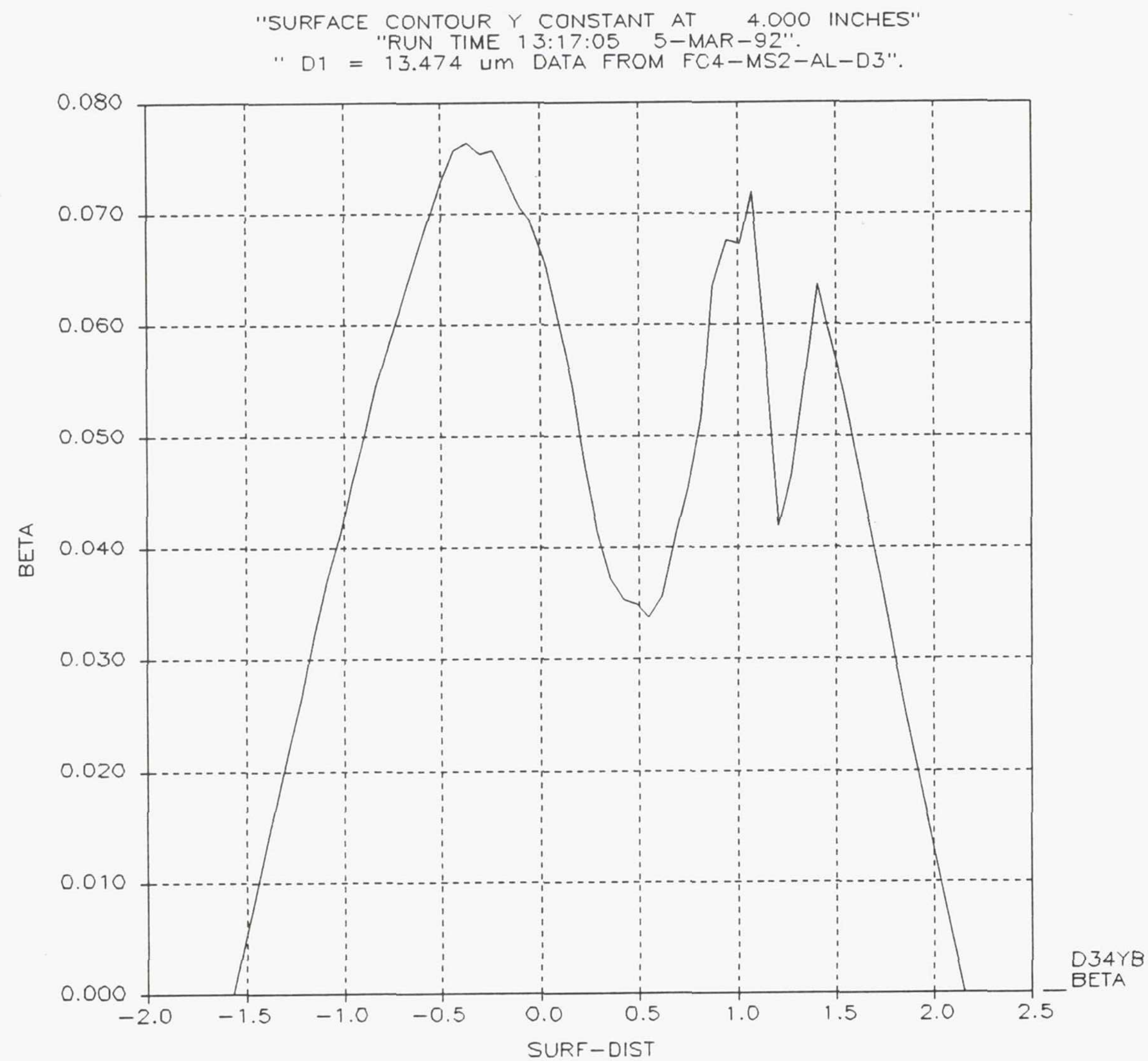

FIGURE D.132

BETA vs SURF-DIST(cm), FC4,Y=4,D=13.5 micron

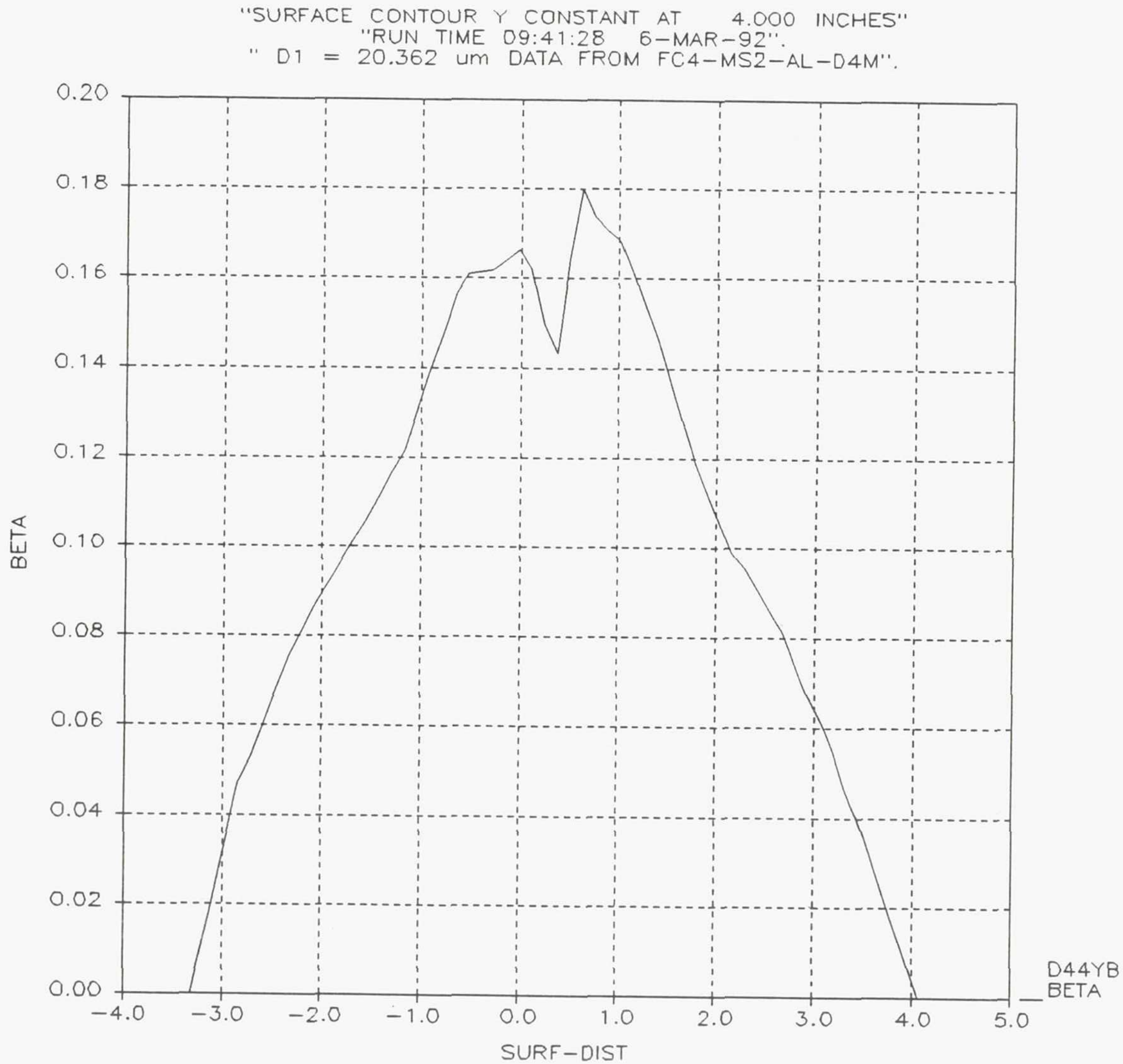

FIGURE D.133

BETA vs SURF-DIST(cm), FC4,Y=4,D=20.4 micron

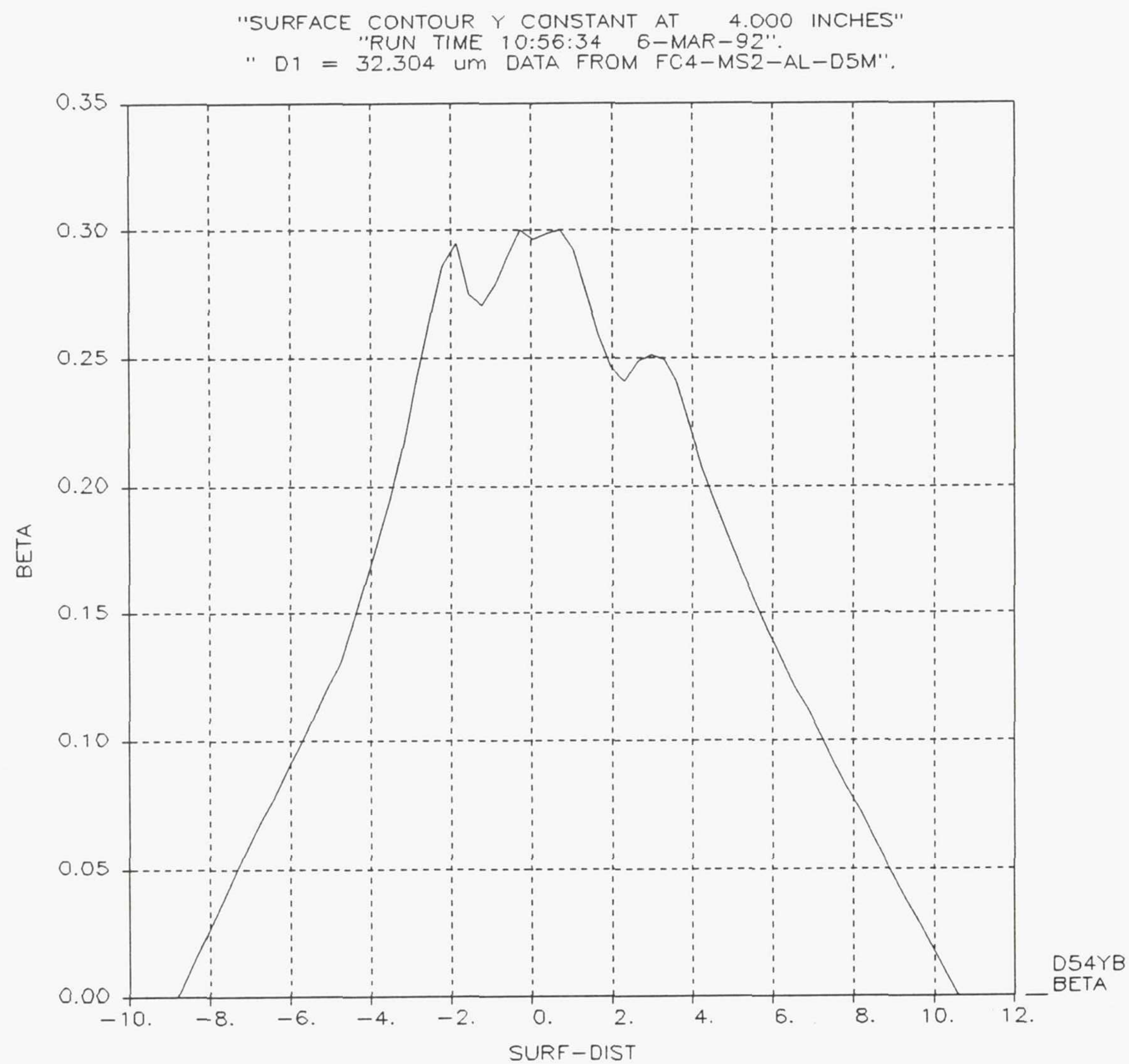

FIGURE D.134

BETA vs SURF-DIST(cm), FC4,Y=4,D=32.3 micron

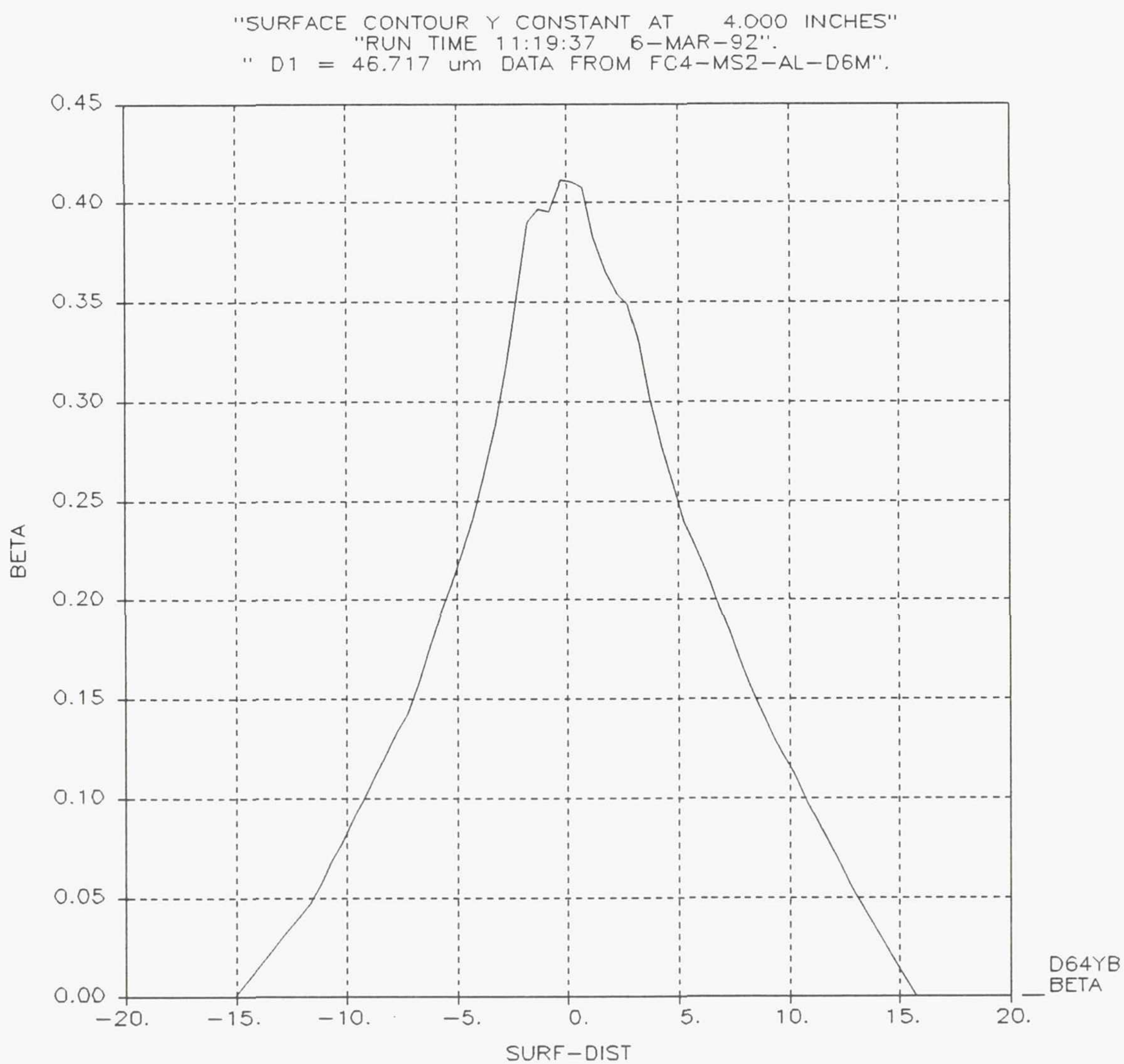

FIGURE D.135

BETA vs SURF-DIST(cm), FC4,Y=4,D=46.7 micron

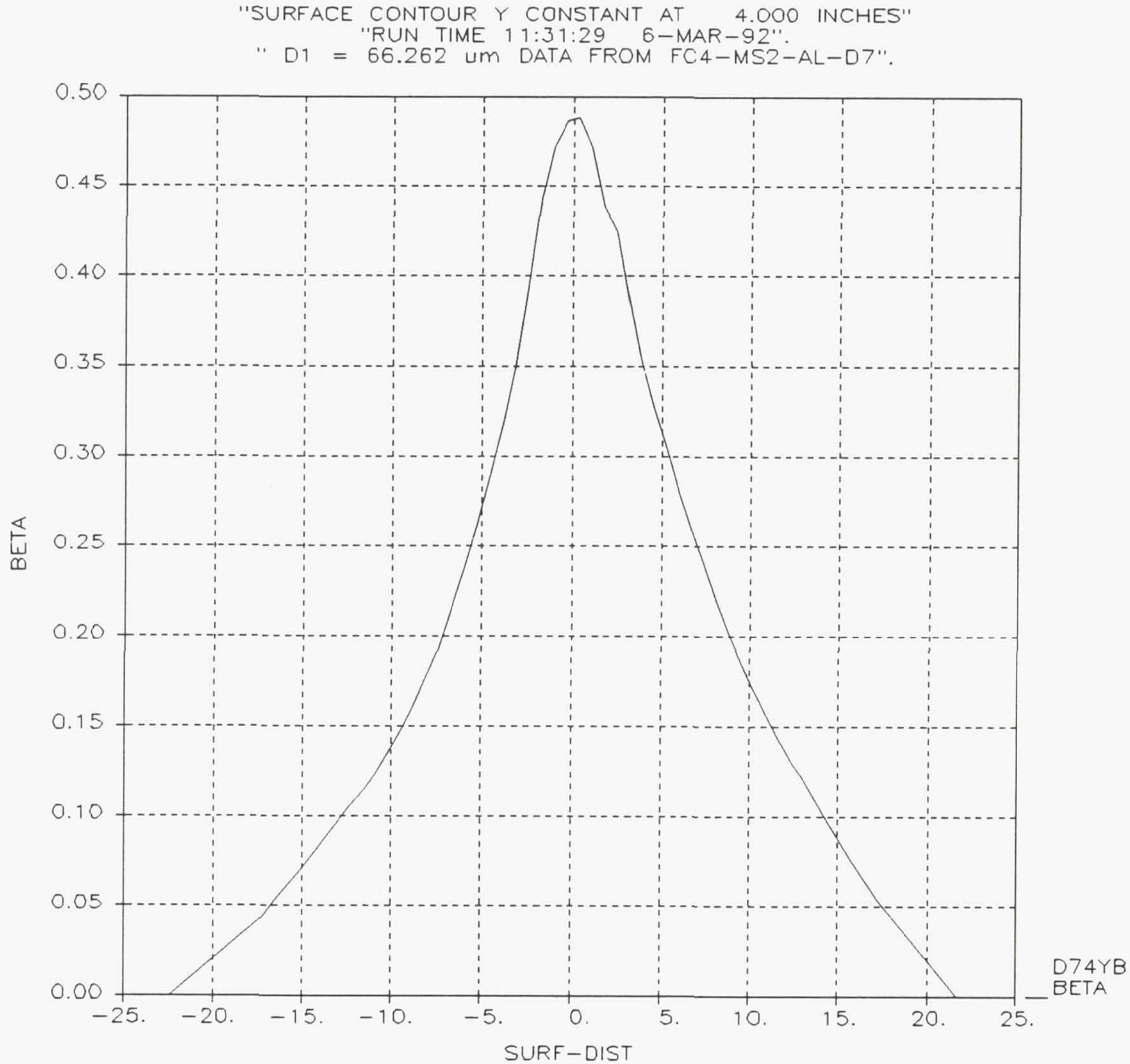

FIGURE D.136

BETA vs SURF-DIST(cm), FC4,Y=4,D=66.3 micron

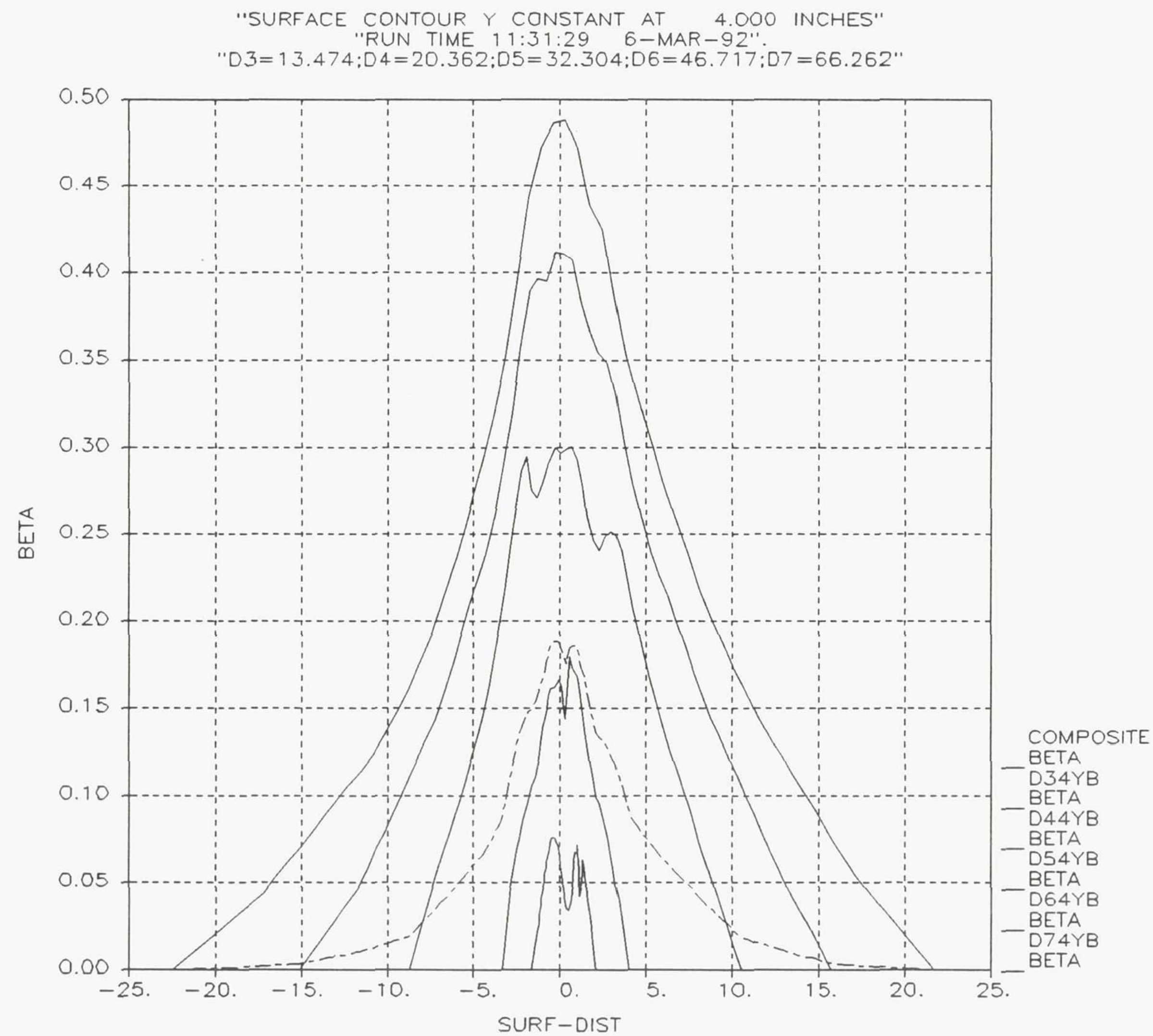

FIGURE D.137

BETA vs SURF-DIST(cm), FC4,Y=4,COMPOSITE AND INDIVIDUAL DROPS

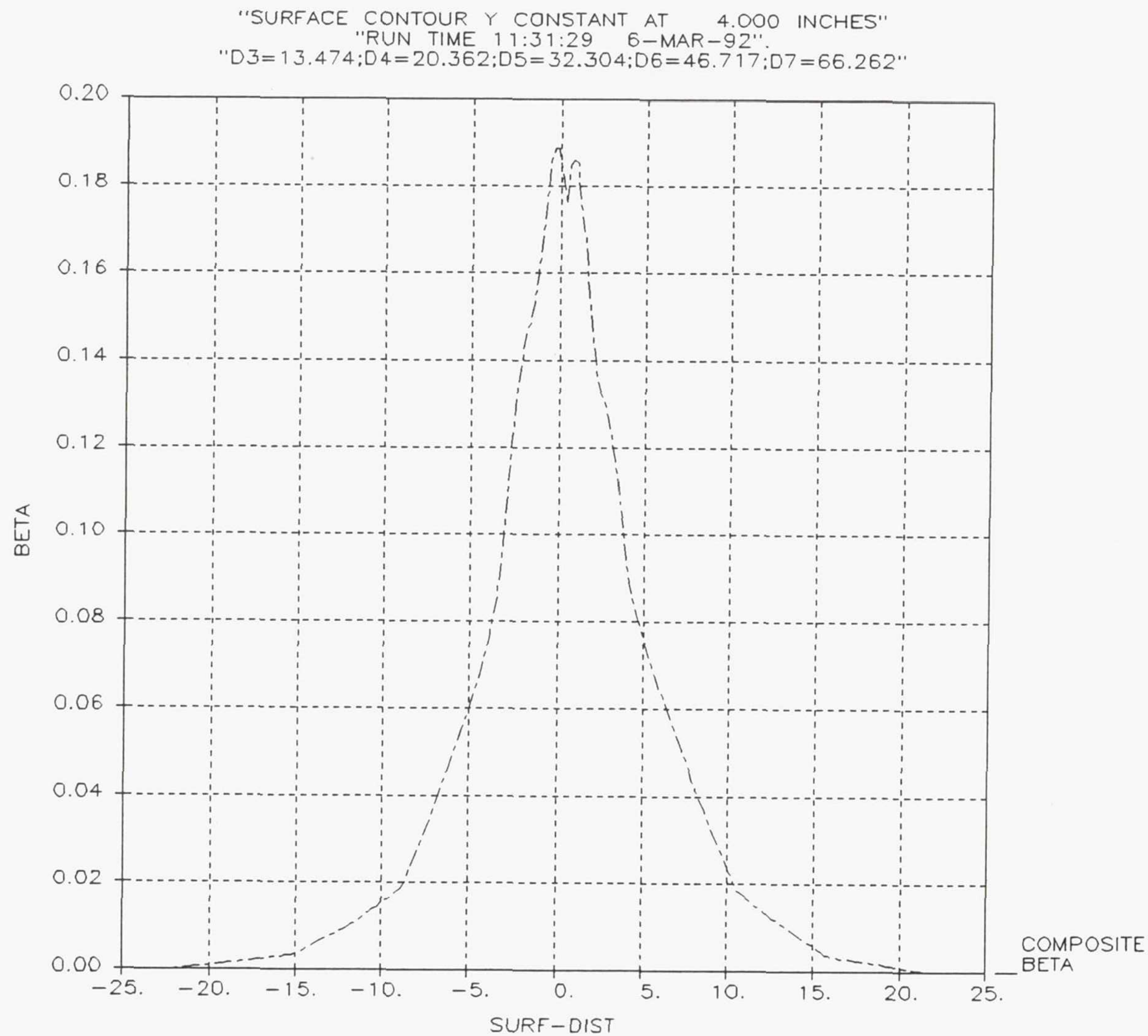

FIGURE D.138

BETA vs SURF-DIST(cm), FC4,Y=4,D=20.4 micron
COMPOSITE DROP

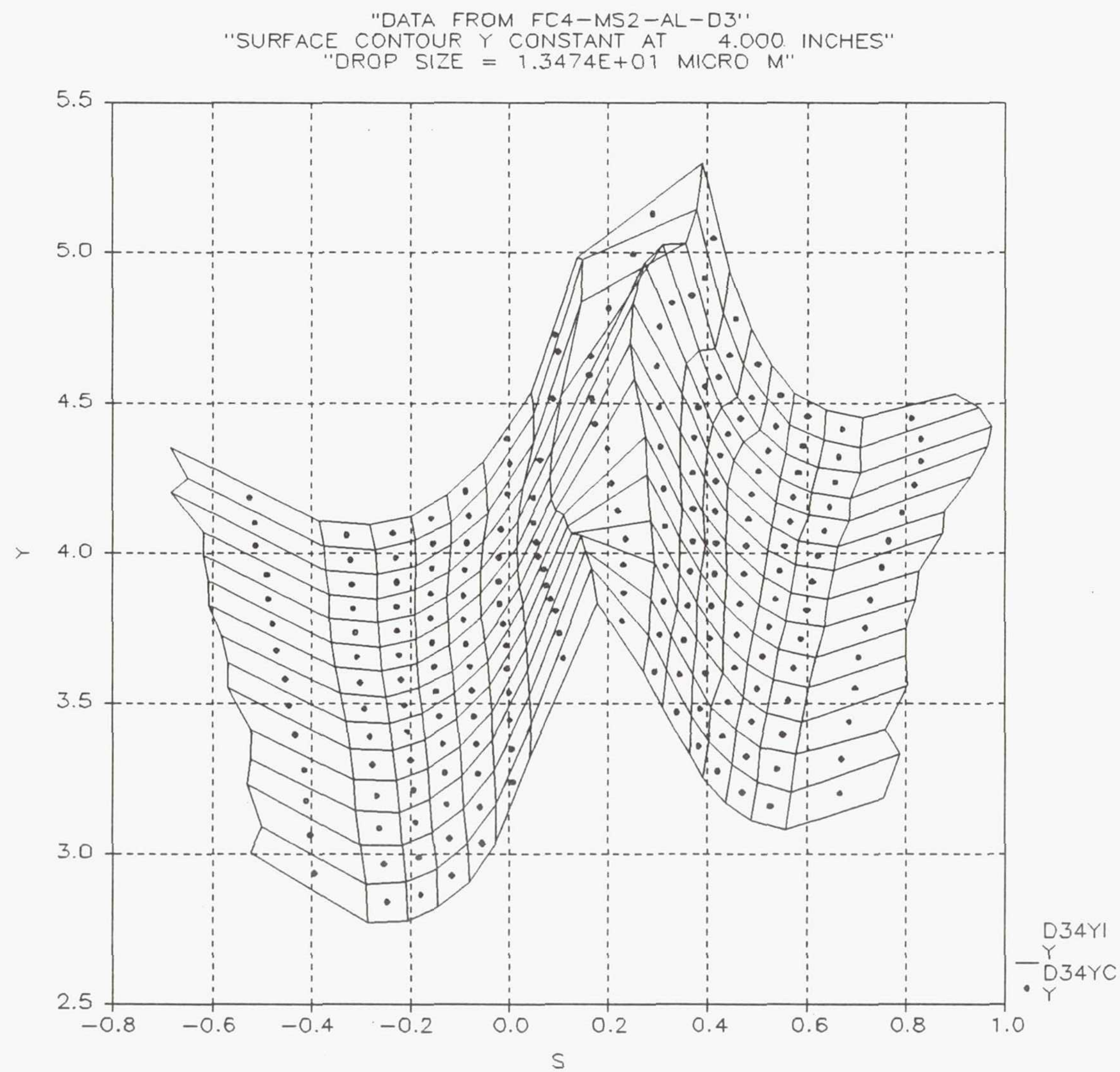

FIGURE D.139

IMPINGEMENT FIELD Y(in) vs S(in), FC4,Y=4,D=13.5 micron

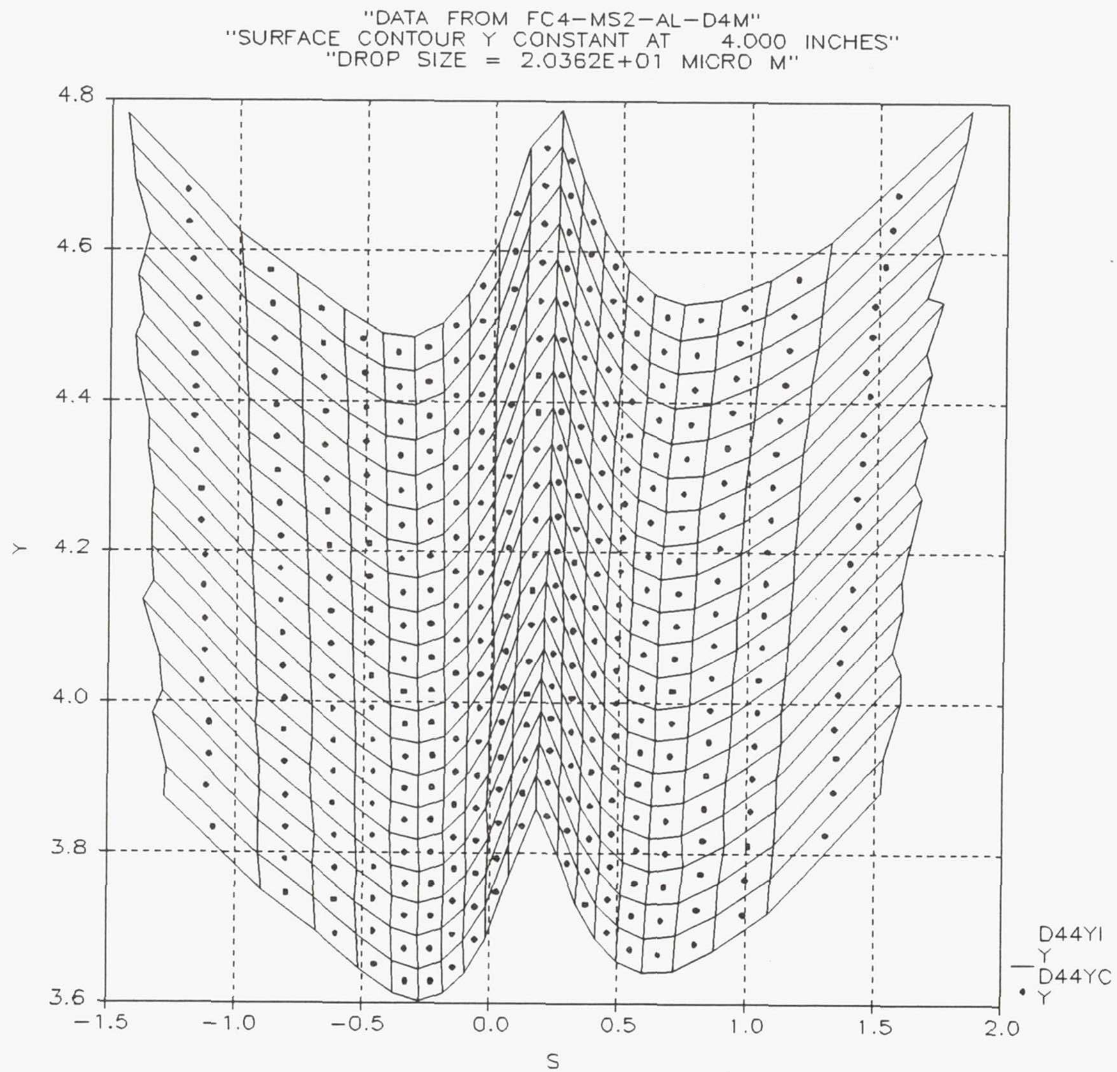

FIGURE D.140

IMPINGEMENT FIELD Y(in) vs S(in), FC4,Y=4,D=20.4 micron

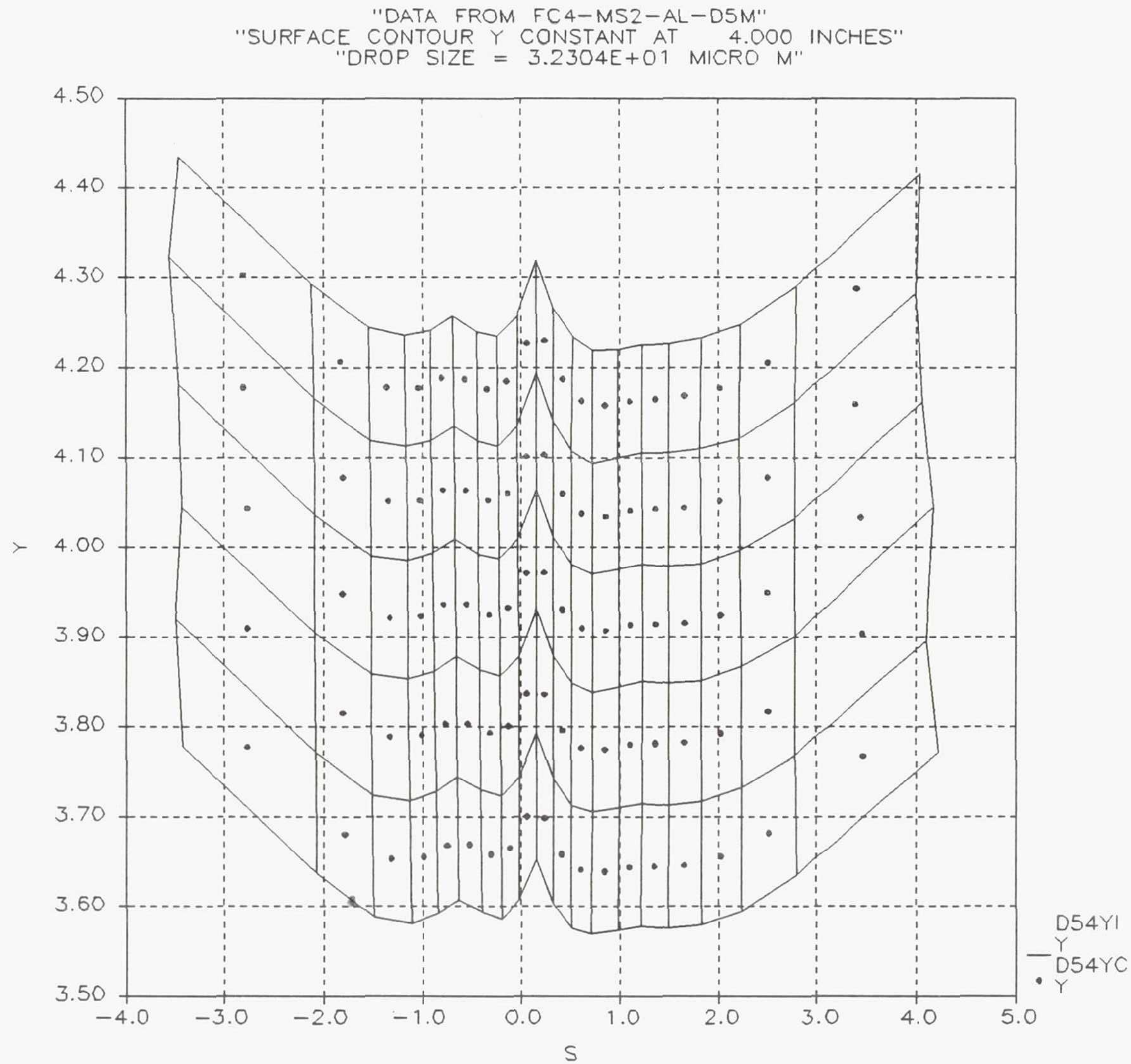

FIGURE D.141

IMPINGEMENT FIELD Y(in) vs S(in), FC4,Y=4,D=32.3 micron

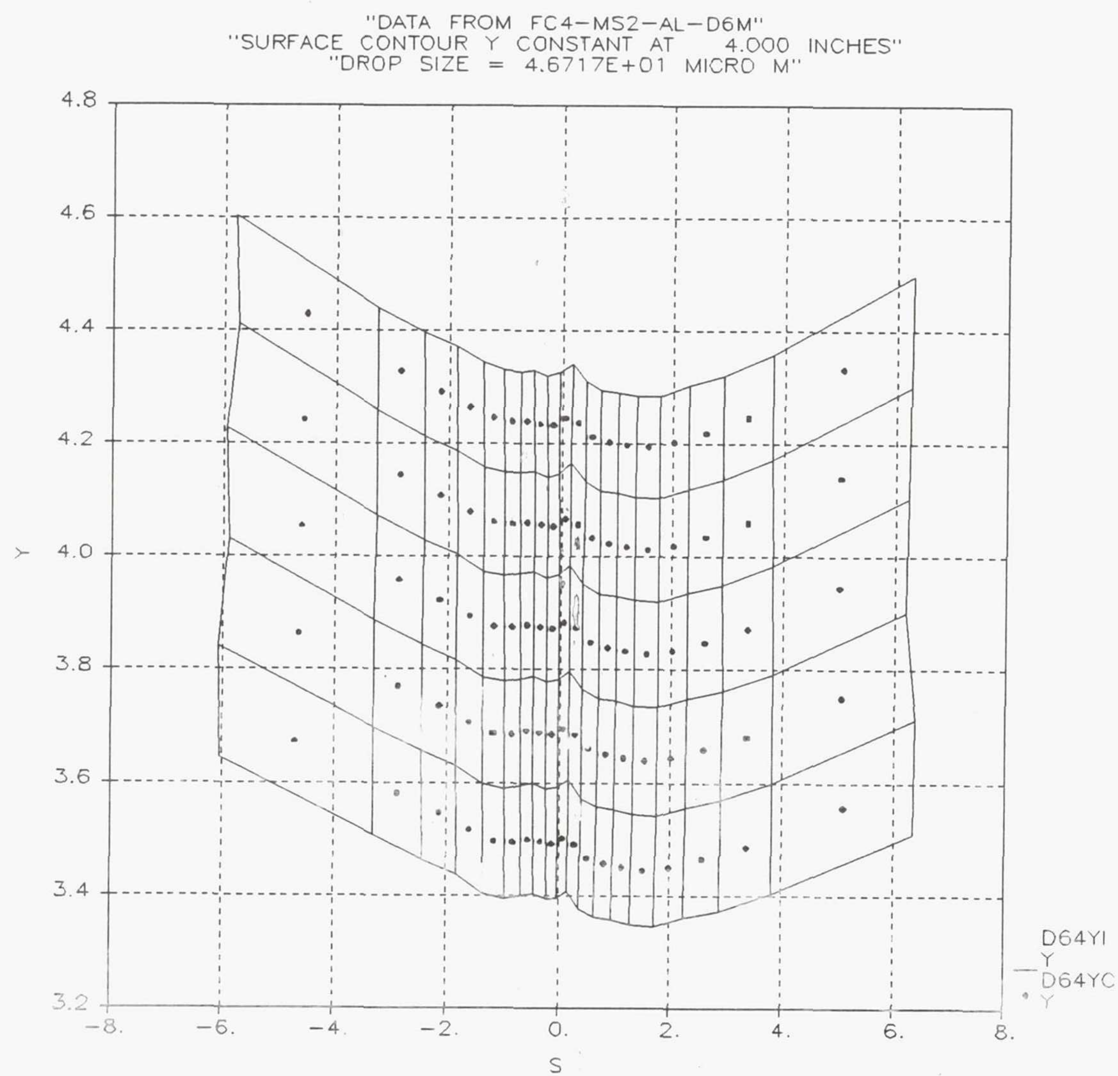

FIGURE D.142

IMPINGEMENT FIELD Y(in) vs S(in), FC4,Y=4,D=46.7 micron

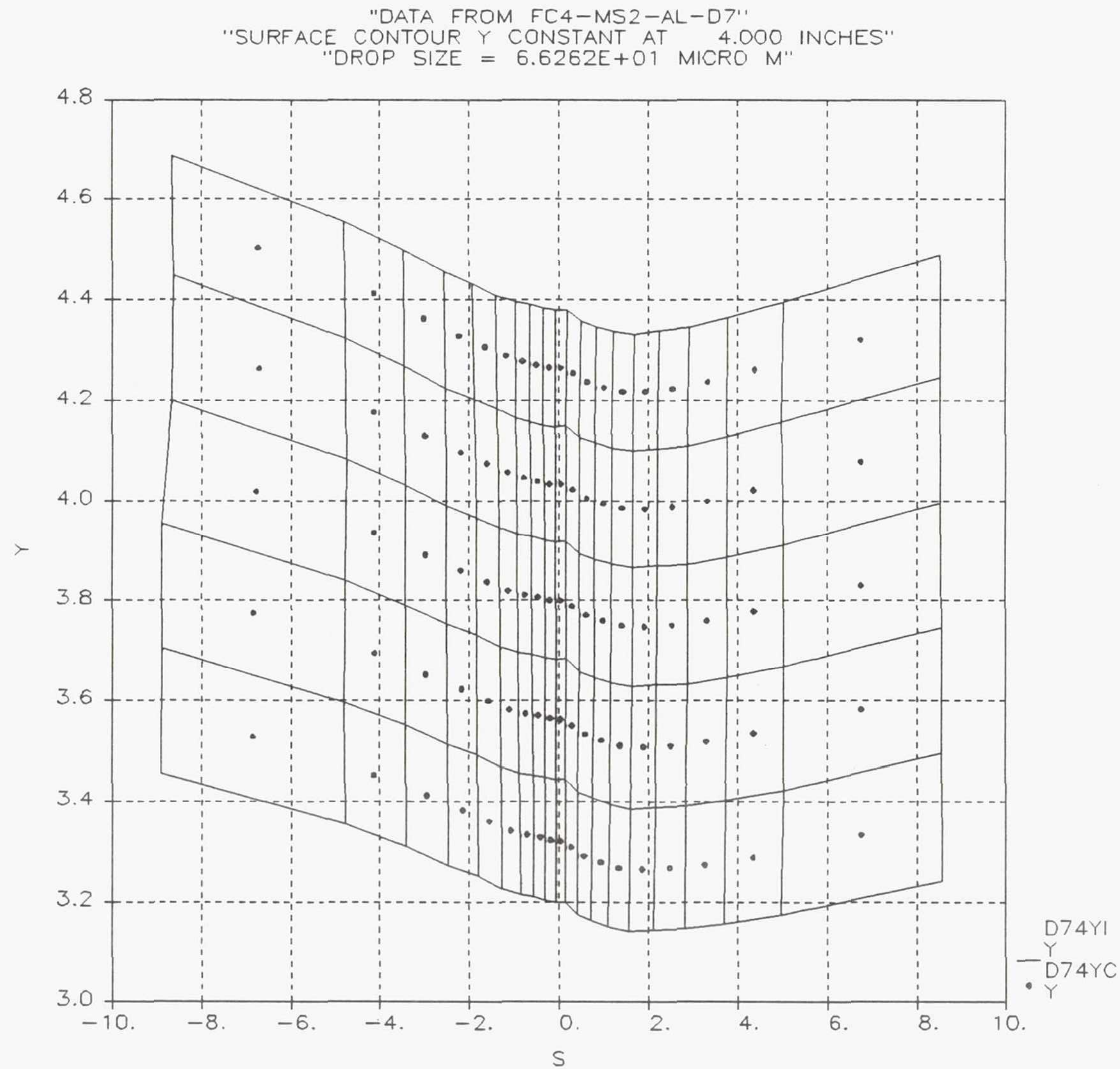

FIGURE D.143

IMPINGEMENT FIELD Y(in) vs S(in), FC4,Y=4,D=66.3 micron

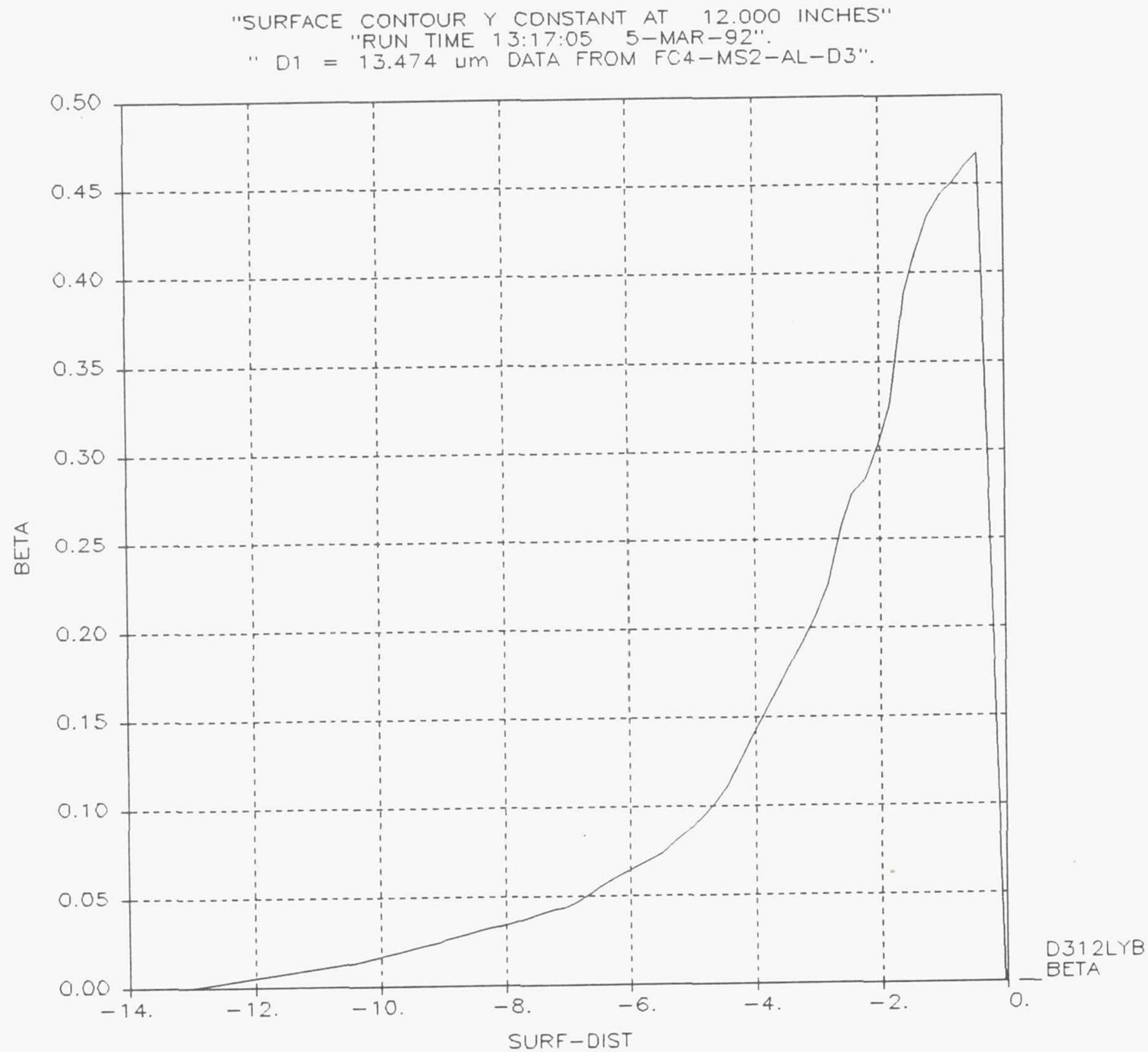

FIGURE D.144

BETA vs SURF-DIST(cm), FC4,Y=12L,D=13.5 micron

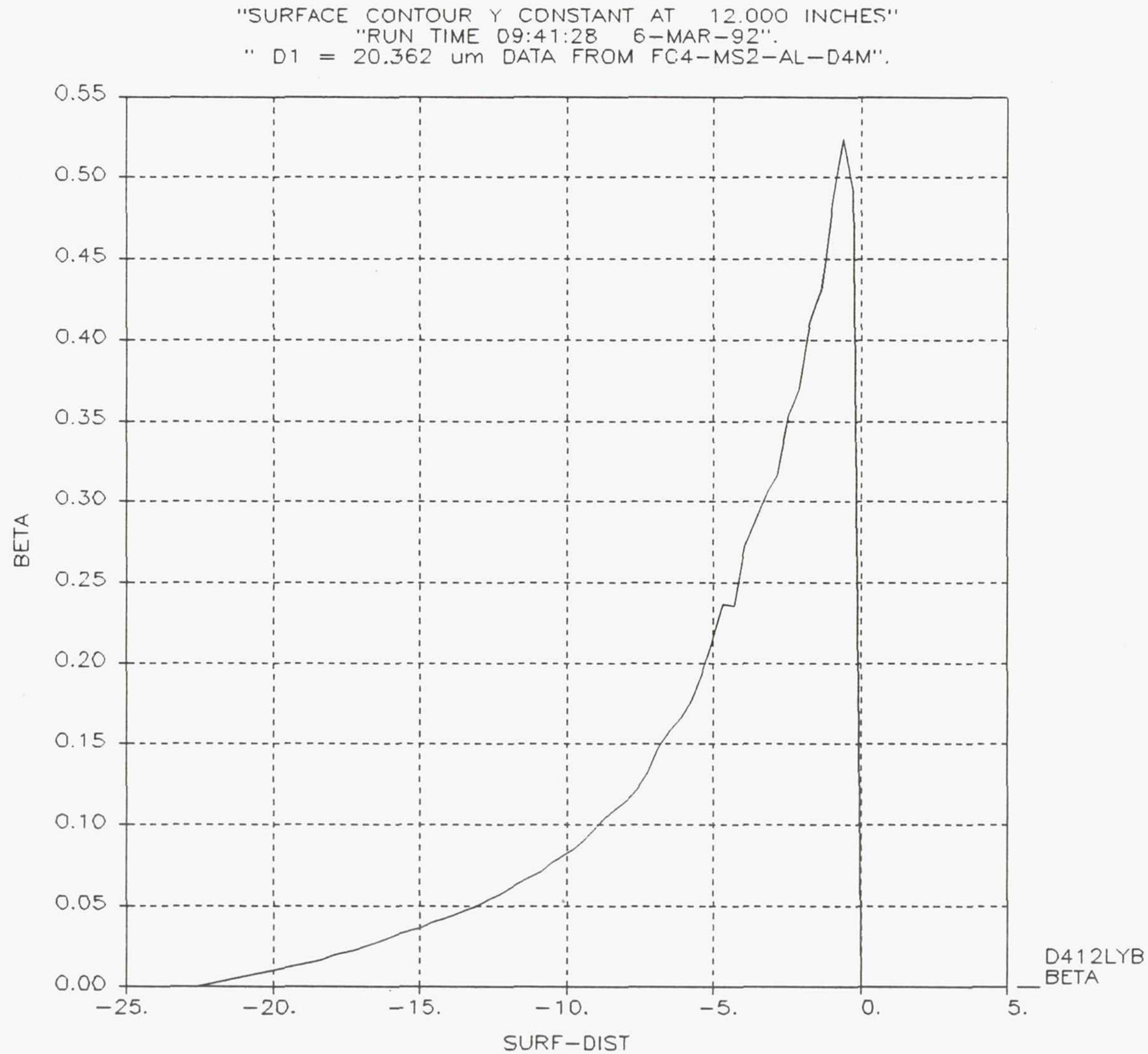

FIGURE D.145

BETA vs SURF-DIST(cm), FC4,Y=12L,D=20.4 micron

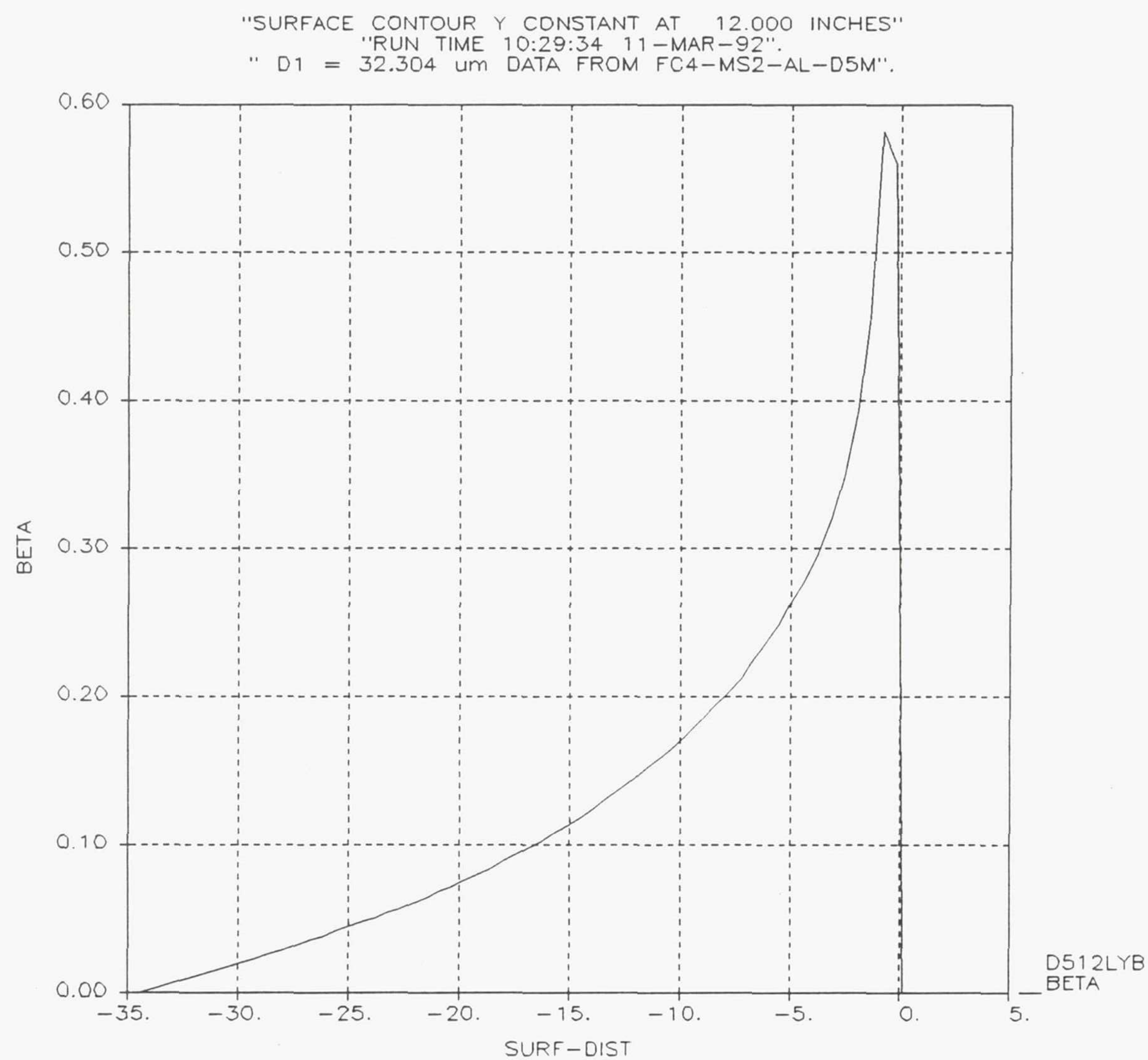

FIGURE D.146

BETA vs SURF-DIST(cm), FC4,Y=12L,D=32.3 micron

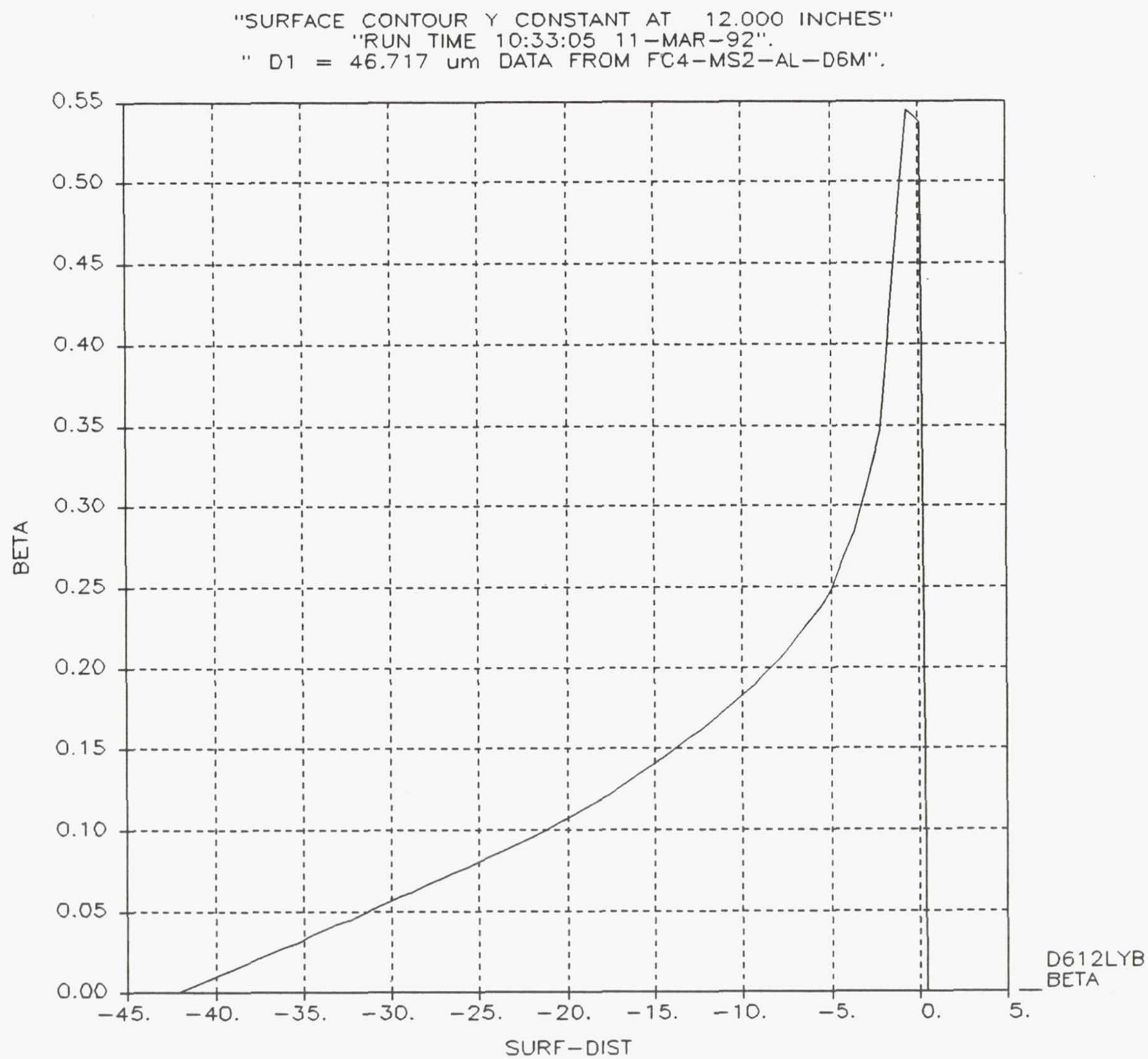

FIGURE D.147

BETA vs SURF-DIST(cm), FC4,Y=12L,D=46.7 micron

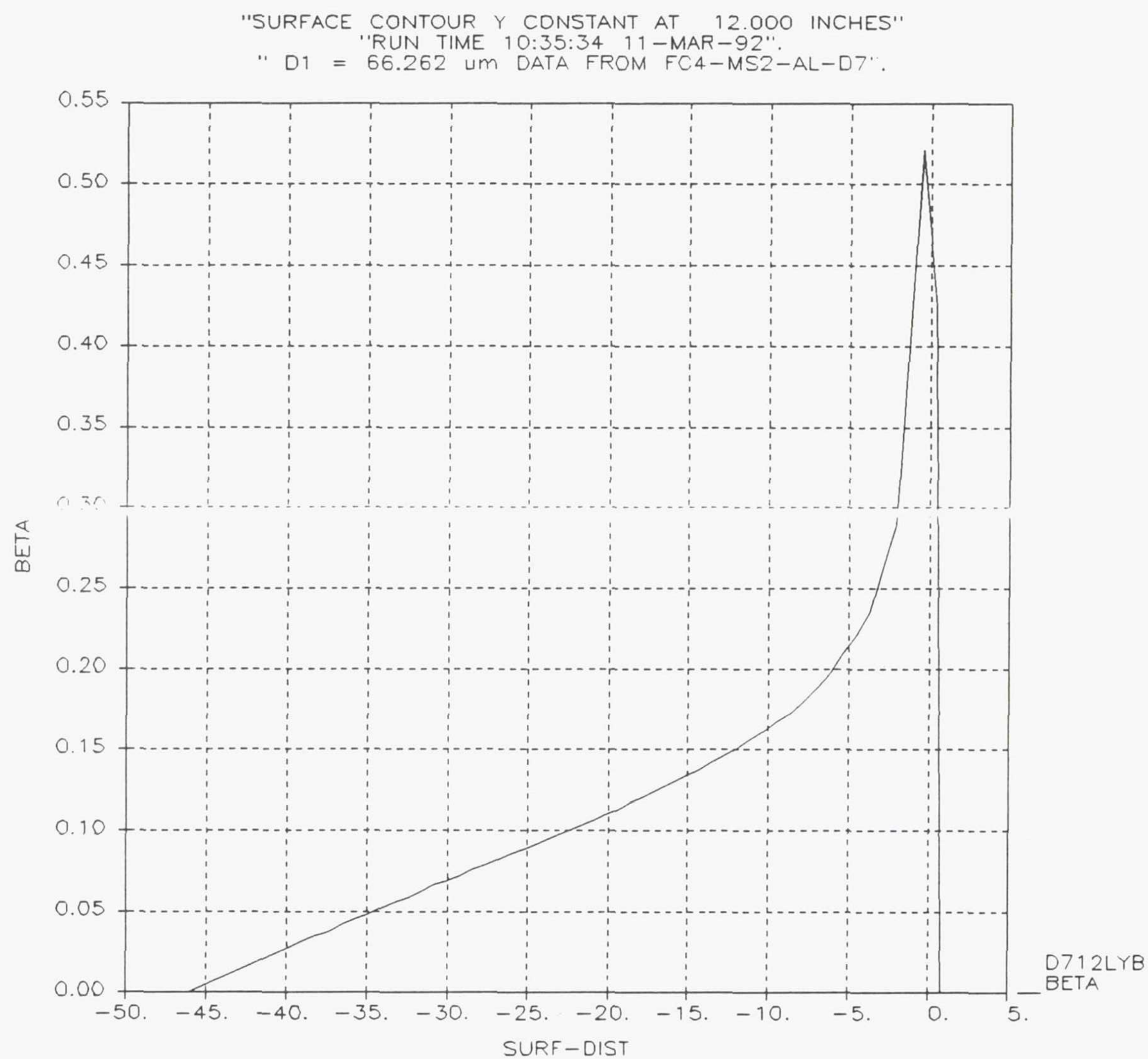

FIGURE D.148

BETA vs SURF-DIST(cm), FC4,Y=12L,D=66.3 micron

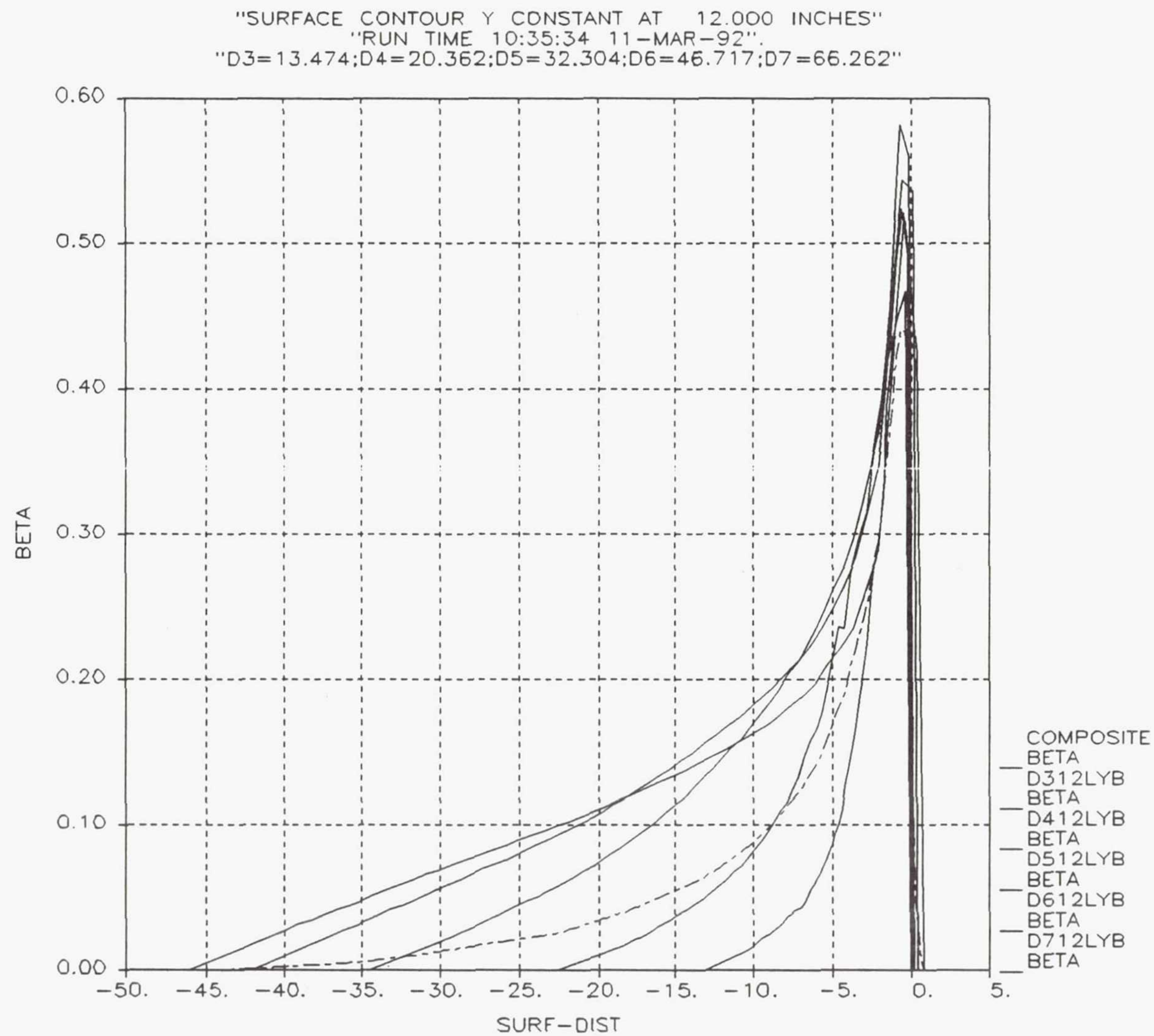

FIGURE D.149

BETA vs SURF-DIST(cm), FC4,Y=12L,COMPOSITE AND INDIVIDUAL DROPS

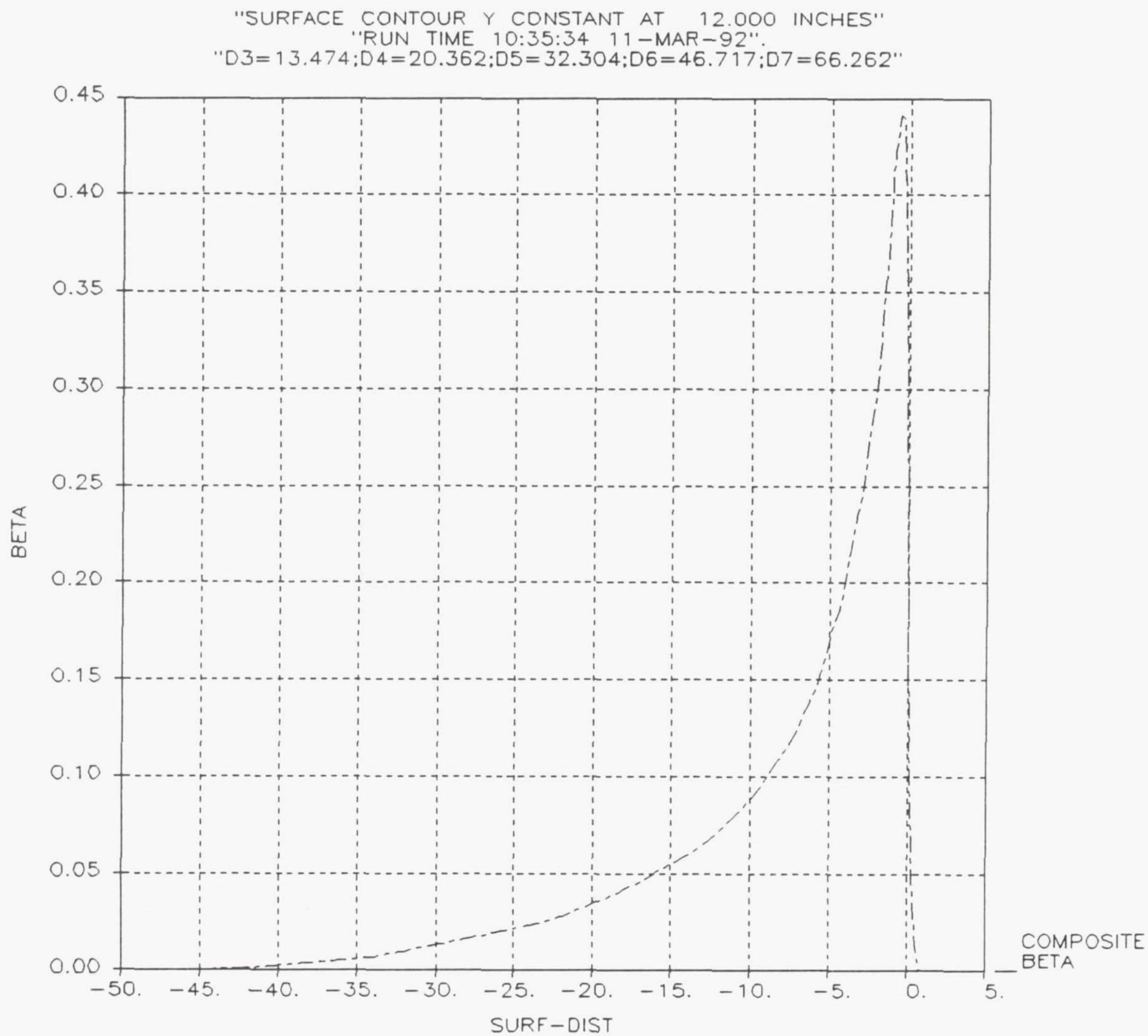

FIGURE D.150

BETA vs SURF-DIST(cm), FC4,Y=12L,D=20.4 micron
COMPOSITE DROP

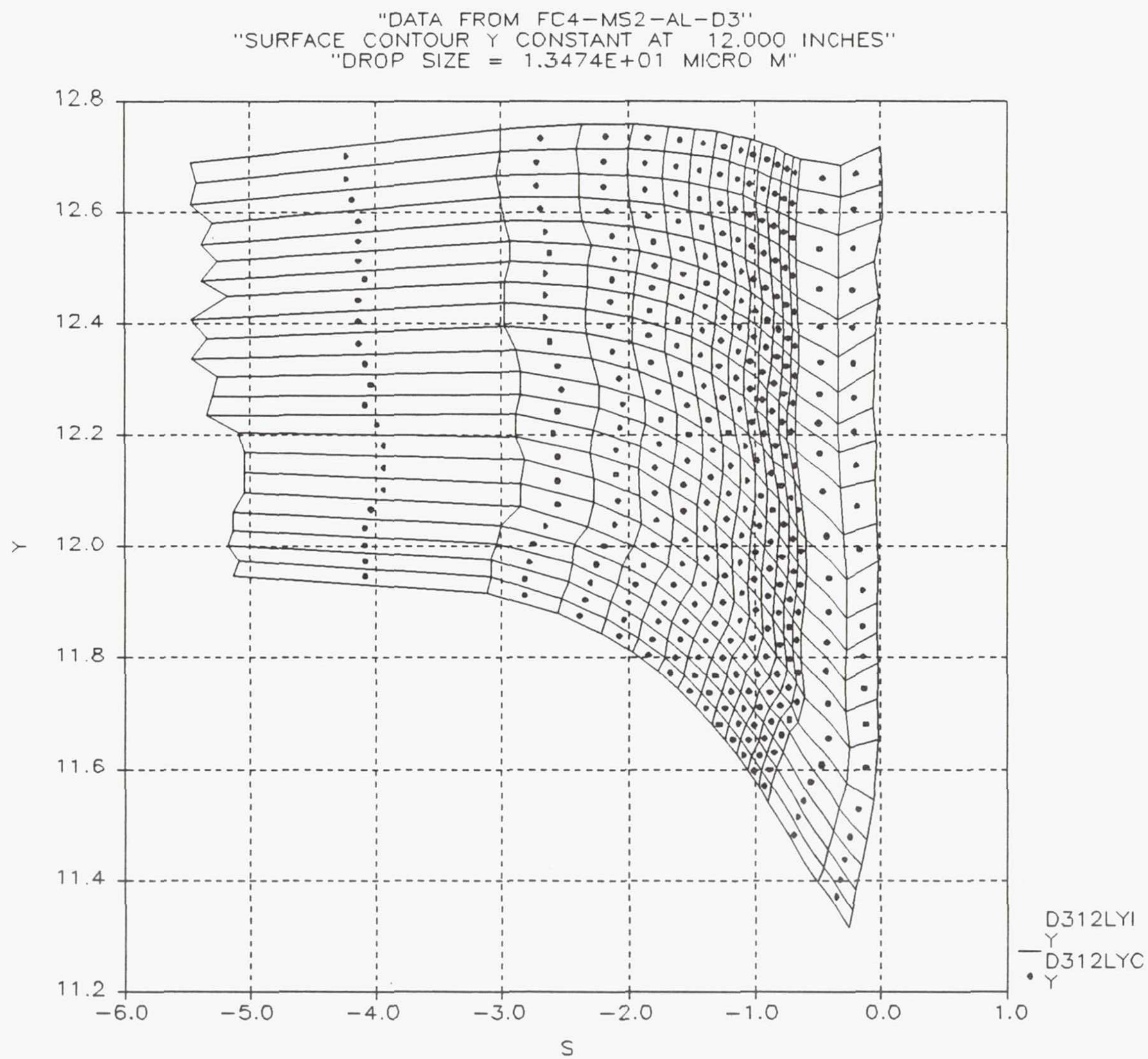

FIGURE D.151

IMPINGEMENT FIELD Y(in) vs S(in), FC4,Y=12L,D=13.5 micron

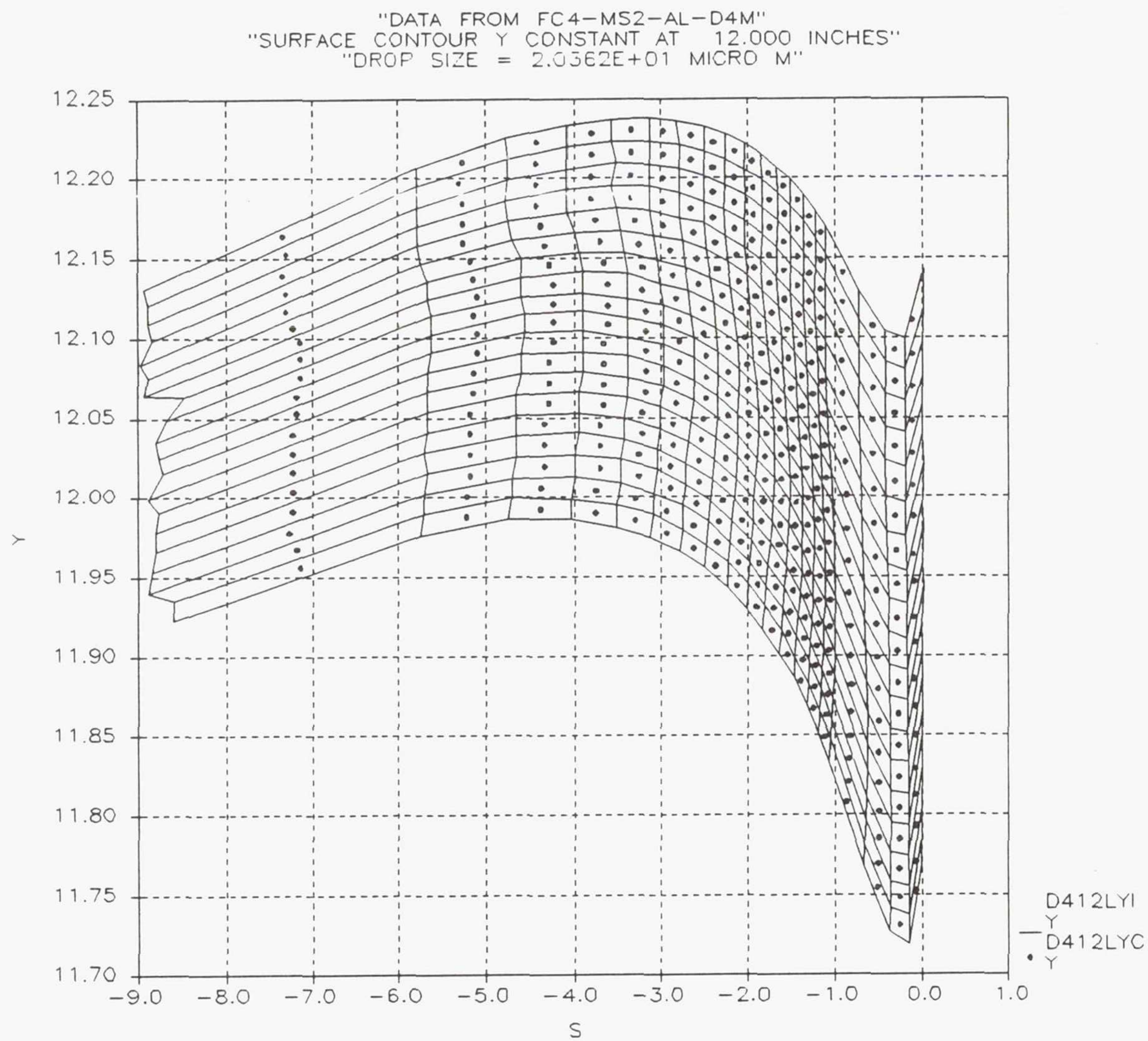

FIGURE D.152

IMPINGEMENT FIELD Y(in) vs S(in), FC4,Y=12L,D=20.4 micron

FIGURE D.153

IMPINGEMENT FIELD Y(in) vs S(in), FC4,Y=12L,D=32.3 micron

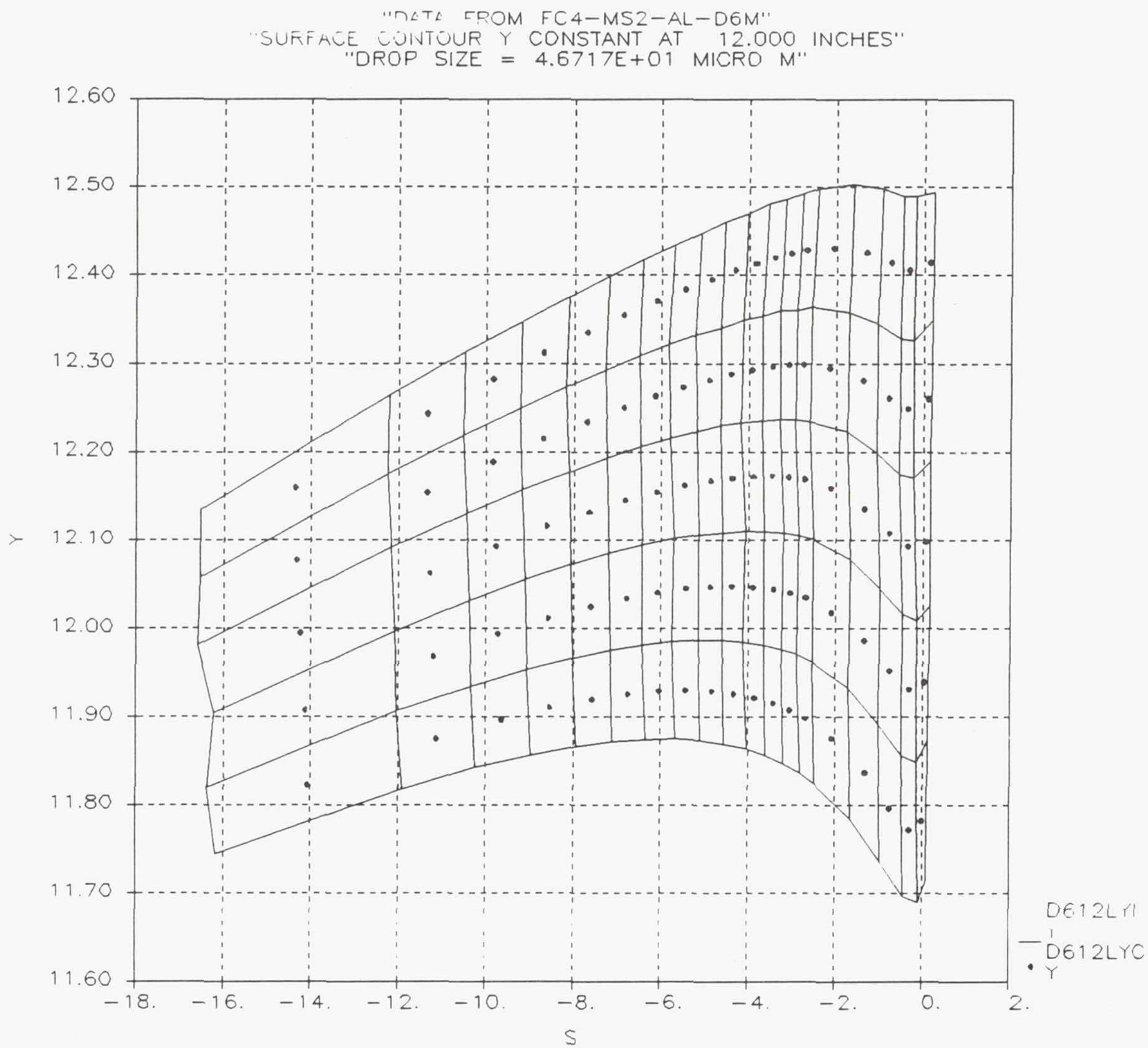

FIGURE D.154

IMPINGEMENT FIELD Y(in) vs S(in), FC4,Y=12L,D=46.7 micron

FIGURE D.155

IMPINGEMENT FIELD Y(in) vs S(in), FC4,Y=12L,D=66.3 micron

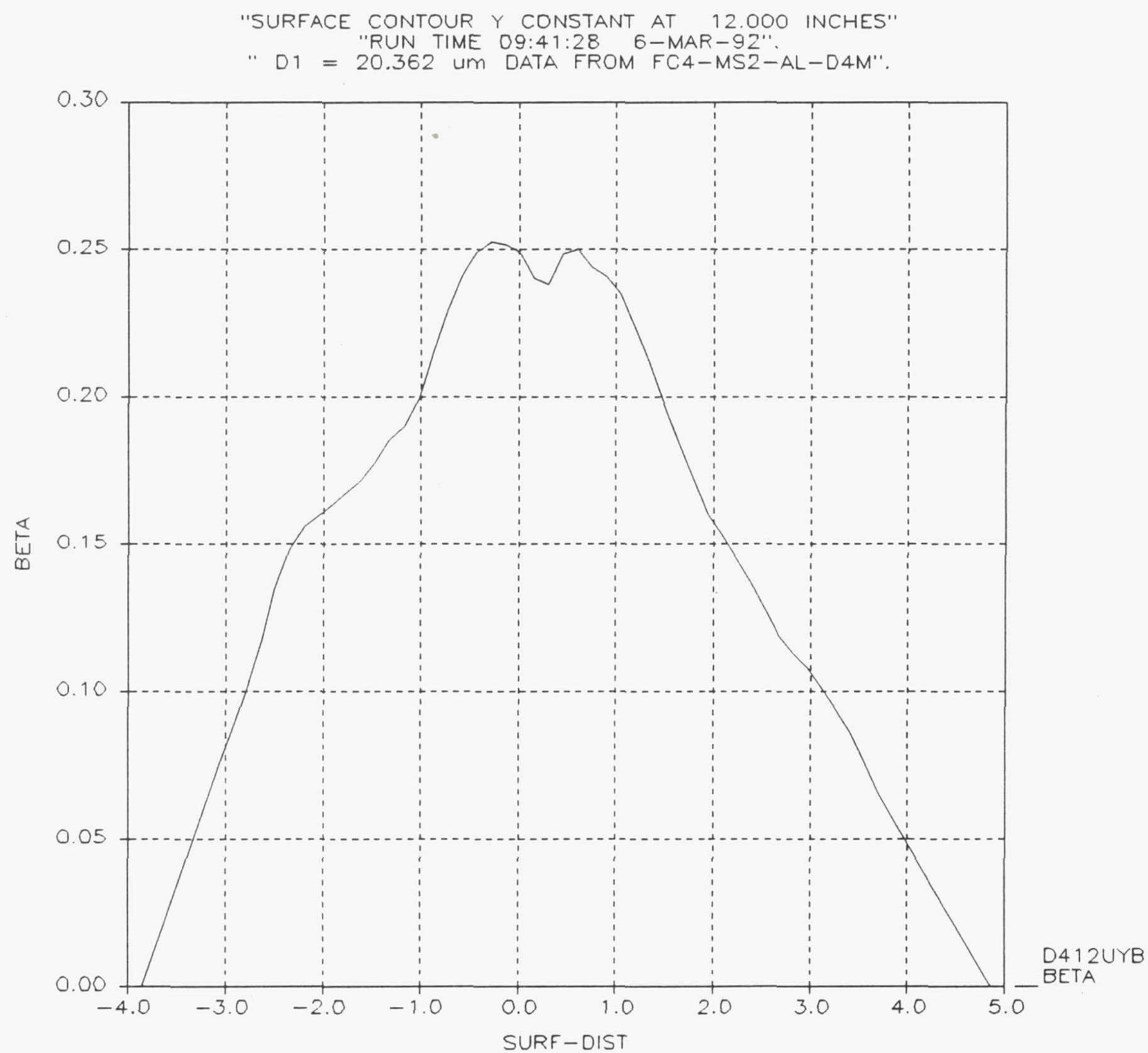

FIGURE D.156

BETA vs SURF-DIST(cm), FC4,Y=12U,D=20.4 micron

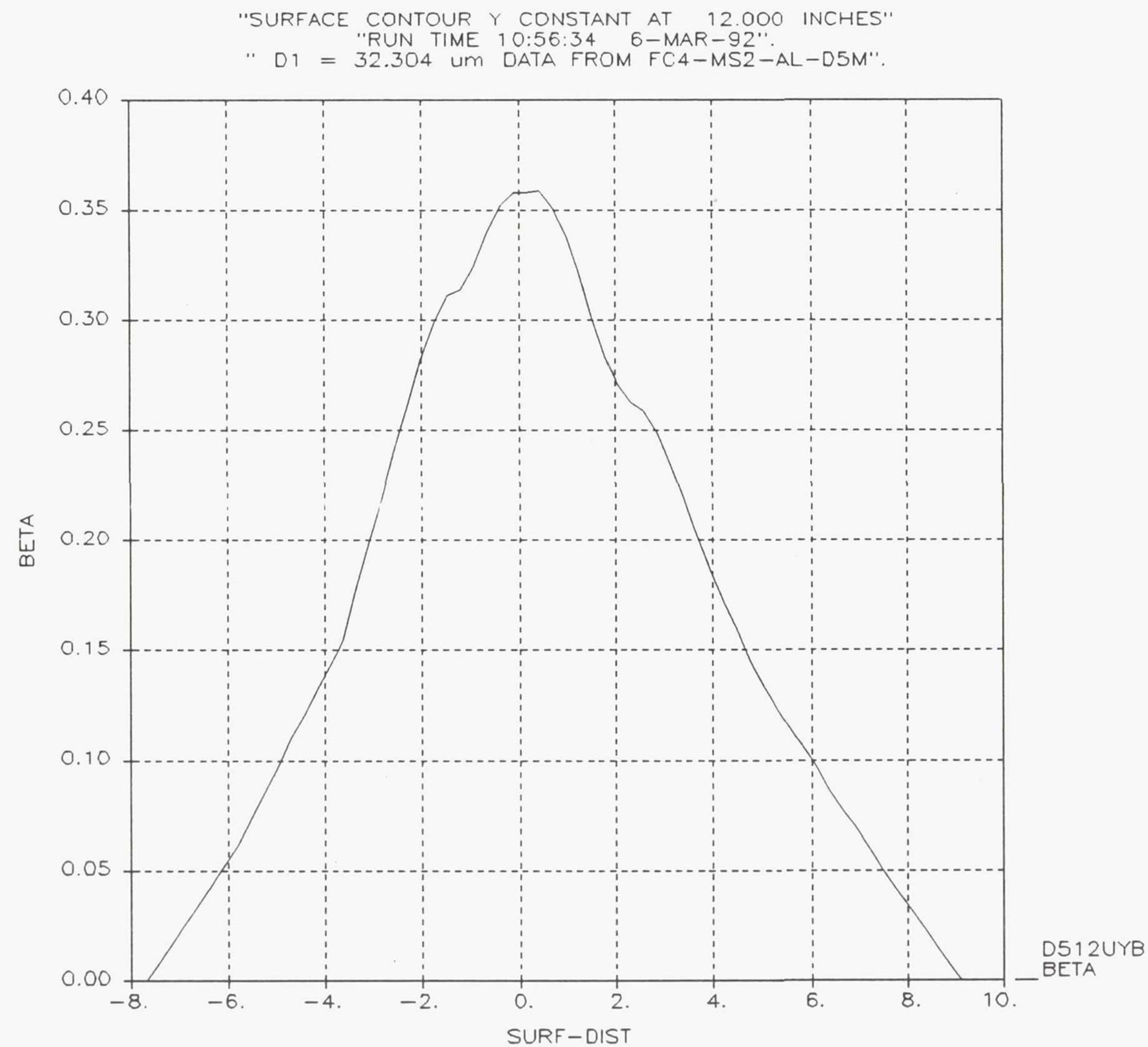

FIGURE D.157

BETA vs SURF-DIST(cm), FC4,Y=12U,D=32.3 micron

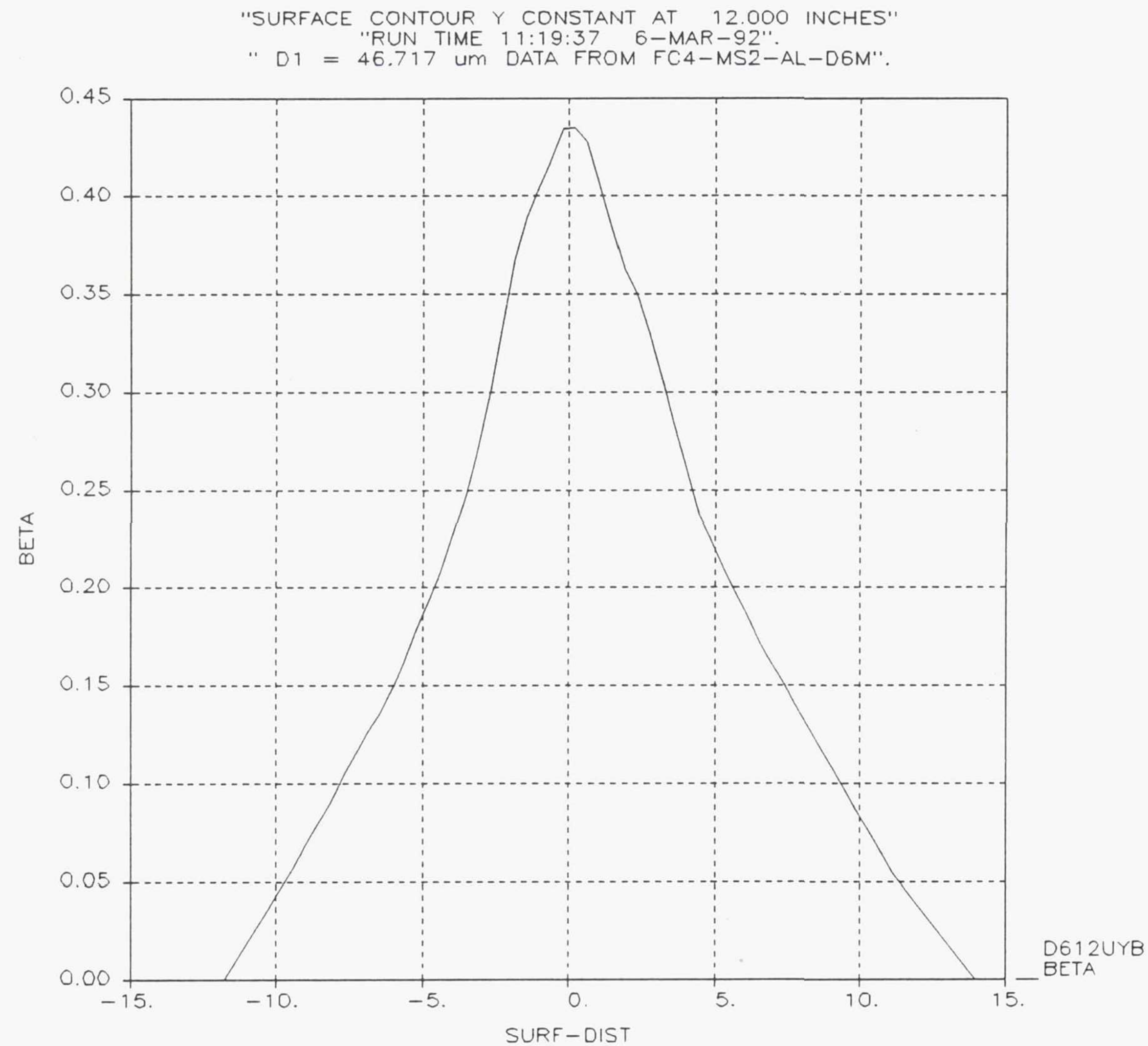

FIGURE D.158

BETA vs SURF-DIST(cm), FC1,Y=12U,D=46.7 micron

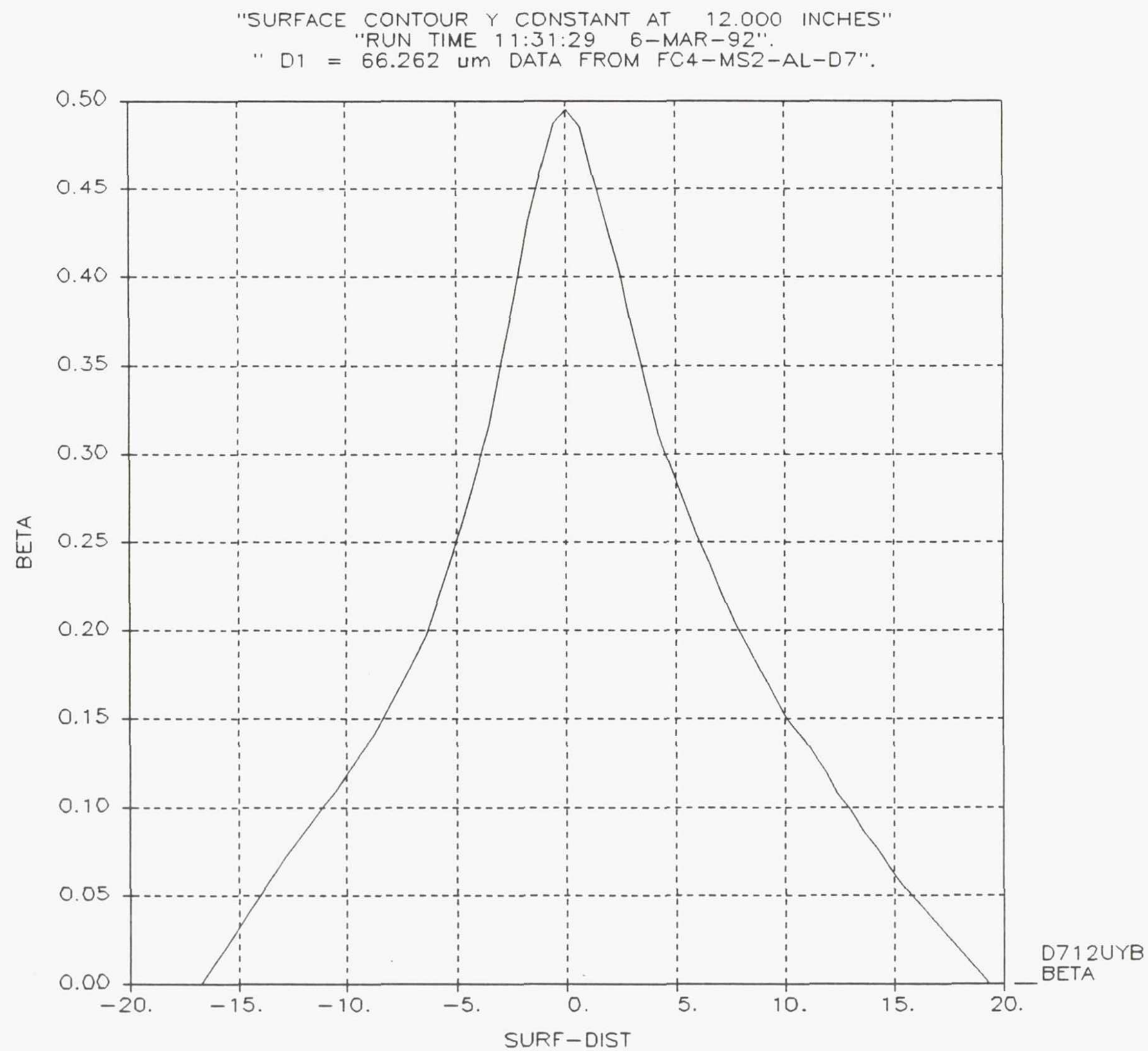

FIGURE D.159

BETA vs SURF-DIST(cm), FC4,Y=12U,D=66.3 micron

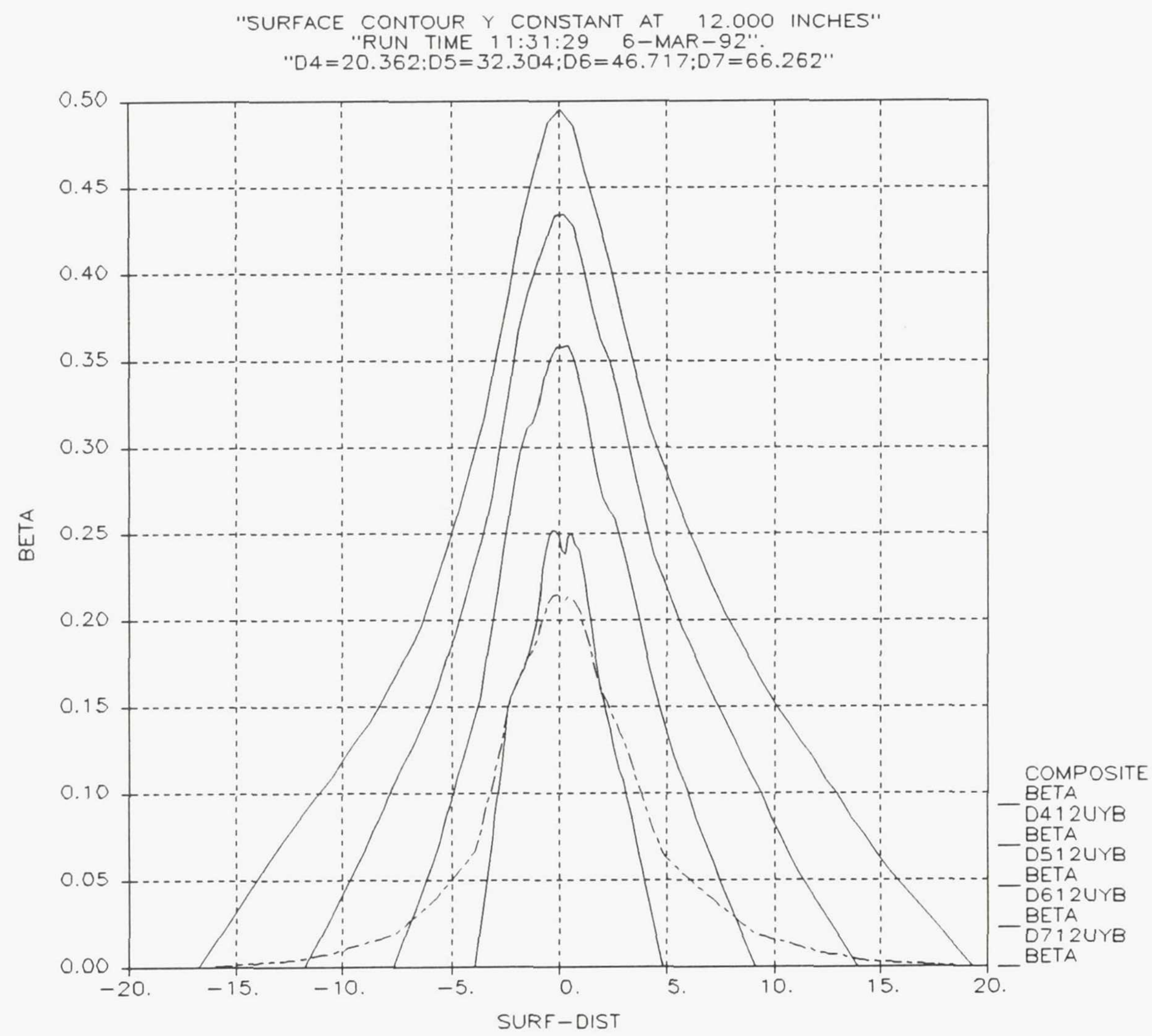

FIGURE D.160

BETA vs SURF-DIST(cm), FC4,Y=12U,COMPOSITE AND INDIVIDUAL DROPS

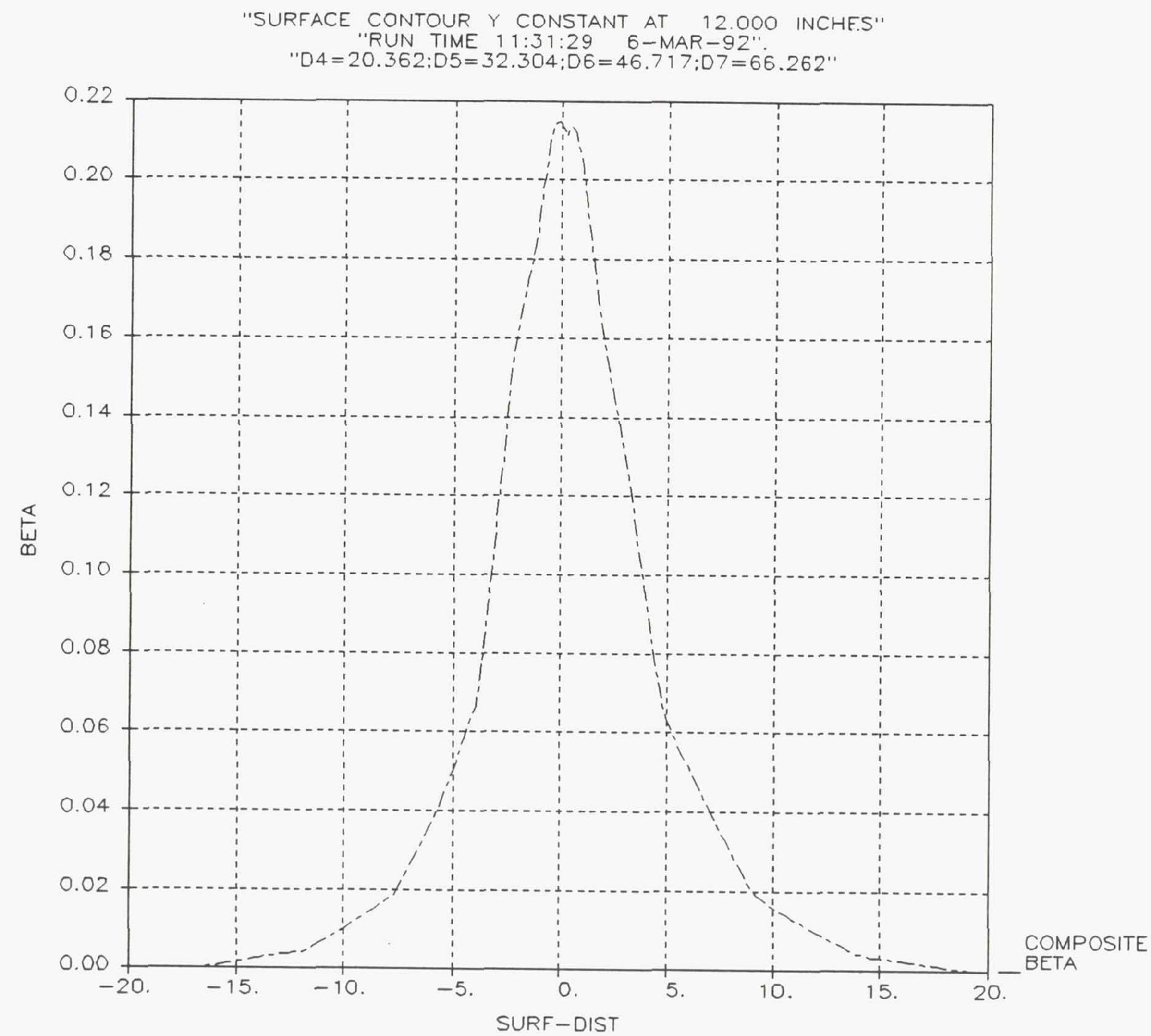

FIGURE D.161

BETA vs SURF-DIST(cm), FC4,Y=12U,D=20.4 micron
COMPOSITE DROP

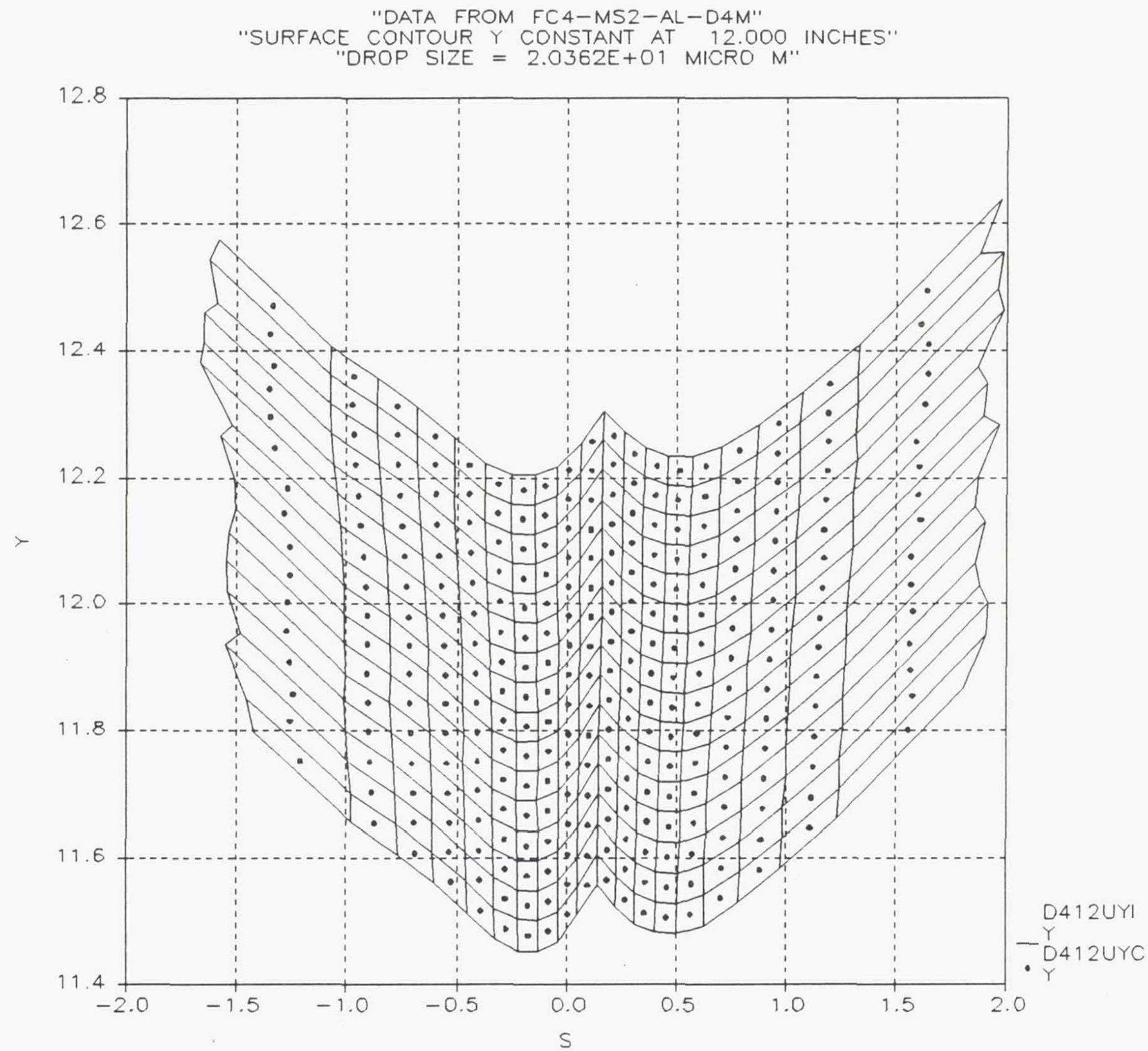

FIGURE D.162

IMPINGEMENT FIELD Y(in) vs S(in), FC4,Y=12U,D=20.4 micron

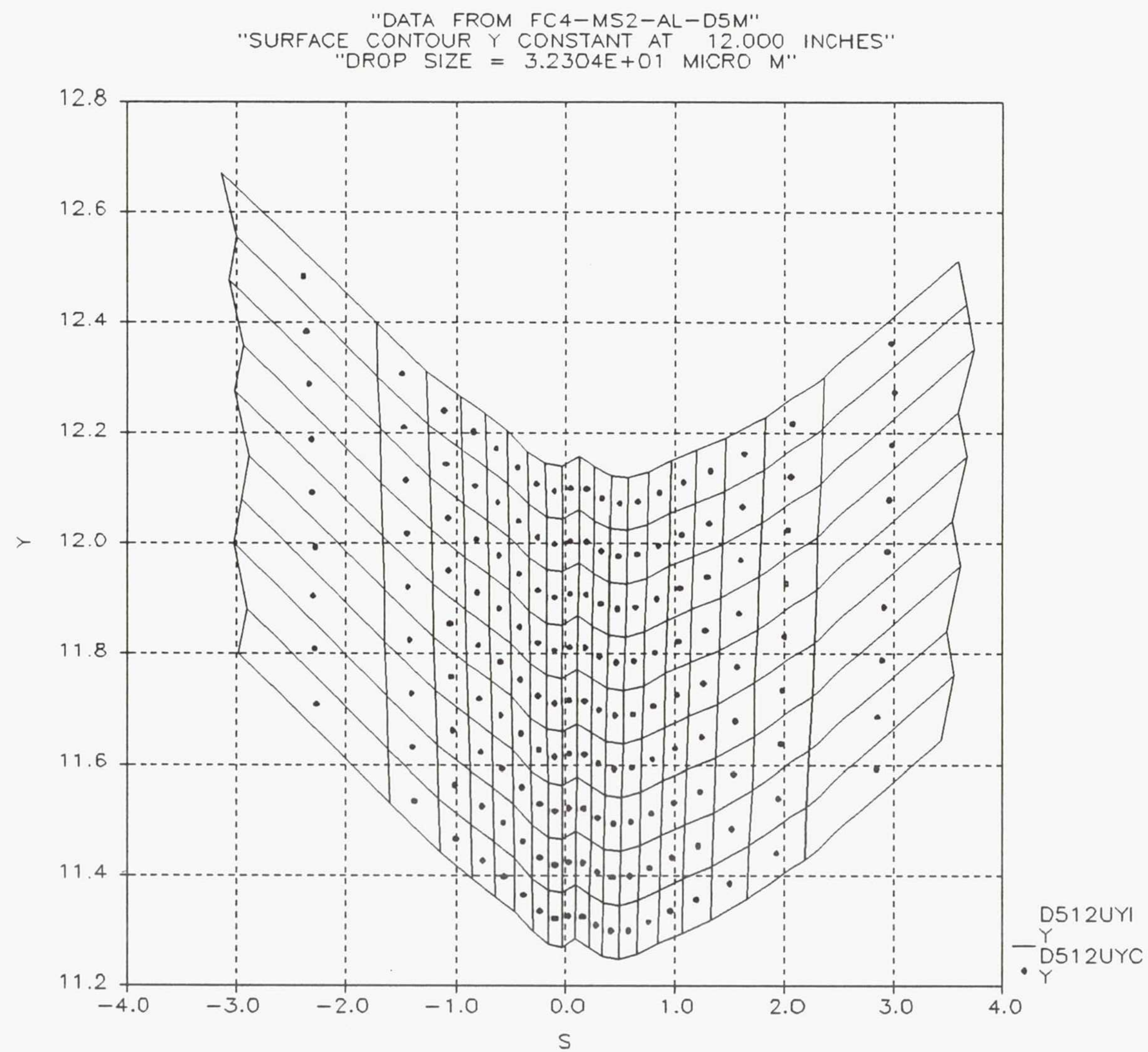

FIGURE D.163

IMPINGEMENT FIELD Y(in) vs S(in), FC4,Y=12U,D=32.3 micron

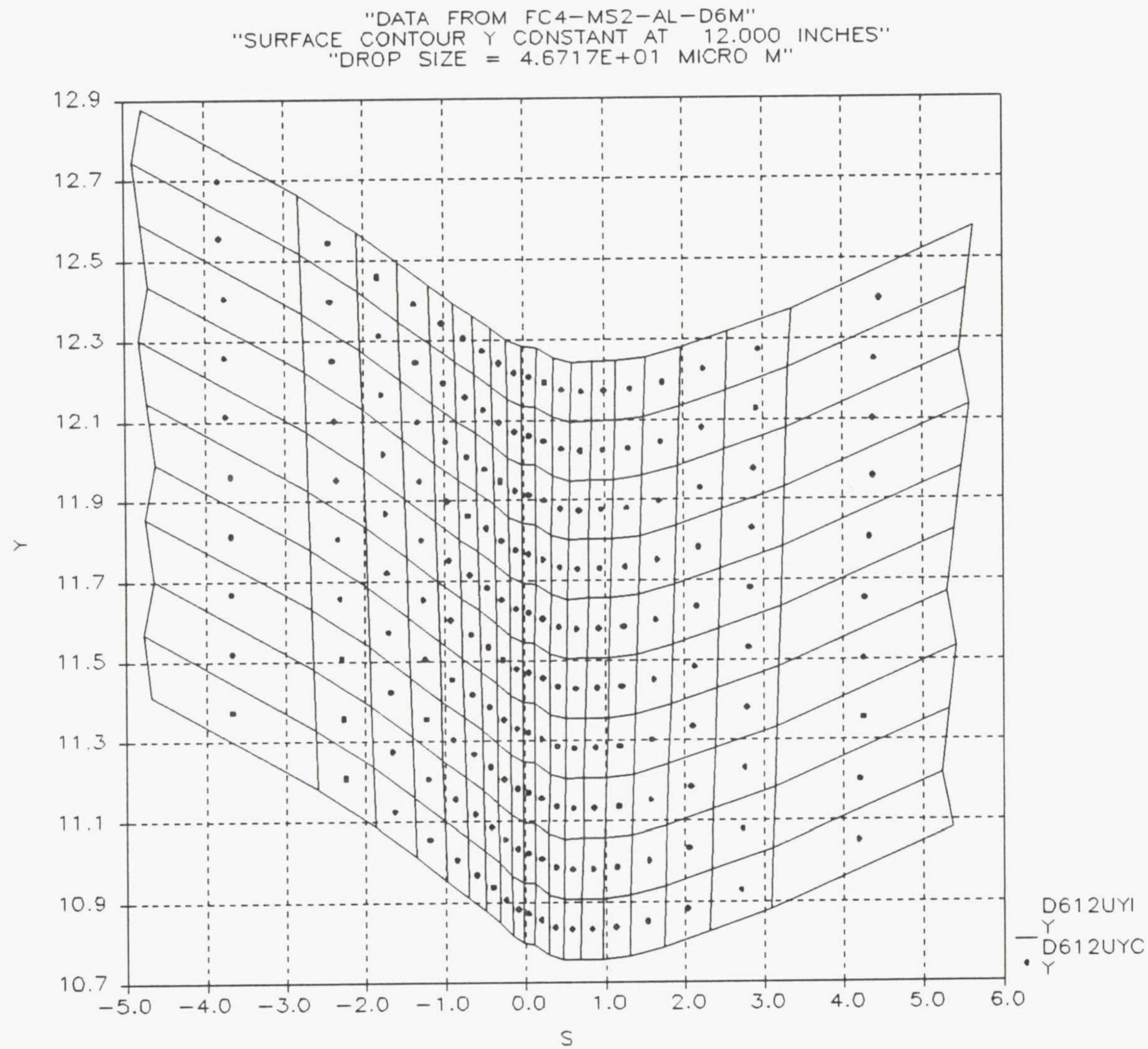

FIGURE D.164

IMPINGEMENT FIELD Y(in) vs S(in), FC4,Y=12U,D=46.7 micron

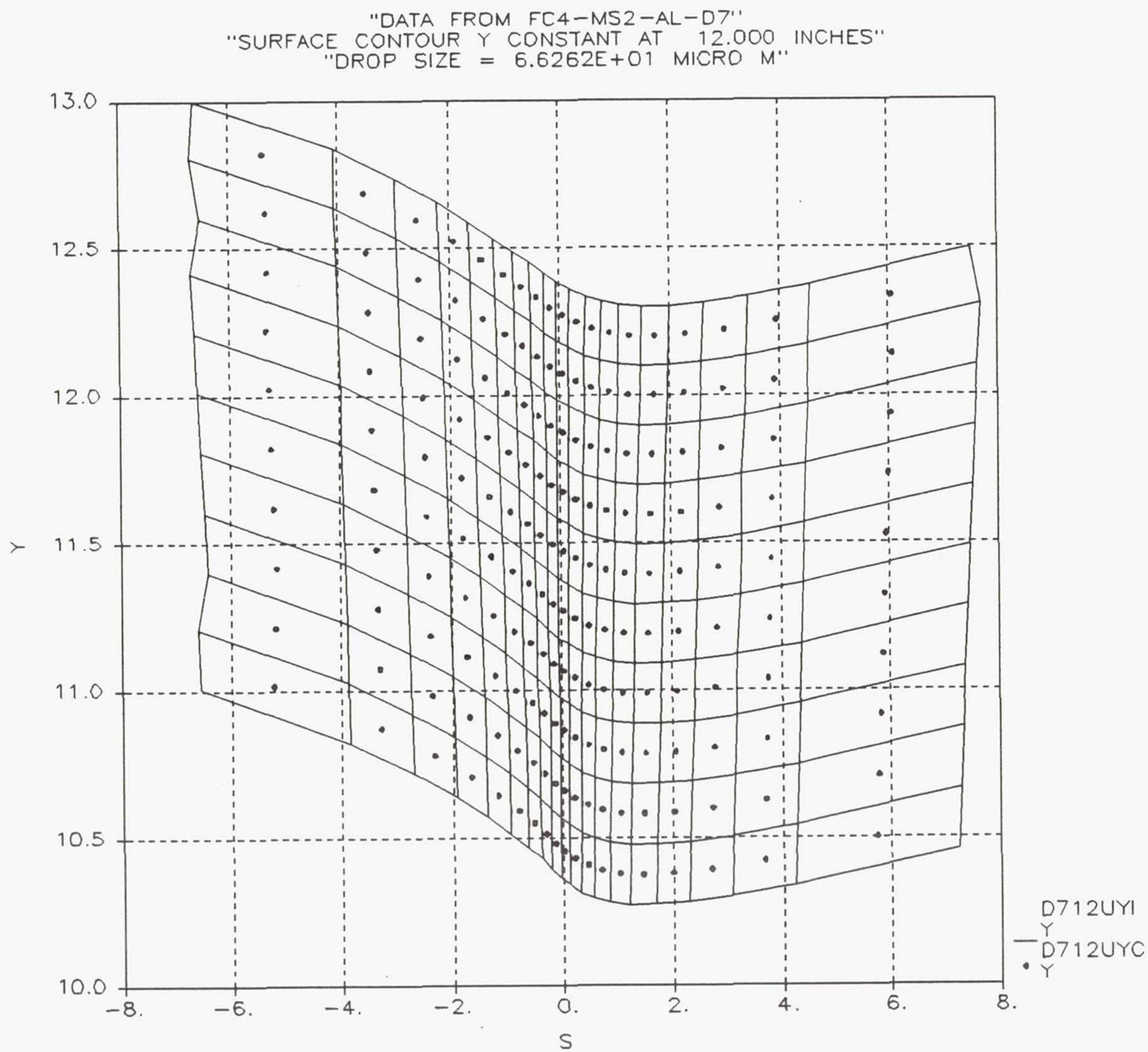

FIGURE D.165

IMPINGEMENT FIELD Y(in) vs S(in), FC4,Y=12U,D=66.3 micron

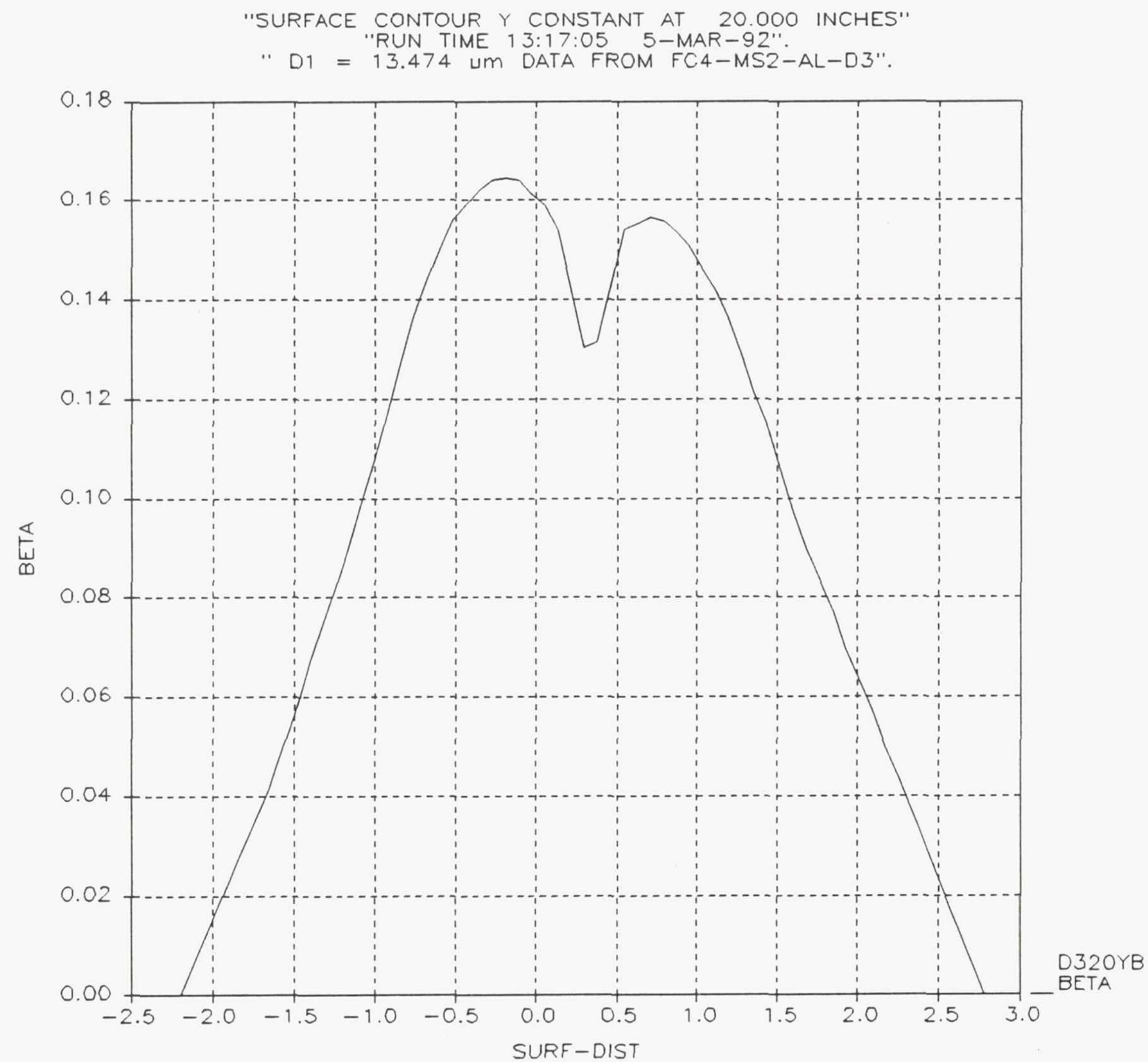

FIGURE D.166

BETA vs SURF-DIST(cm), FC4,Y=20,D=13.5 micron

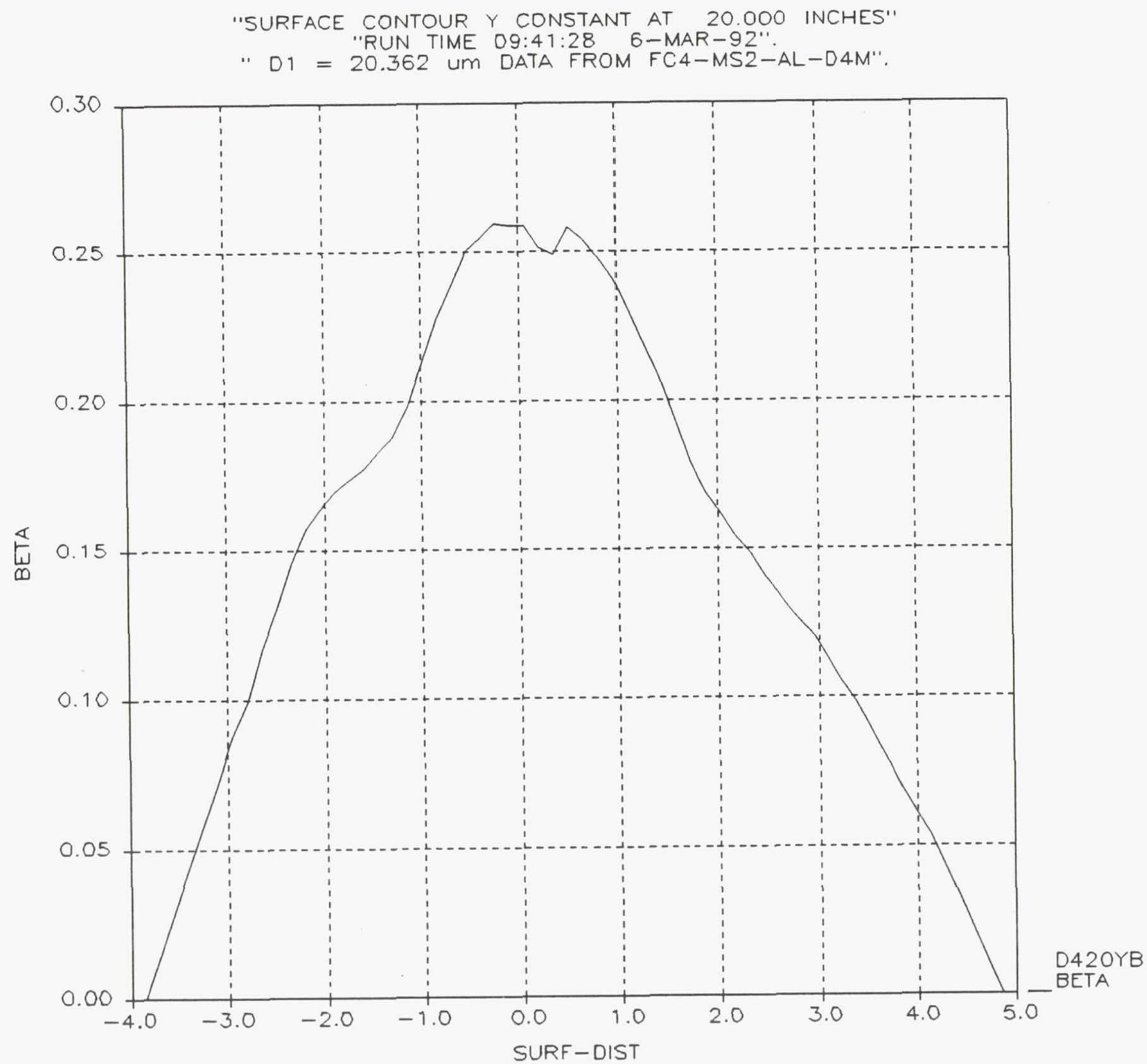

FIGURE D.167

BETA vs SURF-DIST(cm), FC4,Y=20,D=20.4 micron

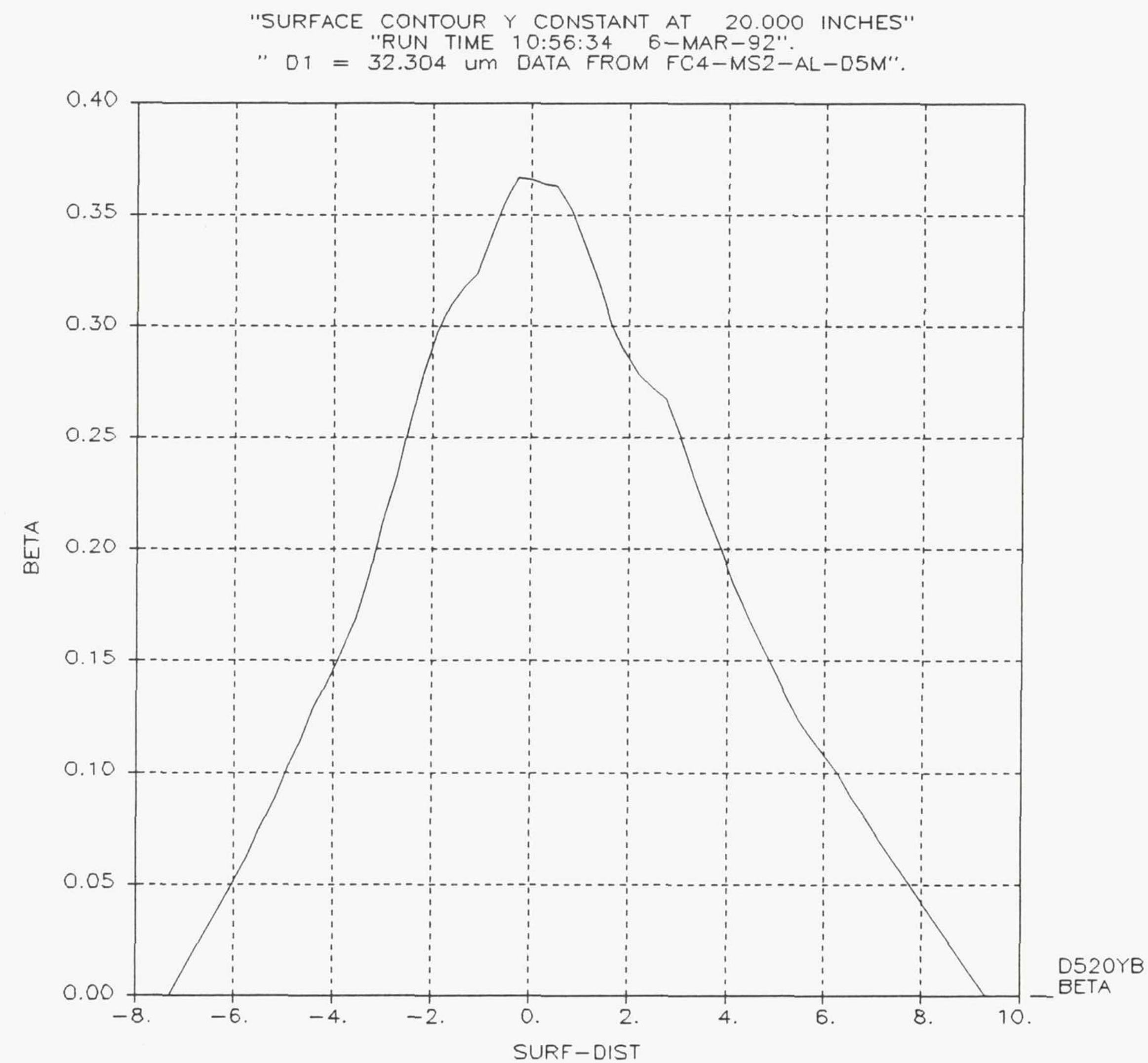

FIGURE D.168

BETA vs SURF-DIST(cm), FC4,Y=20,D=32.3 micron

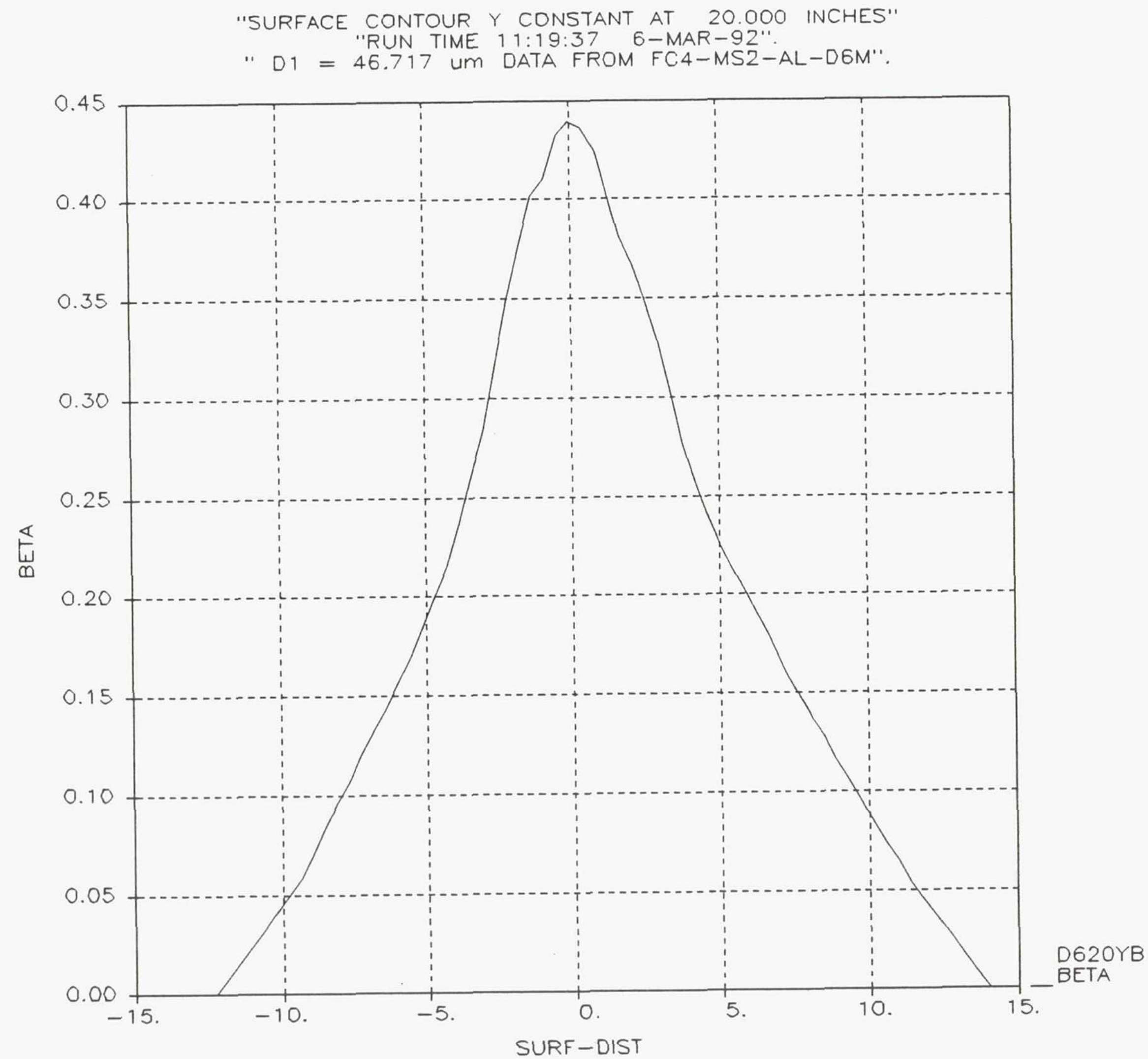

FIGURE D.169

BETA vs SURF-DIST(cm), FC4,Y=20,D=46.7 micron

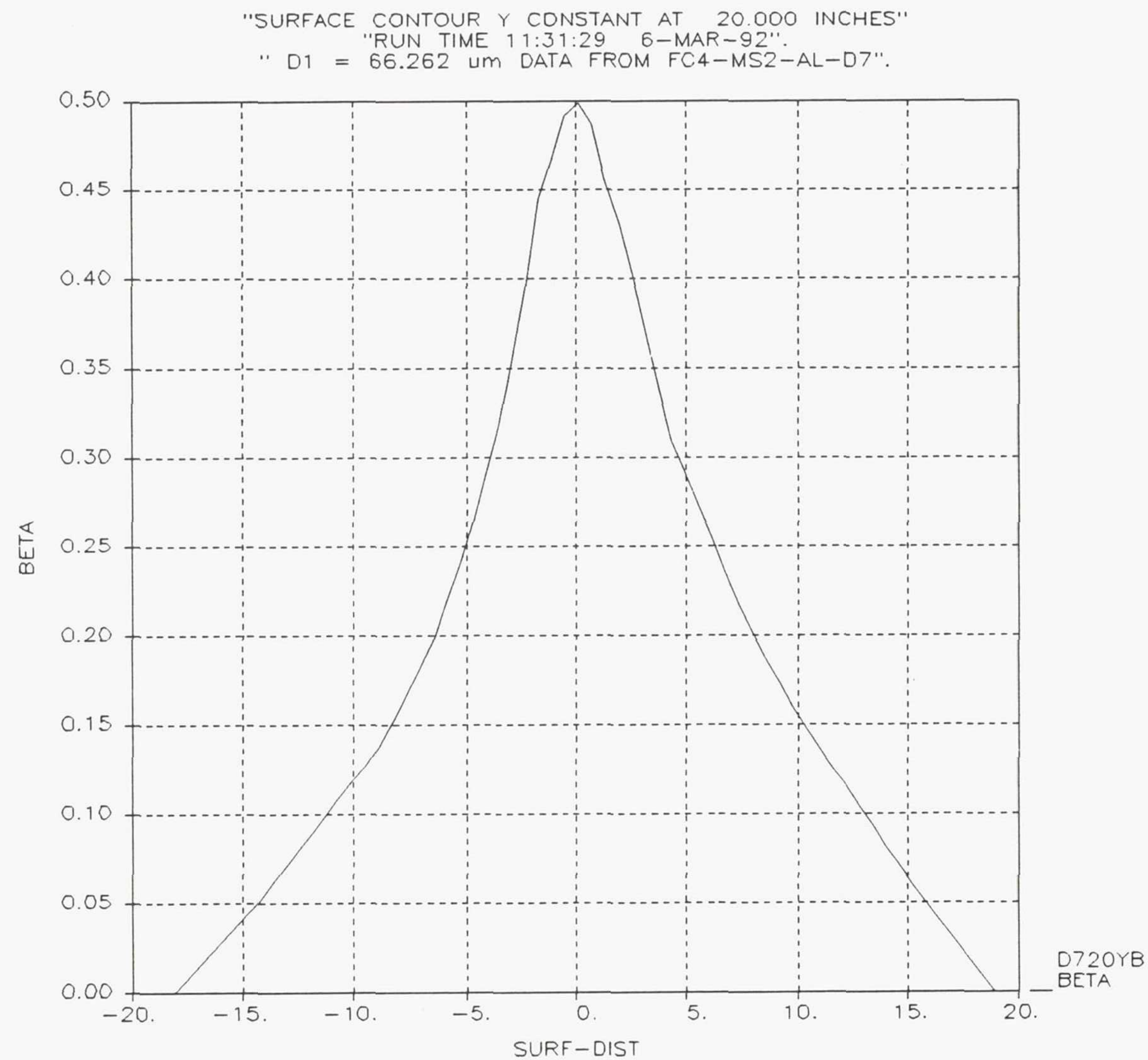

FIGURE D.170

BETA vs SURF-DIST(cm), FC4,Y=20,D=66.3 micron

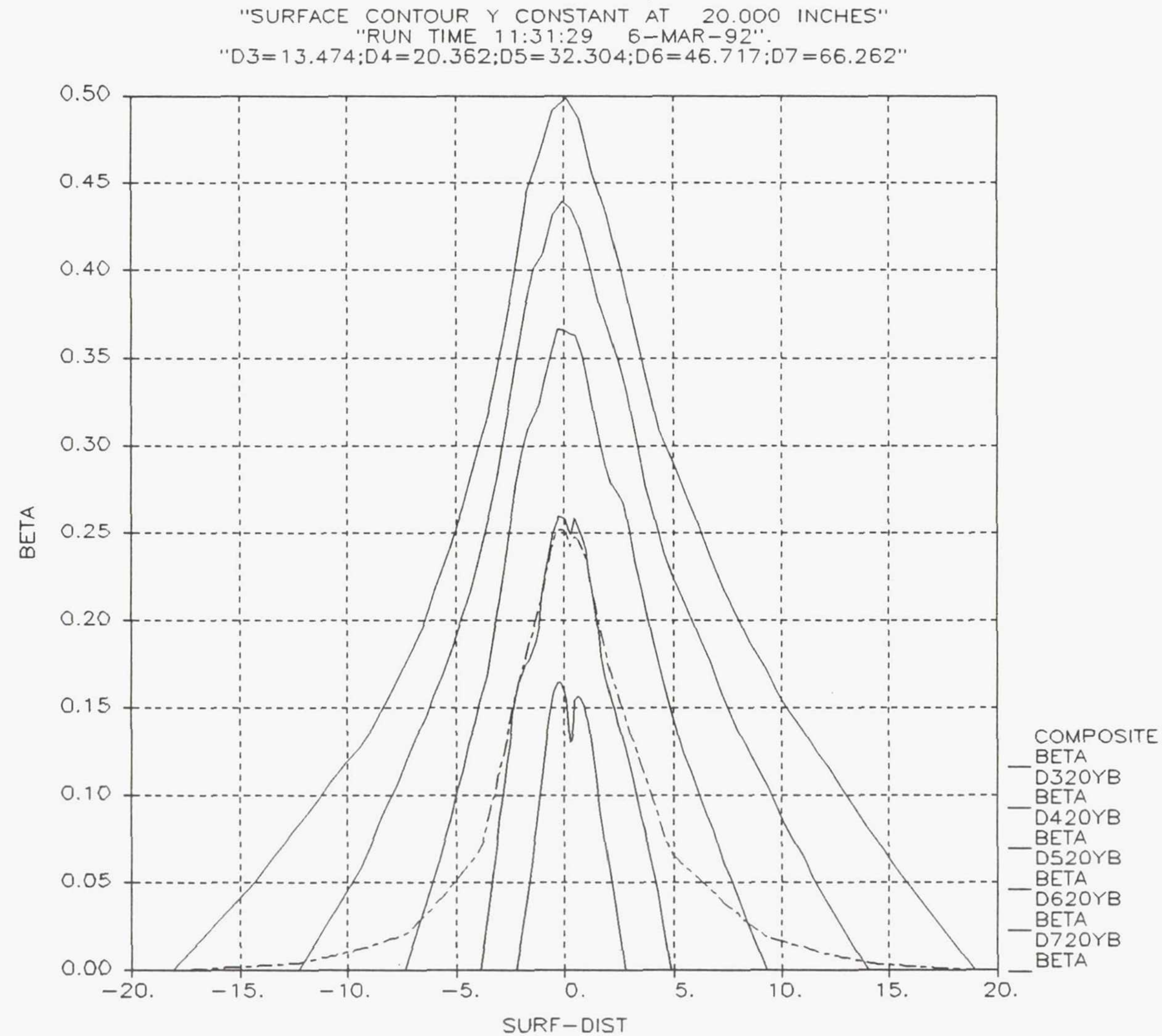

FIGURE D.171

BETA vs SURF-DIST(cm), FC4,Y=20,COMPOSITE AND INDIVIDUAL DROPS

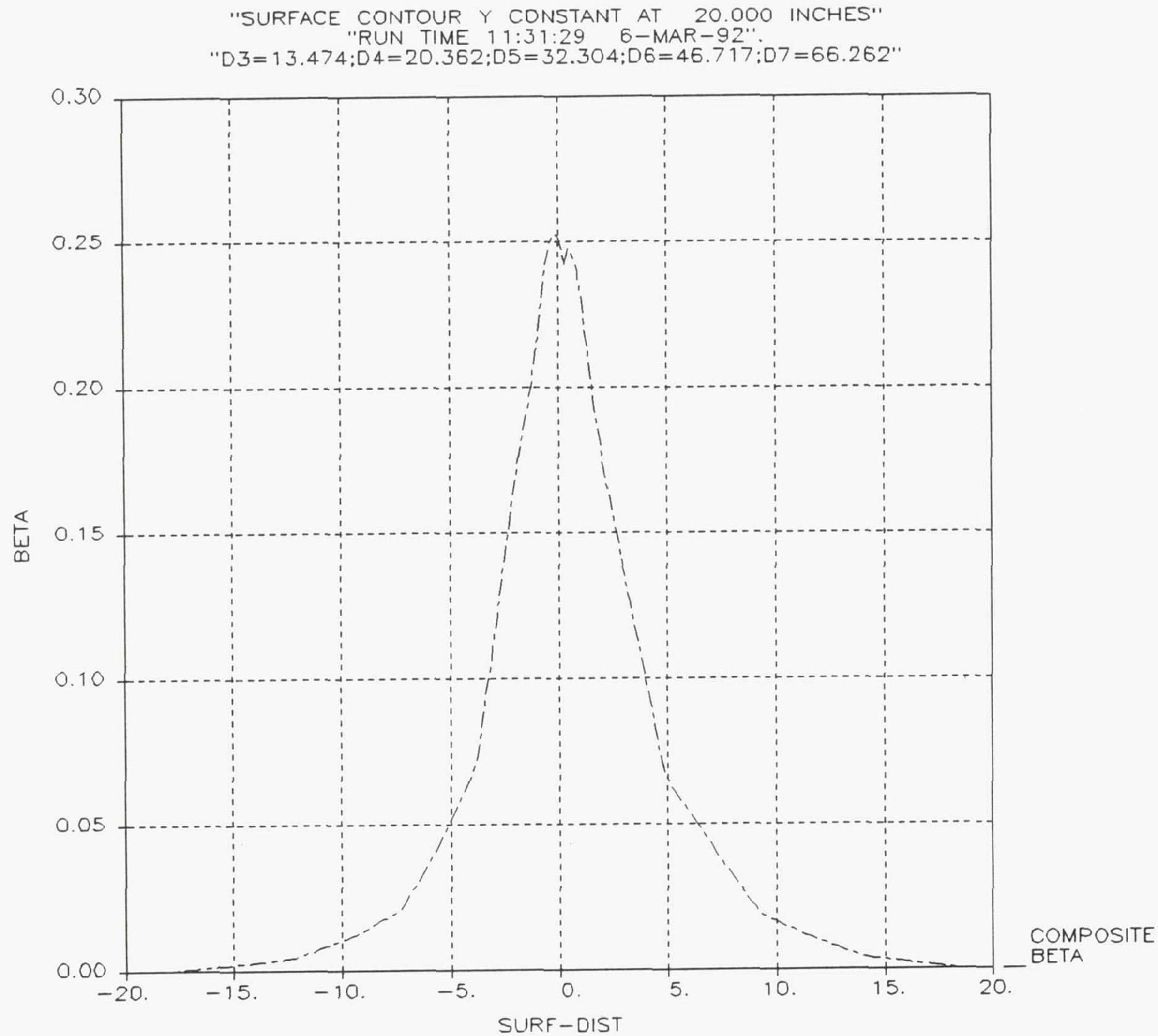

FIGURE D.172

BETA vs SURF-DIST(cm), FC4,Y=20,D=20.4 micron
COMPOSITE DROP

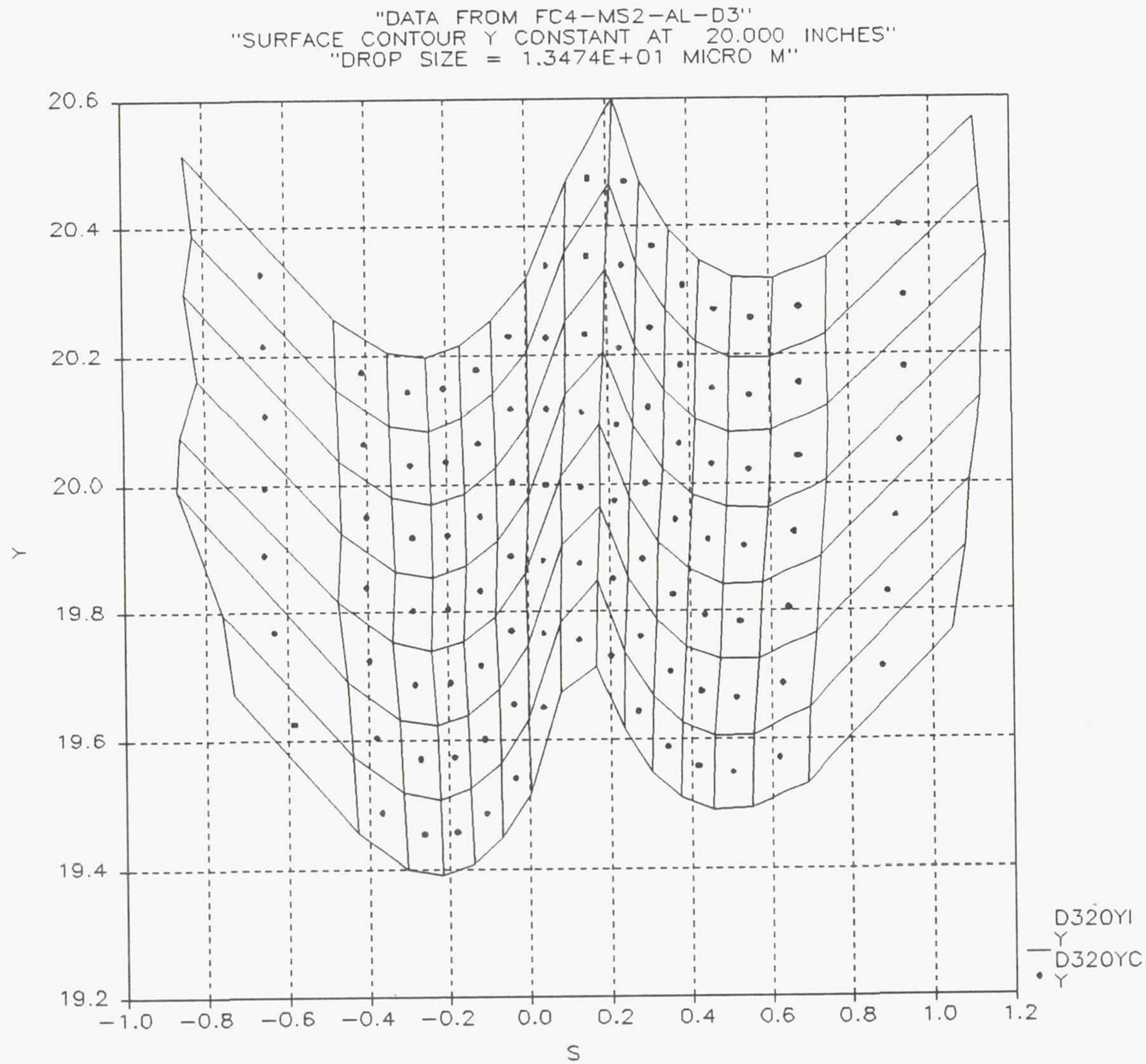

FIGURE D.173

IMPINGEMENT FIELD Y(in) vs S(in), FC4,Y=20,D=13.5 micron

"DATA FROM FC4-MS2-AL-D4M"
"SURFACE CONTOUR Y CONSTANT AT 20.000 INCHES"
"DROP SIZE = 2.0362E+01 MICRO M"

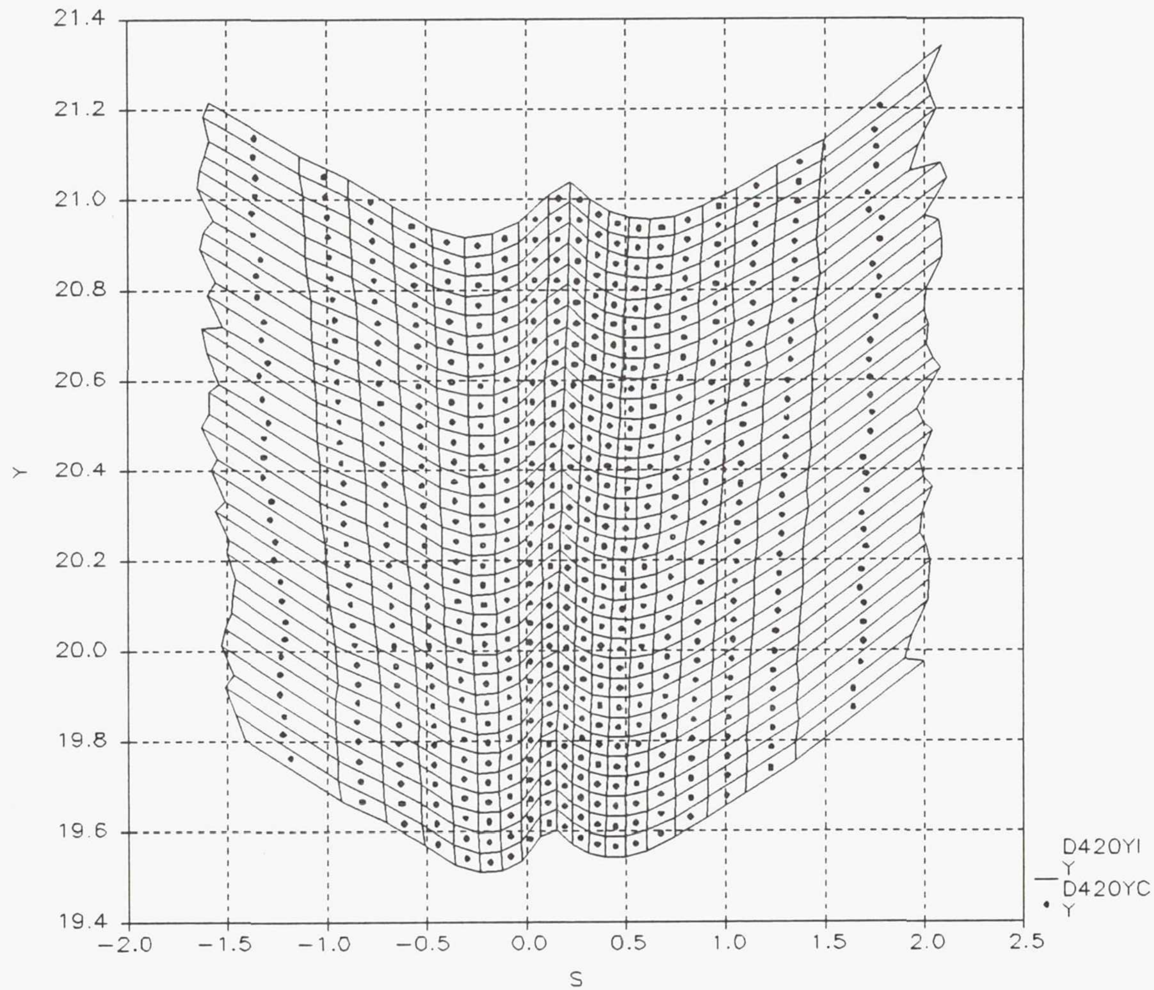

FIGURE D.174

IMPINGEMENT FIELD Y(in) vs S(in), FC4,Y=20,D=20.4 micron

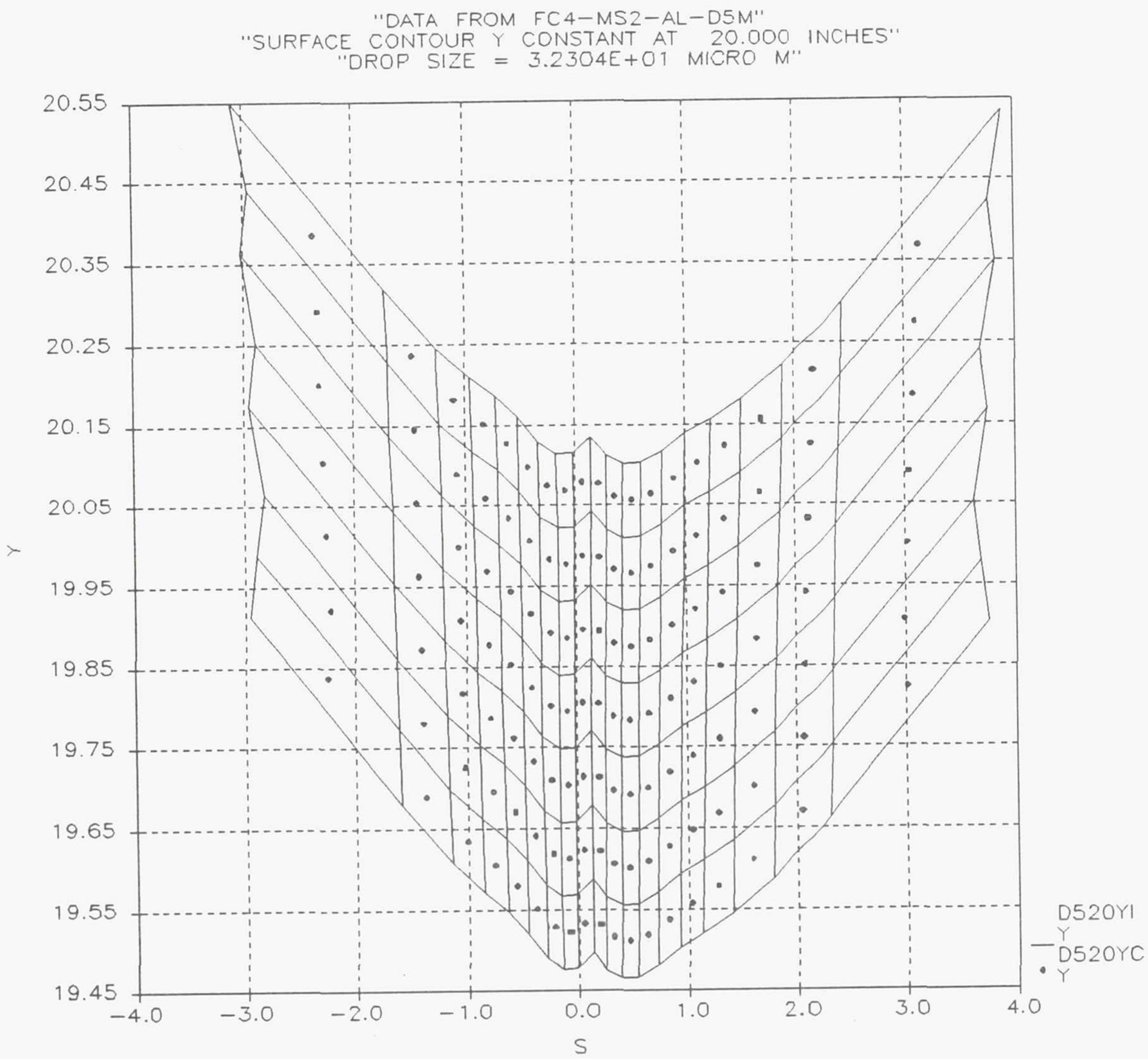

FIGURE D.175

IMPINGEMENT FIELD Y(in) vs S(in), FC4,Y=20,D=32.3 micron

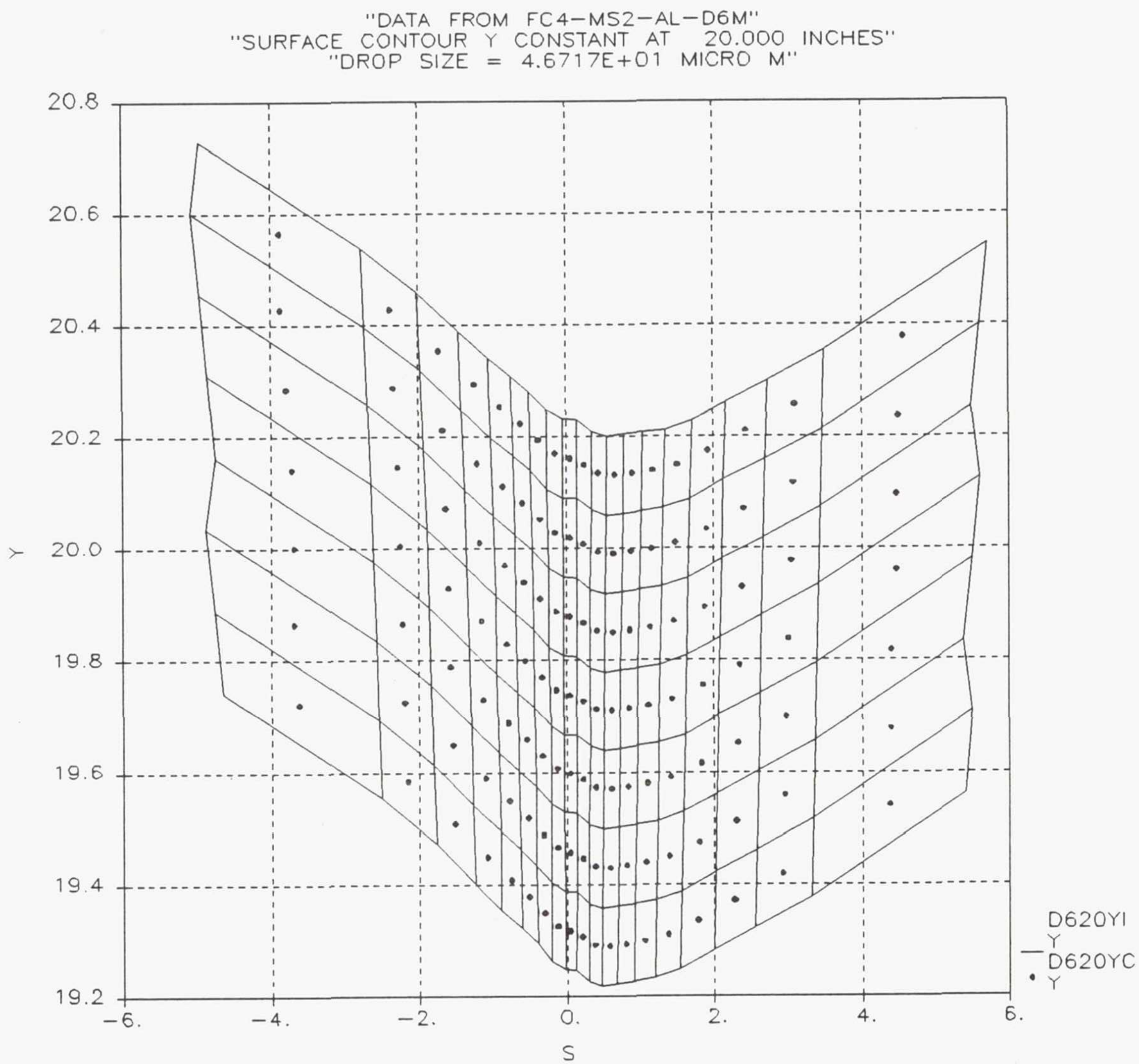

FIGURE D.176

IMPINGEMENT FIELD Y(in) vs S(in), FC4,Y=20,D=46.7 micron

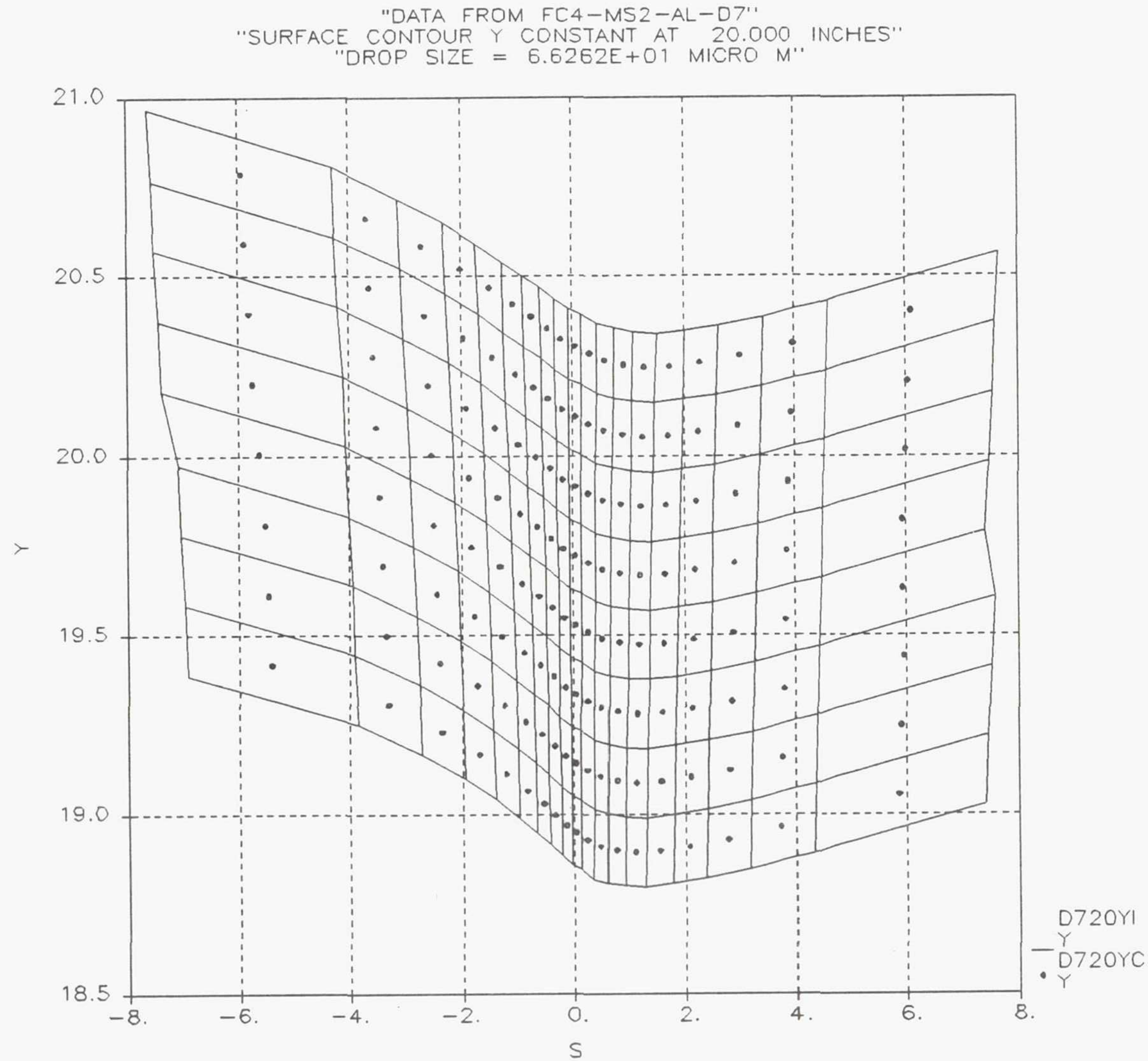

FIGURE D.177

IMPINGEMENT FIELD Y(in) vs S(in), FC4,Y=20,D=66.3 micron

APPENDIX E – COMPOSITE ANALYTICAL, AVERAGED TEST AND INDIVIDUAL TEST IMPINGEMENT EFFICIENCY CURVES FOR EACH LOCATION AND FLIGHT CONDITION

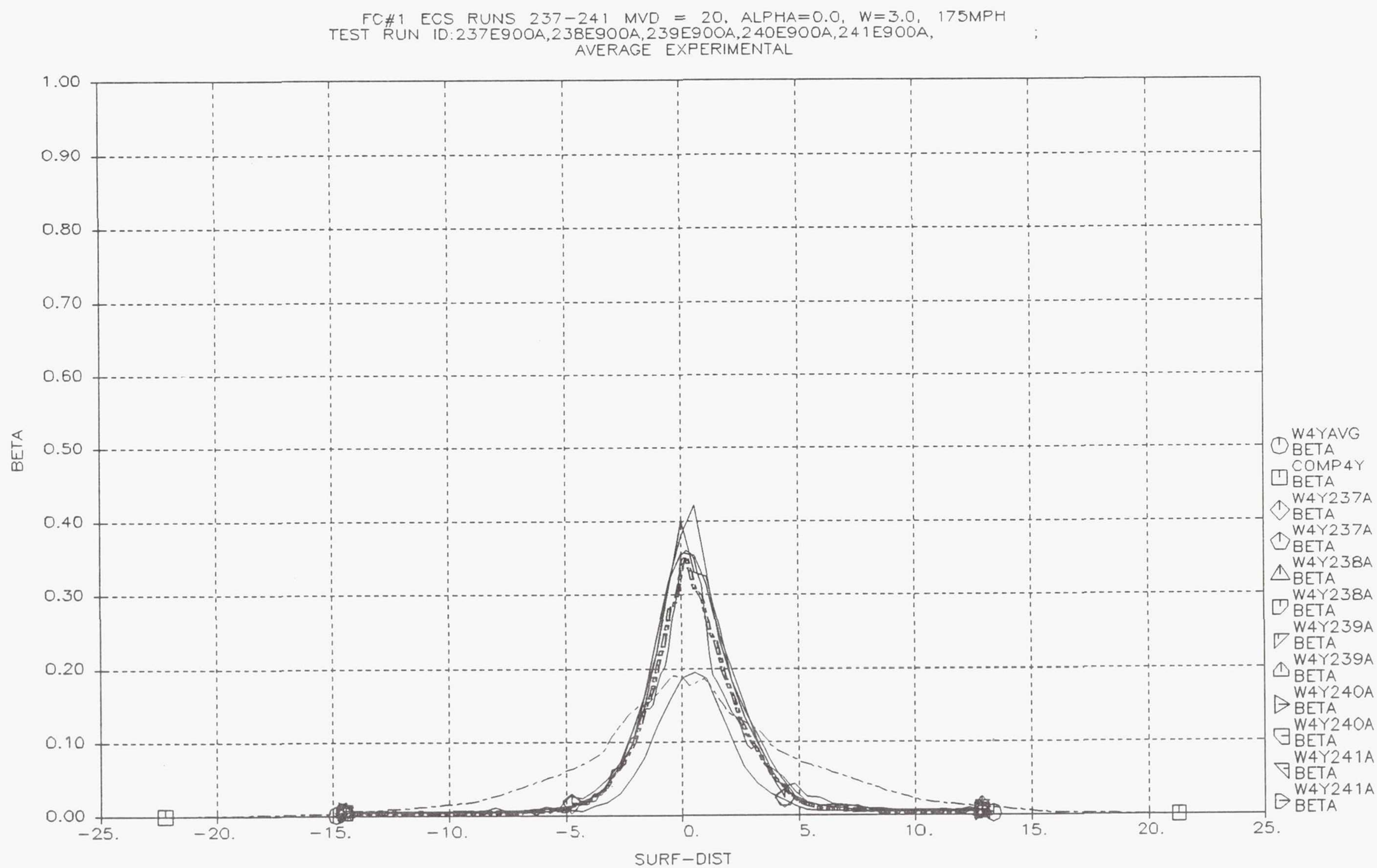

FIGURE E.1

COMPOSITE ANALYSIS AND ALL TEST BETA RESULTS
--BETA(-) vs SURF-DIST(cm), FC1,Y=4

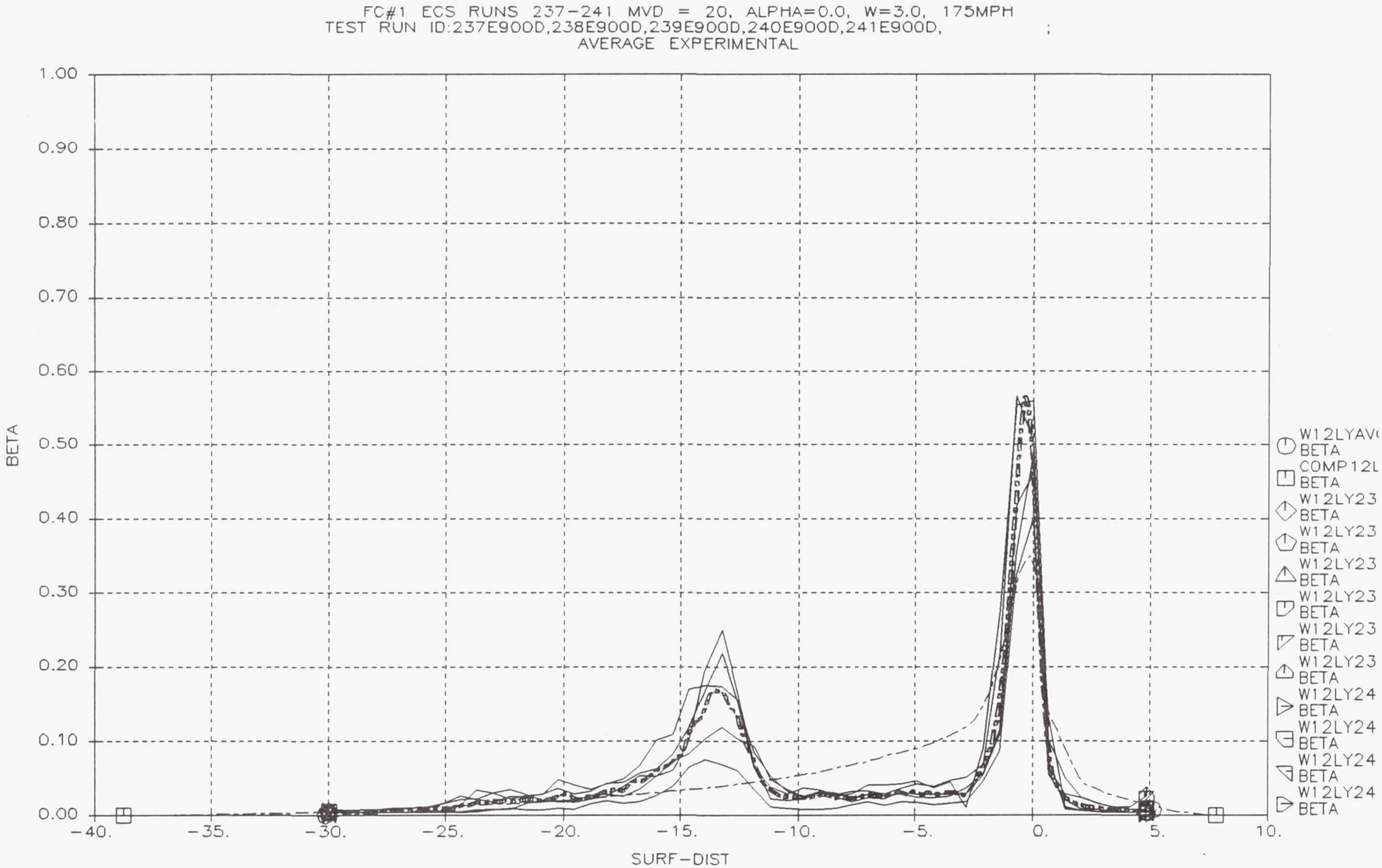

FIGURE E.2

COMPOSITE ANALYSIS AND ALL TEST BETA RESULTS
--BETA(-) vs SURF-DIST(cm), FC1,Y=12L

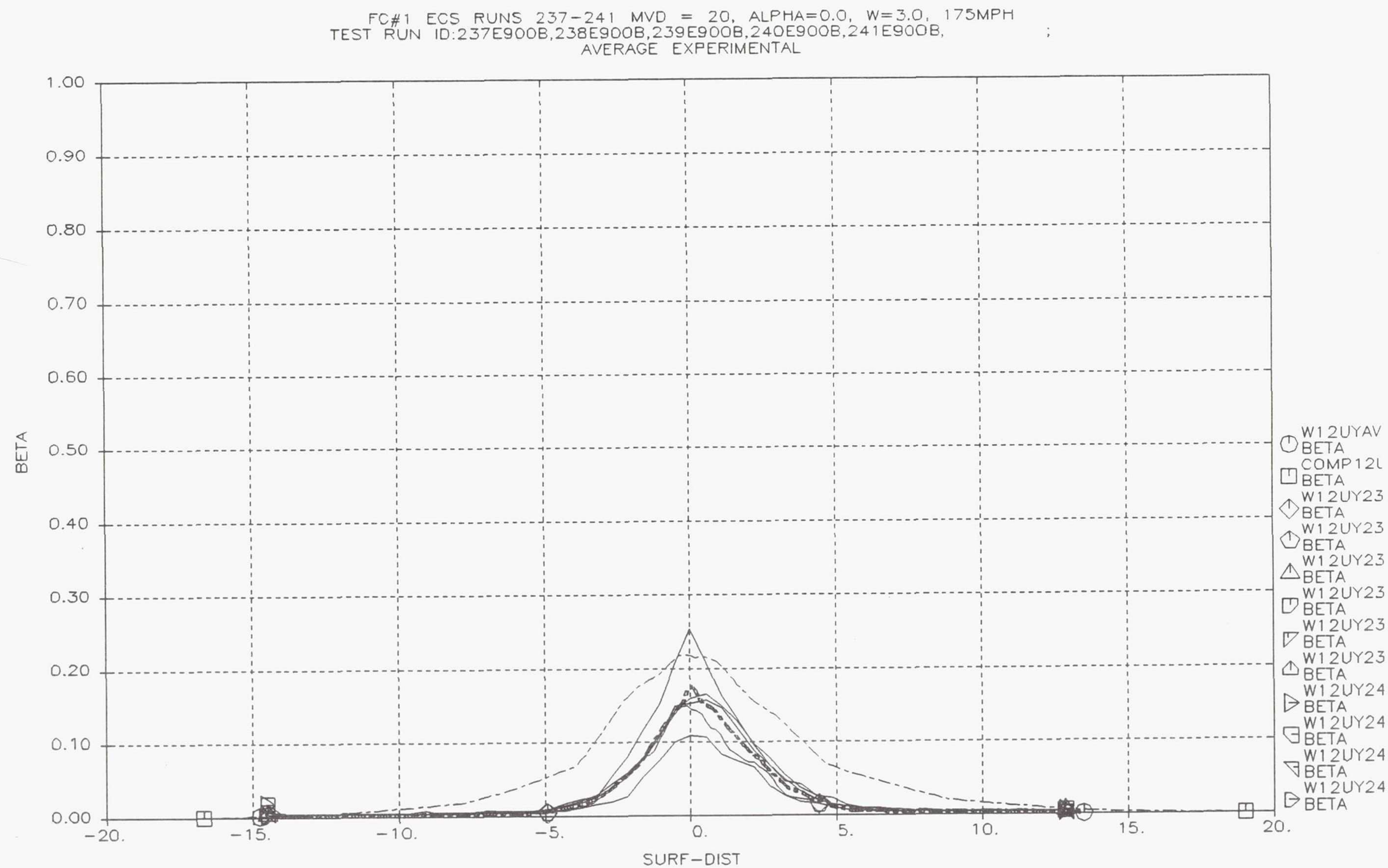

FIGURE E.3

COMPOSITE ANALYSIS AND ALL TEST BETA RESULTS
--BETA(-) vs SURF-DIST(cm), FC1,Y=12U

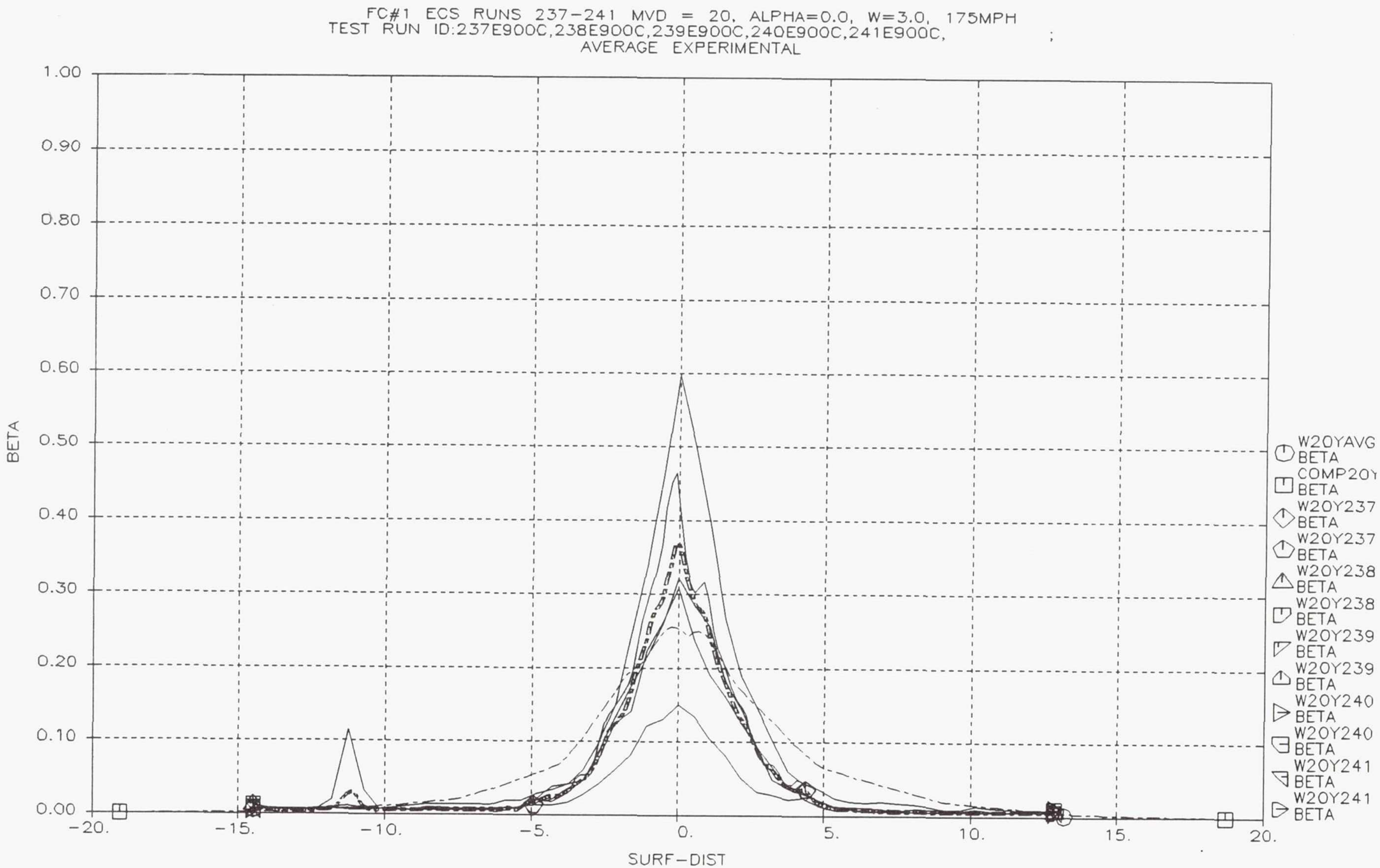

FIGURE E.4

COMPOSITE ANALYSIS AND ALL TEST BETA RESULTS
--BETA(-) vs SURF-DIST(cm), FC1,Y=20

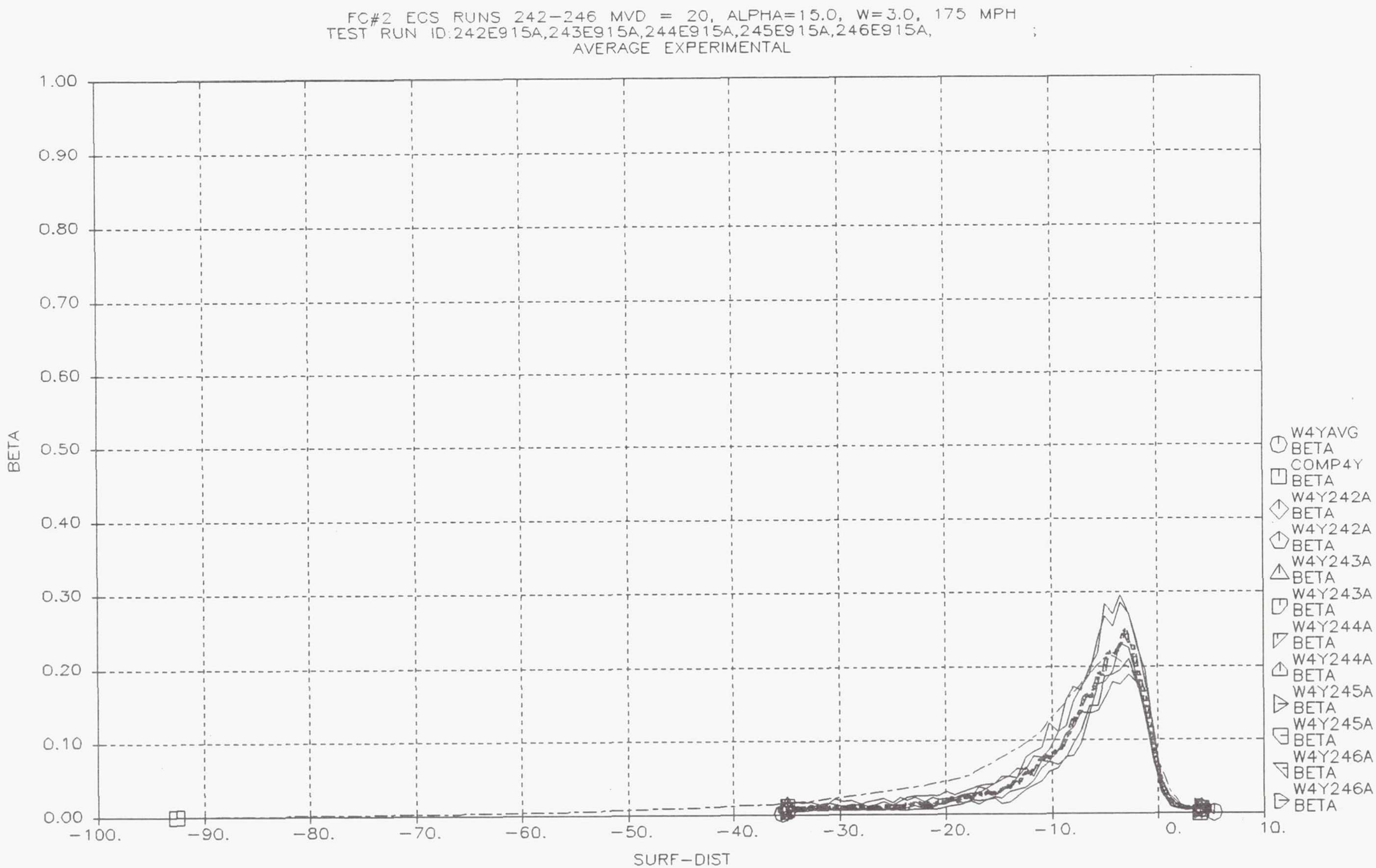

FIGURE E.5

COMPOSITE ANALYSIS AND ALL TEST BETA RESULTS
—BETA(-) vs SURF-DIST(cm), FC2,Y=4

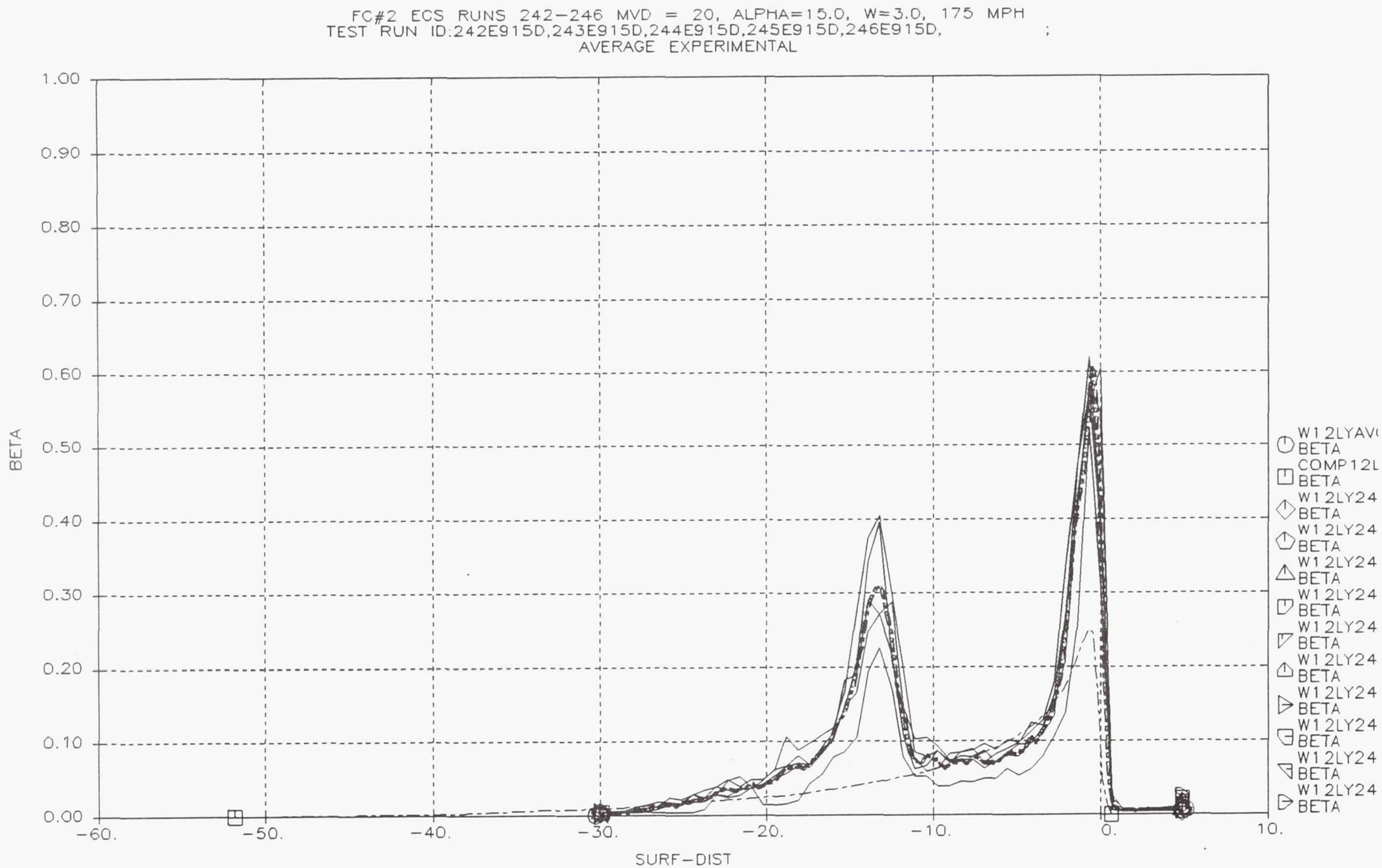

FIGURE E.6

COMPOSITE ANALYSIS AND ALL TEST BETA RESULTS
--BETA(-) vs SURF-DIST(cm), FC2,Y=12L

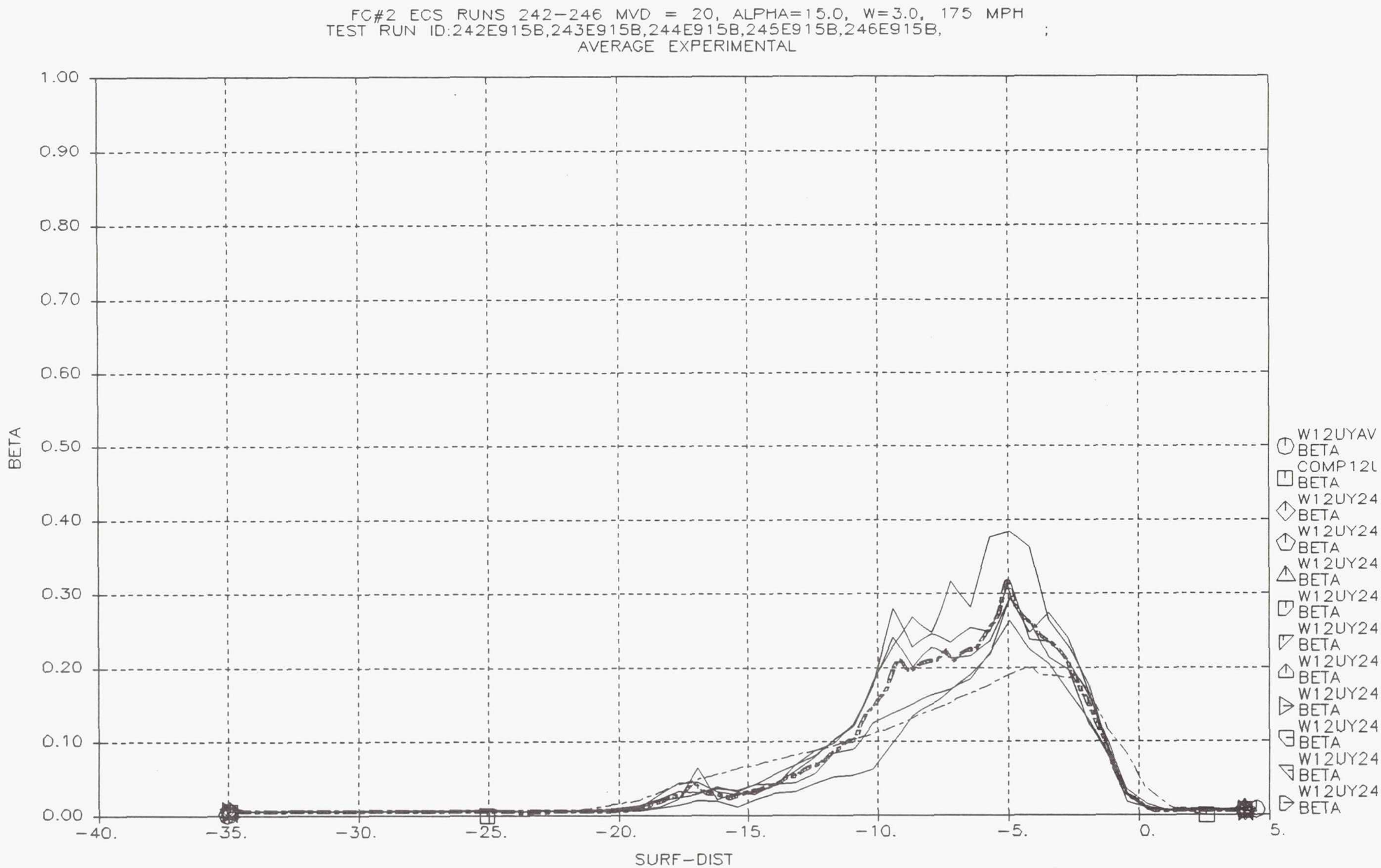

FIGURE E.7

COMPOSITE ANALYSIS AND ALL TEST BETA RESULTS
—BETA(-) vs SURF-DIST(cm), FC2,Y=12U

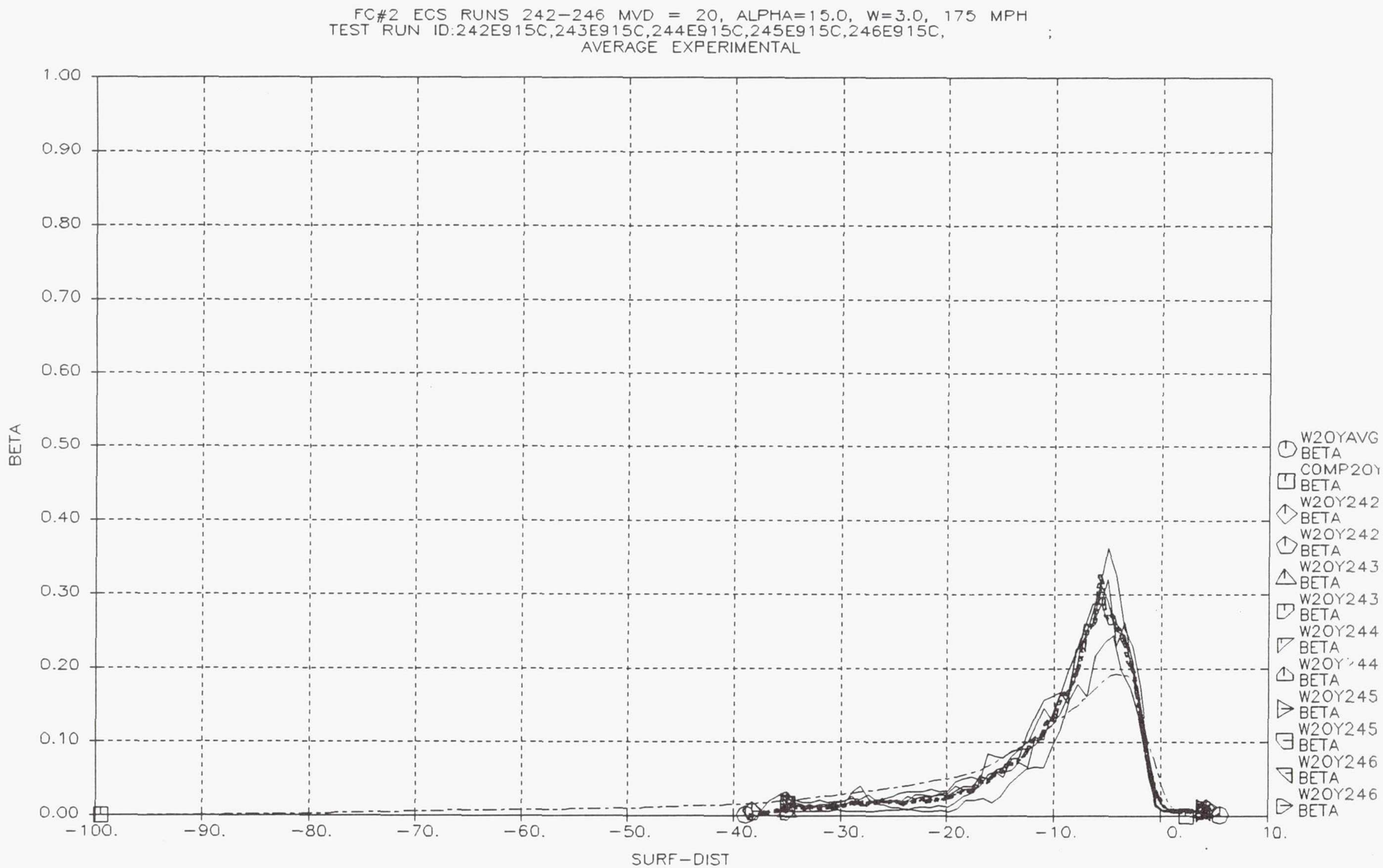

FIGURE E.8

COMPOSITE ANALYSIS AND ALL TEST BETA RESULTS
--BETA(-) vs SURF-DIST(cm), FC2,Y=20

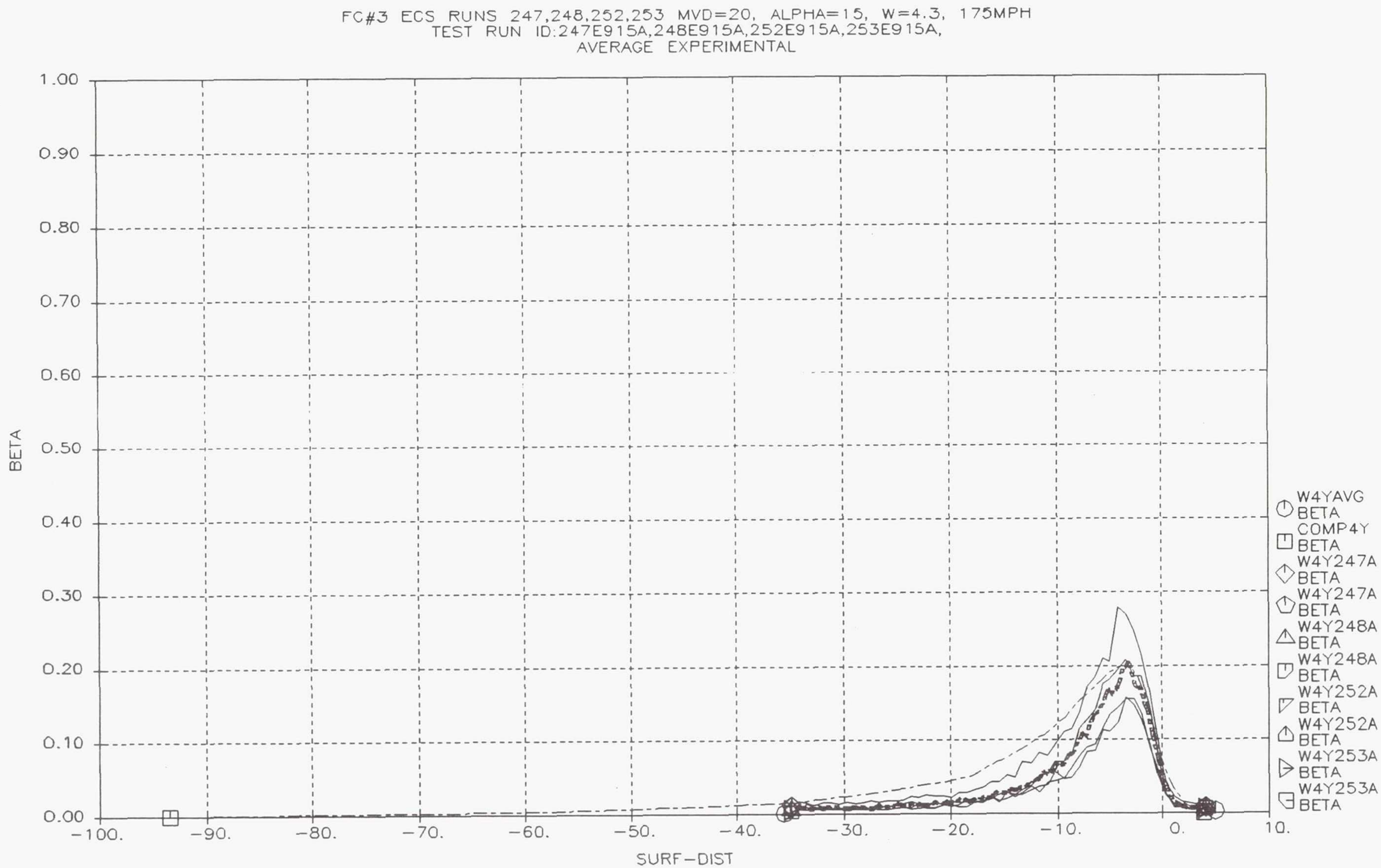

FIGURE E.9

COMPOSITE ANALYSIS AND ALL TEST BETA RESULTS
--BETA(-) vs SURF-DIST(cm), FC3,Y=4

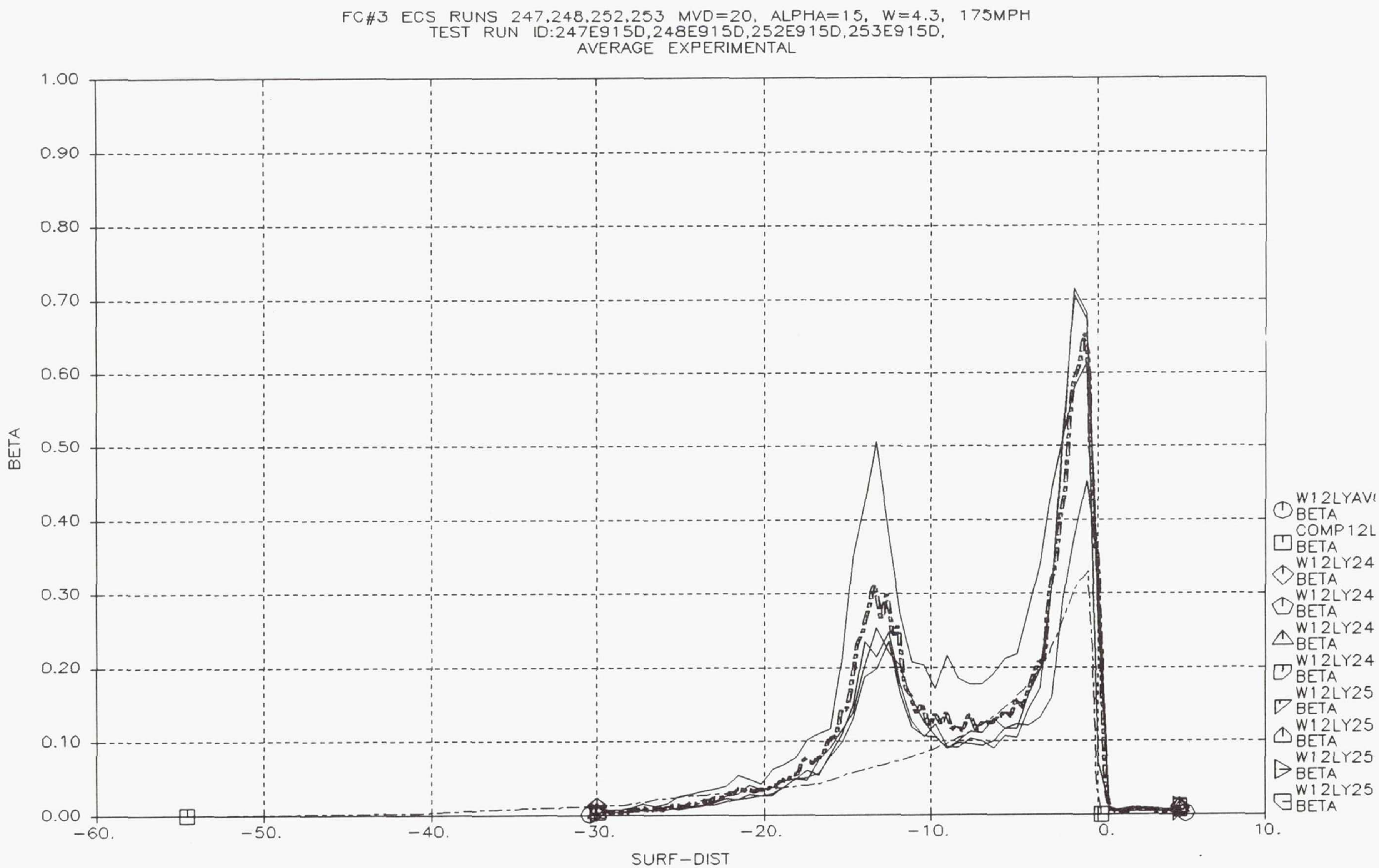

FIGURE E.10

COMPOSITE ANALYSIS AND ALL TEST BETA RESULTS
--BETA(-) vs SURF-DIST(cm), FC3,Y=12L

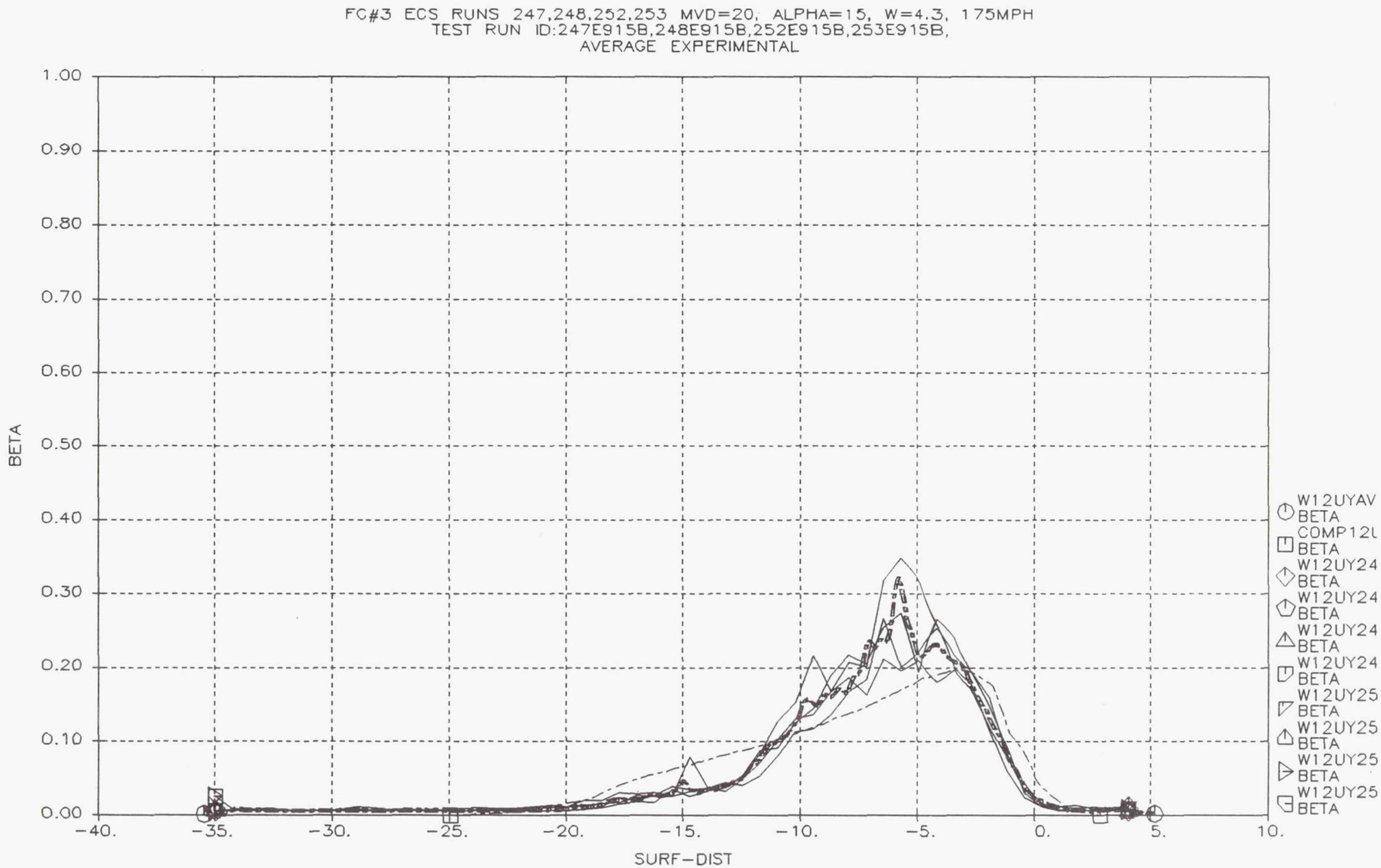

FIGURE E.11

COMPOSITE ANALYSIS AND ALL TEST BETA RESULTS
—BETA(-) vs SURF-DIST(cm), FC3,Y=12U

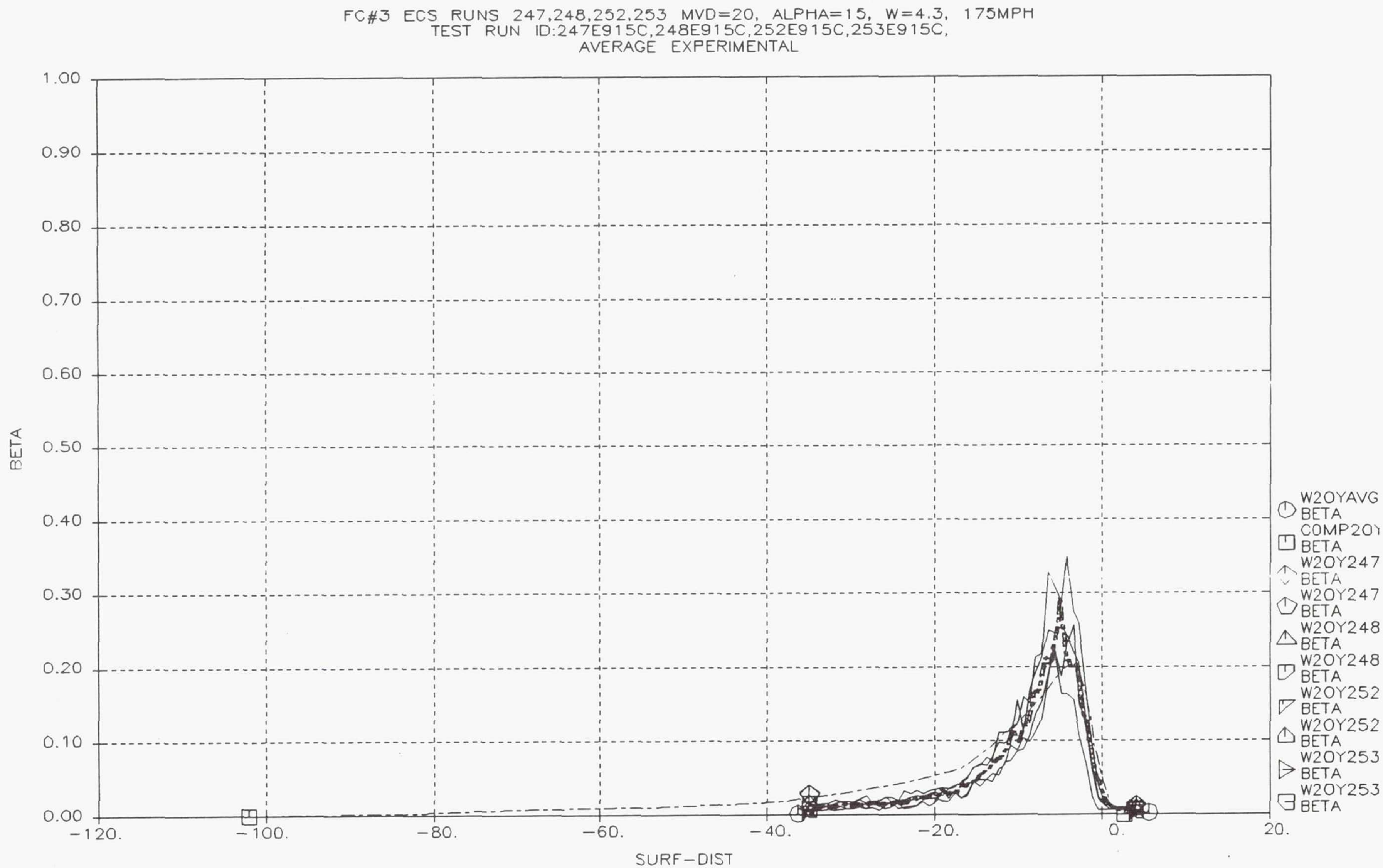

FIGURE E.12

COMPOSITE ANALYSIS AND ALL TEST BETA RESULTS
--BETA(-) vs SURF-DIST(cm), FC3,Y=20

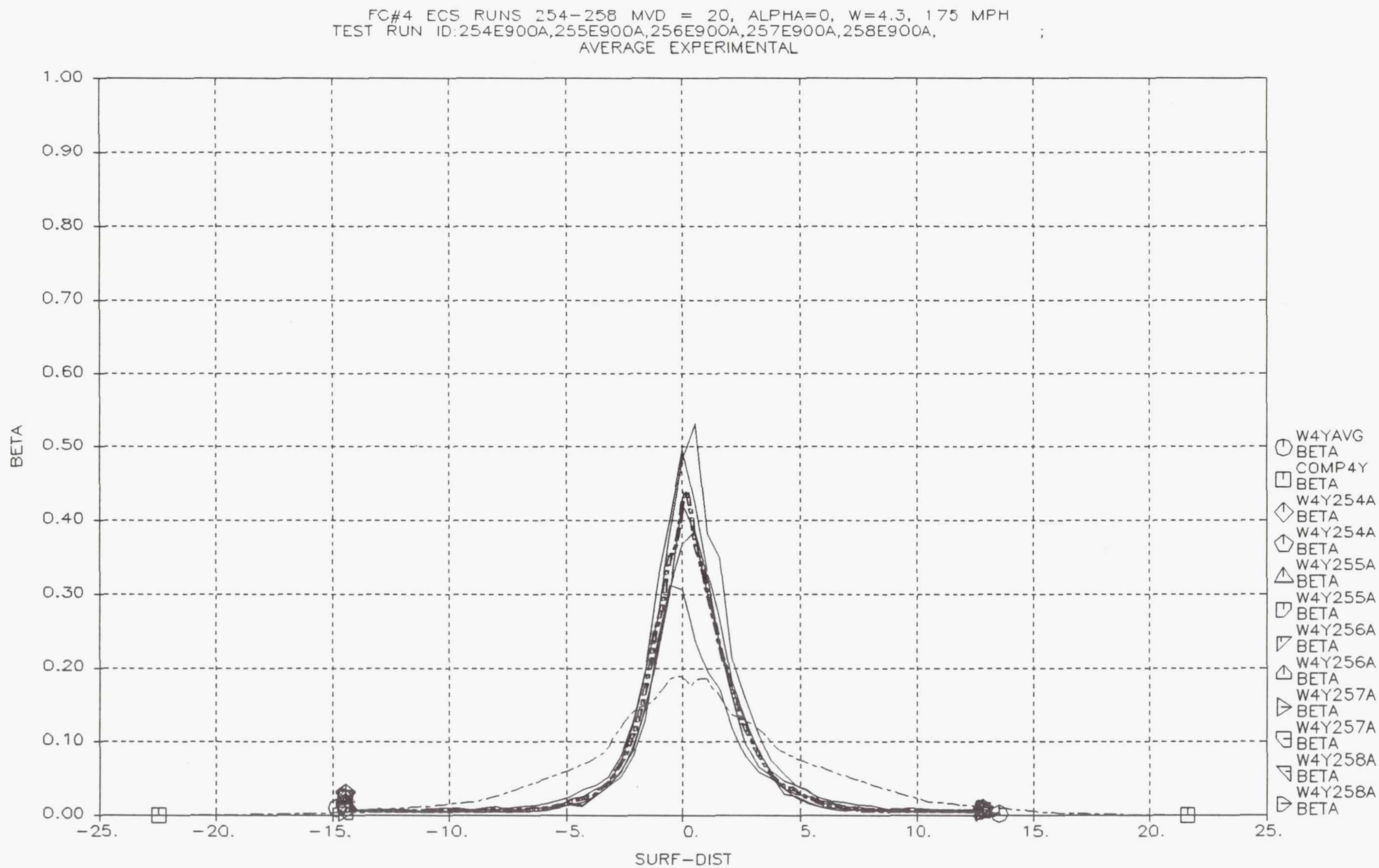

FIGURE E.13

COMPOSITE ANALYSIS AND ALL TEST BETA RESULTS
--BETA(-) vs SURF-DIST(cm), FC4,Y=4

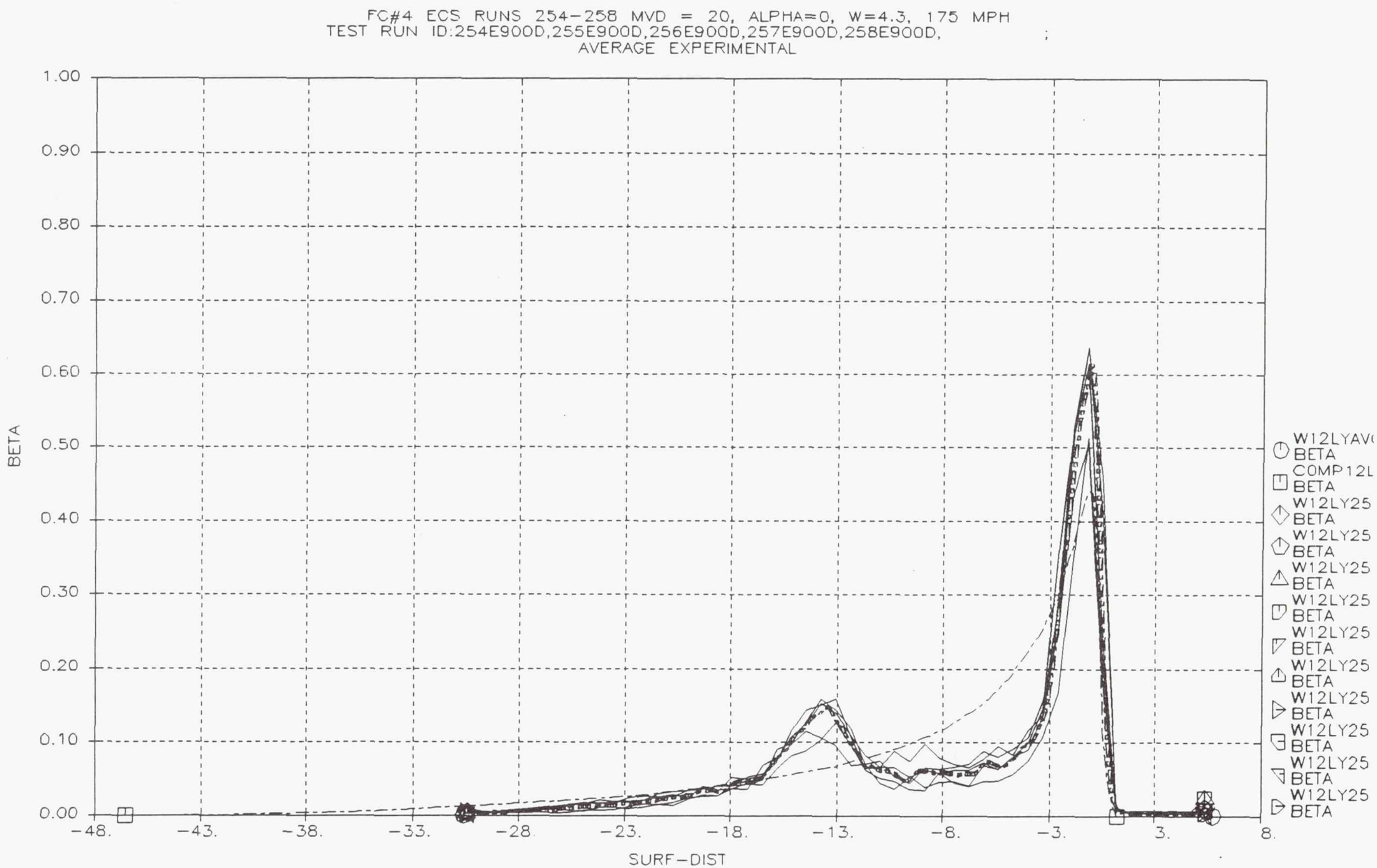

FIGURE E.14

COMPOSITE ANALYSIS AND ALL TEST BETA RESULTS
--BETA(-) vs SURF-DIST(cm), FC4,Y=12L

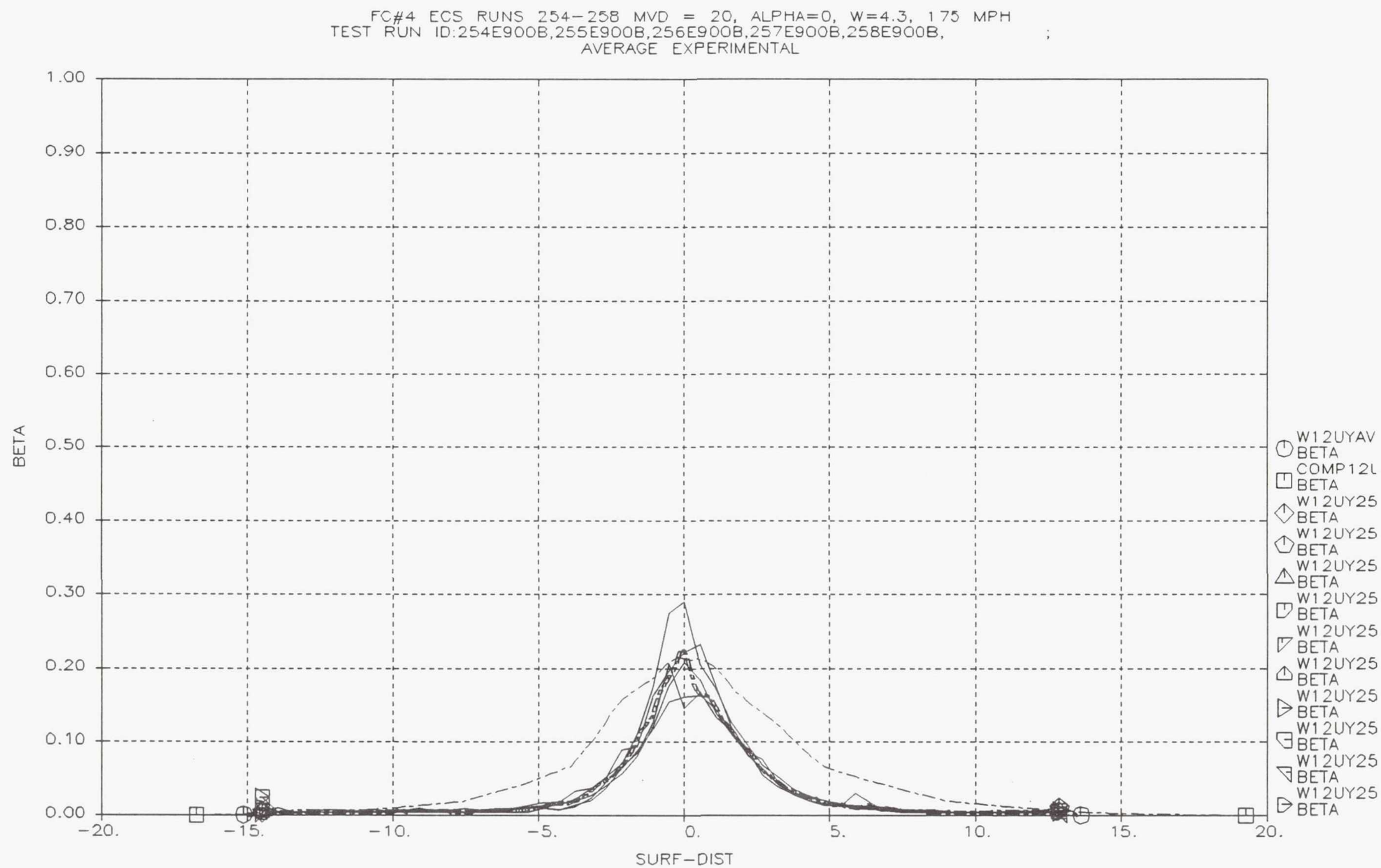

FIGURE E.15

COMPOSITE ANALYSIS AND ALL TEST BETA RESULTS
--BETA(-) vs SURF-DIST(cm), FC4,Y=12U

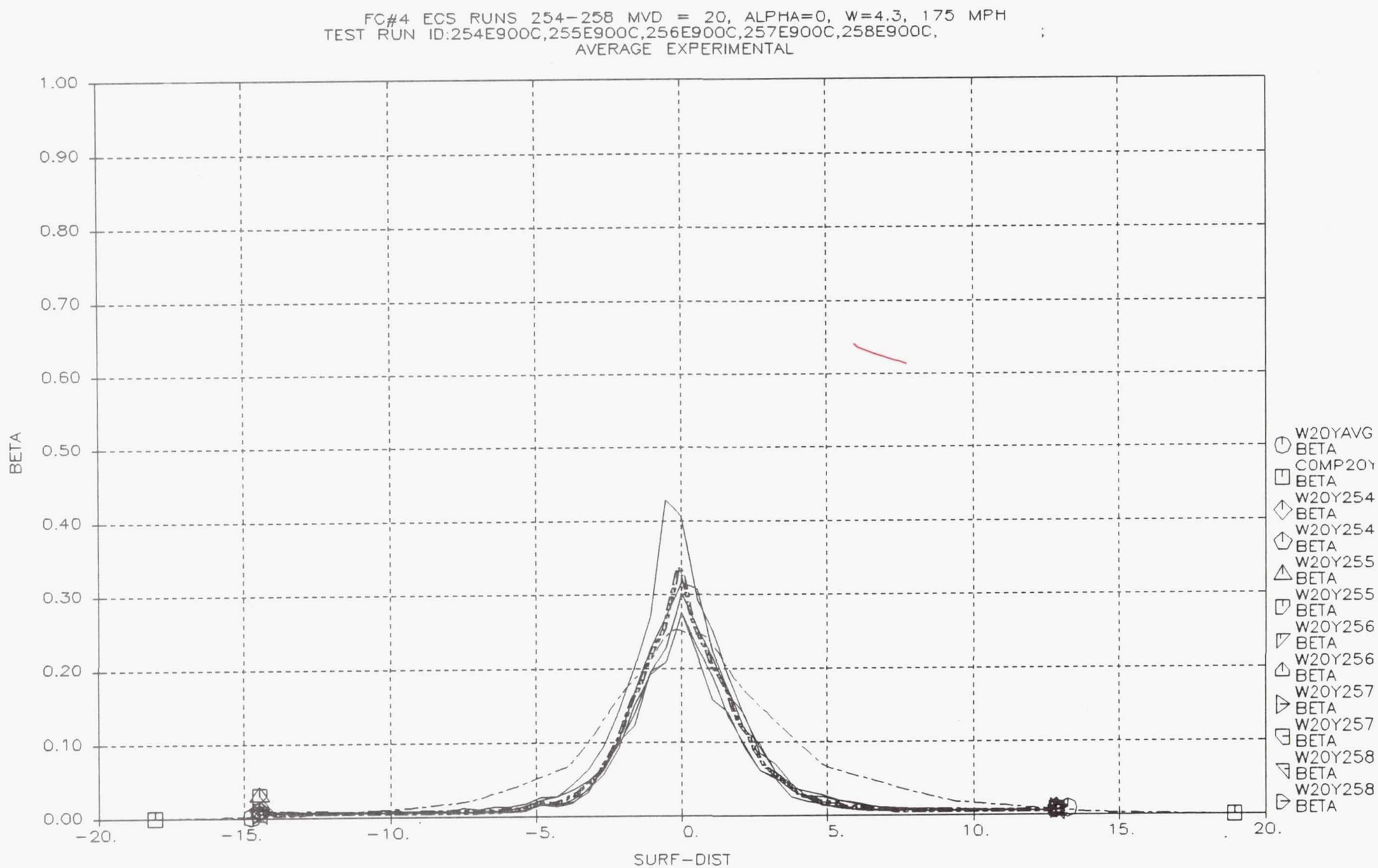

FIGURE E.16

COMPOSITE ANALYSIS AND ALL TEST BETA RESULTS
--BETA(-) vs SURF-DIST(cm), FC4,Y=20

REFERENCES

1. Private Communication to Dr. R. J. Shaw, March 14, 1989.

2. Boeing Document D500-12189-1, "3-D PARTICLE TRAJECTORY ANALYSIS (PTA) CODE - USERS MANUAL", dated February 1990

3. Papadakis, M., Elangovan, R., Freund Jr., G.A., Breer, M.D., Zumwalt, G.W., and Whitmer, L., "AN EXPERIMENTAL METHOD FOR MEASURING WATER DROPLET IMPINGEMENT EFFICIENCY ON TWO- AND THREE-DIMENSIONAL BODIES," NASA Contractor Report 4257, DOT/FAA/CT-87/22, Prepared for NASA-Lewis Research Center under Grant NAG-3-566, November, 1989.

4. Boeing Document D3-9821, "POTENTIAL FLOW (ZEE921) AND DATA PREP (ZEE911) PROGRAMS-USERS MANUAL", dated July 1976

5. Boeing Document D500-11460-1, "2-D/AXI-SYMMETRIC PARTICLE TRAJECTORY COMPUTER PROGRAM-USER MANUAL", dated January 1990

6. BOEING DOCUMENT D6-55342, P582, TRANSONIC POTENTIAL FLOW ABOUT COMPLEX CONFIGURATIONS - USERS GUIDE, dated February 26, 1990.

REPORT DOCUMENTATION PAGE

Form Approved
OMB No. 0704-0188

1. AGENCY USE ONLY (*Leave blank*)	2. REPORT DATE	3. REPORT TYPE AND DATES COVERED
	May 1993	Final Contractor Report

4. TITLE AND SUBTITLE

Three-Dimensional Water Droplet Trajectory Code Validation Using an ECS Inlet Geometry

5. FUNDING NUMBERS

WU–505–62–00
C–NAS3–25820

6. AUTHOR(S)

Marlin D. Breer and Mark P. Goodman

7. PERFORMING ORGANIZATION NAME(S) AND ADDRESS(ES)

Boeing Defense and Space Group
Military Airplanes Division
Seattle, Washington, 25820

8. PERFORMING ORGANIZATION REPORT NUMBER

E–7853

9. SPONSORING/MONITORING AGENCY NAME(S) AND ADDRESS(ES)

National Aeronautics and Space Administration
Lewis Research Center
Cleveland, Ohio 44135–3191

10. SPONSORING/MONITORING AGENCY REPORT NUMBER

NASA CR–191097

11. SUPPLEMENTARY NOTES

Project Manager, Mark G. Potapczuk, Propulsion Systems Division, (216) 433–3919.

12a. DISTRIBUTION/AVAILABILITY STATEMENT

Unclassified - Unlimited
Subject Category 03

12b. DISTRIBUTION CODE

13. ABSTRACT *(Maximum 200 words)*

A task was completed under NASA contract, the purpose of which was to validate a three-dimensional particle trajectory code with existing test data obtained from the Icing Research Tunnel at NASA-Lewis. The geometry analyzed was a flush-mounted ECS inlet. Results of the study indicated good overall agreement between analytical predictions and wind tunnel test results at most flight conditions. Difficulties were encountered when predicting impingement characteristics of the droplets less than or equal to 13.5 microns in diameter. This difficulty was corrected to some degree by modifications to a module of the particle trajectory code; however, additional modifications will be required to accurately predict impingement characteristics of smaller droplets.

14. SUBJECT TERMS

Icing; Trajectory; Droplet; Inlet; Compressible; Three-dimensional

15. NUMBER OF PAGES

306

16. PRICE CODE

A14

17. SECURITY CLASSIFICATION OF REPORT	18. SECURITY CLASSIFICATION OF THIS PAGE	19. SECURITY CLASSIFICATION OF ABSTRACT	20. LIMITATION OF ABSTRACT
Unclassified	Unclassified	Unclassified	